EMERGING INFECTIOUS DISEASES®

CDC
Centers for Disease Control and Prevention

Mycobacteria

March 2020

Charles Laval (1861–1894), *Self-Portrait, Pont-Aven,* 1888. Oil on canvas, 20 in x 23.8 in/50.7 cm × 60.4 cm. Van Gogh Museum, Amsterdam, Vincent van Gogh Foundation

EMERGING INFECTIOUS DISEASES®

Emerging Infectious Diseases is published monthly by the Centers for Disease Control and Prevention, 1600 Clifton Rd NE, Mailstop H16-2, Atlanta, GA 30329-4027, USA. Telephone 404-639-1960, email eideditor@cdc.gov.

EMERGING INFECTIOUS DISEASES®

Mycobacteria **March 2020**

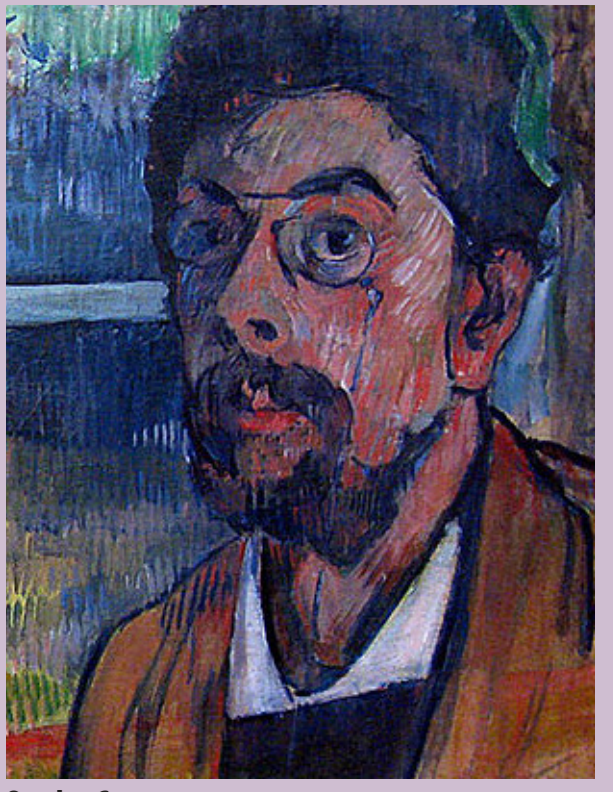

On the Cover

Charles Laval (1861–1894), *Self-Portrait, Pont-Aven*, 1888. Oil on canvas, 20 in x 23.8 in/50.7 cm × 60.4 cm. Van Gogh Museum, Amsterdam, Vincent van Gogh Foundation.

About the Cover p. 634

Synopses

Medscape EDUCATION ACTIVITY

Medscape EDUCATION ACTIVITY

Research

Medscape EDUCATION ACTIVITY

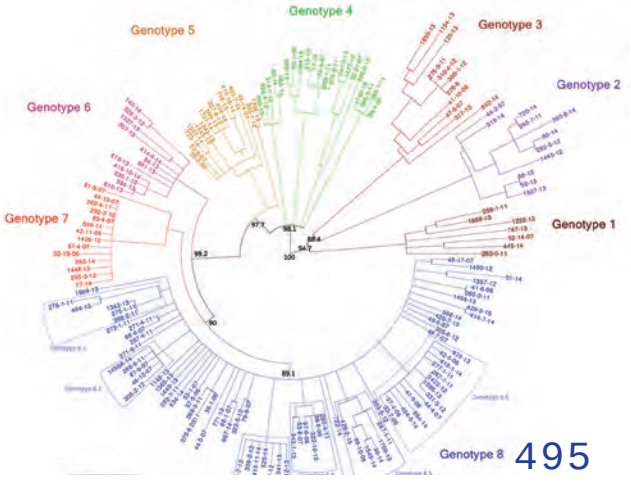

495

EMERGING INFECTIOUS DISEASES®
March 2020


504

Dispatches

EMERGING INFECTIOUS DISEASES®
March 2020

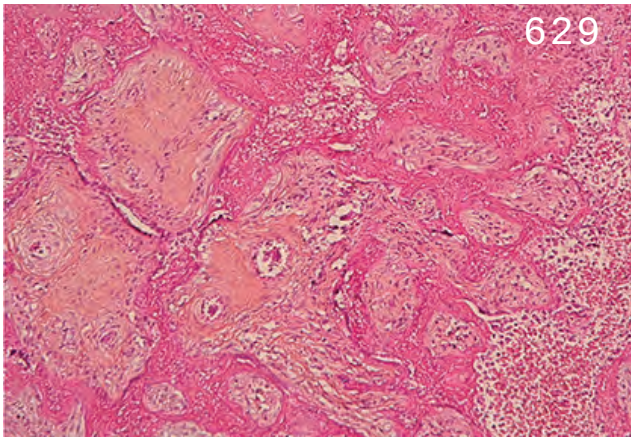

Research Letters

Comment Letters

About the Cover

Online Report

Conference Summary

DECENNIAL 2020

Global Solutions to Antibiotic Resistance in Healthcare

6th Decennial International Conference on Healthcare Associated Infections

March 26–30, 2020
Marriott Marquis
Atlanta, GA

REGISTER TODAY!

Co-Hosted by:

SHEA
The Society for Healthcare Epidemiology of America

CDC
Centers for Disease Control and Prevention

Clinical Characteristics of Disseminated Strongyloidiasis, Japan, 1975–2017

Mitsuru Mukaigawara, Masashi Narita, Soichi Shiiki, Yoshihiro Takayama, Shunichi Takakura, Tomokazu Kishaba

Medscape EDUCATION ACTIVITY

In support of improving patient care, this activity has been planned and implemented by Medscape, LLC and Emerging Infectious Diseases. Medscape, LLC is jointly accredited by the Accreditation Council for Continuing Medical Education (ACCME), the Accreditation Council for Pharmacy Education (ACPE), and the American Nurses Credentialing Center (ANCC), to provide continuing education for the healthcare team.

Medscape, LLC designates this Journal-based CME activity for a maximum of 1.00 ***AMA PRA Category 1 Credit(s)™***. Physicians should claim only the credit commensurate with the extent of their participation in the activity.

Successful completion of this CME activity, which includes participation in the evaluation component, enables the participant to earn up to 1.0 MOC points in the American Board of Internal Medicine's (ABIM) Maintenance of Certification (MOC) program. Participants will earn MOC points equivalent to the amount of CME credits claimed for the activity. It is the CME activity provider's responsibility to submit participant completion information to ACCME for the purpose of granting ABIM MOC credit.

All other clinicians completing this activity will be issued a certificate of participation. To participate in this journal CME activity: (1) review the learning objectives and author disclosures; (2) study the education content; (3) take the post-test with a 75% minimum passing score and complete the evaluation at http://www.medscape.org/journal/eid; and (4) view/print certificate. For CME questions, see page 637.

Release date: February 19, 2020; Expiration date: February 19, 2021

Learning Objectives

Upon completion of this activity, participants will be able to:

- Describe classification of disseminated strongyloidiasis into 3 clinical phenotypes, according to a case series
- Determine clinical and laboratory findings in disseminated strongyloidiasis, according to a case series
- Identify treatment of disseminated strongyloidiasis, according to a case series

CME Editor

Jude Rutledge, BA, Technical Writer/Editor, Emerging Infectious Diseases. *Disclosure: Jude Rutledge has disclosed no relevant financial relationships.*

CME Author

Laurie Barclay, MD, freelance writer and reviewer, Medscape, LLC. *Disclosure: Laurie Barclay, MD, has disclosed no relevant financial relationships.*

Authors

Disclosures: ***Mitsuru Mukaigawara, MD; Masashi Narita, MD; Soichi Shiiki, MD; Yoshihiro Takayama, MD; Shunichi Takakura, MD;*** *and* ***Tomokazu Kishaba, MD, have*** *disclosed no relevant financial relationships.*

Clinical characteristics of disseminated strongyloidiasis, the severest form of strongyloidiasis, are not well described. We conducted a retrospective, consecutive chart review of patients with disseminated strongyloidiasis admitted to Okinawa Chubu Hospital in Okinawa, Japan, during January 1975–December 2017. The 70 patients were classified into 3 clinical phenotypes: dissemination (32 patients [45.7%]), occult dissemination with meningitis caused by enteric organisms (12 patients [17.1%]), and occult dissemination with culture-negative suppurative meningitis (26 patients [37.1%]). Associated mortality rates were 56.3%, 16.7%, and 11.5%, respectively, and sepsis occurred in 40.6%, 58.3%, and 11.5% of cases, respectively. Common symptoms included fever (52.9% of patients), headache (32.9%), and altered mental status (24.3%). Patients were treated with thiabendazole (before 2003) or ivermectin (after 2003). Our findings show that disseminated strongyloidiasis has clinical phenotypes in terms of severity and that identification of occult dissemination, a mild form with prominent neurologic manifestations, is lifesaving.

Author affiliations: Harvard Kennedy School, Cambridge, Massachusetts, USA (M. Mukaigawara); Okinawa Chubu Hospital, Uruma, Okinawa, Japan (M. Mukaigawara, M. Narita, S. Shiiki, Y. Takayama, S. Takakura, T. Kishaba)

DOI: https://doi.org/10.3201/eid2603.190571

Strongyloidiasis is a nematode infection caused by *Strongyloides stercoralis*, a parasitic roundworm. Parasites of the genus *S. stercoralis* are characteristic for their ability to replicate within hosts (*1*). Patients have clinical characteristics of systemic strongyloidiasis when their immune status is impaired (*2*), such as through the use of steroids (*3*), medication associated with organ transplantation (*4*), and initiation of chemotherapy (*5*). Strongyloidiasis has been prevalent in the tropics and subtropics and is reemerging as a critical disease in the immunocompromised patient population (*6*).

The life cycle of the *S. stercoralis* roundworm consists of external and autoinfective cycles (*7*). Infective filariform larvae penetrate the skin, enter the venous circulation, and migrate to the pulmonary circulation. The larvae are then swallowed and remain in the small intestine to mature into the parthenogenic female adult *S. stercoralis* worm (*8*). The noninfectious rhabditiform offspring can develop into infective filariform larvae while still in the intestine and reinfect the host. These autoinfective filariform larvae enable the unique autoinfective life cycle of *S. stercoralis* parasites to continue indefinitely in humans.

When the host immune status is compromised, the autoinfective cycle can be enhanced, enabling increasing numbers of autoinfective larvae to disseminate throughout the body. The clinical complications of disseminated strongyloidiasis are a result of the increasing numbers of autoinfective larvae traveling through the body, with many larvae carrying enteric bacteria from the intestine (*9*). Penetrated larvae carry enteric organisms to multiple organ systems, causing sepsis (*10*–*12*), pneumonia (*10*,*11*,*13*), and meningitis (*10*,*11*,*14*–*18*).

Early recognition of dissemination is essential, yet little has been known about its clinical, laboratory, and microbiological characteristics (*1*). Our study aimed to provide characteristics of patients with disseminated strongyloidiasis. We conducted a retrospective, consecutive chart review of patients diagnosed with disseminated strongyloidiasis in an area of human T-cell lymphotrophic virus type 1 (HTLV-1) infection endemicity in Japan during January 1975–December 2017.

Methods

Study Setting

This study was conducted at Okinawa Chubu Hospital in Okinawa, Japan, which has a subtropical climate; strongyloidiasis is endemic to Okinawa (*19*). The region also has a high prevalence of HTLV-1 infection (*20*). Okinawa Chubu Hospital is one of the largest teaching hospitals in Okinawa.

Study Design and Patients

We consecutively reviewed the charts of adult patients (≥18 years of age) diagnosed with disseminated strongyloidiasis during January 1975–December 2017 and admitted to Okinawa Chubu Hospital. We classified disseminated strongyloidiasis into 3 clinical phenotypes: dissemination, occult dissemination with meningitis caused by enteric organisms (*14*), and occult dissemination with culture-negative suppurative meningitis (*15*).

We defined dissemination as filariform larvae detected from specimens other than the gastrointestinal tract (i.e., feces, duodenal fluid, and gastric juice). We defined occult dissemination with meningitis caused by enteric organisms as meningitis caused by enteric organisms combined rhabditiform larvae detected from the gastrointestinal tract (e.g., in feces and gastric juice); enteric organisms were *Bacteroides* spp., *Enterococcus* spp., *Escherichia coli*, *Enterobacter* spp., *Klebsiella* spp., *Bifidobacterium* spp., *Clostridium perfringens*, *Proteus mirabilis*, *Streptococcus gallolyticus* (*bovis* group), and *Campylobacter* spp. (*21*). We defined occult dissemination with culture-negative suppurative meningitis as cerebrospinal fluid (CSF) culture-negative meningitis with CSF neutrophil-dominant pleocytosis of >500 cells/mm^3 (*16*) combined with rhabditiform larvae detected from the gastrointestinal tract (e.g. in feces and gastric juice).

Patients with nosocomial meningitis and meningitis patients with prior receipt of antibiotics (within 7 days of performing lumbar puncture) were excluded from the analysis. We performed parasitologic examinations by direct microscopic examinations, formalin–ether concentration technique, or both interchangeably on the basis of clinical symptoms.

Ethics Statement

We collected demographic data, clinical characteristics, clinical diagnosis, and microbiologic data for all patients in a secure database after identifying information of included patients was removed. This study was approved by the Institutional Review Board of Okinawa Chubu Hospital (approval no. H29–75).

Results

Patient Population

We identified 70 patients during the study period (Table 1); 42 (60%) were men. Median age of patients

Table 1. Demographic characteristics of patients with disseminated strongyloidiasis, Okinawa Chubu Hospital, Uruma, Japan, 1975–2017*

Characteristic	All patients	Dissemination	Occult dissemination with meningitis/enteric organisms	Occult dissemination with culture-negative suppurative meningitis
No. patients	70/70 (100)	32/70 (45.7)	12/70 (17.1)	26/70 (37.1)
Sex				
M	42 (60)	19 (59.4)	6 (50)	17 (65.3)
F	28 (40)	13 (40.6)	6 (50)	9 (34.7)
Median age, y (range)	61 (21–96)	67 (25–96)	47 (21–84)	57 (38–92)
Immunocompromised status				
HTLV-1 infection†	36/40 (90.0)	17/20 (85.0)	8/9 (88.9)	11/11 (100)
Steroid use	6 (8.6)	5 (15.6)	1 (8.3)	0 (0)
Solid organ malignancy	6 (8.6)	4 (12.5)	2 (16.7)	0 (0)
Diabetes mellitus	4 (5.7)	4 (12.5)	0 (0)	0 (0)
Cirrhosis	2 (2.9)	2 (6.3)	0 (0)	0 (0)
Death	23 (32.9)	18 (56.3)	2 (16.7)	3 (11.5)

*Values are no. (%) unless indicated. HTLV-1, human T-cell lymphotrophic virus type 1.
†Serologic test for HTLV-1 infection was not available until the 1980s.

was 61 years (range 21–96 years); all patients were born before 1964. Thirty-two patients (32/70 [45.7%]) had dissemination, 12 (12/70 [17.1%]) had occult dissemination with meningitis caused by enteric organisms, and 26 (26/70 [37.1%]) had occult dissemination with culture-negative suppurative meningitis. Thirty-six tested patients (36/39 [92.3%]) had positive serologic assay results for HTLV-1. Six patients (6/70 [8.6%]) had solid organ malignancy, 5.7% (4/70) had diabetes mellitus, and 2.9% (2/70) had cirrhosis. Six patients (8.6%) regularly used steroids; doses were equivalent to 5–30 mg of daily prednisolone. The mortality rate was highest in the dissemination group (18/32 [56.3%]), followed by the occult dissemination with meningitis caused by enteric organisms (2/12 [16.7%]) group and the occult dissemination with culture-negative suppurative meningitis (3/26 [11.5%]) group.

The number of annually reported cases was decreasing during the study period. The maximum number of annual cases was 7 (Figure). Most strongyloidiasis cases in the last decade of the study period were classified as dissemination.

Clinical Manifestations

Common symptoms included fever (37/70 [52.9%] patients), headache (23/70 [32.9%]), altered mental status (17/70 [24.3%]), and nausea/vomiting (10/70 [14.3%]) (Table 2). In terms of laboratory findings, the average absolute eosinophil count was 225 cells/μL (range 0–1,482 cells/μL).

The main clinical diagnoses included meningitis, pneumonia, sepsis, and paralytic ileus (Table 2). Twenty-three patients (32.9%) had clinical manifestations of sepsis caused by enteric organisms, 22 patients (31.4%) had clinical manifestations of meningitis caused by enteric organisms, and 34 patients (48.6%) had clinical manifestations of culture-negative suppurative meningitis. Nine patients had highly critical conditions with evidence of multiorgan involvement, including the gastrointestinal (paralytic ileus), pulmonary (pneumonia caused by enteric organisms), central nervous (meningitis), and circulatory (sepsis caused by enteric organisms) systems. The mortality rate was 77.8% (7/9) in these patients. Such clinical features (22) have been referred to as "full-blown" dissemination at our institution (*10*).

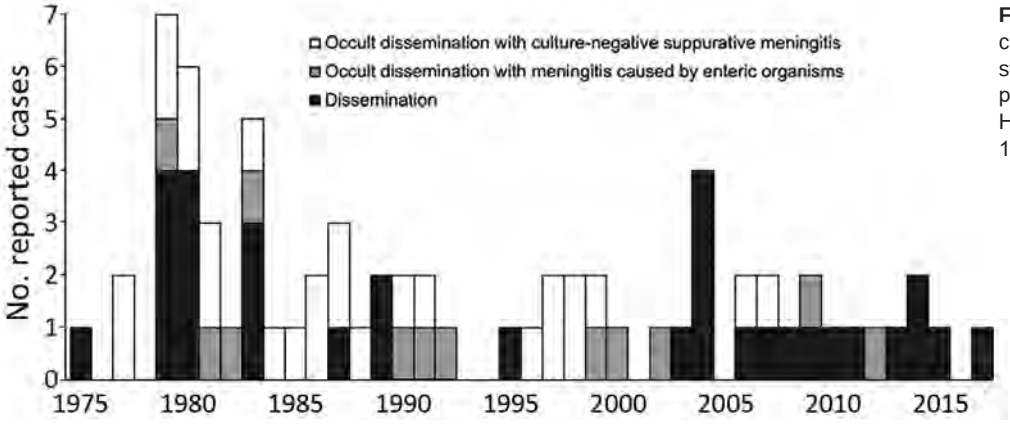

Figure. Number of reported cases of disseminated strongyloidiasis, by clinical phenotype, Okinawa Chubu Hospital, Uruma, Japan, 1975–2017.

Table 2. Symptoms and clinical diagnoses of patients with disseminated strongyloidiasis, Okinawa Chubu Hospital, Uruma, Japan, 1975–2017

Characteristic	No. patients			
	All patients	Dissemination	Occult dissemination with meningitis/enteric organisms	Occult dissemination with culture-negative suppurative meningitis
No. patients	70 (100)	32 (45.7)	12 (17.1)	26 (37.1)
Symptoms*				
Fever	37 (52.9)	15 (46.9)	8 (66.7)	14 (53.8)
Headache	23 (32.9)	3 (9.4)	7 (58.3)	13 (50.0)
Altered mental status	17 (24.3)	7 (21.9)	3 (25.0)	7 (26.9)
Nausea or vomiting	10 (14.3)	4 (12.5)	1 (8.3)	5 (19.2)
Abdominal pain	6 (8.6)	2 (6.3)	2 (16.7)	2 (7.7)
Anorexia	5 (7.1)	4 (12.5)	1 (8.3)	0 (0)
Constipation	1 (1.4)	0 (0)	1 (8.3)	0 (0)
Diarrhea	1 (1.4)	0 (0)	0 (0)	1 (3.8)
Clinical diagnosis†				
Full-blown dissemination‡	9 (12.9)	9 (28.1)	0 (0)	0 (0)
Sepsis	23 (32.9)	13 (40.6)	7 (58.3)	3 (11.5)
Meningitis (enteric)	22 (31.4)	10 (31.3)	12 (100)	0 (0)
Meningitis (culture-negative)	34 (48.6)	8 (25)	0 (0)	26 (100)
Pneumonia	27 (38.6)	26 (81.3)	0 (0)	1 (3.8)
Paralytic ileus	17 (24.3)	15 (46.9)	1 (8.3)	1 (3.8)

*Other symptoms that were only noted in patients with dissemination included cough (2 cases), and rash, fatigue, convulsion, and syncope (1 case each).
†Other diagnoses that were only identified in patients with dissemination included peritonitis (6 cases), dermatitis (5 cases), and esophagitis (1 case).
‡Full-blown dissemination is the severest form of dissemination and hyperinfection, referring to patients with paralytic ileus and pneumonia caused by enteric organisms, as well as either sepsis or meningitis caused by enteric organisms.

One case-patient with full-blown dissemination, a woman in her 60s, had fever, vomiting, headache, and altered mental status. On arrival to the hospital, the patient was obtunded, and neck stiffness was noted. The results of lumbar puncture were suggestive of bacterial meningitis caused by gram-negative bacilli. On direct microscopic examination, multiple larvae were identified in feces, sputum, CSF, ascites, and gastric juice. The patient's condition deteriorated despite treatment for both strongyloidiasis and bacterial meningitis. Her clinical course also was complicated by paralytic ileus and bacterial pneumonia caused by *K. pneumoniae*. Gram staining of CSF was notable for gram-negative bacilli, and both blood and CSF cultures yielded *E. coli*. The patient died on hospital day 11. On autopsy, larvae were identified in the skin and lungs (*11*).

The clinical course of patients with occult dissemination with bacterial meningitis caused by enteric organisms was less severe than full-blown dissemination, yet remained critical without appropriate treatment. One such patient, a man in his 50s, sought care at our emergency department in the 1980s for a 1-day history of headache, vomiting, shaking, and chills. On examination, the patient had neck stiffness. Results of lumbar puncture were notable for a white blood cell count of 4,104 cells/μL (77% of polymorphonuclear neutrophils). Larvae were detected in feces. The patient was started on thiabendazole, chloramphenicol, and ampicillin. Gram staining of CSF samples was negative, but culture later yielded *E. coli*. Blood culture obtained on admission was negative. The patient responded well to the treatment, and larvae were no longer detected in feces by hospital day 6 (*14*).

Occult dissemination with culture-negative suppurative meningitis occurred in less critical conditions. One case-patient, a woman in her 90s, was brought to our hospital in the 1980s for altered mental status and chills. The patient was obtunded, and results of CSF analysis was consistent with suppurative meningitis (white blood cell count of 3,812/cells/μL [73% of polymorphonuclear neutrophils]). Gram staining of CSF was negative for organisms, and culture results were sterile. Parasitologic examination was positive only in feces. The patient responded well to antibiotics and thiabendazole and was discharged to home on hospital day 9 (*15*).

Parasitologic and Microbiologic Results

Larvae were identified from samples including stool (from 60/70 [85.7%] patients), sputum (30/70 [42.9%]), gastric juice (24/70 [34.3%]), ascites (4/70 [5.7%]), urine (3/70 [4.3%]), CSF (2/70 [2.9%]), and biopsy specimens (Table 3). No antibody testing or PCR was used in making a diagnosis, except for 1 patient who had necrotizing esophagitis (*23*).

E. coli, *K. pneumoniae*, and *S. gallolyticus* were the most common organisms detected from blood and CSF cultures, causing 7%–10% of bacteremia. Other organisms that caused bacteremia included *E. aerogenes*, *S. infantarius*, and *Enterococcus* spp.

Table 3. Parasitologic investigation and culture results of patients with disseminated strongyloidiasis, Okinawa Chubu Hospital, Uruma, Japan, 1975–2017*

Characteristic	No. (%) patients			
	All patients	Dissemination	Occult dissemination with meningitis/enteric organisms	Occult dissemination with culture-negative suppurative meningitis
No. patients	70 (100)	32 (45.7)	12 (17.1)	26 (37.1)
Specimens with larvae†				
Stool	60 (85.7)	22 (68.8)	12 (100)	26 (100)
Sputum	30 (42.9)	30 (93.8)	0 (0)	0 (0)
Gastric juice	24 (34.3)	16 (50)	3 (25)	5 (19.2)
Blood culture results‡				
Escherichia coli	6 (8.6)	4 (12.5)	2 (16.7)	0 (0)
Klebsiella pneumoniae	7 (10.0)	4 (12.5)	1 (8.3)	2 (7.7)
Streptococcus gallolyticus	5 (7.1)	1 (3.1)	3 (25)	1 (3.8)
CSF culture results‡				
E. coli	9/65 (13.8)	4/27 (14.8)	5 (41.7)	0 (0)
K. pneumoniae	6/65 (9.2)	3/27 (11.1)	3 (25)	0 (0)
S. gallolyticus	5/65 (7.7)	1/27 (3.7)	4 (33.3)	0 (0)

*CSF, cerebrospinal fluid.
†In dissemination, larvae also were detected from ascites (4 cases), urine (3 cases), CSF (2 cases), and skin, bronchoalveolar lavage, and biopsies of the lung, duodenum, and liver (1 case each).
‡In dissemination, blood cultures also were positive for *Enterobacter aerogenes*, *Enterococcus* spp., and *S. infantarius* (1 case each), and CSF cultures were positive for *E. aerogenes* and *Streptococcus* spp. (1 case each). In occult dissemination with meningitis (enteric organisms), blood cultures also were positive for *E. agglomerans* (1 case), and CSF cultures were positive for *Enterococcus* spp. (1 case).

Treatment

Before 2002, patients were treated with thiabendazole. Thiabendazole was administered at the conventional dose of 50 mg/kg/day (not exceeding 3 g/d) for ≥3 days. Patients in critical conditions were given double doses (100 mg/kg/d) for the first 1–2 days. Thiabendazole was tapered off when clinical improvement or disappearance of larvae in feces was confirmed.

After 2003, all patients were treated with ivermectin at the dose of 200 μg/kg/day. Two patients with critical conditions received 2 or 1.5 times the conventional dose. Ivermectin was administered either 1–2 weeks apart or consecutively until the confirmation of clinical improvement or disappearance of larvae from feces. A combination of oral and rectal forms of ivermectin was administered in 3 patients.

One patient in 1980 initially received pyrvinium pamoate at a dose of 20 mL/day because thiabendazole was not available. Another patient with occult dissemination with culture-negative suppurative meningitis did not receive anthelmintics because meningitis was suspected to be caused by the central nervous system involvement of adult T-cell leukemia.

Discussion

Disseminated strongyloidiasis is a medical emergency. Because of its rarity, most previous reports consist of single cases (*24*), making it difficult to determine its clinical phenotypes. Previous reports identified atypical suppurative meningitis, defined as community-acquired meningitis caused by enteric organisms or culture-negative suppurative meningitis, as a form of occult dissemination (*10*,*14*–*16*). Our study corroborates preceding analyses and extends their findings by demonstrating that early recognition of occult dissemination is lifesaving.

Demographic characteristics in our study, such as age distribution and male-to-female ratio, were in keeping with previous reports (*24*). However, our patients all were born before 1964, and the number of annually reported cases was decreasing during the study period. These findings were consistent with a report from another institution in Okinawa (*25*) and suggest that patients, predominantly men, in this region in the past became infected from contaminated soil during farming and by walking barefoot (*26*). Improved farming environments and changes in lifestyle might have reduced the risk for exposure. Another trend we noted was that 9 of 11 reported cases during the last 10 years of the study period were classified as dissemination and only 2 out of 11 as occult dissemination. The median age of patients in these 11 cases was 80 years, implying that the elderly who had been exposed to *S. stercoralis* parasites in their youth developed systemic strongyloidiasis at advanced age, which quickly disseminated because of their impaired immune status.

In this case series, few patients had risk factors for strongyloidiasis other than HTLV-1 infection, including recent steroid use (*3*), organ transplant (*4*), or cirrhosis (*27*,*28*). In areas with HTLV-1 endemicity, HTLV-1 infection is the major risk factor for both chronic strongyloidiasis and dissemination (*29*).

Table 4. Involvement of larvae and enteric organisms in disseminated strongyloidiasis reported in previous studies*

Characteristic	Dissemination	Occult dissemination with meningitis/enteric organisms	Occult dissemination with culture-negative suppurative meningitis
Involvement of larvae	Confirmed (rhabditiform and filariform larvae)	Confirmed (rhabditiform larvae)	Confirmed (rhabditiform larvae)
Involvement of enteric organisms	Confirmed	Confirmed	Not detected

*References *11*, *14*, and *15*.

Although diabetes mellitus has been reported to be a risk factor for strongyloidiasis treatment failure (*30*), the prevalence in our series remained low.

Considering the mortality rates and the various symptoms and clinical diagnoses, dissemination is the most severe form of strongyloidiasis, followed by occult dissemination with meningitis caused by enteric organisms and then occult dissemination with culture-negative suppurative meningitis. Evidence of multiorgan involvement was less common in occult dissemination, which might reflect the degree of involvement of larvae and enteric organisms in these 3 phenotypes. Previous studies have identified different degrees of their involvement (*11*,*14*,*15*) (Table 4).

Despite the low mortality rate associated with occult dissemination with culture-negative suppurative meningitis, it is critical for clinicians to identify concomitant strongyloidiasis because patients might later have recurrent meningitis in more critical conditions (*18*) if not properly treated. Culture-negative suppurative meningitis should prompt the immediate consideration of performing a parasitologic examination in areas where strongyloidiasis and HTLV-1 are endemic. Previous reports have suggested that culture-negative suppurative meningitis is a form of dissemination (*10*,*15*,*17*).

Limited data are available about the optimal treatment of dissemination. Treatment options consist of reducing immunosuppressive therapies and initiating antihelmintics and antibiotics. Reducing immunosuppressive therapies is recommended because immunosuppressive therapies can induce dissemination (*6*). In a systematic review comparing ivermectin, albendazole, and thiabendazole, ivermectin resulted in better parasitologic cure than albendazole and fewer adverse effects than thiabendazole (*31*). The conventional dose of ivermectin is 200 μg/kg/day orally for 2 days, either consecutively or 2 weeks apart (*32*). In dissemination, the dose and duration are determined clinically. Repeated or prolonged administration are preferred until patients respond or until larvae are no longer detected (*33*). For patients who are unable to take oral ivermectin, a rectal (*34*), veterinary subcutaneous (*35*), or parenteral (*36*) formula is administered. The use of veterinary ivermectin is considered in critical cases. Some studies have also reported the use of a combination of ivermectin and albendazole (*37*). In our study, several critical patients received an increased dose of thiabendazole or ivermectin. No patients received a combination of ivermectin and thiabendazole. Anthelmintic agents were continued until patients responded or until larvae disappeared.

Initiation of antibiotics that target enteric organisms is essential. The antibiotics must penetrate into the central nervous system when meningitis is suspected. The spectrum should be based on the local antibiogram. In our study, no patients had bacterial infection that produced extended spectrum β-lactamases or AmpC β-lactamases. Clinicians should also notice that the results of blood and CSF cultures differed in 4 patients (4/70 [5.7%]), suggesting that larvae might have carried multiple enteric organisms. Empiric antibiotics that sufficiently cover most enteric organisms, such as third-generation cephalosporins, are recommended. The administration of dexamethasone for bacterial meningitis should carefully be considered because it might induce dissemination (*9*).

Our investigation has several limitations. First, the retrospective nature of this study might have resulted in distortions in the accuracy of the retrieved information. Second, patients with disseminated strongyloidiasis have also been admitted to other medical centers in Okinawa (*38*); hence, we might have underreported the prevalence of dissemination in this region. Third, the findings cannot be generalizable to regions where HTLV-1 infection is not endemic.

In summary, we classified disseminated strongyloidiasis into 3 phenotypes on the basis of their severity and various symptoms: dissemination, occult dissemination with meningitis caused by enteric organisms, and occult dissemination with culture-negative suppurative meningitis. Early identification of occult dissemination is lifesaving. Treatment options consist of reduction of immunosuppressive therapies, initiation of anthelmintic agents with a higher dose and longer duration depending on the severity of symptoms, and concurrent use of antimicrobial agents against enteric organisms.

Acknowledgment

We thank Kiyofumi Ohkusu for conducting real-time PCR analysis.

About the Author

Dr. Mukaigawara was a chief medical resident at Okinawa Chubu Hospital when he conducted this research. He is now a graduate student in public policy at Harvard Kennedy School. His primary research interests include global health governance and socioeconomic determinants of health.

References

1. Olsen A, van Lieshout L, Marti H, Polderman T, Polman K, Steinmann P, et al. Strongyloidiasis—the most neglected of the neglected tropical diseases? Trans R Soc Trop Med Hyg. 2009;103:967–72. https://doi.org/10.1016/j.trstmh.2009.02.013
2. Igra-Siegman Y, Kapila R, Sen P, Kaminski ZC, Louria DB. Syndrome of hyperinfection with *Strongyloides stercoralis*. Rev Infect Dis. 1981;3:397–407. https://doi.org/10.1093/clinids/3.3.397
3. Fardet L, Généreau T, Poirot JL, Guidet B, Kettaneh A, Cabane J. Severe strongyloidiasis in corticosteroid-treated patients: case series and literature review. J Infect. 2007;54:18–27. https://doi.org/10.1016/j.jinf.2006.01.016
4. Marty FM. Strongyloides hyperinfection syndrome and transplantation: a preventable, frequently fatal infection. Transpl Infect Dis. 2009;11:97–9. https://doi.org/10.1111/j.1399-3062.2009.00383.x
5. Sánchez PR, Guzman AP, Guillen SM, Adell RI, Estruch AM, Gonzalo IN, et al. Endemic strongyloidiasis on the Spanish Mediterranean coast. QJM. 2001;94:357–63. https://doi.org/10.1093/qjmed/94.7.357
6. Keiser PB, Nutman TB. *Strongyloides stercoralis* in the immunocompromised population. Clin Microbiol Rev. 2004;17:208–17. https://doi.org/10.1128/CMR.17.1.208-217.2004
7. US Centers for Disease Control and Prevention. Parasites: *Strongyloides*. Biology [cited 2019 Feb 1]. https://www.cdc.gov/parasites/strongyloides/biology.html
8. Mansfield LS, Alavi A, Wortman JA, Schad GA. Gamma camera scintigraphy for direct visualization of larval migration in *Strongyloides stercoralis*-infected dogs. Am J Trop Med Hyg. 1995;52:236–40. https://doi.org/10.4269/ajtmh.1995.52.236
9. Pukkila-Worley R, Nardi V, Branda JA. Case records of the Massachusetts General Hospital. Case 28-2014. A 39-year-old man with a rash, headache, fever, nausea, and photophobia. N Engl J Med. 2014;371:1051–60. https://doi.org/10.1056/NEJMcpc1405886
10. Kishaba T. Disseminated strongyloidiasis. In: Shiroma Y, Sato Y, editors. *Strongyloides stercoralis* and strongyloidiasis in Japan [in Japanese]. Fukuoka (Japan): Kyushu University Press; 1997. p. 55–78.
11. Kishaba T. Strongyloidiasis and infections due to enteric organisms: sepsis, pneumonia and meningitis caused by Gram-negative bacteria associated with disseminated strongyloidiasis [in Japanese]. Infection. 1982;12:180.
12. Jain AK, Agarwal SK, el-Sadr W. *Streptococcus bovis* bacteremia and meningitis associated with *Strongyloides stercoralis* colitis in a patient infected with human immunodeficiency virus. Clin Infect Dis. 1994;18:253–4. https://doi.org/10.1093/clinids/18.2.253
13. Chu E, Whitlock WL, Dietrich RA. Pulmonary hyperinfection syndrome with *Strongyloides stercoralis*. Chest. 1990;97:1475–7. https://doi.org/10.1378/chest.97.6.1475
14. Kishaba T, Uchihara T, Ueno K, Goeku C, Shimabukuro Y. Gram-negative rod meningitis probably caused by occult disseminated strongyloidiasis [in Japanese]. Okinawa Medical Journal. 1985;22:3.
15. Kishaba T, Suginohara K, Tamaki K, Miyara Y, Endo K, Taira Y, et al. Culture negative suppurative meningitis probably caused by occult disseminated strongyloidiasis [in Japanese]. Okinawa Medical Journal. 1989;26:219.
16. Mukaigawara M, Nakayama I, Gibo K. Strongyloidiasis and culture-negative suppurative meningitis, Japan, 1993–2015. Emerg Infect Dis. 2018;24:2378–80. https://doi.org/10.3201/eid2412.180375
17. Sasaki Y, Taniguchi T, Kinjo M, McGill RL, McGill AT, Tsuha S, et al. Meningitis associated with strongyloidiasis in an area endemic for strongyloidiasis and human T-lymphotropic virus-1: a single-center experience in Japan between 1990 and 2010. Infection. 2013;41:1189–93. https://doi.org/10.1007/s15010-013-0483-2
18. Shimasaki T, Chung H, Shiiki S. Five cases of recurrent meningitis associated with chronic strongyloidiasis. Am J Trop Med Hyg. 2015;92:601–4. https://doi.org/10.4269/ajtmh.14-0564
19. Toma H, Shimabukuro I, Kobayashi J, Tasaki T, Takara M, Sato Y. Community control studies on *Strongyloides* infection in a model island of Okinawa, Japan. Southeast Asian J Trop Med Public Health. 2000;31:383–7.
20. Sagara Y, Iwanaga M, Morita M, Sagara Y, Nakamura H, Hirayama H, et al. Fine-scale geographic clustering pattern of human T-cell leukemia virus type 1 infection among blood donors in Kyushu-Okinawa, Japan. J Med Virol. 2018;90:1658–65. https://doi.org/10.1002/jmv.25239
21. Cresci GA, Bawden E. Gut microbiome: what we do and don't know. Nutr Clin Pract. 2015;30:734–46. https://doi.org/10.1177/0884533615609899
22. Scowden EB, Schaffner W, Stone WJ. Overwhelming strongyloidiasis: an unappreciated opportunistic infection. Medicine (Baltimore). 1978;57:527–44. https://doi.org/10.1097/00005792-197811000-00004
23. Tomori M, Mukaigawara M, Narita M. Acute esophageal necrosis associated with *Strongyloides stercoralis* hyperinfection. Am J Trop Med Hyg. 2019;100:1037–8. https://doi.org/10.4269/ajtmh.18-0664
24. Geri G, Rabbat A, Mayaux J, Zafrani L, Chalumeau-Lemoine L, Guidet B, et al. *Strongyloides stercoralis* hyperinfection syndrome: a case series and a review of the literature. Infection. 2015;43:691–8. https://doi.org/10.1007/s15010-015-0799-1
25. Tanaka T, Hirata T, Parrott G, Higashiarakawa M, Kinjo T, Kinjo T, et al. Relationship among *Strongyloides stercoralis* infection, human T-cell lymphotropic virus type 1 infection, and cancer: a 24-year cohort inpatient study in Okinawa, Japan. Am J Trop Med Hyg. 2016;94:365–70. https://doi.org/10.4269/ajtmh.15-0556
26. Schär F, Trostdorf U, Giardina F, Khieu V, Muth S, Marti H, et al. *Strongyloides stercoralis*: global distribution and risk factors. PLoS Negl Trop Dis. 2013;7:e2288. https://doi.org/10.1371/journal.pntd.0002288
27. Teixeira MC, Pacheco FT, Souza JN, Silva ML, Inês EJ, Soares NM. *Strongyloides stercoralis* infection in alcoholic patients. BioMed Res Int. 2016;2016:4872473. https://doi.org/10.1155/2016/4872473

28. de Oliveira LC, Ribeiro CT, Mendes DM, Oliveira TC, Costa-Cruz JM. Frequency of *Strongyloides stercoralis* infection in alcoholics. Mem Inst Oswaldo Cruz. 2002;97:119–21. https://doi.org/10.1590/S0074-02762002000100021
29. Gotuzzo E, Terashima A, Alvarez H, Tello R, Infante R, Watts DM, et al. *Strongyloides stercoralis* hyperinfection associated with human T cell lymphotropic virus type-1 infection in Peru. Am J Trop Med Hyg. 1999;60:146–9. https://doi.org/10.4269/ajtmh.1999.60.146
30. Hays R, Esterman A, McDermott R. Type 2 diabetes mellitus is associated with *Strongyloides stercoralis* treatment failure in Australian aboriginals. PLoS Negl Trop Dis. 2015;9:e0003976. https://doi.org/10.1371/journal.pntd.0003976
31. Henriquez-Camacho C, Gotuzzo E, Echevarria J, White AC Jr, Terashima A, Samalvides F, et al. Ivermectin versus albendazole or thiabendazole for *Strongyloides stercoralis* infection. Cochrane Database Syst Rev. 2016;(1):CD007745. https://doi.org/10.1002/14651858.CD007745.pub3
32. Zaha O, Hirata T, Kinjo F, Saito A, Fukuhara H. Efficacy of ivermectin for chronic strongyloidiasis: two single doses given 2 weeks apart. J Infect Chemother. 2002;8:94–8. https://doi.org/10.1007/s101560200013
33. Mejia R, Nutman TB. Screening, prevention, and treatment for hyperinfection syndrome and disseminated infections caused by *Strongyloides stercoralis*. Curr Opin Infect Dis. 2012; 25:458–63. https://doi.org/10.1097/QCO.0b013e3283551dbd
34. Tarr PE, Miele PS, Peregoy KS, Smith MA, Neva FA, Lucey DR. Case report: Rectal adminstration of ivermectin to a patient with *Strongyloides hyperinfection* syndrome. Am J Trop Med Hyg. 2003;68:453–5. https://doi.org/10.4269/ajtmh.2003.68.453
35. Barrett J, Broderick C, Soulsby H, Wade P, Newsholme W. Subcutaneous ivermectin use in the treatment of severe *Strongyloides stercoralis* infection: two case reports and a discussion of the literature. J Antimicrob Chemother. 2016;71:220–5. https://doi.org/10.1093/jac/dkv315
36. Marty FM, Lowry CM, Rodriguez M, Milner DA, Pieciak WS, Sinha A, et al. Treatment of human disseminated strongyloidiasis with a parenteral veterinary formulation of ivermectin. Clin Infect Dis. 2005;41:e5–8. https://doi.org/10.1086/430827
37. Pornsuriyasak P, Niticharoenpong K, Sakapibunnan A. Disseminated strongyloidiasis successfully treated with extended duration ivermectin combined with albendazole: a case report of intractable strongyloidiasis. Southeast Asian J Trop Med Public Health. 2004;35:531–4.
38. Kishimoto K, Hokama A, Hirata T, Ihama Y, Nakamoto M, Kinjo N, et al. Endoscopic and histopathological study on the duodenum of *Strongyloides stercoralis* hyperinfection. World J Gastroenterol. 2008;14:1768–73. https://doi.org/10.3748/wjg.14.1768

Address for correspondence: Mitsuru Mukaigawara, Harvard Kennedy School, 79 John F. Kennedy St, Cambridge, MA 02138 USA; email: mitsuru_mukaigawara@hks.harvard.edu

Epidemiology of Cryptosporidiosis, New York City, New York, USA, 1995–2018[1]

Lisa Alleyne, Robert Fitzhenry, Kimberly A. Mergen, Noel Espina, Erlinda Amoroso, Daniel Cimini, Sharon Balter,[2] Ana Maria Fireteanu, Anne Seeley, Lorraine Janus, Bruce Gutelius,[3] Susan Madison-Antenucci, Corinne N. Thompson

Medscape EDUCATION ACTIVITY

In support of improving patient care, this activity has been planned and implemented by Medscape, LLC and Emerging Infectious Diseases. Medscape, LLC is jointly accredited by the Accreditation Council for Continuing Medical Education (ACCME), the Accreditation Council for Pharmacy Education (ACPE), and the American Nurses Credentialing Center (ANCC), to provide continuing education for the healthcare team.

Medscape, LLC designates this Journal-based CME activity for a maximum of 1.00 ***AMA PRA Category 1 Credit(s)™***. Physicians should claim only the credit commensurate with the extent of their participation in the activity.

Successful completion of this CME activity, which includes participation in the evaluation component, enables the participant to earn up to 1.0 MOC points in the American Board of Internal Medicine's (ABIM) Maintenance of Certification (MOC) program. Participants will earn MOC points equivalent to the amount of CME credits claimed for the activity. It is the CME activity provider's responsibility to submit participant completion information to ACCME for the purpose of granting ABIM MOC credit.

All other clinicians completing this activity will be issued a certificate of participation. To participate in this journal CME activity: (1) review the learning objectives and author disclosures; (2) study the education content; (3) take the post-test with a 75% minimum passing score and complete the evaluation at http://www.medscape.org/journal/eid; and (4) view/print certificate. For CME questions, see page 638.

Release date: February 20, 2020; Expiration date: February 20, 2021

Learning Objectives

Upon completion of this activity, participants will be able to:

- Analyze the clinical effect and treatment of cryptosporidiosis
- Distinguish the trends in the prevalence of cryptosporidiosis over time in New York, New York
- Assess the effect of cryptosporidiosis on specific populations
- Evaluate the effect of foreign travel and new diagnostic tools on the prevalence of cryptosporidiosis

CME Editor

Thomas J. Gryczan, MS, Technical Writer/Editor, Emerging Infectious Diseases. *Disclosure: Thomas J. Gryczan, MS, has disclosed no relevant financial relationships.*

CME Author

Charles P. Vega, MD, Health Sciences Clinical Professor of Family Medicine, University of California, Irvine School of Medicine. *Disclosures: Charles P. Vega, MD, has disclosed the following relevant financial relationships: served as an advisor or consultant for GlaxoSmithKline; Johnson & Johnson Pharmaceutical Research & Development, L.L.C.; served as a speaker or a member of a speakers bureau for Genentech, Inc.; GlaxoSmithKline.*

Authors

Disclosures: ***Lisa Alleyne, MPA; Robert Fitzhenry, PhD; Kimberly Mergen, MS; Noel Espina, PhD; Erlinda Amoroso, MBBS; Daniel Cimini, MPH; Sharon Balter, MD, MPH; Ana Maria Fireteanu, MPH; Anne Seeley, MPH; Lorraine L. Janus, PhD; Bruce Gutelius, MD;*** *and* ***Corinne Thompson, PhD,*** *have disclosed no relevant financial relationships.* ***Susan Madison-Antenucci, PhD,*** *has disclosed the following relevant financial relationships: received grants for clinical research from Grifols.*

Author affiliations: New York City Department Health and Mental Hygiene, Long Island City, New York, USA (L. Alleyne, R. Fitzhenry, E. Amoroso, D. Cimini, S. Balter, A.M. Fireteanu, B. Gutelius, C.N. Thompson); New York State Department of Health, Albany, New York, USA (K.A. Mergen, N. Espina, S. Madison-Antenucci); New York City Department of Environmental Protection, Corona, New York, USA (A. Seeley, L. Janus)

DOI: https://doi.org/10.3201/eid2603.190785

[1]Preliminary results were presented at the annual meeting of the Council of State and Territorial Epidemiologists, June 11–13, 2018; West Palm Beach, Florida, USA.

[2]Current affiliation: Los Angeles County Department of Health, Los Angeles, California, USA.

[3]Current affiliation: Centers for Disease Control and Prevention, Atlanta, Georgia, USA.

Cryptosporidiosis is a parasitic diarrheal infection that is transmitted by the fecal–oral route. We assessed trends in incidence and demographic characteristics for the 3,984 cases diagnosed during 1995–2018 in New York City, New York, USA, and reported to the New York City Department of Health and Mental Hygiene. Reported cryptosporidiosis incidence decreased with HIV/AIDS treatment rollout in the mid-1990s, but the introduction of syndromic multiplex diagnostic panels in 2015 led to a major increase in incidence and to a shift in the demographic profile of reported patients. Incidence was highest among men 20–59 years of age, who consistently represented most (54%) reported patients. In addition, 30% of interviewed patients reported recent international travel. The burden of cryptosporidiosis in New York City is probably highest among men who have sex with men. Prevention messaging is warranted for men who have sex with men and their healthcare providers, as well as for international travelers.

Cryptosporidiosis is marked by watery diarrhea and caused by parasites of the genus *Cryptosporidium*, which are transmitted by the fecal–oral route (*1*). Known risk factors in the United States include recreational water use, contact with animals, sexual activity in which there might be contact with stool, attendance or employment at child care settings, and consumption of contaminated food and water (*1*–*4*). Infection can cause self-limited diarrhea, although treatment is available and recommended for immunocompetent patients with severe or prolonged symptoms (*5*).

Cryptosporidiosis has been a reportable disease in New York City (NYC), New York, USA, since mid-1994 (*6*), and electronic reporting by laboratories has been required since 2006. As has been seen in other jurisdictions in the United States (*7*), the reported incidence of cryptosporidiosis in NYC has been influenced by the recent introduction of syndromic multiplex diagnostic panels, such as BioFire (https://www.biofiredx.com) and Luminex (https://www.luminexcorp.com). These panels enable physicians to screen for a large number of gastrointestinal pathogens simultaneously and have high sensitivity and specificity for several pathogens, including cryptosporidiosis (*8*,*9*).

This disease is monitored by the NYC Department of Health and Mental Hygiene (DOHMH) in part because NYC has a largely unfiltered water supply (*10*,*11*). Filtration is often used to facilitate *Cryptosporidium* oocyst removal in municipal water systems because the oocysts are resistant to standard concentrations of chemical disinfecting agents such as chlorine (*12*,*13*). Ultraviolet disinfection is now in place for the entire NYC water system, which can reduce the risk for cryptosporidiosis (*14*). Despite intensive surveillance, no evidence of drinking water–related outbreaks has been detected in NYC (*11*).

Although documented risks for cryptosporidiosis specifically in NYC include child care attendance (*15*) and HIV positivity (*16*), a systematic summary of the epidemiology of cryptosporidiosis in this large, urban setting is lacking. We examined all reported cryptosporidiosis cases since the first full year of routine investigations began in NYC in 1995. Trends in incidence, patient characteristics, and potential exposures in a large, urban setting are described, focusing on both the overall trend in annual incidence, as well as incidence trends relative to 2 major milestones in cryptosporidiosis surveillance: the period after widespread uptake of highly active antiretroviral therapy (HAART) for the control of AIDS (2000–2014), and the introduction of the sensitive syndromic multiplex panels for diagnosis (2015–2018).

Methods

A case of cryptosporidiosis was included if it occurred in a person who resided in NYC at the time of diagnosis, was diagnosed during 1995–2018, was reported to the NYC DOHMH, and met the Council of State and Territorial Epidemiologists confirmed or probable case definition (*17*). Cases diagnosed by using a syndromic multiplex diagnostic were classified as confirmed by the 2012 Centers for Disease Control and Prevention/Council of State and Territorial Epidemiologists case definition (*18*). Over the study period, there were 5 separate case definitions. However, these modifications centered on classifying cases as probable versus confirmed and did not substantially affect the number of reported cases in NYC. NYC DOHMH epidemiologists attempted to interview all patients reported with cryptosporidiosis by telephone within several weeks of diagnosis. If a patient could not be located, a chart review or interview with a healthcare provider was performed. Information on diagnostic test type was available for each patient beginning in August 2012.

During an interview, we collected information on patient symptoms; demographic characteristics; and potential risk factors, such as travel, child care attendance, recreational water exposure, sexual activity (for patients ≥18 years of age), food and water consumption history, and HIV/AIDS diagnosis. All exposure information refers to reported exposures that occurred during the period of interest before symptom onset (defined as 1 month for cryptosporidiosis patients given a diagnosis during January 1995–April

2010 or 2 weeks for cryptosporidiosis patients given a diagnosis during and May 2010–December 2018).

Population Data

We linearly interpolated intercensal population estimates for 1995–1999 by using 1990 and 2000 US Census data. Annual citywide, borough-specific, and demographic-specific intercensal population estimates (age group, sex, age/sex group, and race/ethnicity) for 2000–2018 were developed by the NYC DOHMH on the basis of the US Census Bureau's Population Estimates Program, as of November 2019 (*19*–*21*).

To calculate incidence among persons immunocompromised because of HIV/AIDS, we used the number of cases among persons with HIV/AIDS (PLWHA) divided by the total annual population of PLWHA in NYC as determined by the HIV Epidemiology and Field Services Program, NYC DOHMH (*22*,*23*). The number of persons who did not have HIV/AIDS was estimated annually to be the total NYC population minus the population of PLWHA.

Neighborhood-Level Poverty

Neighborhood-level poverty was defined as the percentage of census tract residents with household incomes <100% of the federal poverty level, according to data from the US Census and the American Community Survey (*24*,*25*). Census tract boundaries of the 2000 Census were used for patients given a diagnosis of cryptosporidiosis during 2000–2004, and census tract boundaries of the 2010 Census were used for patients given a diagnosis of cryptosporidiosis during 2005–2018. If a patient was homeless at the time of diagnosis, they were considered to live in very high poverty. Patients incarcerated at the time of diagnosis were excluded from poverty assignment. Population denominator data for neighborhood poverty for 2000–2018 were available from the NYC DOHMH Bureau of Epidemiology Services. These data are based on the American Community Survey; a 5-year pooled population estimate was used, centering on the year of the numerator, or the 5-year period that overlapped most closely in time with the year of the numerator (Table 1).

Demographic and Exposure Comparisons

We compared demographic characteristics for patients who were and were not able to be interviewed by using the χ^2 test. In addition, we compared across age/sex groups the proportion of reported exposures during the patients' incubation period among interviewed patients given a diagnosis during 2000–2018 by using the χ^2 test.

Age Adjustment and Incidence Calculations

Annual incidence during 2000–2018 was age-adjusted by using direct standardization for age at diagnosis and weighting by the US 2000 standard population (*26*). We calculated age-adjusted annual disease rates for the period 1995–2018 for the city and by borough of residence. We also calculated age-adjusted disease rates by demographic strata for 2 periods: the period after widespread adoption of HAART and before the introduction of syndromic multiplex panels (2000–2014) and the period after the introduction of syndromic multiplex panels (2015–2018). The demographic characteristics of interest included age, sex, age/sex group (persons of all sexes <20 years of age, men 20–59 years of age, men >59 years of age, and women >20 years of age), borough of residence, race/ethnicity, and neighborhood poverty level. We also calculated unadjusted cryptosporidiosis rates for persons with and without HIV/AIDS. We provide median annual incidence for the entire surveillance period (1995–2018) and for 2000–2014 and 2015–2018.

We calculated age-adjusted incidence rate ratios (IRRs) with 95% CIs by using negative binomial regression, in which the outcome was annual case count, the exposure of interest was a demographic characteristic (e.g., sex), age group was included as a potential confounder, and the offset term was the log of the population per year. We conducted 2 sets of analyses: the first compared rates among strata of demographic groups in the 2 different periods and the second compared rates of each demographic strata between the 2 periods. We conducted all analyses by using SAS version 9.4 (SAS Institute, https://www.sas.com).

Mapping

We mapped incidence of cryptosporidiosis at the community district (CD) level (n = 59). Annual CD population estimates for 2000–2018 were produced by DOHMH on the basis of the US Census Bureau Population Estimates Program, as of November 2019. Median annual incidence was mapped by CD over time and for specific subsets of age and sex. Age-adjusted incidence rates were mapped by using equal interval breaks. Almost all (98%, 3,894/3,984) patients had a successfully geocoded address.

Results

Trends in Cryptosporidiosis Incidence during 1995–2018

During 1995–2018, a total of 3,984 cryptosporidiosis cases were diagnosed and reported to the NYC

Table 1. Descriptive epidemiology of cryptosporidiosis in New York City, New York, USA, 2000–2014 and 2015–2018*

Category	2000–2014			2015–2018		
	No. cases	Incidence	IRR (95% CI)	No. cases	Incidence	IRR (95% CI)
No. cases	3,244	1.46		740	2.11	
Age group, y†						
<5	261	2.30	1.05 (0.83–1.32)	78	3.13	1.11 (0.76–1.60)
5–9	149	1.26	0.65 (0.50–0.85)	34	1.75	0.55 (0.35–0.86)
10–19	170	0.75	0.37 (0.29–0.48)	57	1.44	0.49 (0.33–0.73)
20–44	1,827	2.17	Referent	413	3.13	Referent
45–59	580	1.41	0.70 (0.57–0.86)	107	1.70	0.52 (0.36–0.74)
>59	254	0.39	0.22 (0.17–0.29)	51	0.69	0.24 (0.16–0.36)
Sex						
M	2,230	2.00	2.06 (1.70–2.49)	484	2.71	1.82 (1.34–2.48)
F	1,014	0.80	Referent	255	1.60	Referent
Sex and age group, y†						
All <20	580	1.26	0.43 (0.35–0.52)	169	2.19	0.57 (0.39–0.84)
Men 20–59	1,789	2.96	Referent	355	3.55	Referent
Men >59	135	0.60	0.22 (0.16–0.30)	33	1.06	0.30 (0.19–0.50)
Women >20	737	0.74	0.24 (0.20–0.30)	182	1.43	0.34 (0.23–0.51)
Borough of residence						
Bronx	583	1.59	0.57 (0.48–0.68)	129	2.09	0.54 (0.38–0.75)
Brooklyn	642	1.11	0.34 (0.28–0.40)	186	1.48	0.39 (0.28–0.54)
Manhattan	1,580	3.18	Referent	314	4.91	Referent
Queens	380	0.60	0.24 (0.19–0.29)	103	1.05	0.29 (0.21–0.41)
Staten Island	51	0.46	0.55 (0.38–0.80)	8	0.43	0.30 (0.13–0.66)
Race/ethnicity‡						
Hispanic	969	1.45	1.16 (0.96–1.40)	194	1.96	0.76 (0.56–1.04)
Non-Hispanic white	1,067	1.18	Referent	310	2.47	Referent
Non-Hispanic black/African American	855	1.77	1.45 (1.20–1.75)	122	1.54	0.65 (0.46–0.91)
Other	161	0.68	0.79 (0.61–1.03)	77	1.39	0.69 (0.47–1.01)
Immune status†‡						
Non-HIV/AIDS	1,349	0.65	Referent	544	1.56	Referent
HIV/AIDS	1,863	55.6	89.0 (70.2–112.3)	190	39.0	23.30 (16.4–33.2)
Neighborhood poverty‡§						
Low	883	1.18	Referent	203	2.10	Referent
Medium	769	1.56	1.03 (0.86–1.25)	197	1.97	0.86 (0.61–1.17)
High	583	1.46	1.23 (1.01–1.49)	151	2.16	0.97 (0.69–1.35)
Very high	917	1.87	1.42 (1.18–1.70)	188	2.45	1.17 (0.85–1.62)

*Incidence is median no. cases/100,000 persons; ACS, American Community Survey; IRR, incidence rate ratio.
†Incidence and IRR not age-adjusted.
‡All categories had <10 missing values with the exception of race/ethnicity during 2000–2014 (n = 192) and 2015–2018 (n = 37), immune status during 2000–2014 (n = 32), and poverty during 2000–2014 (n = 92).
§Classified by percent of census tract residents living below the federal poverty line (low, <10%; medium, 10%–<20%; high, 20%–<30%; very high, ≥30%); population denominator data were as follows for each listed year: 2000–2004 (2000 US Census); 2005–2009 (ACS 2007–2011); 2010 (2010 Census); 2011 (ACS 2009–2013); 2012 (ACS 2010–2014); 2013 (ACS 2011–2015); 2014–2018 (ACS 2012–2016).

DOHMH. Interviews were completed for 3,295 (83%) patients. The most common reasons for failure to interview were because the NYC DOHMH was unable to locate the patient (7%), the patient died (4%), or the patient refused to be interviewed (3%). Because death certificate information was not available, cause of death could not be determined. Several major differences were identified between patients who were and were not interviewed (Appendix Table 1, https://wwwnc.cdc.gov/EID/article/25/3/19-0785-App1.pdf). Patients who were not interviewed during 1995–2018 were more likely to be men 20–59 years of age, to be non-Hispanic black/African American, to have a known diagnosis of HIV/AIDS, and to live in census tracts with high or very high poverty levels. A total of 13 patients were incarcerated and 10 patients were homeless at the time of diagnosis.

The median annual age-adjusted incidence of reported cryptosporidiosis cases in NYC during 1995–2018 was 1.71 cases/100,000 persons (interquartile range 1.31–2.18 cases/100,000 persons). The citywide annual age-adjusted incidence decreased by 65% from 1995 (5.86 cases/100,000 persons) through 2000 (2.07 cases/100,000 persons) (Figure 1, panel A). The rate increased toward the end of the study period from 1.59 cases/100,000 persons in 2015 to 2.99 cases/100,000 persons in 2018. Cryptosporidiosis incidence was highest in Manhattan throughout the study period (Figure 1, panel B). Age-adjusted borough-specific annual incidence decreased in Manhattan most dramatically over time from 15.27 cases/100,000 persons in 1995 to 5.12 cases/100,000 persons in 2000. Rates remained relatively stable in each borough during 2000–2014 and began to increase in Brooklyn, the Bronx, and Queens after 2015 (Figure 1, panel B).

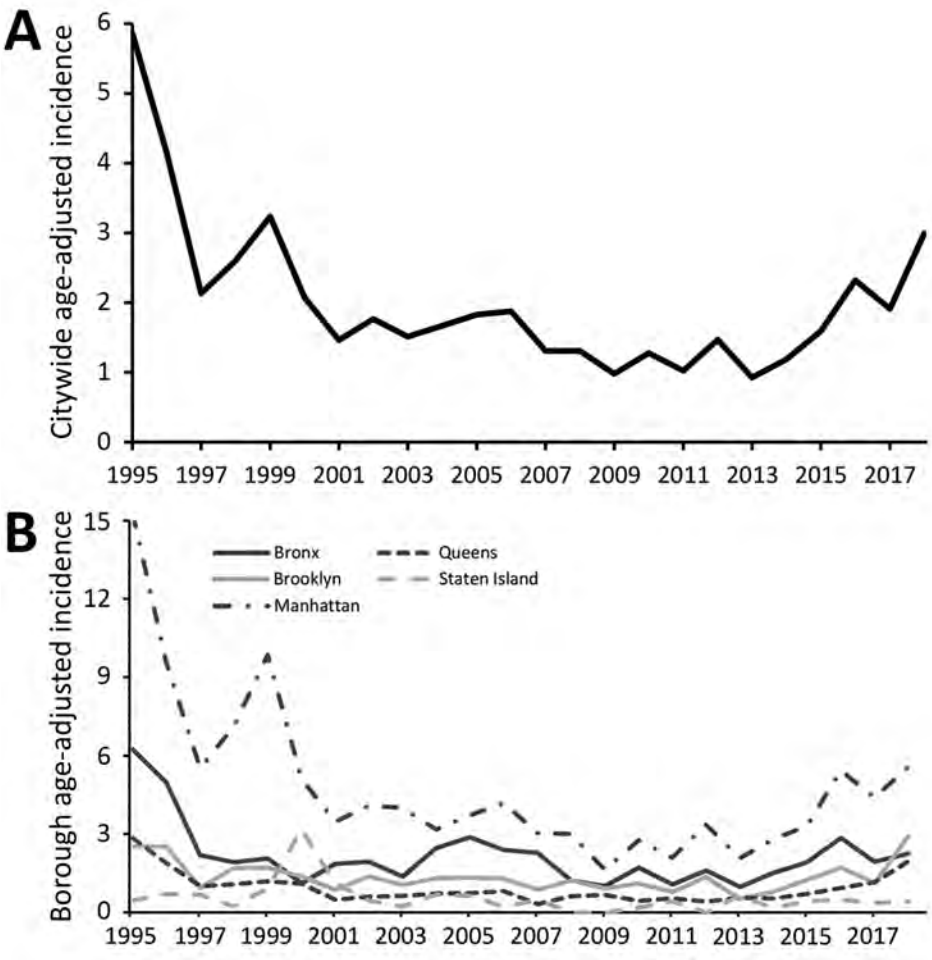

Figure 1. Age-adjusted annual incidence of cryptosporidiosis/100,000 persons, New York City, New York, USA, 1995–2018. A) Citywide; B) by borough of residence.

Trends in Cryptosporidiosis Incidence and Epidemiology during 2000–2018

A total of 2,539 cryptosporidiosis patients were given a diagnosis during 2000–2018 and reported to the NYC DOHMH. Of the 5 boroughs of NYC, cryptosporidiosis patients most often resided in Manhattan (44%), followed by Brooklyn (24%) and the Bronx (19%). Most (54%) patients were men 20–59 years of age; patients were most also frequently non-Hispanic white (33%), followed by Hispanic (any race) (28%) and non-Hispanic black/African American (26%) (Appendix Table 2). The median annual citywide age-adjusted incidence increased from 1.46 cases/100,000 persons during 2000–2014 to 2.11 cases/100,000 persons during 2015–2018. Age group–specific incidence was highest among those <5 years of age, followed by those 20–44 years of age during both periods (Table 1). The proportion of cryptosporidiosis patients with a known diagnosis of HIV/AIDS decreased over time from 60% during 2000–2004 to 26% during 2015–2018 (Appendix Table 2); the incidence was higher among PLWHA throughout 2000–2018 (Table 1).

Cryptosporidiosis among Men during 2000–2018

Incidence among men was higher throughout 2000–2018, and incidence for those 20–59 years of age specifically was consistently higher than for all other age/sex groups during 2000–2014 (median 2.96 cases/100,000 persons) and 2015–2018 (median 3.55 cases/100,000 persons) (Table 1; Figure 2). We identified exposures during the incubation period reported by cryptosporidiosis patients with a completed interview by age and sex group (Table 2). Men 20–59 years of age were more likely to report high-risk sexual practices with an increased risk for fecal contact (43%) compared with older men (16%) and women (17%). In addition, 2 neighborhoods had consistently increased age-adjusted incidence rates before introduction of syndromic multiplex diagnostics; including Chelsea/Greenwich Village and Inwood/Washington Heights in Manhattan (Figure 3, panel A). The geography of age-adjusted incidence among men 20–59 years of age (Figure 3, panel C) differed substantially from other patients (Figure 3, panel D) in that cryptosporidiosis patients

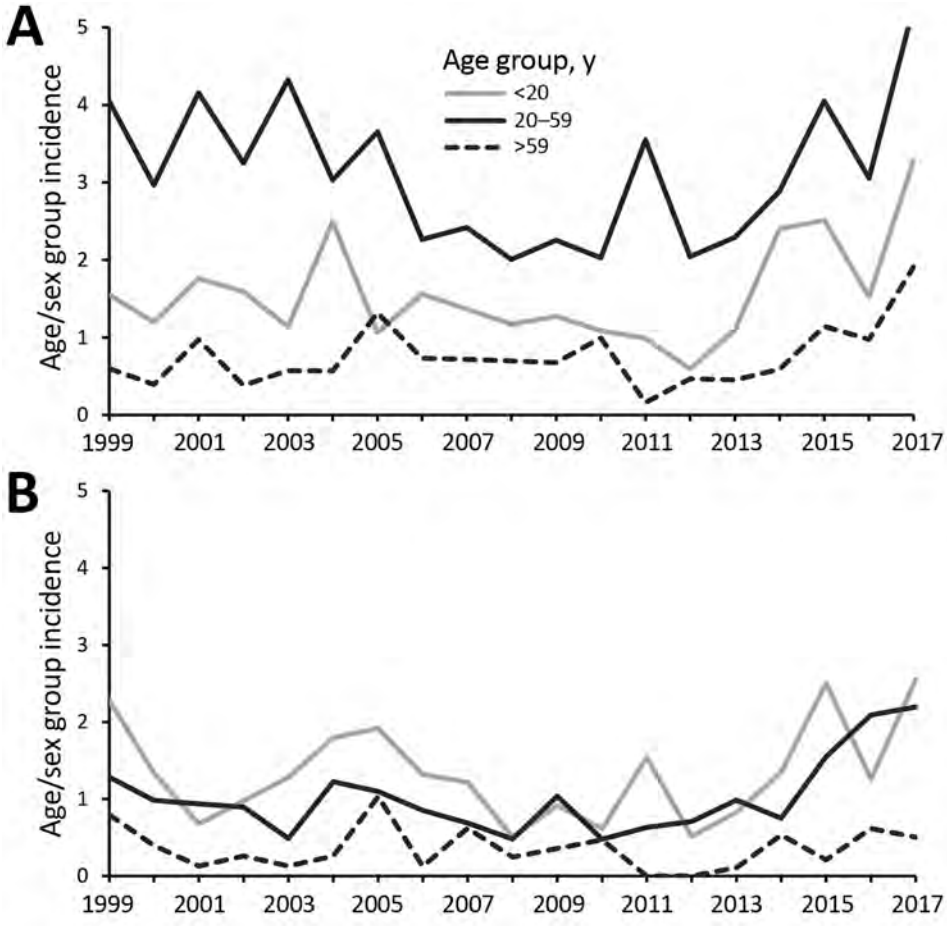

Figure 2. Annual cryptosporidiosis incidence (cases/100,000 persons) by sex and age group, New York City, New York, USA, 2000–2018. A) Male. B) Female

who were men were concentrated again specifically in the Chelsea/Greenwich Village neighborhoods.

International Travel and NYC Tap Water Exposure during 2000–2018

Approximately 30% of patients given a diagnosis during 2000–2018 reported international travel during their incubation period (Table 2). Patients given a diagnosis of cryptosporidiosis during 2015–2018 were more likely to report international travel (34%) compared with patients given a diagnosis during 2000–2014 (23%) ($p<0.0001$). Compared with patients ≥20 years of age (52%), patients <20 years of age (22%) were more likely to have traveled internationally. The most common international destinations were the Dominican Republic (23% of all international destinations) and Mexico (12% of all international destinations). More than two thirds of patients who reported traveling to the Dominican Republic were <20 years of age (68%, 96/142); a similar pattern was not identified for patients with reported travel to Mexico. Finally, patients traveling to the Dominican Republic most often lived in Inwood/Washington Heights in NYC (28%, 39/140).

In terms of NYC municipal water use, most adults reported drinking plain tap water, and >75% of all patients reported using plain tap water for daily activities during their incubation periods. Furthermore, among patients with no reported travel outside NYC, patients <20 years of age were most likely to report recreational water contact (24%).

Impact of Syndromic Multiplex Panels

The median age-adjusted annual incidence increased after introduction of syndromic multiplex panels (IRR for 2015–2018 vs. 2000–2014 1.49, 95% CI 1.17–1.91). Incidence increased during 2015–2018 among most examined demographic groups, most dramatically among those without a known diagnosis of HIV/AIDS (IRR 2.37, 95% CI 1.75–3.22), those 10–19 years of age (IRR 2.07, 95% CI 1.35–3.19), and those who were non-Hispanic white (IRR 1.91, 95% CI 1.46–2.50) (Appendix Table 3). Compared with non-Hispanic whites, the median age-adjusted incidence among non-Hispanic black/African Americans (1.77 cases/100,000 persons) was higher before introduction of syndromic multiplex panels (IRR 1.45, 95% CI

Table 2. Reported exposures of cryptosporidiosis patients stratified by those with and without international or domestic travel outside New York City, New York, USA, during period of interest before symptom onset for patients, 2000–2018*

Characteristic	Age, y/sex group, no. positive/no. tested (%)					p value
	<20/All	20–59/M	>59/M	>20/F	Total	
Interviewed patients	500/555 (90.1)	1,000/1,359 (73.6)	71/87 (81.6)	434/537 (80.8)	2,005/2,538 (79)	<0.001
International travel	254/492 (51.6)	158/993 (15.9)	16/72 (22.2)	155/431 (36.0)	583/1,988 (29.3)	<0.001
Domestic travel	99/445 (22.2)	208/910 (22.9)	12/65 (18.5)	81/395 (20.5)	400/1,815 (22.0)	0.77
No travel	149/474 (31.4)	562/908 (61.9)	39/67 (58.2)	179/401 (44.6)	929/1,850 (50.2)	<0.001
High-risk sex†	ND	234/546 (42.9)	6/37 (16.2)	30/174 (17.2)	270/757 (35.7)	<0.001
Recreational water contact‡	35 (23.5)	46 (8.2)	3 (7.7)	12 (6.7)	96 (10.3)	<0.001
Child care attendee§	14/61 (23.0)	ND	ND	ND	ND	NA
Animal contact¶	36 (24.2)	197 (35.1)	5 (12.8)	64 (35.8)	302 (32.5)	0.02
Ate high-risk food#	61 (40.9)	338 (60.2)	16 (41.0)	113 (63.1)	528 (56.9)	<0.001
Drank NYC tap water	68 (45.6)	403 (71.7)	23 (59.0)	119 (66.5)	613 (66.0)	<0.001
Treated NYC tap water**	53 (35.8)	217 (38.6)	16 (41.0)	73 (40.8)	359 (38.7)	0.50
Used NYC tap water††	117 (78.5)	496 (88.3)	31 (79.5)	165 (92.2)	809 (87.1)	<0.001
Drank high-risk water‡‡	2/145 (1.4)	8/549 (1.5)	0/37 (0)	2/174 (1.1)	12/905 (1.3)	>0.99

*Percentages in parentheses reflect percentage of patients who were interviewed during each period. Period of interest is defined as 1 month for patients given a diagnosis during January 1995–April 2010, and 2 weeks for patients given a diagnosis during May 2010–December 2018. NA, not applicable; ND, no data were collected; NYC, New York City.
†For adults ≥18 years of age, defined as having anal sex (receptive or insertive), insertion of a finger or a tongue in or around a partner's anus, or having oral sex.
‡Defined as water from a hot tub, public or private swimming pool, stream, ocean, or recreational water park.
§For children <5 years of age.
¶Defined as having a pet, being exposed to an animal, changing cat litter, picking up dog stool, visiting a zoo, having a pet, or having a job that required contact with animals.
#Defined as raw or unpasteurized cheese, milk or cider, cooked or uncooked shellfish, and unpeeled fruit or vegetables.
**Patients either boiled or filtered NYC municipal water before drinking.
††Used NYC municipal water to brush teeth, wash vegetables/fruit, make ice, or make juice.
‡‡High-risk water was defined as water from a stream, spring, pond, or private well.

1.20–1.75). However, after introduction of these diagnostics, the incidence in non-Hispanic whites (2.47 cases/100,000 persons) was higher than that for all other race/ethnicity groups (Table 1).

The introduction of syndromic multiplex panels led to an increase in detection across a broader number of neighborhoods across Manhattan (Figure 3, panel B). Before introduction of syndromic multiplex panels, the incidence of cryptosporidiosis was higher among neighborhoods of very high poverty (1.87 cases/100,000 persons) compared with low poverty (IRR 1.42, 95% CI 1.18–1.70). This association is probably driven by an increased number of cases among very high poverty neighborhoods during 2004 (cause unknown). During 2015–2018, neighborhood poverty was not associated with cryptosporidiosis incidence.

Before the introduction of syndromic multiplex panels, cryptosporidiosis diagnoses increased during July–October annually, peaking in August (median 45 cases, range 8–30 cases) and September (median 17 cases, range 7–35 cases) (Figure 4, panel A). After introduction of these diagnostics, the monthly case counts increased substantially in the same months of August (median 30 cases, range 13–35 cases) and September (median 35 cases, range 28–39 cases) (Figure 4, panel B). Patients <20 years of age were most likely to have diagnosis dates in the late summer both before (August: 23%, September 28%) (Figure 4, panel C) and after (August 23%, September 27%) (Figure 4, panel D) introduction of syndromic multiplex panels.

During August 2012–December 2018, a total of 943 patients received a diagnosis of cryptosporidiosis by 992 primary tests at a commercial or hospital laboratory. Before mid-2015, most (76%) patients had only 1 type of positive test result, which consisted of either microscopy or ELISA for *Cryptosporidium* antigen. However, after introduction of syndromic multiplex panels, the proportion of all patients who were given a diagnosis of cryptosporidiosis by these panels increased from 18% (25/137) during 2015 to 76% (190/250) during 2018 (Figure 5). More than 97% (345/355) of patients whose stool specimens were tested by using a syndromic multiplex panel during 2015–2018 were exclusively given a diagnosis by use of this assay rather than through an additional test by microscopy or an antigen ELISA. Most (74%, 255/345) cryptosporidiosis patients given a diagnosis by use of the syndromic multiplex panel did not have another enteric co-infection.

Discussion

An analysis of cryptosporidiosis surveillance data collected in NYC during 1995–2018 suggests that the epidemiology of the parasitic enteric infection in this large, urban, international setting is multifaceted. Although the incidence of cryptosporidiosis in NYC decreased dramatically after the introduction of HAART in the mid-1990s, incidence remained consistently higher among men in NYC, probably reflecting an enduring burden of disease in men who have sex with men (MSM). We also found that cryptosporidiosis

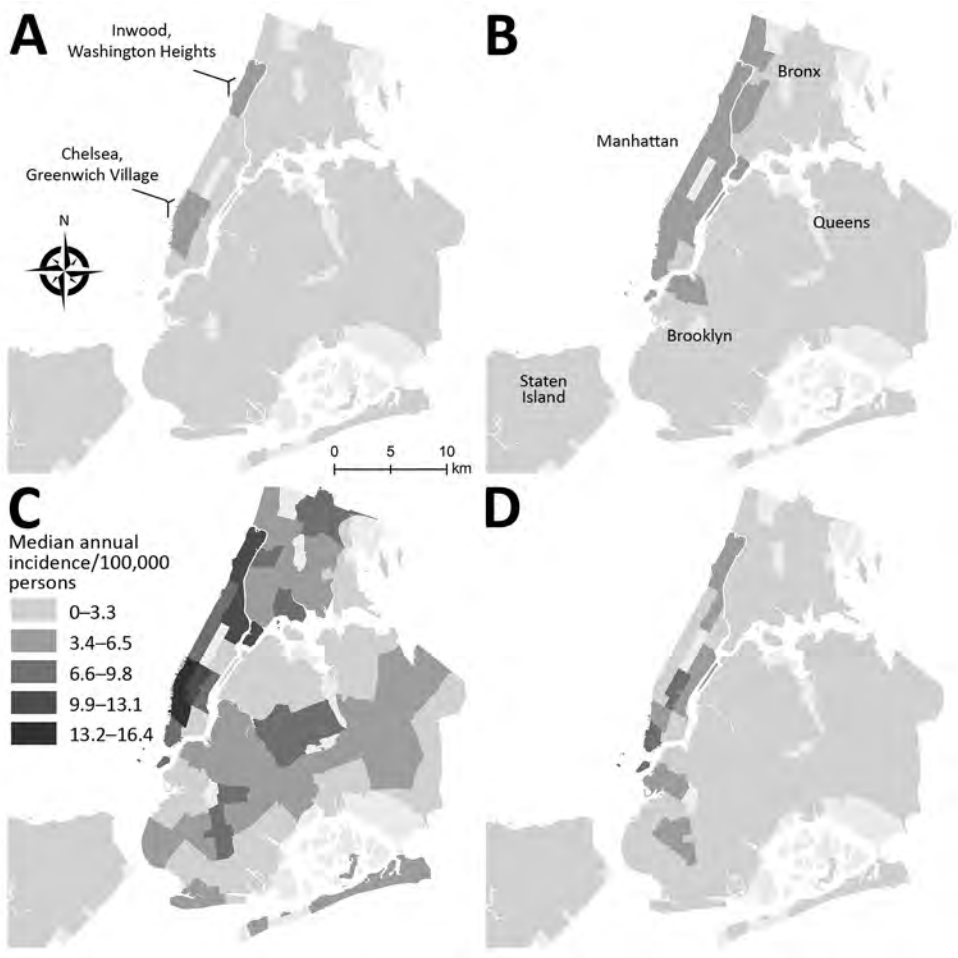

Figure 3. Median annual cryptosporidiosis incidence (cases/100,000 persons) by community district (CD), New York City New York, USA, 1995–2018. A) All persons, age-adjusted, 2000–2014, showing CDs that include Chelsea (Chelsea, Clinton, Hudson Yards) and Greenwich Village (Greenwich Village, Hudson Square, Little Italy, NoHo, SoHo, South Village, West Village). B) All persons, age-adjusted, 2015–2018. C) Men 20–59 years of age, 2015–2018. D) All persons <20 years of age and men >59 years of age, 2015–2018.

was common in children in NYC, probably driven by summertime international travel to disease-endemic areas. Finally, the recent introduction of syndromic multiplex diagnostic panels has led to not only a major increase in the reported incidence of cryptosporidiosis but also to a shift in the demographic makeup of reported cryptosporidiosis patients in NYC.

Our data show that the burden of cryptosporidiosis has been consistently elevated among adult men 20–59 years of age in NYC, probably driven by person-to-person sexual transmission among MSM. Although we did not have reliable data on patient MSM status, high rates of cryptosporidiosis among men were consistently identified in areas known to have an above-average proportion of residents who are MSM, such as Chelsea (*27*). Patients in this age/sex group were more likely to report sexual practices with increased risk for fecal contact during the incubation period than were those in any other age/sex group in NYC. MSM are historically at greater risk for cryptosporidiosis, not only because of a higher prevalence of AIDS in this population (*28*) but also because of sexual practices, such as anilingus, that entail a low risk for HIV transmission but increase the risk for fecal contact (*3*).

The dramatic decrease in citywide cryptosporidiosis incidence observed during 1995–2000 is consistent with the uptake of HAART among PLWHA in NYC. Cryptosporidiosis is a well-known opportunistic infection among PLWHA (*1*,*29*), and restoration of immune function is the recommended therapy (*30*). The number of deaths from all causes among persons who have AIDS peaked in 1994 in NYC and decreased substantially after the introduction of HAART (*31*). Although cryptosporidiosis rates remain high for PLWHA in NYC, patients without HIV/AIDS now represent most reported patients. This finding is likely not only because of high HAART coverage among patients with HIV/AIDS (*32*) but also because of increased case finding in the general population after introduction of syndromic multiplex diagnostics. Before introduction of these new diagnostics, physicians needed to specifically request cryptosporidiosis testing as part of the traditional ova and parasite testing. Given the dramatic consequences of cryptosporidiosis

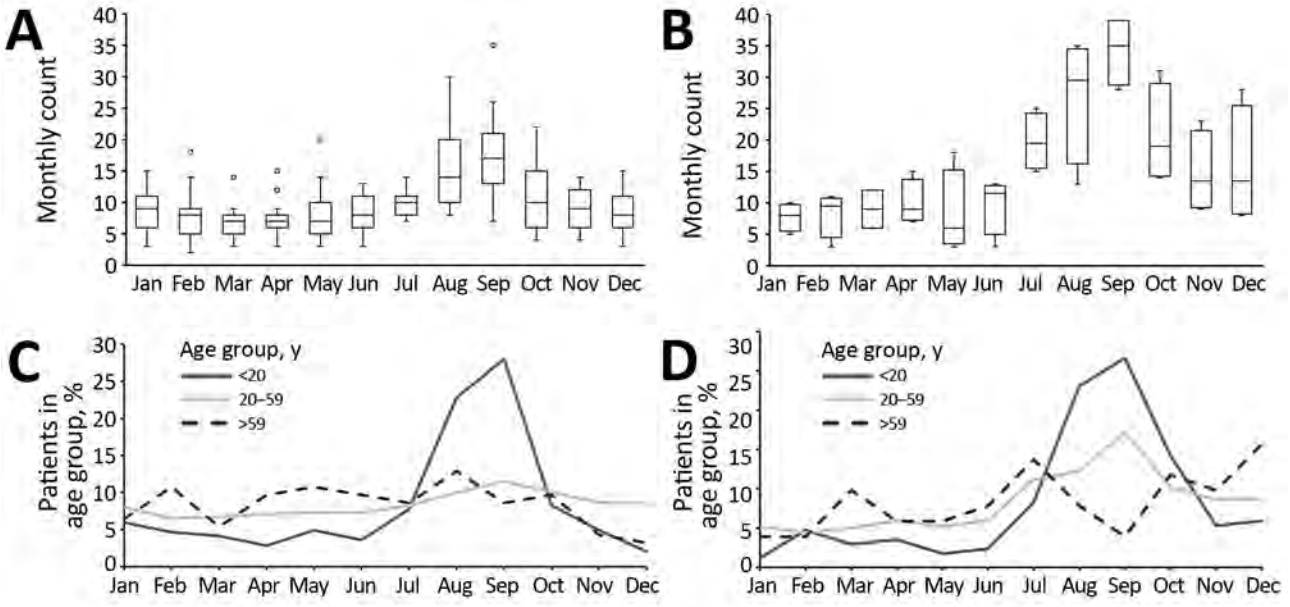

Figure 4. Seasonality of cryptosporidiosis in New York City, New York, USA, 1995–2018. A, B) Count of cryptosporidiosis cases by month during 2000–2014 (A) and 2015–2018 (B). Horizontal bars within boxes indicate median case count by month; box bottoms and tops indicate 25th and 75th percentiles; dots indicate outliers (>95th percentile); and error bars indicate 95% CIs. C, D) Percentage of patients by month of diagnosis and age group during 2000–2014 (C) and 2015–2018 (D).

among PLWHA, clinicians treating cryptosporidiosis in this population would have likely been more aware of the need to specifically request testing for this parasite before presyndromic multiplex panels were introduced.

In addition to patients who were HIV negative, the introduction of syndromic multiplex testing led to an increase in reported cases among persons who were non-Hispanic white. This finding might reflect the populations residing in the specific catchment areas of the laboratories that use syndromic multiplex panels, as well as disparities in healthcare access by race/ethnicity (*33*). We also identified a higher and increasing burden of cryptosporidiosis among children in NYC, especially after introduction of syndromic multiplex panels. Because children with diarrhea are more likely to be taken to a healthcare facility than adults (*34*), the increasing incidence of cryptosporidiosis in the younger age group probably reflects healthcare-seeking behavior along with the improved diagnostic sensitivity of syndromic multiplex panels.

Our data also show that children were more likely to be given a diagnosis of cryptosporidiosis during the summer months and were most likely to

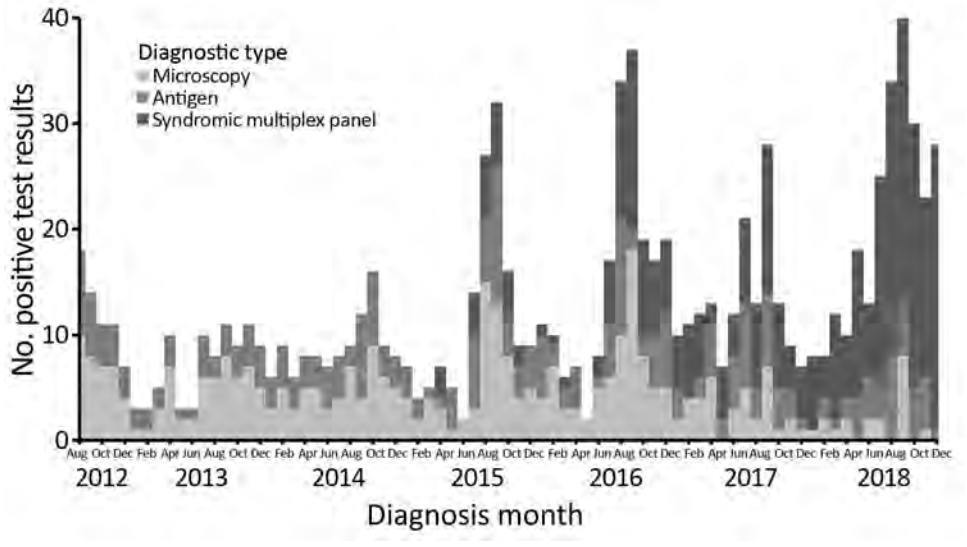

Figure 5. Count of positive diagnostic tests for cryptosporidiosis by month, New York City, New York, USA, August 2012–December 2018. Diagnostic tests include microscopy (stain or ova and parasite test), antigen ELISA for *Cryptosporidium* antigen, and syndromic multiplex test. A patient can have >1 diagnostic test/disease episode.

report recreational water contact and international travel, particularly to the Dominican Republic, where they might be in contact with contaminated food or water (*35*). Although recreational water contact is a known risk factor for cryptosporidiosis (*2*), no large pool-related outbreaks have been detected in NYC. In addition, most cryptosporidiosis patients reported drinking NYC municipal tap water and using it for household needs. Extensive surveillance is in place to monitor for citywide waterborne cryptosporidiosis and giardiasis outbreaks (*11*). To date, there have been no outbreaks of waterborne disease related to the NYC municipal tap water.

Our study has several limitations. Interviewed patients tended to be of higher socioeconomic status than those who were not interviewed, which might bias our results because wealthier patients might have different risk exposures than patients who live in neighborhoods of high poverty. Furthermore, the period of interest for risk factor exposure decreased during 2010, which might have reduced the proportion of persons reporting risk factors over time. Finally, some race and ethnicity data were not collected by self-report and therefore might not accurately capture self-identified race and ethnicity of patients. Notwithstanding these limitations, the epidemiology of cryptosporidiosis merits continued attention because the incidence will probably continue to increase in NYC, as well as in other jurisdictions across the United States (*7*), given the cost-effectiveness of syndromic multiplex panels (*36*). Public health surveillance activities will need to take the improved case detection and increases in hospital/laboratory-specific catchment areas into account when guiding public health action (*37*).

In conclusion, the epidemiology of cryptosporidiosis in NYC reflects the diverse population of this city. The consistently elevated burden in men probably related to sexual transmission among MSM warrants outreach to this community and their providers to increase awareness. Furthermore, messaging related to prevention and treatment for cryptosporidiosis should be targeted to international travelers, particularly parents of children in NYC who travel to the Dominican Republic during the summer months. We anticipate the reported incidence of cryptosporidiosis to continue to increase with the increasing use of syndromic multiplex panels and that the demographic profiles of the patients might also change as these new diagnostics are adopted more widely. These observed patterns of disease might also be present in other urban, diverse jurisdictions, both nationally and internationally.

Acknowledgments

We thank the Bureau of Communicable Disease at the NYC DOHMH, specifically the General Surveillance Unit for interviewing patients and the Reportable Disease Data, Informatics, and Analysis Unit, for cleaning and standardizing laboratory and patient address data, as well as maintaining surveillance databases. We also thank Sharon K. Greene for her analytical suggestions and critical review of the manuscript.

About the Author

Ms. Alleyne is an epidemiologist at the New York City Department of Health and Mental Hygiene, Long Island City, NY. Her primary research interests include waterborne infectious diseases and HIV/AIDS.

References

1. Chen XM, Keithly JS, Paya CV, LaRusso NF. Cryptosporidiosis. N Engl J Med. 2002;346:1723–31. https://doi.org/10.1056/NEJMra013170
2. Yoder JS, Beach MJ. *Cryptosporidium surveillance* and risk factors in the United States. Exp Parasitol. 2010;124:31–9. https://doi.org/10.1016/j.exppara.2009.09.020
3. Hellard M, Hocking J, Willis J, Dore G, Fairley C. Risk factors leading to *Cryptosporidium infection* in men who have sex with men. Sex Transm Infect. 2003;79:412–4. https://doi.org/10.1136/sti.79.5.412
4. Roy SL, DeLong SM, Stenzel SA, Shiferaw B, Roberts JM, Khalakdina A, et al.; Emerging Infections Program FoodNet Working Group. Risk factors for sporadic cryptosporidiosis among immunocompetent persons in the United States from 1999 to 2001. J Clin Microbiol. 2004;42:2944–51. https://doi.org/10.1128/JCM.42.7.2944-2951.2004
5. Checkley W, White AC Jr, Jaganath D, Arrowood MJ, Chalmers RM, Chen X-M, et al. A review of the global burden, novel diagnostics, therapeutics, and vaccine targets for *Cryptosporidium*. Lancet Infect Dis. 2015;15:85–94. https://doi.org/10.1016/S1473-3099(14)70772-8
6. New York City Health Code. Article 11: reportable diseases and conditions; 2019 [cited 2019 Dec 5]. ttps://www1.nyc.gov/assets/doh/downloads/pdf/about/healthcode/health-code-article11.pdf
7. Marder EP, Cieslak PR, Cronquist AB, Dunn J, Lathrop S, Rabatsky-Ehr T, et al. Incidence and trends of infections with pathogens transmitted commonly through food and the effect of increasing use of culture-independent diagnostic tests on surveillance: Foodborne Diseases Active Surveillance Network, 10 U.S. Sites, 2013–2016. MMWR Morb Mortal Wkly Rep. 2017;66:397–403. https://doi.org/10.15585/mmwr.mm6615a1
8. Buss SN, Leber A, Chapin K, Fey PD, Bankowski MJ, Jones MK, et al. Multicenter evaluation of the BioFire FilmArray gastrointestinal panel for etiologic diagnosis of infectious gastroenteritis. J Clin Microbiol. 2015;53:915–25. https://doi.org/10.1128/JCM.02674-14
9. Navidad JF, Griswold DJ, Gradus MS, Bhattacharyya S. Evaluation of Luminex xTAG gastrointestinal pathogen analyte-specific reagents for high-throughput, simultaneous detection of bacteria, viruses, and parasites of clinical and public health importance. J Clin Microbiol. 2013;51:3018–24. https://doi.org/10.1128/JCM.00896-13

10. New York City Department of Environmental Protection. Filtration avoidance determination (FAD) Reports; 2018 [cited 2019 Dec 5]. http://www.nyc.gov/html/dep/html/watershed_protection/fad.shtml
11. Alleyne L, Thompson C, Fitzhenry R, Seeley A, Mathes R, Janus L. Waterborne disease risk assessment program 2018 annual report; 2019 [cited 2019 Dec 5]. https://www1.nyc.gov/html/dep/pdf/reports/fad-8.1-waterborne-disease-risk-assessment-program-annual-report-03-19.pdf
12. United States Environmental Protection Agency. Interim enhanced surface water treatment rule; December 1998 [cited 2019 Dec 5]. https://www.epa.gov/dwreginfo/surface-water-treatment-rules
13. Meinhardt PL, Casemore DP, Miller KB. Epidemiologic aspects of human cryptosporidiosis and the role of waterborne transmission. Epidemiol Rev. 1996;18:118–36. https://doi.org/10.1093/oxfordjournals.epirev.a017920
14. Morita S, Namikoshi A, Hirata T, Oguma K, Katayama H, Ohgaki S, et al. Efficacy of UV irradiation in inactivating *Cryptosporidium parvum* oocysts. Appl Environ Microbiol. 2002;68:5387–93. https://doi.org/10.1128/AEM.68.11.5387-5393.2002
15. Crawford FG, Vermund SH, Ma JY, Deckelbaum RJ. Asymptomatic cryptosporidiosis in a New York City day care center. Pediatr Infect Dis J. 1988;7:806–7. https://doi.org/10.1097/00006454-198811000-00013
16. Spencer KL, Soave R, Acosta A, Gellin B, Prince A, Ramos L, et al. Cryptosporidiosis in HIV-infected persons: prevalence in a New York City population. International Journal of Infectious Diseases. 1997;1:217–21. https://doi.org/10.1016/S1201-9712(97)90041-2
17. Council of State and Territorial Epidemiologists. Cryptosporidiosis (*Cryptosporidium* spp.) case definition. Position statement; 2012 [cited 2019 Dec 5]. https://wwwn.cdc.gov/nndss/conditions/cryptosporidiosis/case-definition/2012
18. Centers for Disease Control and Prevention. Cryptosporidiosis (*Cryptosporidium* spp.): case definition(s). National Notifiable Diseases Surveillance System; 2017 [cited 2019 Dec 5]. https://wwwn.cdc.gov/nndss/conditions/cryptosporidiosis
19. New York City Department of City Planning. Decennial census; 2010 [cited 2019 Dec 5]. https://www1.nyc.gov/site/planning/data-maps/nyc-population/census-2010.page
20. New York City Department of City Planning. Decennial census; 2000 [cited 2019 Dec 5]. http://www1.nyc.gov/site/planning/data-maps/nyc-population/census-2000.page
21. New York City Department Of Health and Mental Hygiene. EpiQuery census 1990–2000 and 2010 modules; 2018 [cited 2019 Dec 5]. https://www1.nyc.gov/site/doh/data/data-sets/epi-census.page
22. New York City Department of Health and Mental Hygiene HIV Epidemiology and Field Services Program. AIDS diagnosis and persons living with HIV/AIDS by year, Pre-1981 to 2016, New York City; 2016 [cited 2019 Dec 5]. https://www1.nyc.gov/assets/doh/downloads/pdf/ah/surveillance-trend-tables.pdf
23. New York City Department of Health and Mental Hygiene. HIV surveillance annual report 2017; 2018 [cited 2019 Dec 5]. https://www1.nyc.gov/assets/doh/downloads/pdf/dires/hiv-surveillance-annualreport-2017.pdf
24. US Census Bureau. American community survey (ACS); 2016 [cited 2019 Dec 5]. https://census.gov/programs-surveys/acs/data.html
25. Toprani A, Hadler J. Selecting and applying a standard area-based socioeconomic status measure for public health data: analysis for New York City. New York City Department of Health and Mental Hygiene: Epi Research Report; May 2013 [cited 2019 Dec 5]. https://www1.nyc.gov/assets/doh/downloads/pdf/epi/epiresearch-SES-measure.pdf
26. Klein RJ, Schoenborn CA. Age adjustment using the 2000 projected US population. Hyattsville (MD): Centers for Disease Control and Prevention, National Center for Health Statistics; 2001.
27. Bureau of Epidemiology Services New York City Department of Health and Mental Hygiene. Prevalence of men Who had sex with men in the past 12 months in NYC by United Hospital Fund Neighborhood, community health survey, 2012–2016; 2017 [cited 2019 Dec 5]. http://www1.nyc.gov/site/doh/data/data-sets/community-health-survey-public-use-data.page
28. Centers for Disease Control and Prevention. Epidemiology of HIV/AIDS—United States, 1981–2005. MMWR Morb Mortal Wkly Rep. 2006;55:589–92.
29. Hunter PR, Nichols G. Epidemiology and clinical features of *Cryptosporidium* infection in immunocompromised patients. Clin Microbiol Rev. 2002;15:145–54. https://doi.org/10.1128/CMR.15.1.145-154.2002
30. Sparks H, Nair G, Castellanos-Gonzalez A, White AC Jr. Treatment of *Cryptosporidium*: what we know, gaps, and the way forward. Curr Trop Med Rep. 2015;2:181–7. https://doi.org/10.1007/s40475-015-0056-9
31. Nash D, Katyal M, Shah S. Trends in predictors of death due to HIV-related causes among persons living with AIDS in New York City: 1993–2001. J Urban Health. 2005;82:584–600. https://doi.org/10.1093/jurban/jti123
32. Sackoff JE, Hanna DB, Pfeiffer MR, Torian LV. Causes of death among persons with AIDS in the era of highly active antiretroviral therapy: New York City. Ann Intern Med. 2006;145:397–406. https://doi.org/10.7326/0003-4819-145-6-200609190-00003
33. Bailey ZD, Krieger N, Agénor M, Graves J, Linos N, Bassett MT. Structural racism and health inequities in the USA: evidence and interventions. Lancet. 2017;389:1453–63. https://doi.org/10.1016/S0140-6736(17)30569-X
34. Van Cauteren D, De Valk H, Vaux S, Le Strat Y, Vaillant V. Burden of acute gastroenteritis and healthcare-seeking behaviour in France: a population-based study. Epidemiol Infect. 2012;140:697–705. https://doi.org/10.1017/S0950268811000999
35. Steffen R, Hill DR, DuPont HL. Traveler's diarrhea: a clinical review. JAMA. 2015;313:71–80. https://doi.org/10.1001/jama.2014.17006
36. Goldenberg SD, Bacelar M, Brazier P, Bisnauthsing K, Edgeworth JD. A cost benefit analysis of the Luminex xTAG gastrointestinal pathogen panel for detection of infectious gastroenteritis in hospitalised patients. J Infect. 2015;70:504–11. https://doi.org/10.1016/j.jinf.2014.11.009
37. Peterson ER, Fireteanu AM, Greene SK. Adapting reportable disease cluster detection. Methods for increased use of culture-independent diagnostic testing. Presented at: Annual Meeting of the Council of State and Territorial Epidemiologists; 2018 Jun 11–13; West Palm Beach, Florida, USA [cited 2019 Dec 5]. https://cste.confex.com/cste/2018/meetingapp.cgi/Paper/9135

Address for correspondence: Corinne N. Thompson, New York City Department of Health and Mental Hygiene, 42-09 28th St, CN22A, Long Island City, NY 11101, USA; email: cthompson2@health.nyc.gov

Public Health Response to Tuberculosis Outbreak among Persons Experiencing Homelessness, Minneapolis, Minnesota, USA, 2017–2018

Kelzee K. Tibbetts, Randy A. Ottoson, Dean T. Tsukayama

Tuberculosis (TB) is a greater risk for populations experiencing homelessness. When a TB exposure occurs in a homeless shelter, evaluation of contacts is both urgent and challenging. In 2017, local public health workers initiated a response to a TB outbreak in homeless shelters in Minneapolis, Minnesota, USA. In this contact investigation, we incorporated multiple techniques to identify, evaluate, and manage patients, including the concentric-circle method to characterize amount of contact, identifying the most frequent sites of sporadic medical care, using electronic medical records, and engaging with medical providers treating this population. Of 298 contacts evaluated, 41 (14%) had latent TB infection and 2 had active TB disease. Our analysis indicated a significant relationship between duration of exposure and positive TB test result (p = 0.001). We encourage local public health departments to expand beyond traditional contact tracing techniques by leveraging partnerships and existing systems to reach contacts exposed in shelters.

In 2017, a total of 9,093 new cases of active tuberculosis (TB) were reported in the United States, and ≈4.5% of these occurred in persons experiencing homelessness (PEH) in the year preceding their diagnosis (*1*). The incidence of TB in PEH populations is >10 times that of the general population (i.e., 36–47 vs. 2.8 cases/100,000 population during 2006–2010) (*2*) because risk factors, such as HIV infection, mental illness, substance abuse, and barriers to accessing healthcare, put them at higher risk. In addition, PEH often use homeless shelters, and congregate in environments where the risk for TB transmission is greatly increased (*3*).

A priority for TB control and prevention is the screening of persons exposed to transmissible TB (*4*). Locating and fully evaluating contacts, essential components of a contact investigation, is difficult but especially urgent for controlling TB among PEH populations. Homelessness at the time of diagnosis indicates the need for a prompt contact investigation; however, guidance or consensus on how to identify contacts in these situations is lacking. Interviews of PEH persons with active TB are not always reliable sources for contact information. An analysis of ≈3,000 PEH and non-PEH TB patients in New York, New York, USA, demonstrated that experiencing homelessness in the year before diagnosis predicted the likelihood of that person's contacts not being identified during interviews (*5*). Shelter rosters can also be incomplete and unreliable, often changing over the course of a single night.

Guidelines for contact prioritization in congregate settings have been established but are impractical to apply to large, complex populations because priority is assigned primarily by likelihood of infection and progression to active disease, which is difficult to determine in these settings (*6*). Mass screenings for latent TB infection (LTBI) eliminate the need for contact prioritization but are resource intensive and decrease the public health value of positive test results. In the absence of readily available information about a person's susceptibility, duration of exposure to an infectious person has been used to prioritize contacts. Although this benchmark for exposure is linked to risk for transmission (*7*,*8*), the measure is not well defined.

In 2017, a total of 70 cases of TB were diagnosed in Hennepin County, the largest county in Minnesota,

Author affiliations: Hennepin County Public Health Department, Minneapolis, Minnesota, USA (K.K. Tibbetts, R.A. Ottoson, D.T. Tsukayama); Hennepin County Medical Center, Minneapolis (D.T. Tsukayama)

DOI: https://doi.org/10.3201/eid2603.190643

USA (population of 1.3 million). This area has experienced an ongoing cluster of genotypically linked TB cases among long-term PEH. The cluster, confirmed by whole-genome sequencing, could have been circulating in Hennepin County as early as 1992 (*9*) but was not identified until the Centers for Disease Control and Prevention (CDC) began providing TB genotyping services to state health departments in 2004. During 2008–2016, a total of 18 cases of this genotype cluster were identified, resulting in multiple complicated contact investigations (Figure 1, panel A).

In 2016, Hennepin County Public Health (HCPH) was notified of 3 newly identified active TB cases matching the cluster previously found in its PEH population. The most infectious person had experienced coughing, night sweats, and weight loss, and testing revealed acid-fast bacilli (AFB)–positive sputum samples and a cavitary lesion on chest radiograph. The contact investigation for this person identified 180 shelter residents at high risk for infection in need of testing, 85% of whom were evaluated.

In 2017, the HCPH was notified of another set of 3 newly identified active TB cases, which prompted another contact investigation. In this report, we review our experience conducting this contact investigation to prevent and control for a potential TB outbreak in Minneapolis homeless shelters during 2017–2018. We incorporated several methods that are not well described in the literature to identify, evaluate, and treat contacts. We specifically examined whether shelter rosters can be used to meaningfully quantify TB risk when multiple persons with TB have overlapping exposure periods and how outreach and partner strategies could be used to identify persons in need of TB testing.

Characteristics of Case-Patients in 2017

In the spring of 2017, case-patient 1 was reported to HCPH and identified as having 48 nights of exposure to a person with active TB in a homeless shelter during the 2016 contact investigation. However, he had not been available for follow-up investigation. When located, he reported hemoptysis, had a cavitary lesion on chest radiograph, and was smear positive for TB (i.e., AFB-positive on sputum smears).

Case-patient 2 was also identified as a contact in the 2016 investigation and was fully evaluated >8 weeks after the date of last exposure; this case-patient had a negative interferon-γ release assay (IGRA) test

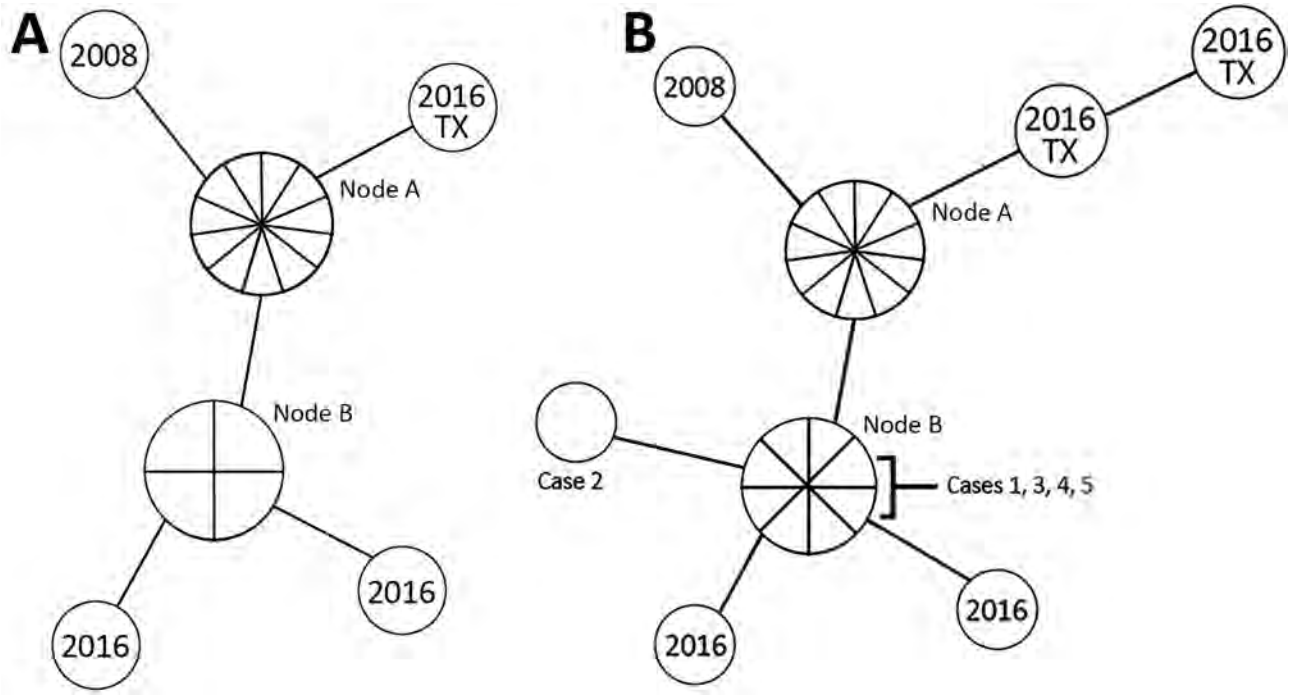

Figure 1. Whole-genome sequencing map of Hennepin County tuberculosis (TB) case cluster, Minneapolis, Minnesota, USA, including cases identified in Texas, USA, in 2016. A) 2008–2016 case cluster, which included 18 cases; B) updated 2008–2018 case cluster, totaling 24 cases. Isolates with the same genome sequence are displayed together in 1 node. Nodes are connected by lines proportional in length to the number of single-nucleotide polymorphism differences between isolates (n = 1, for all). No epidemiologic link to Minnesota was identified for the cases in Texas. Node A contains 10 cases diagnosed during 2008–2015 and the most recent common ancestor reference point. In panel A, node B contains 4 cases diagnosed during 2014–2016, and in panel B, node B contains 8 cases diagnosed during 2014–2018.

result and a clear chest radiograph. Later in 2016, however, a repeat IGRA gave a positive test result, but LTBI treatment was deferred because of elevated liver enzymes and issues with compliance. Whether the IGRA conversion was caused by a subsequent exposure or an initial false-negative test result could not be determined. By the spring of 2017, this case-patient had findings on chest radiograph; no AFB was identified on sputum smears, but *Mycobacterium tuberculosis* was found on sample culturing.

Three weeks after the first 2 cases were diagnosed, a third was reported. Case-patient 3 had AFB-positive sputum smears, a noncavitary lesion on chest radiograph, and a cough complicated by untreated HIV. According to shelter rosters, case-patient 3 had brief shelter-based exposures to case-patients 1 and 2, but contact occurred around the time of case-patient 3's symptom onset. No known exposure occurred between case-patient 3 and case-patients from the 2016 contact investigation. We identified only a weak epidemiologic link between case-patient 3 and the other case-patients identified in 2017, but whole-genome sequencing later confirmed that case-patient 3 was part of the same cluster.

Methods

We interviewed case-patients about all sites of exposure during their infectious period, which was determined on the basis of their symptom onset and available clinical and radiologic evidence (*5*). Information gathered during these interviews suggested that exposures predominantly occurred at 3 homeless shelters in Minneapolis. Capacity of these shelters was 35–170 adult men per night; shelters had common sleeping areas, and no administrative controls were in place at these locations requiring TB screening at entry.

To determine the level of exposure within shelters, we informally collaborated with the Institute for Community Alliances, the Minnesota administrator for the Homeless Management Information System (HMIS), an electronic data collection tool that tracks services accessed by PEH. Staff of all single-adult shelters in Hennepin County manage client data with HMIS, providing complete information about shelter use. After receiving consent from case-patients, epidemiologists disclosed those patients' names to HMIS staff, who compiled dates and locations of their shelter access and assembled full shelter rosters of all their contacts.

We adopted the concentric-circle approach for prioritizing contacts (*10*), using the number of nights of exposure to each case-patient (differing on the basis of perceived level of contagiousness) as a proxy for transmission risk; the first of the concentric circles included contacts with >10 days of exposure to smear-positive case-patients and >20 days exposure to smear-negative case-patients (Table 1). First-ring contacts underwent screening at a variety of locations (the Hennepin County Public Health Clinic and other county public health clinics, shelters, correctional facilities, hospitals, and primary care facilities) and were evaluated with either an IGRA or a tuberculin skin test (TST). If the initial TB test was conducted <8 weeks after the date of last exposure to the case-patient and the test results were negative, a second test was administered after ≥8 weeks had elapsed. All contacts, regardless of test results, were recommended to undergo chest radiography. Contacts who had symptoms or chest radiograph results compatible with active TB underwent clinical evaluation, and if indicated, they were asked to provide 3 sputum samples for smear, PCR, and culture testing. Persons with positive IGRA or TST results and for whom active disease was ruled out were encouraged to start LTBI treatment with daily isoniazid for 9 months, daily rifampin for 4 months, or once-weekly isoniazid/rifapentine for 12 weeks (*11*). Immunocompromised contacts and contacts previously treated for LTBI >10 years ago were also given physical examinations and the option to receive treatment for LTBI.

HCPH's Healthcare for the Homeless program staff assisted with LTBI treatment case management by piloting a directly observed preventive therapy project in which they dispensed medication refills and tracked treatment at an on-site shelter clinic. To engage the medical community, HCPH relied on its collaboration with the Hennepin County Medical Center, a public hospital in Minneapolis. Because Hennepin County Medical Center is a safety-net healthcare facility, PEH regularly use its services and, therefore, have existing electronic health records (EHR). Of 890 adults identified by HMIS as accessing shelters for >2 weeks during September 2016–November 2017, a total of 84% had a Hennepin County Medical Center EHR. For first-ring contacts with a Hennepin County Medical Center EHR, we documented their exposure and the recommended screening procedures they needed to receive in their

Table 1. Exposure criteria used to determine first concentric circle of contacts for case-patients 1–3 of Hennepin County tuberculosis case cluster, Minneapolis, Minnesota, USA, 2017

Case-patient no.	No. nights case-patient in shelter	Exposure criterion, no. nights
1	47	>10
2	28	>20
3	72	>10
1 and 3		>10

EHR and set a best-practice alert that would notify providers entering their record that the patient was a close TB contact. In addition, the alert also requested healthcare staff to update patient demographics and acquire patient contact information to provide HCPH epidemiologists. When the EHRs of these persons were accessed, epidemiologists received an immediate notification through the medical record system, providing real-time opportunities for communication between primary care and public health, if needed.

Last, we shared contact lists with relevant community partners, including shelter managers, staff at drop-in or advocacy centers, and clinic staff at jails and detoxification facilities. We asked partners to notify HCPH if contacts sought help at any of these locations.

After completing the contact investigation, we analyzed outcome data by using the χ^2 statistic to determine any relationship between duration of exposure and positive test results. We also reviewed how our methods contributed to contact identification and evaluation, captured transmission within a shelter setting, and facilitated LTBI treatment completion. Human subjects review for this synopsis was not required by our institutional review board, provided that the work involved a public health response, data were not traceable to individual patients, and informed consent was obtained from participants.

Results

We identified 830 persons as having shelter-based exposure to the 3 TB case-patients identified in 2017; of these, 285 met the first-ring criteria for nights of contact and were recommended to undergo evaluation. Screening of these contacts began in late July 2017. By mid-September, 106 persons had completed evaluations; results for 78 were negative and 28 positive by either TB test administered. Of the contacts with positive test results, 10 had no recollection or documentation of prior testing, and 18 had histories of negative test results.

We identified 1 case of pulmonary disease (case-patient 4) during this early phase of screening. This US-born man had 32 nights of cumulative exposure to both smear-positive case-patients. He had a history of a negative TST result but during this investigation had a positive IGRA result and findings on chest radiograph. This case-patient reported a cough of <1 week and night sweats for 1–2 months. All 3 of his sputum samples were smear negative for AFB, but *M. tuberculosis* was confirmed by culture. Rapid genotyping data showed a minor difference with previous cases, but given whole-genome sequencing results and the strong epidemiologic link, he was included in the cluster, in consultation with CDC. Case-patient 4 accessed only 1 shelter during his infectious period.

An estimated 16%–31% of the PEH population in the United States has LTBI (*12*–*14*). During the 2016 shelter contact investigation, in which 180 contacts of smear-positive case-patients were identified, HCPH found a positivity rate of 23%. Given a preliminary positivity rate of 26% in our investigation, including 1 new case of disease, transmission exceeding the expected rate was evident; hence, we expanded our contact investigation into the second concentric circle of contacts.

First-ring contacts who were newly TB positive could all be epidemiologically linked to case-patient 1 during a short date range at a single shelter, the same (and only) shelter accessed by case-patient 4. Therefore, inclusion in the second ring was based on exposure to case-patient 1, and the exposure cutoff was decreased to ≥5 nights. Using these criteria, we identified 51 additional contacts.

Case-patient 5 had 5 nights of exposure to case-patient 1 and was evaluated in November 2017. He had a negative IGRA result, no TB symptoms, and findings on chest radiograph that had been stable since 2014. In August 2018, a follow-up radiograph showed more pronounced opacities, prompting a bronchoalveolar lavage, which was AFB smear negative but culture positive for *M. tuberculosis*. Genotyping of this case-patient's isolate showed a match with the Hennepin County TB cluster (Figure 1, panel B).

In total, 338 first- and second-ring contacts were identified, and 298 (88%) were fully evaluated, a higher number than in other contact investigations done in this population (Table 2) (*6*,*15*). Of those evaluated, 227 had screening results that were negative for LTBI or active disease, 41 had positive test results but no disease (newly identified LTBIs), and 2 had positive TB test results and active disease and received TB diagnoses.

Percentage positivity trended downward as nights of exposure to case-patient 1 decreased. We analyzed data for a relationship between nights of exposure to case-patient 1 and TB test result by using the χ^2 statistic and the cutoff of >15 nights of exposure and found a significant association ($p = 0.001$). The positivity rate of the high exposure group was 22%, and the positivity rate of the low exposure group was 9%. Overall, the positivity rate was 14%.

Chest radiographs were obtained for 276 contacts at the time of their TB screening (Figure 2). Healthcare providers noted findings on 20 radiographs and recommended sputum sample collection for 14 of these patients. Two (case-patients 4 and 5) were positive for *M. tuberculosis* by culture.

Table 2. Test results for first- and second-ring contacts, by number of nights of exposure to case-patient 1 of Hennepin County tuberculosis case cluster, Minneapolis, Minnesota, USA, 2017–2018*

No. nights exposed to case-patient 1	No. contacts	No. (%) contacts evaluated	Test results*		
			No. (%) positive	No. negative	No. other†
26–31	34	33 (97)	9 (27)	19	6
21–25	59	54 (92)	11 (20)	41	7
16–20	39	36 (92)	7 (19)	26	6
11–15	57	54 (95)	4 (7)	43	10
6–10	76	59 (78)	8 (14)	43‡	25
1–5	54	47 (87)	2 (4)	43	9
0	19	15 (79)	1 (7)	13	5
Total	338	298 (88)	42 (14)	228	68

*Contacts were tested by either the tuberculin skin test or interferon-γ release assay.
†Contacts with history of a positive result by either tuberculosis test and those lost to follow-up.
‡Includes case-patient 5, who received an active tuberculosis diagnosis because his sputum was culture positive.

Treatment for newly identified LTBI was recommended to 41 contacts, and 32 started treatment. Of these, 21 (66%) completed treatment, 9 stopped treatment against medical advice, and 2 did not complete follow-up monitoring. The 3 LTBI patients who were treated through the Healthcare for the Homeless onsite directly observed preventive therapy clinic completed treatment.

Discussion

This contact investigation was initiated after 3 genotypically related cases of TB were diagnosed among PEH and was expanded when 1 case of pulmonary disease and a high positivity rate were found. In total, 5 TB cases were identified. Our work demonstrates a relationship between duration of exposure and TB transmission and uses innovative techniques to identify, test, and treat contacts in homeless shelters.

In shelter environments, contact identification and prioritization are well-known challenges to a successful contact investigation (*13*). In our investigation, no close shelter contacts were identified during case-patient interviews, and bed rosters were not maintained in a way that was conducive to timely analysis. As an alternative to paper rosters kept by many shelter staff, the HMIS database provided electronic spreadsheets from which dates of stay, a proxy measurement for duration of contact, could be quantified. This database enabled HCPH staff to quickly identify persons at greatest risk for TB infection and begin locating them.

Using the concentric circle approach, we prioritized contacts on the basis of their duration of exposure to case-patients, setting first-ring inclusion thresholds at >10 nights for smear-positive case-patients and >20 nights for smear-negative case-patients. Most contacts in this contact investigation had exposure to multiple case-patients, and attributing infection to any 1 case-patient was not possible. However, the 2 secondary active TB cases and 40 of the 41 new LTBI cases were identified in contacts exposed to case-patient 1. The remaining LTBI patient (who had 16 nights of exposure to case-patient 3) was unable to recall ever having a past TB test but confirmed a history of homelessness and incarceration.

We found that degree of contagiousness was linked to transmission and that transmission generally decreased as nights of exposure to case-patient 1 decreased. This finding legitimizes our prioritization methods and demonstrates the value of focusing resources on the evaluation of contacts of highly contagious TB case-patients. The expansion of the contact investigation was also validated, as shown by the 8 cases of newly identified LTBI in persons with 6–10 nights of exposure to case-patient 1. Contacts in the second concentric circle might have had a high positivity rate because many were exposed to case-patient 1 in the days immediately preceding his diagnosis, when he was believed to be most contagious. Therefore, public health officials should consider not only the duration of exposure but also the timing of it.

Establishing relationships with healthcare services accessed by our contacts was essential for successful screening. EHRs conveyed exposure messages to providers and enabled epidemiologists to view historical TB testing and any treatment outcomes. The best practice alert, which contained instructions for evaluation, prompted screening for 33% of contacts. For enhanced contact tracing in future contact investigations, we recommend that public health departments learn where their contacts receive healthcare services and build strong partnerships with the staff at those locations.

PEH face many barriers when accessing healthcare, which were acknowledged as we developed screening strategies. IGRAs were the primary screening tool used in this investigation and are preferable to TSTs for groups that have historically low rates of returning to have their TSTs read (*16*). Likewise, we conducted chest radiography at the time of TB testing.

According to CDC guidelines (*3*), chest radiographs would not have been obtained for contacts with negative TB tests and no symptoms unless the persons were known to have concurrent medical conditions that increased risk (e.g., HIV, diabetes mellitus, substance abuse). Chest radiographs provided additional information that contributed to the diagnosis of active disease in 1 contact (case-patient 5). In addition, with this population's high risk for TB exposure, the baseline films obtained become of great value in future contact investigations. Additional measures to reduce healthcare barriers included the Hennepin County Public Health Clinic offering incentives to contacts for completing screening tests and, later, the Healthcare for the Homeless staff facilitating annual IGRAs for shelter residents.

LTBI treatment completion is one of the best interventions for preventing cases of TB disease, but homelessness has been found to be significantly associated with incomplete treatment (*17*). We used 2 solutions to help contacts complete their treatments. First, the Healthcare for the Homeless project demonstrated that intensive case management combining medication tracking, dispensing, and education can prevent treatment failure. When using directly observed preventive therapy for patients at high risk for noncompliance along with the 12-week regimen, we saw 80% treatment completion, a level similar to that seen in a large-scale analysis of treatment completion among PEH (*18*).

Public health investigations in homeless shelters are not without their limitations, the most critical of which is locating contacts for evaluation. We were unable to coomplete follow-up with nearly 12% of our contacts, some of whom were accessing shelters outside of Hennepin County. HMIS is used statewide, but flagging records with exposure information was ultimately deemed too time consuming and had privacy concerns. EHRs can be useful to TB investigators and should be used to their full potential while still considering patient confidentiality and the urgency of a contact investigation. In addition, although partnering with shelter and day center staff provided opportunities for TB education and demonstrated transparency, these partnerships ultimately yielded no contacts.

Epidemiologists received no verification from case-patients about their exposures to contacts in shelters, and we could not exclude exposures that contacts might have had to these case-patients outside the shelter setting. Likewise, the results here were reported under the assumption that case-patient 1 had the only case with transmission potential. However, exposure to additional unidentified persons with TB infections might have occurred. When prioritizing contacts, we also did not give weight to the shelter environments (e.g., ventilation, bed proximity, and congregate areas within the shelter) of the facilities affected by the outbreak, although these factors could have affected transmission (*19*).

Despite our comprehensive approach to treating new cases of LTBI, treatment completion was low overall, a challenge not unique to this study (*20*,*21*).

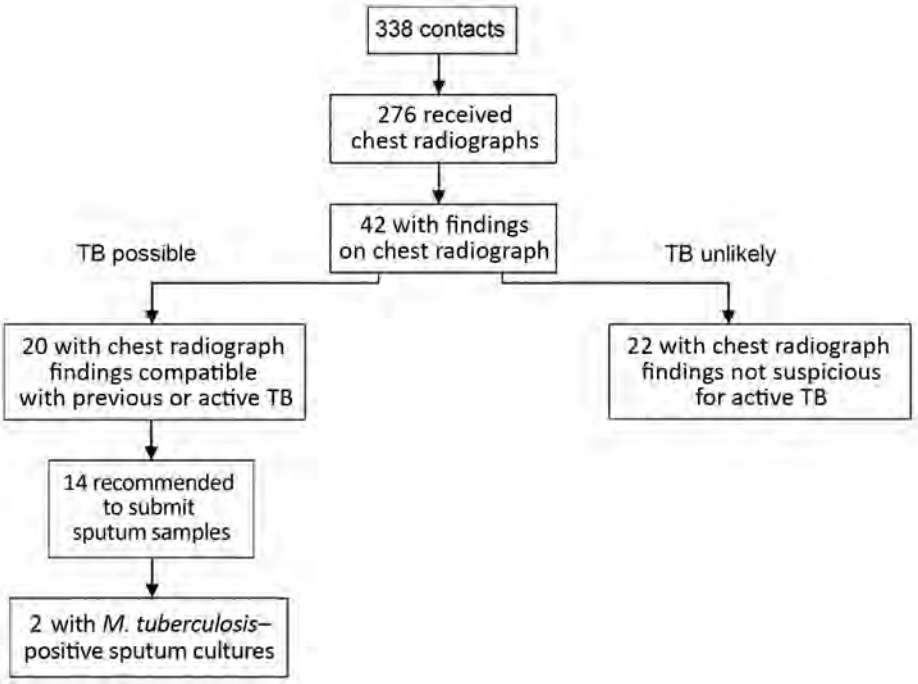

Figure 2. Chest radiograph findings and TB test results of contacts for case-patients 1–3 of Hennepin County TB case cluster, Minneapolis, Minnesota, USA, 2017–2018. At the initial screening, contacts were evaluated by either an interferon-γ release assay or a tuberculin skin test and recommended to undergo chest radiography. Those with suspected active TB were requested to provide sputum samples for further diagnostics (smear test, *Mycobacterium tuberculosis* culturing, and interferon-γ release assay). Two contacts were identified as having active pulmonary disease. TB, tuberculosis.

Although our work can inform contact identification, prioritization, and screening methods, unless LTBI treatment completion rates improve, which requires intensive resources, we expect to see a continuation of this TB cluster in Hennepin County in the PEH population.

Acknowledgments

We acknowledge the support provided to us by the staff of HCPH (especially those in epidemiology), the Hennepin County Public Health Clinic, and Healthcare for the Homeless. We thank the staff of the Minnesota Department of Health TB program and other local partners for their contributions to this investigation.

About the Author

Ms. Tibbetts is an epidemiologist at Hennepin County Public Health in Minneapolis, Minnesota, USA. Her work includes conducting TB contact investigations and performing general infectious disease epidemiology.

References

1. Stewart RJ, Tsang CA, Pratt RH, Price SF, Langer AJ; Centers for Disease Control and Prevention. Tuberculosis—United States, 2017. MMWR Morb Mortal Wkly Rep. 2018;67:317–23. https://doi.org/10.15585/mmwr.mm6711a2
2. Bamrah S, Yelk Woodruff RS, Powell K, Ghosh S, Kammerer JS, Haddad MB. Tuberculosis among the homeless, United States, 1994–2010. Int J Tuberc Lung Dis. 2013;17:1414–9. https://doi.org/10.5588/ijtld.13.0270
3. National Center for HIV/AIDS, Viral Hepatitis, STD, and TB Prevention. Workshop on tuberculosis and homelessness: infection control measures in homeless shelters and other overnight facilities that provide shelter: summary of the workshop held September 28–29, 2015 [cited 2019 May 2]. https://www.cdc.gov/tb/topic/populations/homelessness/TB_and_Homelessness_2015_Summit.pdf
4. Centers for Disease Control and Prevention. Screening for tuberculosis and tuberculosis infection in high-risk populations. Recommendations of the Advisory Council for the Elimination of Tuberculosis. MMWR Recomm Rep. 1995;44(RR-11):19–34.
5. National Tuberculosis Controllers Association; Centers for Disease Control and Prevention. Guidelines for the investigation of contacts of persons with infectious tuberculosis. Recommendations from the National Tuberculosis Controllers Association and CDC. MMWR Recomm Rep. 2005;54(RR-15):1–47.
6. Li J, Driver CR, Munsiff SS, Fujiwara PI. Finding contacts of homeless tuberculosis patients in New York City. Int J Tuberc Lung Dis. 2003;7(Suppl 3):S397–404.
7. Munn MS, Duchin JS, Kay M, Pecha M, Thibault CS, Narita M. Analysis of risk factors for tuberculous infection following exposure at a homeless shelter. Int J Tuberc Lung Dis. 2015;19:570–5. https://doi.org/10.5588/ijtld.14.0648
8. Bailey WC, Gerald LB, Kimerling ME, Redden D, Brook N, Bruce F, et al. Predictive model to identify positive tuberculosis skin test results during contact investigations. JAMA. 2002;287:996–1002. https://doi.org/10.1001/jama.287.8.996
9. Kline SE, Hedemark LL, Davies SF. Outbreak of tuberculosis among regular patrons of a neighborhood bar. N Engl J Med. 1995;333:222–7. https://doi.org/10.1056/NEJM199507273330404
10. Iseman MD, Bentz RR, Fraser RI, Locks MO, Ostrow JH, Sewell EM; American Thoracic Society. Guidelines for the investigation and management of tuberculosis contacts. Am Rev Respir Dis. 1976;114:459–63.
11. American Thoracic Society. Targeted tuberculin testing and treatment of latent tuberculosis infection. MMWR Recomm Rep. 2000;49(RR-6):1–51.
12. Parriott A, Malekinejad M, Miller AP, Marks SM, Horvath H, Kahn JG. Care cascade for targeted tuberculosis testing and linkage to care in homeless populations in the United States: a meta-analysis. BMC Public Health. 2018;18:485. https://doi.org/10.1186/s12889-018-5393-x
13. McAdam JM, Bucher SJ, Brickner PW, Vincent RL, Lascher S. Latent tuberculosis and active tuberculosis disease rates among the homeless, New York, New York, USA, 1992–2006. Emerg Infect Dis. 2009;15:1109–11. https://doi.org/10.3201/eid1507.080410
14. Dewan PK, Grinsdale J, Liska S, Wong E, Fallstad R, Kawamura LM. Feasibility, acceptability, and cost of tuberculosis testing by whole-blood interferon-gamma assay. BMC Infect Dis. 2006;6:47. https://doi.org/10.1186/1471-2334-6-47
15. Yun LW, Reves RR, Reichler MR, Bur S, Thompson V, Mangura B, et al. Outcomes of contact investigation among homeless persons with infectious tuberculosis. Int J Tuberc Lung Dis. 2003;7(Suppl 3):S405–11.
16. Mazurek GH, Jereb J, Vernon A, LoBue P, Goldberg S, Castro K; IGRA Expert Committee; Centers for Disease Control and Prevention. Updated guidelines for using interferon gamma release assays to detect *Mycobacterium tuberculosis infection – United States, 2010.* MMWR Recomm Rep. 2010;59(RR05):1–25.
17. Malejczyk K, Gratrix J, Beckon A, Moreau D, Williams G, Kunimoto D, et al. Factors associated with noncompletion of latent tuberculosis infection treatment in an inner-city population in Edmonton, Alberta. Can J Infect Dis Med Microbiol. 2014;25:281–4. https://doi.org/10.1155/2014/349138
18. Nwana N, Marks SM, Lan E, Chang AH, Holcombe M, Morris SB. Treatment of latent *Mycobacterium tuberculosis* infection with 12 once weekly directly-observed doses of isoniazid and rifapentine among persons experiencing homelessness. PLoS One. 2019;14:e0213524. https://doi.org/10.1371/journal.pone.0213524
19. Taylor JG, Yates TA, Mthethwa M, Tanser F, Abubakar I, Altamirano H. Measuring ventilation and modelling *M.* tuberculosis transmission in indoor congregate settings, rural KwaZulu-Natal. Int J Tuberc Lung Dis. 2016;20:1155–61. https://doi.org/10.5588/ijtld.16.0085
20. Hirsch-Moverman Y, Shrestha-Kuwahara R, Bethel J, Blumberg HM, Venkatappa TK, Horsburgh CR, et al.; Tuberculosis Epidemiologic Studies Consortium. Latent tuberculous infection in the United States and Canada: who completes treatment and why? Int J Tuberc Lung Dis. 2015;19:31–8. https://doi.org/10.5588/ijtld.14.0373
21. Holland DP, Alexander S, Onwubiko U, Goswami ND, Yamin A, Mohamed O, et al. Response to isoniazid-resistant tuberculosis in homeless shelters, Georgia, USA, 2015–2017. Emerg Infect Dis. 2019;25:593–5. https://doi.org/10.3201/eid2503.181678

Address for correspondence: Kelzee K. Tibbetts, Hennepin County Public Health Department, 525 Portland Ave, 3rd Fl, Minneapolis, MN 55415, USA; email: kelzee.tibbetts@hennepin.us

Mycobacterium tuberculosis Complex Lineage 3 as Causative Agent of Pulmonary Tuberculosis, Eastern Sudan[1]

Yassir A. Shuaib, Eltahir A.G. Khalil, Lothar H. Wieler, Ulrich E. Schaible, Mohammed A. Bakheit, Saad E. Mohamed-Noor, Mohamed A. Abdalla, Glennah Kerubo, Sönke Andres, Doris Hillemann, Elvira Richter, Katharina Kranzer, Stefan Niemann,[2] Matthias Merker[2]

Pathogen-based factors associated with tuberculosis (TB) in eastern Sudan are not well defined. We investigated genetic diversity, drug resistance, and possible transmission clusters of *Mycobacterium tuberculosis* complex (MTBC) strains by using a genomic epidemiology approach. We collected 383 sputum specimens at 3 hospitals in 2014 and 2016 from patients with symptoms suggestive of TB; of these, 171 grew MTBC strains. Whole-genome sequencing could be performed on 166 MTBC strains; phylogenetic classification revealed that most (73.4%; n = 122) belonged to lineage 3 (L3). Genome-based cluster analysis showed that 76 strains (45.9%) were grouped into 29 molecular clusters, comprising 2–8 strains/patients. Of the strains investigated, 9.0% (15/166) were multidrug resistant (MDR); 10 MDR MTBC strains were linked to 1 large MDR transmission network. Our findings indicate that L3 strains are the main causative agent of TB in eastern Sudan; MDR TB is caused mainly by transmission of MDR L3 strains.

Tuberculosis (TB) remains a major global health problem; 10 million new cases were reported in 2018 (*1*). In Sudan, the estimated national TB incidence in 2018 was 71/100,000 persons; a total of 20,638 cases were reported (*1*). However, the TB burden is by no means homogeneous across the country. For instance, in eastern Sudan, TB notifications reached 275/100,000 persons in 2012 (*2*,*3*). Prevalence of multidrug-resistant TB (MDR TB) (i.e., resistant to isoniazid and rifampin) was estimated at 2.9% in new and 13% in retreatment cases; however, studies have reported MDR TB rates of 6%–22% (*1*,*4*–*10*).

Ongoing transmission is one of the key challenges for TB control programs, especially in countries with a high TB burden (*1*,*11*). In recent years, molecular techniques have been increasingly used to clarify and trace transmission of *Mycobacterium tuberculosis* complex (MTBC) strains and to direct and guide targeted TB control actions (*12*,*13*). However, availability of molecular techniques is limited in many countries in Africa with a high TB burden (*11*).

In Sudan, drug-resistant TB often goes undetected, resulting in inadequate treatment, illness, death, and ongoing transmission (*1*,*14*). Local laboratories have limited access to mycobacterial culture and drug susceptibility testing (DST) or DNA-based techniques (*14*). Therefore, MDR TB rates might be underestimated in eastern Sudan. In addition, mutations that mediate drug resistance have not been investigated.

Taken together, these factors indicate that, although TB is a huge health problem in eastern Sudan, precise data on the phylogeny and transmission dynamics of MTBC strains, as well as on resistance patterns, is sparsely available (*2*,*3*,*7*,*8*,*15*). Studies using molecular epidemiologic tools are rare and have used classical genotyping techniques, such as

Author affiliations: Freie Universität Berlin, Berlin, Germany (Y.A. Shuaib, L.H. Wieler); Research Center Borstel, Borstel, Germany (Y.A. Shuaib, U.E. Schaible, S. Andres, D. Hillemann, S. Niemann, M. Merker); Sudan University of Science and Technology, Khartoum, Sudan (Y.A. Shuaib, S.E. Mohamed-Noor, M.A. Abdalla); University of Khartoum, Khartoum (E.A.G. Khalil, M.A. Bakheit); Robert Koch Institute, Berlin (L.H. Wieler); Kenyatta University, Nairobi, Kenya (G. Kerubo); Labor Limbach, Heidelberg, Germany (E. Richter); London School of Hygiene and Tropical Medicine, London, UK (K. Kranzer); German Center for Infection Research, Borstel Site, Borstel (S. Niemann, M. Merker)

DOI: https://doi.org/10.3201/eid2603.191145

[1]Preliminary results from this study were presented at the 39th Annual Congress of the European Society of Mycobacteriology, July 1–4, 2018, Dresden, Germany.

[2]These authors contributed equally to this article.

spoligotyping, which cannot deduce direct transmission events (*5*,*15*). New techniques, such as whole-genome sequencing (WGS), offer the highest resolution for MTBC genotyping and provide precise information on resistance mutations (*16*,*17*). We applied state-of-the-art phenotypic and molecular assays to investigate specimens collected from patients with symptoms suggestive of pulmonary TB, including new and retreatment cases, to analyze the MTBC population structure, putative transmission events, and DST profiles in eastern Sudan.

Methods

Study Design and Setting

We recruited patients with symptoms suggestive of pulmonary TB who had positive sputum smears and agreed to participate in this cross-sectional study. Patients had been treated in the outpatient departments at public hospitals in Kassala, Port Sudan, and El-Gadarif in eastern Sudan over 2 recruitment periods, June–October 2014 and January–July 2016. We collected spot and early morning sputum samples. If 1 sample was smear positive, the 2 samples were pooled and stored for ≤6 months at –20°C. Shortly before we shipped each sample to the National Reference Center (NRC) for Mycobacteria, Borstel, Germany, we transferred a volume of ≤2 mL to a screw-capped Eppendorf tube; the samples were shipped in 2 separate batches.

Mycobacterial Culture and Identification

Sample decontamination, smear microscopy, and mycobacterial culture were performed at the NRC (*18*,*19*). We extracted DNA using a QIAamp DNA Mini Kit 250 (QIAGEN, https://www.qiagen.com) according to the instructions of the manufacturer for quantitative PCR (qPCR). We extracted DNA by the boiling/sonication method for conducting line probe assays (LPAs) such as GenoType *Mycobacterium* CM and GenoType *Mycobacterium* MTBC (Hain Lifescience, https://www.hain-lifescience.de) (*19*). We used cetyl trimethylammonium bromide for DNA extraction for WGS (*20*). We transferred the extracted DNA to new Eppendorf tubes and stored it at –20°C until used.

We used an in-house qPCR detecting MTBC and nontuberculous mycobacteria (NTM) DNA to test available culture-negative/contaminated samples (*21*). We ran the qPCR experiments using the Rotor-Gene 2000 (Corbett Research Pty Ltd, http://www.australianexporters.net). We used LPAs (Hain Lifescience, https://www.hain-lifescience.de) according to the manufacturer's instructions to classify isolated mycobacteria into MTBC or NTM and to differentiate the MTBC species.

We identified NTM species using 16S rRNA, internal transcribed spacer (ITS) DNA fragment sequencing, or both (*22*). We sequenced the complete PCR products on an automated DNA sequencer (ABI 377; Applied Biosystems, https://www.thermofisher.com) by cycle sequencing using the Big Dye RR Terminator Cycle Sequencing Kit (Applied Biosystems). We aligned the resulting sequences and compared them with the sequences of the International Nucleotide Sequence Database Collaboration.

Drug Susceptibility Testing

We performed phenotypic DST (pDST) for resistance to streptomycin 1 μg/mL, isoniazid 0.1 μg/mL, rifampin 1 μg/mL, ethambutol 5 μg/mL, and pyrazinamide 100 μg/mL for all MTBC isolates (*18*). We further investigated isolates with resistance to ≥1 first-line drug for resistance to ofloxacin 2 μg/mL, amikacin 1 μg/mL, and capreomycin 2.5 μg/mL (*23*).

We further evaluated strains that had a mutation in the *embB* codons 306, 406, or 497 (as detected by WGS) but tested phenotypically susceptible to ethambutol at the critical concentration by determining ethambutol MICs. We assessed concentrations of 1.25, 2.5, 3.75, and 5.0 μg/mL in the BACTEC MGIT 960 system (Becton Dickinson, https://www.bd.com) (*24*,*25*).

WGS

We performed WGS using the Illumina Nextera (XT) kit (https://www.illumina.com) (*26*). We sequenced isolates with a minimum average genome coverage of 50×. We used single-nucleotide polymorphisms (SNPs) occurring in ≥4 forward and ≥4 reverse reads, 4 reads calling the allele with a Phred score ≥20, and a minimum variant frequency of 75% for a concatenated sequence alignment (*27*). In the comparative genomic analysis, we allowed 5% of all samples to miss these coverage and frequency thresholds at individual positions and called the majority allele (>50% variant frequency) to not lose sequence information in genome regions with lower average coverage. We excluded repetitive region and drug resistance associated genes for phylogenetic reconstruction.

Phylogenetic Inference

We calculated a maximum-likelihood tree with FastTree using the concatenated sequence alignment and a general time-reversible substitution model (*28*). We conducted inspection and rooting of the

maximum likelihood tree using FigTree software and performed the graphical presentation using the online tool EvolView (*29*). We calculated maximum parsimony trees with BioNumerics version 7.6 (Applied Maths, https://www.applied-maths.com) using the concatenated sequence alignment (*30*).

Molecular Drug Resistance Prediction

We screened the *rpsL*, *rrs*, and *gidB* genes for mutations that confer resistance to streptomycin and the *katG* and *inhA* genes and the *fabG1-inhA* promoter for resistance to isoniazid (*31*). We inferred rifampin resistance by mutations in the *rpoB* gene. Moreover, we also noted putative compensatory mutations in the *rpoA* and *rpoC* genes (for rifampin resistance) and the *ahpC* gene (for isoniazid resistance). We investigated the *embA*, *embB*, and *embC* genes for resistance conferring mutations to ethambutol and screened the *pncA* gene for mutations associated with resistance to pyrazinamide (*31*). We investigated the *gyrA* and *gyrB* genes for resistance to fluoroquinolones and investigated the *rrs* gene for resistances against kanamycin, amikacin, and capreomycin. In addition, we screened the *eis* promoter region for resistance against KAN and the *tlyA* for resistance against capreomycin. For ethionamide, we investigated the *ethA* and *inhA* genes and the *fabG1-inhA* promoter and for para-aminosalicylic acid, we investigated the *ribD*, *thyA*, *thyX*, and *folC* genes (*31*).

Statistics

We used SPSS version 20.0 (https://www.ibm.com) for all appropriate statistical analyses. We obtained descriptive statistics of the variables, including frequencies and proportions. We analyzed differences between groups by using the χ^2 or Fisher exact test; $p \leq 0.05$ denoted statistical significance (*32*).

Ethics Considerations

Scientific and ethics approval for the study was provided by the National Research Ethics Committee, Federal Ministry of Health, Khartoum, Sudan, and by the Institutional Review Board of the Institute of Endemic Diseases, University of Khartoum, Khartoum, Sudan (no. 85–03–09). We obtained written informed consent for participation in the study from participants or, in case of children or illiterate patients, their guardians.

Results

Study Population

Sputum samples were provided by smear-positive patients with TB from 3 areas in eastern Sudan in 2014 (n = 101) and 2016 (n = 282) (Figure 1). Based on hospital records, we included 10%–20% of all patients who received diagnoses of TB during the study period. We collected patient-derived samples from 161 patients (42%) in El-Gadarif, 133 patients (34.7%) in Kassala, and 89 patients (23.3%) in Port Sudan hospitals. Patients who provided samples had a median age of 35 years (interquartile range 25–45 years); most (245/383; 66%) were male. In addition, 81.5% (312/383) were new and 5.5% (21/383) were retreatment TB cases; data on TB treatment history were unavailable for 13.0% (50/383) (Table 1). Comparison of the 2 patient cohorts revealed no significant difference between the proportions of L3 strains (p = 0.068 by Fisher exact test) but the 2014 cohort contained more drug-resistant (p = 0.019 by Fisher exact test) and clustered (p = 0.016 by Fisher exact test) strains (Table 2).

Mycobacterium Isolation and Species Identification

Of all collected specimens, 51.2% (196/383) were culture positive for mycobacteria; LPAs identified most (n = 171, 87.2%) as MTBC (Figure 1). The rest of the specimens were either culture negative or contaminated; we tested them with qPCR and Sanger sequencing for mycobacterial DNA detection and species identification (Figure 1) (*14*).

MTBC Population Structure and Genome-Based Clusters

We performed WGS successfully on 166 MTBC strains. We built a maximum-likelihood phylogeny upon a concatenated sequence alignment comprising 11,932 SNPs to investigate the MTBC population structure (Figure 2). We performed MTBC (sub)lineage (L) classification with an SNP bar code nomenclature that was recently introduced (*33*). Strains of L3 (Delhi/CAS) were predominant (73.5%, 122/166), followed by L4 (Euro-American) strains (23.5%, 39/166). We further classified L4 strains into several sublineages (Appendix 1 Figure 1, https://wwwnc.cdc.gov/EID/article/26/3/19-1145-App1.pdf). The remaining isolates belonged to L1 (2.4%, 4/166) and L2 (0.6%, 1/166).

To obtain an indication about putative recent transmission events, we conducted a cluster analysis based on a pairwise SNP distance of ≤12 SNPs between any 2 strains (*12*,*34*). Overall, 45.9% (76/166) of the strains were grouped in 29 clusters comprising 2–8 isolates/patients (Appendix 1 Figure 2). L3 strains were observed with a higher clustering rate (52.5%, 64/122) than L4 isolates (28.2%, 11/39) (p = 0.016 by Fisher exact test). Two of the 4 L1 strains were clustered; no L2 strains were assigned to a WGS

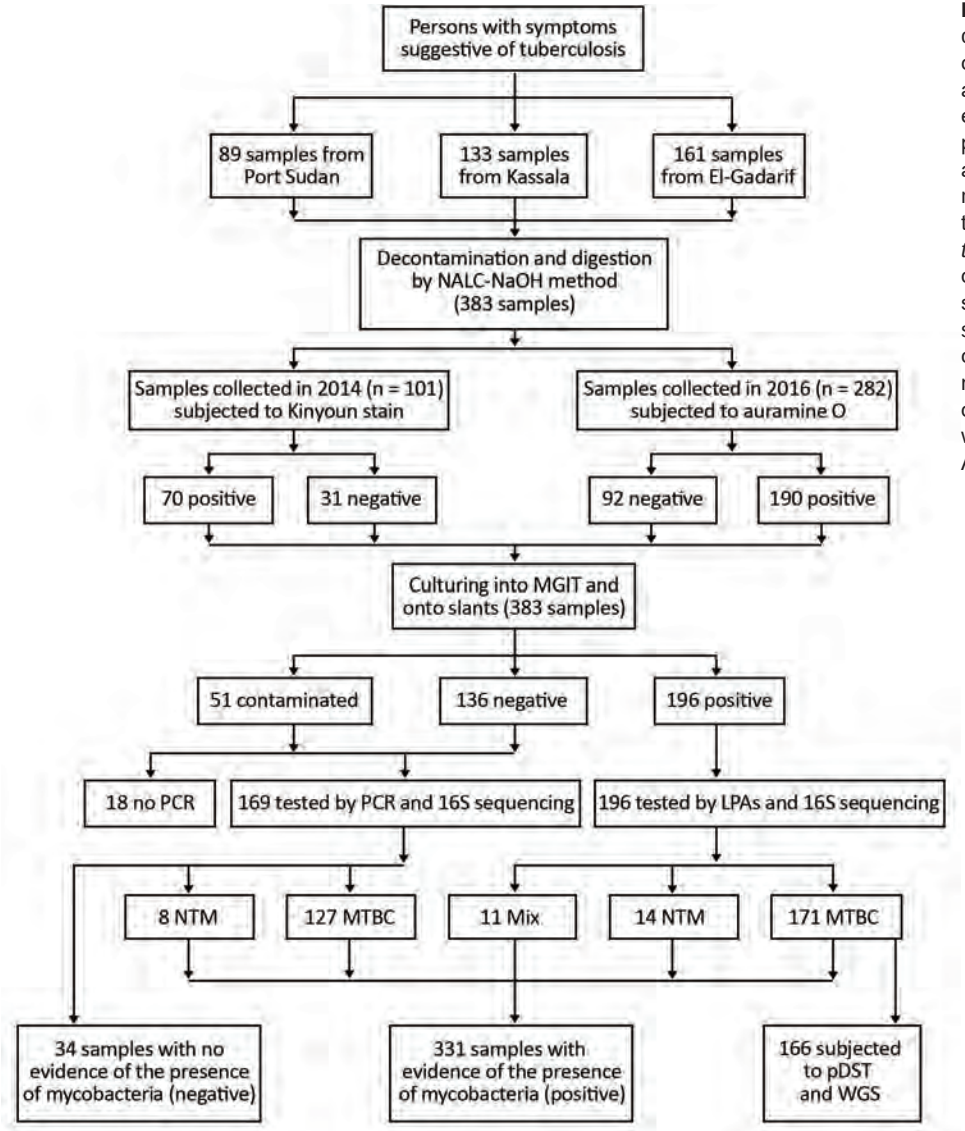

Figure 1. Work flow for study of *Mycobacterium tuberculosis* complex lineage 3 as causative agent of pulmonary tuberculosis, eastern Sudan. LPAs, HAIN line probe assay for GenoType CM and GenoType MTBC; MGIT, mycobacteria growth indicator tube; MTBC, *Mycobacterium tuberculosis* complex; mix, 2 different bacteria grew on the same culture; NALC-NaOH, sodium hydroxide/N-acetyl-cysteine; NTM, nontuberculous mycobacteria; pDST, phenotypic drug susceptibility testing; WGS, whole genome sequencing. Adopted from Shuaib et al. (*14*).

cluster. Moreover, considering a stricter threshold (≤5 SNPs), 36.7% (61/166) isolates were still connected in 24 clusters comprising 2–8 isolates/patients (Appendix 1 Figure 3).

pDST and Genotypic DST

To determine resistance levels and related genomic variants, we performed pDST and genomic resistance predictions or genotypic DST (gDST) and compiled detailed data on resistances and resistance conferring mutations (Tables 3, 4; Appendix 1 Table). Overall, 21.7% (36/166) of the strains showed resistance to ≥1 of the tested first-line antimicrobial drugs by pDST, including 15 (9.0%) MDR and 21 (12.7%) non-MDR strains (Appendix 2, https://wwwnc.cdc.gov/EID/article/26/3/19-1145-App2.xlsx). Strikingly, all MDR and 76.1% of non-MDR strains belonged to L3. Furthermore, beyond the MDR classification, we found that L3 strains in eastern Sudan were more often found with drug resistances as compared with L4 strains (L3, 31/122, 25.4%; L4, 4/39, 10.3%; p = 0.048 by Fisher exact test).

We detected resistance to streptomycin in 19.9% (33/166) of the strains, mediated by mutations in *rspL* (Lys43Arg, Lys88Arg, and Lys88Met), *gidB* (e.g., Ala138Val), and *rrs* (514, a/c) genes. We observed all isoniazid-resistant strains (10.2%, 17/166) either with a mutation in *katG* (Ser315Thr and Ser315Asn) that changes catalase–peroxidase activities or in the promoter region of the drug target InhA, *fabG1-inhA* (–15 c/t), which also confers resistance to the second-line drug ETH. Resistance to rifampin was found in 10.2% (17/166) of the strains and was mediated by mutations in the *rpoB* gene (Ser450Leu, His445Tyr,

His445Asn, and His445Asp). We found 1 ethambutol-resistant strain (0.6%) with the mutation *embB* Gln497Arg. However, we also detected 11 additional mutations associated with ethambutol resistance in the *embB* gene (10 Met306Ile and 1 Met306Val) but with MICs ranging from 1.25 to 5 μg/mL, classifying these strains as phenotypically susceptible based on the recommended critical concentration for ethambutol. With regard to pyrazinamide, we identified 1 strain (0.6%) with the mutation *pncA* Gln10Arg, coinciding with phenotypic pyrazinamide resistance.

A detailed comparison of the pDST and gDST results revealed a high sensitivity and specificity for isoniazid, rifampin, and pyrazinamide resistance prediction by WGS (Table 4). For ethambutol, we determined high-confidence resistance SNPs at codon 306, 406, or 497; however, varying levels of ethambutol MICs in the strains with mutations resulted in a very low positive predictive value. For streptomycin, we considered the *gidB* mutations (Phe12Ser, Arg39Pro, Trp45STP, Ser136STP, Iso114Ser, and deletions at positions 4408101, 4408017, and 4408116) to be mutations with an unclear effect. However, these strains eventually tested phenotypically resistant to streptomycin, leading to a reduced sensitivity.

All strains with resistances to ≥1 first-line antimicrobial drug were phenotypically and genotypically susceptible to ofloxacin, capreomycin, and amikacin. We identified no genotypic resistance marker mediating para-aminosalicylic acid resistance.

Based on a 12-bp SNP threshold between any 2 strains, 80.0% (12/15) of the MDR strains were clustered or connected (i.e., associated with recent transmission); based on ≤5 SNPs distance, 60% (9/15) of the MDR strains were clustered (Appendix 1 Figure 4, panel A). Most of the clustered strains at ≤12 SNPs were isolated from patients in Kassala and grouped in clusters 4 and 29. These strains also shared the same *rpsL* (Lys43Arg) and the *katG* (Ser315Thr) mutations but harbored different mutations in the *rpoB* gene; strains of cluster 4 had the Ser450Leu mutation, whereas strains of cluster 29 exhibited a His445Tyr mutation. This finding points toward a close relationship between the strains of both clusters that likely emerged from a common recent ancestor already being polyresistant to streptomycin and isoniazid (Appendix 1 Figure 4, panel B). Furthermore, all 5 strains of cluster 29 had the *embB* Met306Ile mutation, but 1 of them also had the mutation *embB* Gly406Asp. Within cluster 4, two strains acquired the mutation *embB* Met306Ile independently, and 1 acquired *embB* Met306Val, as judged by the tree topology (Appendix 1 Figure 4, panel B). Moreover, among all drug-resistant strains, only 1 strain was identified with resistance to pyrazinamide mediated by the mutation *pncA* Gln10Arg.

Table 1. Demographic characteristics of tuberculosis patients investigated in eastern Sudan

Characteristic	No. recruited patients	% Recruited patients
Origin		
Kassala	133	34.7
El-Gadarif	161	42.0
Port Sudan	89	23.3
Sex		
M	245	64.0
F	123	32.1
Not available	15	3.9
Age, y		
<25	76	19.8
25–40	170	44.4
>40	108	28.2
Not available	29	7.6
Treatment history		
Retreatment	21	5.5
New	312	81.5
Not available	50	13.0
All patients	383	100

Discussion

By using conventional diagnostics and WGS, we showed that pulmonary TB in eastern Sudan is caused predominantly by L3 strains (Delhi/CAS). Drug resistance and recent transmission were associated with L3 strains, accentuating the key role of L3 strains in TB epidemiology in eastern Sudan. In addition, most

Table 2. Comparison of *Mycobacterium tuberculosis* complex isolates sampled in eastern Sudan, 2014 and 2016*

Variable	Year of sample collection, no. (%) isolates		Total no.	p value
	2014	2016		
Lineage				0.068
L3	51 (82.3)	71 (68.3)	122	
Non-L3	11 (17.7)	33 (31.7)	44	
DST				0.019
Any drug resistance	20 (32.3)	16 (15.4)	36	
No drug resistance	42 (67.7)	88 (84.6)	120	
≤12 SNP cluster				0.016
Clustered	36 (58.1)	40 (38.5)	76	
Not clustered	26 (41.9)	64 (61.5)	90	
All patients	62 (100)	104 (100)	166	

*DST, drug susceptibility testing; L, lineage; SNP, single-nucleotide polymorphism.

MDR TB cases were connected in 2 closely related molecular clusters (denoting recent transmission of MDR strains). This finding suggests that more focused infection control measures and contact tracing of patients with MDR TB need to be introduced to break the transmission chains at an early stage.

In this study, we found that a high proportion of culture-positive pulmonary TB cases (73.4%) were

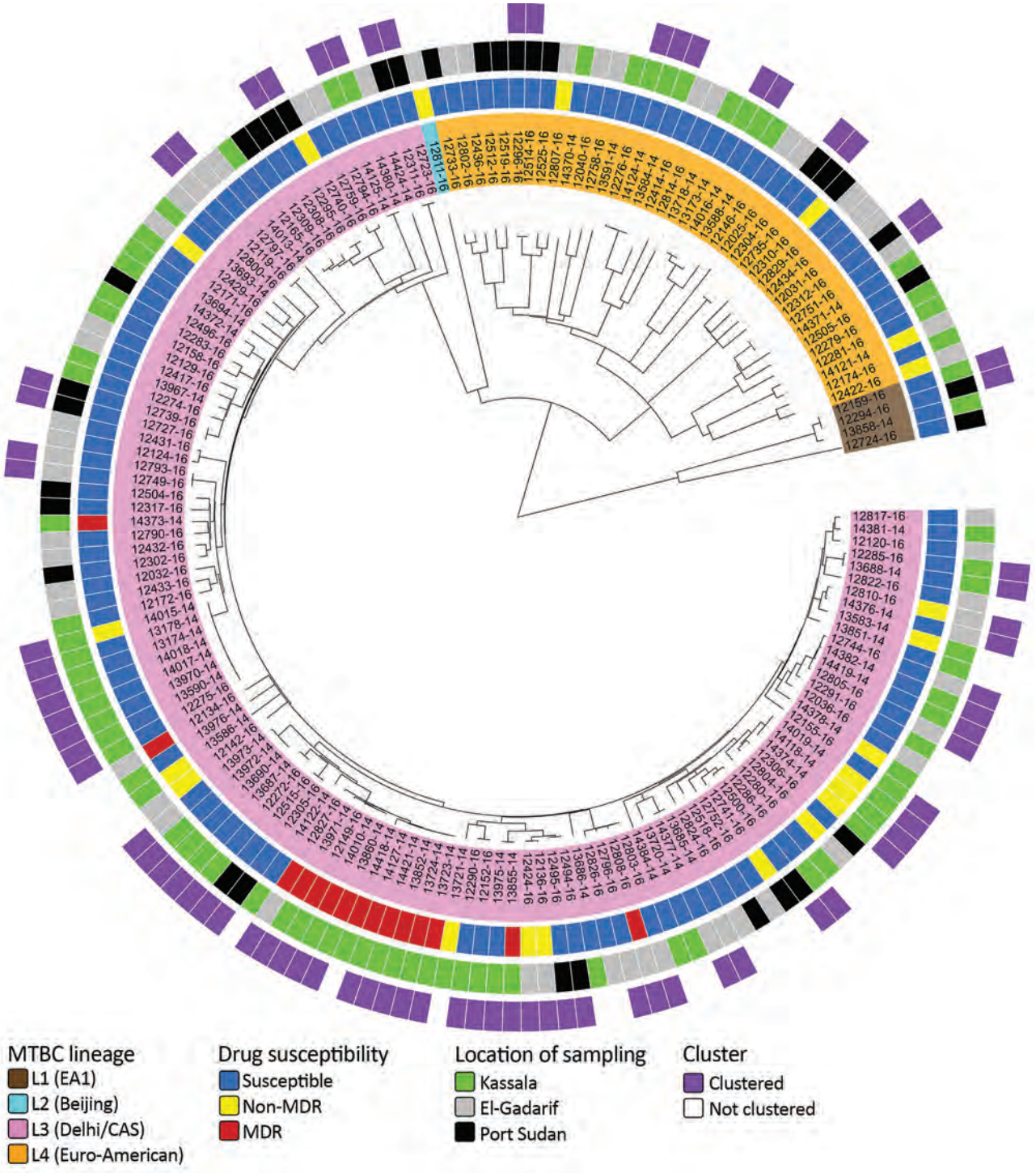

Figure 2. MTBC population structure in eastern Sudan. Maximum-likelihood tree based on 11,932 concatenated single-nucleotide polymorphisms (SNPs) using a general time-reversible substitution model. Colored bars code for (inner to outer ring) MTBC lineages (L1–4); genotypic DST results stratified to MDR, non-MDR, and pansusceptible; sampling location; and clustered and nonclustered strains (SNP distance ≤12). MDR, multidrug resistant; MTBC, *Mycobacterium tuberculosis* complex.

Table 3. Mutations conferring drug resistance among *Mycobacterium tuberculosis* complex genotypes identified in eastern Sudan, 2014 and 2016*

Genotype	No. (%) strains	No. (%) strains with mutations for drug					No. (%) mutations/genotype	No. (%) strains/genotype	
		SM	INH	RIF	EMB	PZA		Non-MDR	MDR
Delhi/CAS	122 (73.5)	28 (85.0)	17 (100)	17 (100)	12 (100)	1 (100)	75 (93.75)	16 (76.1)	15 (100)
EAI	4 (2.4)	0	0	0	0	0	0	0	0
LAM	5 (3.0)	0	0	0	0	0	0	0	0
Uganda	4 (2.4)	1 (3.0)	0	0	0	0	1 (1.25)	1 (4.8)	0
S-type	2 (1.2)	0	0	0	0	0	0	0	0
Haarlem	5 (3.0)	0	0	0	0	0	0	0	0
Sudan H37Rv-like	4 (2.4)	0	0	0	0	0	0	0	0
X-type	2 (1.2)	1 (3.0)	0	0	0	0	1 (1.25)	1 (4.8)	0
Cameroon	2 (1.2)	0	0	0	0	0	0	0	0
Euro-American	15 (9.0)	2 (6.0)	0	0	0	0	2 (2.5)	2 (9.5)	0
Beijing	1 (0.6)	1 (3.0)	0	0	0	0	1 (1.25)	1 (4.8)	0
Total	166 (100)	33 (100)	17 (100)	17 (100)	12 (100)	1 (100)	80 (100)	21 (100)	15 (100)

*CAS, Central Asian strain; EAI, East African Indian; EMB, ethambutol; INH, isoniazid; LAM, Latin American Mediterranean; MDR, multidrug-resistant; PZA, pyrazinamide; RIF, rifampin; SM, streptomycin.

caused by L3 strains. This finding is in line with previous studies that have been based on classical genotyping methods and reported rates of 40% or higher of the so-called Central Asia spoligotype family in central and eastern Sudan (*5*,*15*,*35*). Moreover, Couvin et al. (*36*) identified Sudan as an L3 hotspot in Africa. In this regard, it is intriguing to speculate whether L3 strains in general or certain subgroups have developed particular pathobiologic properties rendering them more virulent in East Africa host populations. Recently, Stucki et al. (*37*) hypothesized a concept of generalists and specialist among L4 strains based on the width of their geographic distribution. For L3 strains, larger studies are needed to reveal their global genetic diversity and geographic prevalence, which might inform about particular successful L3 subgroups and related causative variants in their genomes.

In addition to the general dominance of L3 strains in eastern Sudan, we found that all MDR TB cases were caused exclusively by L3 strains. Of major concern is that 10 of 15 MDR strains were part of 2 genetically related clusters isolated mainly from patients treated in 2014 in Kassala hospital. At first glance, this finding suggested nosocomial transmission. However, 2 strains of these clusters were isolated in 2016, including a strain from a patient treated in El-Gadarif hospital who had also acquired resistance to ethambutol and pyrazinamide. This patient was the first patient in our study cohort infected with a fully first-line drug-resistant strain, clearly emphasizing the importance of adopting focused TB control measures, including rapid detection and effective treatment of patients with MDR TB, to better contain transmission of MDR strains and prevent development of further drug resistances in the region. However, these measures are far from reality because proper TB diagnostics are virtually absent in eastern Sudan; other impeding factors are social stigma, lack of motivation, and poor awareness of TB treatment,

Table 4. Performance of genotypic drug resistance prediction to first-line tuberculosis drugs in *Mycobacterium tuberculosis* complex strains, eastern Sudan*

Drug	Resistant			Susceptible			Se, %† (95% CI)	Sp, %‡ (95% CI)	PPV, %§ (95% CI)	NPV, %¶ (95% CI)	Unknown mutations (%)
	gR (TP)	gS (FN)	gU (FN)	gR (FP)	gS (TN)	gU (TN)					
SM	24	0	9	0	133	0	72.7 (54.5–86.7)	100	100	93.7 (89.4–96.3)	9/166 (5.4)
INH	17	0	0	0	149	0	100	100	100	100	0/166 (0.0)
RIF	17	0	0	0	149	0	100	100	100	100	0/166 (0.0)
EMB	1	0	0	10*	155	0	100	93.9 (89.1–97.1)	9.10 (5.2–15.4)	100	0/166 (0.0)
PZA	1	0	0	0	165	0	100	100	100	100	0/166 (0.0)

*See MICs in the Methods section. EMB, ethambutol; FN, false negative; FP, false positive; gR, genetically resistant; gS, genetically susceptible; gU, genetic resistance unknown; INH, isoniazid; NPV, negative predictive value; PPV, positive predictive value; PZA, pyrazinamide; RIF, rifampin; Se, sensitivity; Sp, specificity; SM, streptomycin; TN, true negative; TP, true positive.
†Se = TP ÷ TP + FN.
‡Sp = TN ÷ TN + FP.
§PPV = TP ÷ (TP + FP).
¶NPV = TN ÷ (TN + FN).

with default rates of 14%–57% (*38*, *39*). This situation may even lead to a further aggravation of the drug resistance problem through selection of MDR clones with additional drug resistances in failing treatment regimens and further transmission of fully first-line resistant MDR strains (*14*,*39*). However, our WGS analysis revealed that MDR isolates did not exhibit mutations mediating resistances to second-line drugs (except for isoniazid/ETH cross resistance), leaving reasonable therapeutic options for patients in eastern Sudan with MDR TB.

Former studies in central and eastern Sudan reported drug resistances in 39%–67% and MDR in 6%–22% of the strains investigated (*4*–*10*). Those variations could possibly be attributed to dissimilarities in study design, sample size, and characteristics of study populations. In former studies, 53–235 samples from only new or new and retreatment TB cases with unknown HIV status or with a proportion of HIV-positive cases were investigated (*4*–*10*). Additionally, variations could also be linked to the laboratory technique used for pDST; for example, discordant results have been noticed between the BACTEC MGIT 960 and the proportion methods for streptomycin and ethambutol (*40*). In Sudan, only 1 study used the BACTEC MGIT 960; the remaining studies used the proportion method on Löwenstein–Jensen slants (*4*–*10*).

Considering the lack of pDST and the technical challenges associated with its implementation in Sudan, introduction of rapid molecular diagnostics to find patients with MDR TB is crucial for timely detection, treatment, and control. Moreover, rapid diagnostics will ultimately strengthen the national TB control program in Sudan. In line with previous studies, our data demonstrate an excellent performance of gDST for molecular resistance prediction (*16*,*17*,*41*). One example of the benefits of molecular assays is the correction of false ethambutol susceptibility results based on pDST in strains that harbor high-confidence *embB* resistance (*42*). Previous studies already revealed a low performance of ethambutol pDST, attributable mainly to the small difference between the wild-type and mutant MIC levels, leading to the effect that strains with canonical *embB* mutations show ethambutol MICs around the defined breakpoint of 5.0 μg/mL, resulting in a low reproducibility of phenotypic results (*24*,*25*,*42*). Therefore, classical Sanger sequencing of the *embB* codons 306, 354, and 406 was recently proposed to overrule phenotypic ethambutol susceptibility results in cases of presence of mutations in these codons (*42*). Furthermore, Cepheid GeneXpert and Hain MTBDR*plus* version 2.0 would have recognized all rifampin-resistant mediating mutations in our study setting and, therefore, offer a rapid solution for identification of patients with MDR/rifampin-resistant TB in eastern Sudan.

This multisite study was conducted in 3 public hospitals in eastern Sudan, comprising 10%–20% of the TB cases in the region during the study period; it thus represents a snapshot of the population diversity and transmission dynamics of MTBC strains in eastern Sudan. An additional strength of this study is that cultures, DSTs, and WGS were done in a World Health Organization–certified NRC in a high-resource setting in Germany, enabling maximum resolution for characterization of MTBC strains.

This study had ≥2 limitations. First, the prolonged transit time of patient-derived samples from Sudan to the NRC in Germany affected the viability of the MTBC bacteria; therefore, no mycobacterial growth was detected for some samples. Furthermore, the unavailability of clinical data, such as HIV status and treatment outcomes, prohibited further linking of bacteriological results to these clinical data.

In conclusion, L3 strains play a pivotal role in the epidemiology and transmission of TB, particularly MDR TB, in eastern Sudan. Transmission of MDR TB could possibly be an emerging concern for local TB departments and hospitals. Therefore, to contain MDR TB transmission, rapid molecular diagnostics, such as Cepheid GeneXpert or Hain MTBDR*plus* v2.0, are desirable in combination with focused tracing of contacts of patients with MDR TB. In addition, early onset of MDR TB therapy would be an ideal approach to reduce the number of secondary cases.

Acknowledgments

We thank all the patients with TB who participated in this study as well as the physicians, technicians, and the working staff at the outpatient departments of public hospitals and local TB laboratories in eastern Sudan and at the Research Center Borstel in Germany for their assistance. In particular, we are grateful to I. Razio, P. Vock, B. Schlüter, T. Ubben, J. Zallet, K. Ott, A.-K. Witt, D. Sievert, and V. Mohr for providing excellent technical assistance. The contribution of the Ministry of Health in Kassala, in El-Gadarif, and in Port Sudan, eastern Sudan, and the Research Center Borstel, Borstel, Germany, in accomplishing this work is appreciated.

Y.A.S. is a DAAD (Deutscher Akademischer Austauschdienst or the German Academic Exchange Service) stipend recipient, funding program no. 57076385. Parts of this

work have been supported by Deutsche Forschungsgemeinschaft (DFG, German Research Foundation) under Germany's Excellence Strategy EXC 22167-390884018, the Leibniz Science Campus EvoLUNG, and the German Center for Infection Research.

About the Author

Mr. Shuaib is a PhD student at the Research Center Borstel and Freie Universität Berlin in Germany and a teaching staff member at Sudan University of Science and Technology. He is interested in the epidemiology of infectious diseases, particularly zoonotic and transboundary animal diseases.

References

1. World Health Organization. Global tuberculosis report. 2019 Sep 26 [cited 2019 Oct 30]. https://apps.who.int/iris/bitstream/handle/10665/329368/9789241565714-eng.pdf
2. World Health Organization. Global tuberculosis report. 2012 Oct 17 [cited 2019 Mar 10]. https://www.who.int/tb/publications/global_report/gtbr12_main.pdf
3. Abdallah TM, Ali AA. Epidemiology of tuberculosis in eastern Sudan. Asian Pac J Trop Biomed. 2012;2:999–1001. https://doi.org/10.1016/S2221-1691(13)60013-1
4. Muna OA. Determination of the prevalence of tuberculosis with drug-resistant strains of *Mycobacterium tuberculosis* in Khartoum, Gazira and camps for displaced people, Sudan. Oslo: Faculty of Medicine, University of Oslo; 2002.
5. Sharaf Eldin GS, Fadl-Elmula I, Ali MS, Ali AB, Salih AL, Mallard K, et al. Tuberculosis in Sudan: a study of *Mycobacterium tuberculosis* strain genotype and susceptibility to anti-tuberculosis drugs. BMC Infect Dis. 2011;11:219. https://doi.org/10.1186/1471-2334-11-219
6. Hassan SO, Musa MT, Elsheikh HM, Eleragi AM, Saeed OK. Drug resistance in *Mycobacterium tuberculosis* isolates from northeastern Sudan. Br J Med Res. 2012;2:424–33. https://doi.org/10.9734/BJMMR/2012/1404
7. Abdul-Aziz AA, Elhassan MM, Abdulsalam SA, Mohammed EO, Hamid ME. Multi-drug resistance tuberculosis (MDR-TB) in Kassala state, eastern Sudan. Trop Doct. 2013;43:66–70. https://doi.org/10.1177/0049475513490421
8. Khalid FA, Hamid ZA, Mukhtar MM. Tuberculosis drug resistance isolates from pulmonary tuberculosis patients, Kassala state, Sudan. Int J Mycobacteriol. 2015;4:44–7. https://doi.org/10.1016/j.ijmyco.2014.11.064
9. Nour EMM, Saeed EMA, Zaki AZSA, Saeed NS. Drug resistance patterns of *Mycobacterium tuberculosis* isolates from patients with pulmonary tuberculosis in the Sudan. IOSR Journal of Dental and Medical Sciences. 2015;14:17–9. https://doi.org/10.9790/0853-14881719
10. Eldirdery MM, Intisar EA, Mona OA, Fatima AK, Asrar MA, Nuha YI, et al. Prevalence of multidrug-resistant tuberculosis among smear positive pulmonary tuberculosis patients in eastern Sudan. Am J Microbiol Res. 2017;5:32–6. https://doi.org/10.12691/ajmr-5-2-2
11. Auld SC, Kasmar AG, Dowdy DW, Mathema B, Gandhi NR, Churchyard GJ, et al. Research roadmap for tuberculosis transmission science: where do we go from here and how will we know when we're there? J Infect Dis. 2017;216(suppl_6):S662–8. https://doi.org/10.1093/infdis/jix353
12. Walker TM, Ip CL, Harrell RH, Evans JT, Kapatai G, Dedicoat MJ, et al. Whole-genome sequencing to delineate *Mycobacterium tuberculosis* outbreaks: a retrospective observational study. Lancet Infect Dis. 2013;13:137–46. https://doi.org/10.1016/S1473-3099(12)70277-3
13. Merker M, Kohl TA, Niemann S, Supply P. The evolution of strain typing in the *Mycobacterium tuberculosis* complex. Adv Exp Med Biol. 2017;1019:43–78. https://doi.org/10.1007/978-3-319-64371-7_3
14. Shuaib YA, Khalil EAG, Schaible UE, Wieler LH, Bakheit MAM, Mohamed-Noor SE, et al. Smear microscopy for diagnosis of pulmonary tuberculosis in eastern Sudan. Tuberc Res Treat. 2018;2018:8038137. https://doi.org/10.1155/2018/8038137
15. Khalid FA, Gasmelseed N, Hailu E, Eldirdery MM, Abebe M, Berg S, et al. Molecular identification of *Mycobacterium tuberculosis* causing pulmonary tuberculosis in Sudan. Eur Acad Res. 2016;4:7842–55.
16. Gröschel MI, Walker TM, van der Werf TS, Lange C, Niemann S, Merker M. Pathogen-based precision medicine for drug-resistant tuberculosis. PLoS Pathog. 2018; 14:e1007297. https://doi.org/10.1371/journal.ppat.1007297
17. Meehan CJ, Goig GA, Kohl TA, Verboven L, Dippenaar A, Ezewudo M, et al. Whole genome sequencing of *Mycobacterium tuberculosis*: current standards and open issues. Nat Rev Microbiol. 2019;17:533–45. https://doi.org/10.1038/s41579-019-0214-5
18. Siddiqi S, Rüsch-Gerdes S. MGIT TM Procedure Manual. Geneva: Foundation for Innovative New Diagnostics (FIND); 2006.
19. Deutsches Institut für Normung. Medical microbiology—diagnosis of tuberculosis. Part 3: detection of mycobacteria by culture methods. Berlin: The Institute; 2011.
20. Somerville W, Thibert L, Schwartzman K, Behr MA. Extraction of *Mycobacterium tuberculosis* DNA: a question of containment. J Clin Microbiol. 2005;43:2996–7. https://doi.org/10.1128/JCM.43.6.2996-2997.2005
21. Hillemann D, Warren R, Kubica T, Rüsch-Gerdes S, Niemann S. Rapid detection of *Mycobacterium tuberculosis* Beijing genotype strains by real-time PCR. J Clin Microbiol. 2006;44:302–6. https://doi.org/10.1128/JCM.44.2.302-306.2006
22. Richter E, Niemann S, Gloeckner FO, Pfyffer GE, Rüsch-Gerdes S. *Mycobacterium holsaticum* sp. *nov*. Int J Syst Evol Microbiol. 2002;52:1991–6.
23. Rüsch-Gerdes S, Pfyffer GE, Casal M, Chadwick M, Siddiqi S. Multicenter laboratory validation of the BACTEC MGIT 960 technique for testing susceptibilities of *Mycobacterium tuberculosis* to classical second-line drugs and newer antimicrobials. J Clin Microbiol. 2006;44:688–92. https://doi.org/10.1128/JCM.44.3.688-692.2006
24. Ängeby K, Juréen P, Kahlmeter G, Hoffner SE, Schön T. Challenging a dogma: antimicrobial susceptibility testing breakpoints for *Mycobacterium tuberculosis*. Bull World Health Organ. 2012;90:693–8. https://doi.org/10.2471/BLT.11.096644
25. Heyckendorf J, Andres S, Köser CU, Olaru ID, Schön T, Sturegård E, et al. What is resistance? Impact of phenotypic versus molecular drug resistance testing on therapy for multi- and extensively drug-resistant tuberculosis. Antimicrob Agents Chemother. 2018;62:e01550–17. https://doi.org/doi: 10.1128/AAC.01550-17
26. Merker M, Barbier M, Cox H, Rasigade JP, Feuerriegel S, Kohl TA, et al. Compensatory evolution drives multidrug-resistant tuberculosis in Central Asia. eLife. 2018;7:e38200. https://doi.org/10.7554/eLife.38200

27. Kohl TA, Utpatel C, Schleusener V, De Filippo MR, Beckert P, Cirillo DM, et al. MTBseq: a comprehensive pipeline for whole genome sequence analysis of *Mycobacterium tuberculosis* complex isolates. PeerJ. 2018; 6:e5895. https://doi.org/10.7717/peerj.5895
28. Price MN, Dehal PS, Arkin AP. FastTree 2—approximately maximum-likelihood trees for large alignments. PLoS One. 2010;5:e9490. https://doi.org/10.1371/journal.pone.0009490
29. He Z, Zhang H, Gao S, Lercher MJ, Chen WH, Hu S. Evolview v2: an online visualization and management tool for customized and annotated phylogenetic trees. Nucleic Acids Res. 2016;44:W236–41. https://doi.org/10.1093/nar/gkw370
30. Kannan L, Wheeler WC. Maximum parsimony on phylogenetic networks. Algorithms Mol Biol. 2012;7:9. https://doi.org/10.1186/1748-7188-7-9
31. Feuerriegel S, Schleusener V, Beckert P, Kohl TA, Miotto P, Cirillo DM, et al. PhyResSE: a Web tool delineating *Mycobacterium tuberculosis* antibiotic resistance and lineage from whole-genome sequencing data. J Clin Microbiol. 2015;53:1908–14. https://doi.org/10.1128/JCM.00025-15
32. Kim HY. Statistical notes for clinical researchers: chi-squared test and Fisher's exact test. Restor Dent Endod. 2017; 42:152–5. https://doi.org/10.5395/rde.2017.42.2.152
33. Coll F, McNerney R, Guerra-Assunção JA, Glynn JR, Perdigão J, Viveiros M, et al. A robust SNP barcode for typing *Mycobacterium tuberculosis* complex strains. Nat Commun. 2014;5:4812. https://doi.org/10.1038/ncomms5812
34. Meehan CJ, Moris P, Kohl TA, Pečerska J, Akter S, Merker M, et al. The relationship between transmission time and clustering methods in *Mycobacterium tuberculosis* epidemiology. EBioMedicine. 2018;37:410–6. https://doi.org/10.1016/j.ebiom.2018.10.013
35. Eldirdery MM, Alrayah IE, ElkareIm MOA, Khalid FA, Elegail AMA, Ibrahim NY, et al. Genotyping of pulmonary *Mycobacterium tuberculosis* isolates from Sudan using spoligotyping. Am J Microbiol Res. 2015;3:125–8.
36. Couvin D, Reynaud Y, Rastogi N. Two tales: worldwide distribution of Central Asian (CAS) versus ancestral East-African Indian (EAI) lineages of *Mycobacterium tuberculosis* underlines a remarkable cleavage for phylogeographical, epidemiological and demographical characteristics. PLoS One. 2019;14:e0219706. https://doi.org/10.1371/journal.pone.0219706
37. Stucki D, Brites D, Jeljeli L, Coscolla M, Liu Q, Trauner A, et al. *Mycobacterium tuberculosis* lineage 4 comprises globally distributed and geographically restricted sublineages. Nat Genet. 2016;48:1535–43. https://doi.org/10.1038/ng.3704
38. Abu Shanab ME. Defaulting to anti-tuberculosis treatment: proportional and associated factors among internally displaced people around Khartoum state. Khartoum (Sudan): Faculty of Public and Environmental Health, University of Khartoum; 2003.
39. Ali AO, Prins MH. Patient non adherence to tuberculosis treatment in Sudan: socio demographic factors influencing non adherence to tuberculosis therapy in Khartoum state. Pan Afr Med J. 2016;25:80. https://doi.org/10.11604/pamj.2016.25.80.9447
40. Giampaglia CM, Martins MC, Vieira GB, Vinhas SA, Telles MA, Palaci M, et al. Multicentre evaluation of an automated BACTEC 960 system for susceptibility testing of *Mycobacterium tuberculosis.* Int J Tuberc Lung Dis. 2007;11:986–91.
41. CRyPTIC Consortium and the 100,000 Genomes Project. Prediction of susceptibility to first-line tuberculosis drugs by DNA sequencing. N Engl J Med. 2018;379:1403–15. https://doi.org/10.1056/NEJMoa1800474
42. Andres S, Gröschel MI, Hillemann D, Merker M, Niemann S, Kranzer K. A diagnostic algorithm to investigate pyrazinamide and ethambutol resistance in rifampin-resistant *Mycobacterium tuberculosis* isolates in a low-incidence setting. Antimicrob Agents Chemother. 2019;63:e01798–18. https://doi.org/10.1128/AAC.01798-18

Address for correspondence: Yassir A. Shuaib or Matthias Merker, Research Center Borstel, Parkallee 1-40, 23845 Borstel, Germany; email: vet.aboamar@gmail.com or mmerker@fz-borstel.de

Norovirus Outbreak Surveillance, China, 2016–2018

Miao Jin,[1] Shuyu Wu,[1] Xiangyu Kong, Huaping Xie, Jianguang Fu, Yaqing He, Weihong Feng, Na Liu, Jingxin Li, Jeanette J. Rainey, Aron J. Hall, Jan Vinjé, Zhaojun Duan

CaliciNet China, a network of provincial, county, and city laboratories coordinated by the Chinese Centers for Disease Control and Prevention, was launched in October 2016 to monitor the epidemiology and genotype distribution of norovirus outbreaks in China. During October 2016–September 2018, a total of 556 norovirus outbreaks were reported, and positive fecal samples from 470 (84.5%) outbreaks were genotyped. Most of these outbreaks were associated with person-to-person transmission (95.1%), occurred in childcare centers or schools (78.2%), and were reported during November–March of each year (63.5%). During the 2-year study period, 81.2% of all norovirus outbreaks were typed as GII.2[P16]. In China, most norovirus outbreaks are reported by childcare centers or schools; GII.2[P16] is the predominant genotype. Ongoing surveillance by CaliciNet China will provide information about the evolving norovirus genotype distribution and outbreak characteristics important for the development of effective interventions, including vaccines.

Human noroviruses are the leading cause of outbreaks of acute gastroenteritis, associated with ≈50% of all outbreaks worldwide (*1*). Norovirus outbreaks are frequently reported in semiclosed institutions, such as hospitals, nursing homes, schools, and childcare centers (*2*). The virus is primarily transmitted directly from person to person or indirectly through contaminated surfaces, food, or water (*1*). The relative stability of noroviruses on environmental surfaces makes infection control challenging (*3*). Several candidate norovirus vaccines are in clinical trials (*4*).

Noroviruses are single-stranded RNA viruses that belong to the genus *Norovirus*, family *Caliciviridae*. The genome is organized into 3 open reading frames (ORFs): ORF1 encodes polyprotein, ORF2 encodes the major capsid protein (VP1), and ORF3 encodes the minor (VP2) capsid protein. The viruses are classified into at least 7 genogroups (G), of which viruses from GI, GII, and GIV infect humans (*5*,*6*). On the basis of the diversity of VP1, these genogroups can be further divided into at least 33 genotypes: 9 GI, 22 GII, and 2 GIV (*7*). In addition, on the basis of the diversity of the polymerase region of ORF1, >14 GI polymerase (GI.P) types and 27 GII.P types have been described (*7*). Because of the frequent recombination at the ORF1/ORF2 junction region, a dual-typing system has been proposed for GI and GII noroviruses (*7*). Since 2002, genogroup II, genotype 4 (GII.4), noroviruses have been associated with most norovirus outbreaks globally, and new GII.4 variants have emerged every 2–3 years (*8*). Monitoring the trends in the distribution of the various genotypes and possible association of certain strains with a more severe disease outcome is important for understanding and controlling norovirus epidemics (*9*).

Several norovirus outbreak surveillance networks, including NoroNet (*10*) and CaliciNet (*7*,*11*), have been developed during the past decade. NoroNet captures molecular and epidemiologic data on norovirus outbreaks and sporadic cases submitted by 19 participating countries across Europe and Asia and by Australia. CaliciNet is a norovirus outbreak surveillance network in the United States in which state and local public health laboratories electronically submit laboratory data, including sequences from norovirus outbreaks, to a central database (https://www.cdc.gov/norovirus/reporting/calicinet/data.html). CaliciNet data are integrated with epidemiologic data

Author affiliations: Chinese Center for Disease Control and Prevention, Beijing, China (M. Jin, X. Kong, N. Liu, J. Li, Z. Duan); US Centers for Disease Control and Prevention, Beijing (S. Wu, J.J. Rainey); Guangzhou Center for Disease Control and Prevention, Guangzhou, China (H. Xie); Jiangsu Provincial Center for Disease Control and Prevention, Nanjing, China (J. Fu); Shenzhen Center for Disease Control and Prevention, Shenzhen, China (Y. He); Wuxi Center for Disease Control and Prevention, Wuxi, China (W. Feng); US Centers for Disease Control and Prevention, Atlanta, Georgia, USA (A.J. Hall, J. Vinjé)

DOI: https://doi.org/10.3201/eid2603.191183

[1]These authors contributed equally to this article.

from the National Outbreak Reporting System, yielding comprehensive surveillance in the United States that enables multifactorial characterization of norovirus outbreaks (*9*).

Since 2004, provincial and local Centers for Disease Control and Prevention (CDCs) in China have been required to report all acute gastroenteritis outbreaks of ≥20 cases, including those caused by noroviruses, to a passive national outbreak surveillance system called Public Health Emergency Event Surveillance System (PHEESS) (*12*). Although PHEESS provides useful information, detailed epidemiologic and molecular data from norovirus outbreaks are typically not included. In October 2016, the National Institute for Viral Disease Control and Prevention at the China CDC launched CaliciNet China as a surveillance network to monitor the epidemiology and molecular characteristics of norovirus outbreaks. We describe this new network and report data from the first 2 years of surveillance.

Materials and Methods

CaliciNet China

For the surveillance of norovirus outbreaks, CaliciNet China relies on contributions from laboratory and epidemiologic staff at county, city, and provincial CDCs. County CDCs are responsible for acute gastroenteritis outbreak investigations and collection of clinical specimens. Laboratories of city and provincial CDCs perform norovirus detection and genotyping on the specimens. The national laboratory at China CDC receives and aggregates findings and provides overall quality control. Laboratory staff at these CDCs received training on using the standardized methods of norovirus detection and typing (*7*). Each laboratory performs proficiency testing once a year for quality assurance.

Outbreak Reporting

CaliciNet China defines norovirus outbreaks as ≥5 acute gastroenteritis cases within 3 days after exposure in a common setting where >2 samples (whole fecal, rectal swab, or vomitus) had been laboratory confirmed as norovirus. Acute gastroenteritis was defined as >3 events involving loose feces, vomiting, or both within a 24-hour period. The data were collected in collaboration with the local epidemiologists investigating the outbreaks using national guidelines (*13*). Local CDCs aggregated epidemiologic data for each outbreak, including date of first illness onset, setting, transmission route, number of cases, and type of specimens collected. All data were entered into Microsoft Excel (Microsoft, https://www.microsoft.com). City, county, and provincial CDCs also submitted laboratory results from real-time reverse transcription PCR (rRT-PCR), conventional RT-PCR, and sequences into a BioNumerics version 6.6 database (Applied Maths, https://www.applied-maths.com) using CaliciNet scripts provided by CaliciNet USA (*7*). Each month, data were sent electronically to China CDC.

rRT-PCR and Genotyping

For fecal samples, laboratories prepared a 10% fecal suspension by mixing 0.1 g feces with 1.0 mL phosphate-buffered saline (pH 7.2). For swab or vomitus samples, nucleic acid was extracted directly. Laboratories tested viral RNA for GI and GII norovirus using the Ag-Path kit (Applied Biosystems, https://www.fishersci.com) (*7*,*14*) in a duplex rRT-PCR with primers (Cog1F, Cog1R, Cog2F, and Cog2R) (*11*) and TaqMan probe (Ring 1E and Ring 2) (*14*,*15*). The cycling conditions were described previously (*7*). Some laboratories also used commercial norovirus rRT-PCR kits (BioPerfectus Technology Co., http://www.s-sbio.net; Da An GENE Co., http://en.daangene.com). Norovirus-positive samples were then amplified by conventional RT-PCR, which amplifies a partial region of ORF1 and a partial region of ORF2 (*7*,*16*). The RT-PCR conditions and the primers used (MON432, G1SKR, MON431, and G2SKR) have been described previously (*7*,*16*).

Data Management and Analysis

We merged epidemiologic and genotype outbreak data at China CDC and then imported them into SPSS Statistics 25 software (IBM, https://www.ibm.com) for data cleaning and analysis. We generated descriptive statistics on reported outbreaks by setting, transmission route, outbreak size, and province and examined differences between genotypes and mode of transmission, outbreak size, setting, and season using χ^2 tests. We used an α value of $p<0.05$ to assess statistical significance. Genotypes were assigned by phylogenetic analysis using the UPGMA method with reference sequences used by CaliciNet for capsid typing.

Ethics Review

The China CDC Ethical Review Committee approved CaliciNet China as routine surveillance for norovirus. Because CaliciNet China collects only aggregate data on norovirus outbreaks, we did not analyze any personal identifying information as part of this project. Linkage of specimens to patient name was maintained by provincial-level CDCs and not submitted into the CaliciNet China database.

Results

Epidemiologic Characteristics of Norovirus Outbreaks

In 2016, CaliciNet China started with 9 laboratories in 3 provinces (Beijing, Guangdong, and Jiangsu) and by 2018 increased to 17 laboratories in 6 provinces (adding Shanghai, Hunan, and Liaoning) distributed across eastern, central, and western China (Figure 1). During October 2016–September 2018, a total of 556 norovirus outbreaks were reported to CaliciNet China. Of these, 320 (57.6%) were reported from Guangdong Province, 101 (18.2%) from Jiangsu Province, 79 (14.2%) from Beijing, 38 (6.8%) from Hunan Province, 12 (2.2%) from Liaoning Province, and 6 (1.1%) from Shanghai. Most outbreaks occurred during the winter season (November–March) (Figure 2). Information about the outbreak size was reported for 427 (76.7%) outbreaks, among which the median size was 15 persons (interquartile range 12–81.5) per outbreak. Five outbreaks each had >200 cases. Three of those occurred in universities and 2 in vocational schools; 4 were caused by person-to person transmission and 1 by foodborne transmission (Table 1). Of the 556 outbreaks, 280 (50.4%) occurred in childcare centers; 155 (27.9%) occurred in primary schools, 61 (11.0%) in middle schools, and 24 (4.3%) in universities (Appendix Table, https://wwwnc.cdc.gov/EID/article/26/3/19-1183-App1.pdf). Of 452 (81.3%) outbreaks in which transmission mode was identified, person-to-person transmission predominated (430 [95.1%]), followed by foodborne transmission (13 [2.9%]) and waterborne transmission (6 [1.3%]) (Table 2).

Genotypes

We obtained genotype information for 470 (84.5%) of the 556 outbreaks. Of the 86 (15.5%) outbreaks with no genotyping results, 72 were not further genotyped by network laboratories and 14 were positive by rRT-PCR but negative by conventional RT-PCR and thus could not be genotyped. Of the typed outbreaks, 430 (91.5%) were GII, 26 (5.5%) were GI, and 14 (2.5%) comprised both GI- and GII-positive samples. Overall, 5 GI genotypes and 12 GII genotypes were detected (Appendix Table). Of 470 genotyped outbreaks, GI genotypes included GI.2[P2] (11 [2.3%]), GI.6[P11] (6 [1.3%]), and GI.3[P13] (5 [1.1%]). Among

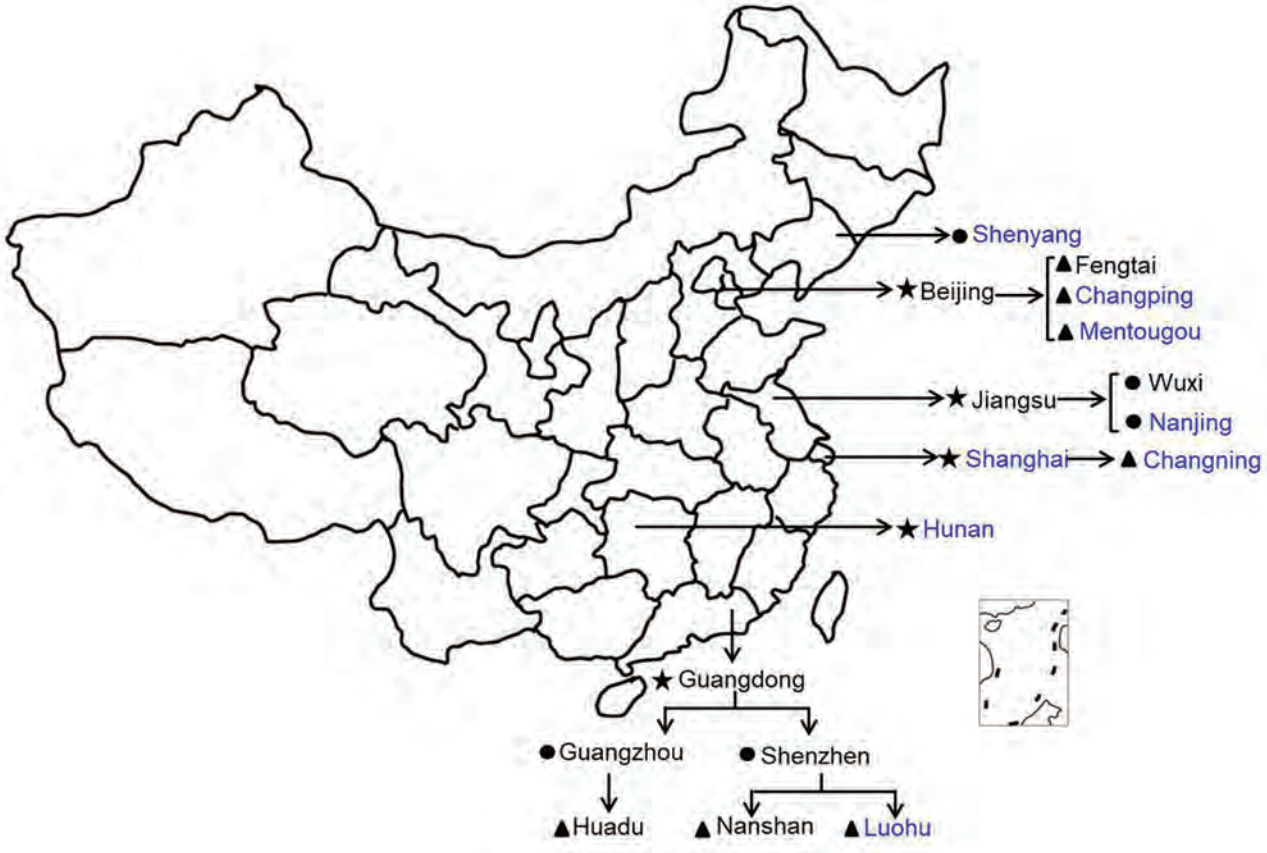

Figure 1. Geographic location of participating local Centers for Disease Control and Prevention in CaliciNet China, October 2016–September 2018. Star indicates provincial/municipality laboratories; circle, city laboratories; triangle, district/county laboratories. Laboratories that participated in CaliciNet China: black, April 2016; blue, April 2017.

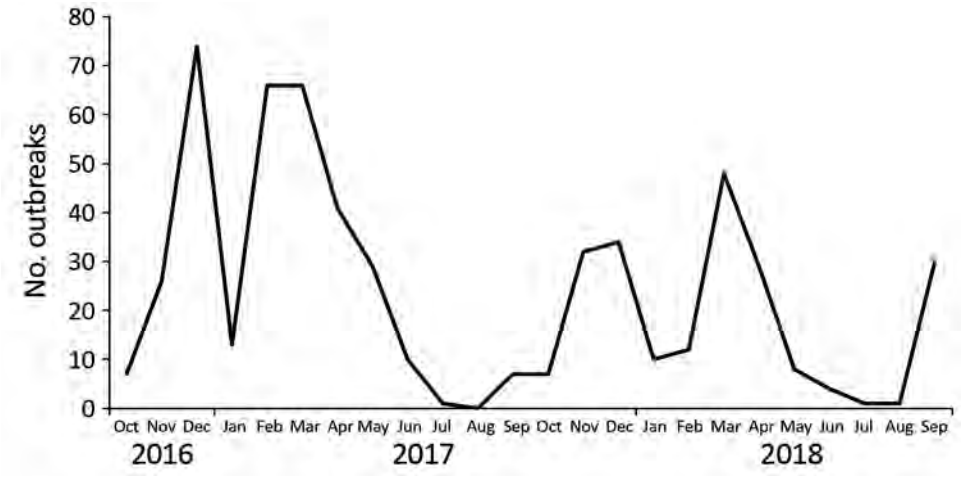

Figure 2. Monthly distribution of norovirus outbreaks reported to CaliciNet China, October 2016–September 2018.

GII outbreaks, 349 (74.3%) were typed as GII.2[P16], which was detected throughout the study period and peaked during winter 2016–17 (Figure 3). Other GII genotypes were GII.3[P12] (25 [5.3%]), GII.17[P17] (18 [3.8%]), GII.6[P7] (16 [3.4%]), and GII.4 Sydney[P31] (11 [2.3%]) (Appendix Table). Genotypes detected in <1% of the outbreaks were GI.1[P1], GI.3[P13], GI.3[P13], GI.5[P12], and GI.6[P11] among GI viruses and GII.1[P33], GII.2[P2], GII.8[P8], GII.13[P21], GII.14[P7], GIX.1[P15], and GII.17[P31] among GII viruses. In the GII.2[P16] epidemic during winter 2016–17, GI viruses were rarely detected (1 [0.3%] of 298), whereas during the following seasons (2017–2018), GI viruses were detected in 24 (13.9%) of 172 outbreaks and peaked in March 2018 (10 [40.0%] of 25). Outbreaks caused by multiple genotypes were mainly detected in March 2018 (9 [64.3%] of 14); GII.17[P17] viruses were mainly detected during January–April 2018 (9 [64.3%] of 14); and GII.6[P7] viruses were detected primarily in the 2017–18 winter season (13 [81.3%] of 16).

Table 1. Genotype of cases in 556 norovirus outbreaks reported to CaliciNet China, October 2016–September 2018

Genotype	No. outbreaks with known size	No. cases or range	Median no. cases
GII.1[P33]	1	43	43
GII.2[P2]	1	15	15
GII.2[P16]	262	3–236	18
GII.3[P12]	21	3–72	7
GII.4 Sydney[P31]	7	3–50	43
GII.6[P7]	12	4–72	12
GII.8[P8]	2	11–13	12
GII.13[P21]	1	14	14
GII.14[P7]	0	0	0
GIX.1[P15]	1	17	17
GII.17[P17]	14	3–360	33
GII.17[P31]	2	6	6
GII untypeable	11	7–115	15
GI.1[P1]	0	0	0
GI.2[P2]	11	5–122	31
GI.3[P13]	5	5–72	16
GI.5[P12]	1	5	5
GI.6[P11]	5	6–117	30
Multiple genotypes	11	5–348	60
Not determined*	59	3–106	10
Total	427	3–360	15

*The genotyping reverse transcription PCR for these outbreaks was not conducted by network laboratories.

Genotypes Associated with Epidemiologic Characteristics

Among the GII.2[P16] outbreaks, foodborne transmission was reported for 10 (3.6%) of 276 and person-to-person transmission for 266 (96.4%) of 276; no waterborne outbreaks were reported (χ^2 10.5; p = 0.003) (Table 3). Outbreaks with multiple genotypes were more often associated with waterborne and foodborne transmission than were outbreaks with a single genotype.

GII.2[P16] outbreaks predominated across all childcare centers and school settings (Appendix Table). GII.3[P12] outbreaks occurred in childcare centers (19 [6.8%] of 280), primary schools (3 [1.9%] of 155), and middle schools (1 [1.6%] of 61). GII.17[P17] outbreaks occurred in universities (2 [8.3%] of 24), middle schools (4 [6.6%] of 61), primary schools (7 [4.5%] of 155), and childcare centers (2 [0.7%] of 280). GI.2[P2] outbreaks were most commonly detected in middle schools (5 [8.2%] of /61) (χ^2 12.907; p = 0.002) (Appendix Table). Of the 14 outbreaks with samples containing multiple genotypes, 4 occurred in universities, 6 in middle schools, 1 in a primary school, and 3 in childcare centers (Appendix Table).

Discussion

CaliciNet China was launched in October 2016 for the surveillance of norovirus outbreaks in China. By using more sensitive inclusion criteria for reporting

Table 2. Number of norovirus outbreaks reported to CaliciNet China for each transmission route and outbreak setting, October 2016–September 2018

Setting	Person-to-person	Foodborne	Waterborne	Unknown	Total
Childcare center	227	2	0	51	280
Primary school	121	3	0	31	155
Middle school	40	3	5	13	61
University	15	3	1	5	24
Company	7	1	0	1	9
Restaurant	2	0	0	2	4
Hospital	3	0	0	0	3
Hotel	1	0	0	1	2
Party	0	0	0	1	1
Multiple school types*	14	1	0	1	16
Unknown	0	0	0	1	1
Total	430	13	6	107	556

*Fifteen outbreaks occurred in schools that combine primary school and middle school, and 1 outbreak occurred in a school that combines a childcare center, a primary school, and a middle school.

acute gastroenteritis outbreaks than PHEESS, CaliciNet China captured more norovirus outbreaks, especially in the catchment area where the network laboratories are located. In addition, the participating laboratories implemented standardized genotyping protocols, which enabled comparison across jurisdictions of norovirus sequences, including emerging strains. The sequence data are accessible only within CaliciNet China.

As found in studies in other countries in the Northern Hemisphere, we found the number of norovirus outbreaks was highest during October–March (*17*,*18*). Person-to-person transmission was the dominant route (95.1%), even higher than has been reported in other countries (*11*,*19*). Almost all (93.7%) outbreaks in our study occurred in childcare centers and schools (primary schools, middle schools, and universities). These outbreak settings have likewise been identified in other Asia countries, such as Japan and South Korea (*18*,*20*), as the most common settings for norovirus outbreaks. In contrast, in the United States and Europe, healthcare facilities (primarily nursing homes and hospitals) are the most commonly reported setting for norovirus outbreaks (*11*,*21*,*22*). The high proportion of norovirus outbreaks in childcare centers and schools seems unique to China and might be associated with the high population density in these settings (*23*) and the enhanced monitoring and reporting of any outbreaks in schools in China. In 2006, the national government started to require school officials to check and screen children attending kindergarten, primary school, and middle schools each morning for fever, vomiting, or diarrhea (*24*). This program has helped facilitate the detection and reporting of infectious diseases, including norovirus, at kindergartens and schools. However, we received few norovirus outbreak reports from other settings involving more adults and elderly persons (such as companies, restaurants, and nursing homes). This difference in the collection of norovirus outbreaks between school and other settings may cause potential bias of the strain patterns of norovirus.

Previous data from CaliciNet and NoroNet have suggested a correlation of certain genotypes with

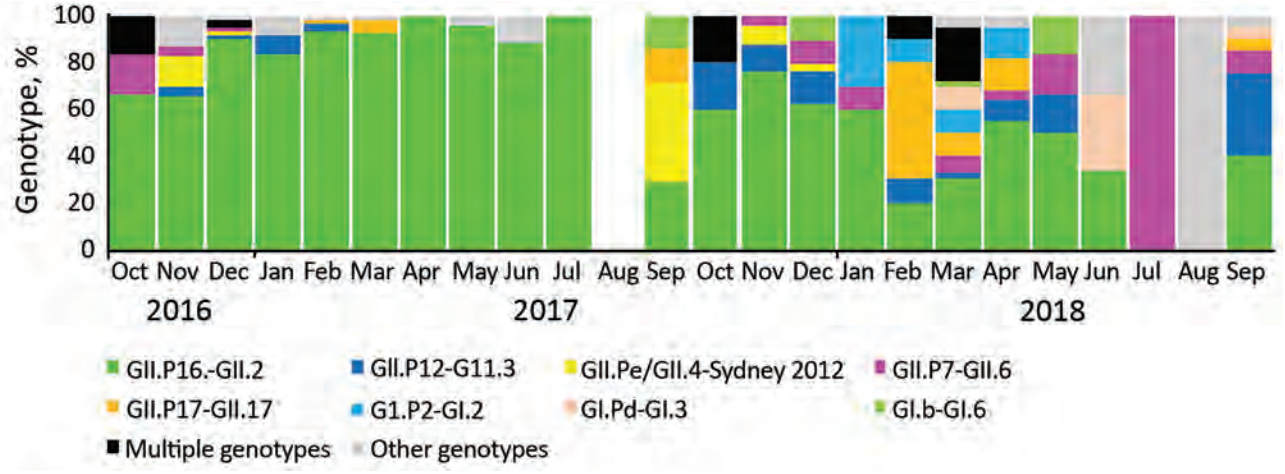

Figure 3. Genotype distribution of 470 norovirus outbreaks reported to CaliciNet China, October 2016–September 2018. No outbreaks were reported in August 2017.

Table 3. Transmission routes of genotypes in norovirus outbreaks reported to CaliciNet China, October 2016–September 2018

Genotype	Person-to-person	Foodborne	Waterborne	Unknown	Total
GII.1[P33]	1	0	0	0	1
GII.2[P16]	266	10	0	73	349
GII.2[P2]	1	0	0	1	2
GII.3[P12]	20	0	0	5	25
GII.4 Sydney[P31]	6	0	0	4	10
GII.Pe-GII.4	1	0	0	0	1
GII.6[P7]	11	1	0	4	16
GII.8[P8]	2	0	0	0	2
GII.13[P21]	1	0	0	0	1
GII.14[P7]	0	0	0	1	1
GIX.1[P15]	1	0	0	1	2
GII.17[P17]	13	0	0	5	18
GII.17[P31]	2	0	0	0	2
GII untypeable	14	0	0	0	14
GI.1[P1]	1	0	0	0	1
GI.2[P2]	10	0	0	1	11
GI.3[P13]	4	0	1	1	6
GI.5[P12]	2	0	0	0	2
GI.6[P11]	5	0	0	1	6
Multiple	6[a]	1	5	2	14
Unknown	63	1	0	8	72
Total	430	13	6	107	556

different transmission modes and outbreak settings. Specifically, GII.4 viruses have been associated with person-to-person transmission, whereas non-GII.4 viruses, such as GI.3, GI.6, GI.7, GII.3, GII.6, and GII.12, are more often associated with foodborne transmission (*25*). Other studies reported that GI genotypes more frequently caused waterborne transmission than GII genotypes (*26*). In our study, all outbreaks caused by GII.4 Sydney[P31] were transmitted from person to person; however, GII.2[P16] viruses predominated among both person-to-person and foodborne outbreaks. A recent study also reported that GII.2 outbreaks were transmitted from person to person (77.8%) and food (17.5%) (*27*). The outbreaks caused by multiple genotypes were more often associated with waterborne transmission than foodborne or person-to-person transmission.

The dominant genotype in our study, GII.2[P16], was mainly associated with outbreaks in childcare centers and schools, consistent with a study in Japan, which found GII.2 was the most prevalent genotype in childcare facilities and schools for multiple years (*28*). In other parts of the world, GII.4 viruses have been reported as the dominant genotype among adults and elderly persons, especially in outbreaks in long-term care facilities (*29*,*30*). Our study had only 11 GII.4 outbreaks, and they mainly occurred in childcare centers and primary schools. GII.3[P12] mainly occurred among children in this study, similar to other studies where GII.3 was one of the most common genotypes associated with sporadic norovirus infection, particularly among children (*29*,*31*–*34*). We also found that GII.17 outbreaks tended to infect older children and adults rather than younger children. Previous reports indicated that the median age of persons infected by GII.17 (49, range 9–75 years) was significantly higher than that of GII.4 cases (1, range 1–8 years) (*35*).

During winter 2014–15, GII.17 was reported as the predominant norovirus strain in China, accounting for 67.2% of outbreaks, whereas during the following winter (2015–16), the proportion of GII.17 outbreaks decreased to 25.0% (*36*). We found that GII.2[P16] viruses caused an increase in the number of norovirus outbreaks during winter 2016–17. The first GII.2[P16]–positive sample was detected in August 2016 in Guangdong Province (*36*,*37*), and the number subsequently increased, with GII.2[P16] accounting for 70%–100% of norovirus outbreaks during winter 2016–17 in different provinces (*38*–*40*). Previous studies suggested that reemerging GII.2[P16] virus most likely evolved from strains emerging during 2012–2013 (*41*). Although the antigenicity and histo-blood group antigen binding profile of the early 2016–2017 and pre-2016 GII.2 noroviruses were similar, 1 GII.2[P16] strain with single Val256Ile mutation and the conventionally orientated Asp382 in VP1 showed an expanded histo-blood group antigen binding spectrum in China (*41*). Unlike previously emergent GII.4 viruses, GII.2[P16] did not become a globally predominant genotype; however, this emerging virus was also detected in other countries, such as Germany, Italy, Japan, France, and the United States (*42*–*44*).

Since 2002, GII.4 has been the predominant norovirus genotype in outbreaks in many countries, and every 2–4 years, new GII.4 variants have emerged, displacing previous variants, several of which have

been associated with increased norovirus outbreaks worldwide (*8*). Previous studies indicated that global epidemics, including in China, were caused by GII.4 Den Haag (2006b) variant in 2006–2007, New Orleans variant in 2009–2010, and GII.4 Sydney variant in 2012–2013. Although GII.4 Sydney has predominated globally, non-GII.4 strains (GII.17[P17] and GII.2[P16]) have caused 2 recent norovirus epidemics in China (*36*,*45*). These observations highlight the need for enhanced global surveillance for potential epidemics of emerging norovirus genotypes, which may have different regional impacts.

CaliciNet China uses database scripts provided by CaliciNet USA (*16*) and updated detection and dual genotyping protocols (*14*). The dual-typing method is helpful in clarifying the molecular epidemiology of noroviruses, including the identification of newly emerging recombinant viruses. For example, GII.4 Sydney[P31] predominated since it was first recognized in 2012 and subsequently became one of the most successful genotypes causing epidemics globally (*8*). In November 2015, this virus was gradually, although not completely, replaced by a new recombinant GII.4 virus, GII.P16-GII.4 Sydney (*7*), and has since caused ≈50% of all norovirus outbreaks in the United States (https://www.cdc.gov/norovirus/reporting/calicinet/data.html).

Our study has several limitations. First, participation in the network was voluntary, so the distribution of the network does not represent the entire country. Currently, network laboratories are located primarily in eastern and southern China, which generally have better infrastructure. Second, the epidemiologic information for each outbreak collected by CaliciNet China is still limited; however, China CDC is making efforts to include more epidemiologic staff in the network and collect more complete and accurate epidemiologic data. Third, the timeliness of the data reporting in CaliciNet needs to be improved. For a variety of reasons, not all network laboratories were able to submit data to China CDC on a monthly basis. In the future, submission of epidemiologic and laboratory data through a Web-based information system will enable uploading of data in near real time.

CaliciNet China's use of the same protocols as other norovirus surveillance networks, such as CaliciNet USA, enables comparison of data internationally and potentially provides an early warning when new strains emerge that have the potential to cause global epidemics. In addition, monitoring changes in the distribution of genotypes can help inform the development and assessment of norovirus vaccines, several of which are in clinical trials (*46*,*47*).

In conclusion, we collected information about 556 norovirus outbreaks using standardized epidemiologic definitions and laboratory testing procedures in 6 provinces in China. Person-to-person was the predominant transmission route, and childcare centers and schools were the most common settings for reported norovirus outbreaks. The large number of outbreaks during winter 2016–17 was attributable at least in part to the emergence of the new recombinant genotype GII.2[P16]. CaliciNet China provides essential information about the evolving strain distribution and epidemiologic characteristics of norovirus outbreaks, which can contribute to the development of effective vaccines.

Acknowledgments

We thank Jing Wang for generating the laboratory and epidemiologic data presented in this article. We gratefully acknowledge all the members of CaliciNet China.

This study was supported by the Key Project of Science and Technology (grant no. 2017ZX10104001-003), and China–US Collaborative Program on Emerging and Re-emerging Infectious Disease (1U01GH002224), National Natural Science Foundation (grant no. 21934005), Scientific Research Project (SZGW2017017) and Basic Research Project (JCYJ20170306160421143), Health and Family Planning Commission (grant no. MS201617), and Foundation for Development of Science and Technology (grant no: CSE31N1611).

About the Author

Dr. Jin is a professor at China CDC. Her research focuses on molecular epidemiology of norovirus gastroenteritis. Dr. Wu is a medical research scientist at the US Centers for Disease Control and Prevention in Beijing. Her research focuses on surveillance of infectious diseases.

References

1. Patel MM, Hall AJ, Vinjé J, Parashar UD. Noroviruses: a comprehensive review. J Clin Virol. 2009;44:1–8. http://dx.doi.org/10.1016/j.jcv.2008.10.009
2. Hall AJ, Wikswo ME, Manikonda K, Roberts VA, Yoder JS, Gould LH. Acute gastroenteritis surveillance through the National Outbreak Reporting System, United States. Emerg Infect Dis. 2013;19:1305–9. http://dx.doi.org/10.3201/eid1908.130482
3. Teunis PF, Moe CL, Liu P, Miller SE, Lindesmith L, Baric RS, et al. Norwalk virus: how infectious is it? J Med Virol. 2008;80:1468–76. http://dx.doi.org/10.1002/jmv.21237
4. Cortes-Penfield NW, Ramani S, Estes MK, Atmar RL. Prospects and challenges in the development of a norovirus vaccine. Clin Ther. 2017;39:1537–49. http://dx.doi.org/10.1016/j.clinthera.2017.07.002
5. Kroneman A, Vega E, Vennema H, Vinjé J, White PA, Hansman G, et al. Proposal for a unified norovirus nomenclature and genotyping. Arch Virol. 2013;158:2059–68. http://dx.doi.org/10.1007/s00705-013-1708-5

6. Vinjé J. Advances in laboratory methods for detection and typing of norovirus. J Clin Microbiol. 2015;53:373–81. http://dx.doi.org/10.1128/JCM.01535-14
7. Cannon JL, Barclay L, Collins NR, Wikswo ME, Castro CJ, Magaña LC, et al. Genetic and epidemiologic trends of norovirus outbreaks in the United States from 2013 to 2016 demonstrated emergence of novel GII.4 recombinant viruses. Erratum in: J Clin Microbiol. 2019. J Clin Microbiol. 2017;55:2208–21. http://dx.doi.org/10.1128/JCM.00455-17
8. van Beek J, de Graaf M, Al-Hello H, Allen DJ, Ambert-Balay K, Botteldoorn N, et al.; NoroNet. Molecular surveillance of norovirus, 2005-16: an epidemiological analysis of data collected from the NoroNet network. Lancet Infect Dis. 2018;18:545–53. http://dx.doi.org/ 10.1016/S1473-3099(18)30059-8
9. Burke RM, Shah MP, Wikswo ME, Barclay L, Kambhampati A, Marsh Z, et al. The norovirus epidemiologic triad: predictors of severe outcomes in US norovirus outbreaks, 2009–2016. J Infect Dis. 2019;219: 1364–72. http://dx.doi.org/10.1093/infdis/jiy569
10. Koopmans M, Vennema H, Heersma H, van Strien E, van Duynhoven Y, Brown D, et al.; European Consortium on Foodborne Viruses. Early identification of common-source foodborne virus outbreaks in Europe. Emerg Infect Dis. 2003;9:1136–42. http://dx.doi.org/10.3201/eid0909.020766
11. Vega E, Barclay L, Gregoricus N, Williams K, Lee D, Vinjé J. Novel surveillance network for norovirus gastroenteritis outbreaks, United States. Emerg Infect Dis. 2011;17:1389–95.
12. Lian Y, Wu S, Luo L, Lv B, Liao Q, Li Z, et al. Epidemiology of norovirus outbreaks reported to the Public Health Emergency Event Surveillance System, China, 2014–2017. Viruses. 2019;11:E342. http://dx.doi.org/10.3390/v11040342
13. Liao Q, Ran L, Jin M, Cui S, Yuan J, Ma H, et al. Guidelines on outbreak investigation, prevention and control of norovirus infection (2015) [in Chinese]. Zhonghua Yu Fang Yi Xue Za Zhi. 2016;50:7–16.
14. Park GW, Chhabra P, Vinje J. Swab sampling method for the detection of human norovirus on surfaces. J Vis Exp. 2017;(120). http://dx.doi.org/10.3791/55205
15. Ettayebi K, Crawford SE, Murakami K, Broughman JR, Karandikar U, Tenge VR, et al. Replication of human noroviruses in stem cell-derived human enteroids. Science. 2016;353:1387–93. http://dx.doi.org/10.1126/science.aaf5211
16. Kojima S, Kageyama T, Fukushi S, Hoshino FB, Shinohara M, Uchida K, et al. Genogroup-specific PCR primers for detection of Norwalk-like viruses. J Virol Methods. 2002;100:107–14. http://dx.doi.org/10.1016/S0166-0934(01)00404-9
17. Vega E, Barclay L, Gregoricus N, Shirley SH, Lee D, Vinjé J. Genotypic and epidemiologic trends of norovirus outbreaks in the United States, 2009 to 2013. J Clin Microbiol. 2014;52:147–55. http://dx.doi.org/10.1128/JCM.02680-13
18. Thongprachum A, Khamrin P, Maneekarn N, Hayakawa S, Ushijima H. Epidemiology of gastroenteritis viruses in Japan: prevalence, seasonality, and outbreak. J Med Virol. 2016;88:551–70. http://dx.doi.org/10.1002/jmv.24387
19. Wikswo ME, Cortes J, Hall AJ, Vaughan G, Howard C, Gregoricus N, et al. Disease transmission and passenger behaviors during a high morbidity norovirus outbreak on a cruise ship, January 2009. Clin Infect Dis. 2011;52:1116–22. http://dx.doi.org/10.1093/cid/cir144
20. Cho HW, Chu C. Norovirus outbreaks occurred in different settings in the Republic of Korea. Osong Public Health Res Perspect. 2015;6:281–2. http://dx.doi.org/10.1016/j.phrp.2015.11.001
21. Loury P, Le Guyader FS, Le Saux JC, Ambert-Balay K, Parrot P, Hubert B. A norovirus oyster-related outbreak in a nursing home in France, January 2012. Epidemiol Infect. 2015;143:2486–93. http://dx.doi.org/10.1017/S0950268814003628
22. Barret AS, Jourdan-da Silva N, Ambert-Balay K, Delmas G, Bone A, Thiolet JM, et al. Surveillance for outbreaks of gastroenteritis in elderly long-term care facilities in France, November 2010 to May 2012. Euro Surveill. 2014;19:20859. http://dx.doi.org/10.2807/1560-7917.ES2014.19.29.20859
23. Qin SW, Chan TC, Cai J, Zhao N, Miao ZP, Chen YJ, et al. Genotypic and epidemiological trends of acute gastroenteritis associated with noroviruses in China from 2006 to 2016. Int J Environ Res Public Health. 2017;14:E1341. http://dx.doi.org/10.3390/ijerph14111341
24. China Ministry of Health and Ministry of Education. Criterion for reporting infectious diseases in schools and child-care institutions (for trial implementation) [cited 2017 Mar 5]. http://www.nhc.gov.cn/zhjcj/s9139/200804/b7fc75fdc7ee43afaadc76803dbbbaff.shtml
25. Verhoef L, Hewitt J, Barclay L, Ahmed SM, Lake R, Hall AJ, et al. Norovirus genotype profiles associated with foodborne transmission, 1999-2012. Emerg Infect Dis. 2015;21:592–9. http://dx.doi.org/10.3201/eid2104.141073
26. Lysén M, Thorhagen M, Brytting M, Hjertqvist M, Andersson Y, Hedlund KO. Genetic diversity among food-borne and waterborne norovirus strains causing outbreaks in Sweden. J Clin Microbiol. 2009;47:2411–8. http://dx.doi.org/10.1128/JCM.02168-08
27. Zhang M, Long YF, Guo LM, Wu SL, Fang L, Yang F, et al. Epidemiological characteristics of outbreaks of norovirus-GII.2, GII.17 and GII.4/Sydney in Guangdong province, 2013–2017 [in Chinese]. Zhonghua Liu Xing Bing Xue Za Zhi. 2018;39:1210–5.
28. Sakon N, Yamazaki K, Nakata K, Kanbayashi D, Yoda T, Mantani M, et al. Impact of genotype-specific herd immunity on the circulatory dynamism of norovirus: a 10-year longitudinal study of viral acute gastroenteritis. J Infect Dis. 2015;211:879–88. http://dx.doi.org/10.1093/infdis/jiu496
29. Bok K, Abente EJ, Realpe-Quintero M, Mitra T, Sosnovtsev SV, Kapikian AZ, et al. Evolutionary dynamics of GII.4 noroviruses over a 34-year period. J Virol. 2009;83:11890–901. http://dx.doi.org/10.1128/JVI.00864-09
30. Bull RA, Eden JS, Rawlinson WD, White PA. Rapid evolution of pandemic noroviruses of the GII.4 lineage. Erratum in: PLoS Pathog. 2010;6(4), PLoS Pathog. 2010; 6:e1000831. http://dx.doi.org/10.1371/journal.ppat.1000831
31. Barreira DM, Ferreira MS, Fumian TM, Checon R, de Sadovsky AD, Leite JP, et al. Viral load and genotypes of noroviruses in symptomatic and asymptomatic children in southeastern Brazil. J Clin Virol. 2010;47:60–4. http://dx.doi.org/10.1016/j.jcv.2009.11.012
32. Dey SK, Phathammavong O, Okitsu S, Mizuguchi M, Ohta Y, Ushijima H. Seasonal pattern and genotype distribution of norovirus infection in Japan. Pediatr Infect Dis J. 2010;29:e32–4. http://dx.doi.org/10.1097/INF.0b013e3181d742bf
33. Dove W, Cunliffe NA, Gondwe JS, Broadhead RL, Molyneux ME, Nakagomi O, et al. Detection and characterization of human caliciviruses in hospitalized children with acute gastroenteritis in Blantyre, Malawi. J Med Virol. 2005;77:522–7. http://dx.doi.org/10.1002/jmv.20488
34. Phan TG, Nguyen TA, Nishimura S, Nishimura T, Yamamoto A, Okitsu S, et al. Etiologic agents of acute gastroenteritis among Japanese infants and children: virus diversity and genetic analysis of sapovirus. Arch Virol. 2005;150:1415–24. http://dx.doi.org/10.1007/s00705-005-0514-0
35. Chan MC, Lee N, Hung TN, Kwok K, Cheung K, Tin EK, et al. Rapid emergence and predominance of a broadly

recognizing and fast-evolving norovirus GII.17 variant in late 2014. Nat Commun. 2015;6:10061. http://dx.doi.org/10.1038/ncomms10061
36. Ao Y, Wang J, Ling H, He Y, Dong X, Wang X, et al. Norovirus GII.P16/GII.2-associated gastroenteritis, China, 2016. Emerg Infect Dis. 2017;23:1172–5. http://dx.doi.org/10.3201/eid2307.170034
37. Lu J, Fang L, Sun L, Zeng H, Li Y, Zheng H, et al. Association of GII.2[P16] recombinant norovirus strain with increased norovirus outbreaks, Guangdong, China, 2016. Emerg Infect Dis. 2017;23:1188–90. http://dx.doi.org/10.3201/eid2307.170333
38. Fu JG, Shi C, Xu C, Lin Q, Zhang J, Yi QH, et al. Outbreaks of acute gastroenteritis associated with a re-emerging GII.2[P16] norovirus in the spring of 2017 in Jiangsu, China. PLoS One. 2017;12:e0186090. http://dx.doi.org/10.1371/journal.pone.0186090
39. Han J, Wu X, Chen L, Fu Y, Xu D, Zhang P, et al. Emergence of norovirus GII.2[P16] strains in patients with acute gastroenteritis in Huzhou, China, 2016–2017. BMC Infect Dis. 2018;18:342. http://dx.doi.org/10.1186/s12879-018-3259-6
40. Wang C, Ao Y, Yu J, Xie X, Deng H, Jin M, et al. Complete genome sequence of a novel recombinant GII.P16-GII.1 norovirus associated with a gastroenteritis outbreak in Shandong province, China, in 2017. Genome Announc. 2018;6:e01483–17. http://dx.doi.org/10.1128/genomeA.01483-17
41. Ao Y, Cong X, Jin M, Sun X, Wei X, Wang J, et al. Genetic analysis of reemerging GII.2[P16] noroviruses in 2016–2017 in China. J Infect Dis. 2018;218:133–43. http://dx.doi.org/10.1093/infdis/jiy182
42. Nagasawa K, Matsushima Y, Motoya T, Mizukoshi F, Ueki Y, Sakon N, et al. Phylogeny and immunoreactivity of norovirus GII.2[P16], Japan, winter 2016–17. Emerg Infect Dis. 2018;24:144–8. http://dx.doi.org/10.3201/eid2401.170284
43. Niendorf S, Jacobsen S, Faber M, Eis-Hübinger AM, Hofmann J, Zimmermann O, et al. Steep rise in norovirus cases and emergence of a new recombinant strain GII.2[P16], Germany, winter 2016. Euro Surveill. 2017;22:30447. http://dx.doi.org/10.2807/1560-7917.ES.2017.22.4.30447
44. Bidalot M, Théry L, Kaplon J, De Rougemont A, Ambert-Balay K. Emergence of new recombinant noroviruses GII.p16-GII.4 and GII.2[P16], France, winter 2016 to 2017. Euro Surveill. 2017;22:30508. http://dx.doi.org/10.2807/1560-7917.ES.2017.22.15.30508
45. Jin M, Zhou YK, Xie HP, Fu JG, He YQ, Zhang S, et al. Characterization of the new GII.17 norovirus variant that emerged recently as the predominant strain in China. J Gen Virol. 2016;97:2620–32. http://dx.doi.org/10.1099/jgv.0.000582
46. Heinimäki S, Malm M, Vesikari T, Blazevic V. Parenterally administered norovirus GII.4 virus–like particle vaccine formulated with aluminum hydroxide or monophosphoryl lipid A adjuvants induces systemic but not mucosal immune responses in mice. J Immunol Res. 2018;2018:3487095.
47. Ball JP, Springer MJ, Ni Y, Finger-Baker I, Martinez J, Hahn J, et al. Intranasal delivery of a bivalent norovirus vaccine formulated in an in situ gelling dry powder. PLoS One. 2017;12:e0177310. http://dx.doi.org/10.1371/journal.pone.0177310

Address for correspondence: Zhaojun Duan, China CDC, National Institute for Viral Disease Control and Prevention, Department of Viral Diarrhea, 155 Changbai Rd, Chang-ping District, Beijing 102206, China; email: zhaojund@126.com

Methicillin-Resistant *Staphylococcus aureus* Bloodstream Infections and Injection Drug Use, Tennessee, USA, 2015–2017

Meghana P. Parikh, Rany Octaria, Marion A. Kainer

Medscape EDUCATION ACTIVITY

In support of improving patient care, this activity has been planned and implemented by Medscape, LLC and Emerging Infectious Diseases. Medscape, LLC is jointly accredited by the Accreditation Council for Continuing Medical Education (ACCME), the Accreditation Council for Pharmacy Education (ACPE), and the American Nurses Credentialing Center (ANCC), to provide continuing education for the healthcare team.

Medscape, LLC designates this Journal-based CME activity for a maximum of 1.00 ***AMA PRA Category 1 Credit(s)™***. Physicians should claim only the credit commensurate with the extent of their participation in the activity.

Successful completion of this CME activity, which includes participation in the evaluation component, enables the participant to earn up to 1.0 MOC points in the American Board of Internal Medicine's (ABIM) Maintenance of Certification (MOC) program. Participants will earn MOC points equivalent to the amount of CME credits claimed for the activity. It is the CME activity provider's responsibility to submit participant completion information to ACCME for the purpose of granting ABIM MOC credit.

All other clinicians completing this activity will be issued a certificate of participation. To participate in this journal CME activity: (1) review the learning objectives and author disclosures; (2) study the education content; (3) take the post-test with a 75% minimum passing score and complete the evaluation at http://www.medscape.org/journal/eid; and (4) view/print certificate. For CME questions, see page 639.

Release date: February 12, 2020; Expiration date: February 12, 2021

Learning Objectives

Upon completion of this activity, participants will be able to:

- Describe the prevalence of life-threatening IDU-related MRSA BSI in Tennessee in 2015–2017, according to an analysis of data from the NHSN and the Tennessee Hospital Discharge Data System
- Determine the demographics and clinical characteristics of IDU-related MRSA BSI in Tennessee in 2015– 2017, according to an analysis of data from the NHSN and the Tennessee Hospital Discharge Data System
- Identify clinical and public health implications of the association of IDU practices with life-threatening MRSA BSI in Tennessee, according to an analysis of data from the NHSN and the Tennessee Hospital Discharge Data System

CME Editor

Deborah Wenger, MBA, Copyeditor, Emerging Infectious Diseases. *Disclosure: Deborah Wenger, MBA, has disclosed no relevant financial relationships.*

CME Author

Laurie Barclay, MD, freelance writer and reviewer, Medscape, LLC. *Disclosure: Laurie Barclay, MD, has disclosed no relevant financial relationships.*

Authors

Disclosures: ***Meghana Pendurthi Parikh, VMD, MPH;*** *and* ***Rany Octaria, MD, MPH,*** *have disclosed no relevant financial relationships.* ***Marion Kainer, MBBS, MPH,*** *has disclosed the following relevant financial relationships: served as an advisor or consultant for Infectious Disease Consulting Corporation; Pfizer Inc.*

Author affiliations: Tennessee Department of Health, Nashville, Tennessee, USA (M.P. Parikh, R. Octaria, M.A. Kainer); Vanderbilt University, Nashville (R. Octaria)

DOI: https://doi.org/10.3201/eid2603.191408

Recently, Tennessee, USA, has seen an increase in the use of commonly injected drugs, such as heroin and fentanyl. Injection drug use (IDU) practices can lead to life-threatening methicillin-resistant *Staphylococcus aureus* (MRSA) bloodstream infections (BSIs) and other serious diseases. We matched MRSA BSIs identified through the National Healthcare Safety Network to the Tennessee Hospital Discharge Data System to characterize the prevalence, demographics, and clinical characteristics associated with IDU in this disease population. Of the 7,646 MRSA BSIs identified during 2015–2017, we found that 1,839 (24.1%) were IDU-related. IDU-related BSIs increased by 118.9%; the greatest rise occurred among emergency department–onset infections (197.4%). IDU was more often associated with white, female, 18–49-year-old, and uninsured persons (p<0.001). We found ≥1 additional IDU-related diagnoses in 84.2% of IDU-related BSIs. Targeted harm reduction strategies for persons at high risk of IDU are necessary to reduce MRSA BSIs in acute care settings.

Methicillin-resistant *Staphylococcus aureus* (MRSA) continues to be a prominent healthcare-associated pathogen causing illness and death (*1*,*2*). As a result of the widespread implementation of infection control practices in acute-care hospitals, nationwide decreases in hospital-onset MRSA (HO MRSA) bloodstream infections (BSIs) were seen during 2005–2012. However, recent data show that since then there has been no change in the incidence of HO MRSA BSIs (*3*). Surveillance data on MRSA BSIs from acute care hospitals in Tennessee show similar patterns in decline and stabilization of HO BSIs; however, state trends in community-onset (CO) BSIs vary greatly from reported national patterns. Nationwide estimates suggest that incidence of CO MRSA BSIs has remained stable during 2005–2016 (*3*), whereas Tennessee's statewide surveillance showed a 37.2% increase in CO MRSA BSI events during 2011–2016 (*4*).

CO MRSA BSIs, classified as having a positive blood sample collected on or before day 3 of hospitalization or during an emergency department (ED) visit (*5*), are often associated with previous healthcare procedures and hospitalizations (*6*,*7*). Additional risk factors for CO MRSA among previously healthy persons include, but are not limited to, close contact with colonized or infected persons (*8*), shared equipment that is not cleaned between users (*9*), and skin trauma (*10*,*11*). We postulate that Tennessee's unique epidemiology of CO MRSA BSIs might be reflective of geographic differences in injection drug use (IDU) practices associated with the opioid epidemic. These patients might have clinical manifestations and risk factors that vary from those identified in previous literature. In the 2000s, opioid use was largely associated with abuse of prescription opioids, but during the past decade, the rise in opioid use and overdose deaths has been attributed to an increase in commonly injected drugs such as heroin and fentanyl (*12*–*14*). In Tennessee, although prescription opioids are still responsible for the greatest number of opioid deaths, overdose deaths associated with synthetic opioids increased by 666% and overdose deaths associated with heroin increased by 522% during 2012–2017 (*15*).

IDU has long been identified as a risk factor for invasive MRSA infections, including skin and soft tissue infections (*16*–*18*), osteomyelitis and septic arthritis (*19*–*21*), bacteremia (*17*,*18*,*22*), and endocarditis (*18*,*23*,*24*). Data from 6 sites of the Centers for Disease Control and Prevention's Emerging Infections Program (Division of Preparedness and Emerging Infections, National Center for Emerging and Zoonotic Infectious Diseases) have shown that persons who inject drugs are >16 times more likely to develop invasive MRSA infections than persons who do not inject drugs and that the proportion of invasive MRSA associated with IDU has risen from 4.1% in 2012 to 9.2% in 2016 (*10*).

We sought to describe the prevalence of IDU-related MRSA BSI cases in acute-care hospitals across Tennessee. In addition, we examined the demographic and clinical characteristics of IDU-related and non–IDU-related cases. With these data, we aim to inform targeted efforts to improve clinical response to high-risk MRSA BSI patients in both outpatient and inpatient settings. Furthermore, increased knowledge of the indirect impacts of the opioid epidemic is imperative for the development of policy-based prevention initiatives.

Methods

Data Sources

We identified MRSA BSIs using the National Healthcare Safety Network (NHSN), a nationwide reporting system through which acute care hospitals in Tennessee track laboratory-identified MRSA BSIs from inpatient (IP) units and EDs (*5*). NHSN includes details on specimen collection and facility characteristics, in addition to limited patient identifiers, such as sex, date of birth, and name (optional to report).

The Tennessee Hospital Discharge Data System (HDDS) was used to further characterize demographics and clinical characteristics of MRSA BSIs identified in NHSN. HDDS captures administrative data on patient demographics, diagnoses, and procedures

performed during all IP hospitalizations and ED encounters occurring in Tennessee hospitals during January 2014–June 2018 (*25*). In that time frame, all hospital visits for MRSA BSI patients were identified by matching records on patient names, dates of birth, or medical record numbers when other identifiers were unavailable. Beginning in January 2016, all HDDS diagnosis codes were documented using the International Classification of Diseases (ICD), 10th Revision, Clinical Modification (ICD-10-CM). Prior to that, codes from ICD-10-CM or the ICD's Ninth Revision, Clinical Modification (ICD-9-CM) were allowed in HDDS.

Our study cohort included MRSA BSIs from patients ≥13 years of age with onset of infection during January 2015–December 2017 and with >1 IP or ED visit to any Tennessee hospital during July 2014–June 2018, as identified in HDDS. HDDS observations were excluded if full patient names or dates of birth were missing.

Variables

We classified a case of MRSA BSI as IDU-related if any HDDS visit in the 6 months before or after blood specimen collection contained a diagnosis code for drug use (primary or secondary). The list of ICD codes used included diagnoses for dependence, abuse, poisoning, or accidental death caused by commonly injected illicit drugs (e.g., cocaine, opioids, methamphetamine) (Appendix Table 1, https://wwwnc.cdc.gov/EID/article/26/3/19-1408-App1.pdf). These codes have been used in peer-reviewed literature to estimate IDU associated with hospitalizations for other infectious diseases, such as infective endocarditis (*23*,*24*,*26*).

In accordance with NHSN guidelines, we classified a BSI event as CO if the culture was obtained on or before hospital day 3 and as HO if obtained on hospital day 4 or later, with the admission date being day 1 (*5*). We further classified CO infections as either CO-ED or CO-IP on the basis of the patient's location at the time of culture collection. We classified same-day cultures collected in both ED and IP locations as a single CO-ED event.

We also evaluated cases for the presence of other IDU-related diagnoses in the 6 months before or after blood collection, including hospitalization for MRSA BSI. Thus, these cases could have occurred as a part of the same or different disease process as the BSI event. IDU-related diagnosis codes included endocarditis, acute or chronic hepatitis C, osteomyelitis or septic arthritis, and skin and soft tissue infections (Appendix Table 2).

Statistical Analysis

We evaluated differences in baseline characteristics between IDU-related and non–IDU-related BSIs using a χ^2 or Fisher exact test for categorical variables and 2-sample *t*-test for continuous variables. We further analyzed IDU-related MRSA BSI events by onset group, using a χ^2 or Fisher exact test for categorical variables and 1-way analysis of variance for continuous variables. We performed database linkages and statistical analyses using SAS 9.4 (SAS Institute Inc., https://www.sas.com). We defined statistical significance as $p<0.05$. This study was approved by the Tennessee Department of Health (TDH) Institutional Review Board (project no. 1148777-1).

Results

After excluding patients <13 years of age at the time of culture, we identified 8,251 NHSN MRSA BSI cases from 7,076 patients during 2015–2017. Of those patients, 6,548 (92.5%) were located within HDDS. In total, the matched patients represented 7,646 MRSA BSI cases included in the study cohort. We identified only 1 BSI case per person in 87.5% of patients; the maximum number of BSI events per person over the study timeframe was 8. Tennessee state residents had 89.7% of BSIs.

MRSA BSI cases increased 17.7% over the study period, from 2,333 cases in 2015 to 2,746 in 2017 (Figure). Most cases (57%) were CO-ED. During 2015–2017, CO-ED BSIs increased by 51.8%, as compared with decreases in CO-IP (-17.9%) and HO (-11.4%) BSIs.

IDU-related cases represented 24.1% of the study cohort; the prevalence of these cases increased from 16.1% in 2015 to 29.9% in 2017 (Table 1). The proportion of IDU-related cases was highest among the CO-ED group (26.5%) compared with other onset groups ($p<0.001$). Age was associated with IDU status ($p<0.001$); the median age of patients with

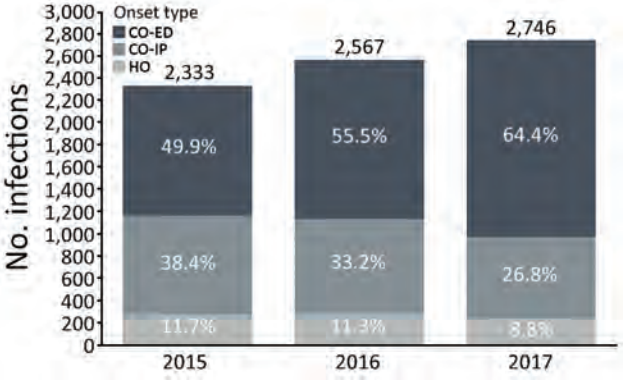

Figure. Annual cases of methicillin-resistant *Staphylococcus aureus* bloodstream infections in hospitals, stratified by onset type, Tennessee, USA, 2015–2017. CO, community onset; ED, emergency department; HO, hospital onset; IP, inpatient.

Table 1. Demographic and clinical characteristics of patients with methicillin-resistant *Staphylococcus aureus* bloodstream infections, by IDU status, Tennessee, USA, 2015–2017*

Characteristic	IDU status		p value	Overall
	IDU	Non-IDU		
Total	1,839 (24.1)	5,807 (75.9)	<0.001	7,646 (100)
Onset year			<0.001	
2015	375 (16.1)	1,958 (83.9)		2,333 (30.5)
2016	643 (25.0)	1,924 (75.0)		2,567 (33.6)
2017	821 (29.9)	1,925 (70.1)		2,746 (35.9)
Onset type			<0.001	
CO-ED	1,156 (62.9)	3,202 (55.1)		4,358 (57.0)
CO-IP	572 (31.1)	1,911 (32.9)		2,483 (32.5)
HO	111 (6.0)	694 (12.0)		805 (10.5)
Age range, y			<0.001	
13–17	1 (0.1)	24 (0.4)		25 (0.3)
18–34	617 (33.6)	387 (6.7)		1,004 (13.1)
35–49	665 (36.2)	912 (15.7)		1,577 (20.63)
50–64	436 (23.7)	1,789 (30.8)		2,225 (29.1)
≥65	120 (6.5)	2,695 (46.4)		2,815 (36.8)
Median (range, Q1–Q3)	40 (31–51)	63 (51–74)	<0.001	
Sex			<0.001	
M	910 (49.5)	3,435 (59.2)		4,345 (56.8)
F	929 (50.5)	2,372 (40.8)		3,301 (43.2)
Race			<0.001	
White	1,635 (88.9)	4,511 (77.7)		6,146 (80.4)
Black	168 (9.1)	1,193 (20.5)		1,361 (17.8)
Other	15 (0.8)	56 (1.0)		71 (0.9)
Unknown	21 (1.1)	47 (0.8)		68 (0.9)
Ethnicity			0.820	
Hispanic	6 (0.3)	22 (0.4)		28 (0.4)
Non-Hispanic	1,768 (96.1)	5,563 (95.8)		7,331 (95.9)
Unknown	65 (3.5)	222 (3.8)		287 (3.8)
Insurance			<0.001	
Commercial	109 (5.9)	648 (11.2)		757 (9.9)
Medicaid	570 (31.0)	655 (11.3)		1,225 (16.0)
Medicare	452 (24.6)	3,688 (63.5)		4,140 (54.2)
Self-pay/uninsured	612 (33.3)	476 (8.2)		1,088 (14.2)
Other/unknown	96 (5.2)	340 (5.9)		436 (5.7)

*Values are no. (%) except as indicated. CO, community onset; ED, emergency department; HO, hospital onset; IDU, injection drug use; IP, inpatient.

IDU-related BSIs was 40 years versus 63 years for patients with non–IDU-related BSI cases. Among IDU-related cases, 69.7% of BSIs occurred in 18–49-year-olds, whereas the same age range made up only 22.4% of non–IDU-related BSIs. Gender was also correlated with IDU status (p<0.001); men accounted for a smaller proportion of IDU-related BSIs (49.5%) than non–IDU-related BSIs (59.2%). Of all MRSA BSIs, 80.4% occurred in white patients and 17.8% in black patients. The proportion of white patients was higher among IDU-related cases than among non–IDU-related cases (88.9% versus 77.7%; p<0.001). Usage of Medicare and commercial insurance was higher among non–IDU-related BSIs (63.5% vs. 11.2% for IDU-related BSIs), whereas Medicaid usage and self-pay/uninsured status were higher among IDU-related cases (31.0% vs. 33.3% for non–IDU-related cases).

Among all patients with MRSA BSIs, 4,604 (61.8%) had ≥1 IDU-related diagnoses documented within 6 months before or after MRSA onset. Prevalence of IDU-related diagnoses was 84.2% among patients with IDU-related BSIs and 54.7% among those with non–IDU-related BSIs. The prevalence of endocarditis (40.4%), hepatitis C infections (50.7%), osteomyelitis/septic arthritis (28.1%), and skin and soft tissue infections (46.9%) were all significantly greater (p<0.001 for all) among IDU-related BSIs than among non–IDU-related BSIs (Table 2).

Among IDU-related cases stratified by onset type, 62.9% were CO-ED (Table 3). The proportion of

Table 2. Prevalence of IDU-related diagnoses among patients with methicillin-resistant *Staphylococcus aureus* bloodstream infections, by IDU status, Tennessee, USA, 2015–2017*

Diagnosis	IDU, no. (%), n = 1,839	Non-IDU, no. (%), n = 5,807	p value	Overall, no. (%), n = 7,646
Endocarditis	743 (40.4)	626 (10.8)	<0.001	1,369 (17.9)
Hepatitis C	932 (50.7)	377 (6.5)	<0.001	1,309 (17.1)
Osteomyelitis/septic arthritis	516 (28.1)	1,340 (23.1)	<0.001	1,856 (24.3)
Skin/soft tissue infection	863 (46.9)	2,227 (38.4)	<0.001	3,090 (40.4)

*IDU, injection drug use.

Table 3. Selected characteristics of patients with injection drug use–related methicillin-resistant *Staphylococcus aureus* bloodstream infections, by onset type, Tennessee, USA, 2015–2017*

Characteristic	MRSA onset			p value	Overall
	CO-ED	CO-IP	HO		
Total	1,156 (62.9)	572 (31.1)	111 (6.0)	<0.001	1,839 (100)
Onset year				<0.001	
2015	192 (51.2)	153 (40.8)	30 (8.0)		375 (20.4)
2016	393 (61.1)	211 (32.8)	39 (6.1)		643 (35.0)
2017	571 (69.5)	208 (25.3)	42 (5.1)		821 (44.6)
Age range, y				<0.001	
13–17	0	1 (0.2)	0		1 (0.0)
18–34	431 (37.3)	164 (28.7)	22 (19.8)		617 (33.6)
35–49	405 (35.0)	226 (39.5)	34 (30.6)		665 (36.2)
50–64	245 (21.2)	149 (26.0)	42 (37.8)		436 (23.7)
≥65	75 (6.5)	32 (5.6)	13 (11.7)		120 (6.5)
Median (Q1–Q3)	38 (31–51)	42 (33–52)	49 (37–59)	<0.001	
Race				<0.001	
White	1,059 (91.6)	501 (87.6)	75 (67.6)		1,635 (88.9)
Black	83 (7.2)	56 (9.8)	29 (26.1)		168 (9.1)
Other	6 (0.5)	7 (1.2)	2 (1.8)		15 (0.8)
Unknown	8 (0.7)	8 (1.4)	5 (4.5)		21 (1.1)
Insurance				0.001	
Commercial	69 (6.0)	32 (5.6)	8 (7.2)		109 (5.9)
Medicaid	347 (30.0)	192 (33.6)	31 (27.9)		570 (31.0)
Medicare	256 (22.1)	154 (26.9)	42 (37.8)		452 (24.6)
Self-pay/uninsured	422 (36.5)	164 (28.7)	26 (23.4)		612 (33.3)
Other/unknown	62 (5.4)	30 (5.2)	4 (3.6)		96 (5.2)

*Values are no. (%) except as indicated. CO, community onset; ED, emergency department; HO, hospital onset; IP, inpatient.

CO-ED cases increased by 18.4% during 2015–2017, whereas the proportion of CO-IP cases among IDU-related BSIs decreased by 15.5% and the proportion of HO cases among IDU-related BSIs decreased by 2.9%. CO-ED IDU-related BSIs had the youngest patients, with a median age of 38 years (p<0.001). Onset type among IDU-related BSIs was associated with insurance status (p = 0.001); the greatest usage of Medicare (37.8%) and commercial insurance (7.2%) occurred among HO cases, whereas self-pay/uninsured status was highest among CO-ED cases (36.5%). Medicaid was used most often among patients with CO-IP IDU-related BSIs (33.6%).

Discussion

We found an alarming increase in the extent of all MRSA BSIs in Tennessee during 2015–2017. This rise is attributed largely to the increase in the number of CO-ED cases, as CO-IP and HO cases have steadily declined. Increasing IDU over the study timeframe, as well as the high prevalence of IDU among CO-ED BSIs, suggests an association between the drug use crisis and MRSA BSIs. These trends are consistent with reports of increasing use of commonly injected drugs in Tennessee based on the surveillance of overdose deaths (*14*,*15*), which might provide an incomplete picture of current drug use practices. The use of hospital discharge billing data in our study enabled us to assess IDU among all patients entering the hospital system, including those who survived.

Using this methodology, we described common demographic characteristics of MRSA BSI patients and stratified them by IDU status. Consistent with previously reported demographics associated with IDU (*12*), we observed that IDU in our population was more common among patients who were 18–49 years of age, female, white, and uninsured. Furthermore, although still observed in the CO-IP and HO groups, IDU and those demographics were most strongly associated with ED-onset BSIs. Our findings demonstrate a shift in patient demographics typically associated with MRSA. Whereas previous studies have shown that invasive MRSA infections occur predominantly in men >49 years of age, with a larger proportion of patients being black (*27*), our study highlights an emerging at-risk population.

Currently, most public health MRSA BSI prevention and treatment strategies are targeted at HO infections (*3*,*28*). The results of this study provide a compelling argument to enhance our MRSA BSI reduction efforts by devoting resources and creating policies targeting CO BSIs. First, this new knowledge can be used to heighten awareness in ED staff of potential IDU among patients with clinical signs consistent with MRSA BSIs. These patients have a high prevalence of other IDU-related diagnoses, including endocarditis and hepatitis C, which might affect clinical progression and, ultimately, patient outcomes. Identifying patients at risk for IDU-related MRSA BSIs enables prompt diagnosis,

treatment, and increased emphasis on feasible follow-up care solutions.

A key difference between both CO groups in this study was the larger utilization of Medicaid among CO-IP IDU-related cases, compared with the higher rates of uninsurance among IDU-related CO-ED BSIs. This contrast has implications for follow-up care, because patients with IDU-related disease might be less likely to afford and pursue required follow-up treatment. In addition to the high potential for illness and death, these patients demonstrate higher rates of IDU-related infections and readmission (*29*), which are often also associated with uninsured status (*19*).

Our findings also raise a question about the role of ED and IP healthcare services in facilitating treatment for drug use and addiction. Despite evidence that interventions such as medication-assisted therapy and screening, brief intervention, and referral to treatment are both feasible and effective in acute care settings (*30*–*32*), pharmacotherapies and psychotherapies are heavily underused (*29*,*33*). Implementing interventions for substance abuse in ED settings has a large potential impact on reducing CO MRSA BSIs and other devastating consequences of IDU.

Our findings are subject to some limitations. The events included in our analyses were laboratory-identified cases from acute care hospitals sourced from Tennessee statewide surveillance data. In addition, only patients who were able to be matched to HDDS were included in the analyses; the match rate of 92.5% indicates a possible underrepresentation of the true burden of disease. We also recognize that because ICD codes do not differentiate between routes of administration for drug use, we might be overestimating the prevalence of IDU compared with overall substance abuse. Similarly, because of stigmas surrounding substance abuse, ICD codes documenting the practice might provide an underestimation of true prevalence. Although we were unable to access medical records to validate our approach, this series of diagnostic codes has previously been used to identify IDU related to infections and hospitalizations (*23*,*24*,*26*). In addition, given that hepatitis C is strongly correlated with IDU (*34*,*35*), the high prevalence of hepatitis C infections among IDU-related MRSA BSI cases in this study lends support to the validity of the diagnostic codes used. For these reasons, it is feasible that our findings are reflective not only of patterns of substance abuse, but also of IDU in Tennessee.

Our study is unique in its linkage of NHSN MRSA BSI surveillance to hospital discharge data for retrospective evaluation of IDU without conducting time-consuming chart reviews. The use of statewide laboratory-based surveillance data provides the additional benefit of a more reliable, complete picture of MRSA BSIs across Tennessee. Previous studies relied on extrapolating data from smaller jurisdictions to estimate the burden of infection and describe patient characteristics, leaving the potential for inaccurate estimation and interpretation of state trends (*10*, *27*). Our technique is advantageous for state public health agencies seeking to investigate the evolving clinical and demographic risk factors associated with reportable diseases. Despite reported national trends of unchanged CO MRSA BSIs (*3*), with the widespread nature of the opioid epidemic, we suspect that other jurisdictions, especially those with similar population characteristics as Tennessee, might see similar trends of rising CO MRSA BSIs associated with IDU. Replicating this study elsewhere would be valuable to identify any local variations in risk factors.

In summary, Tennessee is undergoing a major change in the epidemiology of MRSA BSIs, having a growing population of young, white, uninsured, female patients with CO BSIs as a consequence of IDU. Our findings can be used to inform public health policies and clinical practice, particularly in the ED setting, to introduce prevention and harm reduction strategies to reduce the widespread impacts of this deadly disease within our communities.

Acknowledgments

We thank the acute care hospitals in Tennessee for performing surveillance and reporting MRSA BSI data to NHSN.

Development of this manuscript and contents were supported through the Centers for Disease Control and Prevention (CDC) Epidemiology and Laboratory Capacity (grant no. 6NU50CK000386) and the CDC Emerging Infections Program (grant no. 6NU50CK000491).

About the Author

Dr. Parikh is an epidemiologist at the Tennessee Department of Health's Healthcare Associated Infections and Antimicrobial Resistance Program in Nashville, Tennessee, USA. Her primary research interests include surveillance of infectious diseases.

References

1. van Hal SJ, Jensen SO, Vaska VL, Espedido BA, Paterson DL, Gosbell IB. Predictors of mortality in *Staphylococcus aureus* bacteremia. Clin Microbiol Rev. 2012;25:362–86. https://doi.org/10.1128/CMR.05022-11
2. Sharma A, Rogers C, Rimland D, Stafford C, Satola S, Crispell E, et al. Post-discharge mortality in patients

hospitalized with MRSA infection and/or colonization. Epidemiol Infect. 2013;141:1187–98. https://doi.org/10.1017/S0950268812001963
3. Kourtis AP, Hatfield K, Baggs J, Mu Y, See I, Epson E, et al.; Emerging Infections Program MRSA Author Group. Vital signs: epidemiology and recent trends in methicillin-resistant and in methicillin-susceptible *Staphylococcus aureus* bloodstream infections—United States. MMWR Morb Mortal Wkly Rep. 2019;68:214–9. https://doi.org/10.15585/mmwr.mm6809e1
4. Centers for Disease Control and Prevention. CDC Vital Signs town hall on staph infections can kill: prevention at the front lines; 2019 [cited 2019 Sep 10]. https://www.cdc.gov/publichealthgateway/townhall/2019/downloads/3-mar-presentation.pdf
5. National Center for Emerging and Zoonotic Infectious Diseases. Multidrug-resistant organism and *Clostridioides difficile* infection (MDRO/CDI) module. 2019 [cited 2019 Aug 6]. https://www.cdc.gov/nhsn/pdfs/pscmanual/12pscmdro_cdadcurrent.pdf
6. Huang SS, Platt R. Risk of methicillin-resistant *Staphylococcus aureus* infection after previous infection or colonization. Clin Infect Dis. 2003;36:281–5. https://doi.org/10.1086/345955
7. Huang SS, Hinrichsen VL, Datta R, Spurchise L, Miroshnik I, Nelson K, et al. Methicillin-resistant *Staphylococcus aureus* infection and hospitalization in high-risk patients in the year following detection. PLoS One. 2011; 6:e24340. https://doi.org/10.1371/journal.pone.0024340
8. Campbell KM, Vaughn AF, Russell KL, Smith B, Jimenez DL, Barrozo CP, et al. Risk factors for community-associated methicillin-resistant *Staphylococcus aureus* infections in an outbreak of disease among military trainees in San Diego, California, in 2002. J Clin Microbiol. 2004;42:4050–3. https://doi.org/10.1128/JCM.42.9.4050-4053.2004
9. Centers for Disease Control and Prevention. Methicillin-resistant *Staphylococcus aureus* infections among competitive sports participants—Colorado, Indiana, Pennsylvania, and Los Angeles County, 2000–2003. MMWR Morb Mortal Wkly Rep. 2003;52:793–5.
10. Jackson KA, Bohm MK, Brooks JT, Asher A, Nadle J, Bamberg WM, et al. Invasive methicillin-resistant *Staphylococcus aureus* infections among persons who inject drugs—six sites, 2005–2016. MMWR Morb Mortal Wkly Rep. 2018;67:625–8. https://doi.org/10.15585/mmwr.mm6722a2
11. Centers for Disease Control and Prevention (CDC). Methicillin-resistant *Staphylococcus aureus* skin infections among tattoo recipients—Ohio, Kentucky, and Vermont, 2004–2005. MMWR Morb Mortal Wkly Rep. 2006;55:677–9.
12. Cicero TJ, Ellis MS, Surratt HL, Kurtz SP. The changing face of heroin use in the United States: a retrospective analysis of the past 50 years. JAMA Psychiatry. 2014;71:821–6. https://doi.org/10.1001/jamapsychiatry.2014.366
13. Rudd RA, Seth P, David F, Scholl L. Increases in drug and opioid-involved overdose deaths—United States, 2010–2015. MMWR Morb Mortal Wkly Rep. 2016;65:1445–52. https://doi.org/10.15585/mmwr.mm655051e1
14. Cicero TJ, Ellis MS, Harney J. Shifting patterns of prescription opioid and heroin abuse in the United States. N Engl J Med. 2015;373:1789–90. https://doi.org/10.1056/NEJMc1505541
15. National Institute on Drug Abuse. Tennessee opioid summary: opioid-related overdose deaths. 2018 [cited 2019 Aug 25]. https://www.drugabuse.gov/drugs-abuse/opioids/opioid-summaries-by-state/tennessee-opioid-summary.
16. Ebright JR, Pieper B. Skin and soft tissue infections in injection drug users. Infect Dis Clin North Am. 2002;16:697–712. https://doi.org/10.1016/S0891-5520(02)00017-X
17. Bassetti S, Battegay M. *Staphylococcus aureus* infections in injection drug users: risk factors and prevention strategies. Infection. 2004;32:163–9. https://doi.org/10.1007/s15010-004-3106-0
18. Gordon RJ, Lowy FD. Bacterial infections in drug users. N Engl J Med. 2005;353:1945–54. https://doi.org/10.1056/NEJMra042823
19. Ronan MV, Herzig SJ. Hospitalizations related to opioid abuse/dependence and associated serious infections increased sharply, 2002–12. Health Aff (Millwood). 2016;35:832–7. https://doi.org/10.1377/hlthaff.2015.1424
20. Chandrasekar PH, Narula AP. Bone and joint infections in intravenous drug abusers. Rev Infect Dis. 1986;8:904–11. https://doi.org/10.1093/clinids/8.6.904
21. Allison DC, Holtom PD, Patzakis MJ, Zalavras CG. Microbiology of bone and joint infections in injecting drug abusers. Clin Orthop Relat Res. 2010;468:2107–12. https://doi.org/10.1007/s11999-010-1271-2
22. Chua T, Moore CL, Perri MB, Donabedian SM, Masch W, Vager D, et al. Molecular epidemiology of methicillin-resistant *Staphylococcus aureus* bloodstream isolates in urban Detroit. J Clin Microbiol. 2008;46:2345–52. https://doi.org/10.1128/JCM.00154-08
23. Cooper HLF, Brady JE, Ciccarone D, Tempalski B, Gostnell K, Friedman SR. Nationwide increase in the number of hospitalizations for illicit injection drug use-related infective endocarditis. Clin Infect Dis. 2007;45:1200–3. https://doi.org/10.1086/522176
24. Wurcel AG, Anderson JE, Chui KKH, Skinner S, Knox TA, Snydman DR, et al. Increasing infectious endocarditis admissions among young people who inject drugs. Open Forum Infect Dis. 2016;3:ofw157. https://doi.org/10.1093/ofid/ofw157
25. Tennessee Department of Health. Hospital discharge data system. August 2018 [cited 2019 Aug 25]. https://www.tn.gov/health/health-program-areas/statistics/special-reports/hdds.html
26. Miller AC, Polgreen PM. Many opportunities to record, diagnose, or treat injection drug-related infections are missed: a population-based cohort study of inpatient and emergency department settings. Clin Infect Dis. 2019;68:1166–75. https://doi.org/10.1093/cid/ciy632
27. Dantes R, Mu Y, Belflower R, Aragon D, Dumyati G, Harrison LH, et al.; Emerging Infections Program–Active Bacterial Core Surveillance MRSA Surveillance Investigators. National burden of invasive methicillin-resistant *Staphylococcus aureus* infections, United States, 2011. JAMA Intern Med. 2013;173:1970–8.
28. Centers for Disease Control and Prevention. What CDC is doing to combat MRSA. 2019 [cited 2019 Nov 25]. https://www.cdc.gov/mrsa/tracking
29. Rosenthal ES, Karchmer AW, Theisen-Toupal J, Castillo RA, Rowley CF. Suboptimal addiction interventions for patients hospitalized with injection drug use-associated infective endocarditis. Am J Med. 2016;129:481–5. https://doi.org/10.1016/j.amjmed.2015.09.024
30. Hawk KF, Vaca FE, D'Onofrio G. Reducing fatal opioid overdose: prevention, treatment and harm reduction strategies. Yale J Biol Med. 2015;88:235–45.
31. Madras BK, Compton WM, Avula D, Stegbauer T, Stein JB, Clark HW. Screening, brief interventions, referral to treatment (SBIRT) for illicit drug and alcohol use at multiple healthcare sites: comparison at intake and 6

months later. Drug Alcohol Depend. 2009;99:280–95. https://doi.org/10.1016/j.drugalcdep.2008.08.003
32. Trowbridge P, Weinstein ZM, Kerensky T, Roy P, Regan D, Samet JH, et al. Addiction consultation services—linking hospitalized patients to outpatient addiction treatment. J Subst Abuse Treat. 2017;79:1–5. https://doi.org/10.1016/j.jsat.2017.05.007
33. Knudsen HK, Abraham AJ, Roman PM. Adoption and implementation of medications in addiction treatment programs. J Addict Med. 2011;5:21–7. https://doi.org/10.1097/ADM.0b013e3181d41ddb
34. Nelson PK, Mathers BM, Cowie B, Hagan H, Des Jarlais D, Horyniak D, et al. Global epidemiology of hepatitis B and hepatitis C in people who inject drugs: results of systematic reviews. Lancet. 2011;378:571–83. https://doi.org/10.1016/S0140-6736(11)61097-0
35. Zibbell JE, Iqbal K, Patel RC, Suryaprasad A, Sanders KJ, Moore-Moravian L, et al.; Centers for Disease Control and Prevention. Increases in hepatitis C virus infection related to injection drug use among persons aged ≤30 years—Kentucky, Tennessee, Virginia, and West Virginia, 2006–2012. MMWR Morb Mortal Wkly Rep. 2015;64:453–8.

Address for correspondence: Meghana P. Parikh, Tennessee Department of Health, Healthcare Associated Infections and Antimicrobial Resistance Program, 710 James Robertson Pkwy, Andrew Johnson Tower 3.421C, Nashville, TN 37203, USA; email: Meghana.Parikh@tn.gov

Randomized Trial of 2 Schedules of Meningococcal B Vaccine in Adolescents and Young Adults, Canada[1]

Joanne M. Langley, Soren Gantt, Caroline Quach, Julie A. Bettinger, Scott A. Halperin, Jill Mutch, Shelly A. McNeil, Brian J. Ward, Donna MacKinnon-Cameron, Lingyun Ye, Kim Marty, David Scheifele, Erin Brown, Joenel Alcantara, and The Canadian Immunization Research Network

Emergency vaccination programs often are needed to control outbreaks of meningococcal disease caused by *Neisseria meningitidis* serogroup B (MenB) on college campuses. Such campaigns expend multiple campus and public health resources. We conducted a randomized, controlled, multicenter, observer-blinded trial comparing immunogenicity and tolerability of an accelerated vaccine schedule of 0 and 21 days to a longer interval of 0 and 60 days for 4-component MenB vaccine (MenB-4C) in students 17–25 years of age. At day 21 after the first MenB-4C dose, we observed protective human serum bactericidal titers ≥4 to MenB strains 5/99, H44/76, and NZ 98/254 in 98%–100% of participants. Geometric mean titers increased >22-fold over baseline. At day 180, >95% of participants sustained protective titers regardless of their vaccine schedule. The most common adverse event was injection site pain. An accelerated MenB-4C immunization schedule could be considered for rapid control of campus outbreaks.

Campus outbreaks of meningococcal disease caused by *Neisseria meningitidis* serogroup B (MenB) are rare, but case-fatality rates are 5.3%–10.0%, and 10%–20% of survivors have long-term health effects (*1*). In addition, MenB outbreaks cause public distress and anxiety (*2*). Enhanced person-to-person transmission among young persons living in close quarters and having close social contacts on college campuses is thought to increase risk of outbreaks (*3*). During 2008–2017, a total of 12 campus-based clusters of MenB occurred at residential universities in North America (*4*), 11 in the United States (*4*) and 1 in Canada (*5*).

The public health response to a MenB outbreak includes education about prevention and early recognition of disease, antimicrobial drug prophylaxis for close contacts, and either preexposure or early postexposure vaccination (*3*). Two MenB vaccines are now available, a 4-component protein-based vaccine (MenB-4C [Bexsero; GlaxoSmithKline, https://www.gsk.com]) and a bivalent factor H binding protein-based vaccine (MenB-FHbp [Trumenba; Pfizer Inc., https://www.pfizer.com]). In Canada, MenB-4C was approved for use in 2013 for persons 2 months–17 years of age. MenB-4C is given as 2 doses ≥1 month apart (*6*). MenB-FHbp was authorized in 2017 and is given as 3 doses at 0, 1–2, and 6 months, or 2 doses 6 months apart. During MenB outbreaks, MenB-4C has been administered in 2 doses at varying schedules, including 0 and 30 days, 0 and 6–8 weeks, 0 and 2 months, and 0 and 10 weeks (*7*–*9*). However, few controlled studies have investigated the immunogenicity and reactogenicity of MenB-4C in older adolescents and young adults to compare various vaccination schedules (*10*–*13*).

Management of organization-based outbreaks on college campuses demands considerable resources (*3*,*14*), and disease transmission must be interrupted

Author affiliations: Canadian Center for Vaccinology, Dalhousie University, IWK Health Centre, and Nova Scotia Health Authority, Halifax, Nova Scotia, Canada (J.M. Langley, S.A. Halperin, J. Mutch, S.A. McNeil, D. MacKinnon-Cameron, L. Ye); Vaccine Evaluation Center, University of British Columbia, Vancouver, British Columbia, Canada (S. Gantt, J.A. Bettinger, K. Marty, D. Scheifele); University of Montreal, Montreal, Quebec, Canada (C. Quach); Research Institute of the McGill University Health Centre, Montreal, Quebec, Canada (C. Quach, B.J. Ward); University of Calgary, Calgary, Alberta, Canada (E. Brown, J. Alcantara)

DOI: https://doi.org/10.3201/eid2603.190160

[1]Preliminary results from this study were presented at IDWeek, October 26–30, 2016, New Orleans, LA, USA; and at the Meningitis Research Foundation Conference, November 14–15, 2017, London, England, UK.

quickly. A shorter dosing schedule might provide more rapid individual direct protection and be easier to schedule around exams and school breaks. When MenB-4C vaccine was authorized in Canada, public health stakeholders identified a need to assess shorter dosing schedules for outbreak control to reduce the strain on public health resources by implementing the vaccine campaign in a single condensed period instead of 2 separate deployments. In a study supported by the Canadian Immunization Research Network (CIRN), we compared immunogenicity and tolerability of an accelerated MenB-4C vaccine schedule of 2 doses at 0 and 21 days to a longer interval of 0 and 60 days to facilitate outbreak control.

Methods

We conducted a randomized, 1:1, observer-blind, controlled clinical trial to evaluate reactogenicity and immunogenicity of MenB-4C in 2 different vaccine schedules in Canada. We enrolled participants in Halifax, Nova Scotia; Montreal, Quebec; and Vancouver, British Columbia, during September 21–October 27, 2015. The last participant completed the final visit, day 180, on April 28, 2016.

The study was performed in compliance with Good Clinical Practice guidelines ICH E6 (R2), the World Medical Association Declaration of Helsinki (https://www.wma.net), and national regulatory requirements of Canada. The study protocol was approved by local institutional review boards in each city. The trial is registered at ClinicalTrials.gov (https://clinicaltrials.gov) under NCT02583412.

Participants

We recruited study volunteers by advertising through social and traditional media on university campuses and through electronic mail to distribution lists of each study site. Eligible participants were 17–25 years of age, in good health, and attending school or university during the 2015–16 academic year. Volunteers were excluded if they were pregnant, planning pregnancy during the study period, or lactating; if they had a known medical illness, immunodeficiency, or autoimmune disease; if they previously received a MenB vaccine or had bacteriologically confirmed *N. meningitidis* disease; or if they had hypersensitivity to any components of vaccine products of MenB-4C or hepatitis A vaccine (HAV) used in the study.

Vaccines

MenB-4C contains 4 *N. meningitidis* protein antigens adsorbed on aluminum hydroxide: factor H binding protein (fHbp), Neisserial adhesin A (NadA), Neisserial heparin binding antigen (NHBA), and Porin A P1.4 (PorA) from outer membrane vesicles. MenB-4C is provided in a sterile suspension for intramuscular injection of 0.5 mL/dose (*6*). For control, we used the HAV vaccine Havrix (GlaxoSmithKline Inc.). Havrix contains formaldehyde-inactivated hepatitis A virus adsorbed onto aluminum hydroxide and is provided in a sterile suspension for intramuscular injection in the deltoid of 1.0 mL/dose for this age group (*15*). Both vaccines are stored at 2°C–8°C. The first dose was given in the nondominant arm and the second dose was given in the contralateral arm.

Study Procedures

Participants went to the study site on days 0, 21, 42, 60, 81, and 180. After the study nurse determined eligibility, obtained signed informed consent, and collected demographic characteristics on day 0, participants were randomly allocated 1:1 to the accelerated or longer intervals in blocks of 4 by site. On day 0, all participants received an unblinded first dose of MenB-4C vaccine. On day 21, participants received a second, blinded injection of MenB-4C if they were in the accelerated vaccine schedule group or HAV if they were in the longer interval group. On day 60, the accelerated schedule participants received HAV and the longer interval participants received MenB-4C. Study nurses drew 13 mL of blood at each visit to evaluate human serum bactericidal assay (hSBA) and factor H responses.

At days 21 and 60, an unblinded nurse concealed vaccine identity from participants by covering the vaccine label, laying an opaque cloth over the administration tray, and prohibiting anyone except the unblinded nurse in the room with the participant for vaccine administration. The study participant was not told whether the vaccination was MenB-4C or HAV at the time of the observer-blinded injections. Participants who had not completed a prior 2-dose series of HAV were offered the second dose beginning at day 236.

Outcome Measures

Our primary objective was to measure protective immune responses to the MenB vaccine by using hSBA titers against 3 meningococcal strains: strain New Zealand (NZ) 98/254 for the PorA P1.4 antigen of outer membrane vesicles, strain 5/99 for NadA, and strain H44/76 for fHbp. We did not evaluate the immune response to the NHBA component of the vaccine because a suitable indicator strain that matches this component is not available.

The US Food and Drug Administration noted the unavailability of a suitable strain for assessing bactericidal activity of NHBA-specific antibodies in its licensing correspondence (*16*).

Dominique A. Caugant of the World Health Organization Collaborating Centre for Reference and Research on Meningococci at the Norwegian Institute of Public Health provided *N. meningitidis* serogroup B strains NZ 98/254, 5/99, and H44/76. The Alberta Children's Hospital Research Institute of the University of Calgary performed hSBA by using standard methods (*17*) and human serum as a complement source. Laboratory staff were unaware of study group assignment. We assessed immune responses before MenB-4C vaccine and on days 21, 42, 81, and 180.

Our secondary objective was to compare the reactogenicity of MenB-4C given in an accelerated schedule to dosing on a longer interval. Study participants reported on solicited local adverse events (AE), such as redness, swelling, and pain, and on systemic AEs, including fever, drowsiness, nausea, diarrhea, vomiting, and generalized muscle aches. Participants recorded severity of AEs 0–6 days after each vaccination on a memory aid provided by study nurses (Appendix Table 1, https://wwwnc.cdc.gov/EID/article/26/3/19-0160-App1.pdf). Participants also recorded unsolicited AEs 0–21 days after each vaccination on a memory aid. Serious AEs were collected throughout the study.

We selected the sample size of 60 participants/study group on the basis of feasibility. Previous studies of MenB-4C in adolescents indicated that high bactericidal activity was likely after 1 vaccine dose (*18*). By using a margin of noninferiority of 0.15, and assuming that the probability of achieving a 1:4 hSBA titer with the standard schedule was 0.95, we estimated a sample size of 60 participants/group to provide a power of >0.76 to declare noninferiority, if the probability of 1:4 activity with the accelerated schedule was >0.91.

We considered all participants who received ≥1 dose of vaccine part of the total vaccinated cohort (TVC). We also had an according to protocol (ATP) cohort, which included all participants in the TVC who met the inclusion criteria and received vaccination according to the administration route and vaccination site of the protocol through the end of the study.

We assessed baseline comparability of treatment groups by using binomial estimates and Fisher exact test for binary variables and Student *t*-tests and CIs for continuous variables. We analyzed continuous variables of point estimates and interval estimates for means, and assessed differences between groups by using Student *t*-test and analysis of variance.

We calculated geometric mean titers (GMTs) for hSBA and 2-sided 95% CIs by group. We calculated hSBA results by using the proportion of participants at each serologic point with a titer >1:4, which is considered protective against each MenB strain (*19*). We did not stratify the analysis by baseline titer.

We used the Fisher exact test to assess differences in rates of solicited adverse events between treatment groups. We performed all statistical analyses by using 2-sided tests with a type I error of 5%. We did not include missing values in the analyses, imputation of missing values, or adjustments for multiple comparisons. We used a secure, internet-based data management platform (Dacima Software, https://www.dacimasoftware.com) to assemble study data and SAS version 9.4 or higher (SAS Institute, Inc., https://www.sas.com) to conduct analyses.

Results

Among 121 participants, we had a retention rate of 99% (119/121); 2 participants did not complete follow-up. We had 116 participants in the ATP cohort and we analyzed results from 58 participants in each vaccination group (Figure 1).

Of 121 participants, 84 were female and 37 male. We allocated 60 participants to the accelerated vaccine group and 61 to the longer interval group according to the study protocol. The mean age for participants was 21.4 years. Participant's body mass index, tobacco exposure, concomitant medication use, concurrent health conditions, and previous receipt of nonserogroup B meningococcal vaccines were similar between the 2 study groups (Table 1).

Immunogenicity

At baseline, participants had hSBA titers against all 3 strains, but titers were lowest for strain H44/76 (≥20.7%) and highest for strain 5/99 (<89.7%). Titers rose quickly after the first MenB-4C dose; 98%–100% of participants had titers ≥1:4 for all 3 antigens by day 21 (Table 2; Figure 2). The lower limit of the 95% CI for any hSBA strain at day 21 was 90.8% (Table 2). Titers remained high in >95% of participants in both study groups at day 180.

GMTs increased up to 22-fold from baseline 21 days after the first dose of MenB-4C (Table 3). At day 42, GMTs to the NZ 98/254 and the H44/76 strains were much higher for participants in the accelerated schedule group than for those in the longer interval, but both groups had similar GMTs to all 3 strains thereafter (Table 3; Figure 3).

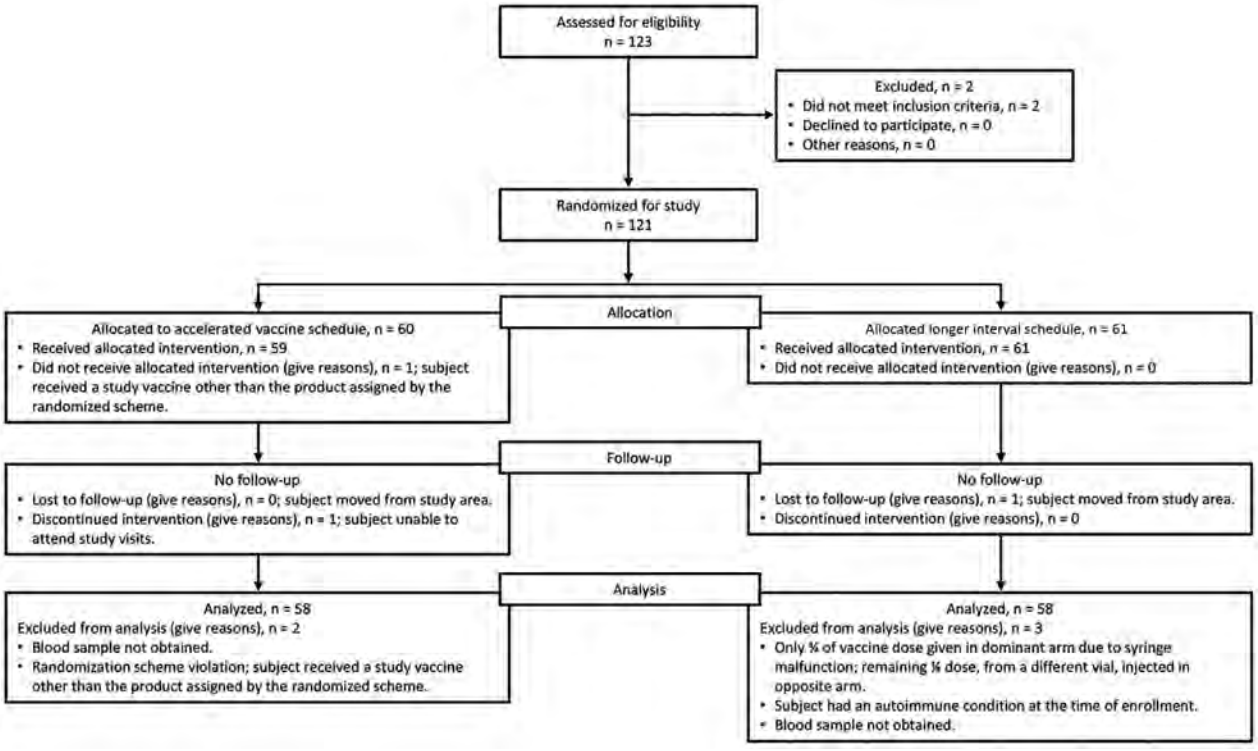

Figure 1. Flowchart of participant inclusion and follow-up for a trial of 4-component protein-based meningococcal B vaccine, Canada.

We compared the percentage of participants achieving an hSBA titer >1:4 to the 3 MenB-4C strains in the accelerated schedule group against the longer interval group at each study visit (Appendix Table 2). We found the schedules were at all points comparable to the longer interval after vaccination.

Reactogenicity

The most common solicited injection site AE was pain, which occurred in 95%–100% of participants after each dose of MenB-4C, and 8.3–32.8% of participants rated their pain as grade 3, interferes with normal activity (Figure 4, panel A). Of participants receiving HAV, 30%–46.6% reported injection site pain; none reported grade 3 pain. The most common systemic AE was muscle aches, reported by 46.7%–55.2% of MenB-4C recipients and 11.7%–24.1% of HAV recipients. In the accelerated schedule group, 2 participants had fever after the second dose of MenB-4C (Figure 4, panel B). The rate of unsolicited

Table 1. Characteristics of study participants in trial of MenB-4C vaccine, Canada*

Characteristic	Study groups		Total	p value
	Accelerated	Longer interval		
Mean age, y (SD)	21.2 (2.9)	20.7 (2.9)	20.6 (2.9)	0.44
Age range, y†	17–26	1 –26	17– 6	
Sex, no. (%)				
M	18 (30)	19 (31.1)	37 (30.6)	1.0
F	42 (70)	42 (68.9)	84 (69.4)	
Body mass index, median	23	22.8	22.9	0.17
Concurrent health conditions, no. (%)‡	29 (48.3)	49 (30)	59 (48.8)	1.0
Concomitant medication, no. (%)§	50 (83.3)	52 (85.2)	102 (84.3)	0.8
Tobacco use, no. (%)	9 (15)	8 (13.1)	17 (14.1)	0.79
Prior receipt of non-MenB vaccine, no. (%)#	49 (90.7)	46 (90.2)	95 (90.5)	1.0

*The accelerated schedule was MenB-4C vaccine at 0 and 21 days. The longer interval schedule was MenB-4C vaccine at 0 and 60 days. MenB, *Neisseria meningitidis* serotype B; MenB-4C, 4-component protein-based menB.
†The first day of the birth month used to calculate age for inclusion criteria of 17–25 years of age,
‡The most common medical conditions were asthma, migraine headaches, seasonal allergies, and musculoskeletal complaints.
§The most common concomitant medications were annual influenza vaccine, contraceptive medications, over-the-counter pain and cold preparations, and asthma and allergy medications.
#In Canada, the public health vaccine program includes a monovalent meningococcal C conjugate vaccine at 12 months of age and quadrivalent or monovalent meningococcal C conjugate vaccine in adolescence.

Table 2. Percentage of participants with hSBA titers ≥1:4 by strain in a trial of MenB-4C vaccine from day 0 to day 180, Canada*

Meningococcal strain	Participants with hSBA, % (95% CI)				
	Day 0	Day 21	Day 42	Day 81	Day 180
5/99					
Accelerated	67.2 (53.7–79.0)	100 (93.8–100)	100 (93.7–100)	100 (93.7–100)	100 (93.7–100)
Longer interval	89.7 (78.8–96.1)	98.3 (90.8–100)	98.3 (90.8–100)	100 (93.8–100)	100 (93.7–100)
H44/76					
Accelerated	20.7 (11.2–33.4)	98.3 (90.8–100)	98.2 (90.6–100)	98.2 (90.6–100)	96.5 (87.9–99.6)
Longer interval	43.1 (30.2–56.8)	98.3 (90.8–100)	96.6 (88.1–99.6)	100 (93.8–100)	100 (93.7–100)
NZ98/254					
Accelerated	51.7 (38.2–65.0)	98.3 (90.8–100)	100 (93.7–100)	100 (93.7–100)	98.2 (90.6–100)
Longer interval	65.5 (51.9–77.5)	100 (93.8–100)	100 (93.8–100)	100 (93.8–100)	98.2 (90.6–100)

*The accelerated schedule was MenB-4C vaccine at 0 and 21 days. The longer interval schedule was MenB-4C vaccine at 0 and 60 days. 5/99, Neisserial adhesin A surface proteins; H44/76, factor H binding protein; hSBA, human serum bactericidal antibody; MenB, *Neisseria meningitidis* serotype B; MenB-4C, 4-component protein-based menB; NZ98/254, New Zealand outer membrane vesicle.

AEs did not differ by dosing schedule or dose (data not shown). One participant had a serious AE (fractured patella) unrelated to vaccination.

Discussion

Invasive meningococcal disease outbreaks cause high levels of distress about the risk for secondary cases from common affiliation in the organization or by a shared, geographically defined community where the outbreak is occurring (*3*). Investigating and managing suspected outbreaks is a time-consuming and resource-intensive effort (*14*). When resources are directed to a mass vaccination program, other public health or healthcare delivery activities might be suspended. Mass vaccination programs in educational settings require planning around midterm and final examinations, school breaks, and the academic year. Immunization programs that rely on multiple doses of vaccine given months apart are even more challenging.

A variety of MenB-4C dosing intervals, from 30–70 days, have been used to control meningococcal outbreaks on college campuses since the vaccine's licensure. Limited data have been reported on the immunogenicity of these schedules among students 17–25 years of age (*13*), and few studies have assessed

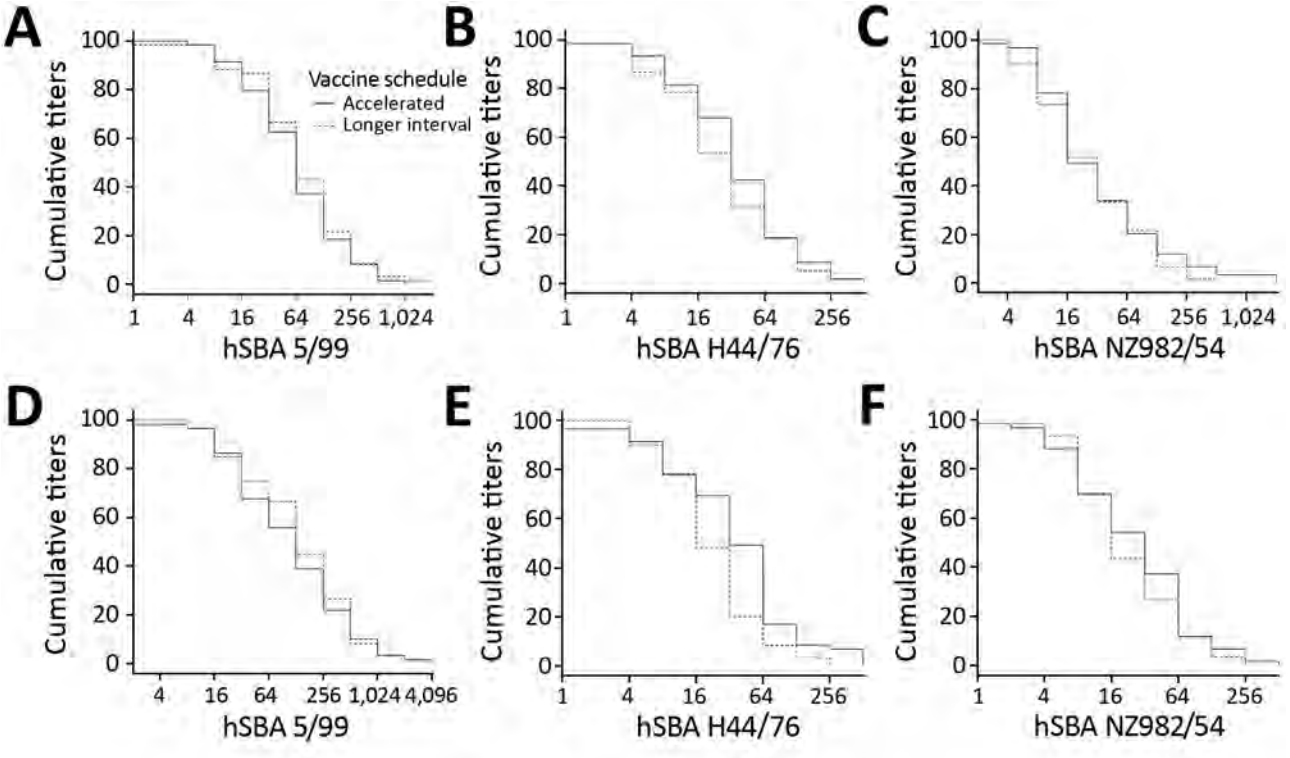

Figure 2. Reverse cumulative distribution curves of hSBA titers to 3 vaccine strains in recipients in trial of 4-component protein-based meningococcal B vaccine administered at 0 and 21 days compared with 0 and 60 days, Canada. A-C) Comparisons made at day 21. D-F) Comparisons made at day 180. hSBA, human serum bactericidal antibody; hSBA 5/99, Neisserial adhesin A surface proteins; hSBA H44/76, factor H binding protein; hSBA 982/54, New Zealand outer membrane vesicle.

Table 3. Geometric mean titers of human serum bactericidal antibody to meningococcal B strains in recipients of a longer interval dosing schedule compared with an accelerated dosing schedule in a trial of MenB-4C vaccine, from day 0 to 180 postvaccine, Canada*

MenB strain	Geometric mean titers (95% CI)				
	Day 0	Day 21	Day 42	Day 81	Day 180
5/99					
Accelerated	5.86 (4.03–8.54)	63.24 (45.87–87.19)	310.99 (207.74–465.55)	262.30 (183.72–374.50)	114.73 (79.32–165.95)
Longer interval	9.34 (6.78–12.87)	74.76 (52.86–105.72)	162.56 (114.85–230.09)	482.30 (15.61–737.02)	144.55 (99.88–209.2)
H44/76					
Accelerated	1.50 (1.25–1.80)	34.38 (24.93–47.42)	79.66 (54.86–115.67)	77.75 (54.02– 111.90)	35.7 (24.8– 51.39)
Longer interval	2.10 (1.66– 2.66)	27.40 (19.74–38.01)	22.9 (15.68–33.45)	85.26 (62.47–116.37)	23.33 (17.94–3.33)
NZ98/254					
Accelerated	3.08 (2.29–413)	32.38 (22.19–47.25)	75.88 (53.30–108.02)	48.98 (33.12–72.43)	25.71 (18.38–35.96)
Longer interval	4.05 (3.00–5.47)	28.06 (20.28–38.82)	25.81 (19.35–34.42)	69.58 (51.27–94.45)	22.22 (16.41–30.09)

*Geometric mean titers of serum bactericidal antibody using human serum as a complement source. 5/99, Neisserial adhesin A surface proteins; H44/76, factor H binding protein; hSBA, human serum bactericidal antibody; MenB, *Neisseria meningitidis* serotype B; MenB-4C, 4-component protein-based menB; NZ98/254, New Zealand outer membrane vesicle.

duration of protection. Shorter dosing schedules can improve compliance and lead to higher vaccine coverage (*11*). An accelerated dosing schedule for MenB-4C vaccine in a campus setting would reduce the time required to conduct the vaccine campaign and the resources required.

We conducted a randomized, controlled, multicenter study in students 17–25 years of age in Canada to assess an accelerated MenB-4C schedule of 2 doses administered 21 days apart. We found the accelerated schedule produced high immunogenicity comparable to 2 doses administered 60 days apart. We observed that >95% of participants in the accelerated and the longer interval groups had protective antibody responses at day 180. We did not observe an increase in AEs with the accelerated schedule, and the most frequent AEs were injection site pain and muscle aches, which were more common after MenB-4C than the control vaccine regardless of the vaccine schedule.

Baseline protective titers to the 3 MenB vaccine components among participants ranged from 20.7% to 89.9%. Naturally acquired serum antibodies can occur after asymptomatic nasopharyngeal carriage of pathogenic and nonpathogenic *Neisseria* strains, and cross-reacting antibodies might be elicited to non-*Neisseria* strains in the gut flora (*20*). Beginning in 2002, children in Canada have received an oligosaccharide meningococcal C protein conjugate vaccine (MenC) at 12 months of age. Provincial and territorial programs in Canada provide a MenC vaccine or a quadrivalent MenC-ACYW-135 vaccine to adolescents. The participants in our study likely would have had exposure only to a MenC vaccine. The possibility that exposure to either of these vaccines can induce cross-reactive antibodies to MenB-4C vaccine components is unknown.

Although the approved schedule for MenB-4C vaccine is 2 doses, we noted a rapid and robust immune response to the first dose of MenB-4C vaccine in our study group by day 21. We hypothesize that a single dose could be considered for the purpose of outbreak management in persons 17–25 years of age when short-term protection is needed during an academic year. No direct evidence has been reported on the duration of individual protection against invasive meningococcal disease in this age group after a single

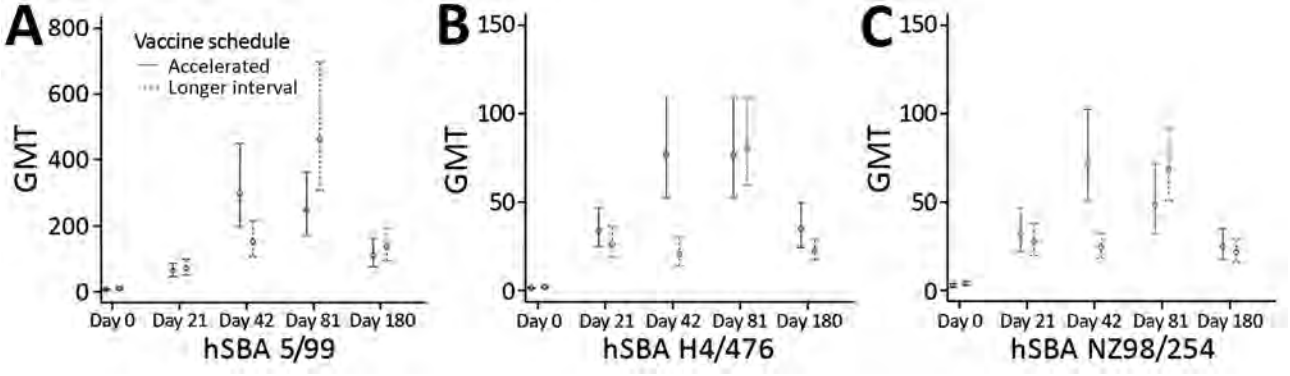

Figure 3. GMTs of hSBA titers to 3 vaccine strains in recipients in trial of 4-component protein-based meningococcal B vaccine administered at 0 and 21 days compared with 0 and 60 days, Canada. A) hSBA 5/99; B) hSBA H44/76; C) hSBA 982/54. Error bars indicate 95% CIs. GMT, geometric mean titer; hSBA, human serum bactericidal antibody; hSBA 5/99, Neisserial adhesin A surface proteins; hSBA H44/76, factor H binding protein; hSBA 982/54, New Zealand outer membrane vesicle.

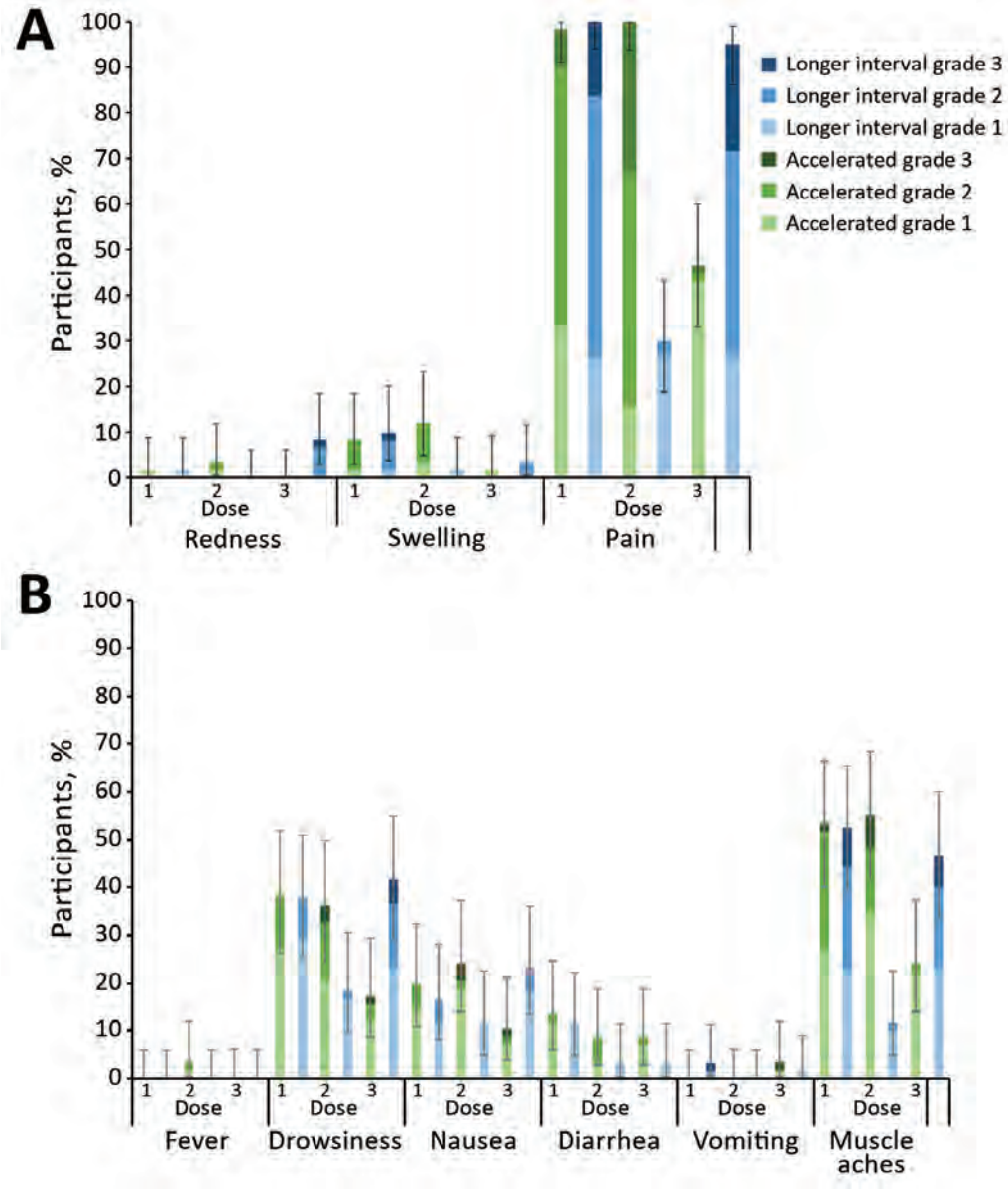

Figure 4. Percent of participants reporting solicited local and systemic adverse events on days 0 through 6 after each vaccine dose in trial of 4-component protein-based meningococcal B vaccine, Canada. A) Adverse events localized at injection site. B) General adverse events. Grade 1: mild, easily tolerated by participant; grade 2: moderate, sufficiently discomforting to interfere with normal everyday activities; grade 3: severe, prevents normal, everyday activities. Error bars indicate 95% CIs.

dose of MenB-4C vaccine. In a trial of children 11–17 years of age randomized to different schedules, investigators noted protective titers ≥4 in 69%–81% of 1-dose participants at 6 months (*18*). In that study, only 57% (95% CI 49%–65%) of participants who did not have protective titers at baseline had protective titers at 6 months.

Coverage for MenB in university-based mass immunization campaigns in the United States during 2013–2018 was variable; 14%–98% of the population received the first dose (*4*), and <50% of the population returned for the second dose in half of those campaigns. If future research demonstrates acceptable short-term protection and outbreak control with a single-dose strategy, resource and opportunity cost savings could allow investigators to focus on increasing coverage rates for the first dose.

Our study had some limitations. First, we assessed immunogenicity to MenB-4C vaccine by using hSBA responses to 3 reference strains, but these strains might differ in antigen expression from diverse circulating strains (*21*). However, even if responses to other strains had been tested, negative hSBA results do not necessarily indicate susceptibility to disease because the assay underestimates immunity (*22*–*24*). Second, we did not evaluate hSBA responses beyond 180 days, so the durability of protection beyond the study period and into the subsequent academic year is unknown.

In summary, we conducted a randomized, controlled, observer-blinded multicenter trial of MenB-4C

vaccination in students 17–25 years of age. We demonstrated that an accelerated immunization schedule of 0 and 21 days had comparable immunogenicity to a longer interval schedule of 0 and 60 days. We also observed that protective hSBA titers were sustained for >6 months. An accelerated vaccine schedule could be considered to control outbreaks, would be easier to schedule within the constraints of the academic year, and can optimize public health and campus resources by deploying human resources to implement the program in a condensed period. Our data support the use of an accelerated MenB-4C vaccine schedule of 2 doses given at 0 and 21 days to rapidly control meningococcal disease outbreaks on college campuses.

Funding for this study was provided by the Canadian Institutes for Health Research (CIHR) and the Public Health Agency of Canada (PHAC).

About the Author

Dr. Langley is a pediatric infectious disease physician and Professor of Pediatrics and Epidemiology based at the Dalhousie University Canadian Center for Vaccinology, and the lead for the Canadian Immunization Research Network Clinical Trials Network, which performed this study.

References

1. National Advisory Committee on Immunization. Canadian immunization guide for health professionals: meningococcal vaccine 2015 [cited 2018 November 28, 2018]. https://www.canada.ca/en/public-health/services/publications/healthy-living/canadian-immunization-guide-part-4-active-vaccines/page-13-meningococcal-vaccine.html
2. Schaffner W, Baker CJ, Bozof L, Engel J, Offit PA, Turner JC. Addressing the challenges of serogroup B meningococcal disease outbreaks on campuses: a report by the National Foundation for Infectious Diseases. Infect Dis Clin Pract. 2014;22:245–52. https://doi.org/10.1097/IPC.0000000000000197
3. US Centers for Disease Control and Prevention. Guidance for the evaluation and public health management of suspected outbreaks of meningococcal disease, version 1.0. Atlanta: The Centers; 2017.
4. Soeters HM, McNamara LA, Blain AE, Whaley M, MacNeil JR, Hariri S, et al.; Serogroup B Meningococcal Disease University Outbreak Group. University-based outbreaks of meningococcal disease caused by serogroup B, United States, 2013–2018. Emerg Infect Dis. 2019;25:434–40. https://doi.org/10.3201/eid2503.181574
5. Langley JM, MacDougall DM, Halperin BA, Swain A, Halperin SA, Top KA, et al. Rapid surveillance for health events following a mass meningococcal B vaccine program in a university setting: A Canadian Immunization Research Network study. Vaccine. 2016;34:4046–9. https://doi.org/10.1016/j.vaccine.2016.06.025
6. Novartis Vaccines and Diagnostics Inc. Product Monograph. Bexsero multicomponent meningococcal B vaccine (recombinant, adsorbed). Mississauga (ON, Canada): GlaxoSmithKline Inc.; 2013.
7. Patel M. Outbreaks of serogroup B meningococcal disease on university campuses–2013. Presented at: Advisory Committee on Immunization Practices Meeting on Meningococcal Vaccines, February 26, 2014 [cited 2015 Feb 20]. https://stacks.cdc.gov/view/cdc/62196
8. McNamara LA, Shumate AM, Johnsen P, MacNeil JR, Patel M, Bhavsar T, et al. First use of a serogroup B meningococcal vaccine in the US in response to a university outbreak. Pediatrics. 2015;135:798–804. https://doi.org/10.1542/peds.2014-4015
9. Basta NE, Mahmoud AA, Wolfson J, Ploss A, Heller BL, Hanna S, et al. Immunogenicity of a meningococcal B vaccine during a university outbreak. N Engl J Med. 2016;375:220–8. https://doi.org/10.1056/NEJMoa1514866
10. Meningococcal B Pilot Project Task Group. The recommended use of the multicomponent meningococcal B (4CMenB) vaccine in Canada: a common guidance statement. Ottawa (ON, Canada): Pan-Canadian Public Health Network; 2014.
11. Nolan T, O'Ryan M, Wassil J, Abitbol V, Dull P. Vaccination with a multicomponent meningococcal B vaccine in prevention of disease in adolescents and young adults. Vaccine. 2015;33:4437–45. https://doi.org/10.1016/j.vaccine.2015.06.011
12. Bexsero (Meningococcal Group B Vaccine) suspension, for intramuscular injection [package insert]. Research Triangle Park (NC, USA): GlaxoSmithKline; 2018.
13. Flacco ME, Manzoli L, Rosso A, Marzuillo C, Bergamini M, Stefanati A, et al. Immunogenicity and safety of the multicomponent meningococcal B vaccine (4CMenB) in children and adolescents: a systematic review and meta-analysis. Lancet Infect Dis. 2018;18:461–72. https://doi.org/10.1016/S1473-3099(18)30048-3
14. Ritscher AM, Ranum N, Malak JD, Ahrabi-Fard S, Baird J, Berti AD, et al. Meningococcal serogroup B outbreak response University of Wisconsin-Madison. J Am Coll Health. 2018;67:191–6. http://doi.org/10.1080/07448481.2018.1469502
15. Harvix [package insert]. Mississauga (ON, Canada): GlaxoSmithKline Inc; 2011.
16. US Food and Drug Administration. Bexsero—summary basis for regulatory action. Washington: The Administration; 2015.
17. Maslanka SE, Gheesling LL, Libutti DE, Donaldson KB, Harakeh HS, Dykes JK, et al. Standardization and a multilaboratory comparison of *Neisseria meningitidis* serogroup A and C serum bactericidal assays. The Multilaboratory Study Group. Clin Diagn Lab Immunol. 1997;4:156–67.
18. Santolaya ME, O'Ryan ML, Valenzuela MT, Prado V, Vergara R, Muñoz A, et al.; V72P10 Meningococcal B Adolescent Vaccine Study group. Immunogenicity and tolerability of a multicomponent meningococcal serogroup B (4CMenB) vaccine in healthy adolescents in Chile: a phase 2b/3 randomised, observer-blind, placebo-controlled study. Lancet. 2012;379:617–24. https://doi.org/10.1016/S0140-6736(11)61713-3
19. Frasch CE, Borrow R, Donnelly J. Bactericidal antibody is the immunologic surrogate of protection against meningococcal disease. Vaccine. 2009;27(Suppl 2):B112–6. https://doi.org/10.1016/j.vaccine.2009.04.065
20. Granoff DM, Pelton S, Harrison LH. Meningococcal vaccines. In: Plotkin SA, Orenstein WA, Offit PA, editors. Vaccines. Philadelphia: Elsevier Inc; 2008. p. 388–418.

21. Poolman JT, Richmond P. Multivalent meningococcal serogroup B vaccines: challenges in predicting protection and measuring effectiveness. Expert Rev Vaccines. 2015; 14:1277–87. https://doi.org/10.1586/14760584.2015.1071670
22. Welsch JA, Granoff D. Immunity to *Neisseria meningitidis* group B in adults despite lack of serum bactericidal antibody. Clin Vaccine Immunol. 2007;14:1596–602. https://doi.org/10.1128/CVI.00341-07
23. Rappuoli R. Meningococcal B vaccine during a university outbreak. N Engl J Med. 2016;375:1594–5. https://doi.org/10.1056/NEJMc1610666
24. Goldschneider I, Gotschlich EC, Artenstein MS. Human immunity to the meningococcus. I. The role of humoral antibodies. J Exp Med. 1969;129:1307–26. https://doi.org/10.1084/jem.129.6.1307

Address for correspondence: Joanne M. Langley, Dalhousie University and IWK Health Center, Division of Infectious Diseases, Department of Pediatrics, 5850 University Ave, POB 9700, Halifax, NS B3K 6R8 Canada; email: joanne.langley@dal.ca

Human Immune Responses to Melioidosis and Cross-Reactivity to Low-Virulence *Burkholderia* Species, Thailand[1]

Patpong Rongkard, Barbara Kronsteiner, Viriya Hantrakun, Kemajittra Jenjaroen, Manutsanun Sumonwiriya, Panjaporn Chaichana, Suchintana Chumseng, Narisara Chantratita, Vanaporn Wuthiekanun, Helen A. Fletcher, Prapit Teparrukkul, Direk Limmathurotsakul, Nicholas P.J. Day, Susanna J. Dunachie

Melioidosis is a neglected tropical disease with an estimated annual mortality rate of 89,000 in 45 countries across tropical regions. The causative agent is *Burkholderia pseudomallei*, a gram-negative soil-dwelling bacterium. In Thailand, *B. pseudomallei* can be found across multiple regions, along with the low-virulence *B. thailandensis* and the recently discovered *B. thailandensis* variant (BTCV), which expresses *B. pseudomallei*–like capsular polysaccharide. Comprehensive studies of human immune responses to *B. thailandensis* variants and cross-reactivity to *B. pseudomallei* are not complete. We evaluated human immune responses to *B. pseudomallei*, *B. thailandensis*, and BTCV in melioidosis patients and healthy persons in *B. pseudomallei*–endemic areas using a range of humoral and cellular immune assays. We found immune cross-reactivity to be strong for both humoral and cellular immunity among *B. pseudomallei*, *B. thailandensis*, and BTCV. Our findings suggest that environmental exposure to low-virulence strains may build cellular immunity to *B. pseudomallei*.

Melioidosis is a neglected tropical disease with an estimated annual global mortality rate of 89,000 (*1*). Its cause is the gram-negative bacterium *Burkholderia pseudomallei*, which is found in environmental soil and water in Southeast Asia and northern Australia and is increasingly recognized across tropical regions (*2*). Known underlying risk factors that contribute to increased susceptibility to infection include diabetes, chronic kidney diseases, and alcohol abuse (*3*). The rapid expansion of type 2 diabetes, especially in low- and middle-income countries, is likely to exacerbate the situation further (*4*). In Thailand, *B. pseudomallei* is highly distributed in the environment in the northeast, where most of the country's melioidosis cases have been reported (*5*). However, *B. pseudomallei* is also isolated from soil in the eastern and central parts of Thailand. A closely related species of minimal virulence, *B. thailandensis*, and a *B. thailandensis* variant (BTCV) expressing the *B. pseudomallei*–like capsular polysaccharide (CPS) are also present in the soil in Thailand (*6*). The genomic composition of *B. thailandensis* shows >85% similarity with *B. pseudomallei* (*7*). However, there are a few key differences, including the lack of virulence factors, such as capsular polysaccharide, and the presence of the arabinose assimilation operon (*8*) in *B. thailandensis* and BTCV. The hybrid BTCV exhibits several features found in *B. pseudomallei*, including resistance to decomposition by the complement system, intracellular survival inside macrophages, and colony morphology that resembles that of *B. pseudomallei* (*9*). Although BTCV has acquired *B. pseudomallei*–like CPS gene clusters, it has been shown to be nonpathogenic in mouse models (*9*).

Immune cross-protection conferred by *B. thailandensis* variants has been demonstrated in animal models (*10*). In particular, mice immunized with the BTCV isolate E555 showed superior cross-protection to that from the noncapsulated strain against a lethal dose of *B. pseudomallei* challenge, resulting in high

Author affiliations: University of Oxford, Oxford, UK (P. Rongkard, B. Kronsteiner, N.P.J. Day, S.J. Dunachie); Mahidol-Oxford Tropical Medicine Research Unit, Bangkok, Thailand (P. Rongkard, V. Hantrakun, K. Jenjaroen, M. Sumonwiriya, P. Chaichana, S. Chumseng, N. Chantratita, V. Wuthiekanun, D. Limmathurotsakul, N.P.J. Day, S.J. Dunachie); Mahidol University, Bangkok (N. Chantratita, D. Limmathurotsakul); London School of Hygiene and Tropical Medicine, London, UK (H.A. Fletcher); Sunpasitthiprasong Hospital, Ubon Ratchathani, Thailand (P. Teparrukkul)

DOI: https://doi.org/10.3201/eid2603.190206

[1]Preliminary results from this study were presented at the European Melioidosis Congress, March 19–21, 2018, Oxford, UK.

CPS-specific IgG levels and decreased bacterial prevalence (*10*). To date, comprehensive immune cross-reactivity to *B. thailandensis* and BTCV has not been studied in humans.

Protective adaptive immunity in human melioidosis is complex, but defense against its intracellular pathogen is likely to require competent cellular immune responses largely mediated by T lymphocytes (*11*,*12*). Our team and others have shown that surviving melioidosis patients have elevated CD4 and CD8 T-cell–mediated interferon γ (IFN-γ) responses to *B. pseudomallei* compared with deceased case-patients (*13*,*14*). Along with key protective immunity conferred by cellular immune responses, humoral immunity against BP infection has been demonstrated to be a component of protection in rodent models (*15*), although antibody levels measured by indirect hemagluttination assay were not significantly associated with survival ($p>0.05$) in human patients after adjusting for other parameters (*16*). Our study aimed to characterize the relationship between the human *B. pseudomallei*–specific immune response and responses to *B. thailandensis* and BTCV. We evaluated humoral and cellular immune responses to *B. pseudomallei*, *B. thailandensis*, and BTCV in patients with acute melioidosis, in patients with other gram-negative bacterial infections, and in exposed populations in the endemic region with and without diabetes.

Materials and Methods

Study Design

We conducted a prospective observational study during 2015–2017 at Sunpasitthiprasong Hospital, Ubon Ratchathani, Thailand, to evaluate human immune responses to *B. pseudomallei*, *B. thailandensis*, and BTCV. We recruited 4 cohorts: inpatients >20 years of age who had culture-confirmed melioidosis (melioidosis cohort; n = 99), patients who had positive cultures for other gram-negative bacterial infections (OGNI cohort; n = 48), patients who attended the hospital's diabetes outpatient clinic for diabetes mellitus (DM cohort; n = 98), and healthy control participants from the melioidosis-endemic areas who were household contacts of the melioidosis case-patients (HH cohort; n = 96). The number of samples varied between assays due to sample availability (Table 1). We determined 28-day survival status using the hospital death records and by telephone. We collected blood samples during enrollment and processed them as described previously (*13*). We measured humoral and cellular immune responses using indirect hemagglutination assay (IHA), IgM and IgG ELISA, ex vivo IFN-γ enzyme-linked immunospot assay (IFN-γ ELISpot), and a whole-blood stimulation assay (WBA). The ethics committees of the Faculty of Tropical Medicine, Mahidol University (TMEC 12–014); Sunpasitthiprasong Hospital, Ubon Ratchathani (017/2559); and the Oxford Tropical Research Ethics Committee (OXTREC35–15) approved the study protocol.

Antigen Preparation

We prepared antigens in accordance with published methods, unless otherwise stated (*17*,*18*). For IHA, we used crude culture filtrate antigens from pooled isolates with the following specifications: *B. pseudomallei* Thai clinical isolates 199a and 207a (*19*), *B. thailandensis* Thai environmental isolates E264 (ATCC700388) and STBCC006 (*20*), and BTCV Thai environmental E555 and USA clinical isolate CDC3015869. We prepared *B. thailandensis* and BTCV antigens following a traditional IHA antigen preparation as described previously (*17*). For ELISA, we prepared whole-cell heat-killed antigens from *B. pseudomallei* Thai clinical isolate K96243, BT E264, and BTCV E555 as described previously (*18*). For IFN-γ ELISpot and whole-blood stimulation assay, we used a single culture filtrate antigen of each strain, *B. pseudomallei* 199a, *B. thailandensis* E264, and BTCV E555.

IHA and ELISA

We determined serologic responses to *B. pseudomallei*, *B. thailandensis*, and BTCV by IHA, as well as IgM and IgG ELISA (*18*). We performed IHA as described previously (*17*), with an IHA titer of ≥1:80 considered positive (*21*).

IFN-γ ELISpot

We used a commercial IFN-γ ELISpot assay (Mabtech AB, https://www.mabtech.com) to quantify secreted

Table 1. Proportions of samples from 4 patient and control cohorts used to evaluate immune responses to melioidosis, Thailand*

Cohort	No. (%) samples by assay		
	IHA or ELISA	IFN-γ ELISpot	WBA
Melioidosis, n = 99	73 (74)	82 (83)	13 (13)
Healthy household contacts, n = 96	35 (36)	93 (97)	8 (8)
Diabetes control, n = 98	54 (55)	95 (97)	NA
Other gram-negative bacterial infections, n = 48	10 (20)	42 (88)	NA

*IFN-γ ELISpot, interferon-γ enzyme-linked immunospot assay; IHA, indirect hemagglutination assay; NA, not available; WBA, whole-blood stimulation assay.

IFN-γ from peripheral blood mononuclear cell (PBMC) in response to *B. pseudomallei*, *B. thailandensis*, and BTCV antigens as described previously (*13*). In brief, we added PBMC at a density of 2×10^5 cells per well to each of 2 antibody-coated plates and incubated them either in media only or in the presence of antigen for 18–20 h at 37°C: final concentration for *B. pseudomallei* was 88 μg/mL; for *B. thailandensis*, 78 μg/mL; for BTCV, 83 μg/mL; and for purified protein derivative (PPD), 20 μg/mL. We added 1 μg/mL of detector antibody and incubated for 3 h at room temperature, then for 2 h with streptavidin-conjugated ALP at room temperature. We used the AP Conjugate Substrate Kit (Bio-Rad, https://www.bio-rad.com) to develop spots for up to 20 min. We analyzed plates on the CTL ELISpot Reader (CTL Analyzers, http://www.immunospot.com) using the proprietary Smartcount automated settings. Results were reported as spot-forming units (SFU) per million PBMC. Background (PBMC in media only) responses in unstimulated control wells were typically <20 spots and were subtracted from those measured in antigen-stimulated wells. We used phytohemagglutinin (PHA) at a concentration of 10 μg/mL as a positive control.

WBA

For antigen stimulation, we added 500 μL heparinized blood to a 5 mL polystyrene round-bottom tube (Corning, https://www.corning.com) containing a final concentration of 1 μL/mL anti-human CD28 and CD49d (Becton Dickinson, https://www.bd.com), along with *B. pseudomallei*, *B. thailandensis*, or BTCV antigens, all at a final concentration of 1 mg/mL. We used staphylococcal enterotoxin B (SEB) at a final concentration of 10 μg/mL as positive control and RPMI medium supplemented with 10% fetal bovine serum (FBS) (R10 medium) as negative control. We incubated the tubes at 37°C, 5% CO_2, 95% humidity. After 18 h, we added a final concentration of 10 μL/mL Brefeldin A (eBioscience, https://www.thermofisher.com) and incubated the assay for another 4–5 h under the same conditions. We then incubated samples with Live/Dead (LD) Fixable Near-IR Dead Cell Stain (Life Technologies, https://www.thermofisher.com) according to the manufacturer's instructions, followed by a single 10-min incubation with FACS Lysing solution at room temperature for red cell removal (Becton Dickinson). We cryopreserved lysed blood cells in FBS with 10% dimethylsulfoxide (DMSO) (Sigma Aldrich, https://www.sigmaaldrich.com) and stored at –80°C until flow cytometry staining.

Flow Cytometry

We thawed frozen cells at 37°C and washed them twice with R10 medium, then fixed for 20 min followed by 5 min of permeabilization using BD Cytofix/Cytoperm kit (Becton Dickinson). Then, we stained samples with fluorescently labeled human antibodies for 20 min on ice in the dark: CD3-PerCP (clone: UCHT1; BioLegend, https://www.biolegend.com), CD4-V450 (clone: L200, Becton Dickinson), CD8-BV510 (clone: RPA-T8; BioLegend), CD56-VioBrightFITC (clone: AF12–7H3; Miltenyi Biotec, https://www.miltenyibiotec.com), and IFN-γ-PE (clone: 4S.B3; BioLegend). We then analyzed using a MACSQuant Analyzer 10 (Miltenyi Biotec) and performed flow cytometry analysis using FlowJo software version 10.2 on Mac OS X (Becton Dickinson, https://www.flowjo.com).

Statistical Analysis

The outcomes of interest were correlation between level of immune responses (measured by IHA titers, optical density of IgM and IgG by ELISA and levels of cytokine-producing cells, and IFN-γ SFU) against 3 antigens: *B. pseudomallei*, *B. thailandensis*, and BTCV. We used Spearman's correlation coefficient (ρ) to determine the correlation between the levels of immune responses against the 3 antigens. We compared ordinal and continuous variables using a nonparametric Mann-Whitney test (comparing 2 independent groups) and Wilcoxon matched-pairs signed rank test (comparing multiple tests on matched cases). We performed all statistical tests using GraphPad Prism version 7.0b for Mac OS X (GraphPad Software, https://www.graphpad.com).

Results

Participants

We enrolled a total of 100 patients with culture-confirmed melioidosis during April 2016–November 2017 into the melioidosis cohort. We excluded 1 patient because of a positive concurrent diagnosis of tuberculosis. We recruited participants at a median of 5 days after admission (interquartile range [IQR] 4–6 days) (Table 2). Diabetes was an underlying condition for two thirds (67%) of the melioidosis cohort. The overall 28-day mortality rate was 30% (30/99), with no significant difference ($p = 0.9$) for patients with and without diabetes.

Humoral Immune Responses by IHA against *B. pseudomallei*, *B. thailandensis*, and BTCV

We observed seropositivity against *B. pseudomallei* in 58% (42/73) of the melioidosis cohort, 26% (9/35) of

Table 2. Characteristics of patients and controls in study of immune responses to melioidosis and cross-reactivity to low-virulence *Burkholderia* species, by cohort, Thailand*

Baseline characteristics	Cohort			
	Melioidosis, n = 99	Healthy controls, n = 96	Diabetes controls, n = 98*	Other gram-negative bacterial infections, n = 48
Sex				
M	63 (64)	27 (28)	25 (26)	27 (56)
F	36 (36)	69 (72)	73 (74)	21 (44)
Age, y, median (range)	55 (20–84)	48 (25–69)	53 (41–60)	64 (24–95)
Diabetes†	66 (67)	NA	98 (100)	NA
Died‡	30 (30)	NA	NA	NA
Survived	69 (70)	NA	NA	NA

*Values are no. (%) except as indicated.
†Includes patients who were previously diagnosed with diabetes or who have a hemoglobin A1C level ≥6.5% at time of recruitment.
‡Died within 28 days of study enrollment.

HH, 7% (4/54) of DM, and none (0/10) of OGNI. The median IHA titer against *B. pseudomallei* in the melioidosis cohort (median 1:80, interquartile range [IQR] 1:10–1:320) was higher than that from all control cohorts (HH, median ≤1:10, IQR ≤1:10–1:80; DM and OGNI, median ≤1:10, IQR ≤1:10–1:10; p<0.01). We observed detectable IHA titer against BTCV only in the melioidosis cohort (median 1:80, IQR 1:10–1:320); this result was significantly higher than that for all control cohorts (p<0.01) (Figure 1). We observed strong correlation between *B. pseudomallei* and BTCV IHA in the melioidosis cohort (ρ = 0.96; p<0.01) and the HH cohort (ρ = 0.84; p<0.01). We observed moderate correlation between *B. pseudomallei* and *B. thailandensis* IHA (ρ = 0.53; p<0.01) only in the melioidosis cohort (Appendix Table 1, https://wwwnc.cdc.gov/EID/article/26/3/19-0206-App1.pdf). We detected no responses against *B. thailandensis* in any of the other cohorts (median ≤1:10).

Humoral Immune Responses by IgG and IgM ELISA against *B. pseudomallei*, *B. thailandensis*, and BTCV

The melioidosis cohort showed significantly higher IgG responses to *B. pseudomallei* (median of optical density [OD] = 1.42), *B. thailandensis* (median OD = 1.12), and BTCV (median OD = 1.43) than any of the control cohorts (p<0.01) (Figure 2, panel A). IgM responses to *B. pseudomallei* (median OD = 0.48) in the melioidosis cohort, similar to IgG responses, were higher than the control cohorts (median OD ranges 0.19–0.28, p≤0.02). In contrast, IgM responses to *B. thailandensis* and BTCV in the melioidosis cohort were similar to responses in the HH cohort but higher than those in DM and OGNI (p<0.05) (Figure 2, panel B). In the melioidosis cohort, we observed a strong correlation from both IgM and IgG responses between *B. pseudomallei*, *B. thailandensis*, and BTCV (ρ>0.9; p<0.01) (Appendix Tables 2, 3).

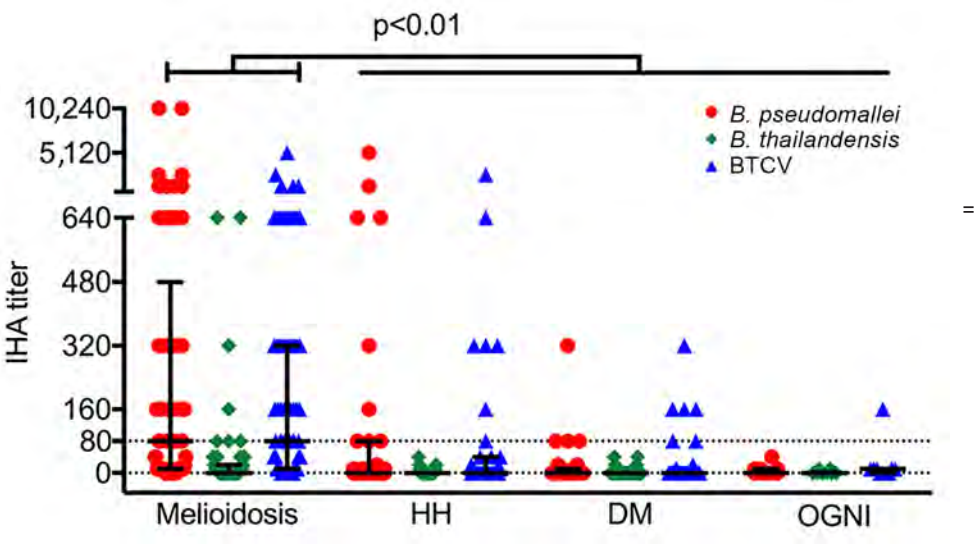

Figure 1. Humoral immune responses to *Burkholderia pseudomallei*, *B. thailandensis*, and BTCV by indirect hemagglutination assay, Thailand. IHA titers are shown for acute melioidosis patients (n = 73) and 3 control cohorts, HH (n = 35), DM (n 54), and OGNI (n = 10), against culture-filtrate antigen of *B. pseudomallei*, *B. thailandensis*, and BTCV. Each symbol represents an IHA titer response from a patient. Dotted line indicates the IHA cutoff titer for seropositivity. Medians (horizontal lines) and interquartile ranges (error bars) are provided. p values were calculated by using the nonparametric Mann-Whitney test. Horizontal bars at top of figure indicate comparisons across cohorts. BTCV, *B. thailandensis* CPS variant; CPS, capsular polysaccharide; DM, patients with diabetes mellitus; HH, healthy household contacts of the melioidosis case-patients; IHA, indirect hemagglutination assay.

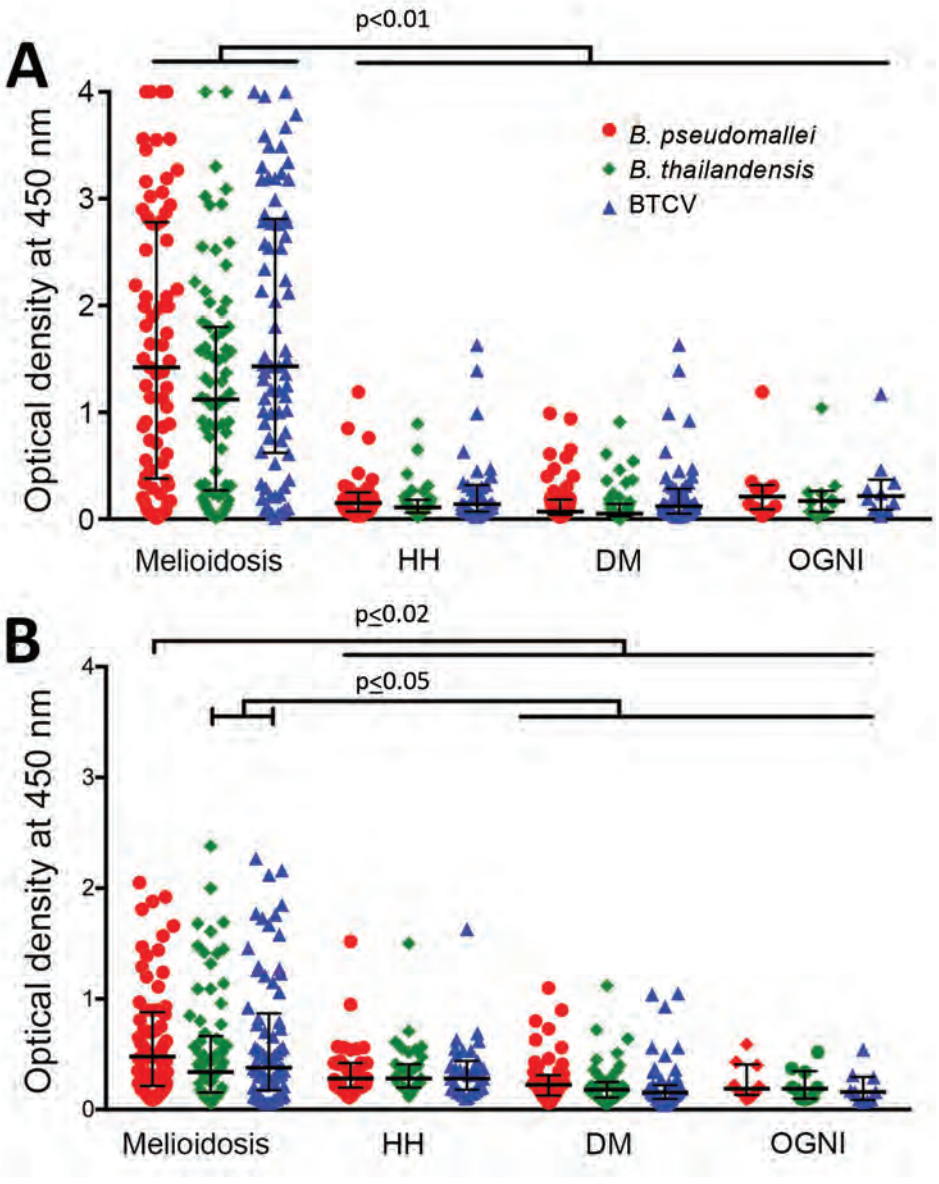

Figure 2. Human humoral immune responses to *Burkholderia pseudomallei*, *B. thailandensis*, and BCTV by IgG and IgM ELISAs, Thailand. IgG-specific (A) and IgM-specific (B) responses are shown for acute melioidosis patients (n = 73) and 3 control cohorts, HH (n = 35), DM (n = 54), and OGNI (n = 10), against culture-filtrate antigen of *B. pseudomallei*, *B. thailandensis*, and BTCV. Each symbol represents an IgM or IgG antibody response from a patient. Medians (horizontal lines) and interquartile ranges (error bars) are shown. p values were calculated by using the nonparametric Mann-Whitney test. Horizontal bars at top of figure indicate comparisons across cohorts. BTCV, *B. thailandensis* CPS variant; CPS, capsular polysaccharide; DM, patients with diabetes mellitus; HH, healthy household contacts of melioidosis case-patients.

Interferon-γ ELISpot Responses to *B. pseudomallei*, *B. thailandensis*, and BTCV

Quantitatively, IFN-γ responses against *B. pseudomallei* in the melioidosis and HH cohorts were significantly higher than those for the DM and OGNI cohorts ($p<0.03$). We observed similar outcomes in the responses to *B. thailandensis* and BTCV (Figure 3). Of interest, the melioidosis and HH cohorts showed comparable IFN-γ responses against *B. pseudomallei* and *B. thailandensis*, but not to BTCV ($p = 0.02$) (Figure 3). In the melioidosis cohort, we observed strong correlations between IFN-γ responses to *B. pseudomallei*, *B. thailandensis*, and BTCV ($\rho>0.9$; $p<0.01$). We observed similar correlations ($\rho>0.7$; $p<0.01$) for the HH, OGNI, and DM cohorts (Appendix Table 4).

Cellular Immune Responses to *B. pseudomallei*, *B. thailandensis*, and BTCV by Whole-Blood Stimulation Assay Using Flow Cytometry

To determine the contribution of CD4 T, CD8 T, DN T, and NK cells to total IFN-γ responses in the melioidosis and HH cohorts, we performed multicolor flow cytometry on WBA samples. In the melioidosis cohort, about half of the IFN-γ responses, on average, came from CD4 T cells for all 3 *Burkholderia* antigens (Figure 4), which was significantly higher than for the HH cohort ($p<0.03$), suggesting a strong contribution of antigen-specific memory responses (Appendix Figure 1, panels A, E). In contrast, the IFN-γ responses in the HH cohort were primarily driven by NK cells (about one third), followed by a balanced mix of

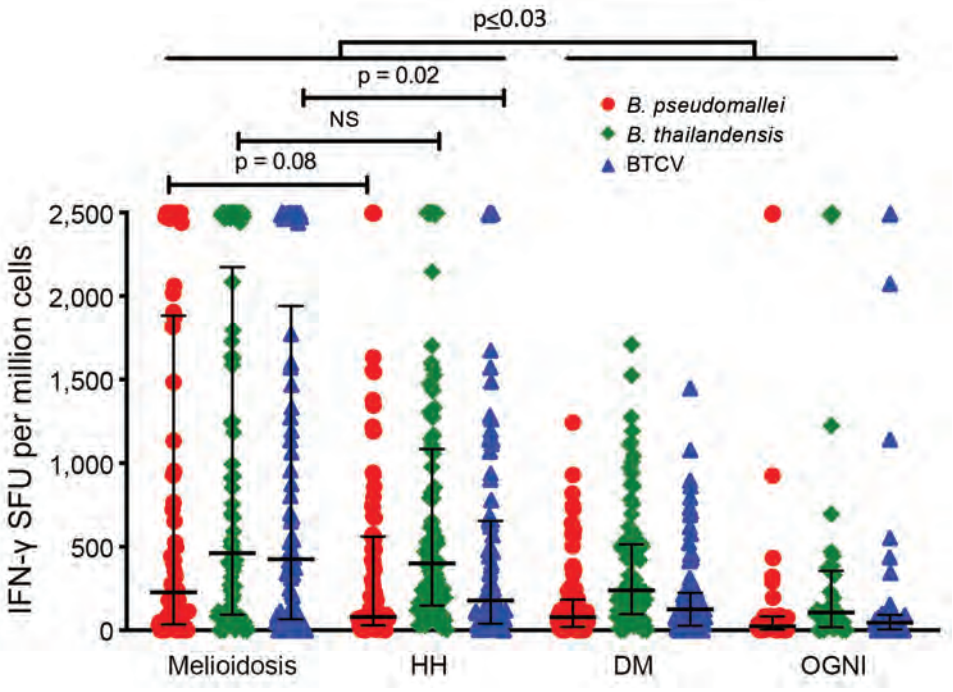

Figure 3. Ex vivo IFN-γ ELISpot responses to *Burkholderia pseudomallei*, *B. thailandensis*, and BTCV, Thailand. IFN-γ responses were quantified for acute melioidosis patients (n = 82) and 3 control cohorts: HH, n = 93), diabetic patients (DM, n = 95), and patients with other gram-negative infections (OGNI, n = 42) against whole-cell heat-killed antigens of *Burkholderia pseudomallei* (BP, red dots), *Burkholderia thailandensis* (BT, green diamonds), and *Burkholderia thailandensis* CPS variant (BTCV, blue triangles) are shown. Each symbol represents the average number of SFU per subject. Medians (horizontal lines) and interquartile ranges (error bars) are shown. p values were calculated by using the nonparametric Mann-Whitney test. Horizontal bars at top of figure indicate comparisons across cohorts. BTCV, *B. thailandensis* CPS variant; CPS, capsular polysaccharide; DM, patients with diabetes mellitus; HH, healthy household contacts of melioidosis case-patients; IFN-γ, interferon-γ; NS, not significant; SFU, spot-forming units.

DN T, CD4 T, and other cells (Figure 4). In particular, the contribution of IFN-γ responses from DN T cells against all *Burkholderia* antigens in the HH cohort was significantly higher than in the melioidosis cohort (p<0.01) (Appendix Figure 1, panel C). In the melioidosis cohort, we observed a strong correlation of IFN-γ responses against *B. pseudomallei*, *B. thailandensis*, and BTCV in CD4 T cells (ρ>0.8; p<0.01) (Appendix Table 5). In contrast, the HH cohort showed strong correlation between IFN-γ responses toward *B. pseudomallei*, *B. thailandensis*, and BTCV in CD8 T and NK cells (ρ>0.9; p<0.01) (Appendix Table 6).

Discussion

Our results demonstrate that melioidosis patients show strong humoral and cellular cross-immunity between the pathogenic *B. pseudomallei* and the less pathogenic *B. thailandensis* and BTCV. On the other hand, the HH cohort and control cohorts in general had relatively low humoral immune responses to all 3 *Burkholderia* antigens but profound cellular immune responses. We showed that just over half of the acute melioidosis patients were positive by IHA; previous work in our group has shown that a significant proportion (12.6%) of melioidosis patients never seroconvert (*16*). We do not have enough information to confirm whether the persistence of seropositivity against *B. pseudomallei* in healthy persons is associated with latent infection or with successful clearance of *B. pseudomallei* after exposure events.

Seropositivity against *B. pseudomallei* is associated with repeated environmental exposure to the organism (*19*). In addition, a recent epidemiologic study showed high prevalence of environmental *B. pseudomallei* in rice paddy fields across multiple regions of Thailand, especially in the east (*6*). Subsequent serologic responses against *B. pseudomallei* in healthy rice farmers are associated with exposure to environmental *B. pseudomallei* rather than *B. thailandensis* and BTCV (*20*); the cause could be a higher prevalence of *B. pseudomallei*. It is impossible to distinguish between the serologic responses to *B. pseudomallei* and BTCV because CPS components are highly cross-reactive (*9*).

Humoral immune responses against CPS components have been found to be associated with protection against experimental melioidosis in mice (*22*,*23*). In a previous study, Tiyawisutsri et al. used modified IHA to detect cross-reactivity between *B. pseudomallei*, *B. thailandensis*, and *B. mallei*, the causative agent of glanders, in melioidosis patients (*24*). Tiyawisutsri et al. reported poor cross-reactivity between *B. pseudomallei* and *B. thailandensis* and saw cross-reactivity to *B. mallei*, which expresses similar CPS components

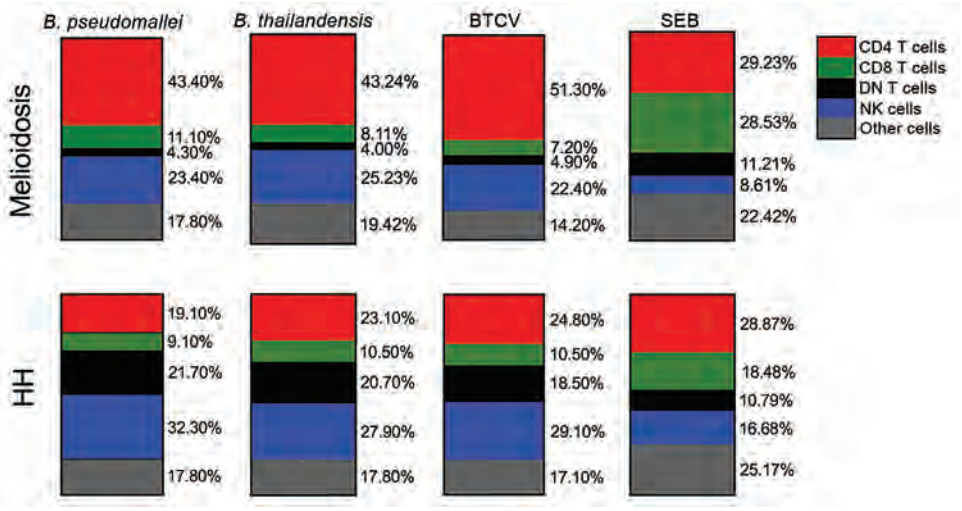

Figure 4. Cellular immune responses to *Burkholderia pseudomallei, B. thailandensis*, and BTCV by whole blood stimulation assay using flow cytometry between melioidosis patients and healthy persons in *B. pseudomallei*–endemic areas, Thailand. Whole blood samples from 14 patients with acute melioidosis and 8 HH contacts were stimulated with culture-filtrate antigens of *B. pseudomallei, B. thailandensis*, BTCV, and SEB (positive control). Frequencies of CD4, CD8, and DN T cells; NK cells; and other cells within total IFN-γ–producing cells are shown. Medians were used to generate each vertical slice graph. BTCV, *B. thailandensis* CPS variant; CPS, capsular polysaccharide; DM, patients with diabetes mellitus; DN, double negative (CD4–CD8–); HH, healthy household contacts of melioidosis case-patients; IFN-γ, interferon-γ; SEB, *Staphylococcus* enterotoxin B.

(*24*,*25*). Consistent with these findings, we report strong cross-reactivity between *B. pseudomallei* and BTCV, and to a lesser extent to *B. thailandensis* in the melioidosis and HH cohorts. Moreover, we suggest that the IHA responses may be primarily specific to CPS components that are not present in *B. thailandensis* (*9*). We explored the humoral responses by IgM and IgG; we report strong IgG responses in acute melioidosis patients but marginal IgM responses. A possible cause of the low IgM responses in acute melioidosis patients is that disease onset occurred some time before admission; reported incubation period is 1–21 days (*26*). Another possibility is that preexisting immunity to *B. pseudomallei* resulted in a burst of IgG responses around the time of study enrollment, which is consistent with a previous report (*27*). Thus, the IgG ELISA could be an improved diagnostic method for melioidosis (*28*).

Cell-mediated immune responses by IFN-γ and type I immune responses (e.g., interleukin [IL] 12, IL-18, tumor necrosis factor α) are essential for the host immune system in fighting against intracellular infections (*29*–*31*). Nithichanon et al. showed that most of an exposed healthy population has acquired cellular immunity against broad immunogenic *B. pseudomallei* epitopes (*32*). Our IFN-γ ELISpot experiments suggest that both melioidosis patients and HH contacts engage strong cross-immune IFN-γ responses between *B. pseudomallei*, *B. thailandensis*, and BTCV, despite low humoral responses in the HH cohort. The IFN-γ responses predominantly from T cells during melioidosis are associated with protection and survival against *B. pseudomallei* infection (*13*). We demonstrate that IFN-γ responses to all 3 antigens are a mix of T and NK cell responses, with different contribution of T-cell subsets in the melioidosis cohort compared with the HH cohort. Whereas melioidosis patients predominantly exhibit CD4 T-cell IFN-γ responses, the HH cohort is characterized by a mix of double negative and CD4 T-cell responses and increased NK cell responses, suggesting an innate or innate-like driven immune response.

Low-dose exposure to *B. pseudomallei* in healthy persons may also contribute to immune responses. *B. pseudomallei*–specific cellular immunity in seronegative healthy participants showed detectable IFN-γ ELISpot responses in some subjects to virulent factors in *B. pseudomallei*, such as bopE (Type III secreted protein), pilO (Type IV pilus biosynthesis protein), and flgK (flagellar hook-associated protein) (*12*). Another possibility would be cross-reactivity to other gram-negative bacteria, as demonstrated by some OGNI participants exhibiting high IFN-γ responses to whole-cell heat-killed *Burkholderia* antigens (Figure 3).

In a previous study in this population, we demonstrated that acute melioidosis patients elicited strong cellular immune responses in both the CD4 and CD8 T-cell compartments (*13*). Cellular immune responses by CD4 T cells against *B. pseudomallei* antigen (AhpC) have been associated with survival (*33*). HIV positivity does not seem to be a major risk factor for melioidosis; a surge in melioidosis incidence and severity was not seen during the HIV epidemic in the 1990s in

Thailand (*34*) although cases of tuberculosis and other opportunistic infections such as cryptococcal meningitis did increase. During this time, 2.8% (95% CI 0.8%–4.7%) of 286 patients in Ubon Ratchathani with *B. pseudomallei* tested positive for HIV, compared with 0.6%–1.1% of blood donors, but this difference was not significant (*35*). However, HIV infection is known to increase the risk for other gram-negative infections, such as *Salmonella* and *Escherichia coli*, and it is likely that a relationship between HIV and melioidosis could be demonstrated by sufficiently powered studies. To date, host immune responses by CD4 T cells in HIV-positive persons with melioidosis remain unknown. Host immune responses during acute melioidosis associated with survival have been shown to be dominated by CD8 T and NK cells (*36*,*37*), and some redundancy may occur to allow compensation of low CD4 counts in HIV.

In conclusion, patients with melioidosis in Thailand demonstrate immune cross-reactivity between *B. pseudomallei*, *B. thailandensis*, and BTCV in both humoral and cellular immune compartments. Healthy persons who live in melioidosis-endemic areas, on the other hand, primarily demonstrate cellular immune cross-reactivity. We recommend further investigation of human immune responses in healthy persons where the less pathogenic strains are prevalent, such as in the central and eastern parts of Thailand (*20*). It is possible that exposure to the less virulent *B. thailandensis* and BTCV generates immune cross-reactivity, which could confer some protection against melioidosis. Nevertheless, cross-protection against *B. pseudomallei* infection through immune cross-reactivity in humans requires further study. Understanding the consequences of naturally acquired immunity to *B. pseudomallei* or *B. thailandensis* variants in previously exposed populations is particularly needed for the development of an efficacious vaccine.

Acknowledgments

We thank all the participants and staff at Sunpasitthiprasong Hospital. We thank Premjit Amornchai, Sayan Langla, Weerawat Wongasa, Ampai Tanganuchitcharnchai, and Widanan Khumhaeng for their laboratory and administrative support.

The authors declare no conflicts of interest.

P.R. was supported by a Master's Fellowship in Public Health and Tropical Medicine by the Wellcome Trust (108395/Z/15/Z). S.J.D. is grateful for the support of a Wellcome Trust Intermediate Clinical Fellowship award (ref. WT100174/Z/12/Z).

About the Author

Mr. Rongkard is doctoral candidate at the Centre for Tropical Medicine and Global Health, University of Oxford, Oxford, UK. His current research interests focus on the immunology of tropical infectious diseases, particularly melioidosis.

References

1. Limmathurotsakul D, Golding N, Dance DAB, Messina JP, Pigott DM, Moyes CL, et al. Predicted global distribution of *Burkholderia pseudomallei* and burden of melioidosis. Nat Microbiol. 2016;1:15008. https://doi.org/10.1038/nmicrobiol.2015.8
2. Currie BJ, Dance DA, Cheng AC. The global distribution of *Burkholderia pseudomallei* and melioidosis: an update. Trans R Soc Trop Med Hyg. 2008;102(Suppl 1):S1–4. https://doi.org/10.1016/S0035-9203(08)70002-6
3. Stewart JD, Smith S, Binotto E, McBride WJ, Currie BJ, Hanson J. The epidemiology and clinical features of melioidosis in Far North Queensland: implications for patient management. PLoS Negl Trop Dis. 2017;11:e0005411. https://doi.org/10.1371/journal.pntd.0005411
4. Zheng Y, Ley SH, Hu FB. Global aetiology and epidemiology of type 2 diabetes mellitus and its complications. Nat Rev Endocrinol. 2018;14:88–98. https://doi.org/10.1038/nrendo.2017.151
5. Trakulsomboon S, Vuddhakul V, Tharavichitkul P, Na-Gnam N, Suputtamongkol Y, Thamlikitkul V. Epidemiology of arabinose assimilation in *Burkholderia pseudomallei* isolated from patients and soil in Thailand. Southeast Asian J Trop Med Public Health. 1999;30:756–9.
6. Hantrakun V, Rongkard P, Oyuchua M, Amornchai P, Lim C, Wuthiekanun V, et al. Soil nutrient depletion is associated with the presence of *Burkholderia pseudomallei*. Appl Environ Microbiol. 2016;82:7086–92. https://doi.org/10.1128/AEM.02538-16
7. Kim HS, Schell MA, Yu Y, Ulrich RL, Sarria SH, Nierman WC, et al. Bacterial genome adaptation to niches: divergence of the potential virulence genes in three *Burkholderia* species of different survival strategies. BMC Genomics. 2005;6:174. https://doi.org/10.1186/1471-2164-6-174
8. Moore RA, Reckseidler-Zenteno S, Kim H, Nierman W, Yu Y, Tuanyok A, et al. Contribution of gene loss to the pathogenic evolution of *Burkholderia pseudomallei* and *Burkholderia mallei*. Infect Immun. 2004;72:4172–87. https://doi.org/10.1128/IAI.72.7.4172-4187.2004
9. Sim BM, Chantratita N, Ooi WF, Nandi T, Tewhey R, Wuthiekanun V, et al. Genomic acquisition of a capsular polysaccharide virulence cluster by non-pathogenic *Burkholderia isolates*. Genome Biol. 2010;11:R89. https://doi.org/10.1186/gb-2010-11-8-r89
10. Scott AE, Laws TR, D'Elia RV, Stokes MG, Nandi T, Williamson ED, et al. Protection against experimental melioidosis following immunization with live *Burkholderia thailandensis* expressing a manno-heptose capsule. Clin Vaccine Immunol. 2013;20:1041–7. https://doi.org/10.1128/CVI.00113-13
11. Tippayawat P, Saenwongsa W, Mahawantung J, Suwannasaen D, Chetchotisakd P, Limmathurotsakul D, et al. Phenotypic and functional characterization of human memory T cell responses to *Burkholderia pseudomallei*. PLoS Negl Trop Dis. 2009;3:e407. https://doi.org/10.1371/journal.pntd.0000407

12. Dunachie SJ, Jenjaroen K, Reynolds CJ, Quigley KJ, Sergeant R, Sumonwiriya M, et al. Infection with *Burkholderia pseudomallei*–immune correlates of survival in acute melioidosis. Sci Rep. 2017;7:12143. https://doi.org/10.1038/s41598-017-12331-5
13. Jenjaroen K, Chumseng S, Sumonwiriya M, Ariyaprasert P, Chantratita N, Sunyakumthorn P, et al. T-cell responses are associated with survival in acute melioidosis patients. PLoS Negl Trop Dis. 2015;9:e0004152. https://doi.org/10.1371/journal.pntd.0004152
14. Ketheesan N, Barnes JL, Ulett GC, VanGessel HJ, Norton RE, Hirst RG, et al. Demonstration of a cell-mediated immune response in melioidosis. J Infect Dis. 2002;186:286–9. https://doi.org/10.1086/341222
15. Healey GD, Elvin SJ, Morton M, Williamson ED. Humoral and cell-mediated adaptive immune responses are required for protection against *Burkholderia pseudomallei* challenge and bacterial clearance postinfection. Infect Immun. 2005;73:5945–51. https://doi.org/10.1128/IAI.73.9.5945-5951.2005
16. Chaichana P, Jenjaroen K, Amornchai P, Chumseng S, Langla S, Rongkard P, et al. Antibodies in melioidosis: the role of the indirect hemagglutination assay in evaluating patients and exposed populations. Am J Trop Med Hyg. 2018;99:1378–85. https://doi.org/10.4269/ajtmh.17-0998
17. Alexander AD, Huxsoll DL, Warner AR Jr, Shepler V, Dorsey A. Serological diagnosis of human melioidosis with indirect hemagglutination and complement fixation tests. Appl Microbiol. 1970;20:825–33.
18. Chantratita N, Wuthiekanun V, Thanwisai A, Limmathurotsakul D, Cheng AC, Chierakul W, et al. Accuracy of enzyme-linked immunosorbent assay using crude and purified antigens for serodiagnosis of melioidosis. Clin Vaccine Immunol. 2007;14:110–3. https://doi.org/10.1128/CVI.00289-06
19. Wuthiekanun V, Chierakul W, Langa S, Chaowagul W, Panpitpat C, Saipan P, et al. Development of antibodies to *Burkholderia pseudomallei* during childhood in melioidosis-endemic northeast Thailand. Am J Trop Med Hyg. 2006;74:1074–5. https://doi.org/10.4269/ajtmh.2006.74.1074
20. Hantrakun V, Thaipadungpanit J, Rongkard P, Srilohasin P, Amornchai P, Langla S, et al. Presence of *B. thailandensis* and *B. thailandensis* expressing *B. pseudomallei*–like capsular polysaccharide in Thailand, and their associations with serological response to *B. pseudomallei*. PLoS Negl Trop Dis. 2018;12:e0006193. https://doi.org/10.1371/journal.pntd.0006193
21. Suttisunhakul V, Chantratita N, Wikraiphat C, Wuthiekanun V, Douglas Z, Day NPJ, et al. Evaluation of polysaccharide-based latex agglutination assays for the rapid detection of antibodies to *Burkholderia pseudomallei*. Am J Trop Med Hyg. 2015;93:542–6. https://doi.org/10.4269/ajtmh.15-0114
22. Burtnick MN, Shaffer TL, Ross BN, Muruato LA, Sbrana E, DeShazer D, et al. Development of subunit vaccines that provide high-level protection and sterilizing immunity against acute inhalational melioidosis. Infect Immun. 2017;86:e00724-17. https://doi.org/10.1128/IAI.00724-17
23. Scott AE, Burtnick MN, Stokes MG, Whelan AO, Williamson ED, Atkins TP, et al. *Burkholderia pseudomallei* capsular polysaccharide conjugates provide protection against acute melioidosis. Infect Immun. 2014;82:3206–13. https://doi.org/10.1128/IAI.01847-14
24. Tiyawisutsri R, Peacock SJ, Langa S, Limmathurotsakul D, Cheng AC, Chierakul W, et al. Antibodies from patients with melioidosis recognize *Burkholderia mallei* but not *Burkholderia thailandensis* antigens in the indirect hemagglutination assay. J Clin Microbiol. 2005;43:4872–4. https://doi.org/10.1128/JCM.43.9.4872-4874.2005
25. Heiss C, Burtnick MN, Wang Z, Azadi P, Brett PJ. Structural analysis of capsular polysaccharides expressed by *Burkholderia mallei* and *Burkholderia pseudomallei*. Carbohydr Res. 2012;349:90–4. https://doi.org/10.1016/j.carres.2011.12.011
26. Currie BJ, Fisher DA, Howard DM, Burrow JN, Selvanayagam S, Snelling PL, et al. The epidemiology of melioidosis in Australia and Papua New Guinea. Acta Trop. 2000;74:121–7. https://doi.org/10.1016/S0001-706X(99)00060-1
27. Currie BJ, Fisher DA, Anstey NM, Jacups SP. Melioidosis: acute and chronic disease, relapse and re-activation. Trans R Soc Trop Med Hyg. 2000;94:301–4. https://doi.org/10.1016/S0035-9203(00)90333-X
28. Suttisunhakul V, Wuthiekanun V, Brett PJ, Khusmith S, Day NP, Burtnick MN, et al. Development of rapid enzyme-linked immunosorbent assays for detection of antibodies to *Burkholderia pseudomallei*. J Clin Microbiol. 2016;54:1259–68. https://doi.org/10.1128/JCM.02856-15
29. Trinchieri G. Cytokines acting on or secreted by macrophages during intracellular infection (IL-10, IL-12, IFN-gamma). Curr Opin Immunol. 1997;9:17–23. https://doi.org/10.1016/S0952-7915(97)80154-9
30. Dinarello CA, Fantuzzi G. Interleukin-18 and host defense against infection. J Infect Dis. 2003;187(Suppl 2):S370–84. https://doi.org/10.1086/374751
31. Barnes JL, Williams NL, Ketheesan N. Susceptibility to *Burkholderia pseudomallei* is associated with host immune responses involving tumor necrosis factor receptor-1 (TNFR1) and TNF receptor-2 (TNFR2). FEMS Immunol Med Microbiol. 2008;52:379–88. https://doi.org/10.1111/j.1574-695X.2008.00389.x
32. Nithichanon A, Rinchai D, Buddhisa S, Saenmuang P, Kewcharoenwong C, Kessler B, et al. Immune control of *Burkholderia pseudomallei* – common, high-frequency T-cell responses to a broad repertoire of immunoprevalent epitopes. Front Immunol. 2018;9:484. https://doi.org/10.3389/fimmu.2018.00484
33. Reynolds C, Goudet A, Jenjaroen K, Sumonwiriya M, Rinchai D, Musson J, et al. T cell Immunity to the alkyl hydroperoxide reductase of *Burkholderia pseudomallei:* a correlate of disease outcome in acute melioidosis. J Immunol. 2015;194:4814–24. https://doi.org/10.4049/jimmunol.1402862
34. Chierakul W, Wuthiekanun V, Chaowagul W, Amornchai P, Cheng AC, White NJ, et al. Short report: disease severity and outcome of melioidosis in HIV coinfected individuals. Am J Trop Med Hyg. 2005;73:1165–6. https://doi.org/10.4269/ajtmh.2005.73.1165
35. Chierakul W, Rajanuwong A, Wuthiekanun V, Teerawattanasook N, Gasiprong M, Simpson A, et al. The changing pattern of bloodstream infections associated with the rise in HIV prevalence in northeastern Thailand. Trans R Soc Trop Med Hyg. 2004;98:678–86. https://doi.org/10.1016/j.trstmh.2004.01.011
36. Kronsteiner B, Chaichana P, Sumonwiriya M, Jenjaroen K, Chowdhury FR, Chumseng S, et al. Diabetes alters immune response patterns to acute melioidosis in humans. Eur J Immunol. 2019;49:1092–106. https://doi.org/10.1002/eji.201848037
37. Lertmemongkolchai G, Cai G, Hunter CA, Bancroft GJ. Bystander activation of CD8+ T cells contributes to the rapid production of IFN-gamma in response to bacterial pathogens. J Immunol. 2001;166:1097–105. https://doi.org/10.4049/jimmunol.166.2.1097

Address for correspondence: Susanna J. Dunachie, University of Oxford—Tropical Medicine, Peter Medawar Building for Pathogen Research, South Parks Rd, Oxford, OX1 3SY, UK; email: susie.dunachie@ndm.ox.ac.uk

Role of Live-Duck Movement Networks in Transmission of Avian Influenza, France, 2016–2017

Claire Guinat, Benoit Durand, Timothee Vergne, Tifenn Corre, Séverine Rautureau, Axelle Scoizec, Sophie Lebouquin-Leneveu, Jean-Luc Guérin, Mathilde C. Paul

The relative roles that movement and proximity networks play in the spread of highly pathogenic avian influenza (HPAI) viruses are often unknown during an epidemic, preventing effective control. We used network analysis to explore the devastating epidemic of HPAI A(H5N8) among poultry, in particular ducks, in France during 2016–2017 and to estimate the likely contribution of live-duck movements. Approximately 0.2% of live-duck movements could have been responsible for between-farm transmission events, mostly early during the epidemic. Results also suggest a transmission risk of 35.5% when an infected holding moves flocks to another holding within 14 days before detection. Finally, we found that densely connected groups of holdings with sparse connections between groups overlapped farmer organizations, which represents important knowledge for surveillance design. This study highlights the importance of movement bans in zones affected by HPAI and of understanding transmission routes to develop appropriate HPAI control strategies.

Infectious diseases commonly spread among animal premises by different transmission pathways, including live-animal movement networks that can cause outbreaks in widespread locations or through proximity networks, leading to spatial clusters of outbreaks (*1*,*2*). High-quality data on the spatial distribution of premises have enabled development of transmission models in which the proximity network assumes that any given infectious premises can infect all susceptible premises within a geographic range (*3*,*4*). Increased monitoring of trade-related movement data has enabled the emergence of innovative modeling approaches based on social network analysis (*5*,*6*). Such an approach has been widely used to quantify how animal movement networks have contributed to disease transmission between animal premises (*7*,*8*) and relies on the assumption that premises intensively connected within the network are more likely to become infected and spread infection. Accordingly, efforts have focused on integrating movement and local spread components into models when the dynamics of past epidemics are explored, the effects of control strategies evaluated, and the pattern of future epidemics predicted (*9*–*11*).

However, the relative contribution of movement networks to the overall transmission risks remains poorly understood, compromising assessments of accurate and realistic disease spread modeling and control efforts. First, to assess the likelihood that the infection was acquired from movement networks, tracing of live-animal movement is required but might be challenging, especially in resource-poor settings where movement data are not regularly recorded as part of flock management systems. Then, the order or time at which animal premises become infected must be statistically related to their position in the movement network or in geographic space. However, these dates of infection are often inaccurate because reporting is delayed or completely lacking, particularly when tracking chronic diseases or wildlife populations, or when resources are limited.

In 2016–2017, Europe was hit hard by an unprecedented wave of highly pathogenic avian influenza (HPAI) A(H5N8) outbreaks that had severe socioeconomic effects on poultry production, global trade, and human livelihoods (*12*). Most outbreaks were reported in France; ducks were the most affected poultry species (*13*,*14*). The epidemic was contained by the end of March 2017 in France by timely application

Author affiliations: École Nationale Vétérinaire de Toulouse, Toulouse, France (C. Guinat, T. Vergne, T. Corre, J.-L. Guérin, M.C. Paul); Institut National de Recherche pour l'Agriculture, l'Alimentation et l'Environnement, Toulouse (C. Guinat, T. Vergne, T. Corre, J.-L. Guérin, M.C. Paul); Agence Nationale de Sécurité Sanitaire de l'Alimentation, Université Paris-Est, Maisons-Alfort, France (B. Durand); Direction Générale de l'Alimentation, Paris, France (S. Rautureau); Agence Nationale de Sécurité Sanitaire de l'Alimentation, Ploufragan, France (A. Scoizec, S. Lebouquin-Leneveu)

DOI: https://doi.org/10.3201/eid2603.190412

of measures after detection of the first outbreaks, as provided for by European Union legislation (*15*–*17*). These measures included culling all birds on the infected holdings, establishing a 3-km protection zone and 10-km surveillance zone with stringent ingoing and outgoing movement bans, testing before movements, and increasing biosecurity measures for holdings in these zones. Spatiotemporal analysis of HPAI outbreaks has shown that the disease spread was partly driven by transmission events between poultry holdings in close proximity in space and time (*14*). Although these previous results helped generate hypotheses about possible routes of infection, they did not enable weighting their relative contribution. Duck movement networks were also identified as underlying factors for the spatial distribution of HPAI outbreaks (*18*), suggesting that these factors should be considered to appropriately describe the epidemic spread. Accurate data on the location and date of suspicion (i.e., onset of clinical signs and increased death rates) of infected holdings and live-duck movements between holdings were collected in France, providing a unique opportunity to unravel the spatial and network dimensions of the epidemic. Our objectives were to analyze live-duck movement networks during the 2016–2017 H5N8 epidemic in France and investigate their likely contribution to disease spread.

Methods

Data Collection

Outbreak Data

We obtained data on the H5N8 outbreaks in ducks in France during the 2016–2017 epidemic (November 28, 2016–March 23, 2017) from the Direction Générale de l'Alimentation of the French Ministry of Agriculture (Paris, France). An outbreak was defined as detection of ≥1 H5N8-infected animal (confirmed by virus isolation or PCR) in a duck holding. Only outbreaks that occurred in holdings that sent or received duck flocks during the study period were retained for the analysis. Data comprised the list of laboratory-confirmed outbreaks, holding identification number, geographic locations (EPSG:2154/RGF93/Lambert-93 [https://epsg.io/2154]), and date of suspicion available by clinical or active surveillance.

Trade Movement Data

We considered only duck movements because they represented the most affected poultry species (81.6%) during the epidemic (*14*). The French organization of fattening duck producers (Comité Interprofessionnel des Palmipèdes à Foie Gras [CIFOG]) requires duck producers to report movements from and onto their holdings within 1–2 days of the movement. We thus obtained data on live-duck movements and holdings' characteristics from the professional database of the CIFOG, under the appropriate confidential data transfer agreements. Data included the list of movement records (defined as movement of a flock between 2 different holdings on the same day), which consisted of the date of movement, identification number of the departure and arrival holdings, and number of ducks moved. The incubation period (i.e., time between virus introduction and onset of clinical signs) ranges from ≈1 to ≈5 days at the individual level and could be longer at the flock level because of the transmission process (*19*). Because such duration is difficult to estimate, a 14-day incubation period was assumed at the flock level (we conducted a sensitivity analysis using a 21-day incubation period and showed that it did not affect the results). Consequently, movements within 14 days before the detection of an infected holding might be responsible for between-holding transmission events (*19*). Thus, we retained only movement data during November 1, 2016–March 31, 2017, between holdings for the analysis; movements to slaughterhouses were excluded. Holdings' characteristics included the geographic locations (EPSG:2154/RGF93/Lambert-93), group of farmer organization, and type of production: rearing (1-day-old ducklings are reared for ≈3 weeks), breeding (1-day to 3-week-old ducks are bred for ≈9–12 weeks), and force-feeding (12-week-old ducks are force-fed for ≈12 days). For holdings with no available coordinates (9.5%), we used the coordinates of the center of the commune (smallest administrative unit in France, with a median area of 10 km^2).

Data Analysis

Spatiotemporal Description of Movements

We first generated descriptive statistics for the number of active holdings (i.e., holdings that received or sent ducks during the study period), the number of flocks moved, and the distances covered by movements (i.e., using Euclidean distance in kilometers between the departure and arrival holdings) per pair of holdings. We removed holdings without available coordinates from the Euclidean distance estimations. Finally, we mapped the number of movements from/to holdings between departments by aggregating movements at the department level (administrative unit in France corresponding to NUTS [Nomenclature of Territorial Units for Statistics] level 3).

Network Analysis

We built directed and weighted networks for data from November 1, 2016–March 31, 2017, considering each duck holding as a node and a movement of a flock between 2 holdings as an edge. We assigned directions to each edge according to the date on which ducks were moved between 2 nodes and assigned weights to each edge according to the number of ducks moved between 2 nodes. We identified trade communities (i.e., densely connected groups of nodes, with only sparse connections between groups [*20*]) over the whole study period using a walktrap algorithm (*21*) based on random walks through the edges in the network. We selected the 15 largest communities on the basis of their respective numbers of holdings and typed them according to holding production types. We mapped holdings belonging to the 15 largest communities and performed a bootstrapped version of the Fisher exact test with 10,000 replicates (*22*) to test whether dependence existed between the trade community and the organization to which farmers belong.

Next, we assessed the likely contribution of live-duck movements in the distribution of H5N8 outbreaks in the network using a permutation-based approach (*23*–*25*). The rationale behind this approach was that if the outbreaks resulted from disease spread through the movement networks, the mean number of infected holdings in contact with an infected holding in the network would be significantly greater than expected if infected holdings were randomly distributed in the network. Again, duck holdings were assumed to become infected through the movement networks if they had received movements from infected holdings within an at-risk period of 14 days before their date of suspicion. Hence, we assumed the mean number of potential transmission events through the movement networks corresponded with the mean number of at-risk movements defined by movements originating from an infected holding (the sender) within 14 days before its date of suspicion and directed to a distinct infected duck holding (the receiver) within 14 days before the receiver's date of suspicion. We then compared this statistic (i.e., the mean number of transmission events per infected holding) with the distribution of the expected statistic under the null hypothesis according to which the dates of suspicion were randomly distributed among infected holdings in the network (n = 1,000), with the p value corresponding to the proportion of permutations for which the expected statistic is higher than the observed statistic. Similarly, to assess the role of proximity networks, we also conducted the test by calculating the following statistic: the mean number of infected duck holdings close in time (differences of infection dates within 14 days) and space (both located within a 10-km radius [*14*]) per infected duck holding. We selected this space–time window on the basis of previous spatiotemporal analysis conducted on the dataset (*14*). Finally, we identified the likely origins of holding infections by calculating the proportion of infected duck holdings retrieved as receivers in the list of transmission events through the movement network and the proportion of infected duck holdings for which ≥1 infected duck holding close in time and space was retrieved in the proximity network. On the basis of the movement and proximity networks, we thus attributed to each holding a likely origin of infection as follows: ingoing edge in the movement network only, ingoing edge in the proximity network only, ingoing edges in both movement and proximity networks, and no ingoing edge (i.e., other transmission pathways than by movement and proximity; for example, by introduction of infected migratory birds from northern Eurasia [*13*,*26*]). Because movement bans were reinforced on February 2, 2017 (*27*), we retained only movement and outbreak data for November 1, 2016–February 2, 2017, for this analysis. We conducted all analyses in R statistical software version 3.4.2 using the igraph package (*28*).

Results

Spatiotemporal Description

A total of 9,096 movements, involving 10,945,388 ducks moved among 2,098 holdings, occurred during November 1, 2016–March 31, 2017 (Table 1). Most holdings involved in these movements were characterized as force-feeding (48.8%), followed by breeding (35.7%) and breeding plus force-feeding (11.9%). The holdings were located mainly in southwestern and northwestern France (Appendix Figure 1, https://wwwnc.cdc.gov/EID/article/26/3/19-0412-App1.pdf). Overall, most (95.8%) of the flocks were moved

Table 1. Descriptive statistics of duck movements per pair of holdings, France, November 1, 2016–March 31, 2017*

	No. (%) flocks	No. ducks moved				Distance moved, km			
Holding type pair	moved	Mean	Median	IQR	Max	Mean	Median	IQR	Max
Rearing to breeding	382 (4.2)	6,001	4,773	3,016–8,991	15,090	58	36	0.1–101	213
Breeding to force-feeding	8,712 (95.8)	993	958	629–1,188	8,050	50	40	16–71	408

*IQR, interquartile range; max, maximum.

from breeding to force-feeding holdings; only 4.2% of movements occurred from rearing to breeding holdings (Table 1). However, more ducks were moved from rearing to breeding holdings (median 4,773) than from breeding to force-feeding holdings (median 958). Movements clearly clustered in the 2 separate geographic areas, southwestern and northwestern France; a limited amount of movements occurred between these 2 areas (Appendix Figure 2).

Network Analysis

The network analysis identified 99 trade communities comprising 2,098 holdings during November 1, 2016–March 31, 2017. The 15 largest communities in terms of number of holdings included 91.8% of holdings. These communities showed a relatively distinct spatial distribution in northwestern France but completely overlapped in southwestern France (Figure 1). However, the communities were characterized by similar holding compositions, dominated by breeding and force-feeding holdings. The 15 largest communities overlapped significantly with the 15 largest groups of farmer organizations ($p<0.001$) (Appendix Figure 3): For example, community 1 included 80.0% of holdings belonging to organization A, community 2 included 51.7% of holdings belonging to organization I and 44.8% to organization J, and community 5 included 63.1% and community 12 36.0% of organization B.

A total of 6,521 movements between 1,988 holdings (involving 104 infected holdings) occurred during November 1, 2016–February 2, 2017. Among the 104 infected holdings, 40 (38.5%) were identified as senders, 36 (34.6%) as receivers, and 28 (26.9%) as senders and receivers during that period. Most (989 [91.8%] of 6,521) movements occurred between noninfected holdings. We identified 16 (0.2%) of 6,521 movements as at risk (i.e., they were compatible with transmission events through the movement networks) (Figure 2). These movements mostly occurred between breeding and force-feeding holdings from the end of November through the beginning of January, before stringent movement bans were implemented, and were directed to areas where most outbreaks were reported during the following weeks (Figure 2). Some of the at-risk movements originated from the first outbreak, reported at the beginning of the epidemic (end of November 2016). A

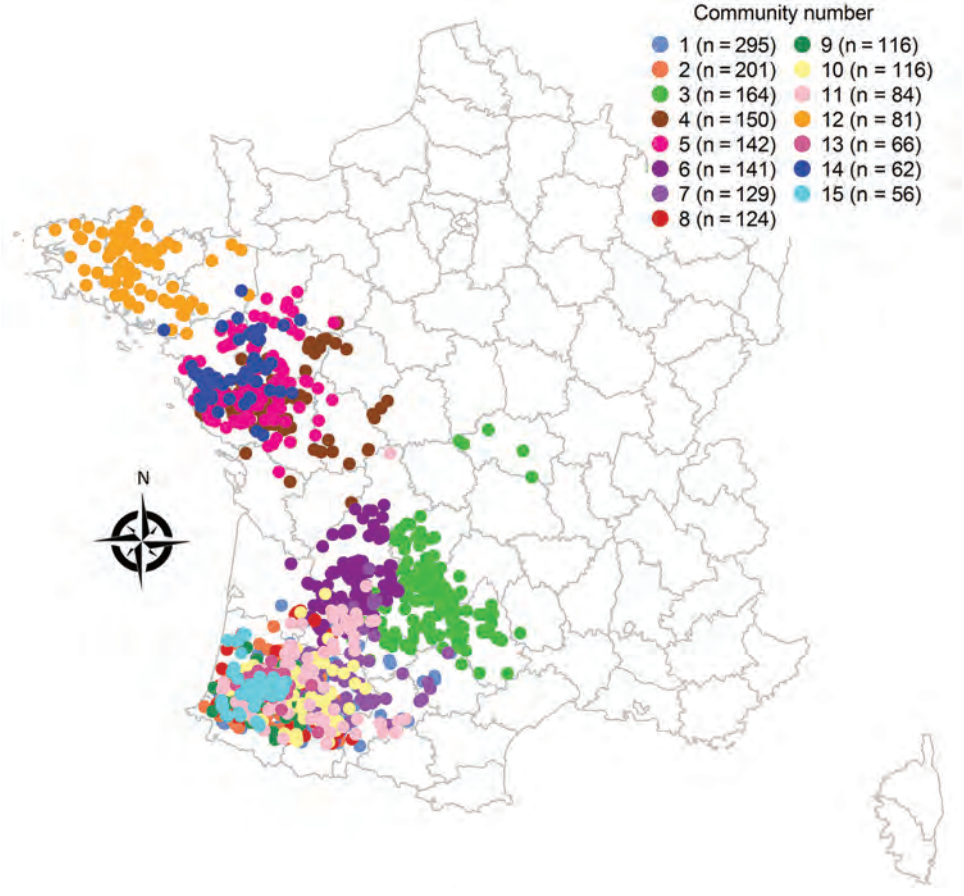

Figure 1. Spatial distribution of the 15 largest live-duck trade communities, France, November 1, 2016–March 31, 2017.

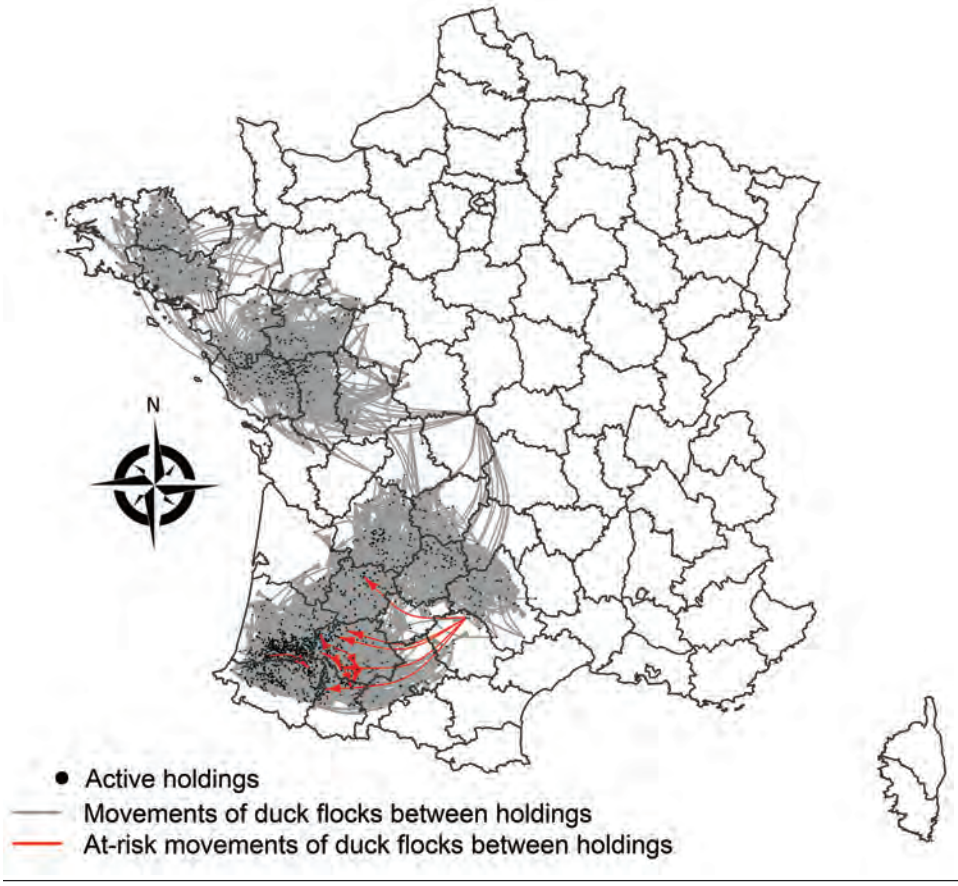

Figure 2. Spatial distribution of live-duck movements identified as responsible for highly pathogenic avian influenza A(H5N8) transmission events between holdings through the movement networks, France, November 1, 2016–February 2, 2017.

few movements (0.4%, 29/6,521) occurred between infected holdings and holdings that did not become infected within 14 days after the movements, from the end of November through the beginning of January, before stringent movement bans were implemented. Therefore, transmission risk through live-duck movements was estimated at 35.5% (16/[16 + 29]), meaning that the likelihood of infection when an infected holding moved flocks to another holding within 14 days before detection was 35.5%. Results from the permutation-based approach indicated the mean number of transmission events per infected holding was significantly greater than under the null hypothesis of an absence of association between movement and infection status (according to which the dates of suspicion should be randomly distributed among network nodes) ($p<0.001$). Moreover, the mean number of infected holdings close in time and space per infected holding was also significantly greater than expected ($p<0.001$). By retrieving holding receivers in the list of transmission events through the movement and proximity networks, most sources of holding infection were attributed to proximity networks (66.3%), followed by movement networks (14.4%), and other unknown means of transmission were possible (23.1%) (Table 2). The 16 at-risk movements could be the likely source of infection for only 15 farms because 1 infected farm received 2 at-risk movements.

Discussion

Using a detailed analysis of live-duck movements and proximity networks, we unraveled the underlying transmission processes of the H5N8 epidemic in ducks in France during 2016–2017. During November 1, 2016–March 31, 2017, which overlaps the H5N8 epidemic period, we observed the most movements from breeding to force-feeding holdings and the largest duck flocks from the rearing to the breeding stage. These findings are consistent with the production cycle and the high specialization in production within which the number of rearing holdings where ducks are first reared and then sent as large flocks to breeding holdings is limited. Flocks are then divided into small flocks to be moved to force-feeding holdings, resulting in a large number of force-feeding holdings reported in the country. Assuming that movement networks influence disease spread, this structure becomes important in terms of disease prevention and control: the dominant role of such superreceiver and

Table 2. Contribution of movement and proximity networks for highly pathogenic avian influenza A(H5N8) transmission events between live-duck holdings, France, November 1, 2016–February 2, 2017

Origin of infection	Infected holdings, no. (%), n = 104	
	14 d before date of suspicion	21 d before date of suspicion
Movement network	11 (10.6)	11 (10.6)
Proximity network	65 (62.5)	72 (69.2)
Movement and proximity networks	4 (3.8)	4 (3.8)
Other	24 (23.1)	17 (16.3)

superspreader holdings indicates that monitoring only a few holdings would be sufficient to reduce disease spread or that targeting sampling in these high-risk holdings would be more effective than random sampling when time and resources are limited (*29*,*30*). This structure supports the recent active surveillance campaign of duck flocks before movements between these 2 production stages, implemented as a result of the devastating H5N8 epidemic (*31*). Overall, most movements were short range (50% cover <40 km and 75% <75 km). This finding is consistent with results from a spatiotemporal analysis (*14*), which provided evidence that local transmission processes mainly drove the spread. Moreover, our study demonstrated that movements clustered mainly in 2 geographic areas (southwestern and northwestern France) and that a limited number of movements occurred between these 2 areas, potentially explaining why the disease did not spread from south to northwest (*14*).

The 15 largest trade communities that comprised most (91.8%) holdings clearly overlapped with the 15 largest farmer organizations. Again, this finding is crucial in terms of disease surveillance because it highlights that targeting sampling of holdings belonging to the trade community of infected holdings would be more effective than random sampling to prevent further disease spread. In terms of disease control, these results indicate that trade within a given group of highly connected holdings could be maintained by disrupting epidemiologic links to other groups of holdings at risk, mainly to minimize disruption of global trade during an epidemic (*32*,*33*). Moreover, being part of a particular farmer organization implies that holdings are connected by other means than movements of live birds, such as shared transport, equipment, feed, animal staff, or catching teams, that could also facilitate transmission events within the community. Our study also highlighted the important role of the community structure in spreading H5N8: the community to which holdings belong (and thus the farmer organization) was significantly associated with the H5N8 holding infection status (data not shown). Again, trade communities did not overlap between northwestern and southwestern France, which could explain why most of outbreaks remained clustered in southwestern France during the 2016–2017 epidemic (*14*).

Results from our permutation-based approach suggested that a limited proportion of holdings (14.4%) became infected through the movement networks before February 2017. We identified some of these transmission events in the movement networks as originating from the first outbreak reported at the beginning of the epidemic (end of November 2016), before stringent movement bans were implemented, and directed to areas where most of the outbreaks were reported during the following weeks (*14*,*34*). Therefore, despite their low number, live-duck movements might have played a crucial role in the onset and spatial extent of the 2016–2017 H5N8 epidemic in the country. The limited contribution of movement networks to disease spread is most likely explained by the timely implementation of control strategies and movement bans after the first outbreaks were detected (*15*,*16*). This limited contribution also is most likely attributed to the duck production characteristics, highly specialized holdings organized in a small pyramidal structure. Results suggest a transmission risk of 35.5% when an infected holding moves flocks to another holding within 14 days before detection. These findings support efforts by authorities in France in collaboration with the farmer organizations to enhance biosecurity during the transport of ducks (*31*) after successive waves of HPAI outbreaks within 2 years (*14*,*35*). Trucks moving flocks are not allowed to load from several different holdings to minimize the risk for contact infections as trucks travel between holdings. It is likely officials will implement new rules, such as using different sets of trucks and cages to move flocks from breeding to force-feeding and from force-feeding to slaughter. A higher proportion of holdings (66.3%) became infected through proximity networks, consistent with previous work that identified local spread as a predominant transmission pathway in the early stage of the epidemic, that is, before February 2017 (*14*). As a result, these findings also support the national biosecurity program that was implemented to prevent the introduction and spread of poultry diseases at the holding level (*36*,*37*).

The 2 recent devastating epidemics of HPAI in France (2015–2016 and 2016–2017) led to major changes in the collection of movement data. Specifically, the farmer organizations require duck producers to timely and accurately report any details on flock movements, leading to the expectation that underreporting remains limited. Data regarding transport, shared equipment, feed, animal staff, carcass rendering, catching teams, or wild birds were not available (*38*,*39*). However, these transmission pathways might be partly reflected by the proximity network (for example, neighboring holdings might share the same equipment or carcass rendering round) or by 23.1% of holdings for which the infection origin was attributed to transmission pathways other than movement or proximity networks (for example, by introduction of infected migratory birds from northern Eurasia [*13*,*26*]). Although the epidemiologic mechanisms that could explain some of these transmission events remain to be explored, one could infer that these transmission pathways might have played a larger role in the spread of H5N8 between holdings than movement of live ducks. Recent studies have shown that wild birds are likely to have played a minor role in the spread of H5N8 between holdings (*18*,*40*), suggesting that the main driver of the epidemic was holding-to-holding transmission. Further work will compare these results with movement networks during a period with no outbreaks reported as to how outbreaks and intervention strategies have modified the structure of the movement networks.

This study provides insights into the likely contribution of live-duck movement networks into the spread of H5N8 at the beginning of the 2016–2017 epidemic in France. This study also highlights the importance of movement bans in affected zones and that understanding transmission routes is paramount for developing appropriate control strategies for HPAI. A new aspect of this study is the inclusion of a permutation-based approach based on the dates of holding infection to evaluate whether the acquisition of holding infection was consistent with virus transmission through the network. This approach has been limitedly applied in the epidemiology of infectious diseases (*23*–*25*), although it outperforms other degree-based statistical methods, such as logistic regression and nonparametric tests. Outcomes about the relative contribution of movement and proximity networks represent a required basis on which predictive models of HPAI spread could be developed. Finally, this study emphasizes the importance of supplementing epidemiologic data with animal movement data and therefore calls for collaborative efforts to report trade movement data and make them available for appropriately targeting surveillance and interventions during future outbreaks.

Acknowledgments

We gratefully acknowledge the Direction Générale de l'Alimentation of the French Ministry of Agriculture and the Comité Interprofessionnel des Palmipèdes à Foie Gras (CIFOG, France) for providing the data, particularly Marie Laborde for providing additional detailed information about the data and interpreting the results.

This work was conducted within the framework of the Chaire de Biosécurité at the École Nationale Vétérinaire de Toulouse, which is funded by the French Ministry of Agriculture and supported by the Unité Mixte de Recherche Interactions Hôtes Agents Pathogènes 1225 École Nationale Vétérinaire de Toulouse, Institut National de la Recherche Agronomique. The research leading to the results was funded by the People Programme (Marie Curie Actions) of the European Union's Seventh Framework Programme (FP7/2007-2013) under Research Executive Agency grant agreement no. PCOFUND-GA-2013-609102, through the PRESTIGE program coordinated by Campus France. This work was also financially supported by the FEDER/Région Occitanie Recherche et Sociétés 2018 — AI-TRACK.

About the Author

Dr. Guinat is a postdoctoral researcher in veterinary epidemiology at the École Nationale Vétérinaire de Toulouse (France). Her major research interest is understanding the spread and maintenance of emerging infectious diseases.

References

1. Fèvre EM, Bronsvoort BMC, Hamilton KA, Cleaveland S. Animal movements and the spread of infectious diseases. Trends Microbiol. 2006;14:125–31. http://dx.doi.org/10.1016/j.tim.2006.01.004
2. Green DM, Kiss IZ, Mitchell AP, Kao RR. Estimates for local and movement-based transmission of bovine tuberculosis in British cattle. Proc Biol Sci. 2008;275:1001–5. http://dx.doi.org/10.1098/rspb.2007.1601
3. Ferguson NM, Donnelly CA, Anderson RM. The foot-and-mouth epidemic in Great Britain: pattern of spread and impact of interventions. Science. 2001;292:1155–60. http://dx.doi.org/10.1126/science.1061020
4. Keeling MJ, Woolhouse MEJ, Shaw DJ, Matthews L, Chase-Topping M, Haydon DT, et al. Dynamics of the 2001 UK foot and mouth epidemic: stochastic dispersal in a heterogeneous landscape. Science. 2001;294:813–7. http://dx.doi.org/10.1126/science.1065973
5. Eubank S, Guclu H, Kumar VS, Marathe MV, Srinivasan A, Toroczkai Z, et al. Modelling disease outbreaks in realistic urban social networks. Nature. 2004;429:180–4. http://dx.doi.org/10.1038/nature02541
6. Riley S, Ferguson NM. Smallpox transmission and control: spatial dynamics in Great Britain. Proc Natl Acad

Sci U S A. 2006;103:12637–42. http://dx.doi.org/10.1073/pnas.0510873103
7. Kao RR, Danon L, Green DM, Kiss IZ. Demographic structure and pathogen dynamics on the network of livestock movements in Great Britain. Proc Biol Sci. 2006;273:1999–2007. http://dx.doi.org/10.1098/rspb.2006.3505
8. Kiss IZ, Green DM, Kao RR. The network of sheep movements within Great Britain: Network properties and their implications for infectious disease spread. J R Soc Interface. 2006;3:669–77. http://dx.doi.org/10.1098/rsif.2006.0129
9. Fournié G, Guitian J, Desvaux S, Cuong VC, Dung H, Pfeiffer DU, et al. Interventions for avian influenza A (H5N1) risk management in live bird market networks. Proc Natl Acad Sci U S A. 2013;110:9177–82. http://dx.doi.org/10.1073/pnas.1220815110
10. Green DM, Kiss IZ, Kao RR. Modelling the initial spread of foot-and-mouth disease through animal movements. Proc Biol Sci. 2006;273:2729–35. http://dx.doi.org/10.1098/rspb.2006.3648
11. Keeling MJ, Eames KTD. Networks and epidemic models. J R Soc Interface. 2005;2:295–307. http://dx.doi.org/10.1098/rsif.2005.0051
12. Napp S, Majó N, Sánchez-Gónzalez R, Vergara-Alert J. Emergence and spread of highly pathogenic avian influenza A(H5N8) in Europe in 2016-2017. Transbound Emerg Dis. 2018;65:1217–26. http://dx.doi.org/10.1111/tbed.12861
13. Alarcon P, Brouwer A, Venkatesh D, Duncan D, Dovas CI, Georgiades G, et al. Comparison of 2016–17 and previous epizootics of highly pathogenic avian influenza H5 Guangdong lineage in Europe. Emerg Infect Dis. 2018;24:2270–83. http://dx.doi.org/10.3201/eid2412.171860
14. Guinat C, Nicolas G, Vergne T, Bronner A, Durand B, Courcoul A, et al. Spatio-temporal patterns of highly pathogenic avian influenza virus subtype H5N8 spread, France, 2016 to 2017. Euro Surveill. 2018;23:23. http://dx.doi.org/10.2807/1560-7917.ES.2018.23.26.1700791
15. Direction Générale de l'Alimentation. Arrêté du 4 janvier 2017 définissant les zones géographiques dans lesquelles un abattage préventif est ordonné en application de l'arrêté du 4 janvier 2017 relatif aux mesures complémentaires techniques et financières pour la maîtrise de l'épizootie d'influenza aviaire due au virus H5N8 dans certains départements [cited 2019 May 20]. https://www.legifrance.gouv.fr/affichTexte.do?cidTexte=JORFTEXT000033793904
16. Direction Générale de l'Alimentation. Arrêté du 31 mars 2017 déterminant des dispositions de prévention, de surveillance et lutte complémentaires contre l'influenza aviaire hautement pathogène dans certaines parties du territoire [cited 2019 May 20]. https://www.legifrance.gouv.fr/affichTexte.do?cidTexte=JORFTEXT000034330812
17. Direction Générale de l'Alimentation. Arrêté du 18 janvier 2008 fixant des mesurestechniques et administratives relatives à la lutte contre l'influenza aviaire [cited 2019 Dec 15]. https://www.legifrance.gouv.fr/affichTexte.do?cidTexte=JORFTEXT000017958300
18. Guinat C, Artois J, Bronner A, Guérin JL, Gilbert M, Paul MC. Duck production systems and highly pathogenic avian influenza H5N8 in France, 2016-2017. Sci Rep. 2019;9:6177. http://dx.doi.org/10.1038/s41598-019-42607-x
19. Pantin-Jackwood MJ, Costa-Hurtado M, Shepherd E, DeJesus E, Smith D, Spackman E, et al. Pathogenicity and transmission of H5 and H7 highly pathogenic avian influenza viruses in mallards. J Virol. 2016;90:9967–82. http://dx.doi.org/10.1128/JVI.01165-16
20. Newman MEJ. Modularity and community structure in networks. Proc Natl Acad Sci U S A. 2006;103:8577–82. http://dx.doi.org/10.1073/pnas.0601602103
21. Pons P, Latapy M. Computing communities in large networks using random walks. In: Computer and information sciences. International Symposium on Computer and Information Sciences [cited 2017 Jun 15]. https://link.springer.com/chapter/10.1007/11569596_31
22. Lin J-J, Chang C-H, Pal N. A revisit to contingency table and tests of independence: bootstrap is preferred to Chi-square approximations as well as Fisher's exact test. J Biopharm Stat. 2015;25:438–58. http://dx.doi.org/10.1080/10543406.2014.920851
23. Bouchez-Zacria M, Courcoul A, Durand B. The distribution of bovine tuberculosis in cattle farms is linked to cattle trade and badger-mediated contact networks in south-western France, 2007–2015. Front Vet Sci. 2018;5:173. http://dx.doi.org/10.3389/fvets.2018.00173
24. Soares Magalhães RJ, Ortiz-Pelaez A, Thi KLL, Dinh QH, Otte J, Pfeiffer DU. Associations between attributes of live poultry trade and HPAI H5N1 outbreaks: a descriptive and network analysis study in northern Vietnam. BMC Vet Res. 2010;6:10. http://dx.doi.org/10.1186/1746-6148-6-10
25. VanderWaal K, Enns EA, Picasso C, Packer C, Craft ME. Evaluating empirical contact networks as potential transmission pathways for infectious diseases. J R Soc Interface. 2016;13:20160166. http://dx.doi.org/10.1098/rsif.2016.0166
26. Sims L, Harder TC, Brown I, Gaidet N, Belot G, von Dobschuetz S, et al. Highly pathogenic H5 avian influenza in 2016 and early 2017—observations and future perspectives. Empres Focus On, 2017;11:1–14 [cited 2019 May 20]. http://www.fao.org/3/a-i8068e.pdf
27. Agence nationale de Sécurité Sanitaire de l'Alimentation, de l'Environnement et du Travail. AVIS de l'Agence nationale de sécurité sanitaire de l'alimentation, de l'environnement et du travail relatif au « périmètre optimal de dépeuplement préventif influenza aviaire IA HP H5N8 ≈ [cited 2017 Apr 12]. https://www.anses.fr/fr/system/files/SABA2017SA0011.pdf
28. Csàrdi G, Nepusz T. The igraph software package for complex network research. InterJournal, Complex Systems. 2006;1695;1–9.
29. Lloyd AL, May RM. Epidemiology. How viruses spread among computers and people. Science. 2001;292:1316–7. http://dx.doi.org/10.1126/science.1061076
30. Pastor-Satorras R, Vespignani A. Epidemic spreading in scale-free networks. Phys Rev Lett. 2001;86:3200–3. http://dx.doi.org/10.1103/PhysRevLett.86.3200
31. Direction Générale de l'Alimentation. Le Pacte de lutte contre l'Influenza Aviaire et de relance de la filière foie gras [cited 2017 May 10]. http://agriculture.gouv.fr/le-pacte-de-lutte-contre-linfluenza-aviaire-et-de-relance-de-la-filiere-foie-gras
32. Ratananakorn L, Wilson D. Zoning and compartmentalisation as risk mitigation measures: an example from poultry production. Rev Sci Tech. 2011;30:297–307. http://dx.doi.org/10.20506/rst.30.1.2029
33. Scott A, Zepeda C, Garber L, Smith J, Swayne D, Rhorer A, et al. The concept of compartmentalisation. Rev Sci Tech. 2006;25:873–9, 881–7, 889–95. http://dx.doi.org/10.20506/rst.25.3.1702
34. Direction Générale de l'Alimentation. Situation de l'Influenza aviaire HP H5N8 en France au 05122016 [cited 2018 Nov 8]. https://www.plateforme-esa.fr/article/situation-de-l-influenza-aviaire-hp-h5n8-en-france-au-05122016

35. Briand F-X, Schmitz A, Ogor K, Le Prioux A, Guillou-Cloarec C, Guillemoto C, et al. Emerging highly pathogenic H5 avian influenza viruses in France during winter 2015/16: phylogenetic analyses and markers for zoonotic potential. Euro Surveill. 2017;22:30473. http://dx.doi.org/10.2807/1560-7917.ES.2017.22.9.30473
36. Delpont M, Blondel V, Robertet L, Duret H, Guerin J-L, Vaillancourt J-P, et al. Biosecurity practices on foie gras duck farms, Southwest France. Prev Vet Med. 2018;158:78–88. http://dx.doi.org/10.1016/j.prevetmed.2018.07.012
37. de l'Alimentation DG. Arrêté du 8 février 2016 relatif aux mesures de biosécurité applicables dans les exploitations de volailles et d'autres oiseaux captifs dans le cadre de la prévention contre l'influenza aviaire [cited 2018 Mar 28]. https://www.legifrance.gouv.fr/affichTexte.do?cidTexte=JORFTEXT000032000273
38. Dent JE, Kao RR, Kiss IZ, Hyder K, Arnold M. Contact structures in the poultry industry in Great Britain: exploring transmission routes for a potential avian influenza virus epidemic. BMC Vet Res. 2008;4:27. http://dx.doi.org/10.1186/1746-6148-4-27
39. Nickbakhsh S, Matthews L, Dent JE, Innocent GT, Arnold ME, Reid SWJ, et al. Implications of within-farm transmission for network dynamics: consequences for the spread of avian influenza. Epidemics. 2013;5:67–76. http://dx.doi.org/10.1016/j.epidem.2013.03.001
40. Andronico A, Courcoul A, Bronner A, Scoizec A, Lebouquin-Leneveu S, Guinat C, et al. Highly pathogenic avian influenza H5N8 in south-west France 2016-2017: A modeling study of control strategies. Epidemics. 2019; 28:100340. http://dx.doi.org/10.1016/j.epidem.2019.03.006

Address for correspondence: Claire Guinat, École Nationale Vétérinaire de Toulouse, UMR INRAE-ENVT 1225–IHAP, 23 chemin des Capelles, 31300 Toulouse, France; email: c.guinat@envt.fr

Multidrug- and Extensively Drug-Resistant *Mycobacterium tuberculosis* Beijing Clades, Ukraine, 2015

Matthias Merker, Elena Nikolaevskaya, Thomas A. Kohl, Barbara Molina-Moya, Olha Pavlovska, Patrik Brännberg, Andrii Dudnyk, Valentyna Stokich, Ivan Barilar, Iryna Marynova, Tetiana Filipova, Cristina Prat, Anders Sjöstedt, Jose Dominguez, Olena Rzhepishevska, Stefan Niemann

Multidrug-resistant (MDR) and extensively drug-resistant (XDR) tuberculosis (TB) is an emerging threat to TB control in Ukraine, a country with the third highest XDR TB burden globally. We used whole-genome sequencing of a convenience sample to identify bacterial genetic and patient-related factors associated with MDR/XDR TB in this country. MDR/XDR TB was associated with 3 distinct *Mycobacterium tuberculosis* complex lineage 2 (Beijing) clades, Europe/Russia W148 outbreak, Central Asia outbreak, and Ukraine outbreak, which comprised 68.9% of all MDR/XDR TB strains from southern Ukraine. MDR/XDR TB was also associated with previous treatment for TB and urban residence. The circulation of Beijing outbreak strains harboring broad drug resistance, coupled with constraints in drug supply and limited availability of phenotypic drug susceptibility testing, needs to be considered when new TB management strategies are implemented in Ukraine.

Each year, approximately half a million new cases of multidrug-resistant (MDR) tuberculosis (TB) challenge global health (*1*,*2*). MDR TB is caused by *Mycobacterium tuberculosis* complex (MTBC) strains, resistant to at least isoniazid and rifampin (*3*). In Europe, Ukraine is a hotspot of drug-resistant TB, with 6,564 laboratory-confirmed MDR and rifampin-resistant cases (*2*) and the third highest burden of extensively drug-resistant (XDR) TB (1,097 laboratory confirmed cases) globally in 2017 (*2*). XDR TB is a complicated form of MDR TB with additional resistances to ≥1 second-line injectable antimicrobial drug and a fluoroquinolone (*1*). Treatment of XDR TB can take up to 2 years (*4*), and treatment of a single XDR TB case has been reported to exceed €100,000 (*5*,*6*), even though treatment success rates remain ≈30% in the European region of the World Health Organization (40 countries reported) (*7*). Improvement of MDR/XDR TB prevention, diagnosis, and treatment is one of the core activities prioritized by WHO and the European Respiratory Society to eliminate TB (*6*).

In addition to shortcomings in TB diagnosis and treatment, bacterial genetic factors might play a role in the epidemiologic success of certain MDR strains, especially of lineage 2 (Beijing) in Eurasia (*8*–*11*). Beijing MDR outbreak strains were shown to acquire fitness-enhancing mutations (i.e., mutations that increase in vitro growth rates) that may result in higher virulence and increased transmissibility, thus fostering the MDR TB epidemic in Eastern Europe (*8*–*10*). In line with this assumption, recent computational models predict that in many high TB incidence countries, person-to-person transmission but not treatment-related acquisition accounts for almost all (95.9%) incident MDR TB cases (*12*). Whole-genome sequencing (WGS) coupled with a molecular drug resistance prediction has provided insight into MTBC transmission networks and the transmissibility of MDR/XDR MTBC strains (*8*–*10*,*13*–*15*). We applied a WGS-based molecular epidemiologic approach to identify molecular resistance patterns, dominant strain types, and

Author affiliations: Research Center Borstel, Borstel, Germany (M. Merker, T.A. Kohl, I. Barilar, S. Niemann); Odessa Regional TB Hospital, Odessa, Ukraine (E. Nikolaevskaya, O. Pavlovska, V. Stokich); Institut d'Investigació Germans Trias i Pujol, Badalona, Spain (B. Molina-Moya, C. Prat, J. Dominguez); Centro de Investigación Biomédica en Red (CIBERES), Badalona (B. Molina-Moya, C. Prat, J. Dominguez); Universitat Autònoma de Barcelona, Barcelona, Spain (B. Molina-Moya, C. Prat, J. Dominguez); Umeå University, Umea, Sweden (P. Brännberg, A. Sjöstedt, O. Rzhepishevska); National Pirogov Memorial Medical University, Vinnytsia, Ukraine (A. Dudnyk); Odessa I.I. Mechnikov National University, Odessa (I. Marynova, T. Filipova); German Center for Infection Research, Hamburg-Lübeck-Borstel-Riems, Germany (S. Niemann)

DOI: https://doi.org/10.3201/eid2603.190525

patient-related factors associated with MDR/XDR TB in a convenience sample from southern Ukraine.

Methods

Study Population

MTBC isolates were collected during January–June 2015 in the clinical laboratory of Odessa Regional TB Hospital (now Odessa Regional Center for Socially Significant Diseases; Odessa, Ukraine), where most clinical MTBC cultures from the region are routinely isolated and analyzed. We completed subculturing and WGS on a subset of culture isolates obtained at the clinical laboratory during the study period. The sampling strategy aimed to include a similar proportion of MDR/XDR TB isolates and non-MDR (polyresistant and pansusceptible) strains. We included samples on the basis of routine phenotypic rifampin and isoniazid susceptibility testing that categorized isolates as MDR or non-MDR TB strains; otherwise, inclusion was unbiased and isolates were included directly from the clinical pipeline when human and technical resources were available. Isolates from both new and retreatment cases were eligible for inclusion; retreatment cases included relapse, reinfection, failure of treatment, or interrupted treatment episode. In accordance with the clinical protocol in the laboratory, all MTBC cultures that were not included in our study were autoclaved and disposed.

Our study was mainly set in the Odessa region, which had the highest TB burden (3,039 cases) in Ukraine, the second highest MDR TB burden (30.5% for new cases and 46.9% for retreatment), and TB incidence twice as high as the country's average (127.9 cases/100,000 population) in 2017 (*16*). In total, we included 186 MTBC isolates, each obtained from 1 patient; most were living in the Odessa region (95.2%). The rest of the samples (4.8%) were from the bordering administrative region of Vinnytsia (Figure 1). Inclusion of these samples supported investigation of epidemiologic links between both regions. Thus, the analysis is focused on the differences between 103 non-MDR and 74 MDR/XDR MTBC strains all isolated from southern Ukraine. Patient characteristics assessed for association with MDR/XDR TB were age, sex, residence, HIV status, and case definition.

Contact Tracing of Patients Infected with a Ukraine Outbreak Strain

We conducted a retrospective review of epidemiologic contact tracing for patients infected with a Ukraine outbreak strain through patient records. Because Ukraine lacks resources for contact tracing and TB is stigmatized, we anticipated that the journal information would yield few contacts. To assist with contact identification, we interviewed physicians providing care for the patients with a Ukraine outbreak strain of TB. We maintained data confidentiality in accordance with regional ethics approvals in Ukraine and Umea, Sweden (N 2012-292-31M). We immediately shared information regarding nosocomial transmission of Ukraine outbreak strains with the administration of Odessa Regional TB Hospital to support infection control measures.

Figure 1. Locations where *Mycobacterium tuberculosis* complex (MTBC) DNA samples were collected in Odessa and Vinnytsia regions. Yellow dots indicate locations of patients infected with a MTBC lineage 2 Ukraine outbreak strain. Green dots indicate major cities.

Phenotypic Characterization of Drug Resistance and DNA Isolation

We performed primary isolation and drug-susceptibility testing of MTBC strains using clinical diagnostics protocol for TB in Ukraine. In brief, we treated sputum samples with the N-acetyl-L-cysteine-NaOH (NALC) method for decontamination and further processed them for Ziehl-Neelsen staining using Gene Xpert-MTB/RIF (Cepheid, https://www.cepheid.com), followed by inoculation on Löwenstein–Jensen (LJ) medium and BACTEC MGIT960 tubes (Becton Dickinson, https://www.bd.com) for culture confirmation and subsequently for phenotypic drug susceptibility testing. We used the following drug concentrations (mg/L, by medium): isoniazid, LJ 0.2, MGIT960 0.1; rifampin, LJ 40.0, MGIT960 1.0; ethambutol, LJ

2.0, MGIT960 5.0; pyrazinamide, MGIT960 100.0; and streptomycin, LJ 4.0, MGIT960 1.0. Individual reagents were not always available for routine drug-susceptibility testing, and resistance profiles in this manuscript are based on molecular markers (Appendix 1 Table 1, https://wwwnc.cdc.gov/EID/article/26/3/19-0525-App1.xlsx). We extracted mycobacterial DNA from LJ cultures as previously described (*17*) using cetyltrimethylammonium bromide.

Whole-Genome Sequencing

We completed WGS using Illumina technology (MiSeq, NextSeq 500, and Nextera XT library preparation kit; Illumina, https://www.illumina.com) according to the manufacturer's instructions. We mapped raw read data (FASTQ files) to the *M. tuberculosis* H37Rv genome (GenBank accession no. NC_000962.3) using Burrows-Wheeler Aligner maximal exact matches (*18*) and refined mappings with the Genome Analysis Toolkit software package (*19*). We detected variants, including single-nucleotide polymorphisms (SNPs) and insertions and deletions (indels), with Samtools mpileup (*20*). For a concatenated sequence alignment, the basis for the phylogenetic reconstruction, we considered only SNPs with minimum thresholds of 4 reads in both forward and reverse orientation, 4 reads calling the SNP with a Phred score ≥20, and 75% SNP frequency. We excluded consecutive SNPs for the phylogenetic reconstruction detected within ≤12 bp, which can occur as artificial variants around indels and which would inflate the genetic distance of individual isolates. We combined all remaining SNP positions that had a clear base call for all strains and matched the threshold levels in >95% of all strains in one FASTA alignment, further excluding repetitive regions and resistance-associated genes.

Phylogenetic Reconstruction

We calculated maximum-likelihood trees with FastTree version 2.1.9 (*21*) using a general time-reversible nucleotide substitution model and 1,000 resamplings. The consensus tree was rooted with the midpoint root option in FigTree version 1.4 (http://tree.bio.ed.ac.uk/software/figtree). We obtained cladograms of outbreak strains and number of branch-specific mutations by maximum parsimony using BioNumerics version 7.6 (Applied Maths, https://www.applied-maths.com).

We inferred phylogenetic lineages from specific SNPs based on Coll et al. (*22*) and Merker et al. (*8*). As proxy for TB cases associated with direct transmission events, we considered a maximum pairwise genetic distance between ≥2 MTBC isolates of 5 SNPs, proposed by Walker et al. as a strict threshold that identified cases associated with household transmission (*23*).

Genotypic Drug Resistance Prediction

We extracted polymorphisms from 37 drug resistance– and bacterial fitness–associated genomic targets (Appendix 1 Table 1). We excluded known and newly identified phylogenetic, non–resistance-related variants (*8,24,25*) from the genotypic drug resistance prediction (Appendix 1 Table 3).

Resistance genotypes were defined as follows: for wild-type alleles (H37Rv reference sequence) for all resistance-associated targets we inferred antimicrobial susceptibility (genotypic wild type, gWT). We classified isolates with unknown mutations as genotypic non–wild-type (non-WT) with no further classification. We considered isolates with known resistance-mediating mutations to be resistant to the respective antimicrobial drug (Appendix 1 Table 1). Using genotypic resistance predictions, we classified the isolates as XDR (known mutations mediating resistance to isoniazid, rifampin, ≥1 second-line injectable drug, and a fluoroquinolone), MDR (isoniazid and rifampin resistance but not XDR), and non-MDR (either pansusceptible or any resistance but not MDR).

Statistical Analysis

We created an association plot in R version 3.3 (https://www.r-project.org) using the vcd package version 1.4. The underlying assumption is that the proportion of MDR/XDR MTBC strains within 1 group resembles the proportion of this group among all analyzed isolates (i.e., the resistance level is independent from the phylogenetic groupings). We calculated Pearson residuals to measure the departure from independence from each cell; values of ±2 represent significant deviation at $\alpha = 0.05$ and values of ±4 deviation at $\alpha = 0.001$ (*26*). We prepared a box plot of pairwise genomic distances of MTBC strains from defined strain groups with R version 3.3 using the ggplot2 package version 2.2 (Appendix 2 Figure 1, https://wwwnc.cdc.gov/EID/article/26/3/19-0525-App2.pdf).

We analyzed factors associated with MDR/XDR TB by logistic regression (univariate and multivariate model) using the glm function in R version 3.3.1 (*27*). We excluded the variable MTBC genotype from multivariate analysis because cell counts included 0. We compared means of pairwise SNP distances with 1-way analysis of variance (ANOVA) and Bonferroni multiple comparison tests.

Results

Study Population

During the study period, TB service identified 1,026 patients with ≥1 culture–positive specimen in the Odessa region. Of these cultures, 330 isolates were identified as MDR.

Our study included 16.17% (169/1,026) of the identified positive cultures. MDR/XDR TB specimens constituted 21.82% (72/330) of all MDR/XDR TB–positive cultures identified during the study period. The remaining 97 isolates were phenotypically non-MDR MTBC strains (50 pansusceptible and 47 monoresistant or polyresistant strains). In addition, we randomly collected and analyzed 6 pansusceptible and 2 MDR/XDR MTBC isolates from TB patients registered in the bordering region of Vinnytsia (Vinnytsia Regional TB Hospital, Vinnytsia).

After completing WGS, we withdrew 4.8% (9/186) of MTBC isolates from analysis because of discrepancies between phenotypic drug susceptibility testing and the applied genome-based drug resistance prediction. Therefore, we included 177 MTBC clinical isolates in analysis.

MDR/XDR MTBC Beijing Outbreak Clades

We classified a total of 177 clinical isolates based on WGS data from 10,339 variable positions, according to a recently proposed SNP barcode (*22*). Furthermore, we classified 89 of the isolates (50.3%) as Beijing genotype (lineage 2.2.1) and the remaining 88 (49.7%) as Euro-American lineage 4. We differentiated lineage 4 strains to the following genotypes and sublineages: 8/88 (9.1%) Ghana (lineage 4.1); 32/88 (36.4%) H37Rv-like (lineages 4.7 and 4.8); 16/88 (18.2%) Haarlem (lineages 4.1.2 and 4.1.2.1); 21/88 (23.9%) LAM (lineages 4.3.3, 4.3.4.1, and 4.3.4.2); and 11/88 (12.5%) Ural (lineage 4.2.1) (Figure 2).

Within Beijing lineage 2.2.1, we identified 3 closely related subgroups that exhibited a lower genetic diversity compared with other lineage 2.2.1 strains, based on intragroup pairwise SNP distances between any 2 strains. Two of those subgroups were previously reported in other settings (*8*); we identified them by clade-specific SNPs, and termed them Central Asia outbreak and Europe/Russia W148 outbreak. The third subgroup, named Ukraine outbreak, had not been previously described. These Beijing clades showed a lower median pairwise SNP distance of

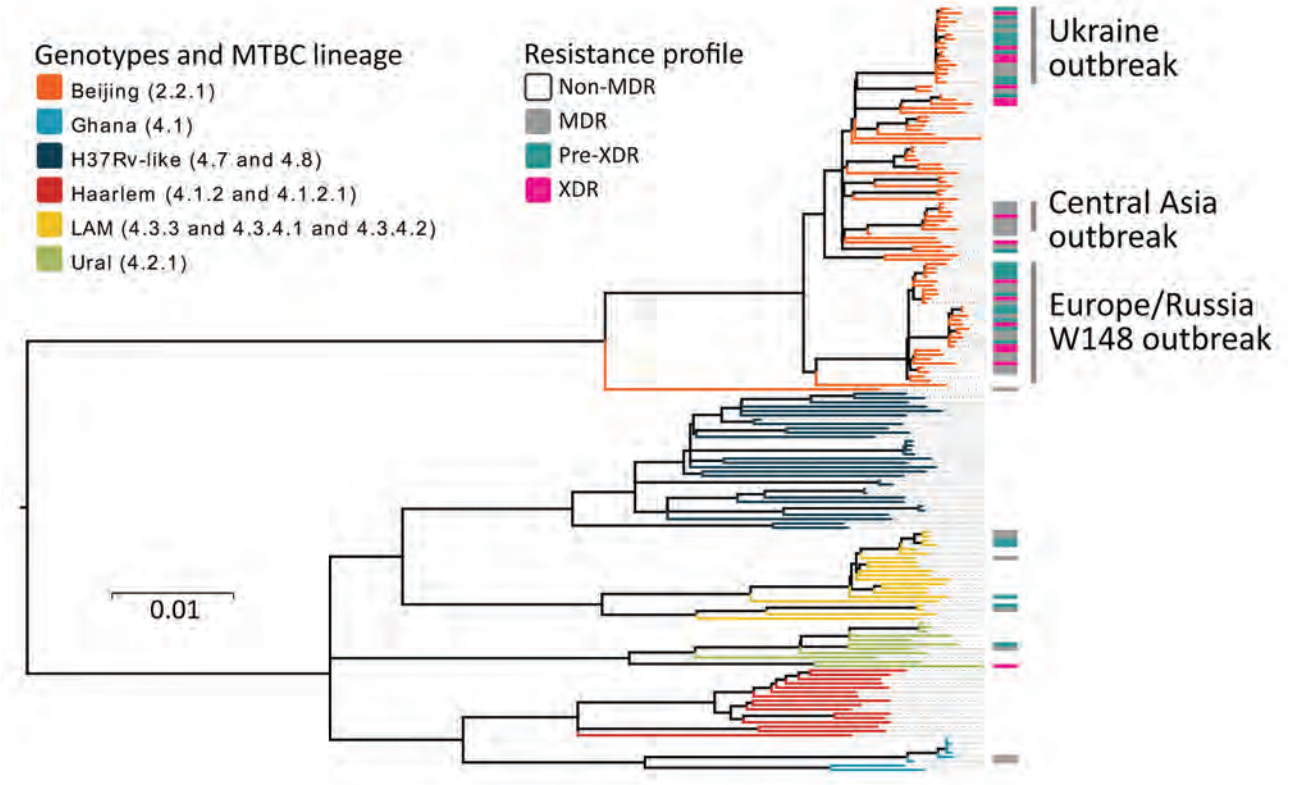

Figure 2. Maximum-likelihood phylogeny based on 10,339 SNPs, and employing general time-reversible substitution model for 177 clinical MDR/XDR and non-MDR *Mycobacterium tuberculosis* complex isolates from southern Ukraine. Branches are color-coded according to the phylogenetic classification from Coll et al. (*22*). Resistance profile bars represent drug resistance classifications based on drug resistance mediating mutations. Scale bar indicates substitutions per site. MDR, multidrug resistant; XDR, extensively drug-resistant.

t25 (interquartile range [IQR] 20.0–32.5) for Central Asia outbreak, 39 (IQR 25.0–48.0) for Europe/Russia W148 outbreak, and 14 (IQR 11.5–18.0) for Ukraine outbreak, contrasting with a distance of 122 (IQR 170.8–139.0) for other Beijing strains ($p<0.05$, one-way ANOVA, Bonferroni multiple comparison test) (Appendix 2 Figure 1).

When we considered a strict threshold of 0–5 SNPs, as previously proposed for MTBC strains isolated from household contacts (*23*), only 9.0% of all patients (16/177) could be linked to 7 putative transmission networks comprising 2–4 patients each. We found these networks or molecular clusters among the 3 Beijing outbreaks (3 transmission events) and other Beijing strains (1 transmission event), and also among Euro-American strains (lineages 4.1 and 4.8; 3 transmission events) (Appendix 1 Table 1).

Contact Tracing Review for Beijing Ukraine Outbreak Cases

Epidemiologic links between clustered patients were partially confirmed by retrospective contact tracing review of patients infected with the Ukraine outbreak strain; of 18 cases, 7 were new and 11 retreatment (Figure 1; Appendix 1 Table 4; Appendix 2 Figure 2). Ukraine outbreak cases were registered in several places (Figure 1); 3 patients had contact through a psychiatric hospital (patient isolate odir-1606, with pairwise SNP distance of 8; odir-1746, SNP distance 10; odir-1747, with distance of 12) and 2 cases (odir-5192 and odir-1636, SNP distance 3) had close contact through their immediate neighborhood (Appendix 1 Table 4; Appendix 2 Figure 2). The neighborhood contact had also been detected by applying the strict SNP threshold. Three other case-patients had a close family MDR TB contact, but bacterial DNA was not available for these cases. No apparent connection could be established among 13 of 18 Ukraine outbreak cases.

Patient Factors Associated with MDR/XDR TB

To pinpoint certain demographic and treatment-related factors associated to MDR/XDR TB in southern Ukraine, we further used logistic regression analysis (Table 1). After multivariate analysis, 3 factors—previous TB treatment (OR 3.5, 95% CI 1.0–12.8; p = 0.04), living in a city (OR 6.0, 95% CI not applicable; p = 0.005), and infection with a Beijing outbreak strain (OR 7.4, 95% CI 1.8–29.9; p≤0.001)—were significantly associated with MDR/XDR TB. Multivariate analysis included the additional variables age, gender, HIV status, and MTBC genotype.

Table 1. Factors associated with MDR/XDR TB in southern Ukraine, analyzed by logistic regression*

Factor	No. (%) cases MDR/XDR TB, n = 74	Univariate analysis OR (95% CI)	Univariate analysis p value	Multivariate analysis† Adjusted OR (95% CI)	Multivariate analysis† Adjusted p value
Age, y					
≤30	15 (20.3)	**3.0 (1.0–8.3)**	**0.04**	0.9 (0.2–4.0)	0.87
30–39	23 (31.1)	1.5 (0.6–3.5)	0.39	0.9 (0.3–3.1)	0.95
40–49	24 (32.4)	1.6 (0.7–3.9)	0.27	0.8 (0.1–5.2)	0.78
≥50	12 (16.2)	Referent			
Case					
Previous treatment	33 (44.6)	**3.3 (1.7–6.5)**	**≤0.001**	**3.5 (1.0–12.8)**	**0.04**
New case	41 (55.4)	Referent			
Sex					
M	50 (67.6)	0.9 (0.5–1.8)	0.85	3.0 (0.6–15.5)	0.12
F	24 (32.4)	Referent			
HIV status					
Positive	24 (32.4)	1.5 (0.8–2.9)	0.23	0.8 (0.1–6.2)	0.81
Negative	50 (67.6)	Referent			
Residence					
Unknown	5 (6.8)	0.5 (0.1–1.5)	0.21	0.7 (NA)†	0.68
City	27 (36.5)	**2.1 (1.1–4.2)**	**0.03**	**6.0 (NA)†**	**0.005**
Village	42 (56.8)	Referent			
Outbreak					
Yes	51 (68.9)	**112 (25.4–493.4)**	**≤0.001**	**7.4 (1.8–29.9)**	**≤0.001**
No	23 (31.1)	Referent			
MTBC genotype†					
Beijing	61 (82.4)	**3.5 (1.3–9.5)**	**0.01**		
H37Rv-like	0 (0)	NA	0.99		
Ghana	2 (2.7)	0.5 (0.1–3.4)	0.51		
Haarlem	0(0)	NA	0.99		
Ural	3 (4.1)	0.6 (0.1–3.0)	0.54		
LAM	8 (10.8)	Referent			

*Bold text indicates significance (p≤0.05). MDR, multidrug-resistant; MTBC, *Mycobacterium tuberculosis* complex; NA, not available; OR, odds ratio; TB, tuberculosis; XDR, extensively drug resistant.
†MTBC genotype contains categories with 0 events; thus, in the multivariate analysis, OR could not be calculated and OR 95% CI reached infinity.

Transmitted and Acquired Drug Resistance among Beijing Outbreak Strains

Consistent with results from the phylogenetic and logistic regression analyses, Beijing outbreak strains were the main carriers of MDR/XDR TB. The Europe/Russia W148, Central Asia, and Ukraine outbreak strains accounted for 29.9% of the cohort, but they contributed to more than two thirds (68.9%) of all MDR/XDR TB cases (Figure 3; Appendix 1 Table 2). The 3 Beijing outbreak strains all harbored high rates of first-line drug resistances to isoniazid (93%–100%), rifampin (93%–100%), streptomycin (93%–100%), ethambutol (86%–100%), and pyrazinamide (75%–100%) (Table 2). In contrast, first-line drug resistance rates among all other Beijing and non-Beijing strains were reduced (8%–33% for individual drugs). Similarly, resistance rates to second-line drugs among the 3 outbreak strains were high (ofloxacin 14%–44%, kanamycin 14%–50%, and prothionamide 57%–100%) compared with other Beijing (ofloxacin 11%, kanamycin 17%, and prothionamide 11%) and non-Beijing (ofloxacin 3%, kanamycin 8%, and prothionamide 15%) strains (Table 2).

An association plot confirmed the results from the logistic regression analysis that demonstrated that MDR/XDR TB among patients in southern Ukraine is clearly linked to the 3 Beijing outbreak clades and that drug resistance is not equally distributed among the MTBC strains, as one would expect from random treatment failures (i.e., acquired resistance) (Figure 3). For example, the Ukraine outbreak strain, constituting 10.2% of the total cohort, was associated with 24.3% of all MDR/XDR TB cases. In contrast, non-Beijing strains, constituting 49.7% of the cohort, were associated with only 17.6% of all MDR/XDR cases.

Strains from the 3 outbreaks demonstrated clade-specific drug resistance–related mutations, mainly to first-line drugs (Figure 4). All Ukraine outbreak strains shared identical mutations mediating resistance to isoniazid (*katG* S315T, *inhA* –15c/t), prothionamide (*inhA* –15c/t), rifampin (*rpoB* S450L), streptomycin (*rpsL* K88R), and ethambutol (*embA* –12 c/t and *embB* Y334H), suggesting that patients have been infected primarily with a strain already resistant to at least these 5 drugs. On the other hand, mutations in the *pncA* gene conferring pyrazinamide resistance were diverse, indicating individual and more recent drug resistance acquisition under selective pressure (e.g., failing treatment regimens) (Figure 4). Similar patterns can be observed for the other 2 outbreaks: shared first-line resistance mediating mutations; unique mutations mediating resistance to kanamycin (*eis* –8 del c, –10 g/a, –12 c/t, –14 c/t, –15 c/g, –35 g/a, –37 g/t); cross-resistance to all injectable drugs (*rrs* 1401 a/g); and resistance to the fluoroquinolones (*gyrA* A90V, S91P, D94G, D94N, D94Y, D94A) (Figure 4; Appendix 1 Table 1). We did not identify any known resistance marker for cycloserine and linezolid (Appendix 1 Table 2).

Strains of the 3 outbreak clades acquired putative compensatory mutations, e.g., in *rpoB* or *rpoC* previously suggested to mitigate the growth deficit of rifampin-resistant strains (*10,11*). These mutations occur either jointly or after the rifampin resistance mediating mutation in the *rpoB* rifampin resistance determining region (Figure 4).

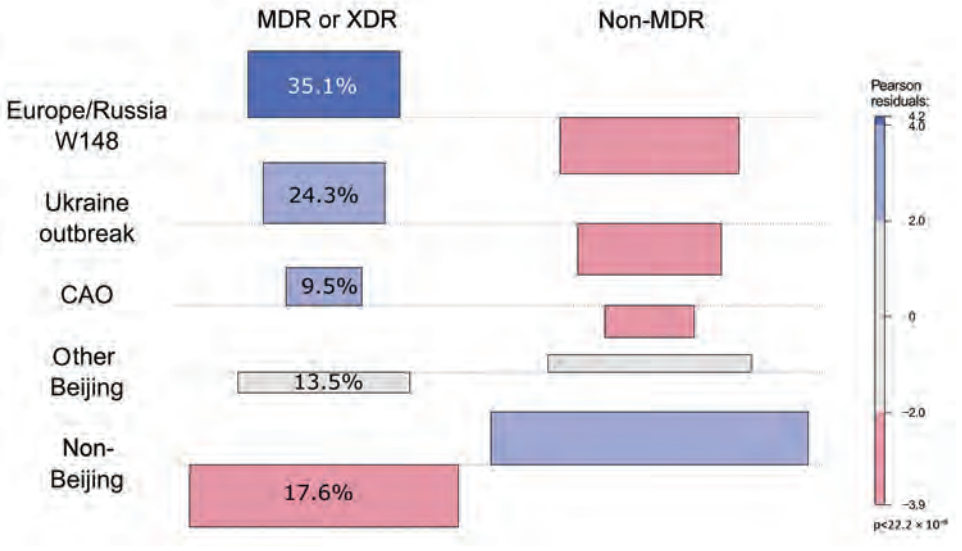

Figure 3. Association plot comparing expected and observed numbers of MDR/XDR and non-MDR strains from different phylogenetic groups. The colors and bar heights reflect the Pearson residuals, the width of the boxes is proportional to the square root of the expected cell counts, blue squares reflect values that are overrepresented, and red squares reflect values that are underrepresented. Pearson values of ±2 represent significant deviation at α = 0.05 level, and values of ±4 represent significant deviation at α = 0.001 level. For example, there are more MDR/XDR TB strains in the Europe/Russia W148 clade (35.1% of all MDR/XDR strains) than expected under the hypothesis of independence. CAO, Central Asian outbreak; MDR, multidrug resistant; XDR, extensively drug-resistant.

Table 2. Percentages of resistance to antimicrobial drugs among *Mycobacterium tuberculosis* strains identified in southern Ukraine*

Drug	All strains, n = 177	Ukraine outbreak, n = 18	Europe/Russia W148 outbreak, n = 28	Central Asia outbreak, n = 7	Other Beijing strains, n = 36	Non-Beijing strains, n = 88
Isoniazid	**48.0** (54.2)	**100** (100)	**92.9** (92.9)	**100** (100)	**27.8** (44.4)	**27.3** (33.0)
Rifampin	**42.9** (44.3†)	**100** (100)	**92.9** (92.9)	**100** (100)	**30.6** (31.4†)	**15.9** (18.2)
Streptomycin	**45.2** (54.8)	**100** (100)	**92.9** (92.9)	**100** (85.7)	**33.33** (47.2)	**19.32 (**34.1)
Ethambutol	**37.3** (36.2)	**100** (66.7)	**85.7** (75.0)	**100** (57.1)	**11.11** (38.9)	**14.77** (14.8)
Pyrazinamide	**31.6**	**88.9**	**75**	**100**	**13.9**	**8.0**
Ofloxacin	**14.7**	**44.4**	**35.7**	**14.3**	**11.1**	**3.4**
Amikacin	**9.6**	**22.22**	**21.43**	**14.3**	**8.3**	**3.4**
Capreomycin	**9.6**	**22.2**	**21.4**	**14.3**	**8.3**	**3.4**
Kanamycin	**19.2**	**50.0**	**39.3**	**14.3**	**16.7**	**8.0**
Prothionamide	**34.5**	**100**	**78.6**	**57.1**	**11.1**	**14.8**
Cycloserine	**0**	**0**	**0**	**0**	**0**	**0**
Linezolid	**1.0**	**0**	**0**	**0**	**0**	**1.1**
PAS	**10.7**	**0**	**39.3**	**0**	**0**	**9.**1

*Percentages of genotypic (parentheses) and phenotypic (bold text) drug resistance for *Mycobacterium tuberculosis* complex strains in southern Ukraine. PAS, para-aminosalicylic acid.
†One phenotypic susceptibility test result was not available.

Discussion

This study demonstrates that MDR/XDR TB patients in southern Ukraine are infected predominantly with strains belonging to 3 distinct MTBC Beijing outbreak clades. The fact that strains belonging to 2 of these outbreaks have been isolated from patients elsewhere in the world indicates long-term transmission and prevalence of these strain types on a broader geographic scale (i.e., Eastern Europe and Central Asia). Each outbreak subgroup harbored specific combinations of mutations mediating drug resistance, a likely result of clonal expansion of a drug-resistant common ancestor giving rise to almost identical clones that individually acquired additional drug resistance mediating mutations.

Considering the mean pairwise distances among the outbreak clades (14 SNPs for Ukraine outbreak, 25 for Central Asia outbreak, and 39 for Europe/Russia outbreak) and a proposed short-term mutation rate for MTBC strains of ≈0.5 SNPs/genome/year (*23*), we estimate that each outbreak progenitor emerged 20–40 years ago. The W148 Europe/Russia outbreak clade and the Central Asia outbreak clade have been described previously in former Soviet Union territories (*8,10*). The Ukraine outbreak clade has not been found in other settings and may be geographically restricted to Ukraine.

Imprisonment has been discussed as the major driver of MDR/XDR TB transmission in Ukraine (*28*–*30*). However, only 1 of the Ukraine outbreak case-patients had been previously imprisoned. The contact tracing review indicates household/neighborhood and nosocomial transmission as modes for the spread of MDR/XDR outbreak strains. The fact that 25 of 53 outbreak strains (Appendix 1 Table 1) have been isolated from new TB cases in our study suggests larger transmission networks in the community. However, because of limitations of the contact tracing review, it is possible that we overlooked some contacts connected to prisons in Ukraine.

The resistance profiles of the outbreak strains indicate that TB treatment regimens including isoniazid, rifampin, pyrazinamide, ethambutol, kanamycin, amikacin, capreomycin, levofloxacin, moxifloxacin, ethionamide, prothionamide, para-aminosalicylic acid, linezolid, and cycloserine (*31*) are not sufficient to effectively treat patients infected with these strains. Indeed, the implementation of rapid Xpert MTB/RIF diagnostics (Cepheid) in the Odessa region has not resulted in substantially improved MDR TB treatment outcomes (*32*). The failing standard MDR TB regimens that include 2–3 active and 2–3 nonactive drugs are still used instead of personalized, laboratory-confirmed treatment (*30*). One reason for this is a lack of the universal access to new or repurposed anti-TB drugs such as bedaquiline, delamanid, and meropenem, and limited funding of palliative TB care that should be used when fewer than 4 active drugs are available (*31*).

Studies in South Africa and Argentina demonstrate that inadequate treatment regimens are drivers for clonal expansion of particular strain types and further drug resistance acquisition (*13,33*), which also holds true for the expansion of the 3 detected Beijing outbreak clades in southern Ukraine. In fact, the observed mutation profiles of the outbreak strains with identical first-line drug resistance–mediating mutations and individual mutations that confer second-line drug resistances are characteristic of an acquired MDR MTBC infection (primary resistance), followed by further resistance development under suboptimal treatment regimens (secondary resistance) during a more recent infection or treatment regimen. The high

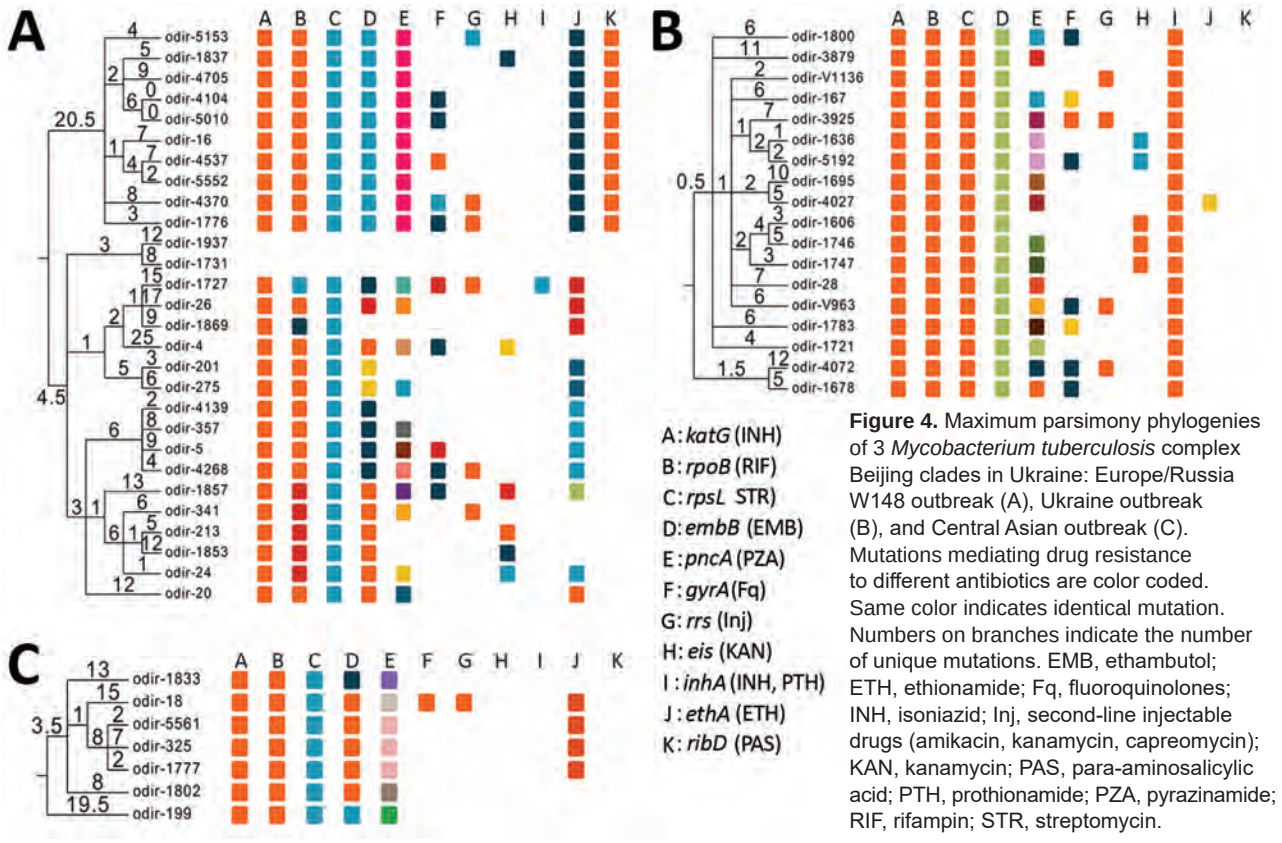

Figure 4. Maximum parsimony phylogenies of 3 *Mycobacterium tuberculosis* complex Beijing clades in Ukraine: Europe/Russia W148 outbreak (A), Ukraine outbreak (B), and Central Asian outbreak (C). Mutations mediating drug resistance to different antibiotics are color coded. Same color indicates identical mutation. Numbers on branches indicate the number of unique mutations. EMB, ethambutol; ETH, ethionamide; Fq, fluoroquinolones; INH, isoniazid; Inj, second-line injectable drugs (amikacin, kanamycin, capreomycin); KAN, kanamycin; PAS, para-aminosalicylic acid; PTH, prothionamide; PZA, pyrazinamide; RIF, rifampin; STR, streptomycin.

prevalence of high-level isoniazid resistance, mediated by *katG* S315T, and also the broad spectrum of pyrazinamide resistance mediating mutations adds Ukraine to the list of countries where the recently proposed standard short MDR TB regimen will have hardly any effect (*34*,*35*).

The main limitation of our study is that only 21.81% of all MDR isolates registered during the study period could be recovered within routine practice because of limited technical and human resources. This shortfall could potentially introduce some uncertainties regarding the true proportions of the outbreak clades. Further, we show that MDR/XDR TB patients in southern Ukraine are infected mainly with 3 distinct MTBC Beijing outbreak clades. However, inhabitants of southeastern Ukraine were indeed at higher risk for primary MDR TB (*36*,*37*). This finding might be linked to the circulation of the Beijing outbreak strains we describe but we cannot extrapolate our results to the whole country which was shown to have an asymmetric distribution of MDR TB (*37*). Finally, the low number of genetically predicted and confirmed transmission events in our study is likely due to the short sampling period.

In conclusion, we demonstrate that distinct MDR outbreak clones in combination with failing regimens have been the main drivers of the MDR/XDR TB epidemic in Ukraine, rather than poor adherence to treatment. Individualized treatment regimens based on laboratory-confirmed resistance profiles are the key to containing MDR/XDR TB in these settings. Access to new drugs such as bedaquiline and delamanid should be supported, but strictly controlled, because resistances are likely to develop (*38*).

M.M. received the Gertrud Meissner Award sponsored by HAIN Lifescience, outside the submitted work; S.N. reports grants from the German Center for Infection Research and the Leibniz Association during the conduct of the study; E.N., I.M., O.P., P.B., J.D., C.P., O.R. report FP7-Marie Curie Sklodowska Actions, grant N 319007, during the study period.

About the Author

Dr. Merker is an assistant professor in the group of molecular and experimental mycobacteriology at the Research Center Borstel, Borsel, Germany. His research is focused on the evolution of drug resistance, *M. tuberculosis* population genetics, and the application of next-generation sequencing techniques for molecular drug resistance assays.

References

1. World Health Organization. Global tuberculosis report 2017. Geneva: The Organization; 2017.
2. World Health Organization. Global tuberculosis report 2018: Geneva: The Organization; 2018.
3. Walker TM, Merker M, Knoblauch AM, Helbling P, Schoch OD, van der Werf MJ, et al.; MDR-TB Cluster Consortium. A cluster of multidrug-resistant *Mycobacterium tuberculosis* among patients arriving in Europe from the Horn of Africa: a molecular epidemiological study. Lancet Infect Dis. 2018;18:431–40. https://doi.org/10.1016/S1473-3099(18)30004-5
4. Lange C, Abubakar I, Alffenaar JW, Bothamley G, Caminero JA, Carvalho AC, et al. TBNET. Management of patients with multidrug-resistant/extensively drug-resistant tuberculosis in Europe: a TBNET consensus statement. Eur Respir J. 2014;44:23–63. https://doi.org/10.1183/09031936.00188313
5. Günther G, Gomez GB, Lange C, Rupert S, van Leth F. TBNET. Availability, price, and affordability of anti-tuberculosis drugs in Europe: a TBNET survey. Eur Respir J. 2015;45:1081–8. https://doi.org/10.1183/09031936.00124614
6. Matteelli A, Rendon A, Tiberi S, Al-Abri S, Voniatis C, Carvalho ACC, et al. Tuberculosis elimination: where are we now? Eur Respir Rev. 2018;27:27. https://doi.org/10.1183/16000617.0035-2018
7. European Centre for Disease Prevention and Control/WHO Regional Office for Europe. Tuberculosis surveillance and monitoring in Europe, 2018, 2016 data. 2018 [cited 2019 Dec 31]. https://www.ecdc.europa.eu/en/publications-data/tuberculosis-surveillance-and-monitoring-europe-2018
8. Merker M, Blin C, Mona S, Duforet-Frebourg N, Lecher S, Willery E, et al. Evolutionary history and global spread of the *Mycobacterium tuberculosis* Beijing lineage. Nat Genet. 2015;47:242–9. https://doi.org/10.1038/ng.3195
9. Cohen KA, Abeel T, Manson McGuire A, Desjardins CA, Munsamy V, Shea TP, et al. Evolution of extensively drug-resistant tuberculosis over four decades: whole-genome sequencing and dating analysis of *Mycobacterium tuberculosis* isolates from KwaZulu-Natal. PLoS Med. 2015;12:e1001880. https://doi.org/10.1371/journal.pmed.1001880
10. Casali N, Nikolayevskyy V, Balabanova Y, Harris SR, Ignatyeva O, Kontsevaya I, et al. Evolution and transmission of drug-resistant tuberculosis in a Russian population. Nat Genet. 2014;46:279–86. https://doi.org/10.1038/ng.2878
11. Comas I, Coscolla M, Luo T, Borrell S, Holt KE, Kato-Maeda M, et al. Out-of-Africa migration and Neolithic coexpansion of *Mycobacterium tuberculosis* with modern humans. Nat Genet. 2013;45:1176–82. https://doi.org/10.1038/ng.2744
12. Kendall EA, Fofana MO, Dowdy DW. Burden of transmitted multidrug resistance in epidemics of tuberculosis: a transmission modelling analysis. Lancet Respir Med. 2015;3:963–72. https://doi.org/10.1016/S2213-2600(15)00458-0
13. Eldholm V, Monteserin J, Rieux A, Lopez B, Sobkowiak B, Ritacco V, et al. Four decades of transmission of a multidrug-resistant *Mycobacterium tuberculosis* outbreak strain. Nat Commun. 2015;6:7119. https://doi.org/10.1038/ncomms8119
14. Lalor MK, Casali N, Walker TM, Anderson LF, Davidson JA, Ratna N, et al. The use of whole-genome sequencing in cluster investigation of a multidrug-resistant tuberculosis outbreak. Eur Respir J. 2018;51:1702313. https://doi.org/10.1183/13993003.02313-2017
15. Nikolayevskyy V, Kranzer K, Niemann S, Drobniewski F. Whole genome sequencing of *Mycobacterium tuberculosis* for detection of recent transmission and tracing outbreaks: A systematic review. Tuberculosis (Edinb). 2016;98:77–85. https://doi.org/10.1016/j.tube.2016.02.009https://www.ncbi.nlm.nih.gov/entrez/query.fcgi?cmd=Retrieve&db=PubMed&list_uids=27156621&dopt=Abstract
16. Public Health Center Ukraine. Tuberculosis in Ukraine [in Ukrainian]. 2018 [cited 2019 Dec 31]. http://aph.org.ua/wp-content/uploads/2018/09/proekt-dovidnika-TB-2018.pdf
17. van Soolingen D, Hermans PW, de Haas PE, Soll DR, van Embden JD. Occurrence and stability of insertion sequences in *Mycobacterium tuberculosis* complex strains: evaluation of an insertion sequence-dependent DNA polymorphism as a tool in the epidemiology of tuberculosis. J Clin Microbiol. 1991; 29:2578–86. https://doi.org/10.1128/JCM.29.11.2578-2586.1991
18. Li H, Durbin R. Fast and accurate short read alignment with Burrows-Wheeler transform. Bioinformatics. 2009;25:1754–60. https://doi.org/10.1093/bioinformatics/btp324
19. McKenna A, Hanna M, Banks E, Sivachenko A, Cibulskis K, Kernytsky A, et al. The Genome Analysis Toolkit: a MapReduce framework for analyzing next-generation DNA sequencing data. Genome Res. 2010;20:1297–303. https://doi.org/10.1101/gr.107524.110
20. Li H, Handsaker B, Wysoker A, Fennell T, Ruan J, Homer N, et al. 1000 Genome Project Data Processing Subgroup. The Sequence Alignment/Map format and SAMtools. Bioinformatics. 2009;25:2078–9. https://doi.org/10.1093/bioinformatics/btp352
21. Price MN, Dehal PS, Arkin AP. FastTree 2—approximately maximum-likelihood trees for large alignments. PLoS One. 2010;5:e9490. https://doi.org/10.1371/journal.pone.0009490
22. Coll F, McNerney R, Guerra-Assunção JA, Glynn JR, Perdigão J, Viveiros M, et al. A robust SNP barcode for typing *Mycobacterium tuberculosis complex strains*. Nat Commun. 2014;5:4812. https://doi.org/10.1038/ncomms5812
23. Walker TM, Ip CL, Harrell RH, Evans JT, Kapatai G, Dedicoat MJ, et al. Whole-genome sequencing to delineate *Mycobacterium tuberculosis* outbreaks: a retrospective observational study. Lancet Infect Dis. 2013;13:137–46. https://doi.org/10.1016/S1473-3099(12)70277-3
24. Coll F, McNerney R, Preston MD, Guerra-Assunção JA, Warry A, Hill-Cawthorne G, et al. Rapid determination of anti-tuberculosis drug resistance from whole-genome sequences. Genome Med. 2015;7:51. https://doi.org/10.1186/s13073-015-0164-0
25. Feuerriegel S, Köser CU, Niemann S. Phylogenetic polymorphisms in antibiotic resistance genes of the *Mycobacterium tuberculosis* complex. J Antimicrob Chemother. 2014;69:1205–10. https://doi.org/10.1093/jac/dkt535
26. Mayer D, Zeileis AKH. Visualizing independence using extended association plots. Presented at: Third International Workshop on Distributed Statistical Computing (DSC 2003); March 20–22, 2003; Vienna, Austria.
27. The R Core Team. R: a language and environment for statistical computing. Reference index. 2019 [cited 2019 Dec 31]. https://cran.r-project.org/manuals.html
28. Daum LT, Konstantynovska OS, Solodiankin OS, Liashenko OO, Poteiko PI, Bolotin VI, et al. Next-generation sequencing for characterizing drug resistance-conferring *Mycobacterium tuberculosis* genes from clinical isolates in the Ukraine. J Clin Microbiol. 2018;56:e00009–00018. https://doi.org/10.1128/JCM.00009-18

29. Nikolayevskyy VV, Brown TJ, Bazhora YI, Asmolov AA, Balabanova YM, Drobniewski FA. Molecular epidemiology and prevalence of mutations conferring rifampicin and isoniazid resistance in *Mycobacterium tuberculosis* strains from the southern Ukraine. Clin Microbiol Infect. 2007;13:129–38. https://doi.org/10.1111/j.1469-0691.2006.01583.x
30. World Health Organization. Review of the national tuberculosis programme in Ukraine. Copenhagen, Denmark: The Organization; 2011.
31. A unified clinical protocol of primary, secondary (specialized) and tertiary (highly specialized) medical care for adults [in Ukrainian]. Tuberculosis. 2014 [cited 2020 Jan 8]. https://www.phc.org.ua/sites/default/files/uploads/files/%D0%9F%D1%80%D0%BE%D1%82%D0%BE%D0%BA%D0%BE%D0%BB%20%D0%A2%D0%91%20%D1%83%20%D0%B2%D0%B7%D1%80%D0%BE%D1%81%D0%BB%D1%8B%D1%85%20620%20%D0%BE%D1%82%20%2004%2009%2014.pdf
32. Nikolayevskyy V, Kontsevaya I, Nikolaevskaya E, Surkova E, Samchenko S, Esipenko S. Diagnostic performance and impact of routinely implemented Xpert® MTB/RIF assay in a setting of high incidence of drug-resistant TB in Odessa Oblast, Ukraine. Clin Microbiol Infect. 2019;25:1040.e1–6. https://doi.org/10.1016/j.cmi.2018.12.013
33. Manson AL, Cohen KA, Abeel T, Desjardins CA, Armstrong DT, Barry CE III, et al.; TBResist Global Genome Consortium. Genomic analysis of globally diverse *Mycobacterium tuberculosis* strains provides insights into the emergence and spread of multidrug resistance. Nat Genet. 2017;49:395–402. https://doi.org/10.1038/ng.3767
34. Lange C, Duarte R, Fréchet-Jachym M, Guenther G, Guglielmetti L, Olaru ID, et al. European MDR-TB database collaboration. Limited benefit of the new shorter multidrug-resistant tuberculosis regimen in Europe. Am J Respir Crit Care Med. 2016;194:1029–31. https://doi.org/10.1164/rccm.201606-1097LE
35. Balabanova Y, Fiebig L, Ignatyeva O, Riekstina V, Danilovits M, Jaama K, et al. Multidrug-resistant TB in Eastern region of the EU: is the shorter regimen an exception or a rule? Thorax. 2017;72:850–2. https://doi.org/10.1136/thoraxjnl-2016-209841
36. Konstantynovska O, Rekrotchuk M, Hrek I, Rohozhyn A, Rudova N, Poteiko P, et al. Severe clinical outcomes of tuberculosis in Kharkiv Region, Ukraine, are associated with Beijing strains of *Mycobacterium tuberculosis*. Pathogens. 2019;8:8. https://doi.org/10.3390/pathogens8020075
37. Pavlenko E, Barbova A, Hovhannesyan A, Tsenilova Z, Slavuckij A, Shcherbak-Verlan B, et al. Alarming levels of multidrug-resistant tuberculosis in Ukraine: results from the first national survey. Int J Tuberc Lung Dis. 2018;22:197–205. https://doi.org/10.5588/ijtld.17.0254
38. Hoffmann H, Kohl TA, Hofmann-Thiel S, Merker M, Beckert P, Jaton K, et al. Delamanid and bedaquiline resistance in *Mycobacterium tuberculosis* ancestral Beijing genotype causing extensively drug-resistant tuberculosis in a Tibetan refugee. Am J Respir Crit Care Med. 2016;193:337–40. https://doi.org/ 10.1164/rccm.201502-0372LE

Address for correspondence: Olena Rzhepishevska, Umea University—Chemistry, Linnaeus väg 10, 901 87 Umea, Sweden; email: olena.rzhepishevska@umu.se; Matthias Merker, National Reference Centre for Mycobacteria, Research Centre—Molecular Mycobacteriology, Parkallee 1, 23845 Borstel, Germany; email: mmerker@fz-borstel.de

Stable and Local Reservoirs of *Mycobacterium ulcerans* Inferred from the Nonrandom Distribution of Bacterial Genotypes, Benin

Clément Coudereau, Alban Besnard, Marie Robbe-Saule, Céline Bris, Marie Kempf, Roch Christian Johnson, Télésphore Yao Brou, Ronald Gnimavo, Sara Eyangoh, Fida Khater, Estelle Marion

Mycobacterium ulcerans is the causative agent of Buruli ulcer, a neglected tropical disease found in rural areas of West and Central Africa. Despite the ongoing efforts to tackle Buruli ulcer epidemics, the environmental reservoir of its pathogen remains elusive, underscoring the need for new approaches to improving disease prevention and management. In our study, we implemented a local-scale spatial clustering model and deciphered the genetic diversity of the bacteria in a small area of Benin where Buruli ulcer is endemic. Using 179 strain samples from West Africa, we conducted a phylogeographic analysis combining whole-genome sequencing with spatial scan statistics. The 8 distinct genotypes we identified were by no means randomly spread over the studied area. Instead, they were divided into 3 different geographic clusters, associated with landscape characteristics. Our results highlight the ability of *M. ulcerans* to evolve independently and differentially depending on location in a specific ecologic reservoir.

Buruli ulcer (BU) is a devastating necrotic human skin disease caused by *Mycobacterium ulcerans* (*1*). It is the third most common mycobacterial disease after tuberculosis and leprosy; ≈2,000 cases are reported each year worldwide, mostly in rural areas of West and Central Africa. The high number of patients with massive skin ulcers is a major problem because treatment of advanced disease is complex, and the consequent long-term disabilities can lead to social stigmatization and economic consequences for families and rural communities (*2*).

BU is characterized by a focal endemicity, and *M. ulcerans* has potential primary environmental reservoirs in wetlands, rivers, and stagnant bodies of water (*3*,*4*). The exact mode of transmission to humans remains unclear, but studies have shown that inoculation into the subcutaneous tissues is required (*5*,*6*). Thus, suspicions have arisen that aquatic insects, mollusks, and fishes are reservoirs and that insect bites are the mode of transmission (*7*–*9*). Transmission through human-to-human contact has been ruled out as a potential mode of transmission because living near an infected family member does not pose a higher risk for infection (*10*). However, fundamental questions remain concerning the participation of humans in dissemination of the bacterium (*11*,*12*).

Developing adapted preventive strategies requires identification of the environment that enables *M. ulcerans* development and the dynamics of the mycobacterium in the environment and in patients. However, because *M. ulcerans* cannot yet be cultured directly from environmental samples, comparison of *M. ulcerans* isolates retrieved in the environment with those in humans is impossible.

Whole-genome sequencing (WGS), coupled with single-nucleotide polymorphism (SNP)–based genotyping, has led to major advances in *M. ulcerans* genomics. This approach was applied recently to provide a description of the *M. ulcerans* population structure in Ghana (*13*). It has also been used to provide insights into the circulating genotypes in BU-endemic regions of Cameroon (*14*) and to study the evolution of *M. ulcerans* in Africa and southeastern

Author affiliations: Université d'Angers, Angers, France (C. Coudereau, A. Besnard, M. Robbe-Saule, M. Kempf, F. Khater, E. Marion); INSERM, Angers (C. Coudereau, A. Besnard, M. Robbe-Saule, M. Kempf, F. Khater, E. Marion); Centre Hospitalo-Universitaire d'Angers, Angers (C. Bris, M. Kempf); Université d'Abomey Calavi, Abomey Calavi, Benin (R.C. Johnson); Fondation Raoul Follereau, Paris, France (R.C. Johnson); Maison de la Télédétection, Montpellier, France (T.Y. Brou); Centre de Diagnostic et Traitement de la Lèpre et de l'Ulcère de Buruli, Pobè, Bénin (R. Gnimavo); International Pasteur Institute Network, Yaoundé, Cameroon (S. Eyangoh)

DOI: https://doi.org/10.3201/eid2603.190573

Australia (*11*,*15*). Recently, Vandelannoote et al. described the bacterial distribution on a local scale in Congo (*12*).

In using a representative collection of 208 *M. ulcerans* isolates, our objective was to identify and track on a local scale the genotypes circulating in the BU-endemic regions of Ouémé and Plateau in southeast Benin and in Ogun State in southwest Nigeria. We evaluated the presence of specific clusters according to the geographic localization of patients and performed local-scale clustering by using a phylogenetic analysis approach based on SNP typing, coupled with spatial scan statistics.

Materials and Methods

Bacterial Isolates and Patients

We conducted WGS on 208 *M. ulcerans* strains isolated from patients diagnosed with and treated for BU during 2007–2016 at the Centre de Diagnostic et Traitement de la Lèpre et de l'Ulcère de Buruli (CDTLUB) in Pobè, Benin. We first sequenced and analyzed 179 strains; then, to perform validation of the model, we sequenced and analyzed a second set of 29 strains.

DNA Sequencing

We cultivated isolates on a Lowenstein-Jensen medium for 5 months. We performed DNA extraction as previously described (*16*). We sequenced genomes by using either MiSeq or HiSeq sequencer (Illumina, https://www.illumina.com) with Nextrera XT DNA preparation kit or Ion Torrent S5XL technology with IonXpress Plus Fragment library kit (Life Technologies, https://www.thermofisher.com/us/en/home/brands/life-technologies.html). We submitted generated reads to the National Center for Biotechnology Information Sequence Read Archive (BioProjectID no. PRJNA499075). (See additional methods in Appendix 1, https://wwwnc.cdc.gov/EID/article/26/3/19-0573-App1.pdf.)

Variant Detection and Maximum-Likelihood Phylogenetics

After checking quality with FastQC version 0.11.7 (*17*), we performed a quality trimming by using Trimmomatic version 0.36 (*18*) and read mapping and SNP detection by using Snippy version 3.2 (*19*). We used the Burrows-Wheeler Aligner version 0.7.12 (*20*) with default parameters to map clipped read-pairs to the Agy99 reference genome (Genbank accession no. CP000325) and to the pMUM001 plasmid (accession no. BX649209) (*21*). Agy99 is the only annotated strain from Africa available for *M. ulcerans* species. By using the alignment of core genome SNPs of the first 179 genomes, we generated a maximum-likelihood phylogenetic tree with PhyML 3.020120412 using the general time-reversible model (*22*). For the second set of sequencing of 29 strains, we generated another tree by using the alignment of all the sequenced genomes. We performed bootstrapping by using 1,000 replicates to assess the reliability of the phylogenies. All phylogenies were rooted by using strains from Mu_A2 lineage. We used TreeCollapseCL 4.0 (*23*) to collapse nodes in the tree with bootstrap values below a set threshold of 70% to soft polytomies, thereby preserving the length of the tree.

Phylogeographic Analysis

We performed a Kulldorf spatial scan statistic, implemented in SaTScan 9.6 (*24*), to verify the presence and location of spatial clusters by identifying spatial clusters on the basis of geographic coordinates (Appendix 1). We used QGIS 2.10 (*25*) to generate figures on the geographic distribution of *M. ulcerans*.

Satellite Data and Processing

We acquired satellite imagery by using Sentinel-2 (European Space Agency, https://www.esa.int). Images used were recorded on January 6, 2018, with a spatial resolution of 10 m. Land use and cover were recovered with a supervised classification using minimum distance algorithm. We created training samples on the basis of expert knowledge of West Africa topography and Google Earth.

Statistical Analysis

We tested for statistical significance by using either Fisher exact test or 1-way analysis of variance. We validated the model by calculating accuracy and Matthews correlation coefficient on the confusion matrices (Appendix 1). We performed data analysis and visualization in R 3.4.4 (*26*) with the ade4, plot3D, seqinr, and ggplot2 packages and data-intensive computations by using a GenOuest computer cluster (https://www.genouest.org).

Results

Presentation of Selected Strains and Areas

We analyzed 179 strains isolated from patients diagnosed with and treated for BU at CDTLUB during 2007–2016. Patients originated from regions of Ouémé (111 [52%]) and Plateau (47 [26%]) in southeast Benin and from Ogun State in southwest Nigeria (21 [12%]). The proportion of genomes selected was in accordance with the geographic origin of patients visiting CDTLUB (Figure 1). Moreover, the 158 bacterial strains

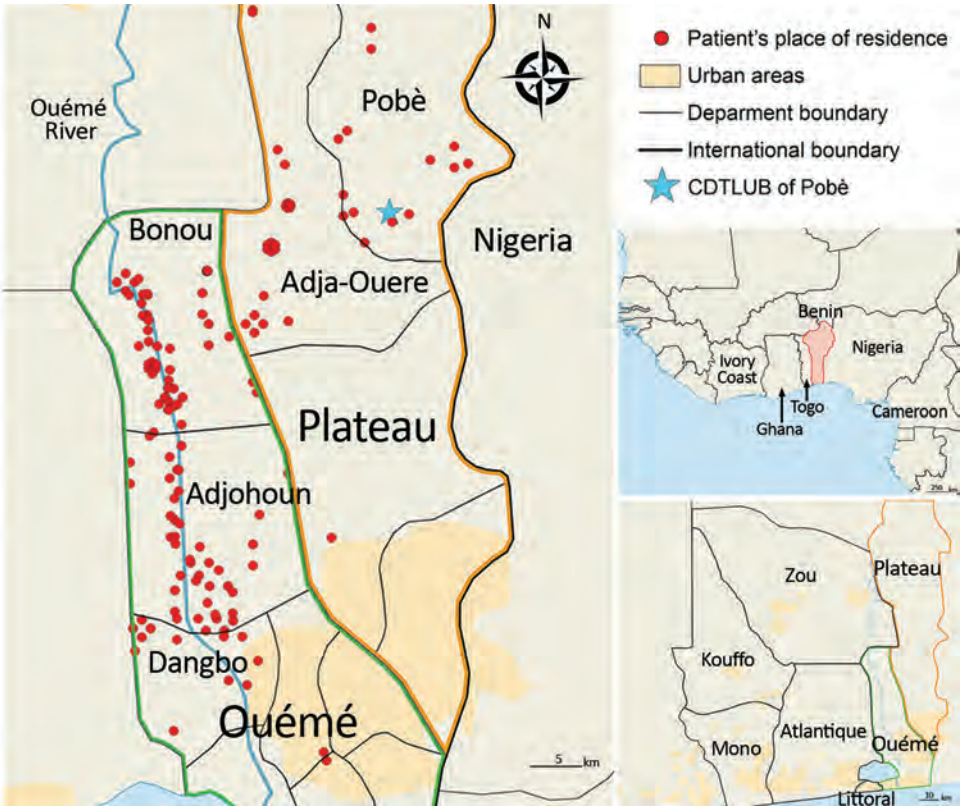

Figure 1. Spatial distribution of Buruli ulcer patients in Benin and Nigeria. The 179 sequenced genomes of *Mycobacterium ulcerans* were isolated from patients in southeastern Benin; 62% came from the Ouémé region, 26% came from the Plateau region, and the remaining genomes originated from patients in Nigeria. Red dots indicate precise locations of patients' declared place of residence. In cases where several patients were from the same village, points were slightly displaced in a circle fashion to obtain the most accurate rendering of geographic density of Buruli ulcer cases. Insets show location of Benin in West Africa and of the Ouémé and Plateau regions in Benin. CDTLUB, Centre de Diagnostic et Traitement de la Lèpre et de l'Ulcère de Buruli.

selected from Benin (Ouémé and Plateau) were representative of the epidemiologic data of BU in patients in Benin (Appendix 2 Tables 1, 2, https://wwwnc.cdc.gov/EID/article/26/3/19-0573-App2.xlsx).

Genome Sequence Comparisons of 179 *M. ulcerans* Strains

SNP Identification on *M. ulcerans* Strains

After WGS, a total of 6,163 core genome SNPs were uncovered after mapping the 179 strains against the referent genome Agy99 (Appendix 2 Table 3a); 35 SNPs (0.5%) were nonsense mutations, 2,544 (41.2%) were missense mutations, 1,539 (25%) were synonymous mutations, and 2,045 (33.2%) were outside of genes. Among these SNPs, 85% (5,223) belonged to 5 isolates identified as coming from Mu_A2 lineage and thus were used as a tree rooting outgroup. The 174 other isolates belonged to the West Africa lineage Mu_A1, and their genomes displayed highly restricted intrastrain genetic variation, having 940 SNP differences across a 5.2 Mbp core genome. Among these 940 SNPs (Appendix 2 Table 3b), 9 (1%) were nonsense, 398 (42%) were missense, 228 were synonymous (24%), and 305 (33%) were outside of genes. Also, although the plasmid accounted for 3.1% of the total amount of the bacterial genome, only 9 SNPs (0.9%) were found, none occurring on genes that encoded enzymes required for mycolactone synthesis. Thus, most (99%) SNPs were located on the bacterial chromosome.

Identification of 8 Genetically Distinct *M. ulcerans* Genotypes

We used an Eigenstrat-like principal component analysis approach to identify groups of genomes based on their SNP. We identified 8 groups with similar genotypic features and defined them as genotypes (Figure 2, panel A). We displayed the 940 SNPs at each genomic position (Figure 2, panel B).

Phylogenetic Inference of the 8 Genetically Distinct *M. ulcerans* Genotypes

The 8 genotypes were also identifiable in the phylogeny of the 174 strains identified as belonging to Mu_A1 lineage (West Africa lineage) (Figure 3; Appendix 1 Figure 1). Almost half (46%) of the strains belonged to genotype 8; the rest belonged to genotypes 1–7 at proportions ranging from 4% to 12% (Figure 2). Each genotype seemed to be a monophyletic group, with the exception of genotypes 4 and 5, which were paraphyletic. Each group had a bootstrap value ranging from 88% to 100%. Therefore, we proposed a mutation profile for each genotype, thereby providing a specific molecular signature as a basis for bacterial

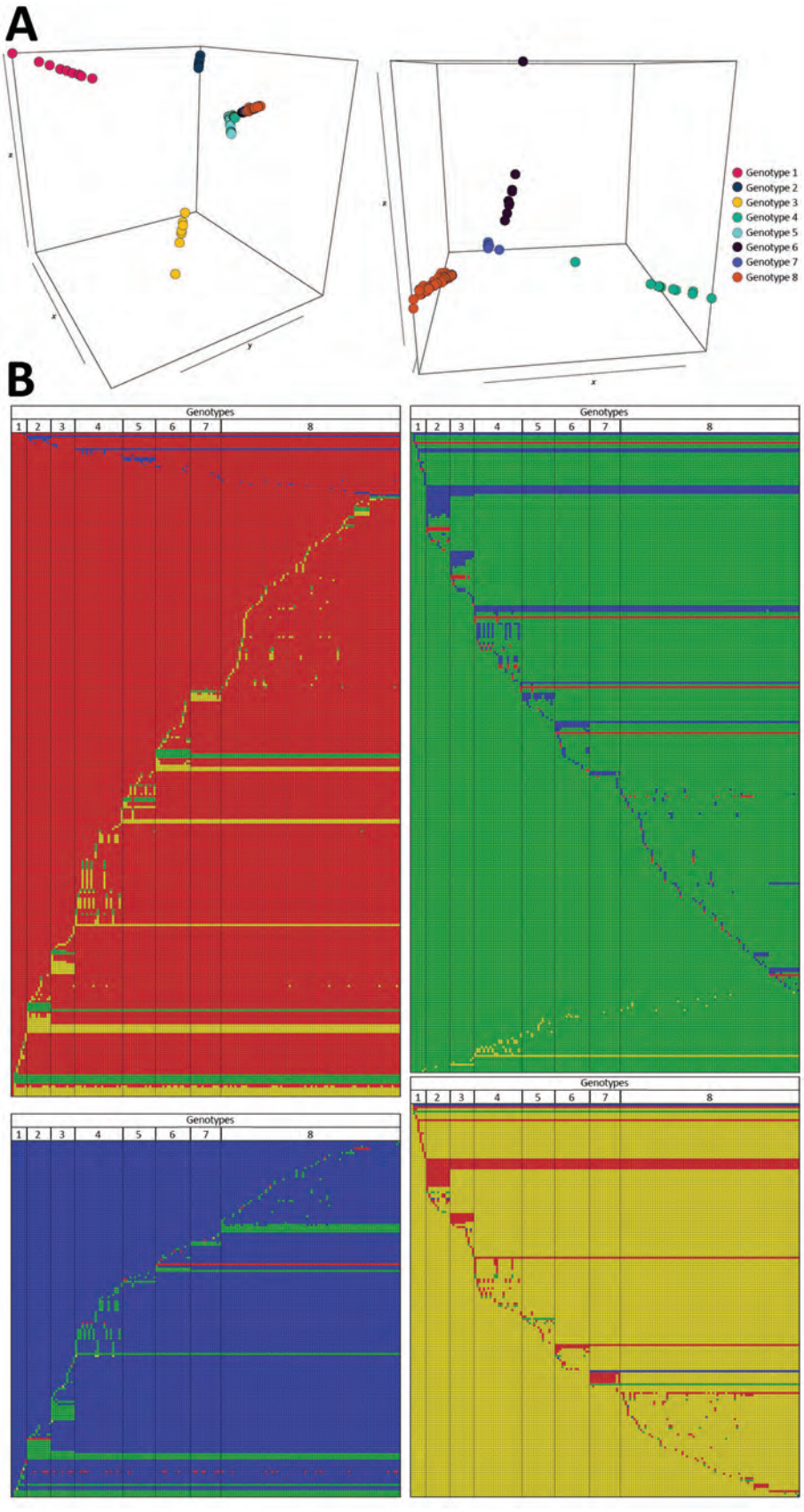

Figure 2. Graphical representations of the 8 *Mycobacterium ulcerans* genomes and their 940 single-nucleotide polymorphisms from Buruli ulcer patients in Benin and Nigeria. A) Principal component analysis (PCA) projection on the first 3 principal components with 8 groups of genomes clustering together, which we defined as genotypes. PCA was performed based on the Eigenstrat algorithm but applied to a haploid organism. Image on the left displays a PCA performed on all 174 genomes; image on the right displays a PCA performed after removing genomes from the first 3 genotypes (shown for better visualization of genome clustering). Axes x, y, and z represent the principal components 1, 2, and 3, respectively; inertia was 7% for component 1, 5% for component 2, and 4% for component 3. B) Graphical representation of the 940 single-nucleotide polymorphisms specific to the 8 genotypes, showing interdifferences and intradifferences of all genomes. Each line represents 1 genomic position, and each column represents 1 *M. ulcerans* genome. A color code has been chosen for each nucleotide (blue, adenine; green, guanine; red, cytosine; yellow, thymine). Each representation has been ordered and referenced against the genome 1232–13 belonging to genotype 1 (first column).

strain genotyping (Appendix 1 Figure 2). We compiled each SNP specific relationship to a genotype (Appendix 2 Table 3).

Effect of Genotype Specificity on Clinical Features

To verify whether the 8 genotypes could be related to any of the basic characteristics of patients, we performed the Fisher exact test to analyze severity and sex and analysis of variance to analyze age. We found no significant association regarding severity, sex, or age (data not shown). We also considered finding an association between genotypes and presence of bone lesions. Our results showed no association between genotype and higher or lower incidence of osteomyelitis (data not shown). However, this lack of finding could be attributable to the limited amount of reported bone damage in our sampling (only 4 cases). We found no association between genotype and the year of strain isolation (Figure 4).

Identification of Spatial Clusters in Benin

To examine the relationship between phylogenetic classification and *M. ulcerans* geographic origin, we used a multinomial spatial scan statistic (Appendix 1). We found a first significant cluster ($p = 0.002$), with a radius of 15.7 km^2, that included 68 cases and was located in northern Ouémé (Figure 5). This cluster contained strains belonging mainly to genotypes 4 and 8;

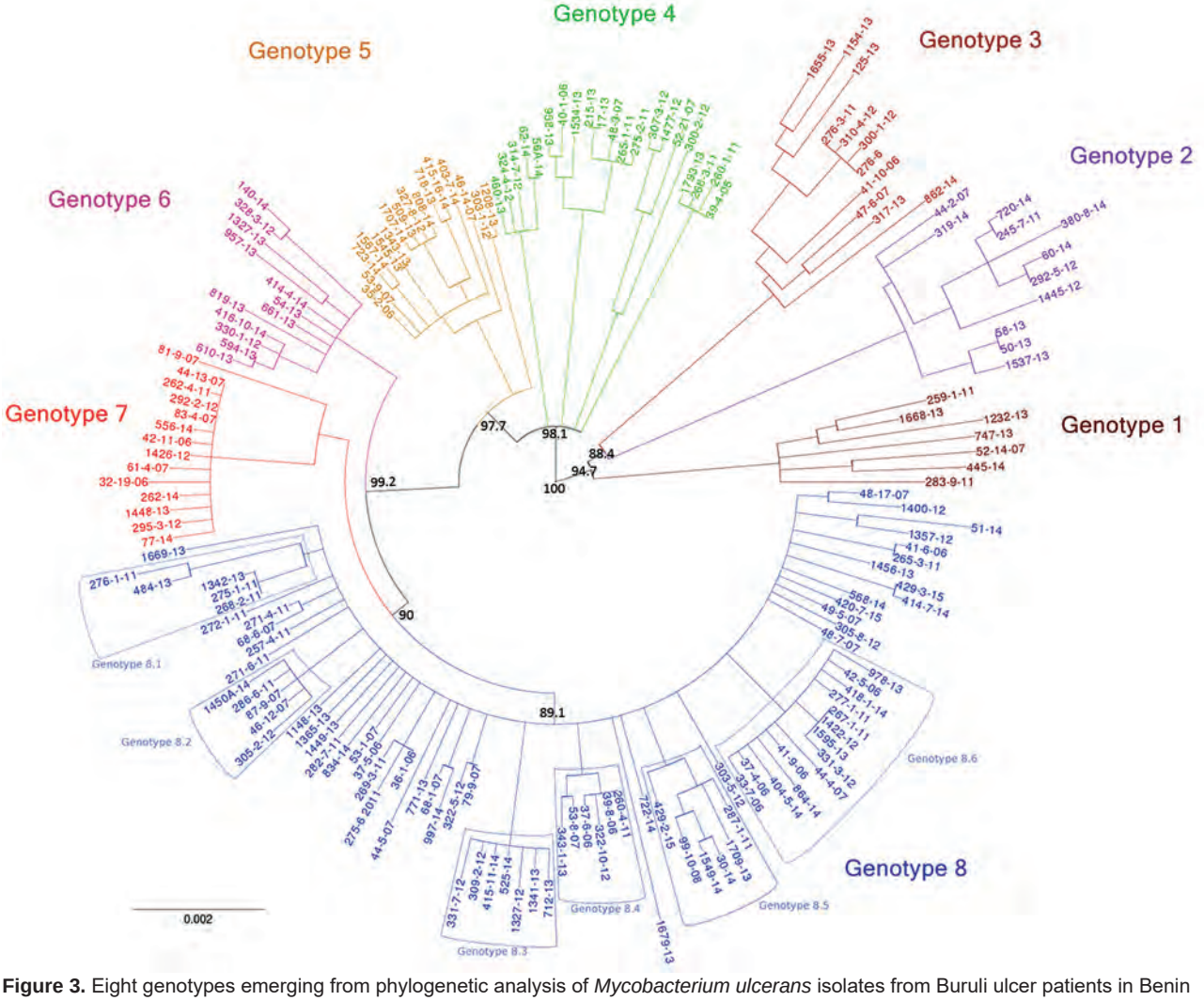

Figure 3. Eight genotypes emerging from phylogenetic analysis of *Mycobacterium ulcerans* isolates from Buruli ulcer patients in Benin and Nigeria. This rooted circular phylogenetic tree was built by using PhyML (*22*) on the basis of the core alignment of all single-nucleotide polymorphisms obtained with Snippy 3.2 (*19*). The bootstrap values are only represented on primitive branches. Branches with bootstrap values <70% were collapsed as polytomies. The outgroup (Papua New Guinea genomes) and the reference genome (Agy99) are not represented (see Appendix 1 Figure 1, https://wwwnc.cdc.gov/EID/article/26/3/19-0573-App1.pdf). On the basis of the segregation indicated by this tree, the genomes were divided in 8 genotypes, which are either monophyletic or paraphyletic. Each taxon was assigned a specific color. Subgenotypes of genotype 8 also are indicated. Scale bar indicates the Nei genetic distance.

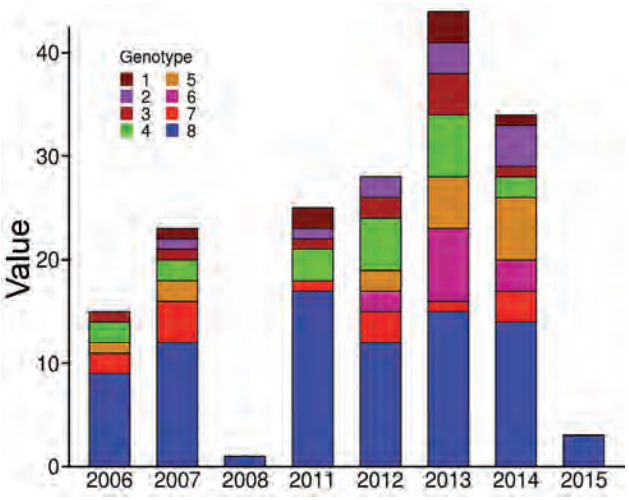

Figure 4. Distribution of *Mycobacterium ulcerans* genotypes according to diagnosis date for Buruli ulcer patients in Benin and Nigeria. The distribution of genotypes was tested on 2 × 8 contingency tables (Fisher exact test) to compare each year to one another.

relative risk (RR) for infection was 1.5 for genotype 4 and 1.9 for genotype 8 (Table 1). In contrast, within this area, the RR for infection with a strain of genotype 2, 3, 5, and 7 was low (RR 0.6, 0.2, 1.0, and 0.4, respectively), and the RR for infection with a strain belonging to genotype 1 or 6 was null. The second significant cluster (p = 0.0024) was located in southern Ouémé, with a radius of 18.8 km^2, and included 17 strains. The most notable feature of this cluster was the high risk for infection with a strain of genotype 7 (Table 1). Indeed, a patient with BU living in this area was 20 times more likely to have been infected with this genotype than a BU person living outside this area. Surprisingly, the multinomial spatial scan statistic did not identify any significant cluster in Plateau, meaning that strains in Plateau are similar to a random distribution of all *M. ulcerans* genotypes (Figure 5). These data suggest a difference in bacterial life cycle between Ouémé and Plateau in terms of bacterial persistence.

Identification and Distribution of Genetic Subgroups Belonging to Genotype 8

Among the 8 genotypes identified from the West Africa lineage, genotype 8 held almost half of the *M. ulcerans* strains and was present in Ouémé and Plateau. We focused on this genotype and found 6 subgenotypes phylogenetically distinguished, with well-supported nodes and bootstrap values ranging from 84% to 99% (Figures 3, 6; Appendix 2 Table 3). Subgenotypes 8.1 to 8.6 contained half of the total strains belonging to genotype 8. The other half was assigned to the denomination 8.0 as not belonging to a particular subgenotype. Because genotype 8 was found mainly near the Ouémé River, we assessed the distribution of subgenotypes in this area by using a spatial scan statistic similar to that we described previously. We found 2 statistically significant clusters along the Ouémé River, 1 in the north (cluster 1) and 1 in the south (cluster 2) (Figure 6). Subgenotypes 8.1, 8.2, 8.3, and 8.5 were found only in cluster 1 (i.e., in the north (Table 2). Subgenotypes 8.1 and 8.3 had higher RRs (4.31 and 2.69, respectively) within this area compared with outside the area. The risk for carrying subgenotype 8.6 strains within this cluster was significantly low (RR 0.1) (Table 2). However, we found only 2 subgenotypes (8.4 and 8.6) in cluster 2 (RR 9.4 for subgenotype 8.6 and 1.7 for subgenotype 8.4) (Table 2). Clusters 1 and 2 (Figure 6) were slightly displaced compared with the northern and southern clusters (Figure 5) but overlapped considerably.

Land Cover and Genotype Distribution

Genotypes were not distributed randomly between southern and northern Ouémé, suggesting that the clusters might be associated with specific land cover. Globally, the 2 regions differed significantly in terms of land use and cover, and a high soil heterogeneity existed between the north and south (Figure 7). Whereas the south has flooded soils suitable for market gardening and marshes for tree cultivation, the north mainly consists of forests and palm groves, and agricultural land is sparse. This difference might indicate that *M. ulcerans* strains of genotype 7 will most likely be found in bare soils and rice fields, whereas *M. ulcerans* strains of genotype 8 will most likely be found in areas with riparian vegetation, herbaceous vegetation, and woodlands.

Specificity of the Nigeria Strains

The CDTLUB in Pobè is located near the Nigeria–Benin border, and several BU patients from Nigeria were treated in the center. Of the 179 strains sequenced in our study, 21 were isolated from patients from Ogun State in southwestern Nigeria. This area is dependent on a different drainage basin than that used by Ouémé, thus providing an opportunity to study *M. ulcerans* diversity and distribution in another independent BU-endemic area. Spatial analysis showed that the most significant cluster (p<0.0001) covered the area of Ogun State. This cluster was drastically different from those found in the Ouémé region of Benin. In this region of Nigeria, the RRs for infection with strains from genotype 1, 2, 3, or 6 were significantly higher than for any other genotype (Figure 8). The

RR for infection with these genotypes was 9.9 times higher for genotype 1, 3.2 times higher for genotype 2, 5 times higher for genotype 3, and 13 times higher for genotype 6 in this area compared with outside the area (Table 1). Furthermore, the RR for infection with genotype 8 was negligible (0.2), even though it was the most widespread genotype along the Ouémé River (Table 1). We observed a similar nonrandom distribution in Ouémé and in Ogun State.

Validation of Multinomial Model Demonstrating Geographic Clusters

To validate the distribution of genotypes in both BU-endemic areas, we developed a spatial model of genotype dispersion on the basis of phylogenetic classification. To verify the power of our model to correctly associate a genotype to a genome given its geographic origin, we performed WGS on 29 additional bacterial strains. These strains were isolated from patients at CDTLUB who had been diagnosed with BU during 2015–2017 and were living in northern Ouémé (11 patients), southern Ouémé (9 patients), Plateau (4 patients), and Nigeria (5 patients). We identified 2 of the 29 strains as part of the MU_A2 lineage and added them to the outgroup to build a new phylogenetic tree. The 27 other strains were easily included in the phylogenetic tree (Figure 2) without altering the classification of the 8 different genotypes or the cluster classifications. Plateau contained no statistically significant clusters.

For each of the 3 significant geographic clusters, we compared the observed repartition of new genomes to the expected distribution given by each cluster. The 2 clusters in Ouémé exhibited strong

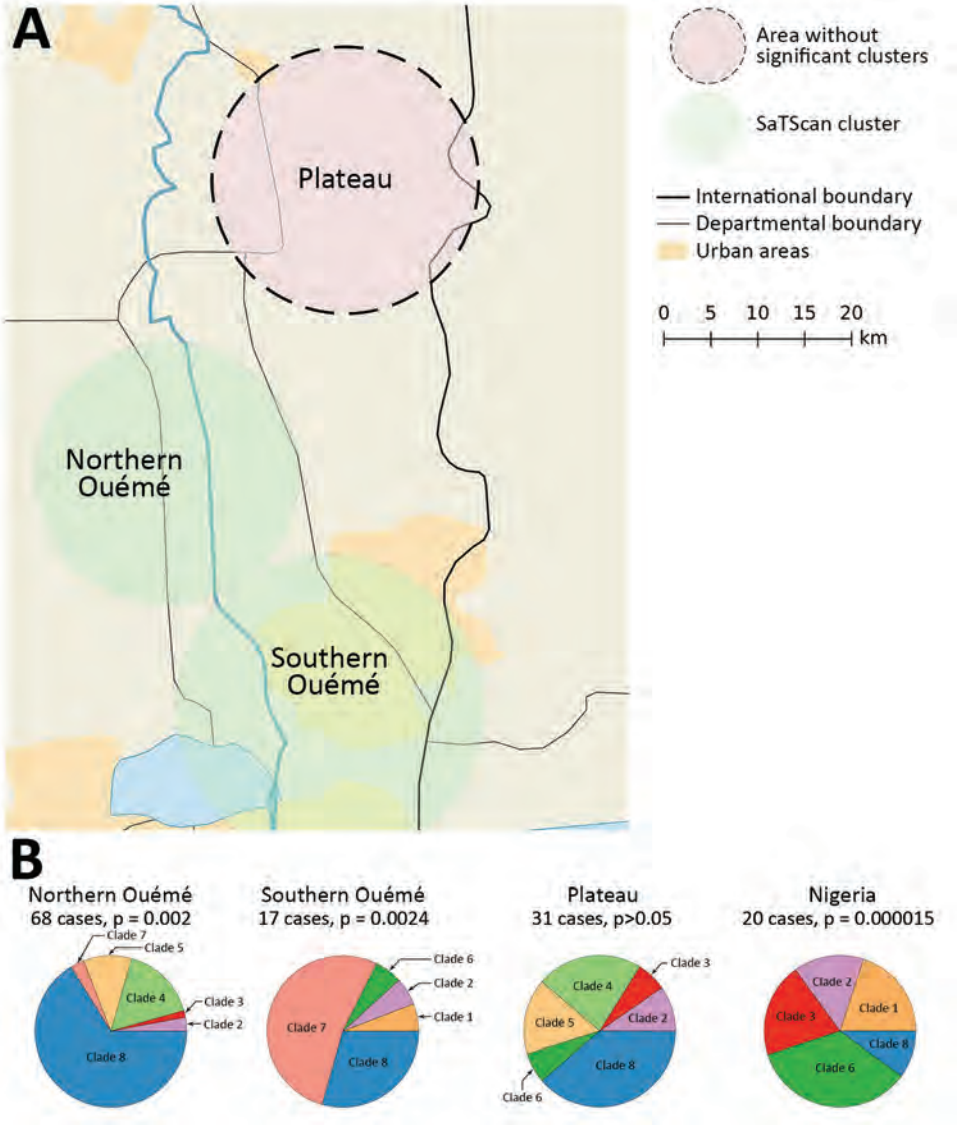

Figure 5. Spatial cluster detection results of *Mycobacterium ulcerans* genotypes for Buruli ulcer patients in Benin and Nigeria. A) Two significant areas detected along the Ouémé River. Three regions of interest are shown on the map. Two (northern Ouémé and southern Ouémé) show significant spatial clustering of genotypes; a nonsignificant area (Plateau) is given for reference. B) Composition of these 3 clusters, compared with the composition that would be expected from a random distribution.

Table 1. Cluster detection analysis for predominance of *Mycobacterium ulcerans* genotypes using the maximum reported spatial window of 50% of the sample population and a univariate scan statistic, Benin and Nigeria*

Spatial cluster	Radius, km^2	LLR	Ob	Genotype 1 RR (%)	2 RR (%)	3 RR (%)	4 RR (%)	5 RR (%)	6 RR (%)	7 RR (%)	8 RR (%)
Northern Ouémé	15.7	19.2	68	0	0.6 (4.1)	0.2 (1.3)	1.5 (15)	1 (9.6)	0	0.4 (4.1)	1.9 (66)
Southern Ouémé	17.9	18.8	17	1.5 (5)	1 (6)	0	0	0	0.9 (6)	20 (53)	0.6 (29)
Nigeria†	54.3	27.1	20	9.9 (20)	3.2 (15)	5 (20)	0	0	13 (35)	0	0.2 (10)

*Percentages indicate falling in each group within a cluster. LLR: log likelihood ratio; Ob, number of observations in a cluster; RR, relative risk, computed as the ratio of the proportions of the number of Buruli ulcer cases in each category out of the total number of cases inside the cluster versus outside.
†Ogun State.

accuracy (91%) and a Matthews coefficient >0.6, corresponding to a strong relationship (Table 3). The Nigeria cluster model showed lower accuracy (85%) and a Matthews coefficient of 0.371, corresponding to a moderately positive relationship. These results support the existence of a spatial cluster of *M. ulcerans* genotypes in some BU-endemic areas.

Discussion

BU occurs in poor rural communities with little economic or political influence. A key epidemiologic feature of this disease is the distribution of cases in very well-delimited foci. However, in these areas, the precise zones of high-risk contamination in environments are not identified. As with other neglected tropical diseases, fighting BU will require integrated approaches to reduce transmission of the causative mycobacterium and ensure earlier patient management.

Socioeconomic factors, environmental changes, ecologic factors, and the conquest of new territories promote infections caused by pathogens with a wildlife origin (*28*–*30*). In the field of BU, all epidemiologic studies show that environmental changes, particularly wetland creation, deforestation, and socioeconomic factors that promote contact with nonprotected water, enhance the spread of the disease (*3*,*28*,*31*–*37*). Although all epidemiologic and environmental studies underline the main role of ecologic factors in *M. ulcerans* transmission, the precise route of *M. ulcerans* transmission to humans remains unclear. Molecular epidemiology studies conducted on a local scale can be adapted to elucidate the structure, diversity, evolution, dissemination, and life of the bacterial population.

The genome of *M. ulcerans* consists of a main chromosome and a giant plasmid containing the gene encoding for enzymes synthesizing the mycolactone. Because this genome has low variation, conventional genetic methods can only differentiate isolates on a continental scale (*38*). WGS offers a much greater resolution and could be used for studying *M. ulcerans* diversity on a local scale by analyzing SNPs (*11*). SNP analysis of our 174 *M. ulcerans* isolates belonging to the West Africa lineage Mu_A1 enabled us to identify 8 genotypes on the basis of 940 SNP positions. This analysis revealed a high conservation, especially on plasmid sequences, highlighting the crucial role of mycolactone toxin to colonize specific environmental niches, including human (*39*,*40*). The main role of mycolactone in host colonization was affirmed because no link could be established between this genomic diversity and clinical manifestations. Furthermore, the distribution of gene mutations based on a functional annotation is similar to the distribution of all the classified genes of *M. ulcerans* (Appendix 1 Figure 3), supporting the hypothesis that acquisition of a mutation has no relation to its ability to colonize a host or with its virulence.

The particularity of our study was the spatial local-scale analysis of the isolates. We used a phylogenetic analysis approach based on SNP-typing, coupled with spatial scan statistics. This method is more suitable for working in a well-defined BU-endemic area in a short period (a few years), whereas a Bayesian phylogenetic approach is suitable for studying temporal distribution of *M. ulcerans* over a much longer period (decades) (*11*,*15*).

Our spatial analysis revealed the existence of a geographic clustering of *M. ulcerans* genotypes in southeastern Benin and southwestern Nigeria. On this scale, our results showed a strong association between hydrologic drainage areas and *M. ulcerans* genotypes, because a clear difference was observed in the distribution of genotypes between BU patients living around Nigeria's Yewa basin and Benin's Ouémé basin. Our clustering revealed that bacteria evolved independently and differentially, depending on their specific ecologic reservoir. Moreover (and more surprisingly), we were able to detect clustering of *M. ulcerans* genotypes along a same drainage basin (in this case the Ouémé basin). Inside the main genotype (genotype 8), we were also able to detect subgenotypes with a similar clustering along the river,

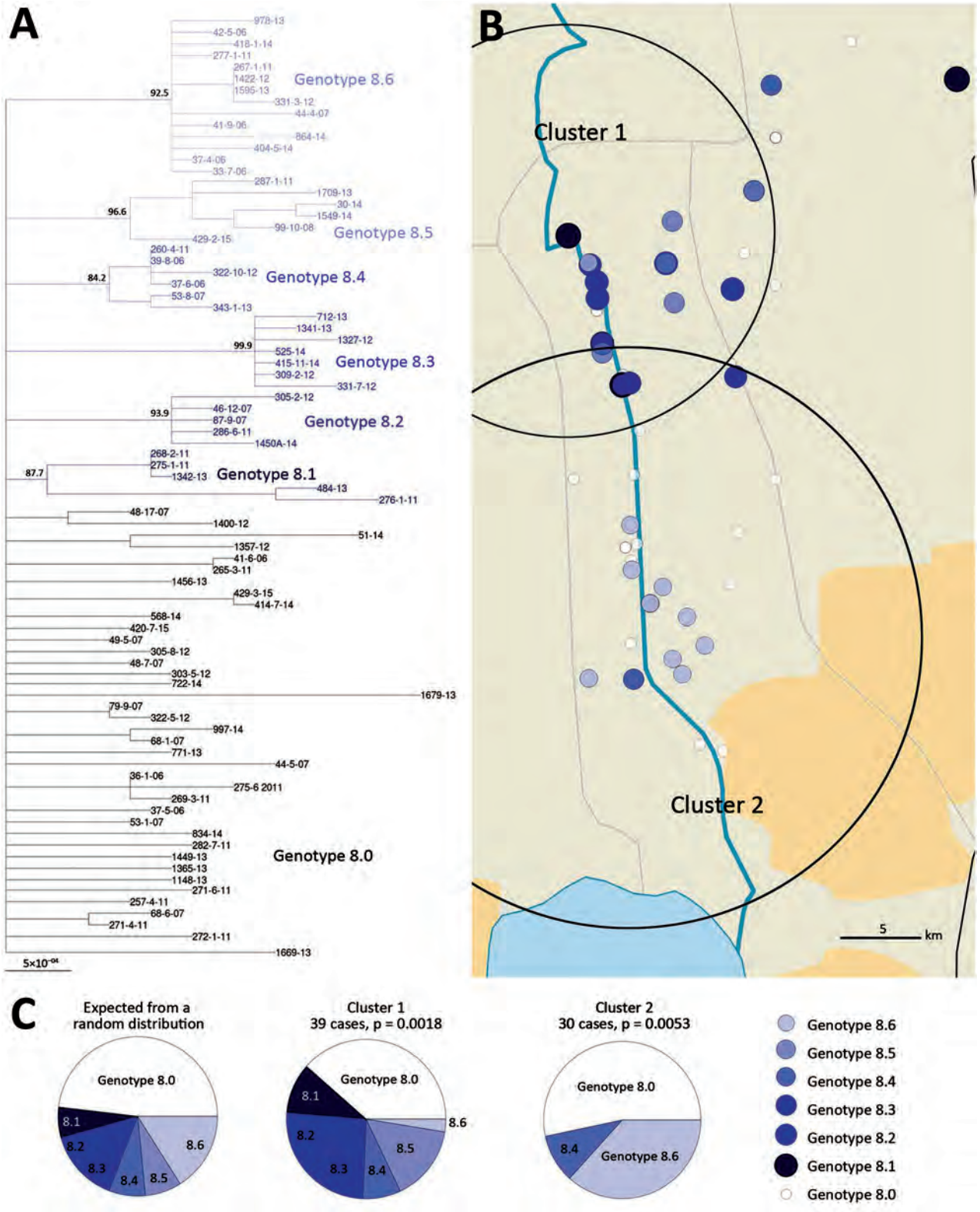

Figure 6. Spatial cluster detection results of *Mycobacterium ulcerans* genotype 8 for Buruli ulcer patients in Benin and Nigeria. Genotype 8 population was identified in 2 clusters along the Ouémé River. A) Phylogenetic tree of genotype 8 reveals the presence of potentially emerging genotypes. B) Location of the clusters. The analysis shows 2 significant clusters where specific subgenotypes are overrepresented compared to outside of these areas. C) Composition of these 2 clusters compared with the composition that would be expected from a random distribution.

Table 2. Cluster detection analysis for predominance of subgenotypes of *Mycobacterium ulcerans* genotype 8, Benin*

Spatial cluster	Radius, km^2	LLR	Ob	Subgenotype 8.0 RR (%)	8.1 RR (%)	8.2 RR (%)	8.3 RR (%)	8.4 RR (%)	8.5 RR (%)	8.6 RR (%)
Cluster 1	14.7	15.7	39	0.7 (38.5)	4.3 (10.3)	Inf (12.8)	2.69 (12.8)	1.08 (7.7)	Inf (15.4)	0.1 (2.6)
Cluster 2	20.0	17.3	30	1.2 (53.3)	0 (0)	0 (0)	0 (0)	1.7 (10)	0 (0)	9.4 (36.7)

*Percentages indicate falling in each group within a cluster. Inf, infinite; LLR: log likelihood ratio; Ob, number of observations in a cluster; RR, relative risk, computed as the ratio of the proportions of the number of Buruli ulcer cases in each category out of the total number of cases inside the cluster versus outside.

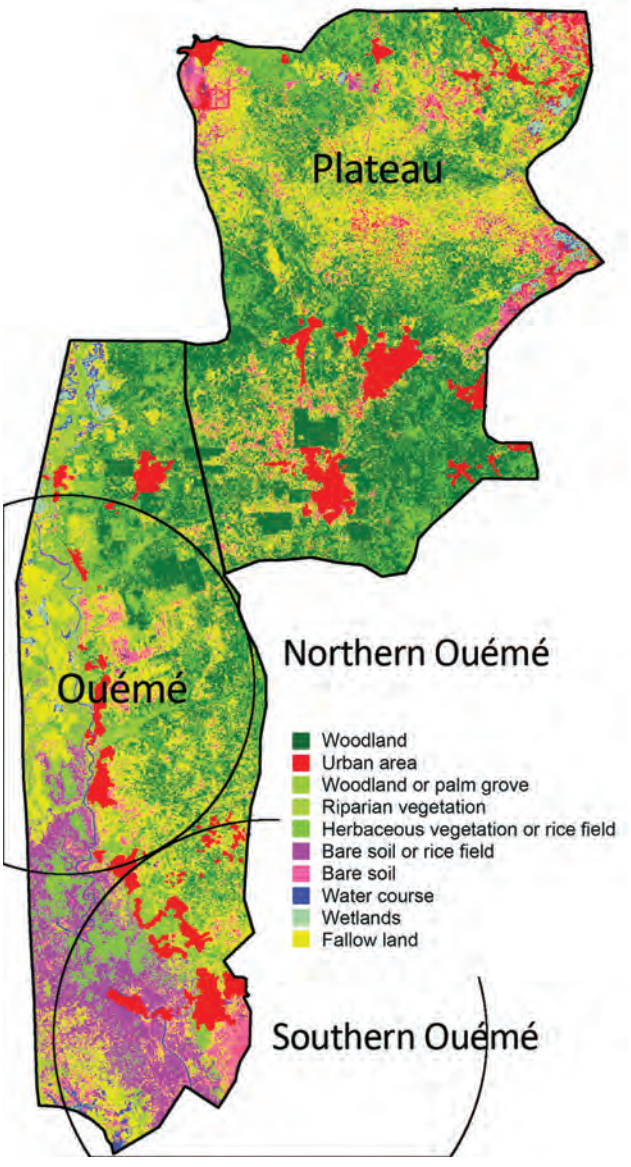

Figure 7. Land use and land cover assessment from Sentinel-2 imaging of Benin. The Ouémé region has specific land and plant formations, such as grassy savanna, grasslands, and swamps. Soils easily become saturated with water because of a shallow water table and the proximity of a river, which causes floods and a natural delta formation in the south of the region. Circles indicate the detected northern and southern Ouémé *Mycobacterium ulcerans* clusters.

indicating dissemination of *M. ulcerans* on a local scale and then a persistence of *M. ulcerans* in independently endemic niches. These findings are consistent with previous scenarios in which *M. ulcerans*, once introduced into a new environment, expands instead of becoming a quiescent pathogen (*11*).

In considering the nature of the land cover, we observed striking heterogeneity along the river, pinpointing the compartmentalization of different environmental niches (Figure 7). On the other hand, the predominance of 1 genotype in 1 area associated with a particular land cover suggests that patients frequent the same type of contamination source, and the hypothesis that acquisition of infection is local has already been proposed (*11*). Altogether, our study gives a precise cartography of *M. ulcerans* genotype distribution, revealing a well delimited high-risk area where preventive strategies, active diagnosis, and epidemiologic surveillance must be focused.

Unlike the Ouémé region and southwestern Nigeria, the lack of any spatial cluster in the Plateau region suggests differences in terms of dissemination and environmental persistence. Plateau separates the Ouémé and Yewa draining basins, and the bacterial genotypes in the Plateau area are a mix of the genotypes in these 2 basins. This signature could be explained by different hypotheses. First, there might be a contamination site different from the place of residence given that persons living on the Plateau might be contaminated in Ouémé or Nigeria during their travels. This hypothesis does not explain all contaminations because patients' histories revealed that some of them had never left their village. Second, there might be a nonpersistent presence of *M. ulcerans* in the Plateau environment, in which *M. ulcerans* might be disseminated from Ouémé and Nigeria to Plateau by mammals (including humans) or flying insects and might be present in aquatic niches for only the few months when wetlands exist just after the rainy seasons (*41*). This situation rules out humans as the main carrier and reservoir of *M. ulcerans* and supports the position that humans with active infection are unlikely to play a major role in the bacterial ecology.

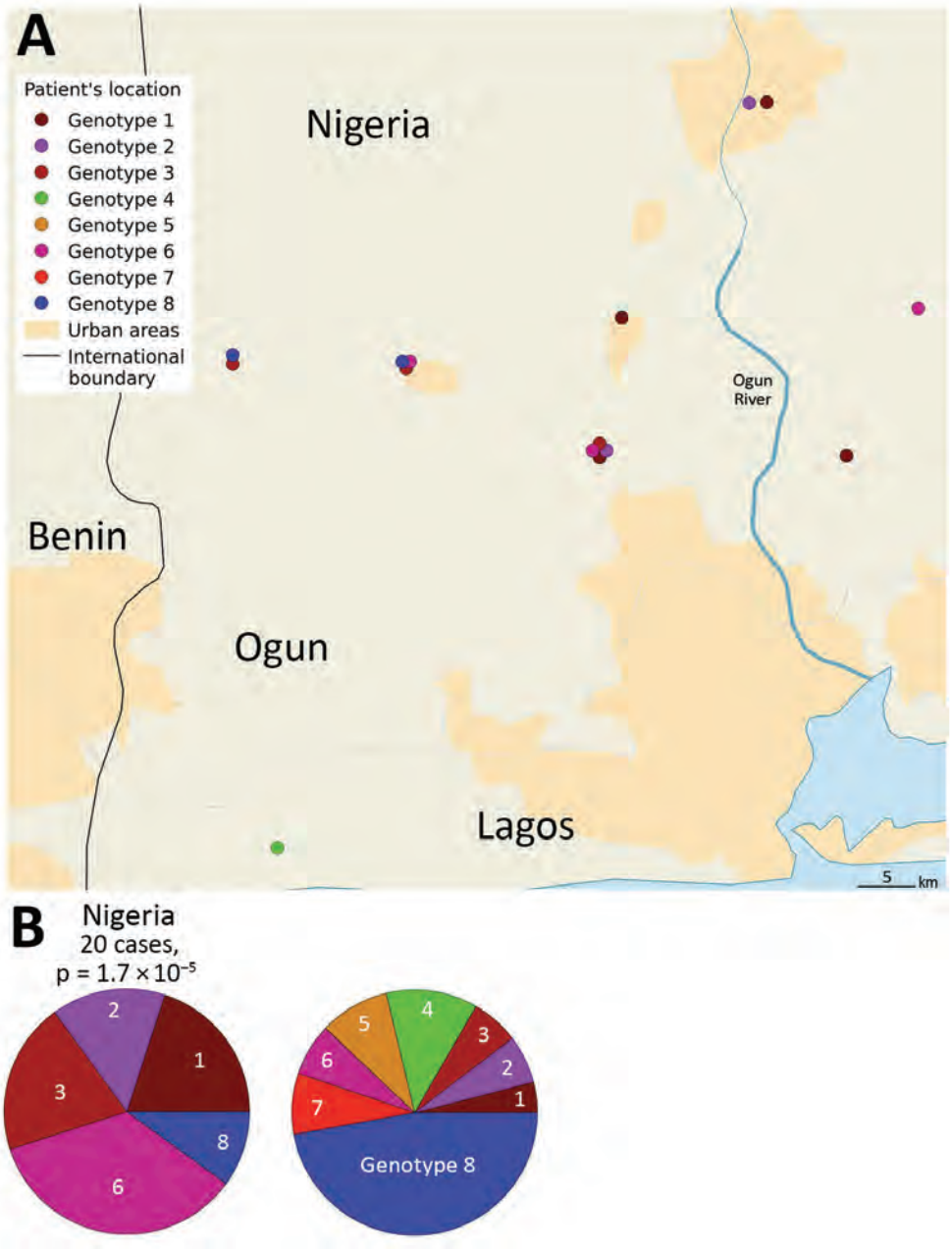

Figure 8. Difference in *Mycobacterium ulcerans* genotype distribution between Ogun State (Nigeria) and Benin. A) Locations of patients and the genotypes of the strains. B) Composition of the cluster in the Ogun area compared with the composition that would be expected from a random distribution. The genotype distribution of the Ogun was fundamentally different from those in Benin.

Moreover, BU is known to be a locally acquired infection rather than an imported one (*42*). Thus, the most plausible hypothesis in the particular case of the Plateau region is based on the inability of the bacterium to develop for a period long enough in transitional aquatic reservoirs, thereby preventing the production of new genotypes. Treating humans against *M. ulcerans* infection might not be sufficient to break disease transmission chains as previously suggested (*12*).

Because only *M. ulcerans* strains isolated from patients were analyzed, it would have been interesting, as a next step, to compare diversity of *M. ulcerans* from

Table 3. Statistical measurements of the performance of the multinomial models on a real dataset of newly sequenced genomes, Benin and Nigeria*

Locale	Accuracy†	Matthews correlation coefficient‡
Northern Ouémé	91.44%	0.608*
Southern Ouémé	91.73%	0.637*
Nigeria (Ogun State)	86.25%	0.371**

†Sum of the true positive and true negative divided by the total population.
‡Contingency matrix method of calculating the Pearson product–moment correlation coefficient (*27*). Its value ranges from −1 to +1 with +1 being a perfect positive prediction model, 0 no better than random prediction, and −1 being a model where predicted class is in total contradiction with observed class. Values indicated the strength of the relationship (*, strong positive relationship; **, moderate positive relationship).

humans and environmental samples to better understand the interactions between this pathogen and the host. Combined with the tools we developed to reveal the genetic diversity of *M. ulcerans* in humans, DNA enrichment techniques, such those reported in studies on *Borrelia* spp., could be improved to meet this challenge (*43*). In conclusion, our approach allowed the identification of delimited high-risk contamination areas, paving a new avenue to develop prevention and intervention strategies.

Acknowledgments

We thank Laurent Marsollier for proofreading and advice, Tim Stinear and Jessica Porter for support with DNA sequencing, all staff at CDTLUB-Pobè in Benin who performed diagnosis and treatment, and David Goudenege and Vincent Procaccio from the Biochemistry and Genetics Department at Angers Hospital, France.

This work was carried out with support from the GenOuest bioinformatics platform.

Funding for this work was provided by Agence Nationale de la Recherche (grants nos. ANR 11 CEPL 00704 EXTRA6MU and 17-BSV3-0013-01), Fondation Raoul Follereau, INSERM, and Agence Nationale de la Recherche Région Pays de la Loire.

Use of patients' data was approved by the CDTLUB Institutional Review Board, the national BU control authorities of Benin (approval no. IRB00006860), and the Ethics Committee of the Angers University Hospital in France (Comité d'Ethique du Centre Hospitalo-Universitaire d'Angers).

About the Author

Dr. Coudereau is a former postdoctoral fellow at the Centre de Recherche en Cancérologie et Immunologie Nantes–Angers (CRCINA) pursuing a career in bioinformatics. His research interests include next-generation sequencing, phylogeny, and spatial analysis related to the genetic population of *M. ulcerans* in endemic regions of Africa.

References

1. Sizaire V, Nackers F, Comte E, Portaels F. *Mycobacterium ulcerans* infection: control, diagnosis, and treatment. Lancet Infect Dis. 2006;6:288–96. https://doi.org/10.1016/S1473-3099(06)70464-9
2. Asiedu K, Etuaful S. Socioeconomic implications of Buruli ulcer in Ghana: a three-year review. Am J Trop Med Hyg. 1998;59:1015–22. https://doi.org/10.4269/ajtmh.1998.59.1015
3. Aiga H, Amano T, Cairncross S, Adomako J, Nanas OK, Coleman S. Assessing water-related risk factors for Buruli ulcer: a case-control study in Ghana. Am J Trop Med Hyg. 2004;71:387–92. https://doi.org/10.4269/ajtmh.2004.71.387
4. Merritt RW, Walker ED, Small PL, Wallace JR, Johnson PD, Benbow ME, et al. Ecology and transmission of Buruli ulcer disease: a systematic review. PLoS Negl Trop Dis. 2010;4:e911. https://doi.org/10.1371/journal.pntd.0000911
5. Wallace JR, Mangas KM, Porter JL, Marcsisin R, Pidot SJ, Howden B, et al. *Mycobacterium ulcerans* low infectious dose and mechanical transmission support insect bites and puncturing injuries in the spread of Buruli ulcer. PLoS Negl Trop Dis. 2017;11:e0005553. https://doi.org/10.1371/journal.pntd.0005553
6. Williamson HR, Mosi L, Donnell R, Aqqad M, Merritt RW, Small PL. *Mycobacterium ulcerans* fails to infect through skin abrasions in a guinea pig infection model: implications for transmission. PLoS Negl Trop Dis. 2014;8:e2770. https://doi.org/10.1371/journal.pntd.0002770
7. Johnson PD, Azuolas J, Lavender CJ, Wishart E, Stinear TP, Hayman JA, et al. *Mycobacterium ulcerans* in mosquitoes captured during outbreak of Buruli ulcer, southeastern Australia. Emerg Infect Dis. 2007;13:1653–60. https://doi.org/10.3201/eid1311.061369
8. Marsollier L, Robert R, Aubry J, Saint André JP, Kouakou H, Legras P, et al. Aquatic insects as a vector for *Mycobacterium ulcerans*. Appl Environ Microbiol. 2002;68:4623–8. https://doi.org/10.1128/AEM.68.9.4623-4628.2002
9. Portaels F, Elsen P, Guimaraes-Peres A, Fonteyne PA, Meyers WM. Insects in the transmission of *Mycobacterium ulcerans* infection. Lancet. 1999;353:986. https://doi.org/10.1016/S0140-6736(98)05177-0
10. van der Werf TS, Stinear T, Stienstra Y, van der Graaf WT, Small PL. Mycolactones and *Mycobacterium ulcerans* disease. Lancet. 2003;362:1062–4. https://doi.org/10.1016/S0140-6736(03)14417-0
11. Buultjens AH, Vandelannoote K, Meehan CJ, Eddyani M, de Jong BC, Fyfe JAM, et al. Comparative genomics shows that *Mycobacterium ulcerans* migration and expansion preceded the rise of Buruli ulcer in southeastern Australia. Appl Environ Microbiol. 2018;84:e02612–7. https://doi.org/10.1128/AEM.02612-17
12. Vandelannoote K, Phanzu DM, Kibadi K, Eddyani M, Meehan CJ, Jordaens K, et al. *Mycobacterium ulcerans* population genomics to inform on the spread of Buruli ulcer across central Africa. MSphere. 2019;4:e00472–18. https://doi.org/10.1128/mSphere.00472-18
13. Wu J, Tschakert P, Klutse E, Ferring D, Ricciardi V, Hausermann H, et al. Buruli ulcer disease and its association with land cover in southwestern Ghana. PLoS Negl Trop Dis. 2015;9:e0003840. https://doi.org/10.1371/journal.pntd.0003840
14. Bolz M, Bratschi MW, Kerber S, Minyem JC, Um Boock A, Vogel M, et al. Locally confined clonal complexes of *Mycobacterium ulcerans* in two Buruli ulcer endemic regions of Cameroon. PLoS Negl Trop Dis. 2015;9:e0003802. https://doi.org/10.1371/journal.pntd.0003802
15. Vandelannoote K, Meehan CJ, Eddyani M, Affolabi D, Phanzu DM, Eyangoh S, et al. Multiple introductions and recent spread of the emerging human pathogen *Mycobacterium ulcerans* across Africa. Genome Biol Evol. 2017;9:414–26. https://doi.org/10.1093/gbe/evx003
16. Kambarev S, Corvec S, Chauty A, Marion E, Marsollier L, Pecorari F. Draft genome sequence of *Mycobacterium ulcerans* S4018 isolated from a patient with an active Buruli ulcer in Benin, Africa. Genome Announc. 2017;5:e00248–17. https://doi.org/10.1128/genomeA.00248-17

17. Andrew S. FastQC: a quality control tool for high throughput sequence data. 2010 [cited 2019 Apr 1].
18. Bolger AM, Lohse M, Usadel B. Trimmomatic: a flexible trimmer for Illumina sequence data. Bioinformatics. 2014;30:2114–20. https://doi.org/10.1093/bioinformatics/btu170
19. Seemann T. Snippy: fast bacterial variant calling from NGS reads. 2015 [cited 2019 Apr 1].
20. Li H, Durbin R. Fast and accurate short read alignment with Burrows-Wheeler transform. Bioinformatics. 2009;25:1754–60. https://doi.org/10.1093/bioinformatics/btp324
21. Stinear TP, Seemann T, Pidot S, Frigui W, Reysset G, Garnier T, et al. Reductive evolution and niche adaptation inferred from the genome of *Mycobacterium ulcerans,* the causative agent of Buruli ulcer. Genome Res. 2007;17:192–200. https://doi.org/10.1101/gr.5942807
22. Guindon S, Dufayard JF, Lefort V, Anisimova M, Hordijk W, Gascuel O. New algorithms and methods to estimate maximum-likelihood phylogenies: assessing the performance of PhyML 3.0. Syst Biol. 2010;59:307–21. https://doi.org/10.1093/sysbio/syq010
23. Hodcroft E. TreeCollapserCL. 2012 [cited 2019 Apr 1].
24. Kulldorff M. SatScan: software for the spatial and space-time scan statistics. 2019 [cited 2019 Apr 1].
25. Team QGIS Development. QGIS Geographic Information System. Project OSGF. 2019 [cited 2019 Apr 1].
26. R Core Team. R: a language and environment for statistical computing. Computing RFfS. 2019 [cited 2019 Apr 1].
27. Powers DMW. Evaluation: from precision, recall and F-Measure to ROC, informedness, markedness, and correlation. J Mach Learn Technol. 2011;2:37–63.
28. Bennett SD, Lowther SA, Chingoli F, Chilima B, Kabuluzi S, Ayers TL, et al. Assessment of water, sanitation and hygiene interventions in response to an outbreak of typhoid fever in Neno District, Malawi. PLoS One. 2018;13:e0193348. https://doi.org/10.1371/journal.pone.0193348
29. Davies HG, Bowman C, Luby SP. Cholera - management and prevention. J Infect. 2017;74(Suppl 1):S66–73. https://doi.org/10.1016/S0163-4453(17)30194-9
30. Mitjà O, Marks M, Bertran L, Kollie K, Argaw D, Fahal AH, et al. Integrated control and management of neglected tropical skin diseases. PLoS Negl Trop Dis. 2017;11:e0005136. https://doi.org/10.1371/journal.pntd.0005136
31. Brou T, Broutin H, Elguero E, Asse H, Guegan JF. Landscape diversity related to Buruli ulcer disease in Côte d'Ivoire. PLoS Negl Trop Dis. 2008;2:e271. https://doi.org/10.1371/journal.pntd.0000271
32. Landier J, Gaudart J, Carolan K, Lo Seen D, Guégan JF, Eyangoh S, et al. Spatio-temporal patterns and landscape-associated risk of Buruli ulcer in Akonolinga, Cameroon. PLoS Negl Trop Dis. 2014;8:e3123. https://doi.org/10.1371/journal.pntd.0003123
33. Marion E, Landier J, Boisier P, Marsollier L, Fontanet A, Le Gall P, et al. Geographic expansion of Buruli ulcer disease, Cameroon. Emerg Infect Dis. 2011;17:551–3. https://doi.org/10.3201/eid1703.091859
34. Nackers F, Johnson RC, Glynn JR, Zinsou C, Tonglet R, Portaels F. Environmental and health-related risk factors for *Mycobacterium ulcerans* disease (Buruli ulcer) in Benin. Am J Trop Med Hyg. 2007;77:834–6. https://doi.org/10.4269/ajtmh.2007.77.834
35. Pouillot R, Matias G, Wondje CM, Portaels F, Valin N, Ngos F, et al. Risk factors for buruli ulcer: a case control study in Cameroon. PLoS Negl Trop Dis. 2007;1:e101. https://doi.org/10.1371/journal.pntd.0000101
36. Raghunathan PL, Whitney EA, Asamoa K, Stienstra Y, Taylor TH Jr, Amofah GK, et al. Risk factors for Buruli ulcer disease (*Mycobacterium ulcerans* Infection): results from a case-control study in Ghana. Clin Infect Dis. 2005;40:1445–53. https://doi.org/10.1086/429623
37. Wagner T, Benbow ME, Burns M, Johnson RC, Merritt RW, Qi J, et al. A Landscape-based model for predicting *Mycobacterium ulcerans* infection (Buruli Ulcer disease) presence in Benin, West Africa. EcoHealth. 2008;5:69–79. https://doi.org/10.1007/s10393-007-0148-7
38. Röltgen K, Stinear TP, Pluschke G. The genome, evolution and diversity of *Mycobacterium ulcerans.* Infect Genet Evol. 2012;12:522–9. https://doi.org/10.1016/j.meegid.2012.01.018
39. Demangel C, Stinear TP, Cole ST. Buruli ulcer: reductive evolution enhances pathogenicity of *Mycobacterium ulcerans.* Nat Rev Microbiol. 2009;7:50–60. https://doi.org/10.1038/nrmicro2077
40. Rondini S, Käser M, Stinear T, Tessier M, Mangold C, Dernick G, et al. Ongoing genome reduction in *Mycobacterium ulcerans.* Emerg Infect Dis. 2007;13:1008–15. https://doi.org/10.3201/eid1307.060205
41. Yerramilli A, Tay EL, Stewardson AJ, Fyfe J, O'Brien DP, Johnson PDR. The association of rainfall and Buruli ulcer in southeastern Australia. PLoS Negl Trop Dis. 2018;12:e0006757. https://doi.org/10.1371/journal.pntd.0006757
42. Tanser FC, Le Sueur D. The application of geographical information systems to important public health problems in Africa. Int J Health Geogr. 2002;1:4. https://doi.org/10.1186/1476-072X-1-4
43. Carpi G, Walter KS, Bent SJ, Hoen AG, Diuk-Wasser M, Caccone A. Whole genome capture of vector-borne pathogens from mixed DNA samples: a case study of *Borrelia burgdorferi.* BMC Genomics. 2015;16:434. https://doi.org/10.1186/s12864-015-1634-x

Address for correspondence: Estelle Marion, ATOMycA Team, CRCINA Inserm U1232, 4 rue Larrey, 49933 Angers, France; email: estelle.marion@inserm.fr

etymologia

Buruli ulcer [boo'rə-le ul'sər]

Ronnie Henry

Named for Buruli County (now Nakasongola District), Uganda, where large numbers of cases were reported in the 1960s, Buruli ulcer (from the Latin *ulcus*, "sore") is a cutaneous infection with *Mycobacterium ulcerans*. This bacterium produces a unique toxin (mycolactone), which causes rapid and extensive skin ulceration that is relatively painless. Buruli ulcer was first described by Sir Albert Cook in 1897. However, in his book *A Walk Across Africa*, describing his participation in the 1860 expedition to find the source of the Nile River, Scottish explorer James Augustus Grant might have earlier described Buruli ulcer:

> "The right leg, from above the knee, became deformed with inflammation, and remained for a month in this unaccountable state, giving intense pain, which was relieved temporarily by a deep incision and copious discharge. For three months, fresh abscesses formed, and other incisions were made; my strength was prostrated; the knee stiff and alarmingly bent, and walking was impracticable."

Australian physician Peter MacCallum identified the causative organism in 1948. More than 33 countries in Africa, Central and South America, and the Western Pacific report cases of Buruli ulcer. Transmission is not well understood, which hampers the ability to prevent infection. Buruli ulcer is considered a public health problem in West Africa, and rates are also high in Victoria, Australia.

Figure. Captain Grant leaving Karague, carried on a wicker stretcher. Note his bent right leg. (From the book *Journal of the Discovery of the Source of the Nile*, by John Hanning Speke, 1863, p. 401.) Source: Wikipedia, https://en.wikipedia.org/wiki/File:James_Augustus_Grant.jpg

Sources

1. Grant JA. A walk across Africa: or, domestic scenes from my Nile journal. Edinburgh: William Blackwood and Sons; 1864.
2. MacCallum P, Tolhurst JC, Buckle G, Sissons HA. A new mycobacterial infection in man. J Pathol Bacteriol. 1948;60:93–122. https://doi.org/10.1002/path.1700600111
3. World Health Organization. Treatment of *Mycobacterium ulcerans* disease (Buruli ulcer): guidance for health care workers, 2012 [cited 2020 Jan 10]. https://apps.who.int/iris/bitstream/handle/10665/77771/9789241503402_eng.pdf
4. Yotsu RR, Suzuki K, Simmonds RE, Bedimo R, Ablordey A, Yeboah-Manu D, et al. Buruli ulcer: a review of current knowledge. Curr Trop Med Rep. 2018;5:247–56. https://doi.org/10.1007/s40475-018-0166-2

Address for correspondence: Ronnie Henry, Centers for Disease Control and Prevention, 1600 Clifton Rd NE, Mailstop V18-2, Atlanta, GA 30329-4027, USA; email: boq3@cdc.gov

DOI: https://doi.org/10.3201/eid2603.ET2603

Genomic and Phenotypic Variability in *Neisseria gonorrhoeae* Antimicrobial Susceptibility, England

Katy Town, Simon Harris, Leonor Sánchez-Busó, Michelle J. Cole, Rachel Pitt, Helen Fifer, Hamish Mohammed, Nigel Field, Gwenda Hughes

Antimicrobial resistance (AMR) in *Neisseria gonorrhoeae* is a global concern. Phylogenetic analyses resolve uncertainties regarding genetic relatedness of isolates with identical phenotypes and inform whether AMR is due to new mutations and clonal expansion or separate introductions by importation. We sequenced 1,277 isolates with associated epidemiologic and antimicrobial susceptibility data collected during 2013–2016 to investigate *N. gonorrhoeae* genomic variability in England. Comparing genetic markers and phenotypes for AMR, we identified 2 *N. gonorrhoeae* lineages with different antimicrobial susceptibility profiles and 3 clusters with elevated MICs for ceftriaxone, varying mutations in the *penA* allele, and different epidemiologic characteristics. Our results indicate *N. gonorrhoeae* with reduced antimicrobial susceptibility emerged independently and multiple times in different sexual networks in England, through new mutation or recombination events and by importation. Monitoring and control for AMR in *N. gonorrhoeae* should cover the entire population affected, rather than focusing on specific risk groups or locations.

Antimicrobial resistance (AMR) in *Neisseria gonorrhoeae* is a global concern and affects all classes of antimicrobial drugs used for treatment. Penicillin, ciprofloxacin, and cefixime were the recommended first-line antimicrobial drug therapies until AMR prevalence breached the World Health Organization (WHO) recommended threshold of ≥5% of local isolates demonstrating resistance; at that point, ceftriaxone became the preferred antimicrobial drug treatment (*1*). However, ceftriaxone resistance has been reported in many countries and frequently in East and Southeast Asia, probably because of poor antimicrobial stewardship (*2*). Ceftriaxone resistance has been linked to mutations in the *penA* gene, which has been reported in several continents, including North America and Europe (*3*–*5*).

To clarify the spread of AMR in *N. gonorrhoeae* and the population groups most at risk, surveillance programs and research studies often link phenotypic susceptibility data with data on the epidemiologic characteristics of cases (*6*,*7*). However, these analyses are limited because isolates with identical phenotypes might not be genetically related. Consequently, determining the extent to which AMR transmission is due to clonal dissemination or separate introductions is challenging and these data are essential to guide the public health response.

Combining phenotypic and genomic data can help resolve uncertainties. Whole-genome sequencing (WGS) enables investigation of genetic determinants for AMR and how these are distributed in the pathogen population (*4*,*5*). WGS also can contribute evidence toward the development of rapid antimicrobial susceptibility tests to improve treatment decisions (*8*,*9*). However, few *N. gonorrhoeae* WGS studies have been conducted in England, and none include representative geographic coverage over time (*10*–*13*).

We investigated the genomic and phenotypic variability in *N. gonorrhoeae* antimicrobial susceptibility in England. We described the epidemiologic characteristics of genetically distinct clusters of infection with reduced susceptibility to cefixime, ceftriaxone, and azithromycin and resistance to ciprofloxacin and penicillin. We focused on *N. gonorrhoeae* with mutations in the *penA* allele, which contribute to reduced susceptibility to ceftriaxone. In addition, we assessed the genetic similarity of *N. gonorrhoeae* in England, Europe, and the United States to determine the

Author affiliations: National Institute for Health Research, London, UK (K. Town, G. Hughes); Public Health England, London (K. Town, M.J. Cole, R. Pitt, H. Fifer, H. Mohammed, G. Hughes); University College London, London (K. Town, N. Field, G. Hughes); Microbiotica Ltd, Cambridge, UK (S. Harris); Wellcome Sanger Institute, Cambridge (S. Harris, L. Sánchez-Busó); University of Oxford, Oxford, UK (L. Sánchez-Busó)

DOI: https://doi.org/10.3201/eid2603.190732

extent to which international travel might influence the spread of AMR in *N. gonorrhoeae*.

Methods

Isolate Selection

We selected *N. gonorrhoeae* isolates from the archives of the Gonococcal Resistance to Antimicrobials Surveillance Programme (GRASP), a sentinel program implemented by Public Health England (PHE) in 2000. GRASP is designed to represent the gonococcal population in England (*14*) and includes clinical, sociodemographic, and behavioral data collected through the GUMCAD STI Surveillance System (https://www.gov.uk/guidance/gumcad-sti-surveillance-system) and directly from clinics. During a 3-month period each year, GRASP tests for antimicrobial susceptibility in consecutive isolates from all culture-positive *N. gonorrhoeae* cases identified in 26 sexual health clinics in England and Wales (*15*). GRASP collects ≈1,200–2,500 isolates annually for antimicrobial susceptibility testing (*16*).

We selected isolates collected from 5 GRASP clinics, 2 in London and 3 in other geographically distinct areas in England: Birmingham, Bristol, and Liverpool. We chose these locations to obtain isolates from cases representing a broad range of sociodemographic and behavioral characteristics, including sex, sexual orientation, age, ethnicity, and HIV status (Appendix Table 1, https://wwwnc.cdc.gov/EID/article/26/3/19-0732-App1.pdf). We sequenced all isolates collected during 2013–2016 by the 5 clinics and stored in the GRASP archive. We chose the most recent years of GRASP data to investigate prevailing trends and patterns. We did not include isolates from a 2015 outbreak of high-level azithromycin-resistant *N. gonorrhoeae* in the United Kingdom in this sampling frame because the isolates did not meet the eligibility criteria of our study.

Ethics Considerations

PHE has permission to process confidential patient data obtained by GRASP under Regulation 3 (Control of Patient Information) of the Health Service Regulations 2002. Information governance advice and ethics approval for this study were granted by the PHE Research Ethics and Governance Group.

Antimicrobial Susceptibility Testing

GRASP tests isolates for antimicrobial susceptibility by using agar dilution methods, records MICs for antimicrobial drugs, and defines AMR by using European Committee on Antimicrobial Susceptibility Testing (EUCAST) breakpoints. For our study, we used data on MICs for ceftriaxone, azithromycin, cefixime, penicillin, and ciprofloxacin (*17*). In GRASP, epidemiologic data were linked to MICs for antimicrobial drugs for each isolate phenotype.

Isolation and WGS

We retrieved selected isolates from the GRASP archive by culturing on nonselective gonococcus agar (Difco BBL GC II Agar Base [Becton, Dickinson and Company, https://www.bd.com] plus 1% Vitox [Oxoid, http://www.oxoid.com]). We extracted DNA from a subculture of a single colony of each isolate by using the automated QIAsymphony DNA Mini Kit (QIAGEN, https://www.qiagen.com). WGS was conducted at the Wellcome Sanger Institute (Cambridge, UK) by using the HiSeq X Ten system (Illumina, https://www.illumina.com) and processed in the routine Sanger WGS data management pipeline (Appendix).

Data Sources from Europe and the United States

We compared the study sample with published WGS and associated metadata for *N. gonorrhoeae* isolates from international studies. The collection from Europe (European Nucleotide Archive (ENA; accession no. PRJEB9227) contained 1,054 isolates from the European Gonococcal Antimicrobial Surveillance Programme (Euro-GASP) (*5*). Isolates were collected in 2013 from 20 countries and included 106 isolates from England. We excluded 21% (22/106) that were duplicates of isolates in the study sample, leaving 948 isolates from Europe. The metadata for isolates from Europe included reporting country, antimicrobial susceptibility profile, MICs for ceftriaxone and cefixime, and the presence of the *penA*-34 allele. We grouped MICs to match the categories used in GRASP.

Isolates from the United States were from 2 previous studies investigating the association between phenotype and genotype for AMR in *N. gonorrhoeae* (*4*,*9*). The collection from the United States contained 1,114 isolates collected during 2000–2013 (ENA accession nos. PRJEB2999 and PRJEB7904). The metadata for the isolates from the United States included antimicrobial susceptibility profiles; 270 had reduced susceptibility to cephalosporin (MIC ≥0.25 mg/L for cefixime or MIC ≥0.125 mg/L for ceftriaxone); 294 had reduced susceptibility to azithromycin (MIC ≥2 mg/L); and 594 were ciprofloxacin-resistant (MIC ≥1 mg/L). Metadata also included sexual orientation of case-patients and the presence of the *penA*-34 allele. We grouped MICs to match the categories used in GRASP.

Phylogenetic Analysis

We created phylogenetic trees and removed genetic recombination events by using default settings in Gubbins version 2.4.0 (*18*), including 5 iterations and ≥3 base substitutions to identify a recombination event, and the RAxML (Geneious, https://www.geneious.com) or FastTree (*19*) tree building option (Appendix). We created 3 phylogenetic trees: isolates from England only, isolates from England and other countries in Europe, and isolates from England and the United States.

We identified known genetic markers of AMR, including mutations in the *penA* allele, by using ARIBA (*20*). We compared MICs to the genetic markers by using the ARIBA micplot module.

We identified the genotype of isolates in large and distinct clusters of *N. gonorrhoeae* with elevated MICs for ceftriaxone (MIC ≥0.015 mg/L) and cefixime (MIC ≥0.03 mg/L) from the phylogenetic trees. We compared the epidemiologic characteristics of cases in the clusters by using the χ^2 or Fisher exact test.

Statistical Analysis

We used univariate and multivariable analyses to assess differences in the epidemiologic characteristics and antimicrobial susceptibility of isolates between lineages identified in the phylogenetic tree. We analyzed the following explanatory variables: year and location the isolate was collected; case-patient information, including gender, sexual orientation, age, ethnicity, country of birth, whether they had a symptomatic *N. gonorrhoeae* infection or previous sexually transmitted infection (STI), HIV status, and the number of sexual partners they had in the United Kingdom or through travel-associated sexual partnerships ≤3 months before diagnosis; and isolate susceptibility data, including reduced susceptibility to ceftriaxone (MIC ≥0.015 mg/L), cefixime (MIC ≥0.03 mg/L), or azithromycin (MIC ≥0.25 mg/L); or resistance to penicillin (MIC >1 mg/L or β-lactamase positive) or ciprofloxacin (MIC >0.06 mg/L). We used elevated MIC thresholds for ceftriaxone, cefixime, and azithromycin to provide a robust sample size for regression analysis.

We also explored the relationship between travel-associated sexual partnerships and reduced susceptibility to antimicrobial drugs by conducting univariate and multivariable analyses with reduced susceptibility or resistance as the outcome and travel-associated sexual partnerships as the primary explanatory variable. We considered CI of the odds ratio (OR) >1.0 and p<0.05 by χ^2 test as statistically significant.

We developed multivariable logistic regression models by using a forward approach and including only statistically significant variables associated with the outcome in the univariate model to control for possible confounding between variables. We used the likelihood ratio test to determine which explanatory variables should remain in the multivariable model by using p<0.05 as the threshold of statistical significance.

Results

Sample Description

Of the eligible isolates, we successfully sequenced 91% (1,277/1,407); the bacteria of the remaining 130 isolates were no longer viable for DNA extraction. For all antimicrobial drugs tested, the MIC distributions of the study isolates were similar to those of all GRASP isolates (Appendix Table 2). We found that 3.6% of isolates were resistant to azithromycin (MIC >0.5 mg/L) and 2 isolates were highly resistant (MIC ≥256 mg/L); 0.6% were resistant to cefixime (MIC >0.125 mg/L), 36.3% to ciprofloxacin (MIC >0.06 mg/L), 16.6% to penicillin (MIC >1 mg/L), and none to ceftriaxone (MIC >0.125 mg/L). The MIC distribution of the isolates not sequenced was similar to the distribution of the sequenced isolates. Most (69%; 881/1,277) isolates were from genital infections, 23.4% (299/1,277) were from rectal infections, and 6.3% (80/1,277) were from pharyngeal infections. Overall, we identified 226 different sequence types (STs) by using *N. gonorrhoeae* multiantigen sequence typing (NG-MAST) (Appendix). We deposited novel sequences extracted for this study into ENA (accession no. ERP022090) and provide metadata (Appendix).

N. gonorrhoeae Lineages Circulating in England

We noted 2 distinct lineages in the phylogenetic tree (Figure 1). Compared with lineage B, lineage A was more likely to contain isolates from clinics in London than those outside of London (outside London:in London adjusted odds ratio [aOR] 1.74, 95% CI 1.27–2.67; p = 0.001). Lineage A also contained more isolates from persons ≥35 years of age than persons ≤24 years of age (aOR 1.68, 95% CI 1.16–2.40; p = 0.006). Asian ethnicity also was associated more frequently with isolates from lineage A compared with white ethnicity (aOR 1.86, 95% CI 1.01–3.45; p = 0.048) (Table 1). Lineage A was less likely to contain isolates from women (aOR 0.14, 95% CI 0.09–0.22; p<0.001) or men who reported having sex with women exclusively (MSW; aOR 0.33, 95% CI 0.23–0.47; p<0.001) compared with MSM. This lineage also was less likely to contain isolates from persons reporting black Caribbean ethnicity compared with persons reporting

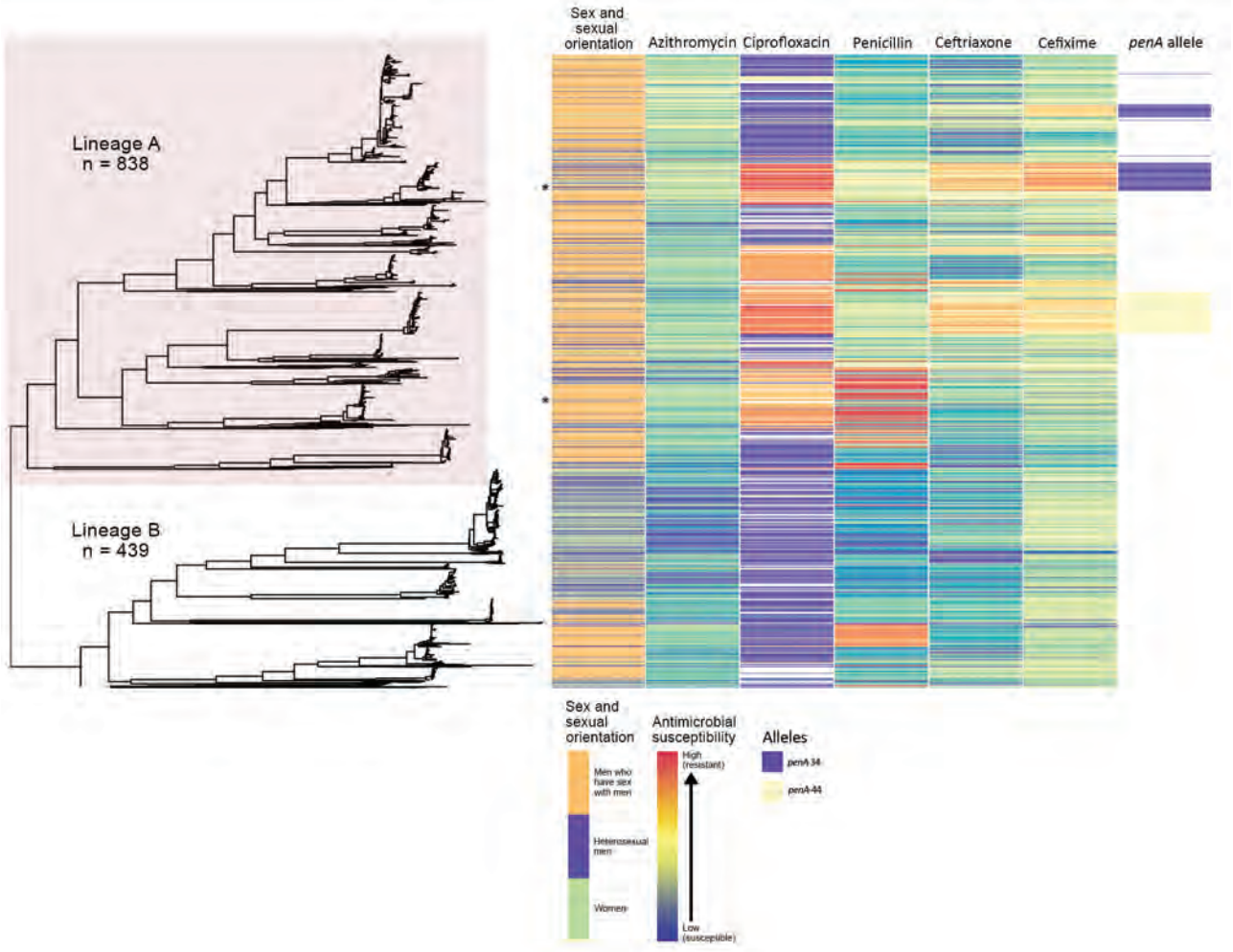

Figure 1. Phylogeny and antimicrobial susceptibility of *Neisseria gonorrhoeae* isolates from England, 2013–2016. Maximum-likelihood phylogeny with recombination events removed of all *N. gonorrhoeae* isolates annotated with gender and sexual orientation, antimicrobial susceptibility phenotype, and *penA* genotype. Asterisks represent location in tree of isolates with high-level azithromycin resistance (MIC ≥256 mg/L). Heterosexual men were those who reported sex with women exclusively.

white ethnicity (aOR 0.49, 95% CI 0.32–0.76; p = 0.001). Lineage A was more likely to contain isolates from persons who reported a travel-associated sexual partnership compared with isolates from lineage B (crude odds ratio [cOR] 1.96, 95% CI 1.20–3.21; p = 0.006), but this association did not persist in the multivariable model (aOR 1.66, 95% CI 0.94–2.91; p = 0.078 adjusting for location, age, sex, sexual orientation, and ethnicity). However, isolates from persons who had a recent travel-associated sexual partnership were more likely to be resistant to ciprofloxacin (aOR 1.83, 95% CI 1.13–2.96; p = 0.015, adjusting for location, age, sex, sexual orientation, and ethnicity). We saw no statistically significant association between recent travel-associated sexual partnerships and *N. gonorrhoeae* with reduced susceptibility to ceftriaxone, cefixime, or azithromycin, or resistance to penicillin.

Isolates with reduced susceptibility to ceftriaxone, cefixime, or azithromycin or resistance to ciprofloxacin and penicillin were dispersed throughout the phylogenetic tree (Figure 1). However, compared with lineage B, isolates in lineage A were more likely to have higher MICs for ceftriaxone (aOR 15.4, 95% CI 8.50–27.8; p<0.001), cefixime (aOR 3.97, 95% CI 2.76–5.76; p<0.001), azithromycin (aOR 7.5, 95% CI 5.37–10.5; p<0.001), and penicillin (aOR 18.2, 95% CI 11.4–29.2; p<0.001) (Table 2).

Distribution of *penA* Alleles across the Phylogeny

Overall, we identified 32 different known mutations in 8 genes associated with resistance to ceftriaxone, cefixime, azithromycin, ciprofloxacin, or penicillin. For all antimicrobial drugs, we noted isolates with the same combination of genotypic markers of

Table 1. Univariate and multivariable analyses comparing the epidemiologic characteristics of cases of *Neisseria gonorrhoeae* between 2 phylogenetic lineages, England*

	Lineage, no.		Lineage A outcomes					
			Univariate			Multivariable		
Characteristics	A	B	cOR	95% CI	p value	aOR	95% CI	p value
Total	838	439						
Year								
2013	220	106	Ref					
2014	210	123	0.82	0.60–1.13	0.234			
2015	260	107	1.17	0.85–1.62	0.339			
2016	148	103	**0.69**	**0.49–0.98**	**0.035**			
Clinic location								
Outside London	630	136	Ref			Ref		
London	463	109	**3.73**	**2.86–4.88**	**<0.001**	**1.74**	**1.27–2.67**	**0.001**
Sex and sexual orientation								
MSM	630	136	Ref			Ref		
MSW	150	154	**0.21**	**0.15–0.29**	**<0.001**	**0.33**	**0.23–0.47**	**<0.001**
F	57	149	**0.08**	**0.05–0.12**	**<0.001**	**0.14**	**0.09–0.22**	**<0.001**
Age, y								
≤24	188	196	Ref			Ref		
25–34	342	161	**2.21**	**1.67–2.93**	**<0.001**	1.14	0.83–1.59	0.413
≥35	308	82	**3.92**	**2.81–5.46**	**<0.001**	**1.68**	**1.16–2.40**	**0.006**
Ethnicity								
White	586	238	Ref			Ref		
Black Caribbean	51	81	**0.26**	**0.17–0.38**	**<0.001**	**0.49**	**0.32–0.76**	**0.001**
Black African	27	20	**0.55**	**0.30–1.00**	**0.046**	0.84	0.43–1.64	0.607
Black Other	6	4	0.61	0.17–2.18	0.442	0.57	0.14–2.37	0.441
Asian	57	17	1.36	0.78–2.39	0.280	**1.86**	**1.01–3.45**	**0.048**
Other	24	8	1.22	0.54–2.75	0.634	0.99	0.41–2.44	0.999
Mixed	62	43	**0.59**	**0.39–0.89**	**0.011**	0.82	0.51–1.32	0.413
Place of birth								
United Kingdom	473	309	Ref					
Not United Kingdom	305	102	**1.95**	**1.49–2.56**	**<0.001**			
Symptomatic infection								
No	219	119	Ref					
Yes	526	277	1.03	0.79–1.35	0.818			
New STI diagnosis ≤1 year, excluding HIV								
No or unknown	615	363	Ref					
Yes	223	75	**1.75**	**1.31–2.35**	**<0.001**			
HIV status								
Negative or unknown	653	398	Ref					
Positive	185	41	**2.75**	**1.91–3.96**	**<0.001**			
Number of partners in the United Kingdom ≤3 months of diagnosis								
0	27	20	Ref					
1	175	162	0.80	0.43–1.48	0.478			
≥2	304	167	1.35	0.73–2.48	0.335			
Travel-associated sexual partnerships ≤3 months of diagnosis								
No	442	325	Ref					
Yes	64	24	**1.96**	**1.20–3.21**	**0.006**			

*The multivariable model was adjusted for location, gender and sexual orientation, age, and ethnicity. Bold text indicates statistical significance (p<0.05 and 95% CI does not cross 1.0). aOR, adjusted odds ratio; cOR, crude odds ratio; MSM, men who have sex with men; MSW, men who reported sexual activity exclusively with women; Ref, referent; STI, sexually transmitted infection.

resistance but differing phenotypic MICs (Appendix Figures 1–5).

The larger, distinct clusters with elevated MICs for ceftriaxone and cefixime contained the *penA*-34 allele and the *penA*-44 allele (Figure 1). All isolates with the *penA*-34 allele (n = 86) had a MIC of ≥0.015 mg/L for cefixime and 67 had a MIC of ≥0.015 mg/L for ceftriaxone. Most (81/84; 96%) isolates with the *penA*-44 allele had a MIC of ≥0.015 mg/L for cefixime, a MIC of ≥0.015 mg/L for ceftriaxone (83/84; 98%), or both (81/84; 96%).

The 2 largest clusters with the *penA*-34 allele (cluster 1, n = 57; cluster 2, n = 26) were genetically distinct from each other and isolates in the 2 groups had statistically significant differences by year, clinic, sexual orientation, and HIV status (Table 3). Most (81%; 21/26) isolates in cluster 2 were from London in 2014–2015, and most (67%; 38/57) in cluster 1 were from outside London but distributed across all 4 years of the study. Most (96%; 25/26) isolates in cluster 2 were from MSM; whereas cluster 1 was more mixed and composed of isolates from women (21%; 12/57), MSW (37%; 21/57), and MSM (42%; 24/57). Cluster 2 had a higher percentage of persons living with HIV (35%; 9/26) than did cluster 1 (7%; 4/57). Most (82%;

69/84) isolates with the *penA*-44 allele were from MSM, persisted over all 4 years of the study, and were found both inside and outside of London. The characteristics of isolates with the *penA*-44 allele were more similar to the characteristics of isolates in cluster 2 of the *penA*-34 group than to isolates in cluster 1 (Appendix Table 3).

Comparison of Isolates from England, Europe, and the United States

Isolates from England were genetically interspersed with isolates from other countries in Europe (Figure 2) or the United States (Figure 3), although some large clades of isolates came only from England or the United States. Isolates in cluster 1 with the *penA*-34 allele in England were clustered with isolates from Europe and the United States (Figures 2–3). Isolates with the *penA*-34 allele in cluster 2 from England that were only found after 2013 were not related genetically to isolates from the United States or from other countries in Europe.

Discussion

We conducted a large study on genomic variability of antimicrobial susceptibility in *N. gonorrhoeae* in England. We sampled isolates from geographically dispersed clinics in England, and our data likely represent patterns at a national level. Our data suggest that *N. gonorrhoeae* with reduced susceptibility to antimicrobial drugs, including ceftriaxone, has emerged in England through novel mutation and recombination events, repeated introduction from overseas, clonal expansion, or a combination of these.

We observed 3 distinct clusters with 2 different *penA* alleles and reduced susceptibility to ceftriaxone and cefixime and found patients in each cluster with differing epidemiologic characteristics. The genetic similarity of isolates from England, Europe, and the United States is consistent with global dissemination of *N. gonorrhoeae* concerning genotypic and phenotypic features. Our data highlight the potential influence of travel-associated sexual partnerships in AMR transmission.

As seen in other *N. gonorrhoeae* studies, the high frequency of DNA recombination requires computational strategies to use single-nucleotide polymorphism differences arising through mutation rather than recombination. We identified and removed recombinant DNA, but some likely remained, which might lead to incorrect inferences about relatedness for some isolates.

We found 2 distinct lineages of *N. gonorrhoeae* with different antimicrobial susceptibility profiles circulating in England. The larger lineage contained isolates with elevated MICs or resistance to all 5 antimicrobial drugs tested, consistent with findings from recent studies in Europe and globally (*5*,*21*). The authors of those studies hypothesized that differing susceptibility profiles of the 2 lineages were associated with different sexual orientation networks, but neither study had complete data on sexual orientation to support the hypothesis. Our study includes sexual orientation data for 99% of cases. Our findings strongly support the hypothesis that MSM are more frequently infected with *N. gonorrhoeae* strains with reduced susceptibility to antimicrobials, whereas MSW and women are more frequently infected with the more susceptible lineage. Nevertheless, many MSW were infected with *N. gonorrhoeae* with reduced susceptibility to antimicrobial drugs and MSM were

Table 2. Association between antimicrobial susceptibility of *Neisseria gonorrhoeae* isolates and presence in lineage A of the phylogeny, England*

Susceptibility	Lineage A, no. isolates	Lineage B, no. isolates	aOR	95% CI	p value
Reduced					
Ceftriaxone, MIC ≥0.015 mg/L					
No	572	418	Referent	–	–
Yes	263	15	**15.4**	**8.50–27.8**	**<0.001**
Cefixime, MIC ≥0.03 mg/L					
No	544	370	Referent	–	–
Yes	291	63	**3.97**	**2.76–5.76**	**<0.001**
Azithromycin, MIC ≥0.25 mg/L					
No	328	367	Referent	–	–
Yes	507	66	**7.50**	**5.37–10.5**	**<0.001**
Resistant					
Penicillin, MIC >1 mg/L or β-lactamase positive					
No	671	378	Referent	–	–
Yes	164	55	1.33	0.92–1.93	0.134
Ciprofloxacin, MIC >0.06 mg/L					
No	400	408	Referent	–	–
Yes	435	25	**18.2**	**11.4–29.2**	**<0.001**

*Each model adjusted for location inside or outside of London, and patient age, sexual orientation, and ethnicity. Nine isolates did not have MIC data. Bold text indicates statistical significance, i.e., p<0.05 and 95% CI does not cross 1. aOR, adjusted odds ratio.

infected by antimicrobial-susceptible *N. gonorrhoeae*, and we noted intralineage variation by sexual orientation. MSM have more bacterial STI diagnoses and greater exposure to antimicrobial drugs, thereby increasing selection pressures for AMR, a hypothesis supported by mathematical models (*21*–*24*). Resistant strains also might persist in the absence of selective pressure because the organism's biologic fitness is unaffected or compensatory mutations mitigate a deleterious effect (*25*–*27*).

By combining WGS, epidemiologic, and phenotypic data, we found that reduced susceptibility to ceftriaxone and cefixime emerged repeatedly in separate sexual networks in England. Without WGS data, we would have grouped all *penA*-34 samples from MSM together. Likewise, if we restricted sequencing to the *penA* gene, we would not have identified unique clusters with the same *penA*-34 allele.

The large group of isolates in England with the *penA*-34 allele clustered with isolates from Europe and the United States that had the same allele. Some of the *penA*-34 allele isolates belonged to the NG-MAST 1407 lineage, a widely disseminated clone associated with elevated MICs for ceftriaxone and cefixime and the catalyst for changing national treatment guidelines in the United Kingdom from cefixime as

Table 3. Epidemiologic characteristics of patients from whom *Neisseria gonorrhoeae* isolates were collected in the 2 largest *penA*-34 clusters, England*

Characteristics	Total	Cluster 1, n = 57, no. (%)	Cluster 2, n = 26, no. (%)	p value†
Year				
2013	26	26 (45.6)	0	**<0.001**‡
2014	29	14 (24.6)	15 (57.7)	
2015	20	10 (17.5)	10 (38.5)	
2016	8	7 (12.3)	1 (3.8)	
Sex and sexual orientation				
MSM	49	24 (42.1)	25 (96.2)	**<0.001**‡
MSW	21	21 (36.8)	0	
F	13	12 (21.1)	1 (3.8)	
Clinic location				
Outside London	43	38 (66.7)	5 (19.2)	**<0.001**‡
London	40	19 (33.3)	21 (80.8)	
Age, y				
≤24	28	23 (40.4)	5 (19.2)	0.081
25–34	29	20 (35.1)	9 (34.6)	
≥35	26	14 (24.6)	12 (46.2)	
Ethnicity				
White	59	37 (68.5)	22 (84.6)	0.408‡
Black Caribbean	6	6 (11.1)	0	
Black, Other	2	2 (3.7)	0	
Asian	5	4 (7.4)	1 (3.8)	
Other	4	2 (3.7)	2 (7.7)	
Mixed	4	3 (5.6)	1 (3.8)	
Place of birth				
United Kingdom	40	30 (52.6)	10 (38.5)	0.262‡
Not United Kingdom	40	26 (45.6)	14 (53.9)	
Unknown	3	1 (1.7)	2 (7.7)	
Symptomatic infection				
No	28	13 (24.5)	15 (57.7)	**0.004**
Yes	51	40 (75.5)	11 (42.3)	
New STI diagnosed ≤1 year, excluding HIV				
No	68	51 (89.5)	17 (65.4)	**0.013**‡
Yes	15	6 (10.5)	9 (34.6)	
HIV status				
Negative or unknown	70	53 (93.0)	17 (65.4)	**0.003**‡
Positive	13	4 (7.0)	9 (34.6)	
Number of sexual partners in the United Kingdom ≤3 mo of *N. gonorrhea* diagnosis				
0	6	6 (13.3)	0	0.675‡
1	19	16 (35.6)	3 (33.3)	
≥2	29	23 (51.1)	6 (66.7)	
Travel-associated sexual partnership				
No	43	34 (75.6)	9 (100)	0.178‡
Yes	11	11 (24.4)	0	

*Bold text indicates statistical significance (i.e., p<0.05 and 95% CI does not cross 1). MSM, men who have sex with men; MSW, men who reported sexual activity exclusively with women.
†Calculated using χ^2 test, except where noted.
‡Calculated using Fisher exact test.

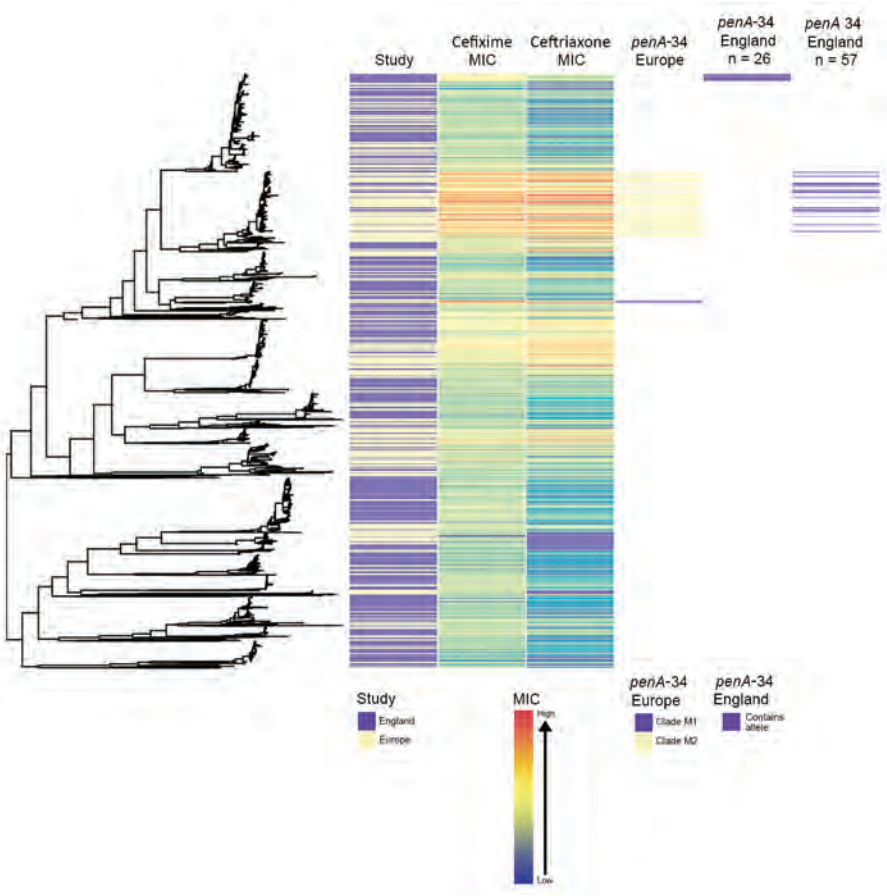

Figure 2. Phylogenetic tree of *Neisseria gonorrhoeae* isolates from England and other countries in Europe in a study of antimicrobial susceptibility, 2013–2016, including metadata for study type, MICs for ceftriaxone and cefixime, and presence of *penA*-34 alleles. We sequenced 1,277 isolates; 948 isolates were from other countries in Europe. The *penA*-34 clades from Europe are labeled M1 and M2, as noted by Harris et al. (*5*).

first-line therapy to ceftriaxone in 2011 (*6*,*22*). Therefore, the larger *penA*-34 group probably represents clonal spread of a previously identified endemic strain of *N. gonorrhoeae*; the smaller *penA*-34 group represents a new strain emerging in a different sexual network largely comprising MSM in London with a history of STIs, including HIV. Consequently, restricting public health resources that measure, prevent, and control AMR in *N. gonorrhoeae* to specific risk groups or geographic locations could be ineffective because AMR appears to emerge independently in different sexual networks and locations.

We found some evidence for importation of AMR. Isolates from persons who recently had a travel-associated sexual partnership were more likely to be infected with *N. gonorrhoeae* that was resistant to ciprofloxacin. Although de novo development of high-level resistance to azithromycin in the United Kingdom has been described, some studies have concluded that importation events probably initiate AMR spread in countries with low population prevalence, such as England (*11*,*27*,*28*). The success of antimicrobial stewardship policies and compliance with treatment guidelines that aim to curtail AMR in the endemic gonococcal population in England could be undermined by the importation and subsequent spread of resistant isolates. These data support the importance of promoting STI prevention messages and testing to international travelers, particularly those visiting countries where AMR *N. gonorrhoeae* is endemic. Quantifying the relationship between *N. gonorrhoeae* circulating in England and internationally also could help parameterize mathematical models exploring the relative contribution of importation and de novo development on AMR prevalence and distribution.

Rapid molecular tests for genetic markers that are highly predictive of an antimicrobial susceptibility phenotype could lead to more effective use of antimicrobials. Tests detecting markers of ciprofloxacin and cephalosporin antimicrobial susceptibility are already in development (*8*,*29*,*30*). However, as found in our study and elsewhere, the association between genotype and phenotype is much stronger for ciprofloxacin resistance than for cephalosporin resistance (*4*,*31*,*32*). Most rapid tests for cephalosporin resistance focus on detecting mutations in the *penA* allele, but reduced susceptibility to cephalosporins also can

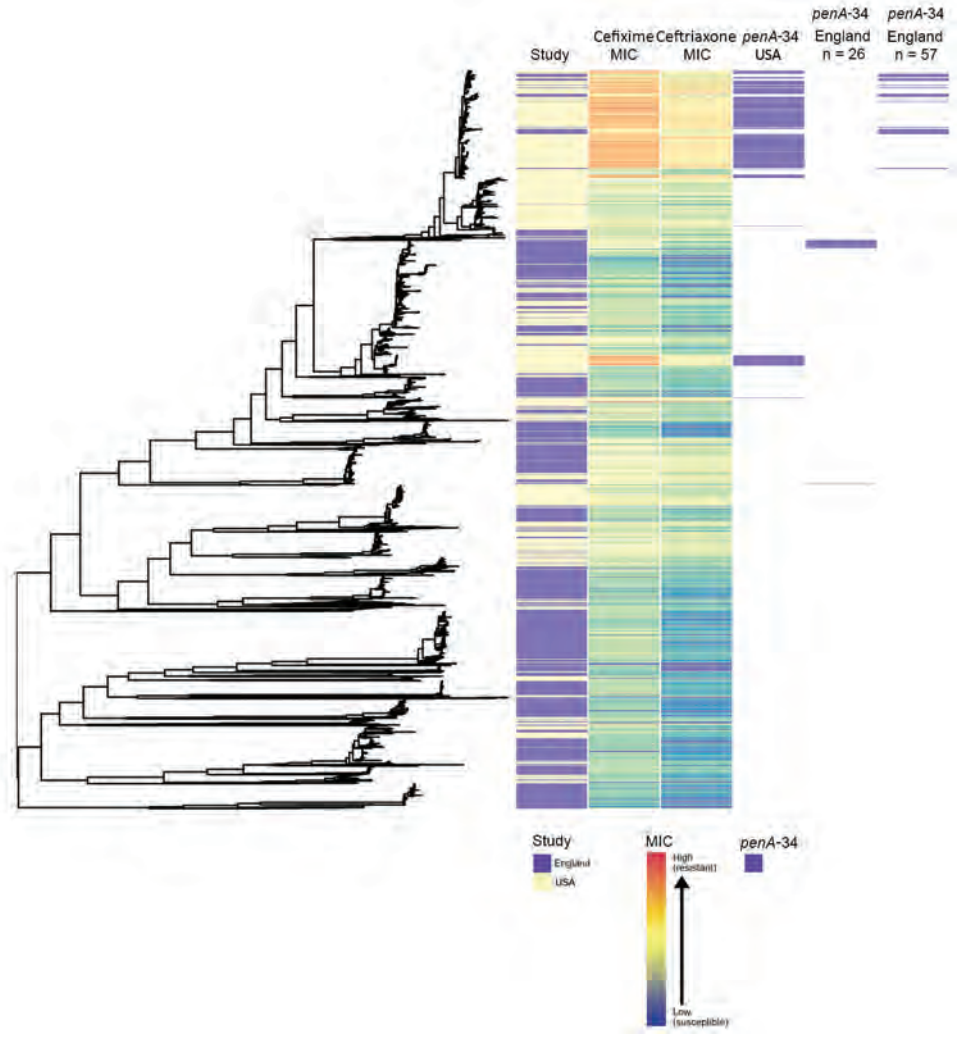

Figure 3. Phylogenetic tree of *Neisseria gonorrhoeae* isolates from England and the United States in a study of antimicrobial susceptibility, 2013–2016, including metadata for study type, MICs for ceftriaxone and cefixime, and presence of *penA*-34 alleles. We sequenced 1,277 isolates; 1,114 isolates were from the United States.

be caused by mutations in the semimosaic *penA* allele, *penA*-35, the nonmosaic *penA* allele, *penA*-44, or even in the *mtrR* and *penB* genes (*30*,*33*).

Molecular tests that focus on the presence or absence of 1 mutation without considering the additive effect of multiple mutations could be insufficient for detecting resistance and predicting treatment failure. Epistasis, in which phenotypic resistance is dependent on complex interactions of multiple mutant genes, is known to occur in *N. gonorrhoeae* (*22*,*31*,*34*). In our study, the antimicrobial susceptibility of isolates with identical genetic markers of resistance varied by >2 doubling dilutions, and most isolates with resistance markers were sensitive. Nonetheless, the presence of 1 mutation that belongs to a complex of mutations required for resistance indicates the potential for phenotypic resistance to develop. Clinicians could prioritize patients infected with these strains for a test of cure or consider use of alternative antimicrobial drugs unaffected by the resistance marker. In any event, mathematical modeling studies have shown that molecular tests should only be implemented if they are highly sensitive; otherwise, they could accelerate the spread of AMR (*23*). Elucidation of the mechanisms and genomic markers of cephalosporin resistance is needed and can be achieved through a combination of microbiologic and genomic studies, including genomewide association studies. WGS cannot replace phenotypic testing for all antimicrobial susceptibility because it can only detect known mutations associated with resistance, and novel mutations associated with resistance develop constantly in *N. gonorrhoeae* (*31*).

In conclusion, phylogenetic analyses with WGS data revealed transmission patterns of *N. gonorrhoeae* with reduced susceptibility in England that would not have been identified by using only epidemiologic and phenotypic data. Reduced susceptibility to

antimicrobial drugs likely has emerged and spread independently in different sexual networks in England through multiple de novo mutation and recombination events and through some repeated importation by persons who have travel-associated sexual partnerships. Consequently, public health actions to limit dissemination of AMR in England should aim to reduce risk behaviors that support *N. gonorrhoeae* transmission and encompass the diffuse distribution and epidemiologic diversity of the population groups affected.

Acknowledgments

We thank our funders, the Blood-Borne and Sexually Transmitted Infections Steering Committee of the National Institute for Health Research Health Protection Research Unit (NIHR HPRU), Caroline Sabin, Anthony Nardone, Catherine Mercer, Gwenda Hughes, Jackie Cassell, Greta Rait, Samreen Ijaz, Tim Rhodes, Kholoud Porter, Sema Mandal, and William Rosenberg; the Wellcome Trust (grant no. 098051); and Public Health England. We also thank the clinical and laboratory staff who contributed to GRASP and Hester Allen for her help with data management and analysis.

This research was funded by the National Institute for Health Research (NIHR) Health Protection Research Unit in Blood Borne and Sexually Transmitted Infections at University College London in partnership with Public Health England, in collaboration with the London School of Hygiene & Tropical Medicine. The views expressed are those of the authors and not necessarily those of the NIHR, the Department of Health and Social Care, or Public Health England.

About the Author

Dr. Town was the senior surveillance scientist on the Gonococcal Resistance to Antimicrobials Surveillance Programme (GRASP) at Public Health England and graduated from University College London with a PhD in epidemiology. Dr. Town's research focuses on investigating new methods for understanding, monitoring, and preventing the spread of *Neisseria gonorrhoeae* and antimicrobial resistance.

References

1. Tapsall JW. Antimicrobial resistance in *Neisseria gonorrhoeae*. Geneva: World Health Organization; 2001.
2. Wi T, Lahra MM, Ndowa F, Bala M, Dillon JR, Ramon-Pardo P, et al. Antimicrobial resistance in *Neisseria gonorrhoeae*: global surveillance and a call for international collaborative action. PLoS Med. 2017;14:e1002344. https://doi.org/10.1371/journal.pmed.1002344
3. Demczuk W, Lynch T, Martin I, Van Domselaar G, Graham M, Bharat A, et al. Whole-genome phylogenomic heterogeneity of *Neisseria gonorrhoeae* isolates with decreased cephalosporin susceptibility collected in Canada between 1989 and 2013. J Clin Microbiol. 2015;53:191–200. https://doi.org/10.1128/JCM.02589-14
4. Grad YH, Harris SR, Kirkcaldy RD, Green AG, Marks DS, Bentley SD, et al. Genomic epidemiology of gonococcal resistance to extended-spectrum cephalosporins, macrolides, and fluoroquinolones in the United States, 2000–2013. J Infect Dis. 2016;214:1579–87. https://doi.org/10.1093/infdis/jiw420
5. Harris SR, Cole MJ, Spiteri G, Sánchez-Busó L, Golparian D, Jacobsson S, et al.; Euro-GASP study group. Public health surveillance of multidrug-resistant clones of *Neisseria gonorrhoeae* in Europe: a genomic survey. Lancet Infect Dis. 2018;18:758–68. https://doi.org/10.1016/S1473-3099(18)30225-1
6. Town K, Obi C, Quaye N, Chisholm S, Hughes G; GRASP Collaborative Group. Drifting towards ceftriaxone treatment failure in gonorrhoea: risk factor analysis of data from the Gonococcal Resistance to Antimicrobials Surveillance Programme in England and Wales. Sex Transm Infect. 2017;93:39–45. https://doi.org/10.1136/sextrans-2016-052583
7. Kirkcaldy RD, Zaidi A, Hook EW III, Holmes KK, Soge O, del Rio C, et al. *Neisseria gonorrhoeae* antimicrobial resistance among men who have sex with men and men who have sex exclusively with women: the Gonococcal Isolate Surveillance Project, 2005–2010. Ann Intern Med. 2013;158:321–8. https://doi.org/10.7326/0003-4819-158-5-201303050-00004
8. Allan-Blitz L-T, Humphries RM, Hemarajata P, Bhatti A, Pandori MW, Siedner MJ, et al. Implementation of a rapid genotypic assay to promote targeted ciprofloxacin therapy of *Neisseria gonorrhoeae in a large health system*. Clin Infect Dis. 2017;64:1268–70. https://doi.org/10.1093/cid/ciw864
9. Grad YH, Kirkcaldy RD, Trees D, Dordel J, Harris SR, Goldstein E, et al. Genomic epidemiology of *Neisseria gonorrhoeae* with reduced susceptibility to cefixime in the USA: a retrospective observational study. Lancet Infect Dis. 2014;14:220–6. https://doi.org/10.1016/S1473-3099(13)70693-5
10. Town K, Bolt H, Croxford S, Cole M, Harris S, Field N, et al. *Neisseria gonorrhoeae* molecular typing for understanding sexual networks and antimicrobial resistance transmission: A systematic review. J Infect. 2018;76:507–14. https://doi.org/10.1016/j.jinf.2018.02.011
11. Fifer H, Cole M, Hughes G, Padfield S, Smolarchuk C, Woodford N, et al. Sustained transmission of high-level azithromycin-resistant *Neisseria gonorrhoeae* in England: an observational study. Lancet Infect Dis. 2018;18:573–81. https://doi.org/10.1016/S1473-3099(18)30122-1
12. Eyre DW, Town K, Street T, Barker L, Sanderson N, Cole MJ et al. Detection in the United Kingdom of the *Neisseria gonorrhoeae* FC428 clone, with ceftriaxone resistance and intermediate resistance to azithromycin, October to December 2018. Euro Surveil. 2019;24.https://doi.org/10.2807/1560-7917.ES.2019.24.10.1900147
13. De Silva D, Peters J, Cole K, Cole MJ, Cresswell F, Dean G, et al. Whole-genome sequencing to determine transmission of *Neisseria gonorrhoeae*: an observational study. Lancet Infect Dis. 2016;16:1295–303. https://doi.org/10.1016/S1473-3099(16)30157-8
14. Hughes G, Nichols T, Ison CA. Estimating the prevalence of gonococcal resistance to antimicrobials in England and Wales. Sex Transm Infect. 2011;87:526–31. https://doi.org/10.1136/sextrans-2011-050071

15. Public Health England. Gonococcal Resistance to Antimicrobials Surveillance Programme (GRASP): protocol. 2014 [22 Jan 2020]. https://www.gov.uk/government/publications/gonococcal-resistance-to-antimicrobials-surveillance-programme-grasp-protocol/gonococcal-resistance-to-antimicrobials-surveillance-programme-grasp-protocol
16. Mohammed H, Ison CA, Obi C, Chisholm S, Cole M, Quaye N, et al.; GRASP Collaborative Group. Frequency and correlates of culture-positive infection with *Neisseria gonorrhoeae* in England: a review of sentinel surveillance data. Sex Transm Infect. 2015;91:287–93. https://doi.org/10.1136/sextrans-2014-051756
17. Cole MJ, Quaye N, Jacobsson S, Day M, Fagan E, Ison C, et al. Ten years of external quality assessment (EQA) of *Neisseria gonorrhoeae* antimicrobial susceptibility testing in Europe elucidate high reliability of data. BMC Infect Dis. 2019;19:281. https://doi.org/10.1186/s12879-019-3900-z
18. Croucher NJ, Page AJ, Connor TR, Delaney AJ, Keane JA, Bentley SD, et al. Rapid phylogenetic analysis of large samples of recombinant bacterial whole genome sequences using Gubbins. Nucleic Acids Res. 2015;43:e15. https://doi.org/10.1093/nar/gku1196
19. Price MN, Dehal PS, Arkin AP. FastTree: computing large minimum evolution trees with profiles instead of a distance matrix. Mol Biol Evol. 2009;26:1641–50. https://doi.org/10.1093/molbev/msp077
20. Hunt M, Mather AE, Sánchez-Busó L, Page AJ, Parkhill J, Keane JA, et al. ARIBA: rapid antimicrobial resistance genotyping directly from sequencing reads. Microb Genom. 2017;3:e000131. https://doi.org/10.1099/mgen.0.000131
21. Sánchez-Busó L, Golparian D, Corander J, Grad YH, Ohnishi M, Flemming R, et al. The impact of antimicrobials on gonococcal evolution. Nat Microbiol. 2019;4:1941–50. https://doi.org/10.1038/s41564-019-0501-y
22. Unemo M, Nicholas RA. Emergence of multidrug-resistant, extensively drug-resistant and untreatable gonorrhea. Future Microbiol. 2012;7:1401–22. https://doi.org/10.2217/fmb.12.117
23. Fingerhuth SM, Bonhoeffer S, Low N, Althaus CL. Antibiotic-resistant *Neisseria gonorrhoeae* spread faster with more treatment, not more sexual partners. PLoS Pathog. 2016; 12:e1005611. https://doi.org/10.1371/journal.ppat.1005611
24. Xiridou M, Soetens LC, Koedijk FD, van der Sande MA, Wallinga J. Public health measures to control the spread of antimicrobial resistance in *Neisseria gonorrhoeae* in men who have sex with men. Epidemiol Infect. 2015;143:1575–84. https://doi.org/10.1017/S0950268814002519
25. Abrams AJ, Kirkcaldy RD, Pettus K, Fox JL, Kubin G, Trees DL. A Case of decreased susceptibility to ceftriaxone in *Neisseria gonorrhoeae* in the absence of a mosaic penicillin-binding protein 2 (*penA*) allele. Sex Transm Dis. 2017;44:492–4. https://doi.org/10.1097/OLQ.0000000000000645
26. Al Suwayyid BA, Coombs GW, Speers DJ, Pearson J, Wise MJ, Kahler CM. Genomic epidemiology and population structure of *Neisseria gonorrhoeae* from remote highly endemic Western Australian populations. BMC Genomics. 2018;19:165. https://doi.org/10.1186/s12864-018-4557-5
27. Hui BB, Whiley DM, Donovan B, Law MG, Regan DG; GRAND Study Investigators. Identifying factors that lead to the persistence of imported *gonorrhoeae* strains: a modelling study. Sex Transm Infect. 2017;93:221–5. https://doi.org/10.1136/sextrans-2016-052738
28. Goldstein E, Kirkcaldy RD, Reshef D, Berman S, Weinstock H, Sabeti P, et al. Factors related to increasing prevalence of resistance to ciprofloxacin and other antimicrobial drugs in *Neisseria gonorrhoeae*, United States. Emerg Infect Dis. 2012;18:1290–7. https://doi.org/10.3201/eid1808.111202
29. Donà V, Smid JH, Kasraian S, Egli-Gany D, Dost F, Imeri F, et al. Mismatch amplification mutation assay-based real-time PCR for rapid detection of *Neisseria gonorrhoeae* and antimicrobial resistance determinants in clinical specimens. J Clin Microbiol. 2018;56:e00365-18. https://doi.org/10.1128/JCM.00365-18
30. Zhao L, Liu A, Li R, Zhao S. Multiplex TaqMan real-time PCR platform for detection of *Neisseria gonorrhoeae* with decreased susceptibility to ceftriaxone. Diagn Microbiol Infect Dis. 2019;93:299–304. https://doi.org/10.1016/j.diagmicrobio.2018.10.013
31. Unemo M, Shafer WM. Antimicrobial resistance in *Neisseria gonorrhoeae* in the 21st century: past, evolution, and future. Clin Microbiol Rev. 2014;27:587–613. https://doi.org/10.1128/CMR.00010-14
32. Chen SC, Yin YP, Dai XQ, Unemo M, Chen XS. First nationwide study regarding ceftriaxone resistance and molecular epidemiology of *Neisseria gonorrhoeae* in China. J Antimicrob Chemother. 2016;71:92–9. https://doi.org/10.1093/jac/dkv321
33. Zhao S, Duncan M, Tomberg J, Davies C, Unemo M, Nicholas RA. Genetics of chromosomally mediated intermediate resistance to ceftriaxone and cefixime in *Neisseria gonorrhoeae.* Antimicrob Agents Chemother. 2009;53:3744–51. https://doi.org/10.1128/AAC.00304-09
34. Tomberg J, Unemo M, Davies C, Nicholas RA. Molecular and structural analysis of mosaic variants of penicillin-binding protein 2 conferring decreased susceptibility to expanded-spectrum cephalosporins in *Neisseria gonorrhoeae:* role of epistatic mutations. Biochemistry. 2010;49:8062–70. https://doi.org/10.1021/bi101167x

Address for correspondence: Katy Town, Public Health England, 61 Colindale Ave, London NW9 5EQ, UK; email: katy.town.15@alumni.ucl.ac.uk

High Prevalence of and Risk Factors for Latent Tuberculosis Infection among Prisoners, Tianjin, China

Guoqin Zhang, Yuhua Zhang, Da Zhong, Sukai Meng, Liqun An, Wenliang Wei, Zhi Zhang, Yanyong Fu, Xiexiu Wang

The high incidence of tuberculosis (TB) among prisoners calls for interventions to identify latent tuberculosis infection (LTBI) before disease onset. To identify LTBI prevalence among prisoners and factors associated with it, we conducted a cross-sectional study in Tianjin. We randomly sampled 959 HIV-negative adult prisoners by ward clusters in 5 prisons and determined LTBI by seropositivity using an interferon-γ release assay. The overall rate of LTBI was 52.0% (499/959) in the 5 facilities and ranged from 41.9% (72/172) to 60.9% (106/174). Age (adjusted odds ratio [aOR] 1.7, 95% CI 1.4–2.0 per 10 years), duration of imprisonment (aOR 1.2, 95 CI% 1.1–1.2 per year), previous incarceration (aOR 2.0, 95% CI 1.5–2.7), and facility-specific TB incidence (aOR 1.9, 95% CI 1.3–2.8) were risk factors for LTBI. These findings indicate possible TB transmission within prisons and suggest the necessity for early TB case detection, as well as prophylaxis.

Tuberculosis (TB) remains a global threat to human health. In 2018, a total of 10 million cases of TB and 1.5 million deaths from TB were reported by the World Health Organization (WHO) (*1*). Globally, TB notification rates for prisoners are 11–81 times higher than those for local general populations (*2*). An estimated 10.4 million persons are held in penal institutions throughout the world, and each year the number of persons passing through prison gates could be 4–6 times higher because of high turnover of inmates (*3*). TB in prisons might spread to the civilian population through staff, visitors, and released prisoners because of inadequate treatment for TB and thus could affect TB control in the general population (*4*,*5*).

Author affiliations: Tianjin Center for Tuberculosis Control, Tianjin, China (G. Zhang, Y. Zhang, D. Zhong, S. Meng, W. Wei, Z. Zhang, X. Wang); Tianjin Centers for Disease Control and Prevention, Tianjin (L. An); Tianjin Third Central Hospital, Tianjin (Y. Fu)

DOI: https://doi.org/10.3201/eid2603.190891

China has the second highest burden of TB in the world (0.9 million incident TB cases during 2018) (*1*). There were ≈1.7 million prisoners in China during 2016 (*3*). However, similar to the situation in other countries, TB control in prisons remained largely neglected (*6*,*7*).

Tianjin, located in northern China, has ≈16 million permanent residents and is one of the pioneering regions for TB control in China. This city had systematically implemented active TB case-finding and directly observed treatment using short-course chemotherapy in all prisons according to the guidelines (*8*,*9*).

However, despite major achievements, TB incidence among prisoners is still much higher than in the general population in Tianjin (*10*). It is essential to conduct interventions to identify latent TB infection (LTBI) through screening and prophylaxis in prisons (*11*). To achieve this goal, we conducted a study to evaluate the prevalence of and risk factors for LTBI by using an interferon-γ release assay (IGRA) in 8 prisons in Tianjin, China.

Methods

We conducted a baseline cross-sectional study in Tianjin during 2016, followed by providing prophylaxis to prisoners with LTBI and consecutive surveillance of TB incidence. We determined the necessary sample size as ≥880 persons by using Epi Info (https://www.cdc.gov/epiinfo) to satisfy a cross-sectional design for estimation of LTBI (≥480 persons) and a community randomized control trial design (≥880 persons). The 8 prisons contained 14,401 prisoners (≥18 years of age) and were composed of separate wards, each containing ≈200 persons.

Sampling was performed by using a 2-stage process and ward clustering; persons in selected wards participated in a screening procedure for the study.

In the first stage of sampling, 5 prisons incarcerating 9,037 men were randomly selected in stratifications representing different levels of reported pulmonary TB incidence in the past 5 years (median 892.7 cases/100,000 persons). In the second stage of sampling, with the proviso that sample size be allocated equally among 5 prisons, 1–3 wards from 1 prison and 8 wards incarcerating persons without HIV infection were randomly selected. Screening for HIV/AIDS routinely occurred at the beginning of imprisonment for each person; HIV-positive prisoners were incarcerated in separate wards and excluded from this study.

We interviewed all participants to obtain a history of TB and treatment. We performed a chest radiograph for all participants at the beginning of the study, and further tested persons with abnormal clinical manifestation by using bacteriological tests according to WHO guidelines (*12*). The inclusion criterion was persons in selected wards with >2 years remaining in their prison terms, which enabled follow-up of pulmonary TB incidence. Exclusion criteria were HIV infection, medical history of TB (either pulmonary or extrapulmonary), anti-TB treatment for >1 month previously or currently, and refusal to participate. A total of 172–224 eligible participants from each prison (959 persons from 5 prisons) were included in the study (Figure).

We collected demographic information by using a questionnaire under the supervision of prison guards. This information included age, ethnicity, residence, employment before imprisonment, height, weight, contact history of TB, concurrent conditions other than TB (e.g., chronic diseases, such as diabetes, silicosis, hypertension, kidney disease), history of previous incarceration, and initiation of the current prison term. We calculated body mass index (BMI) as weight in kilograms divided by the square of height in meters (*13*). Physicians checked for *Mycobacterium bovis* BCG vaccine scars at the time of blood sampling. LTBI was determined by using a seropositive result in an IGRA by using the QuantiFERON-TB Gold Kit (QIAGEN, https://www.qiagen.com).

We collected questionnaires and blood samples after written consent was obtained from the participants; we then deidentified the information. Participants who were seropositive were able to receive free preventive therapy (rifampin and isoniazid) after medical evaluation once they provided consent (*11*). The study protocol was reviewed and approved by the Ethical Committee of Tianjin Centers for Disease Control and Prevention.

We compared frequencies of characteristics of participants between seropositive and seronegative persons by using conventional 2-way contingency tables and the χ^2 test to evaluate statistical significance. We calculated odds ratios (ORs) and 95% CIs for LTBI seropositivity. We used multivariate logistic regression to analyze factors associated with seropositivity and for calculation of adjusted ORs (aORs) and 95% CIs. We performed all statistical analyses by using SAS version 9.3 (SAS Institute Inc., http://support.sas.com).

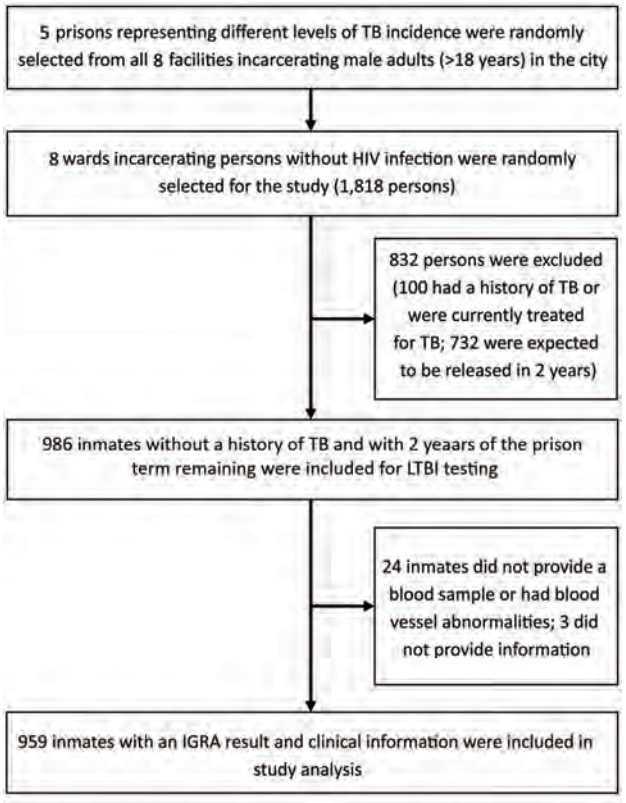

Figure. Recruitment of participants in study of high prevalence of and risk factors for latent tuberculosis among prisoners, Tianjin, China. IGRA, interferon-γ release assay; LTBI, latent tuberculosis infection; TB, tuberculosis.

Results

Study Participants

All 959 participants were men (median age 35 years, age range 19–66 years). A total of 95.2% (913/959) (age range 29–43 years) were ethnic Han, and the remaining 4.8% (46/959) were from minority populations. A total of 46.8% (449/959) had a middle school education (9-year compulsory education practiced nationwide since 1986), 33.5% (321/959) had an education less than middle school, 13.8% (312/959) had a high school education (12 years), and 5.9% (57/959) had a college education or higher. A total of 45.2% (433/595) were local registered residents, and 54.8%

Table 1. IGRA results for prisoners with specific TB incidences in prisons, Tianjin, China*

Prison no.	TB incidence†	No. (%) seropositive	No. (%) seronegative	Total	p value
1	1,945.2	106 (60.9)	68 (39.1)	174	<0.01
2	649.9	72 (41.9)	100 (58.1)	172	NA
3	892.7	91 (47.2)	102 (52.8)	193	NA
4	944.6	129 (57.6)	95 (42.4)	224	NA
5	603.0	101 (51.5)	95 (48.5)	196	NA
Overall	1,028.9	499 (52.0)	460 (48.0)	959	NA

*IGRA, interferon-γ release assay; NA, not applicable; TB, tuberculosis.
†Reported pulmonary TB incidence (cases/100,000 persons) in the past 5 years was based on annual TB screening and case finding through daily healthcare seeking.

(526/959) were migrants. BMI ranged from 14.9 to 33 (median 23.2, interquartile range 21.5–25.2).

A total of 14.1% (135/959) participants reported employment before current imprisonment, and the remaining 85.9% (824/959) were unemployed. A total of 16.3% (156/959) reported a contact history with TB patients and 16.8% (161/959) reported current conditions other than TB. A total of 28.8% (276/959) had a history of imprisonment before the current term, and the other 71.2% (683/959) were incarcerated for the first time. The current prison term ranged from 0.4 to 21.0 years (median term 3.9 years, interquartile range 2.6–5.4 years). A total of 59.5% (571/959) participants had ≥1 BCG vaccine scar.

Comparison of Characteristics between Seropositive and Seronegative Participants

The rate of TB seropositivity was 52.0% (499/959; range 41.9%–60.9%) for all study participants for the 5 prisons with specific TB incidences (Table 1); the difference between seropositive and seronegative participants was significant (p<0.05). We compared frequencies of characteristics between seropositive and seronegative participants (Table 2). More LTBI-positive participants were ≥35 years of age; the difference between the 2 groups was significant (p<0.01). Positivity rates increased with age: <25 years, 18.9%; 25–34 years, 46.6%; 35–44 years, 58.5%; and >45 years, 68.6%. This increasing trend was significant (p<0.01).

The presence of factors other than TB, BCG scar, and history of previous incarceration was significantly higher for seropositive participants (p<0.05). As the level of TB incidence in the past 5 years for each prison increased, the rates of positivity also increased significantly (p<0.01): 47.0% positivity rate for the 2 prisons with low background incidence (603.0 and 649.9 cases/100,000 persons), 52.8% for the 2 prisons with medium background incidence (892.7 and 944.6 cases/100,000 persons), and 61.9% for the prison with high background incidence (1,945.2 cases/100,000 persons).

Longer duration (≥3.9 years) in the current prison term was observed more often among positive participants than among negative participants; however, this difference was not significant (p = 0.07). Differences in ethnicity, education, residency, employment, BMI, and contact history were also not significant between the 2 groups (p>0.05).

Factors Associated with LTBI

We identified several characteristics as factors associated with LTBI among prisoners (Table 3). The risk for LTBI increased with age, and from age <25 years to ≥45 years (aOR 1.7, 95% CI 1.4–2.0/10 years). A longer prison term led to a higher risk for LTBI (aOR 1.2, 95% CI 1.1–1.2 per year). A history of previous incarceration nearly doubled the risk for LTBI among prisoners. The risk for LTBI showed a major increase for prisons that had a higher incidence of TB in the past 5 years. Prisoners in prisons that had an annual TB incidence >1,900 cases/100,000 persons had a 1.9 times higher risk for TB than prisoners from 2 prisons who had an annual TB incidence of 600–650 cases/100,000 persons. Multivariate analysis showed a relationship between BCG scar and positive test results (aOR 1.3, 95% CI 1.0–1.8).

Discussion

Implementation of active case-finding and directly observed treatment using short-course chemotherapy in the prison system in Tianjin, China, led to a major decrease in pulmonary TB incidence, from 2,801.9 cases/100,000 persons (≈80 times the level in the general population) in 2000 to 735.1 cases/100,000 persons (≈30 times the level in the general population) in 2010 (*10*). This decrease confirmed the highly efficient strategy aimed at patients with active TB in crowded environments, which had a high incidence of TB. However, after this striking decrease, the level of TB incidence reached a plateau, still much higher in prisons than in the general population. Thus, prisons remain major TB reservoirs, indicating the limitation of strategies that focus merely on patients who have active TB. Early interventions before TB onset are required to achieve a further decrease in TB incidence in prisons, and management of LTBI in such crowded populations has been recommended by WHO (*11*).

Our study showed that the rate of LTBI among prisoners was >50%. This rate was much higher than that for the general population (13.5%–24.3%) in China, which was reported in recent studies that used IGRA (*14*–*16*). Two studies in Jiangsu Province reported IGRA positivity rates of 20.0% (1,060/5,305) and 24.3% (527/2,169) (*14*,*15*). Another study in Shenzhen reported an IGRA positivity rate of 17.9% (790/4,422) among rural migrant workers (*16*). A more representative multicenter study involving >20,000 participants in China reported an overall IGRA positivity rate of 18.8% (3,955/21,022) among all participants; the adjusted rates of LTBI by age and sex ranged from 13.5% to 19.8% in the 4 study sites (*17*). The higher rate of LTBI in prisoners than in the general population can be an attribution, as well as a consequence, of higher incidence of TB in prisons, which confirms the necessity of interventions for LTBI that target prisoners.

The rates of LTBI reported among prisoners varied in different studies, ranging from 11.7% to 92.5%, and were based mostly on results of the tuberculin skin test (TST). In Brazil, a study reported a TST positivity rate of 22.5% (620/2,752) for male prisoners and 11.7% (60/511) for female prisoners (*18*); these rates were lower than that for an earlier survey in a prison in the same country (49.3% [106/215]) (*19*). In other studies, rates of TST positivity were 17.9% (80/448) in Italy, 48% (204/425) in Pakistan, and 77.6% (643/829) in Colombia (*20*–*22*). In Malaysia, TST positivity rates were 84.7% (117/138) for HIV-infected and 92.5% (137/148) for HIV-uninfected prisoners in 1 prison; the overall positivity rate was 88.8% (254/286) (*23*). A

Table 2. Comparison of characteristics between IGRA-seropositive and IGRA-seronegative prisoners, Tianjin, China*

Characteristic	No. (%) seropositive	No. (%) seronegative	Total	p value by χ^2 test
Age, y				
<25	14 (2.8)	60 (13.0)	74	<0.01
25–34	197 (39.5)	226 (49.1)	423	
35–44	168 (33.7)	119 (25.9)	287	
≥45	120 (24.0)	55 (12.0)	175	
Ethnicity				
Han	470 (94.2)	443 (96.3)	913	0.13
Other	29 (5.8)	17 (3.7)	46	
Education level				
Primary school	172 (34.5)	149 (32.4)	321	0.70
Middle school	233 (46.7)	216 (47)	449	
High school	94 (18.8)	95 (20.7)	189	
Residence				
Local	220 (44.1)	213 (46.3)	433	0.49
Migrant	279 (55.9)	247 (53.7)	526	
Employment				
No	425 (85.2)	399 (86.7)	824	0.49
Yes	74 (14.8)	61 (13.3)	135	
BMI†				
Abnormal: ≥25–<18.5	147 (29.5)	137 (29.8)	284	0.91
Normal: 18.5–25.0	352 (70.5)	323 (70.2)	675	
Contact history				
No	415 (83.2)	388 (84.3)	803	0.62
Yes	84 (16.8)	72 (15.7)	156	
Concurrent condition‡				
No	403 (80.8)	395 (85.9)	798	0.03
Yes	96 (19.2)	65 (14.1)	161	
Mycobacterium bovis BCG scar				
No	180 (36.1)	206 (44.8)	385	<0.01
Yes	319 (63.9)	254 (55.2)	573	
History of incarceration				
No	315 (63.1)	368 (80.0)	683	<0.01
Yes	184 (36.9)	92 (20.0)	276	
Current duration of incarceration, y				
<3.9	227 (45.5)	236 (51.3)	463	0.07
≥3.9	272 (54.5)	224 (48.7)	496	
Facility-specific TB incidence, cases/100,000 persons§				
Low	173 (34.7)	195 (42.4)	368	0.01
Medium	220 (44.1)	197 (42.8)	417	
High	106 (21.2)	68 (14.8)	174	

*BMI, body mass index; TB, tuberculosis.
†By World Health Organization standard (*13*).
‡Chronic diseases, including diabetes, silicosis, hypertension, kidney disease.
§The 2 low-incidence prisons reported 603.0 and 649.9 TB cases/100,000 persons, the 2 medium-incidence prisons 892.7 and 944.6 cases/100,000 persons, and the high-background prison 1,945.2 cases/100,000 persons.

Table 3. Factors associated with LTBI seropositivity among prisoners, Tianjin, China*

Factor	OR (95% CI)	aOR (96% CI)	p value by type 3 test
All age groups	1.79 (1.53–20.9)	1.67 (1.42–1.96)	<0.01
Ethnicity			
Han	Referent	Referent	0.06
Other	1.61 (0.87–2.97)	1.90 (0.98–3.68)	
Education			
Primary school	Referent	Referent	0.76
Middle school	0.94 (0.7–1.25)	1.08 (0.79–1.48)	
High school	0.86 (0.6–1.23)	0.95 (0.63–1.44)	
Residency			
Local	Referent	Referent	0.15
Migrant	1.09 (0.85–1.41)	1.22 (0.93–1.62)	
Employment			
No	Referent	Referent	0.94
Yes	1.14 (0.79–1.64)	0.98 (0.65–1.49)	
BMI			
Normal: 18.5–25.0	Referent	Referent	0.52
Abnormal: >25–<18.5	0.98 (0.74–1.29)	0.91 (0.67–1.22)	
Contact history			
No	Referent	Referent	0.97
Yes	1.09 (0.77–1.54)	1.01 (0.70–1.46)	
Concurrent condition			
No	Referent	Referent	0.49
Yes	1.45 (1.03–2.04)	1.14 (0.78–1.67)	
Mycobacterium bovis BCG scar			
No	Referent	Referent	0.04
Yes	1.44 (1.11–1.86)	1.33 (1.01–1.75)	
History of incarceration			
No	Referent	Referent	<0.01
Yes	2.34 (1.75–3.13)	2.01 (1.48–2.74)	
Current duration of incarceration	1.11 (1.04–1.18)	1.15 (1.07–1.23)	<0.01
Facility-specific TB incidence, cases/100,000 population†			
Low	Referent	Referent	<0.01
Median	1.26 (0.95–1.67)	1.13 (0.83–1.53)	
High	1.76 (1.22–2.54)	1.87 (1.25–2.79)	

*BMI, body mass index; LTBI, latent tuberculosis infection; TB, tuberculosis.
†The 2 low-incidence prisons reported 603.0 and 649.9 TB cases/100,000 persons, the 2 medium-incidence prisons 892.7 and 944.6 cases/100,000 persons, and the high-background prison 1,945.2 cases/100,000 persons.

study that used TST and IGRA in Taiwan reported a positivity rate of 24.6% (594/2416) for IGRA but >82% for TST among the same study participants (*24*).

Discrepancies reported for LTBI incidence in different studies might be related not only to testing methods, but also to the background of TB incidence and BCG vaccination among the general population. Although the rate of LTBI in our study was not directly comparable to those of most other surveys because of different testing methods used, this rate might have been higher if we had used TST instead of IGRA, which might have produced a rate similar to those reported in some other studies.

The risk for LTBI increases with age, regardless of whether TST or IGRA was used, among prisoners and in the general population. In the general population of China, the rate of LTBI detected by IGRA increased from 2.9% (43/1,459) for children 5–9 years of age to 32.4% (590/1,822) for persons ≥70 years of age (*17*). In 2 studies in China, the aOR of age to IGRA positivity was 1.1 (95% CI 1.1–1.1) per 10 years for migrant workers and 1.0 (95% CI 1.0–1.0) per 10 years for village populations (*14*,*16*). In our study, the aOR of age to LTBI was 1.7 (95% CI 1.4–2.0) per 10 years for prisoners, which demonstrated that the cumulative effect of age was even more pronounced for prisoners than for the general population.

The effect of age on TST positivity was also seen in prisons in other studies. In Italy, compared with persons ≤30 years of age, the aOR of age to TST positivity was 4.1 (95% CI 1.5–11.1) for persons 31–40 years of age and 3.8 (95% CI 1.4–10.6) for persons >40 years of age in prisons (*20*). In Barcelona, Spain, the aOR of age to TST positivity among immigrants entering prisons was 2.3 (95% CI 1.4–3.9) for prisoners ≥40 years of age compared with prisoners <40 years of age (*25*). In Pakistan, the aOR was 3.5 (95% CI 1.9–6.7) for prisoners >42 years of age compared with prisoners 18–26 years of age (*21*). The cumulative effect of age to LTBI suggests that being older can be a priority for implementing specific interventions against LTBI in prisons.

History of previous incarceration or duration of current incarceration was found to be a risk factor

for LTBI in previous studies (*18*,*20*–*23*). In a prison in Malaysia, previous frequent incarceration was a risk factor for LTBI (aOR 1.2, 95% CI 1.0–1.4 for every previous incarceration) (*23*). In Italy, although previous imprisonment was not associated with TST positivity, current detention was an independent risk factor (aOR 1.1, 95% CI 1.0–1.2) (*20*). Previous incarceration or duration of current incarceration was also confirmed in studies in Pakistan, Colombia, Brazil, and Chile (*18*,*21*,*22*,*26*). Similar to previous studies, in our study, the history of incarceration and current duration in prison increased the risk for LTBI, which reflected cumulative TB transmission among prisoners. Therefore, LTBI screening and intervention should be prioritized in persons who had previous incarceration.

In this study, although the history of TB contact was not associated with LTBI, prisoners from the facility with the highest incidence of TB in the past 5 years had 1.9 (95% CI 1.3–2.8) times higher risk for LTBI. Similar findings were reported in a study from Colombia, in which contact history was not related to TST positivity (*22*). However, in that study, annual risk for LTBI varied between prison blocks with high and low incidences of TB; infection rates were 5.1% per year for blocks with a high incidence of TB and 2.7% for blocks with a low incidence of TB. Self-reporting of a contact history might be unreliable because of recall bias and variable personal understanding of TB. However, in the congested environment, prisoners could get LTBI without realizing it, and prisons with higher incidences of TB pose a greater threat of TB transmission. This finding suggests that early case finding and timely isolation of contagious TB patients should be intensified to reduce the risk for LTBI.

In this study, the prison with the highest incidence of TB once served as a quarantine facility in the city for contagious TB patients (sputum smear positive) found at entry screening (*10*). This facility also kept healthy inmates in separate wards, which might be the cause of the high incidences of TB and LTBI. After our survey, this situation was changed, and this prison now serves only as a quarantine facility and no longer receives healthy new inmates. This change was a positive step based partly on our TB surveillance and the LTBI survey.

Some studies have reported that LTBI was associated with being foreign-born (OR 4.9) and having a lower level of education (<5 years) (OR 1.90) (*20*,*21*). However, in our study, ethnicity, education, residency, employment before imprisonment, and BMI status were not associated with LTBI. Some studies that used IGRA reported a negative relationship between history of BCG vaccination and positive test results for TB, which was in contrast to results of studies that used TST (*19*,*24*,*27*). Two studies that used IGRA among general populations in China reported that a history of BCG vaccination was a protective factor against LTBI (aOR 0.8 [95% CI 0.7–1.0 in Jiangsu and 0.8 [95% CI 0.7–1.0 in Shenzhen) (*14*,*16*). However, 2 studies that used IGRA in a general population did not report an association between BCG scar and LTBI (*15*,*17*). In our study, BCG scar being a predictive factor of LTBI might be attributed to the age of the prisoners being older than the BCG protection period (75% of the prisoners were >29 years of age); alternatively, prisoners with a BCG scar might induce a better immune reaction in an IGRA, indicating a true TB infection. However, the effect of the aOR was marginal in this study, and the effect of BCG on LTBI among adults still requires stronger evidence.

Although prisons are recognized as major reservoirs of TB, control programs for TB in prison systems are facing several challenges (*7*). Our study was limited by safety concerns for prison administration. Thus, prisoners who committed severely violent crimes were not included in the study, and questions involving privacy and sensitive information, such as drug abuse, were not included in the questionnaire. In such situations, investigators had few opportunities to talk with study participants; instead, prison officers were in charge of quality control interpretation of information. Despite these limitations, the findings in this study provide useful information for control of TB in prisons in Tianjin and can be applied to other prisons.

In conclusion, LTBI prevalence is high in prisons in Tianjin, China. Previous incarceration and high facility-specific TB incidence are risk factors for LTBI. Age and duration of incarceration have cumulative effects on LTBI in prisons. High prevalence of LTBI increases the risk for TB incidence. Also, the high incidence of TB leads to high rates of LTBI. These findings suggest that preventive interventions to reduce LTBI before the onset of active TB among prisoners and to increase early detection of TB and timely quarantine of infectious case-patients will reduce transmission caused by overcrowding and poor ventilation.

Acknowledgments

We thank all prison staff for providing contributions to the field work and Masae Kawamura, Romy Ho, Gang Hu, and Ru Gao for proofreading the manuscript.

The study was supported by the Tianjin Health Area Key Reach Project (grant no. 16KG171).

About the Author

Dr. Guoqin Zhang is an epidemiologist and doctoral candidate at the Tianjin Center for Tuberculosis Control, Tianjin, China. His primary research interest is control of *M. tuberculosis* TB among vulnerable populations.

References

1. World Health Organization. Global tuberculosis report. Geneva: The Organization; 2019.
2. Modvig J. Violence, sexual abuse and torture in prisons. In: Enggist S, Møller L, Galea G, Udesen C, editors. Prisons and health. Copenhagen: World Health Organization Regional Office for Europe; 2014. p. 19–26.
3. Walmsley R. World prison population list, 11 ed. London: Institute for Criminal Policy Research; 2015 [cited 2019 Dec 23]. https://www.prisonstudies.org/sites/default/files/resources/downloads/world_prison_population_list_11th_edition_0.pdf
4. Stuckler D, Basu S, McKee M, King L. Mass incarceration can explain population increases in TB and multidrug-resistant TB in European and central Asian countries. Proc Natl Acad Sci U S A. 2008;105:13280–5. https://doi.org/10.1073/pnas.0801200105
5. Barbour V, Clark J, Jones S, Veitch E; PLoS Medicine Editors. The health crisis of tuberculosis in prisons extends beyond the prison walls. PLoS Med. 2010;7:e1000383. https://doi.org/10.1371/journal.pmed.1000383
6. O'Grady J, Maeurer M, Atun R, Abubakar I, Mwaba P, Bates M, et al. Tuberculosis in prisons: anatomy of global neglect. Eur Respir J. 2011;38:752–4. https://doi.org/10.1183/09031936.00041211
7. Dara M, Acosta CD, Melchers NVSV, Al-Darraji HAA, Chorgoliani D, Reyes H, et al. Tuberculosis control in prisons: current situation and research gaps. Int J Infect Dis. 2015;32:111–7. https://doi.org/10.1016/j.ijid.2014.12.029
8. Maher D, Grzemska M, Coninx Hernan Reyes R, Demeulenaere T, Harries A, Fernandez de la Hoz K, et al. Guidelines for the control of tuberculosis in prisons. Geneva: World Health Organization; 1998.
9. Dara M, Grzemska M, Kimerling ME, Reyes H, Zagorskiy A. Guidelines for control of tuberculosis in prisons. Geneva: Tuberculosis Coalition for Technical Assistance, International Committee of the Red Cross; 2009.
10. Yanyon F, Guoqin Z, Xiexiu W, Wenliang W, Shanglun L, Zhenhua Y, et al. Effect of tuberculosis control among prisoners in Tianjin, 2000–2010 [in Chinese]. Chinese Journal of Public Health. 2015;31:669–72.
11. World Health Organization. Latent tuberculosis infection: updated and consolidated guidelines for programmatic management. Geneva: The Organization; 2018.
12. World Health Organization. Chest radiography in tuberculosis detection: summary of current WHO recommendations and guidance on programmatic approaches. Geneva: The Organization; 2016.
13. World Health Organization. Body mass index—BMI [cited 2019 Nov 30]. http://www.euro.who.int/en/health-topics/disease-prevention/nutrition/a-healthy-lifestyle/body-mass-index-bmi
14. Chen C, Zhu T, Wang Z, Peng H, Kong W, Zhou Y, et al. High latent TB infection rate and associated risk factors in the eastern China of low TB incidence. PLoS One. 2015;10:e0141511. https://doi.org/10.1371/journal.pone.0141511
15. Liu Y, Huang S, Jiang H, Xiong J, Wang Y, Ou M, et al. The prevalence of latent tuberculosis infection in rural Jiangsu, China. Public Health. 2017;146:39–45. https://doi.org/10.1016/j.puhe.2017.01.008
16. Li X, Yang Q, Feng B, Xin H, Zhang M, Deng Q, et al. Tuberculosis infection in rural labor migrants in Shenzhen, China: emerging challenge to tuberculosis control during urbanization. Sci Rep. 2017;7:4457. https://doi.org/10.1038/s41598-017-04788-1
17. Gao L, Lu W, Bai L, Wang X, Xu J, Catanzaro A, et al.; LATENTTB-NSTM study team. Latent tuberculosis infection in rural China: baseline results of a population-based, multicentre, prospective cohort study. Lancet Infect Dis. 2015;15:310–9. https://doi.org/10.1016/S1473-3099(14)71085-0
18. Carbone AS, Paião DS, Sgarbi RV, Lemos EF, Cazanti RF, Ota MM, et al. Active and latent tuberculosis in Brazilian correctional facilities: a cross-sectional study. BMC Infect Dis. 2015;15:24. https://doi.org/10.1186/s12879-015-0764-8
19. Estevan AO, Oliveira SM, Croda J. Active and latent tuberculosis in prisoners in the central-west region of Brazil. Rev Soc Bras Med Trop. 2013;46:515–8. https://doi.org/10.1590/0037-8682-1441-2013
20. Carbonara S, Babudieri S, Longo B, Starnini G, Monarca R, Brunetti B, et al.; GLIP (Gruppo di Lavoro Infettivologi Penitenziari). Correlates of *Mycobacterium tuberculosis* infection in a prison population. Eur Respir J. 2005;25:1070–6. https://doi.org/10.1183/09031936.05.00098104
21. Hussain H, Akhtar S, Nanan D. Prevalence of and risk factors associated with *Mycobacterium tuberculosis* infection in prisoners, North West Frontier Province, Pakistan. Int J Epidemiol. 2003;32:794–9. https://doi.org/10.1093/ije/dyg247
22. Rueda ZV, Arroyave L, Marin D, López L, Keynan Y, Giraldo MR, et al. High prevalence and risk factors associated with latent tuberculous infection in two Colombian prisons. Int J Tuberc Lung Dis. 2014;18:1166–71. https://doi.org/ 10.5588/ijtld.14.0179
23. Al-Darraji HA, Kamarulzaman A, Altice FL. Latent tuberculosis infection in a Malaysian prison: implications for a comprehensive integrated control program in prisons. BMC Public Health. 2014;14:22. https://doi.org/10.1186/1471-2458-14-22
24. Chan P-C, Yang C-H, Chang L-Y, Wang K-F, Kuo Y-C, Lin C-J, et al. Lower prevalence of tuberculosis infection in BCG vaccinees: a cross-sectional study in adult prison inmates. Thorax. 2013;68:263–8. https://doi.org/10.1136/thoraxjnl-2012-202208
25. Solé N, Marco A, Escribano M, Orcau A, Quintero S, Del Baño L, et al. Prevalence of latent tuberculosis infection amongst immigrants entering prison [in Spanish]. Rev Esp Sanid Penit. 2012;14:12–8.
26. Aguilera XP, González C, Nájera-De Ferrari M, Hirmas M, Delgado I, Olea A, et al. Tuberculosis in prisoners and their contacts in Chile: estimating incidence and latent infection. Int J Tuberc Lung Dis. 2016;20:63–70. https://doi.org/10.5588/ijtld.15.0056
27. Schwartz IS, Bach PJ, Roscoe B, Majury A, Hopman WM, Ellis E, et al. Interferon-gamma release assays piloted as a latent tuberculous infection screening tool in Canadian federal inmates. Int J Tuberc Lung Dis. 2014;18:787–92. https://doi.org/10.5588/ijtld.13.0816

Address for correspondence: Xiexiu Wang, General Office, Tianjin Center for Tuberculosis Control, No. 124 Chifeng Rd, Heping District, Tianjin 300041, China; email: wjsttigo@126.com

Whole-Genome Sequencing to Detect Numerous *Campylobacter jejuni* Outbreaks and Match Patient Isolates to Sources, Denmark, 2015–2017

Katrine G. Joensen, Kristoffer Kiil, Mette R. Gantzhorn, Birgitte Nauerby, Jørgen Engberg, Hanne M. Holt, Hans L. Nielsen, Andreas M. Petersen, Katrin G. Kuhn, Gudrun Sandø, Steen Ethelberg, Eva M. Nielsen

In industrialized countries, the leading cause of bacterial gastroenteritis is *Campylobacter jejuni*. However, outbreaks are rarely reported, which may reflect limitations of surveillance, for which molecular typing is not routinely performed. To determine the frequency of genetic clusters among patients and to find links to concurrent isolates from poultry meat, broiler chickens, cattle, pigs, and dogs, we performed whole-genome sequencing on 1,509 *C. jejuni* isolates from 774 patients and 735 food or animal sources in Denmark during 2015–2017. We found numerous clusters; 366/774 (47.3%) clinical isolates formed 104 clusters of ≥2 isolates. A total of 41 patient clusters representing 199/366 (54%) patients matched a potential source, primarily domestic chickens/broilers. This study revealed serial outbreaks and numerous matches to concurrent food and animal isolates and highlighted the potential of whole-genome sequencing for improving routine surveillance of *C. jejuni* by enhancing outbreak detection, source tracing, and potentially prevention of human infections.

Campylobacter jejuni is the most frequent cause of bacterial gastroenteritis in industrialized countries worldwide (*1*,*2*), including in Denmark, where ≈4,000 *Campylobacter* infections are reported annually (*3*). Despite the high notification rates, *Campylobacter* infections are believed to be highly underdiagnosed (*4*,*5*). Denmark's national surveillance system for *Campylobacter* is based on observation of the number of notified human cases (*3*); a substantial number of *Campylobacter* outbreaks may be overlooked because of a lack of routine microbiological typing of isolates. This hypothesis is supported by evidence from a recent study, in which whole-genome sequencing (WGS)–based typing of selected clinical *Campylobacter* isolates from patients in Denmark identified numerous small outbreak-like clusters (*6*). This finding suggests that more outbreaks occur in Denmark than the few typically large outbreaks associated with a single event that are detected by the current surveillance system (*7*–*10*). To achieve a national surveillance system that will detect ongoing *Campylobacter* outbreaks in real time, highly discriminatory subtyping of isolates is needed. Thus, we more comprehensively evaluated the frequency of *Campylobacter* outbreaks among humans in Denmark by using WGS-based typing. To match the clinical isolates with their sources, we compared them with isolates from food and animals, covering the main putative sources of human *Campylobacter* infections (i.e., contact with or consumption of animals or animal products, primarily contaminated poultry meat). Although *Campylobacter* infections are primarily foodborne, a recent case–control study in Denmark found that contact with animals and the environment might account for a substantial proportion of domestic infections (*11*). Several other reported sources of infection include unpasteurized milk, drinking water, bathing water, vegetables, and fruits (*1*,*12*–*14*).

WGS offers high-resolution discriminatory subtyping and has been successfully implemented for

Author affiliations: Statens Serum Institut, Copenhagen, Denmark (K.G. Joensen, K. Kiil, K.G. Kuhn, S. Ethelberg, E.M. Nielsen); Danish Veterinary and Food Administration, Copenhagen (M.R. Gantzhorn, B. Nauerby, G. Sandø); Slagelse Hospital, Slagelse, Denmark (J. Engberg); Odense University Hospital, Odense, Denmark (H.M. Holt); Aalborg University Hospital, Aalborg, Denmark (H.L. Nielsen); Aalborg University, Aalborg (H.L. Nielsen); Hvidovre University Hospital, Hvidovre, Denmark (A.M. Petersen)

DOI: https://doi.org/10.3201/eid2603.190947

public health surveillance of several foodborne pathogens (e.g., *Salmonella*, *Listeria,* and Shiga toxin–producing *Escherichia coli*) in Denmark and abroad (*3*,*15*,*16*). Recent studies have proven WGS to be applicable for *Campylobacter* outbreak investigations (*17*–*22*), and it has recently been shown that WGS could trace back clinical infections directly to chicken slaughter batches (*23*).

For this study, we performed WGS on a large cohort of 1,509 *C. jejuni* isolates collected from patients and food/animal samples in Denmark over 2 years. We clustered the isolates by using core-genome multilocus sequence typing (cgMLST) to determine the frequency of genetic clusters among clinical isolates (i.e., possible outbreaks) and how they matched concurrent isolates from potential sources. We detected numerous clusters among the patients and a large number of matches between clinical isolates and potential food/animal sources.

Materials and Methods

Isolate Collection

During 2015–2017, we collected *Campylobacter* isolates representing human infections and food/animal sources. The collection period for isolates from humans (clinical isolates) and from food/animals overlapped by 18 months (October 2015–March 2017). We present WGS data for 1,509 *C. jejuni* isolates: 774 clinical and 735 food/animal.

The clinical isolates were supplied by 4 clinical microbiological laboratories (Aalborg University Hospital, Slagelse Hospital, Hvidovre University Hospital, and Odense University Hospital), which were performing clinical microbiological services for the regional hospitals and practitioners in 4 of the 5 geographic regions in Denmark. These 4 laboratories diagnosed ≈60% of the *Campylobacter* cases in Denmark. Collection of 904 isolates was timed to best capture seasonal variation. On the basis of data from previous years, each laboratory was to supply the number of isolates that could be expected to constitute a constant fraction of their positive samples per calendar month.

We performed WGS on all collected isolates. After removing 130 sequences because of poor sequence quality, we included in our analysis 774 *C. jejuni* isolates (representing 772 patients), representing ≈10% of the *Campylobacter* cases during the period.

Clinical isolates were collected during September 2015–April 2017 and represented 673 domestically acquired infections, 60 travel-associated infections, and 41 infections in persons of unknown travel status. We also included 14 isolates obtained from a fifth region (Aarhus University Hospital) during an outbreak investigation in June 2017. Of the domestically acquired isolates, 192 had been previously analyzed as part of another study to detect clusters among *Campylobacter* isolates in Denmark (October 2015–June 2016) (*6*).

The *C. jejuni* isolates from food/animals were collected during May 2015–March 2017 by the Danish Veterinary and Food Administration, where a total of 798 food/animal isolates were subjected to WGS. A total of 63 isolates were removed from the study because of poor sequence quality. The remaining 735 isolates represented animals from Denmark, hereafter referred to as domestic (27 pigs, 214 cattle, and 150 broilers [collected as cecal samples at slaughter]) or retail meat (172 domestic chicken, 111 imported chicken, 9 imported turkey, 4 domestic duck, and 22 imported duck). A limited number of isolates were available from 3 domestic retail vegetables, 2 seawater samples, and 21 pet dogs. The food/animal samples were primarily collected as part of official surveillance programs. Some animals, as well as turkey meat and duck meat, were collected specifically for the source attribution study (*24*). Isolates from pet dogs were obtained from healthy dogs and dogs that had diarrhea before sampling.

WGS

Genomic DNA (gDNA) from clinical isolates was purified by using a QIAGEN DNeasy Blood and Tissue kit (https://www.qiagen.com), and gDNA from food/animal isolates was purified by using the Invitrogen Easy-DNA gDNA purification kit (https://www.thermofisher.com). Sequencing was conducted by using Illumina technology (https://www.illumina.com) on either MiSeq or NextSeq sequencing machines and using the Nextera XT Library preparation protocol for paired-end reads of 150 bp or 250 bp. Raw data were deposited in the European Nucleotide Archive (accession no. PRJEB31119).

We processed WGS data by using a QC-pipeline (https://github.com/ssi-dk/SerumQC), in which isolate sequences were removed in case of contamination with >5% of another genus, as well as sequences representing *C. jejuni* isolates with genome sizes outside the range of 1.6–1.9 Mbp. We conducted further analyses by using BioNumerics 7.6 (Applied Maths, https://www.applied-maths.com), in which cgMLST assignment was based on the 1,343-loci cgMLST scheme from the *Campylobacter* Multi Locus Sequence Typing website (https://pubmlst.org/campylobacter) at the University of Oxford (*25*). We removed isolate sequences from the dataset if assemblies

comprised >500 contigs, the cgMLST core-percentage was <95%, or >40 loci were present with multiple consensus sequences. When multiple isolates were available from the same patient, we kept only unique representative sequences. Clusters, or matches, were defined by the unweighted pair group method with arithmetic mean (UPGMA) clustering with cgMLST allele differences as a distance measure and a cluster threshold of 4. This value was chosen after evaluation of the phylogeny, with clustering of potentially related isolates and separation of nonrelated isolates (Appendix, https://wwwnc.cdc.gov/EID/article/26/3/19-0947-App1.pdf). We gave each cluster a unique name in which sequence type (ST) was followed by a number (#1, #2, etc.) to separate different clusters of the same ST.

Rarefaction

We produced a rarefaction curve for the clinical isolates by using the rarefy function from the R vegan library (*26*). For each isolate, we used the specific cluster type as the input type for the rarefaction and assigned sporadic cases their own cluster type. We calculated data points for a subsample of $n_{subsample}$ = 100 to 774, with a step of 100. From a random reordering of the same samples, at the same subsample steps as above, we selected the first $n_{subsample}$ samples and counted the number of clusters of size >1 and >4.

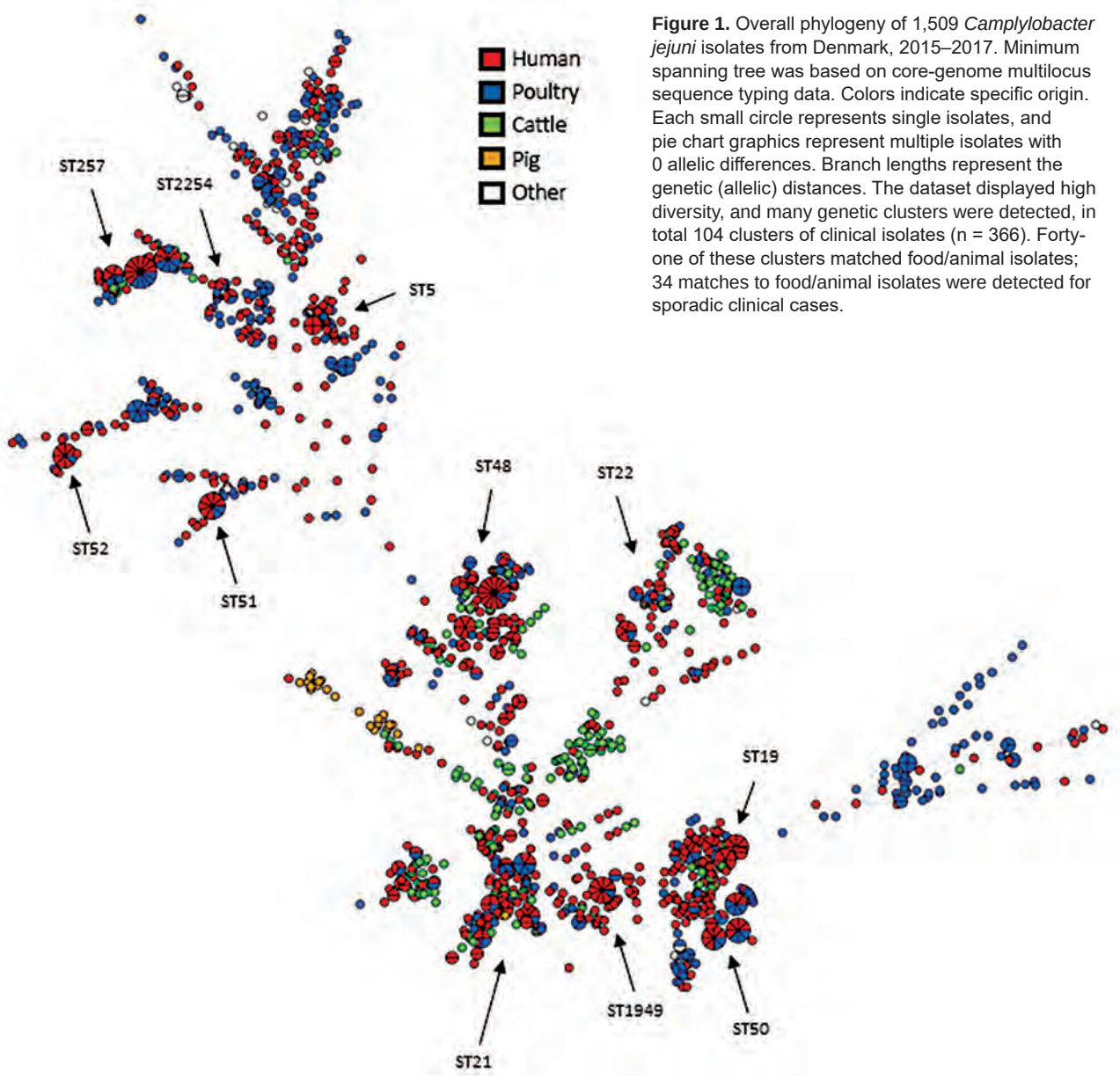

Figure 1. Overall phylogeny of 1,509 *Camplylobacter jejuni* isolates from Denmark, 2015–2017. Minimum spanning tree was based on core-genome multilocus sequence typing data. Colors indicate specific origin. Each small circle represents single isolates, and pie chart graphics represent multiple isolates with 0 allelic differences. Branch lengths represent the genetic (allelic) distances. The dataset displayed high diversity, and many genetic clusters were detected, in total 104 clusters of clinical isolates (n = 366). Forty-one of these clusters matched food/animal isolates; 34 matches to food/animal isolates were detected for sporadic clinical cases.

Cost-effectiveness Calculation

Estimates of outbreak detection frequency were calculated by using the survival function S(cluster_threshold-1) under the binomial distribution $B(N_{cases,fsampling})$. The complete code for the cost-effectiveness calculation is provided (Appendix).

Results

The 1,509 sequenced *C. jejuni* isolates showed high diversity and were distributed over 234 seven-locus multilocus sequence types (MLSTs) (Figure 1). Of the sources represented by numerous isolates, only the isolates from pigs (n = 27) were confined to a single clonal complex (CC), CC403, with the exception of 2 CC21 isolates. The clinical isolates and poultry isolates were generally distributed throughout the tree, although poultry isolates were not present in CC403. Isolates from cattle were abundant in certain clonal complexes (CC21, CC42, CC48, and CC61) and generally present in most parts of the tree. Despite the high genetic diversity of the dataset in general, we identified a large number of genetic clusters.

Genetic Clusters

Analysis of cgMLST results for all 1,509 isolates indicated that 732 of the isolates were part of 204 clusters consisting of ≥2 isolates. Of these, 63 clusters consisted exclusively of clinical isolates (n = 167), 66 consisted exclusively of food/animal isolates (n = 176), and 75 consisted of clinical (n = 233) and food/animal isolates (n = 156).

Clusters of Clinical Isolates

Separate analysis of the 774 clinical isolates showed that 366 (47.3%) formed 104 clusters consisting of ≥2 isolates. A considerably higher concentration of clusters occurred during the summer, when *Campylobacter* incidence peaks (27), whereas the number of sporadic infections was almost constant throughout the year (Figure 2).

Most (82) clusters were small clusters of 2–4 clinical isolates (total 190 isolates); 22 large clusters consisted of 5–17 clinical isolates (total 176 isolates). We detected a direct match to ≥1 isolates of food or animal origin for most (17/22; 77%) of the large patient clusters but only 24 (29%) of the 82 small patient clusters. Thus, 41/104 patient clusters could be matched to a potential source and represented 199/366 (54%) of the patients who were part of a potential outbreak.

The clinical isolates in this study represented ≈10% of the nationwide cases in the period. More extensive sampling would probably lead to detection of more clusters. Typing of all 774 clinical isolates indicated that 47% were part of the 104 identified clusters (Figure 3); had the sample size been reduced to, for example, 400 or 200 isolates, the percentage of isolates in clusters would have decreased to 39% or 25%, respectively.

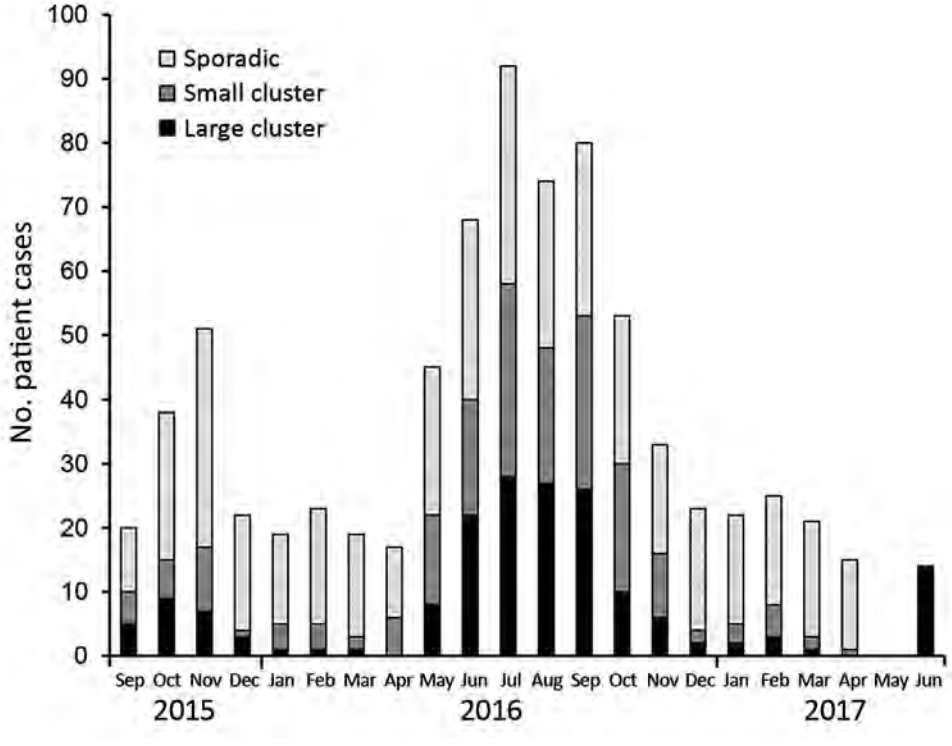

Figure 2. Distribution of clinical *Camplylobacter jejuni* isolates from Denmark over time, 2015–2017. Colors represent isolates in large (≥5 isolates, n = 176) and small (2–4 isolates, n = 190) clusters or as sporadic cases (n = 408). All 774 clinical isolates are shown according to their sample date. A higher concentration of clusters occurred during the summer, and the number of sporadic cases was relatively constant during the year.

To implement cost-effective surveillance of clusters of clinical isolates, it is essential to consistently find large clusters without investigating small insignificant clusters. With a sampling frequency of 10% and an investigation threshold of 4 clustered isolates, we expect to find 99.2% of large outbreaks (of 100 reported cases), and an investigation would be triggered within the first one third of the cases for 42% of the large outbreaks. A small outbreak of 10 reported cases would be observed only 1.3% of the time, and assuming a 1:100 ratio of large:small outbreaks, an average of 1.3 small outbreaks would be investigated per large outbreak.

Clinical Isolates Clustering with Isolates of Food/Animal Origin

A total of 75 clusters contained isolates of both clinical and food/animal origin (Table). Seventeen clusters contained ≥5 clinical isolates, but only 1 clinical isolate matched the source isolate(s) in 34 clusters.

Clinical isolates most often (192/233) matched isolates from domestic chicken meat, broilers, or both, corresponding to 25% of all clinical isolates in the study. In 10 clusters, 18 (2%) clinical isolates matched imported chicken meat, and 8 clusters included isolates from cattle and comprised a total of 16 (2%) clinical isolates. One small cluster matched 2 clinical isolates to an isolate from a dog, and a single cluster included isolates from imported chicken, imported turkey, and a domestic broiler. The chicken meat/broiler isolates in the same cluster were often linked to the same slaughterhouse, and some originated from the same farm. However, it was also common for cluster isolates to originate from different farms, but because complete data were not available, we could not make a systematic assessment.

Clusters often originated with the detection of a food/animal isolate, followed by the presence of several clinical isolates over a few months, as seen in the examples of epidemic curves of large genetic clusters (Figure 4). In some instances, the cluster type disappeared for months and later reappeared in new patients (Figure 4, panels A, C, E). With few exceptions, the clinical isolates present in clusters were detected across the 4 geographic regions.

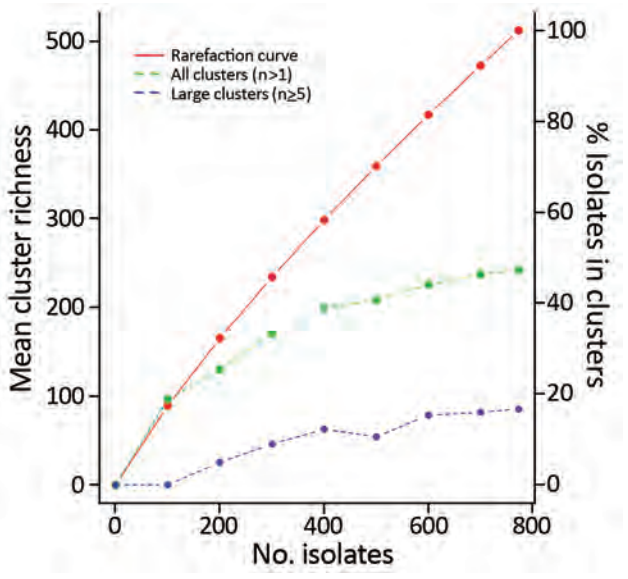

Figure 3. Rarefaction curve of *Campylobacter jejuni* clinical isolates from Denmark, 2015–2017. Curve of cluster types is shown relating to the left y-axis, revealing 512 different cluster types, which encompass the 104 defined clusters as well as the 408 sporadic cases assigned to their own cluster type. The right y-axis indicates the percentage of clinical isolates assigned to any cluster or a large cluster for a given subsample size. The rarefaction curve indicates that only a small fraction of the diversity is sampled; a larger fraction of the sporadic isolates would be included in clusters if a greater fraction of the population had been sampled.

Timeline of the Clusters

Clusters occurred independently and generally reflected the seasonality of *Campylobacter* infections (Figure 2). Most clusters typically occurred over a few months. We determined the distribution of cluster isolates in the 22 large clusters over time (Figure 5).

Table. Genetic clusters of *Campylobacter* isolates with matches between clinical isolates and food/animal isolates, Denmark, 2015–2017

Possible source	No. clusters with clinical isolates (1, 2–4, ≥5 isolates)	Total no. clinical isolates in clusters	Total no. cluster isolates
Domestic cattle	8 (5, 2, 1)	16	24
Imported chicken meat	10 (5, 5, 0)	18	30
Domestic chicken/broiler	55 (24, 16, 15)	192	322
Chicken meat*	13 (4, 4, 5)	69	89
Broiler	21 (14, 6, 1)	37	62
Chicken meat and/or broiler	21 (6, 6, 9)	86	171
Dog (domestic)	1 (0, 1, 0)	2	3
Chicken (imported) + turkey (imported) + broiler (domestic)	1 (0, 0, 1)	5	10
Total	75 (34, 24, 17)	233	389

*One cluster included a *C. jejuni* isolate from a dog.

For most clusters, the isolates were distributed close in time around the median day (t = 0) of the specific cluster. Typically, most isolates were present within a 1-month period (±30 days) before and after this time point. However, it was not uncommon to detect a few cluster isolates outside this time range, and on a few occasions clusters lasted for several months (i.e., ST5#1 spanning 14 months and ST2254#1 spanning 17 months).

Potential Multistrain Outbreaks

In the dataset, we found 2 examples for which distinct genetic clusters could be linked by epidemiologic data. The first example was an identified outbreak in which 14 isolates were sequenced as part of an outbreak investigation. These isolates split into 2 distinct clusters (ST21#9 and ST19#6), consisting of 8 and 6 clinical isolates, respectively. This multistrain outbreak involved ≈100 schoolchildren who had been served unpasteurized milk while visiting a dairy farm.

In the second example, a sample from a patient was positive for 2 strains belonging to distinct clusters (ST51#1 and ST21#2; Figure 4, panel F). The 2 clusters were observed for the same period of 2016, and each matched isolates from domestic chicken meat and broilers within a few weeks and contained

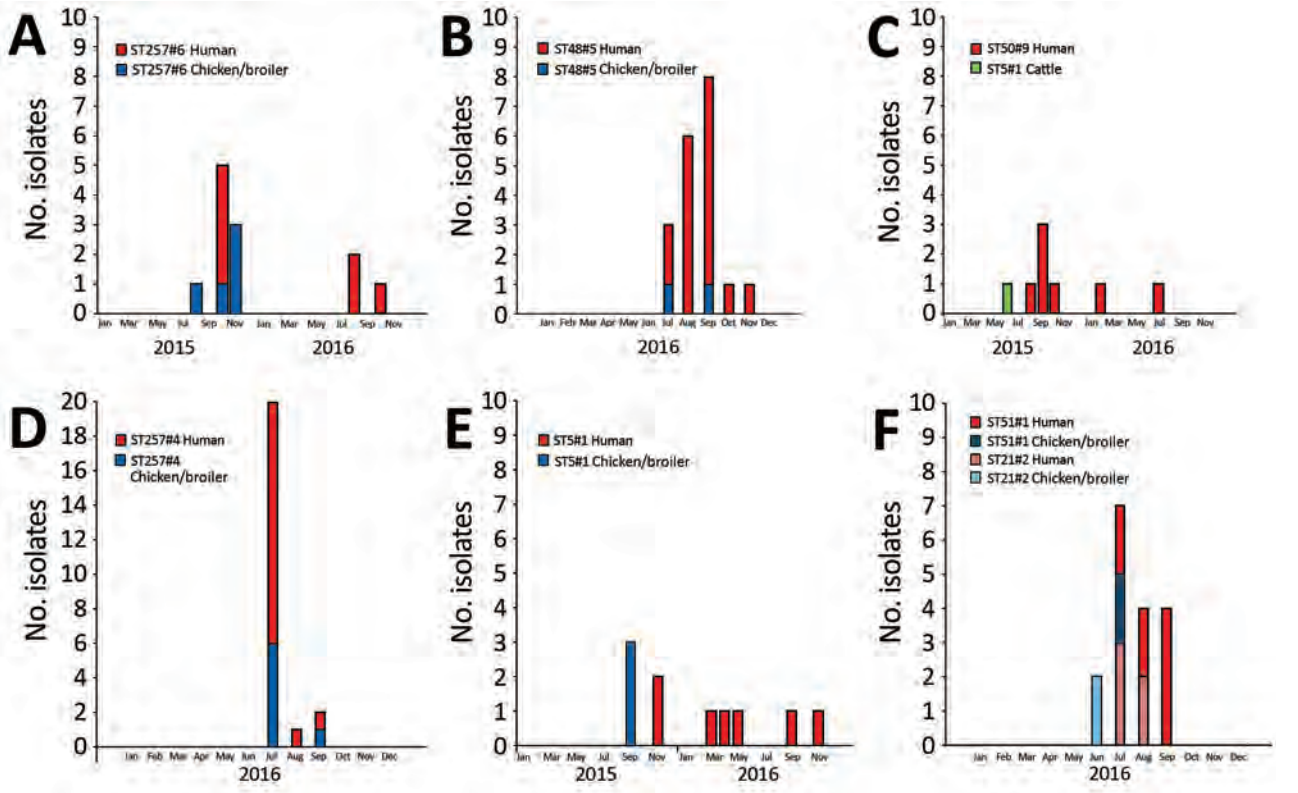

Figure 4. Epidemic curves for 6 large genetic clusters matching clinical *Campylobacter jejuni* isolates to source isolates, Denmark, 2015–2017. Each example shows the number of isolates (vertical) distributed over time (horizontal). All clusters include isolates that are within 4 allelic differences. A) Cluster ST257#6, with 7 human cases and 2 peaks detected roughly a year apart. Patient cases primarily originated from 1 region (clinical microbiological laboratory [CML] Hvidovre, n = 6). The 5 domestic chicken/broiler isolates originated from 2 slaughterhouses, and 3 of these originated from different farms. B) ST48#5, the largest of all detected clusters, with 17 human cases, provided by all 4 CMLs. The cluster contained 2 domestic chicken isolates; however, no information about origin (i.e., slaughterhouse or farm) was available. C) ST50#9, the largest cluster detected with cattle as the potential source. A total of 7 domestically acquired clinical isolates were detected from August 2015 through July 2016; isolates were provided by all 4 CMLs. D) ST257#4, the second-largest cluster, comprising isolates from 16 human cases and 7 domestic chicken/broiler isolates, primarily (6/7) from the same slaughterhouse but from different farms, except for 2 isolates that were sampled 2 days apart. Clinical isolates were obtained from all 4 CMLs, primarily from Aalborg (n = 10). Thirteen infections were registered as domestically acquired; 2 patients had traveled and travel status was unknown for 1. E) ST5#1 genetic cluster with 7 patient cases, all domestically acquired; isolates received from 2 CMLs. The 3 domestic chicken/broiler isolates were obtained at the same slaughterhouse over 3 days; however, they originated from 2 farms only ≈20 km apart. F) ST51#1 and ST21#2, the 2 genetic clusters, each contains an isolate from patient A. Separately, the clusters comprise 8 and 5 isolates, respectively; combined, they cover 12 patients with domestically acquired infections representing all 4 CMLs. Of the 4 chicken/broiler isolates (domestic), 2 were obtained at the same slaughterhouse but originated from 2 farms with the same owner. No information was available for the other 2 isolates. ST, sequence type.

clinical isolates from the 4 regions. The 2 isolates from broilers representing each of the clusters were obtained from the same slaughterhouse; the broilers originated from 2 geographically close farms.

Clusters of Food/Animal Isolates

Of the 66 clusters containing isolates of nonhuman origin, most (n = 59) included isolates from only 1 common source: domestic chicken meat and/or broilers (n = 37), domestic cattle (n = 11), imported chicken meat (n = 7), imported duck meat (n = 1), domestic pig (n = 1), imported turkey meat (n = 1), and domestic vegetables (n = 1). Isolates within each cluster often originated from the same farm, had been through the same slaughterhouse, or came from meat imported from the same country (data not shown). Cluster isolates were often isolated close in time, typically within a few days or months. Seven clusters contained isolates from >1 source: cattle and domestic chicken/broilers (3 clusters), cattle and dog (1 cluster), domestic chicken/broilers and dog(s) (2 clusters), and imported chicken and turkey meat and domestic chicken meat (1 cluster).

Discussion

Our findings show that a large proportion of *Campylobacter* infections are not sporadic. We matched clinical isolates to genetic clusters (i.e., possible outbreaks), comprising almost half of the sequences from human infections during the study period. Given that only ≈10% of the diagnosed *Campylobacter* infections in Denmark were included in the study, we assume that if the remaining infections had been included, the proportion of sporadic cases would have decreased and the cluster sizes would have increased. A large proportion (30%) of all clinical isolates matched contemporary isolates from potential sources. In our WGS-based analysis of 1,509 isolates, a large fraction of the clinical isolates matched isolates from domestic broilers/chicken meat (25%) or imported chicken meat (2%), confirming that chicken is a main source of human infections.

Despite a large number of patient clusters (104), most contained few isolates and only 22 clusters harbored ≥5 isolates. Most (17/22) of the large clusters matched source isolates, primarily from domestic chicken meat and broilers. Only 5 large clusters did not match a source isolate. However, 3 of the 5 clusters

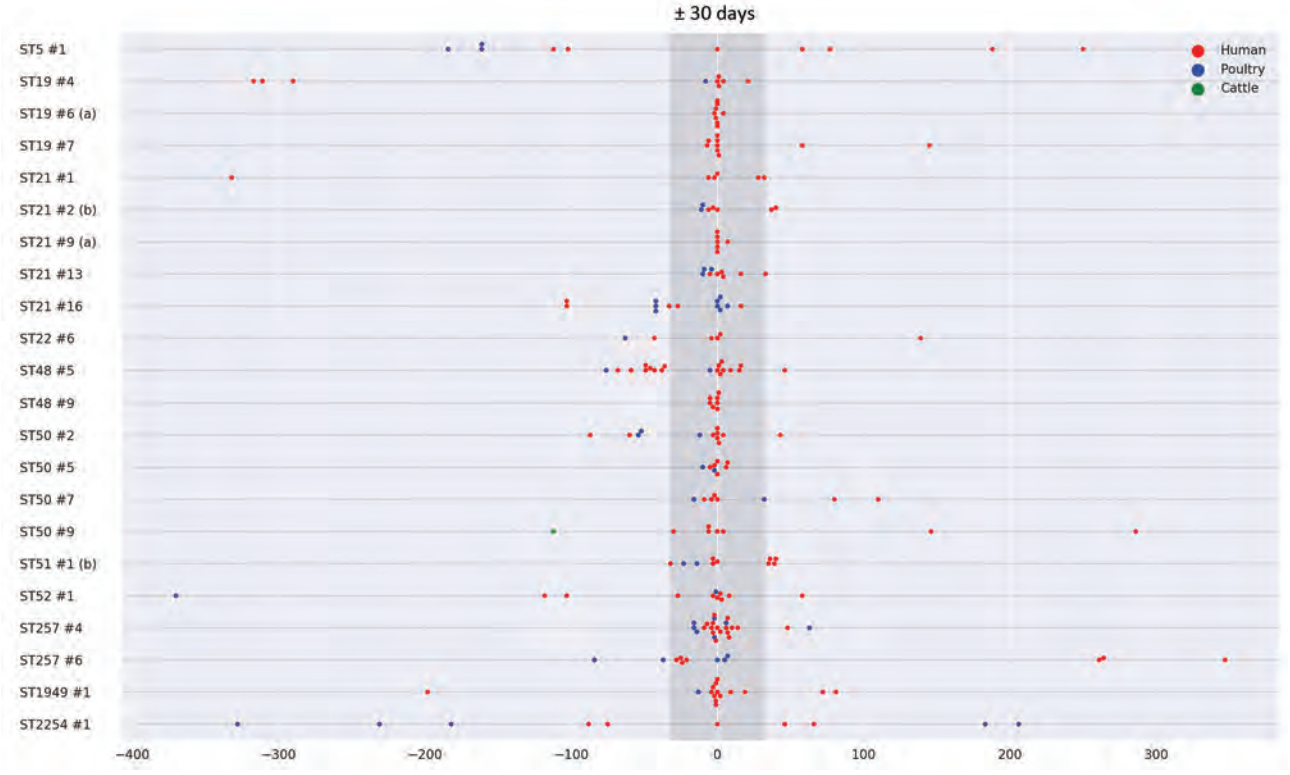

Figure 5. Distribution of large cluster isolates of *Campylobacter jejuni* from Denmark, over time. The 22 large genetic clusters (≥5 clinical isolates) are listed vertically, and the cluster isolates are displayed over time (in days) horizontally. Each cluster is centered at the median date of the cluster isolates (t = 0). Each dot represents an isolate at a certain time, and colors indicate the origin of the isolate. The 6 clusters ST257#6, ST48#5, ST50#9, ST257#4, ST5#1, and ST51#1+ST21#2 are also illustrated in Figure 3. (a) indicates the 2 clusters representing the multistrain outbreak from the fifth CML; (b) indicates the 2 clusters linked by the same patient having an isolate part of each cluster.

represented solved outbreaks without an available source isolate, specifically the multistrain outbreak associated with raw milk (which encompassed 2 clusters) and a geographically confined outbreak for which the suspected source was lettuce (*6*). Thus, only 2 of the 22 large clusters were truly not matched to a source. In contrast, among the small clusters (2–4 clinical isolates), only a minority (29%) matched a source isolate. This finding indicates that domestic chicken meat and broilers are not dominant sources of small clusters and suggests that small clusters may arise from imported food, food with a lower contamination load, small batches of less widely distributed food, or nonfood sources such as direct animal contact or environmental exposures. This indication is supported by the fact that patient matches to sources other than domestic chicken meat/broilers (i.e., cattle, imported chicken, and dogs) were found primarily for clinical isolates in small clusters or isolates from sporadic cases. Because representative isolates from low-prevalence sources are difficult to obtain, we did not sufficiently cover these sources in this study.

The *C. jejuni* genomes in the study showed a high level of genetic diversity, in line with the general knowledge of the *C. jejuni* population structure, which is formed by a high level of horizontal gene transfer (*28*). Clearly, some clones are stable enough to be detected in patients and animals over several months, as indicated by our finding isolates with the same cluster type up to 17 months apart (Figure 5). The high diversity and presence of stable clones were difficult to deduce by previous typing methods. In recent years, WGS-based typing has proven to be a strong tool for detecting outbreaks caused by several bacterial pathogens; however, interpretation is not yet standardized. For cgMLST, the allelic distance that delimits outbreaks may vary among organisms, serotypes, and outbreak etiology and epidemiology. Thus, for most organisms, including *Campylobacter*, a defined cutoff is not established, although a cluster definition of 7 allelic differences has been proposed for *Listeria* outbreaks (*29*). Also for *Listeria*, however, several outbreaks with larger isolate diversity have been described (*30*). In this study, we used a cutoff of 4 allelic differences with UPGMA clustering after evaluating the phylogeny and defining clusters by using the available epidemiologic data (i.e., defined outbreaks and food/animal isolates obtained from the same location) (Appendix). UPGMA clustering limited the merging of closely related clusters seen with single-linkage clustering. The selected cutoff correctly matched the epidemiologically confirmed outbreaks and often clustered with chickens/broiler isolates from the same slaughterhouse/farm while separating isolates without apparent epidemiologic association. For future WGS-based analyses of *C. jejuni* for surveillance and outbreak detection, the available epidemiologic information needs to be considered to ensure correct inclusion and exclusion of isolates with respect to outbreak duration, possible source differences, and differences in genomic stability of the specific clone. Although it is not likely that a definite cutoff can be established, a cutoff of 4 allelic differences, or slightly more, seems to provide a sensible differentiation in a dataset like this one with limited a priori knowledge of the epidemiologic associations. However, UPGMA clustering is not useful in a real-time surveillance setup in which isolates are continuously added to the analysis. In routine surveillance, single-linkage clustering can be used by ensuring that newly added isolates are within a reasonable distance from the main cluster isolates because this method expands clusters and will sometimes join previously separated clusters.

This study shows that WGS is a valuable tool for improved surveillance and outbreak detection of *Campylobacter*, but a limitation is the detection of multistrain outbreaks (*31*). Multistrain outbreaks of *C. jejuni* are common, potentially constituting as much as 50% of reported outbreaks in the United Kingdom (*32*). Furthermore, food products, including chicken meat, may carry several types of *C. jejuni* (*33*). Thus, several clusters may be part of the same outbreak without being detectable in the current setup. For instance, the epidemiologically confirmed multistrain outbreak described in this study, which constituted 2 distinct clusters, would never have been connected without the epidemiologic link. Likewise, the single patient harboring strains from 2 genetic clusters would not have been detected systematically. Establishing the prevalence of multistrain outbreaks in the context of Denmark would be valuable, as would a cost-effective approach for detecting multistrain outbreaks in a routine surveillance setting.

Undertaking a detailed investigation of all clusters would be difficult and costly because many are small and many occur simultaneously. A carefully selected sampling frequency and investigation threshold facilitate a more cost-effective cluster investigation. With the aim of detecting large clusters, our study suggests that a sampling frequency of 10% is sufficient, although a low sampling frequency limits the value of epidemiologic investigations from food exposure data. In our study, most clusters had

source links to chicken, a commonly consumed food source, making exposure investigation less efficient. Domestically produced chicken meat is distributed throughout the country, which is reflected by patient cases in clusters generally not being confined to a single geographic location, often limiting the geographic signal. Although the principal part of the clusters is confined to a short period, the general picture of clusters lasting for a few months offers the potential to prevent some cases through traditional outbreak detection and follow-up. This study indicates that it might be possible to limit some large clusters and probably a substantial part of sporadic cases by using control measures in the poultry industry. However, it is more difficult to identify other sources (e.g., raw milk, vegetables, animal contact, and different kinds of environmental exposures) because doing so would take disproportionate resources to encompass sufficient routine sampling of these sources. Because food/animal isolates are widely distributed in the phylogenetic tree, our study indicates that we cannot expect to be able to predict the source of human infections without having isolates from the specific source. In addition, the *C. jejuni* clones causing the 2 point-source outbreaks with a probable nonpoultry source (i.e., raw milk and lettuce) were also genetically similar, albeit not considered matches, to strains isolated from poultry.

This study confirms previous findings that campylobacteriosis is not a wholly sporadic disease but rather constitutes numerous small clusters with cases geographically distributed across the country, lasting for a few months and then being replaced by other clusters of different strains of *C. jejuni*. As a result of this study, continuous surveillance based on sampling of ≈10% of the patient cases has been initiated in Denmark for the purpose of detecting large outbreaks and linking them to contemporary food/animal sources to improve public health and reduce the incidence of *Campylobacter* infections.

Acknowledgments

We are grateful to all patients whose isolates were used as part of this study and to the laboratory staff at the Statens Serum Institute; the Danish Veterinary and Food Administration in Ringsted, Denmark; and all participating clinical microbiological laboratories.

This study was financially supported by the European Union's Horizon 2020 research and innovation program under grant agreement nos. 773830 (the ORION project under the European Joint Programme One Health) and 643476 (COMPARE).

About the Author

Dr. Joensen is a microbiologist working as a researcher at Statens Serum Institut in Denmark. Her research interests include WGS-based typing, surveillance, and outbreak detection of foodborne pathogens.

References

1. Kaakoush NO, Castaño-Rodríguez N, Mitchell HM, Man SM. Global epidemiology of *Campylobacter* infection. Clin Microbiol Rev. 2015;28:687–720. https://doi.org/10.1128/CMR.00006-15
2. European Food Safety Authority/European Centre for Disease Prevention and Control. The European Union summary report on trends and sources of zoonoses, zoonotic agents and food-borne outbreaks in 2017. EFSA Journal. 2018;16:5500. https://doi.org/10.2903/j.efsa.2018.5500
3. Kuhn KG, Nielsen EM, Mølbak K, Ethelberg S. Epidemiology of campylobacteriosis in Denmark 2000-2015. Zoonoses Public Health. 2018;65:59–66. https://doi.org/10.1111/zph.12367
4. Havelaar AH, Ivarsson S, Löfdahl M, Nauta MJ. Estimating the true incidence of campylobacteriosis and salmonellosis in the European Union, 2009. Epidemiol Infect. 2013:141:293–302.
5. Haagsma JA, Geenen PL, Ethelberg S, Fetch A, Hansdotter F, Jansen A, et al. Community incidence of pathogen-specific gastroenteritis: reconstructing the surveillance pyramid for seven pathogens in seven European Union member states. Epidemiol Infect. 2013;141:1625–39.
6. Joensen KG, Kuhn KG, Müller L, Björkman JT, Torpdahl M, Engberg J, et al. Whole-genome sequencing of *Campylobacter jejuni* isolated from Danish routine human stool samples reveals surprising degree of clustering. Clin Microbiol Infect. 2018;24:201.e5–201.e8. PMID: 28782648
7. Gubbels S-M, Kuhn KG, Larsson JT, Adelhardt M, Engberg J, Ingildsen P, et al. A waterborne outbreak with a single clone of *Campylobacter jejuni* in the Danish town of Køge in May 2010. Scand J Infect Dis. 2012;44:586–94.
8. Kuhn KG, Falkenhorst G, Emborg H-D, Ceper T, Torpdahl M, Krogfelt KA, et al. Epidemiological and serological investigation of a waterborne *Campylobacter jejuni* outbreak in a Danish town. Epidemiol Infect. 2017;145:701–9.
9. Harder-Lauridsen NM, Kuhn KG, Erichsen AC, Mølbak K, Ethelberg S. Gastrointestinal illness among triathletes swimming in non-polluted versus polluted seawater affected by heavy rainfall, Denmark, 2010-2011. PLoS One. 2013;8:e78371. https://doi.org/10.1371/journal.pone.0078371
10. Engberg J, Gerner-Smidt P, Scheutz F, Møller Nielsen E, On SLW, Mølbak K. Water-borne *Campylobacter jejuni* infection in a Danish town—a 6-week continuous source outbreak. Clin Microbiol Infect. 1998;4:648–56. https://doi.org/10.1111/ j.1469-0691.1998.tb00348.x
11. Kuhn KG, Nielsen EM, Mølbak K, Ethelberg S. Determinants of sporadic *Campylobacter* infections in Denmark: a nationwide case-control study among children and young adults. Clin Epidemiol. 2018;10:1695–707. https://doi.org/10.2147/CLEP.S177141
12. Mughini Gras L, Smid JH, Wagenaar JA, de Boer AG, Havelaar AH, Friesema IHM, et al. Risk factors for campylobacteriosis of chicken, ruminant, and environmental origin: a combined case-control and source attribution analysis. PLoS One. 2012;7:e42599. https://doi.org/10.1371/journal.pone.0042599

13. Verhoeff-Bakkenes L, Jansen HAPM, in 't Veld PH, Beumer RR, Zwietering MH, van Leusden FM. Consumption of raw vegetables and fruits: a risk factor for *Campylobacter* infections. Int J Food Microbiol. 2011;144:406–12. https://doi.org/10.1016/j.ijfoodmicro.2010.10.027
14. Domingues AR, Pires SM, Halasa T, Hald T. Source attribution of human campylobacteriosis using a meta-analysis of case-control studies of sporadic infections. Epidemiol Infect. 2012;140:970–81. https://doi.org/10.1017/S0950268811002676
15. Joensen KG, Scheutz F, Lund O, Hasman H, Kaas RS, Nielsen EM, et al. Real-time whole-genome sequencing for routine typing, surveillance, and outbreak detection of verotoxigenic *Escherichia coli.* J Clin Microbiol. 2014; 52:1501–10.
16. Kvistholm Jensen A, Nielsen EM, Björkman JT, Jensen T, Müller L, Persson S, et al. Whole-genome sequencing used to investigate a nationwide outbreak of listeriosis caused by ready-to-eat delicatessen meat, Denmark, 2014. Clin Infect Dis. 2016;63:64–70. https://doi.org/10.1093/cid/ciw192
17. Revez J, Llarena A-K, Schott T, Kuusi M, Hakkinen M, Kivistö R, et al. Genome analysis of *Campylobacter jejuni* strains isolated from a waterborne outbreak. BMC Genomics. 2014;15:768. https://doi.org/10.1186/1471-2164-15-768
18. Revez J, Zhang J, Schott T, Kivistö R, Rossi M, Hänninen M-L. Genomic variation between *Campylobacter jejuni* isolates associated with milk-borne-disease outbreaks. 2014;52: 2782–6. https://doi.org/10.1128/JCM.00931-14
19. Lahti E, Löfdahl M, Ågren J, Hansson I, Olsson Engvall E. Confirmation of a campylobacteriosis outbreak associated with chicken liver pâté using PFGE and WGS. Zoonoses Public Health. 2017;64:14–20. PMID: 27334628
20. Lahti E, Rehn M, Ockborn G, Hansson I, Ågren J, Engvall EO, et al. Outbreak of campylobacteriosis following a dairy farm visit: confirmation by genotyping. Foodborne Pathog Dis.2017;14:326–32. PMID: 28350214
21. Clark CG, Berry C, Walker M, Petkau A, Barker DOR, Guan C, et al. Genomic insights from whole genome sequencing of four clonal outbreak *Campylobacter jejuni* assessed within the global C. jejuni population. BMC Genomics. 2016;17:990. https://doi.org/10.1186/s12864-016-3340-8
22. Kovanen SM, Kivistö RI, Rossi M, Schott T, Kärkkäinen U-M, Tuuminen T, et al. Multilocus sequence typing (MLST) and whole-genome MLST of *Campylobacter jejuni* isolates from human infections in three districts during a seasonal peak in Finland. J Clin Microbiol. 2014; 52:4147–54.
23. Kovanen S, Kivistö R, Llarena A-K, Zhang J, Kärkkäinen U-M, Tuuminen T, et al. Tracing isolates from domestic human *Campylobacter jejuni* infections to chicken slaughter batches and swimming water using whole-genome multilocus sequence typing. Int J Food Microbiol. 2016;226:53–60. https://doi.org/10.1016/j.ijfoodmicro.2016.03.009
24. Pires SM, Christensen J. Source attribution of *Campylobacter* infections in Denmark–technical report [cited 2019 Jul 3]. http://orbit.dtu.dk/en/publications/source-attribution-of-campylobacter-infections-in-denmark--technical-report(4c71814c-db74-481b-b8a5-54f4c6bcd3f5).html
25. Jolley KA, Bray JE, Maiden MCJ. Open-access bacterial population genomics: BIGSdb software, the PubMLST.org website and their applications. Wellcome Open Res. 2018; 3:124. https://doi.org/10.12688/wellcomeopenres.14826.1
26. Oksanen J, Blanchet FG, Friendly M, Kindt R, Legendre P, McGlinn D, et al. vegan: Community Ecology Package [cited 2019 May 3]. https://cran.r-project.org/package=vegan
27. Lake IR, Colón-González FJ, Takkinen J, Rossi M, Sudre B, Dias JG, et al. Exploring *Campylobacter* seasonality across Europe using The European Surveillance System (TESSy), 2008 to 2016. Euro Surveill. 2019;24. https://doi.org/10.2807/1560-7917.ES.2019.24.13.180028
28. Sheppard SK, Maiden MCJ. The evolution of *Campylobacter jejuni* and *Campylobacter coli.* Cold Spring Harb Perspect Biol. 2015;7:a018119. https://doi.org/10.1101/cshperspect.a018119
29. Moura A, Criscuolo A, Pouseele H, Maury MM, Leclercq A, Tarr C, et al. Whole genome-based population biology and epidemiological surveillance of *Listeria monocytogenes.* Nat Microbiol. 2016;2:16185. https://doi.org/10.1038/nmicrobiol.2016.185
30. Pightling AW, Pettengill JB, Luo Y, Baugher JD, Rand H, Strain E; Interpreting whole-genome sequence analyses of foodborne bacteria for regulatory applications and outbreak investigations. Front Microbiol. 2018;10;9:1482.
31. Gerner-Smidt P, Besser J, Concepción-Acevedo J, Folster JP, Huffman J, Joseph LA, et al. Whole genome sequencing: bridging one-health surveillance of foodborne diseases. Front Public Health. 2019;7:365.
32. Frost JA, Gillespie IA, O'Brien SJ. Public health implications of *Campylobacter* outbreaks in England and Wales, 1995–9: epidemiological and microbiological investigations. Epidemiol Infect. 2002; 128:111–8.
33. Kramer JM, Frost JA, Bolton FJ, Wareing DR. *Campylobacter* contamination of raw meat and poultry at retail sale: identification of multiple types and comparison with isolates from human infection. J Food Prot. 2000;63:1654–9. https://doi.org/ 10.4315/0362-028X-63.12.1654

Address for correspondence: Eva M. Nielsen, Statens Serum Institut, Department of Bacteriology, Mycology & Parasitology, Artillerivej 5 Copenhagen 2300, Denmark; email: emn@ssi.dk

US Tuberculosis Rates among Persons Born Outside the United States Compared with Rates in Their Countries of Birth, 2012–2016[1]

Clarisse A. Tsang, Adam J. Langer, J. Steve Kammerer, Thomas R. Navin

The US Centers for Disease Control and Prevention recommends screening populations at increased risk for tuberculosis (TB), including persons born in countries with high TB rates. This approach assumes that TB risk for expatriates living in the United States is representative of TB risk in their countries of birth. We compared US TB rates by country of birth with corresponding country rates by calculating incidence rate ratios (IRRs) (World Health Organization rate/US rate). The median IRR was 5.4. The median IRR was 0.5 for persons who received a TB diagnosis <1 year after US entry, 4.9 at 1 to <10 years, and 10.0 at ≥10 years. Our analysis suggests that World Health Organization TB rates are not representative of TB risk among expatriates in the United States and that TB testing prioritization in the United States might better be based on US rates by country of birth and years in the United States.

In the United States, 9,272–9,940 cases of tuberculosis (TB) were reported annually during 2012–2016; incidence rate was 2.9–3.2 cases/100,000 population (*1*). Most cases occurred among non–US-born persons and were attributed to progression of remotely acquired latent TB infection (LTBI) rather than recent transmission within the preceding 2 years (*2*). US law requires non–US-born persons seeking lawful permanent residency in the United States and refugees resettling in the United States to undergo a medical examination, including screening for TB. These examinations can be done by panel physicians in other countries before the immigrant or refugee arrives in the United States, or they can be done by civil surgeons in the United States for persons with temporary visas who are seeking lawful permanent residency (*3*,*4*). This TB screening requirement is intended to identify otherwise undiagnosed TB among non–US-born persons seeking lawful permanent residency, although it would not identify TB among the substantial proportion of non–US-born residents who are in the United States on temporary visas or who are undocumented. Of note, these required examinations would identify any cases of TB among examinees, but testing of adults for LTBI is not required. Although recent reliable data on visa status of US TB patients are not available, Davidow et al. determined that among non–US-born TB patients reported during 2005–2006, most (61%) were either permanent residents or naturalized citizens who would have been screened for TB either before departure or during visa status change in the United States, whereas 13% were temporary visa holders (student, work, or exchange visas) for whom TB screening is not mandated and 25% were undocumented (*5*).

The US Centers for Disease Control and Prevention (CDC) and the US Preventive Services Task Force recommend that healthcare providers and public health departments offer testing for TB infection in populations at increased risk for exposure to TB or for having TB infection progress to TB. This recommendation encompasses persons who were born in or frequently travel to countries with high numbers of TB cases among their expatriates living in the United States, including Mexico, the Philippines, Vietnam, India, China, Haiti, and Guatemala, as well as other

Author affiliation: Centers for Disease Control and Prevention, Atlanta, Georgia, USA

DOI: https://doi.org/10.3201/eid2603.190974

[1]Preliminary results from this study were presented at the Union–North America Region conference, 2019 Feb 21–23, Vancouver, British Columbia, Canada; and at the National TB Conference, 2019 Apr 23–26, Atlanta, Georgia, USA.

countries where rates of TB are high (*6*). What constitutes high TB rates or how these rates should be calculated is not specified. One option is to use TB incidence rates in countries as reported by the World Health Organization (WHO; hereafter referred to as WHO rates); however, using WHO rates assumes that TB rates in a given country reflect TB rates among persons from that country in the United States (hereafter referred to as US rates). We compared WHO rates with US rates for all countries for which data were available. Our hypothesis was that using US rates by country of birth would provide better data than using WHO rates, which is the current US Preventive Services Task Force recommendation for establishing which countries have a high burden of TB (*7*).

Materials and Methods

We analyzed data from the US National TB Surveillance System (NTSS) for TB cases reported during 2012–2016 for persons born outside the United States. To minimize the effects of yearly fluctuations in rate, we selected a 5-year period; at the time of this analysis, the most recent data were from 2016. NTSS data are compiled from reports of TB cases submitted electronically to CDC by the 50 states and the District of Columbia. Reports include the patient's self-reported country of birth, approximate date of arrival in the United States, other demographic information (e.g., date of birth, sex, race/ethnicity), and clinical information (e.g., site of TB disease and laboratory results). For this analysis, persons born outside the United States included persons born in the US territories (American Samoa, Commonwealth of the Northern Mariana Islands, Guam, Puerto Rico, and US Virgin Islands). Because persons born in the US territories are eligible for US citizenship, they do not report a month or year of arrival in the United States. Persons from the US sovereign freely associated states of the Federated States of Micronesia, the Republic of the Marshall Islands, and the Republic of Palau are classified as born outside the United States but do not require a visa to visit or relocate to the United States. In this way, they are similar to persons born in the US territories. NTSS does not collect travel history or countries of residence other than among pediatric patients (<15 years of age).

To calculate TB rates in the United States by patient's country of birth, we obtained TB case counts by country of birth reported to NTSS during 2012–2016 as well as US population estimates by country of birth from the US Census Bureau, American Community Survey (ACS), Public Use Microdata Sample data, 2012–2016 multiyear file (*8*). ACS is an annual survey of ≈3.5 million US households and includes reported country of birth and year of arrival in the United States. We also calculated rates by years spent in the United States before TB diagnosis (<1 year, 1 to <10 years, and ≥10 years). Case rates were calculated as the number of cases per 100,000 population.

In the ACS, country of birth is based on self-report and coded as a country or region. Persons born outside the United States are asked to report country of birth according to current international boundaries. If there are <10,000 persons from a particular country of birth in the United States, the ACS does not provide population estimates from that particular country but groups the country into a region. The ACS does not provide individual population estimates for North and South Korea but provides a population estimate for Korea as a whole, encompassing the populations of South and North Korea. The ACS also does not provide a population estimate for the state of Palestine. For TB case data for persons born in countries where the ACS does not provide individual country population estimates, we aggregated these cases into regions by using the same regions categorized by the ACS (*8*) and applied the TB rate calculated for the region to all countries included in that region. If a country of birth associated with a case reported to NTSS was not provided as a country of birth or categorized within a region by the ACS, then a rate was not calculated. We compared our US TB rate calculations by country of birth (US rates) with country TB rates published by WHO for 2014 (WHO rates), which was the midpoint year between 2012 and 2016 (*9*).

To compare the WHO and the US rate estimates, we calculated incidence rate ratios (IRRs) for each country of birth. IRRs >1.0 indicated a higher WHO rate than the corresponding US rate. We used 95% CIs from 2014 WHO incidence rates to calculate 95% CIs for each individual country/region-specific IRR by dividing the WHO lower CI limit by the US rate and the WHO upper CI limit by the US rate. We also compared WHO rates with US rates by years since US arrival by calculating median IRRs by year. We used SAS version 9.4 (https://www.sas.com) to conduct the analysis.

Results

During 2012–2016, a total of 47,718 persons in the United States were reported to have TB, of which 32,087 (67.2%) had been born outside the United States. Patients from Mexico, the Philippines, India, Vietnam, and China accounted for 54.0% of persons with reported TB who had been born outside the United States. Rates varied by country and region of birth. US rates

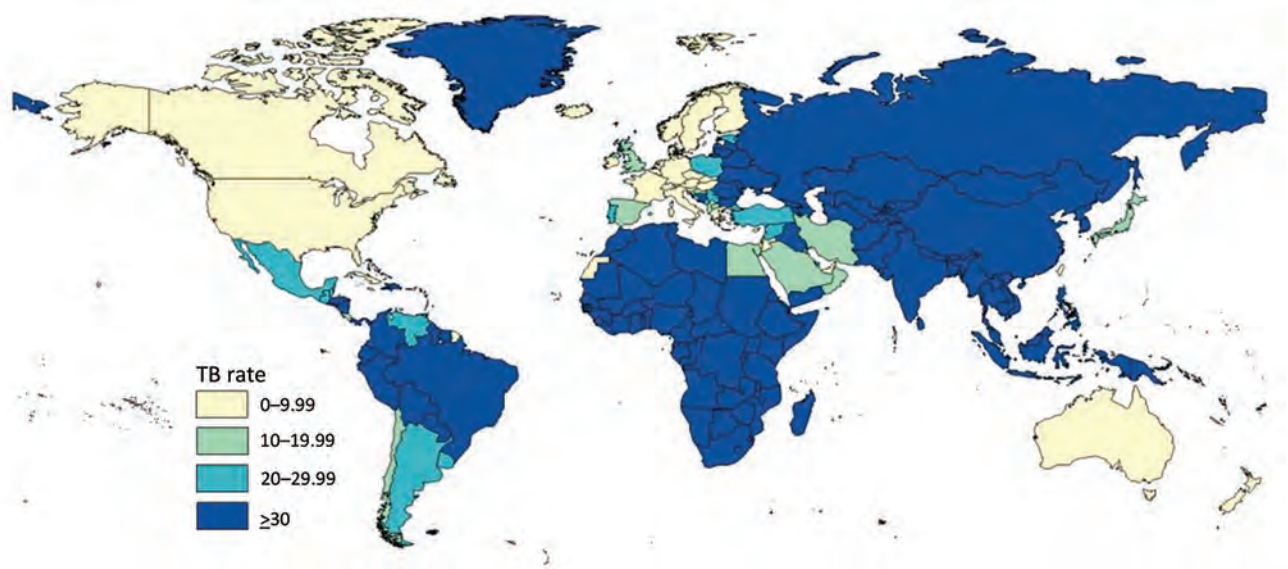

Figure 1. TB rates (per 100,000 population) worldwide, according to World Health Organization reports, 2014. TB, tuberculosis.

were ≥30 cases/100,000 population for far fewer countries than were WHO rates (Figure 1; Figure 2, panel A). Of the 195 countries in the world, the corresponding US rate was ≥30 cases/100,000 population for 65 countries, 20–30/100,000 for 13 countries, 10–20/100,000 for 19 countries, and <10/100,000 for 97 countries; the rate could not be calculated for 1 country. Complete data for month and year of arrival in the United States were available for 90% of persons born outside the United States. Rates were generally higher among persons for whom TB was diagnosed <1 year after arrival in the United States than among those who arrived 1 to <10 years before receiving a TB diagnosis (Figure 2, panels B, C) and higher among those for whom TB was diagnosed 1 to <10 years after US arrival than among those who arrived in the United States >10 years

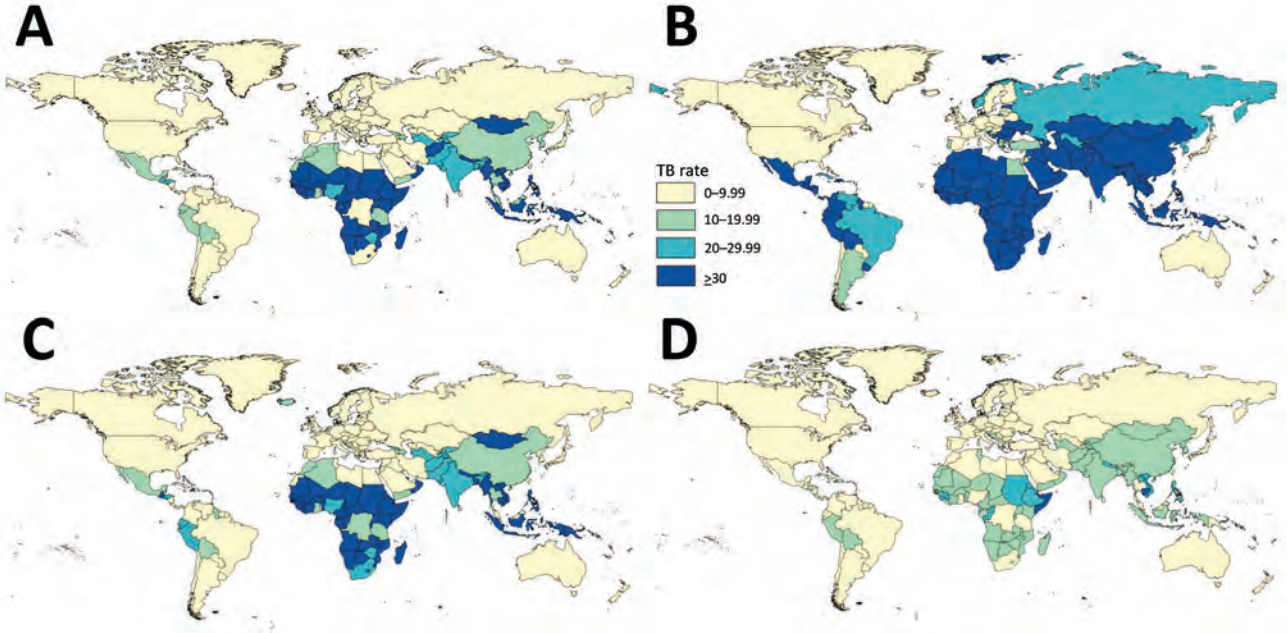

Figure 2. TB rates (per 100,000 population) in the United States, by country of birth and time from US arrival to TB diagnosis, 2012–2016. A) Persons born abroad by their country of birth (note that rates could not be calculated for 1 country); B) persons by their country of birth who lived in the United States <1 year before diagnosis; C) persons by their country of birth who lived in the United States ≥1 to <10 years before diagnosis; D) persons by their country of birth who lived in the United States ≥10 years before diagnosis. Note that the US Census Bureau American Community Survey provides only a combined population estimate for Korea; thus, the rate represented for North Korea and South Korea is calculated as a combined rate for Korea. TB, tuberculosis.

before receiving a TB diagnosis (Figure 2, panels C, D). Rates were ≥30 cases/100,000 population among US residents born in sub-Saharan Africa, South Central Asia, Southeast Asia, Mexico, and parts of Central and South America who received their TB diagnosis <1 year after arrival in the United States. Rates were ≥30 cases/100,000 population among US residents born in parts of sub-Saharan Africa and Southeast Asia who received their TB diagnosis 1 to <10 years after their arrival in the United States. Rates were ≥30 cases/100,000 population among only those US residents from the Republic of the Marshall Islands, Somalia, and Cambodia who had received their TB diagnosis ≥10 years after arrival in the United States. US rates were lower than WHO rates among persons from South America (Figures 1, 2).

Among the 20 countries of birth for which TB case counts in the United States were the highest, the 10 countries for which WHO rates were the highest were the Philippines, Cambodia, Myanmar, Somalia, Pakistan, India, Nigeria, Ethiopia, Haiti, and Laos (range 189–546 cases/100,000 population) (Table 1). In contrast, the 10 areas for which US rates (i.e., among expatriates in the United States) were the highest were Republic of Congo, Republic of the Marshall Islands, Somalia, Bhutan, Myanmar, Nepal, Guinea, Ethiopia, the Federated States of Micronesia, and the countries in the Other Africa region (range 62–150 cases/100,000 population) (Appendix, https://wwwnc.cdc.gov/EID/article/26/3/19-0974-App1.xlsx).

Of the 195 countries represented as members of the United Nations (*10*,*11*), rate data for calculation of IRR were available for 189; for 178 (94%) of those, WHO rates were higher than the corresponding US rates (Figure 3). The median IRR was 5.4 (interquartile range [IQR] 2.6–8.7). The country of birth for which IRRs were highest and for which population estimates were not from a region were South Africa, Lithuania, and Belarus. The country of birth for which TB cases were reported and the IRR was notably below average was United Arab Emirates (Appendix).

We calculated median IRRs by years since entry into the United States before TB diagnosis by using the 189 countries. The median IRR was 0.5 (IQR 0.2–1.1) for persons for whom TB was diagnosed <1 year after US arrival, 4.9 (IQR 2.6–9.4) for 1 to <10 years, and 10.0 (IQR 4.9–19.9) for ≥10 years. Of the 195 countries, the US rate was greater than the WHO rate for 58% of those for whom TB was diagnosed <1 year after US arrival. On average, among persons for whom TB was diagnosed <1 year after US arrival, US rates by country of birth were higher than corresponding WHO rates by country. In contrast, on average among persons for whom TB was diagnosed ≥1 year after US arrival, US rates by country of birth were lower than corresponding WHO rates by country.

Table 1. TB rates in the United States, by country of birth, 2012–2016, compared with World Health Organization rates, 2014, for the 20 countries with the highest TB counts in the United States*

COB	Average annual no. cases	Estimated population†	Rate by years since US arrival			Overall US rate by COB	WHO rate (95% CI)‡	IRR (95% CI)§
			<1	1 to <10	≥10			
Mexico	1,262.2	11,851,810	103.0	11.7	7.9	10.6	21 (16–27)	2.0 (1.5–2.5)
Philippines	788.4	2,048,557	297.4	42.5	26.8	38.5	54 (304–859)	14.2 (7.9–22.3)
India	537	2,235,594	117.1	24.1	14.1	24.0	223 (136–332)	9.3 (5.7–13.8)
Vietnam	487.2	1,340,215	290.7	46.8	23.8	36.4	140 (111–173)	3.9 (3.1–4.8
China	393.2	1,966,551	56.8	16.7	16.7	20.0	68 (58–78)	3.4 (2.9–3.9)
Guatemala	193.4	929,637	220.9	30.4	8.6	20.8	25 (19–31)	1.2 (0.9–1.5)
Haiti	174.8	661,301	311.9	37.3	13.9	26.4	200 (154–253)	7.6 (5.8–9.6)
Ethiopia	151.8	222,559	623.8	80.4	24.5	68.2	207 (134–295)	3.0 (2.0–4.3)
Honduras	135.8	594,066	231.3	25.2	10.9	22.9	40 (30–50)	1.7 (1.3–2.2)
Myanmar	113.8	129,594	707.3	76.5	15.8	87.8	369 (269–484)	4.2 (3.1–5.5)
El Salvador	107.4	1,330,323	87.4	11.8	4.8	8.1	44 (34–56)	5.5 (4.2–6.9)
Somalia	96.2	85,871	1,033.9	105.6	51.0	112.0	274 (177–391)	2.4 (1.6–3.5)
Nepal	83.4	108,099	439.5	67.6	24.4	77.2	158 (139–178)	2.0 (1.8–2.3)
Peru	82.2	450,546	228.9	28.6	11.3	18.2	121 (93–153)	6.6 (5.1–8.4)
Pakistan	80.8	368,845	178.1	20.4	13.9	21.9	270 (175–386)	12.3 (8.0–17.6)
Cambodia	75.2	161,226	187.4	39.1	36.0	46.6	390 (252–557)	8.4 (5.4–11.9)
Laos	72.4	192,908	96.5	46.6	29.7	37.5	189 (122–270)	5.0 (3.3–7.2)
Ecuador	72.2	439,795	127.8	27.4	9.4	16.4	41 (31–51)	2.5 (1.9–3.1)
Nigeria	68.4	289,679	242.3	28.5	8.1	23.6	219 (143–311)	9.3 (6.1–13.2)
Dominican Republic	66.4	1,064,665	55.2	7.4	4.0	6.2	53 (41–67)	8.5 (6.6–10.7)

*Although South Korea has an average annual number of 97.4 cases, it is not listed in the table because the ACS does not provide a population estimate for South Korea. ACS, US Census Bureau American Community Survey; COB, country of birth; IRR, incidence rate ratio; TB, tuberculosis; US, United States, WHO, World Health Organization.
†ACS Public Use Microdata Sample data, 2012–2016 multiyear file, https://www.census.gov/programs-surveys/acs/data/pums.html.
‡World Health Organization TB burden estimates, https://www.who.int/tb/country/data/download/en/.
§Rate in country (WHO rate) divided by overall US rate by COB. An IRR >1.0 indicates that the WHO rate is larger than the US rate.

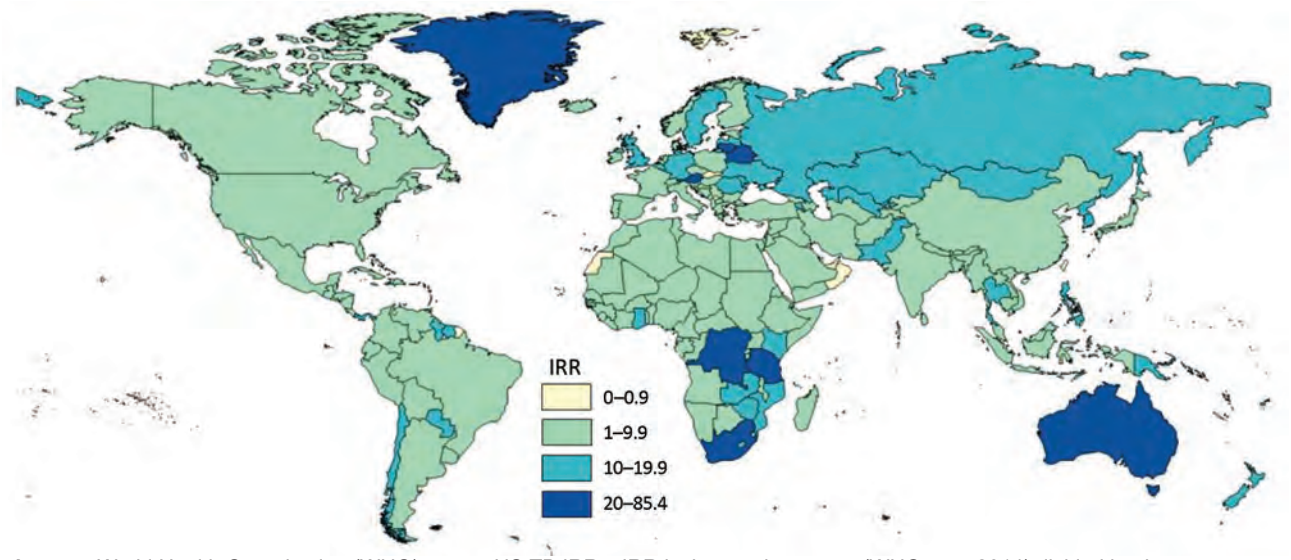

Figure 3. World Health Organization (WHO) versus US TB IRRs. IRR is the rate in country (WHO rate, 2014) divided by the rate by country of birth in the United States (US rate, 2012–2016). IRR >1.0 indicates that the WHO rate is larger than the US rate. IRR, incidence rate ratio; TB, tuberculosis.

Discussion

Our analysis showed that, for 2012–2016, the WHO rate (TB incidence rate for a country as reported by WHO) did not consistently equate to the overall US rate (TB incidence in the United States for persons born in the corresponding country). WHO rates, by country, were a median of 5.4 times higher than US rates among persons born in the corresponding countries. The WHO rate for South Africa (820 cases/100,000 population) was most discrepant with the overall US rate for persons born in South Africa (9.6/100,000). Menzies et al. examined the 30 countries with the highest case counts in the United States from 2003 through 2015 and estimated that TB incidence rates in a country of birth were 6.8 times higher than TB rates among persons born in that country and living in the United States (*12*). A previous analysis of 2004 data by Cain et al. demonstrated that US TB rates among non–US-born persons were highest among persons born in sub-Saharan Africa, followed by South Asia, East Asia, and the Pacific (*13*). Another analysis done by Cain et al. showed that annual TB rates for persons in the United States who had been born in Canada, Australia, New Zealand, countries of western Europe, and Japan were very low (<10/100,000 population) (*14*). Our results are consistent with the previous findings that TB rates are highest among US persons from sub-Saharan Africa, Asia, and the Pacific Islands (Figure 2).

Current US TB screening guidelines recommend TB testing for persons born in countries where TB rates are high (*6*). Although what constitutes high TB rates is not specified universally, several resources use WHO rates to dictate screening practices (*15*,*16*). Our data show that WHO rates differ from US rates. WHO TB rates by country were a median of 5.4 times higher than the TB rate in the United States for persons from the corresponding country of birth (Table 1). Time since arrival in the United States also plays a role in TB rates. On average, among persons for whom TB was diagnosed <1 year after US arrival, US rates for the country of birth were higher than corresponding WHO rates (median IRR 0.5) (Table 2). This finding is consistent with previous findings. Cain et al. showed that TB rates for non–US-born persons were highest for those who had been in the United States ≤1 year before TB diagnosis (121.0 cases/100,000 population) and lowest for those who had been in the United States >5 years before TB diagnosis (11.9/100,000 population) (*13*). Similar to our analysis, that analysis also showed that for most non–US-born persons, rates of TB among those who had been in the United States ≤1 year were higher than rates for their respective countries of birth (*13*). High rates of TB among persons who had been in the United States for <1 year could be attributed in part to selection bias resulting from immigration-related TB screening. Walter et al. demonstrated that 85% of TB cases diagnosed for immigrants from the Philippines in California within 1 year of their preimmigration examination in the Philippines were attributed to imported TB (i.e., prevalent TB at the time of arrival in the United States) (*17*). Cain et al. demonstrated

Table 2. World Health Organization versus US TB IRRs, by years since entry into the United States before TB diagnosis*

Year(s) since entry into the United States	Median IRR†
<1	0.5
1–4	4.0
5–9	6.7
10–14	6.9
15–19	11.0
20–24	11.1
25–29	10.9
30–34	7.2
35–39	7.1
40–44	9.3
45–49	5.5
50–54	6.7
≥55	4.9

*COB, country of birth; IRR, incidence rate ratio; TB, tuberculosis; WHO, World Health Organization.
†IRR is the rate in country (WHO rate, 2014) divided by the rate by COB by years since entry into the United States (US rate, 2012–2016). An IRR >1.0 indicates that the WHO rate is larger than the US rate. Median IRR for each year since entry into the United States category was calculated for the 195 countries defined by the United Nations Member State (https://www.un.org/en/member-states/index.html) and Non–Member States (https://www.un.org/en/sections/member-states/non-member-states/index.html) lists. A WHO rate and a nonzero US rate were available for only 189 of these countries.

that even for non–US-born persons who had lived in the United States for ≥20 years, annual TB case rates were ≥10 cases/100,000 population (*14*). This finding is further supported by the Walter et al. study, in which the rate of LTBI reactivation among immigrants with negative preimmigration examination results (no evidence of TB detected by physical examination, radiography, sputum culture, or sputum microscopy) was 32 cases/100,000 population/year within 9 years of US entry (*17*). Thus, when addressing US rates, it is crucial to examine TB rate by years since arrival in the United States. Despite TB rates being higher among persons who had been in the United States for <1 year than rates reported by WHO for the same country, almost half of non–US-born persons with TB are among those who have lived in the United States for ≥10 years (*18*,*19*). Other age-period-cohort effects might also be useful when comparing US and WHO rates by country of birth. A previous study by Iqbal et al. showed that TB rates decreased as members of a birth cohort aged but were higher among adolescents and young adults (*20*). Another finding from that study was that, among non–US-born persons during 1996–2016, TB rates among black persons were highest for those <45 years of age, but rates among Asians/Pacific Islanders were highest for those ≥45 years of age (*20*). Of note, a study in Canada showed that persons born in countries where TB incidence was lower had arrived in Canada in earlier years than those from countries where TB incidence was higher (*21*).

A strength of examining rates of TB in the United States by country of birth is that US TB surveillance data are relatively complete. Winston et al. conducted an in-depth investigation of 11 US reporting areas that together reported 5,436 TB cases in 2008 and 2009 and did not find a single unreported case (*22*). Furthermore, the US Census Bureau ACS is the largest US household survey with reliable data on demographic, social, economic, and housing measures. Because completion of ACS is mandatory, levels of nonresponse are low (*23*). When examining global data, WHO does not measure TB incidence at national levels because of high costs and challenging logistics. Methods currently used by WHO to estimate TB incidence are based on case notification data combined with expert opinion about case-detection gaps, TB prevalence surveys, notifications in high-income countries adjusted for underreporting and underdiagnosis, and inventory studies and capture–recapture analyses (*24*). WHO uses population estimates from the United Nations, where recent country-level population data may not always be available; thus, standard demographic adjustments are made (*25*). Because US surveillance of TB reporting is complete and the ACS provides detailed population data, we believe that US rates by country of birth are more appropriate than WHO rates for prioritizing TB testing in the United States. In addition, using rates by country of birth might be helpful for local TB programs interested in TB targeted testing within their own jurisdictions (*26*,*27*). Using rates by country of birth, Readhead et al. demonstrated that the highest TB rates in Los Angeles County, California, were among persons born in Myanmar, Ethiopia, and Indonesia (*28*).

Our study has limitations. Incidence rate calculations are based on estimated population denominators. NTSS and the ACS rely on self-report for country of birth. Because numerous foreign country boundaries have changed in the past century, some persons may report country of birth in terms of boundaries that existed at the time of their birth or emigration or in accordance with their own national preference. We used the midpoint WHO year of 2014 to compare with the ACS population denominators from 2012–2016. In addition, the method used by WHO for calculating country rates differs from our approach for calculating rates by country of birth in the United States.

Most TB cases in the United States are in persons born outside the United States (*1*), and most cases are attributed to progression of remotely acquired TB infection. Statistical modeling has shown that the most effective intervention for reducing the overall

US TB rate is treatment of LTBI (*29*); rate reduction is predicted to be greater among non–US-born than among US-born persons (*30*). However, available resources for TB prevention programs remain limited, which highlights the need to ensure that TB testing programs are as cost-effective as possible. Tasillo et al. demonstrated the cost-effectiveness of testing and treating LTBI among non–US-born persons (*31*).

Our analysis emphasizes the value of focusing on country of birth and length of time in the United States to guide how to best expand LTBI testing and treatment. Other factors, such as underlying conditions and socioeconomic disparities, could play a role in TB risk (*32*). Accordingly, populations should be prioritized for TB testing according to their relative risk of being TB infected or having TB develop. This prioritization is especially relevant in a low-incidence country like the United States, where careful consideration must be made with regard to LTBI screening to ensure that the benefits outweigh the harm (*33*). Historically, risk for TB infection in non–US-born populations has been based on WHO TB incidence rates (*15*,*16*); however, our analysis shows the differences between WHO rates by country and US rates by country of birth. We believe that US rates are more relevant than WHO rates for TB screening in the United States because expatriates living in the United States differ from the population of their country of birth. Our analysis, in combination with the accuracy and completeness of NTSS and ACS data compared with reported WHO TB incidence rates (*22*), demonstrates that country of birth–specific US rates provide a better method for prioritizing populations for testing in the United States. A next step would be developing a strategy that uses US country-of-birth rates and length of time in the United States to designate cutoff points to prioritize testing for TB infection among persons born outside the United States.

Acknowledgments

We thank state, local, and territorial health department personnel for providing reported TB data; the US Census Bureau for assistance with population data; Andrew Hill for statistical consultation; and Robert H. Pratt for assistance with data manipulation.

About the Author

Ms. Tsang is an epidemiologist with the Division of Tuberculosis Elimination; National Center for HIV/AIDS, Viral Hepatitis, STD, and TB Prevention; CDC, Atlanta. Her research interests include infectious diseases, surveillance, and epidemiology.

References

1. Centers for Disease Control and Prevention. Reported tuberculosis in the United States, 2016. Atlanta: The Centers; 2017.
2. Yuen CM, Kammerer JS, Marks K, Navin TR, France AM. Recent transmission of tuberculosis—United States, 2011–2014. PLoS One. 2016;11:e0153728. https://doi.org/10.1371/journal.pone.0153728
3. Centers for Disease Control and Prevention. Tuberculosis technical instructions for panel physicians [cited 2019 Oct 11]. https://www.cdc.gov/immigrantrefugeehealth/exams/ti/panel/tuberculosis-panel-technical-instructions.html
4. Centers for Disease Control and Prevention. Tuberculosis technical instructions for civil surgeons [cited 2019 Oct 11]. https://www.cdc.gov/immigrantrefugeehealth/exams/ti/civil/tuberculosis-civil-technical-instructions.html
5. Davidow AL, Katz D, Ghosh S, Blumberg H, Tamhane A, Sevilla A, et al.; Tuberculosis Epidemiologic Studies Consortium. Preventing infectious pulmonary tuberculosis among foreign-born residents of the United States. Am J Public Health. 2015;105:e81–8. https://doi.org/10.2105/AJPH.2015.302662
6. Centers for Disease Control and Prevention. Latent TB infection testing and treatment: summary of U.S. recommendations [cited 2019 Jun 27]. https://www.cdc.gov/tb/publications/ltbi/pdf/CDC-USPSTF-LTBI-Testing-Treatment-Recommendations-508.pdf
7. Bibbins-Domingo K, Grossman DC, Curry SJ, Bauman L, Davidson KW, Epling JW Jr, et al.; US Preventive Services Task Force. Screening for latent tuberculosis infection in adults: US Preventive Services Task Force recommendation statement. JAMA. 2016;316:962–9. https://doi.org/10.1001/jama.2016.11046
8. US Census Bureau. Public Use Microdata Sample (PUMS) documentation [cited 2019 Jul 3]. https://www.census.gov/programs-surveys/acs/technical-documentation/pums.html
9. World Health Organization. Tuberculosis (TB), download data as CSV files [cited 2019 May 29]. http://www.who.int/tb/country/data/download
10. United Nations. Member States [cited 2019 May 29]. https://www.un.org/en/member-states/index.html
11. United Nations. Non-Member States [cited 2019 May 29]. https://www.un.org/en/sections/member-states/non-member-states/index.html
12. Menzies NA, Hill AN, Cohen T, Salomon JA. The impact of migration on tuberculosis in the United States. Int J Tuberc Lung Dis. 2018;22:1392–403. https://doi.org/10.5588/ijtld.17.0185
13. Cain KP, Haley CA, Armstrong LR, Garman KN, Wells CD, Iademarco MF, et al. Tuberculosis among foreign-born persons in the United States: achieving tuberculosis elimination. Am J Respir Crit Care Med. 2007;175:75–9. https://doi.org/10.1164/rccm.200608-1178OC
14. Cain KP, Benoit SR, Winston CA, Mac Kenzie WR. Tuberculosis among foreign-born persons in the United States. JAMA. 2008;300:405–12. https://doi.org/10.1001/jama.300.4.405
15. Centers for Disease Control and Prevention. Latent tuberculosis infection: a guide for primary health care providers; Appendix B: identifying persons from high-risk countries [cited 2013 Apr 3]. https://www.cdc.gov/tb/publications/ltbi/appendixb.htm
16. Stop TB Partnership, High burden countries [cited 2019 Jun 27]. http://www.stoptb.org/countries/tbdata.asp
17. Walter ND, Painter J, Parker M, Lowenthal P, Flood J, Fu Y, et al.; Tuberculosis Epidemiologic Studies Consortium.

Persistent latent tuberculosis reactivation risk in United States immigrants. Am J Respir Crit Care Med. 2014;189:88–95.
18. Talwar A, Tsang CA, Price SF, Pratt RH, Walker WL, Schmit KM, et al. Tuberculosis—United States, 2018. Am J Transplant. 2019;19:1582–8. https://doi.org/10.1111/ajt.15384
19. Tsang CA, Langer AJ, Navin TR, Armstrong LR. Tuberculosis among foreign-born persons diagnosed ≥10 years after arrival in the United States, 2010–2015. MMWR Morb Mortal Wkly Rep. 2017;66:295–8. https://doi.org/10.15585/mmwr.mm6611a3
20. Iqbal SA, Winston CA, Bardenheier BH, Armstrong LR, Navin TR. Age-period-cohort analyses of tuberculosis incidence rates by nativity, United States, 1996–2016. Am J Public Health. 2018;108(S4):S315–20. https://doi.org/10.2105/AJPH.2018.304687
21. Guthrie JL, Ronald LA, Cook VJ, Johnston J, Gardy JL. The problem with defining foreign birth as a risk factor in tuberculosis epidemiology studies. PLoS One. 2019;14:e0216271. https://doi.org/10.1371/journal.pone.0216271
22. Winston CA, Navin TR, Becerra JE, Chen MP, Armstrong LR, Jeffries C, et al. Unexpected decline in tuberculosis cases coincident with economic recession—United States, 2009 [cited 2019 May 29]. BMC Public Health. 2011;11:846. https://doi.org/10.1186/1471-2458-11-846
23. US Census Bureau. American Community Survey design and methodology (January 2014) [cited 2019 May 29]. https://www2.census.gov/programs-surveys/acs/methodology/design_and_methodology/acs_design_methodology_report_2014.pdf
24. World Health Organization. Global tuberculosis report 2017 [cited 2019 May 29]. https://www.who.int/tb/publications/global_report/gtbr2017_main_text.pdf
25. United Nations Department of Economic and Social Affairs/Population Division. World Population prospects: methodology of the united nations population estimates and projections, 2017 revision [cited 2019 May 29]. https://population.un.org/wpp/Publications/Files/WPP2017_Methodology.pdf
26. Stennis NL, Trieu L, Ahuja SD, Harris TG. Estimated prevalence of tuberculosis infection among a New York City clinic population using interferon-gamma release assays. Open Forum Infect Dis. 2014;1:ofu047. https://doi.org/10.1093/ofid/ofu047
27. Desale M, Bringardner P, Fitzgerald S, Page K, Shah M. Intensified case-finding for latent tuberculosis infection among the Baltimore City Hispanic population. J Immigr Minor Health. 2013;15:680–5. https://doi.org/10.1007/s10903-012-9692-5
28. Readhead A, Chang AH, Ghosh JK, Sorvillo F, Detels R, Higashi J. Challenges and solutions to estimating tuberculosis disease incidence by country of birth in Los Angeles County. PLoS One. 2018;13:e0209051. https://doi.org/10.1371/journal.pone.0209051
29. Menzies NA, Cohen T, Hill AN, Yaesoubi R, Galer K, Wolf E, et al. Prospects for tuberculosis elimination in the United States: results of a transmission dynamic model. Am J Epidemiol. 2018;187:2011–20. https://doi.org/10.1093/aje/kwy094
30. Hill AN, Becerra J, Castro KG. Modelling tuberculosis trends in the USA. Epidemiol Infect. 2012;140:1862–72. https://doi.org/10.1017/S095026881100286X
31. Tasillo A, Salomon JA, Trikalinos TA, Horsburgh CR Jr, Marks SM, Linas BP. Cost-effectiveness of testing and treatment for latent tuberculosis infection in residents born outside the United States with and without medical comorbidities in a simulation model. JAMA Intern Med. 2017;177:1755–64. https://doi.org/10.1001/jamainternmed.2017.3941
32. Hayward S, Harding RM, McShane H, Tanner R. Factors influencing the higher incidence of tuberculosis among migrants and ethnic minorities in the UK. F1000Res. 2018;7:461.
33. Campbell JR, Dowdy D, Schwartzman K. Treatment of latent infection to achieve tuberculosis elimination in low-incidence countries. PLoS Med. 2019;16:e1002824. https://doi.org/10.1371/journal.pmed.1002824

Address for correspondence: Clarisse A. Tsang, Centers for Disease Control and Prevention, 1600 Clifton Rd NE, Mailstop US12-4, Atlanta, GA 30329-4027, USA; email: ctsang@cdc.gov

Pregnancy Outcomes among Women Receiving rVSVΔ-ZEBOV-GP Ebola Vaccine during the Sierra Leone Trial to Introduce a Vaccine against Ebola

Jennifer K. Legardy-Williams,[1] Rosalind J. Carter,[1] Susan T. Goldstein, Olamide D. Jarrett, Elena Szefer, Augustin E. Fombah, Sarah C. Tinker, Mohamed Samai,[2] Barbara E. Mahon[2]

Little information exists regarding Ebola vaccine rVSVΔG-ZEBOV-GP and pregnancy. The Sierra Leone Trial to Introduce a Vaccine against Ebola (STRIVE) randomized participants without blinding to immediate or deferred (18–24 weeks postenrollment) vaccination. Pregnancy was an exclusion criterion, but 84 women were inadvertently vaccinated in early pregnancy or became pregnant ≤60 days after vaccination or enrollment. Among immediate vaccinated women, 45% (14/31) reported pregnancy loss, compared with 33% (11/33) of unvaccinated women with contemporaneous pregnancies (relative risk 1.35, 95% CI 0.73–2.52). Pregnancy loss was similar among women with higher risk for vaccine viremia (conception before or ≤14 days after vaccination) (44% [4/9]) and women with lower risk (conception >15 days after vaccination) (45% [10/22]). No congenital anomalies were detected among 44 live-born infants examined. These data highlight the need for Ebola vaccination decisions to balance the possible risk for an adverse pregnancy outcome with the risk for Ebola exposure.

The 2014–2016 West Africa Ebola virus disease outbreak was unprecedented in magnitude and complexity, resulting in >28,000 cases and >11,000 deaths in the 3 highly affected countries (Sierra Leone, Guinea, and Liberia) (*1*). During the outbreak, clinical trials of the investigational Ebola vaccine rVSVΔG-ZEBOV-GP (Merck, https://merck.com) were rapidly implemented. The vaccine, a live-attenuated recombinant vesicular stomatitis virus (rVSV) vaccine, was found to be protective when used in a ring vaccination strategy in Guinea (*2*). This result spurred subsequent use of this vaccine under expanded use protocols as part of the public health response to Ebola outbreaks. As of late November 2019, >250,000 investigational doses had been administered in 2 outbreaks in the Democratic Republic of the Congo during 2018 and 2019 (*3*). The vaccine received conditional marketing approval from the European Medicines Agency and World Health Organization prequalification in November 2019 (*4*). However, little information on the safety of the vaccine for pregnant women is available, making decisions about vaccination during pregnancy challenging.

Pregnancy was an exclusion criterion for all rVSVΔG-ZEBOV-GP clinical trials, not only because so little was known about the safety of the vaccine generally but also because adverse effects on pregnancy were biologically plausible (*5*,*6*). A phase 1 trial was paused because of concerns about postvaccination arthritis associated with dissemination of the vaccine rVSV into the joints, raising concerns that other adverse reactions could occur consequent to vaccine viremia (*7*–*9*). In the Sierra Leone Trial to Introduce a Vaccine against Ebola (STRIVE) (*10*,*11*), some women were enrolled who were inadvertently vaccinated early in pregnancy, and some women became pregnant ≤60 days after enrollment or vaccination. STRIVE followed these women for pregnancy outcomes. We have previously reported preliminary

Author affiliations: Centers for Disease Control and Prevention, Atlanta, Georgia, USA (J.K. Legardy-Williams, R.J. Carter, S.T. Goldstein, O.D. Jarrett, S.C. Tinker, B.E. Mahon); University of Illinois at Chicago, Chicago, Illinois, USA (O.D. Jarrett); The Emmes Corporation (E. Szefer); University of Sierra Leone College of Medicine and Allied Health Sciences, Freetown, Sierra Leone (A.E. Fombah, M. Samai)

DOI: https://doi.org/10.3201/eid2603.191018

[1]These first authors contributed equally to this article.

[2]These authors were co–principal investigators.

analysis of pregnancy outcomes (*10*); we now report a more detailed analysis.

Methods

STRIVE was a phase 2/3, unblinded, individually randomized clinical trial to assess the safety and efficacy of rVSVΔG-ZEBOV-GP; the methods have been detailed previously (*10*). In brief, adult (≥18 years of age) healthcare and Ebola frontline workers were randomized to immediate or deferred (18–24 weeks later) vaccination with a single intramuscular dose (nominal 2×10^7 PFUs) of rVSVΔG-ZEBOV-GP vaccine. No placebo was used; all participants who were eligible for vaccination were offered vaccine by the end of the study. The immediate group was vaccinated from April through August 2015 and the deferred group from September through December 2015. Before the deferred group was vaccinated, they were referred to as the unvaccinated group; once vaccinated, they were referred to as the deferred crossover vaccinated group (Figure 1).

Pregnancy was an exclusion criterion for the study and was assessed during preenrollment screening. At this screening, women of reproductive age (18–49 years of age) were asked if they were pregnant and were required to take a urine pregnancy test. Before deferred vaccination, women 18–49 years of age were again asked if they were pregnant and were required to take another urine pregnancy test. Vaccinated women were counseled to avoid pregnancy for ≤60 days after vaccination. Contraception was available locally but was not provided by the trial. Participants were referred to the Ministry of Health's Family Planning Service Clinics if they requested contraception.

All study participants received monthly calls for 6 months after vaccination to monitor for the onset of Ebola, safety outcomes, and, for women, pregnancy. Home visits were conducted if participants could not be contacted by phone. A STRIVE telephone hotline was also available 24/7 for participants to report any medical issue. Women who reported pregnancy were monitored through their pregnancy outcome.

The Sierra Leone Ethics and Scientific Review Committee, the CDC Institutional Review Board, the Pharmacy Board of Sierra Leone, and the US Food and Drug Administration reviewed and approved the study design. The trial was conducted in accordance with the International Council for Harmonization's Good Clinical Practice standards (https://ich.org). All women signed informed consent forms at screening for pregnancy testing and enrollment.

Pregnancy and Infant Follow-Up

During each monthly follow-up call, we asked female participants about pregnancy. If a woman reported being pregnant, no confirmation (e.g., urine or blood pregnancy test, physical examination, or sonogram) was required. For the purpose of follow-up, we calculated the estimated date of conception (EDC) as the date of the last menstrual period (LMP) plus 14 days. Women whose EDC was ≤60 days after enrollment or vaccination (immediate or deferred crossover) were followed monthly by a STRIVE study nurse until a pregnancy outcome was documented. STRIVE did not provide clinical care for pregnant women; women were referred to free prenatal care provided by the Ministry of Health. For 1 woman whose LMP was not known and who delivered at full term, we used the actual delivery date minus 40 weeks to determine EDC. In this analysis, we include women whose EDC was ≤60 days after enrollment or vaccination.

We categorized pregnancy outcomes as live birth, pregnancy loss, ectopic pregnancy, or unknown. The live birth category included both preterm and term births, as self-reported by the mother. Because STRIVE did not routinely collect exact dates of pregnancy losses, we could not reliably differentiate between spontaneous abortions and stillbirths, so we grouped them into a single pregnancy loss category for the analysis.

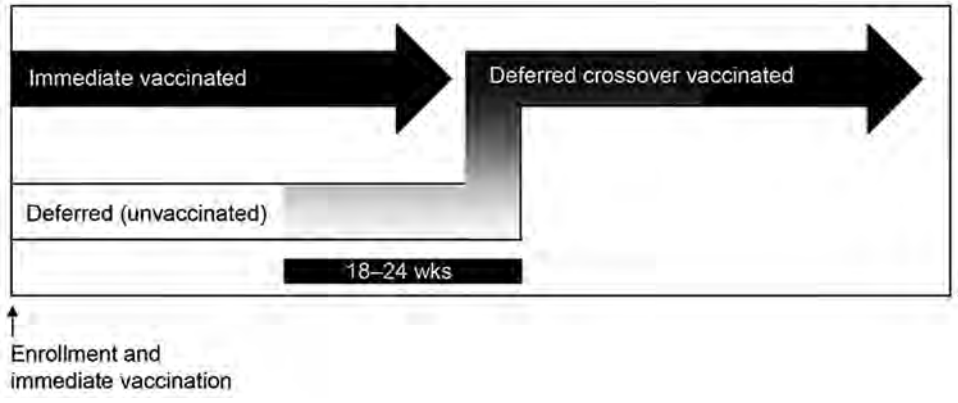

Figure 1. Enrollment and vaccination period for 84 participants in Sierra Leone Trial to Introduce a Vaccine against Ebola (STRIVE). Three participants randomized to the immediate group were unvaccinated. After vaccination, participants in the deferred group were eligible for vaccination at 18–24 weeks postenrollment. Upon vaccination, participants in the deferred group were referred to as the deferred crossover vaccinated group.

Induced abortion is not legal in Sierra Leone but is reported to be available (*12*); women who had an induced abortion might not have reported their pregnancy or might have reported the pregnancy outcome as a spontaneous abortion. The unknown category included women for whom follow-up was not completed and whose pregnancy outcome therefore could not be determined. After delivery, mothers were asked about the date of delivery and the infant's birth weight.

A STRIVE study nurse examined live-born infants at ≥28 days of life. Study nurses received training on infant examination by a team of physicians from Sierra Leone and the United States that included a pediatrician. The infant examination, which was usually conducted at the woman's home, included examination of the infant's general appearance, extremities, head and face, chest, abdomen, anus, genitourinary system, and musculoskeletal system for the presence of external congenital anomalies; no vision or hearing tests were conducted. Nurses were instructed to refer infants to a study physician for further evaluation if the examination raised any concerns, and, if necessary, the infant was then referred to a pediatrician.

Using conservative estimates, we defined pregnancy groups as either high viremia risk (if EDC was before vaccination or ≤14 days after vaccination, including women who were pregnant at the time of vaccination) or low viremia risk (if the EDC was ≥15 days after vaccination). We based these determinations on studies showing that viremia or PCR positivity peaks in healthy adults 1–3 days after vaccination and usually resolves within 7–14 days after vaccination (*7*–*9*,*13*–*15*).

Statistical Methods and Analyses

For comparison of outcomes in vaccinated and unvaccinated women, we included only pregnancies in the immediate vaccinated group and the unvaccinated group. We did not include the deferred crossover vaccinated group in this specific analysis because multiple time-related factors could have affected earlier (immediate and unvaccinated) and later (deferred crossover) pregnancies differently. These potentially confounding factors include differential access to healthcare services, such as prenatal and maternity services, during versus at the end of the Ebola outbreak; infections such as malaria that have strong seasonal patterns; and attitudes toward pregnancy during versus after the Ebola epidemic. For comparison of pregnancy outcomes based on viremia risk, however, we included both the immediate and deferred crossover vaccinated groups separately (because of the confounding we have described) and combined (because of small sample size).

We reported descriptive statistics summarizing maternal and infant characteristics. Counts and percentages are reported for binary characteristics; medians and ranges are reported for continuous characteristics. We computed the relative risk (RR) of pregnancy loss and the associated exact 95% CI, comparing the immediate vaccinated and unvaccinated groups. We used Barnard's unconditional exact test to test for differences in occurrence of pregnancy loss between the immediate vaccination and unvaccinated groups and between viremia risk categories within vaccination groups. Women with unknown outcomes were excluded from primary analyses. However, we conducted sensitivity analyses assuming that all pregnancies with unknown outcome were classified as either pregnancy loss or live birth to understand the maximum potential effect of missing data.

Results

Of the 8,651 participants enrolled in STRIVE, 3,101 were women of reproductive age (18–49 years of age). Eighty-four (2.7%) of these women had a singleton pregnancy (no multiple gestations) with EDC ≤60 days from enrollment or vaccination, including 31 in the immediate vaccinated group, 35 in the unvaccinated group, and 18 in the deferred crossover vaccinated group. At enrollment, the median age of these women was 28 years (range 20–40 years); most of these women were nurses (66 [79%]) or frontline Ebola responders (14 [16%]) (Table 1). Baseline demographic characteristics of vaccinated (immediate and deferred crossover) and unvaccinated pregnant women were generally similar.

The 84 pregnancies led to 51 live births (49 term and 2 preterm) and 30 pregnancy losses (Table 1). For 3 women (2 unvaccinated and 1 deferred crossover vaccinated), the pregnancy outcome was not known. No ectopic pregnancies or neonatal deaths were reported. Of the 51 live births, 29 were in vaccinated women and 22 in unvaccinated women. Most (46 [90%]) infants were delivered in a hospital; 5 (10%) were born at home. The median birth weight was 3,210 g (range 2,400–5,200 g). STRIVE staff obtained consent to examine 44 of the 51 infants (born to 28 vaccinated and 16 unvaccinated women); no external congenital anomalies were documented among these infants.

A total of 7 serious adverse events (SAEs) were reported among pregnant participants. Five SAEs were hospitalizations for a pregnancy-related complication: gestational hypertension (2 cases), prolonged labor (2 cases), and a postpartum hemorrhage (1 case) that resulted in a maternal death. Two pregnant

Table 1. Demographic characteristics and pregnancy outcomes by vaccination group among 84 women with estimated date of conception ≤60 days from vaccination or enrollment, Sierra Leone Trial to Introduce a Vaccine against Ebola*

Characteristic	Immediate vaccinated	Unvaccinated	Deferred crossover vaccinated	Total
Total	31	35	18	84
Median age, y (range)	27 (22–38)	29 (20–40)	28 (20–38)	28 (20–40)
Primary occupation				
Nurse†	24 (77)	29 (83)	13 (72)	66 (79)
Frontline worker	5 (16)	6 (17)	3 (17)	14 (16)
Other‡	2 (7)	0	2 (11)	4 (5)
Prior pregnancy				
No	10 (32)	12 (34)	6 (33)	28 (33)
Yes	21 (68)	23 (66)	12 (67)	56 (67)
Pregnancy outcomes				
Known	31 (100)	33 (94)	17 (94)	81 (96)
Live birth	17 (55)	22 (66)§	12 (71)§	51 (63)
Preterm delivery	2	0	0	2
Term delivery	15	22	12	49
Pregnancy loss¶	14 (45)	11 (33)§	5 (29)§	30 (37)
Unknown	0	2 (6)	1 (6)	3 (4)

*Values are no. (%) except as indicated.
†Includes nurse, nurse aide, maternal–child health aide, nursing student, midwife, community health nurse, and vaccinator.
‡Includes allied health profession, community health worker, dentist, medical counselor, nutritionist, physiotherapist, vaccinator, and surveillance worker.
§Denominator for live birth and pregnancy loss includes number of pregnancies with known outcomes (i.e., unknown outcomes excluded).
¶Pregnancy loss includes spontaneous abortion and stillbirth.

women had hospitalizations for SAEs not related to pregnancy (1 for enteritis and 1 for malaria).

We compiled the number and outcomes of pregnancies by EDC among participants in this analysis (Figure 2). Among the 48 vaccinated women with a known pregnancy outcome based on EDC calculations, 9 were pregnant at the time of vaccination, all with a negative self-report and negative urine pregnancy test. An additional 8 women had an EDC of 0–14 days after vaccination. Thus, a total of 17 women were in the high viremia risk group. We observed no difference in proportions of live births and pregnancy loss between women who were pregnant when vaccinated and those who became pregnant 0–14 days after vaccination (data not shown). The other 31 women, with EDC 15–60 days after vaccination, comprised the low viremia risk group.

Pregnancy Outcome by Vaccination Group

In the comparison of pregnancy outcome in the vaccinated and unvaccinated women with known outcomes, pregnancy loss occurred more frequently in the immediate vaccinated group (45% [14/31]) compared with the unvaccinated group (33% [11/33]), although this difference was not statistically significant (unadjusted RR 1.35 [95% CI 0.73–2.52]; p = 0.34) (Table 1). The calculated gestational ages were similar between vaccination groups (data not shown). A sensitivity analysis that included the 2 pregnancies with unknown outcomes as pregnancy losses reduced the RR to 1.22 (95% CI 0.68–2.17); including them as live births increased the RR to 1.44 (95% CI 0.77–2.68).

Pregnancy Outcome by Viremia Risk Group

Pregnancy loss occurred at similar rates in the high viremia risk group (35% [6/17]) and the low viremia risk group (42% [13/31]; p value for comparison 0.69) and with similar patterns in the immediate vaccinated and deferred crossover vaccinated groups (Table 2). Within the high viremia risk group, pregnancy loss was reported for 3 (33%) of the 9 women who were pregnant when vaccinated and by 3 (38%) of the 8 women whose EDC was 0–14 days after vaccination. In the sensitivity analyses, including the 1 unknown pregnancy outcome in the deferred crossover group as a pregnancy loss or as a live birth did not change the results (data not shown).

Discussion

This analysis of STRIVE clinical trial data provides valuable, although not conclusive, information about pregnancy outcomes in women who were pregnant when they were vaccinated with the investigational Ebola vaccine rVSVΔG-ZEBOV-GP or who became pregnant within 60 days after vaccination. The 45% rate of pregnancy loss in the immediate vaccination group was not significantly higher than the 33% rate in the contemporaneous unvaccinated group. However, only a small number of pregnancies occurred among participants in STRIVE, and data from larger study samples would be needed to rule out a meaningful difference in the percentage of pregnancy losses.

We observed no difference in pregnancy loss when we compared women who had a high likelihood of having been pregnant during the period of postvaccination vaccine viremia to those who

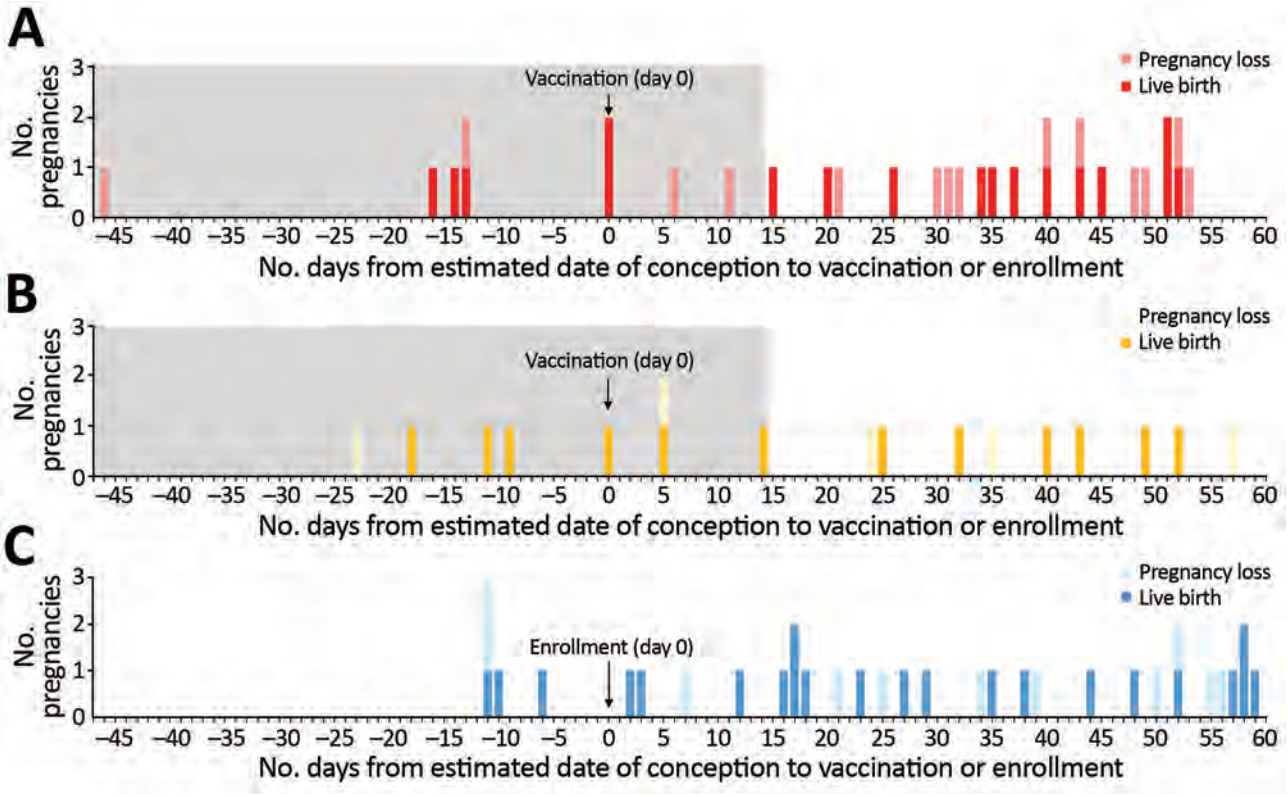

Figure 2. Number of pregnancies by estimated date of conception relative to vaccination or enrollment among 81 participants in the Sierra Leone Trial to Introduce a Vaccine against Ebola (STRIVE). A) Immediate vaccination group (n = 31). B) Deferred crossover vaccination group (n = 17). C) Unvaccinated group (n = 33). Because pregnancy outcome for 3 of the 84 women was unknown, these 3 women are not included in the figure. Outcomes include live birth (term and preterm) and pregnancy loss (early and late loss). Gray shaded area denotes the high viremia risk period (i.e., women who were pregnant when vaccinated or became pregnant 0–14 days after vaccination).

became pregnant later after vaccination. Also, 44 of 51 live-born infants were examined, and no external congenital anomalies were detected, although only a small number of infants were born to vaccinated women and no diagnostic testing was conducted. In the absence of more definitive data, our results can inform consideration of the inclusion of pregnant women in rVSVΔG-ZEBOV-GP vaccination programs, such as in recent and, as of December 2019, ongoing responses to Ebola outbreaks in the Democratic Republic of the Congo (*3*). The limitations of our results highlight the need for ongoing collection of information on pregnancy outcomes in vaccinated women.

The rVSVΔG-ZEBOV-GP vaccine has a vesicular stomatitis virus (VSV) backbone in which the gene encoding the VSV envelope glycoprotein is replaced with the gene encoding the Zaire Ebola virus (Kikwit strain) glycoprotein. VSV normally infects animals; human disease has been reported rarely, and no information exists regarding wild-type VSV infection in human pregnancy (*16*). In 1 study from the 1970s, spontaneous abortion and neonatal death were reported in ferrets experimentally infected with VSV-Indiana, a wild-type VSV strain, and virus was recovered from the placentas of 2 experimentally vaccinated ferrets (*5*). Vaccine VSV might be less virulent than wild-type VSV (*17*). Because rVSVΔG-ZEBOV-GP is a replication-competent vaccine, rVSVΔG-ZEBOV-GP vaccination commonly produces rVSV vaccine viremia within a few days after vaccination (*8*,*9*,*13*,*14*). The detection of vaccine virus in joint fluid and skin lesion in some vaccinated persons in phase 1 studies of this vaccine raised the possibility of adverse effects on pregnancy (*8*,*13*). A total of 20 additional women who were pregnant when vaccinated or became pregnant soon after vaccination with rVSVΔG-ZEBOV-GP have been reported in 3 clinical trials other than STRIVE during 2014–2016. Outcomes for these 20 pregnancies included 2 spontaneous abortions at ≈1 month after conception and 1 stillbirth, for an overall pregnancy loss rate of 15% (*7*,*18*,*19*).

In STRIVE, as in the other phase 2/3 rVSVΔG-ZEBOV-GP trials initiated during the West Africa Ebola epidemic, pregnancy was an exclusion criterion. STRIVE screened women of childbearing age for

Table 2. Pregnancy outcome by risk for vaccine viremia during pregnancy among 48 women with estimated date of conception ≤60 days from vaccination, Sierra Leone Trial to Introduce a Vaccine against Ebola*

Characteristic	Live birth	Pregnancy loss	Total	Barnard's exact p value
Immediate vaccinated, no.	17	14	31	1
High viremia risk	5 (56)	4 (44)	9	NA
Low viremia risk	12 (55)	10 (45)	22	NA
Deferred crossover vaccinated, no.	12	5	17	0.75
High viremia risk	6 (75)	2 (25)	8	NA
Low viremia risk	6 (67)	3 (33)	9	NA
Total vaccinated, no.	29	19	48	0.69
High viremia risk	11 (65)	6 (35)	17	NA
Low viremia risk	18 (58)	13 (42)	31	NA

*Values are no. (%) except as indicated. NA, not applicable.
†High viremia risk is defined as estimated date of conception before vaccination or 0–14 days after vaccination. Low viremia risk is defined as estimated date of conception 15–60 days after vaccination.

pregnancy and counseled vaccinated participants to avoid becoming pregnant for ≤60 days after vaccination. For most women who were inadvertently vaccinated while pregnant, conception was probably too recent for the pregnancy test to be positive or for the woman to realize she was pregnant. Use of a questionnaire, such as the Pregnancy Exclusion Checklist, in combination with the urine pregnancy test might have more effectively identified women who were early in pregnancy (*20*). However, the EDC of 1 of the women with a negative urine pregnancy test was 46 days before vaccination. This woman possibly did not know or did not disclose she was pregnant, or the urine pregnancy test might have been performed incorrectly or was not able to detect the pregnancy. A strength of our analysis was that the design of the trial yielded a contemporaneous unvaccinated group for comparison to the vaccinated group, and that information was available on the outcomes of almost all pregnancies, a result of the identification and comprehensive follow-up of all pregnant women in STRIVE.

Our study had several limitations, however, beyond the small sample size and inability to adjust for confounding factors. In cases of pregnancy loss, information on the timing of the loss was often lacking, limiting our ability to differentiate between early and late pregnancy loss. Also, because we had limited information about the timing of pregnancies (ultrasound dating is rarely available in Sierra Leone), we had to calculate EDCs from LMPs, which is not an ideal method (*21*). Unrecognized or unreported pregnancies that led to pregnancy loss might have occurred, and because we did not confirm the pregnancies, a pregnancy loss might have been reported when a woman was not actually pregnant (i.e., late menstrual cycle reported as spontaneous abortion). Another important limitation is that STRIVE has no information on long-term outcomes in infants.

The few published data on pregnancy loss for Sierra Leone are limited to stillbirths (late pregnancy) (*22*) and do not include spontaneous or induced abortions. However, some conditions common in Sierra Leone, such as malaria, increase the risk for stillbirth and spontaneous abortion (*23*,*24*). A limitation of our data is that we were not able to ascertain the number of pregnancy losses in STRIVE that were caused by induced abortion. Induced abortions are illegal in Sierra Leone, but they occur (*12*). When induced abortions are included in analysis of US pregnancy outcomes, ≈34% of pregnancies end in loss, similar to the loss percentage observed during the STRIVE trial (37%) (*25*). Because the trial was unblinded, women in the immediate vaccinated group and the unvaccinated group knew their vaccination status, which could have affected their decision-making. For instance, vaccinated women might have been concerned about the safety of the vaccine in pregnancy and thus were more likely than unvaccinated women to terminate the pregnancy, and unvaccinated women might have been more likely to terminate in the context of the outbreak. Also, STRIVE was launched during a terrible epidemic that caused enormous social upheaval. This timing might also have affected decision-making about pregnancy termination.

Vaccination with rVSVΔG-ZEBOV-GP has become an integral component of the public health response to recent Ebola outbreaks, including the ongoing outbreak in the Democratic Republic of the Congo (*3*,*26*), underscoring the urgency of obtaining a full understanding of the safety of the vaccine in pregnancy. The World Health Organization's Strategic Advisory Group of Experts on Immunization, recognizing the high risk for maternal and fetal death from Ebola virus infection, has endorsed the need for careful evaluation of risks and benefits in a local context by national regulatory authorities and ethics committees in decision-making about rVSVΔG-ZEBOV-GP vaccination of pregnant women during an Ebola outbreak (*27*). The decision to offer rVSVΔG-ZEBOV-GP vaccine to pregnant women will need to balance the risk for an adverse pregnancy outcome with the risk for exposure to and subsequent infection with Ebola (*28*–*33*). When vaccination is offered to pregnant women, the provision

of culturally appropriate information to assist women in making informed decisions about whether to accept vaccination will be critical. The STRIVE experience contributes information that should be useful for these decisions. It also highlights the urgent need for additional comprehensive and accurate pregnancy outcome information, whether through clinical trials, in which inclusion of pregnant women is increasingly being considered (*32*), or through observational strategies, such as data collection during outbreak response or pregnancy registries.

Acknowledgments

We thank all of the healthcare and frontline workers who were STRIVE participants and the STRIVE staff for their tireless dedication to the execution of the study.

This trial was supported by the Centers for Disease Control and Prevention, the Biomedical Advanced Research and Development Authority, and the National Institutes of Health, with additional support from the CDC Foundation. ClinicalTrials.gov registration no. NCT02378753; Pan African Clinical Trials Registry no. PACTR201502001037220.

About the Author

Ms. Legardy-Williams is a health scientist at the Centers for Disease Control and Prevention's National Center for Immunization and Respiratory Diseases. She serves as the implementation lead for STRIVE, for which she led a team focused on the study operations. Her primary research interests are infectious diseases (e.g., Ebola, vaccine-preventable diseases, and sexually transmitted diseases) and contraceptive methods.

References

1. World Health Organization. Ebola situation report, Mar 30, 2016 [cited 2017 Dec 27]. http://apps.who.int/ebola/current-situation/ebola-situation-report-30-march-2016
2. Henao-Restrepo AM, Longini IM, Egger M, Dean NE, Edmunds WJ, Camacho A, et al. Efficacy and effectiveness of an rVSV-vectored vaccine expressing Ebola surface glycoprotein: interim results from the Guinea ring vaccination cluster-randomised trial. Lancet. 2015;386:857–66. https://doi.org/10.1016/S0140-6736(15)61117-5
3. World Health Organization. Ebola situation reports: Democratic Republic of the Congo. 2019 [cited 2019 Dec 24]. https://www.who.int/publications-detail/ebola-virus-disease-democratic-republic-of-congo-external-situation-report-73-2019
4. Burki T. Ebola virus vaccine receives prequalification. Lancet. 2019;394:1893. https://doi.org/10.1016/S0140-6736(19)32905-8
5. Ezeanolue E, Harriman K, Hunter P, Kroger A, Pellegrini C. General best practice guidelines for immunization. 2017 [cited 2019 Jun 24]. https://www.cdc.gov/vaccines/hcp/acip-recs/general-recs/index.html
6. Suffin SC, Muck KB, Porter DD. Vesicular stomatitis virus causes abortion and neonatal death in ferrets. J Clin Microbiol. 1977;6:437–8.
7. Agnandji ST, Fernandes JF, Bache EB, Obiang Mba RM, Brosnahan JS, Kabwende L, et al.; VEBCON Consortium. Safety and immunogenicity of rVSVΔG-ZEBOV-GP Ebola vaccine in adults and children in Lambaréné, Gabon: a phase I randomised trial. PLoS Med. 2017;14:e1002402. https://doi.org/10.1371/journal.pmed.1002402
8. Huttner A, Dayer JA, Yerly S, Combescure C, Auderset F, Desmeules J, et al.; VSV-Ebola Consortium. The effect of dose on the safety and immunogenicity of the VSV Ebola candidate vaccine: a randomised double-blind, placebo-controlled phase 1/2 trial. Lancet Infect Dis. 2015;15:1156–66. https://doi.org/10.1016/S1473-3099(15)00154-1
9. Regules JA, Beigel JH, Paolino KM, Voell J, Castellano AR, Hu Z, et al.; rVSVΔG-ZEBOV-GP Study Group. A recombinant vesicular stomatitis virus Ebola vaccine. N Engl J Med. 2017;376:330–41. https://doi.org/10.1056/NEJMoa1414216
10. Samai M, Seward JF, Goldstein ST, Mahon BE, Lisk DR, Widdowson MA, et al. The Sierra Leone Trial to Introduce a Vaccine Against Ebola: an evaluation of rVSVΔG-ZEBOV-GP vaccine tolerability and safety during the West Africa Ebola outbreak. J Infect Dis. 2018;217(suppl_1):S6–S15.
11. Widdowson MA, Schrag SJ, Carter RJ, Carr W, Legardy-Williams J, Gibson L, et al. Implementing an Ebola vaccine study—Sierra Leone. MMWR Suppl. 2016;65:98–106. https://doi.org/10.15585/mmwr.su6503a14
12. Paul M, Gebreselassie H, Samai M, Benson J, Kargbo S, Lazzarino MM. Unsafe abortion in Sierra Leone: an examination of costs and burden of treatment on healthcare resources. J Womens Health Care. 2015;4:1–6.
13. Agnandji ST, Huttner A, Zinser ME, Njuguna P, Dahlke C, Fernandes JF, et al. Phase 1 trials of rVSV Ebola vaccine in Africa and Europe. N Engl J Med. 2016;374:1647–60. https://doi.org/10.1056/NEJMoa1502924
14. ElSherif MS, Brown C, MacKinnon-Cameron D, Li L, Racine T, Alimonti J, et al.; Canadian Immunization Research Network. Assessing the safety and immunogenicity of recombinant vesicular stomatitis virus Ebola vaccine in healthy adults: a randomized clinical trial. CMAJ. 2017;189:E819–27. https://doi.org/10.1503/cmaj.170074
15. Kennedy SB, Bolay F, Kieh M, Grandits G, Badio M, Ballou R, et al.; PREVAIL I Study Group. PREVAIL I Study Group. Phase 2 placebo-controlled trial of two vaccines to prevent Ebola in Liberia. N Engl J Med. 2017;377:1438–47. https://doi.org/10.1056/NEJMoa1614067
16. Monath TP, Fast PE, Modjarrad K, Clarke DK, Martin BK, Fusco J, et al.; Brighton Collaboration Viral Vector Vaccines Safety Working Group (V3SWG). rVSVΔG-ZEBOV-GP (also designated V920) recombinant vesicular stomatitis virus pseudotyped with Ebola Zaire glycoprotein: standardized template with key considerations for a risk/benefit assessment. Vaccine X. 2019;1:100009. https://doi.org/10.1016/j.jvacx.2019.100009
17. Mire CE, Miller AD, Carville A, Westmoreland SV, Geisbert JB, Mansfield KG, et al. Recombinant vesicular stomatitis virus vaccine vectors expressing filovirus glycoproteins lack neurovirulence in nonhuman primates. PLoS Negl Trop Dis. 2012;6:e1567. https://doi.org/10.1371/journal.pntd.0001567
18. Halperin SA, Arribas JR, Rupp R, Andrews CP, Chu L, Das R, et al.; V920-012 Study Team. Six-month safety data of recombinant vesicular stomatitis virus-Zaire Ebola virus envelope glycoprotein vaccine in a phase 3 double-blind, placebo-controlled randomized study in healthy adults. J Infect Dis. 2017;215:1789–98. https://doi.org/10.1093/infdis/jix189

19. Juan-Giner A, Tchaton M, Jemmy JP, Soumah A, Boum Y, Faga EM, et al. Safety of the rVSV ZEBOV vaccine against Ebola Zaire among frontline workers in Guinea. Vaccine. 2019;37:7171–7. https://doi.org/10.1016/j.vaccine.2018.09.009
20. Stanback J, Qureshi Z, Sekadde-Kigondu C, Gonzalez B, Nutley T. Checklist for ruling out pregnancy among family-planning clients in primary care. Lancet. 1999;354:566. https://doi.org/10.1016/S0140-6736(99)01578-0
21. Committee on Obstetric Practice, the American Institute of Ultrasound in Medicine, and the Society for Maternal-Fetal Medicine . Committee opinion no 700: methods for estimating the due date. Obstet Gynecol. 2017;129:e150–4. https://doi.org/10.1097/AOG.0000000000002046
22. Statistics Sierra Leone, ICF International. Sierra Leone Demographic and Health Survey 2013. 2014 [cited 2019 Nov 27]. https//dhsprogram.com/pubs/pdf/fr297.pdf
23. Desai M, ter Kuile FO, Nosten F, McGready R, Asamoa K, Brabin B, et al. Epidemiology and burden of malaria in pregnancy. Lancet Infect Dis. 2007;7:93–104. https://doi.org/10.1016/S1473-3099(07)70021-X
24. Giakoumelou S, Wheelhouse N, Cuschieri K, Entrican G, Howie SE, Horne AW. The role of infection in miscarriage. Hum Reprod Update. 2016;22:116–33. https://doi.org/10.1093/humupd/dmv041
25. Curtin SC, Abma JC, Ventura SJ, Henshaw SK. Pregnancy rates for U.S. women continue to drop. NCHS Data Brief. 2013;136:1–8.
26. World Health Organization. Meeting of the Strategic Advisory Group of Experts on Immunization, April 2017—conclusions and recommendations. Wkly Epidemiol Rec. 2017;92:301–20.
27. World Health Organization. Meeting of the Strategic Advisory Group of Experts on Immunization, December 2018—conclusions and recommendations. Wkly Epidemiol Rec. 2018;49:661–80.
28. Bebell LM, Oduyebo T, Riley LE. Ebola virus disease and pregnancy: A review of the current knowledge of Ebola virus pathogenesis, maternal, and neonatal outcomes. Birth Defects Res. 2017;109:353–62.
29. Feldmann H, Geisbert TW. Ebola haemorrhagic fever. Lancet. 2011;377:849–62. https://doi.org/10.1016/S0140-6736(10)60667-8
30. Henwood PC, Bebell LM, Roshania R, Wolfman V, Mallow M, Kalyanpur A, et al. Ebola virus disease and pregnancy: a retrospective cohort study of patients managed at 5 Ebola treatment units in West Africa. Clin Infect Dis. 2017;65:292–9. https://doi.org/10.1093/cid/cix290
31. Mupapa K, Mukundu W, Bwaka MA, Kipasa M, De Roo A, Kuvula K, et al. Ebola hemorrhagic fever and pregnancy. J Infect Dis. 1999;179(Suppl 1):S11–2. https://doi.org/10.1086/514289
32. Krubiner CB, Faden RR, Karron RA, Little MO, Lyerly AD, Abramson JS, et al. Pregnant women and vaccines against emerging epidemic threats: ethics guidance for preparedness, research, and response. Vaccine. 2019;May 3:S0264–410X(19)30045–3.
33. Lyman M, Mpofu JJ, Soud F, Oduyebo T, Ellington S, Schlough GW, et al. Maternal and perinatal outcomes in pregnant women with suspected Ebola virus disease in Sierra Leone, 2014. Int J Gynaecol Obstet. 2018;142:71–7. https://doi.org/10.1002/ijgo.12490

Address of correspondence: Jennifer K. Legardy-Williams, Centers for Disease Control and Prevention, 1600 Clifton Rd NE, Mailstop H24-8, Atlanta, GA 30329-4027, USA; email: yzl3@cdc.gov

Acquisition of Plasmid with Carbapenem-Resistance Gene bla_{KPC2} in Hypervirulent *Klebsiella pneumoniae*, Singapore

Yahua Chen, Kalisvar Marimuthu, Jeanette Teo, Indumathi Venkatachalam, Benjamin Pei Zhi Cherng, Liang De Wang, Sai Rama Sridatta Prakki, Weizhen Xu, Yi Han Tan, Lan Chi Nguyen, Tse Hsien Koh, Oon Tek Ng, Yunn-Hwen Gan

The convergence of carbapenem-resistance and hypervirulence genes in *Klebsiella pneumoniae* has led to the emergence of highly drug-resistant superbugs capable of causing invasive disease. We analyzed 556 carbapenem-resistant *K. pneumoniae* isolates from patients in Singapore hospitals during 2010–2015 and discovered 18 isolates from 7 patients also harbored hypervirulence features. All isolates contained a closely related plasmid (pKPC2) harboring bla_{KPC-2}, a *K. pneumoniae* carbapenemase gene, and had a hypervirulent background of capsular serotypes K1, K2, and K20. In total, 5 of 7 first patient isolates were hypermucoviscous, and 6 were virulent in mice. The pKPC2 was highly transmissible and remarkably stable, maintained in bacteria within a patient with few changes for months in the absence of antimicrobial drug selection pressure. Intrapatient isolates were also able to acquire additional antimicrobial drug resistance genes when inside human bodies. Our results highlight the potential spread of carbapenem-resistant hypervirulent *K. pneumoniae* in Singapore.

The rise of multidrug-resistant (MDR) *Enterobacteriaceae* prompted the World Health Organization to classify carbapenem-resistant *Enterobacteriaceae*, of which *Klebsiella* is the most common genus, on the global priority list of antibiotic-resistant bacteria in 2017 (*1*). Carbapenem-resistant *K. pneumoniae* (CRKP, also including *K. quasipneumoniae*) infections are generally hospital acquired, particularly among elderly and immunocompromised patients (*2*,*3*). The major carbapenemases include *K. pneumoniae* carbapenemase (KPC), New Delhi metallo-β-lactamase, and carbapenem-hydrolyzing class D β-lactamase (OXA), all of which have spread globally (*4*–*7*).

The Carbapenemase-Producing *Enterobacteriaceae* in Singapore (CaPES) study initiated in 2013 revealed that the rate of incident carbapenem-resistant *Enterobacteriaceae* clinical cultures in government hospitals in Singapore increased during 2011–2013 and plateaued thereafter (*8*). The number of cases of hypervirulent *K. pneumoniae* has increased in the past 3 decades in parts of Asia, and likewise, the number of cases of monomicrobial *Klebsiella*-induced liver abscesses has also increased (*9*,*10*).

The prevalence of antimicrobial resistance among hypervirulent *K. pneumoniae* isolates is rare compared with that of standard isolates (*11*,*12*); hypervirulent *K. pneumoniae* and CRKP seem to have their own particular reservoirs and remain mostly segregated from each other. However, hypervirulent *K. pneumoniae* and CRKP isolates can converge in the same organism, leading to the emergence of superbugs resistant to antimicrobial drugs of even the last line of treatment that are capable of infecting healthy persons. This emergence has already been reported in China, Brazil, and the United Kingdom (*13*–*15*). The fatal outbreak that occurred in a hospital in China in 2016 was caused by a carbapenem-resistant hypervirulent *K. pneumoniae* strain that had acquired a virulence plasmid by a classic sequence type (ST) 11 strain (*16*). In a study of a collection of >2,200 *K. pneumoniae* genomes, distinct evolutionary patterns of horizontal gene transfer were observed in MDR isolates versus

Author affiliations: National University of Singapore, Singapore (Y. Chen, Y.H. Tan, L.C. Nguyen, Y.-H. Gan); National Centre for Infectious Diseases, Singapore (K. Marimuthu, L.D. Wang, S.R.S. Prakki, W. Xu, O.T. Ng); Tan Tock Seng Hospital, Singapore (K. Marimuthu, O.T. Ng); National University Hospital, Singapore (J. Teo); Singapore General Hospital, Singapore (I. Venkatachalam, B.P.Z. Cherng, T.H. Koh); Nanyang Technological University, Singapore (O.T. Ng)

DOI: https://doi.org/10.3201/eid2603.191230

hypervirulent isolates (*17*). The authors of that study postulated that hypervirulent clones might be subject to some sort of constraint against horizontal gene transfer and show more conserved pangenomic diversity than MDR clones. If that hypothesis is correct, MDR clones acquiring virulence genes or *K. pneumoniae* virulence plasmids would be more likely than hypervirulent clones acquiring MDR genes. To investigate this hypothesis, we searched for hypervirulent isolates among 556 CRKP isolates collected at public hospitals of Singapore.

Materials and Methods

Bacterial Isolates and Microbiologic Methods

During 2010–2015, all microbiology laboratories in Singapore had been mandated to submit their carbapenem-resistant *Enterobacteriaceae* isolates to the National Public Health Laboratory of Singapore. Using this library, we collected isolates from the CaPES study. We performed species identification, assessed carbapenem resistance, and determined carbapenemase genes as previously described (*8*).

Whole-Genome Sequencing and Data Analysis

We performed whole-genome sequencing using the MiSeq platform (Illumina, https://www.illumina.com) as previously described (*18*). In addition, we sequenced the complete genomes of 5 isolates from 3 patients, obtaining long reads using the GridION X5 system (Oxford Nanopore Technologies, https://nanoporetech.com) to close the gaps. We de novo assembled the Illumina sequence reads using SPAdes 3.11.1 (*19*) and completed genome assembly using a combination of Illumina and Oxford Nanopore Technologies data with the hybrid assembler Unicycler version 0.4.7 (Appendix Table, https://wwwnc.cdc.gov/EID/article/26/3/19-1230-App1.pdf) (*20*). We deposited whole-genome sequencing data in GenBank (BioProject numbers PRJNA342893, PRJNA557813, and PRJNA591409). We screened genome assemblies for virulence loci and *K. pneumoniae* virulence plasmid–associated loci using kleborate (*21*–*23*). We resolved missing loci and ambiguous alleles by mapping short reads to reference sequences using breseq (*24*) and screened assemblies for antimicrobial resistance genes using ResFinder 3.1 (*25*) and CARD (*26*). We resolved any discrepancies between these 2 gene identifiers by searching blastp (https://blast.ncbi.nlm.nih.gov/Blast.cgi?PAGE=Proteins) using translated gene sequences. We identified plasmid replicons in all completely sequenced genomes using PlasmidFinder with default settings (*27*). For all isolates, we performed core-genome single-nucleotide polymorphism (SNP) analysis against reference genome SGH10 chromosome (GenBank accession no. CP025080) using Parsnp 1.2 (*28*). In plasmid analyses, we generated alignments by mapping assemblies to reference plasmids using bowtie2 (*29*) on the REALPHY server (*30*). We inferred approximate maximum-likelihood phylogenetic trees using FastTree 2 (*31*) and screened completed assemblies for origin of transfer (*oriT*) sites and other transfer-related modules using oriTfinder (*32*).

Determining Hypermucoviscosity

We assessed hypermucoviscosity of all isolates using the string test (*33*) and a quantitative centrifugation assay (*34*). We used SGH10 as the positive control and SGH10 with *rmpA* deleted as the negative control.

Mouse Infection

We infected female 7–8-week-old C57BL/6J mice (InVivos, http://www.invivos.com.sg) with 1×10^5 CFU of bacteria diluted in 100 µL phosphate-buffered saline through the intraperitoneal route and assessed for death every 8–16 h. Animal experiments were approved under protocol R18–0252 by the National University of Singapore Institutional Animal Care and Use Committee in accordance with the National Advisory Committee for Laboratory Animal Research guidelines.

Conjugation Experiments

We measured the transmissibility of the bla_{KPC-2}–carrying plasmid using a previously described method (*35*). In this experiment, carbapenem-resistant hypervirulent *K. pneumoniae* isolates were the donors and a kanamycin-resistant *Escherichia coli* MG1655 mutant SLC568 strain (*36*) was the recipient. We carried out conjugation on 0.22-µm nitrocellulose filters with donors and recipients incubated at a 1:1 ratio on lysogeny broth (LB) agar plates for 4 h at 37°C. We enumerated transconjugants on LB agar plates containing carbenicillin (100 µg/mL) and kanamycin (50 µg/mL) and recipients on LB agar plates containing kanamycin only. We confirmed transfer of the bla_{KPC-2} gene by PCR.

Antimicrobial Susceptibility Testing

We performed antimicrobial susceptibility testing following the Clinical and Laboratory Standards Institute guidelines. We determined MICs (*37*) and interpreted breakpoints (*38*) of antimicrobial drugs as described.

Statistical Methods

We performed statistical analyses using GraphPad Prism version 8 (https://www.graphpad.com). We compared samples using the unpaired *t*-test with Welch correction.

Results

Discovery of Hypervirulent Features of CRKP

We retrieved 1,312 carbapenem-resistant *Enterobacteriaceae* collected from 6 public hospitals in Singapore during 2010–2015 through the CaPES program and National Public Health Laboratory of Singapore; 1,251 isolates were whole-genome sequenced with Illumina technology, and 556 isolates were *K. pneumoniae*. We searched *K. pneumoniae* isolate genomes for the presence of *K. pneumoniae* virulence plasmid–associated virulence determinants, *rmpA*, *rmpA2*, *iro* (the salmochelin locus), and *iuc* (the aerobactin locus) by using kleborate. We identified 18 isolates (originating from just 7 patients) harboring all of these loci, and 14 of these isolates came from the same 3 patients. We screened the genome assemblies of these 18 isolates for virulence features and compared the characteristics of these isolates with those of 2 known hypervirulent strains, SGH10 (serotype K1 liver abscess–associated isolate from Singapore) (*6*,*39*) and CG43 (serotype K2 clinical isolate from Taiwan) (*40*). We then performed a phylogenetic analysis of the core genomes of all these isolates.

The differences found among isolates from the same patient were small (0–15 SNPs) (Figure 1, panel A), suggesting that patients with multiple isolates were infected with a single strain. All isolates from patients A2, A4, and A6 were ST23 and serotype K1 (same as SGH10) and, except for ENT1256, carried the same virulence loci as SGH10 (Table 1); ENT1256 had a different allele for *rmpA2*. The core genomes of

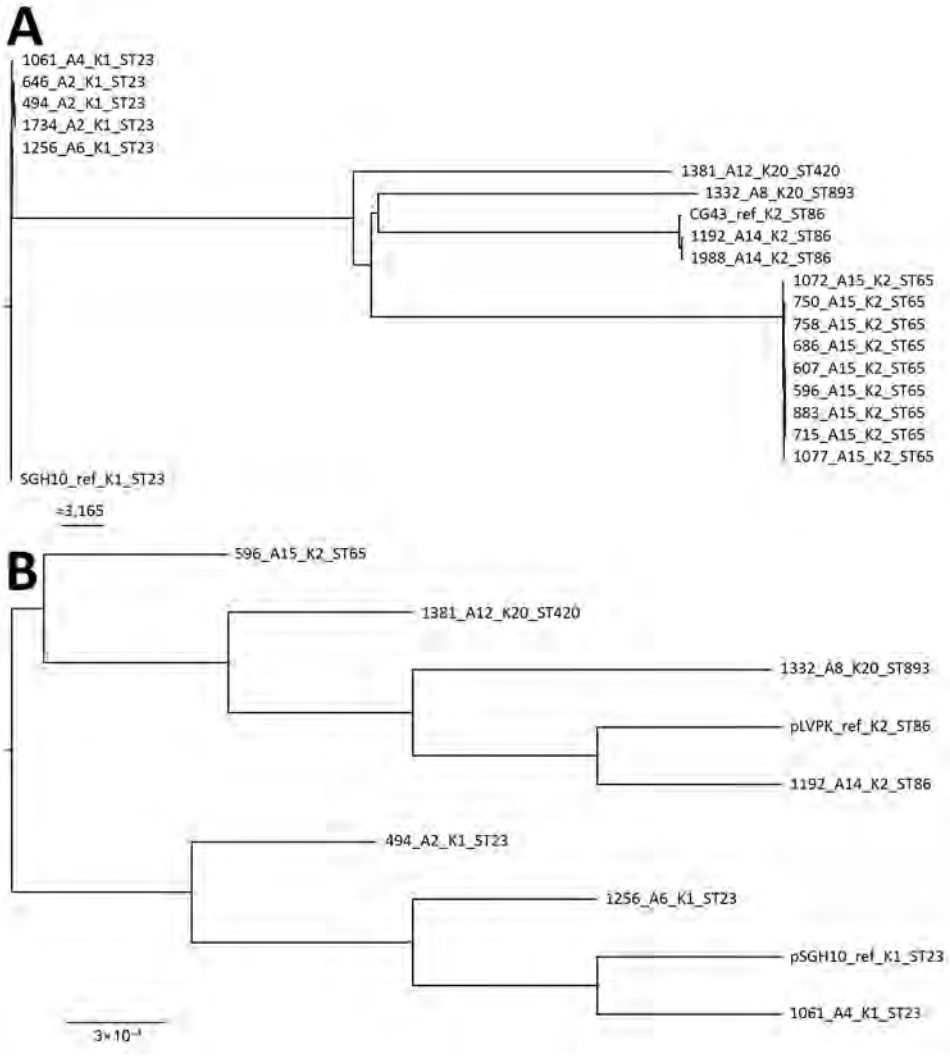

Figure 1. Maximum-likelihood trees of genes from carbapenem-resistant *Klebsiella pneumoniae* isolates, Singapore, 2013–2015. A) Analysis generated using 63,297 single-nucleotide polymorphism sites in the core genome. The chromosomal sequence of SGH10 (GenBank accession no. CP025080) was used as reference. Isolates are closely related to hypervirulent strains SGH10 and CG43. Scale bar indicates number of single-nucleotide polymorphisms. B) Analysis generated from the alignment of *K. pneumoniae* virulence plasmids from the first isolates collected from different patients. The sequences of *K. pneumoniae* virulence plasmid pSGH10 (GenBank accession no. CP025081) was used as reference. Scale bar indicates nucleotide changes per base pair. Trees were drawn using FigTree version 1.4.4 (http://tree.bio.ed.ac.uk/software/figtree) and rooted at the SGH10 branch. Labels indicate isolate no._patient no._K serotype_ sequence type. Ref, reference; ST, sequence type.

Table 1. Classifications and virulence characteristics of 18 carbapenem-resistant *Klebsiella pneumoniae* isolates harboring KPVP-associated genes, Singapore, 2013–2015*

Isolate	Patient no.	K locus	ST	Virulence score	Locus					
					Yersiniabactin	Colibactin	Aerobactin	Salmochelin	*rmpA*	*rmpA2*
ENT494	A2	1	23	5	*ybt* 1, ICEKP10	*clb* 2	*iuc* 1	*iro* 1	2(KPVP-1)	6
ENT646	A2	1	23	5	*ybt* 1, ICEKP10	*clb* 2	*iuc* 1	*iro* 1	2(KPVP-1)	6
ENT1734	A2	1	23	5	*ybt* 1, ICEKP10	*clb* 2	*iuc* 1	*iro* 1	2(KPVP-1)	6
ENT1061	A4	1	23	5	*ybt* 1, ICEKP10	*clb* 2	*iuc* 1	*iro* 1	2(KPVP-1)	6
ENT1256	A6	1	23	5	*ybt* 1, ICEKP10	*clb* 2	*iuc* 1	*iro* 1	2(KPVP-1)	5
ENT1332	A8	20	893	4	*ybt* unknown	–	*iuc* 1	*iro* 1	1(KPVP-1)	2
ENT1381	A12	20	420	4	*ybt* 9, ICEKP3	–	*iuc* 1	*iro* 1	1(KPVP-1)	5
ENT1192	A14	2	86	4	*ybt* 9, ICEKP3	–	*iuc* 1	*iro* 1	2(KPVP-1)	6
ENT1988	A14	2	86	4	*ybt* 9, ICEKP3	–	*iuc* 1	*iro* 1	2(KPVP-1)	6
ENT596	A15	2	65	5	*ybt* 17, ICEKP10	*clb* 3	*iuc* 1	*iro* 1	2(KPVP-1)	6
ENT607	A15	2	65	5	*ybt* 17, ICEKP10	*clb* 3	*iuc* 1	*iro* 1	2(KPVP-1)	6
ENT686	A15	2	65	5	*ybt* 17, ICEKP10	*clb* 3	*iuc* 1	*iro* 1	2(KPVP-1)	6
ENT715	A15	2	65	5	*ybt* 17, ICEKP10	*clb* 3	*iuc* 1	*iro* 1	2(KPVP-1)	6
ENT750	A15	2	65	5	*ybt* 17, ICEKP10	*clb* 3	*iuc* 1	*iro* 1	2(KPVP-1)	6
ENT758	A15	2	65	5	*ybt* 17, ICEKP10	*clb* 3	*iuc* 1	*iro* 1	2(KPVP-1)	6
ENT883	A15	2	65	5	*ybt* 17, ICEKP10	*clb* 3	*iuc* 1	*iro* 1	2(KPVP-1)	6
ENT1072	A15	2	65	5	*ybt* 17, ICEKP10	*clb* 3	*iuc* 1	*iro* 1	2(KPVP-1)	6
ENT1077	A15	2	65	5	*ybt* 17, ICEKP10	*clb* 3	*iuc* 1	*iro* 1	2(KPVP-1)	6
ENT495†		66	841	0	–	–	–	–	–	–
SGH10‡		1	23	5	*ybt* 1, ICEKP10	*clb* 2	*iuc* 1	*iro* 1	2(KPVP-1)	6
CG43§		2	86	3	–	–	*iuc* 1	*iro* 1	1(KPVP-1)	1

*ICEKP, integrative conjugative element *K. pneumoniae*; KPVP, *K. pneumoniae* virulence plasmid; ST, sequence type.
†Control carbapenem-resistant *K. pneumoniae* isolate (classified as *K. quasipneumoniae* by GenBank).
‡GenBank accession nos. CP025080 and CP025081.
§GenBank accession nos. CP006648 and AY378100.

these isolates were also similar to SGH10, as shown by the phylogenetic analysis (Figure 1, panel A). However, the differences between isolates from patients A2, A4, and A6 were much greater (200–300 SNPs) than the differences between isolates from patient A2 (15 SNPs), indicating that the bacteria from these patients were unlikely to have originated from the same strain. The isolates from patients A14 and A15 were the same serotype (K2) but different sequence types (Table 1), and their core genomes contained many differences (>20,000 SNPs). The isolates from patient A14 were phylogenetically close to the other hypervirulent strain, CG43 (Figure 1, panel A); however, unlike CG43, which carried no yersiniabactin (*ybt*) and colibactin (*clb*) loci, 2 A14 isolates (ENT1192 and ENT1988) had a *ybt* 9 locus on integrative conjugative element *K. pneumoniae* 3 (Table 1). The isolates from the remaining 2 patients (A8 and A12) were the same serotype (K20) but had different sequence types and many core genome differences (>20,000 SNPs). ENT1332 had an unknown *ybt* locus, and ENT1381 had a *ybt* 9 locus on integrative conjugative element *K. pneumoniae* 3. Both of these isolates did not have the *clb* locus. All isolates had hypervirulence backgrounds.

We also performed a whole-genome phylogenetic analysis on the *K. pneumoniae* virulence plasmid carried in the first isolates obtained from all patients, using the *K. pneumoniae* virulence plasmid sequence from SGH10 (pSGH10) as reference. The *K. pneumoniae* virulence plasmids appeared to form 2 separate clades, 1 for all K1 isolates and the other for K2 and K20 isolates (Figure 1, panel B).

The virulence potentials of all isolates were high (Table 1); the virulence scores predicted by kleborate for all isolates (≥4) were higher than the score (3) predicted for the hypervirulent K2 reference strain CG43. Hypervirulent *K. pneumoniae* isolates are generally defined as carrying *K. pneumoniae* virulence plasmid–associated loci and having a hypermucoviscous phenotype (including a positive string test result), which is dependent on regulator RmpA (*40*,*41*). We measured the hypermucoviscosity of the first isolates from all patients using both the string test and a centrifugation assay; 6 of 7 isolates formed strings, and 5 of 7 isolates were hypermucoviscous according to the centrifugation assay (Figure 2, panel A). Only ENT596 was negative by both tests.

The virulence potential of the carbapenem-resistant hypervirulent *K. pneumoniae* isolates was further determined in an intraperitoneal mouse infection model. The first isolates from 6 of 7 patients killed >50% of the infected mice within 96 hours; only ENT596 (like control isolate ENT495, a CRKP strain carrying pKPC2 but not hypervirulent) did not kill any mice (Figure 2, panel B). Serotype K1 isolates were the most virulent, and serotype K20 isolates took longer to kill. The virulence of ENT596 did not correlate with its predicted score; this isolate demonstrated concurrent loss of hypermucoviscosity and virulence in mice

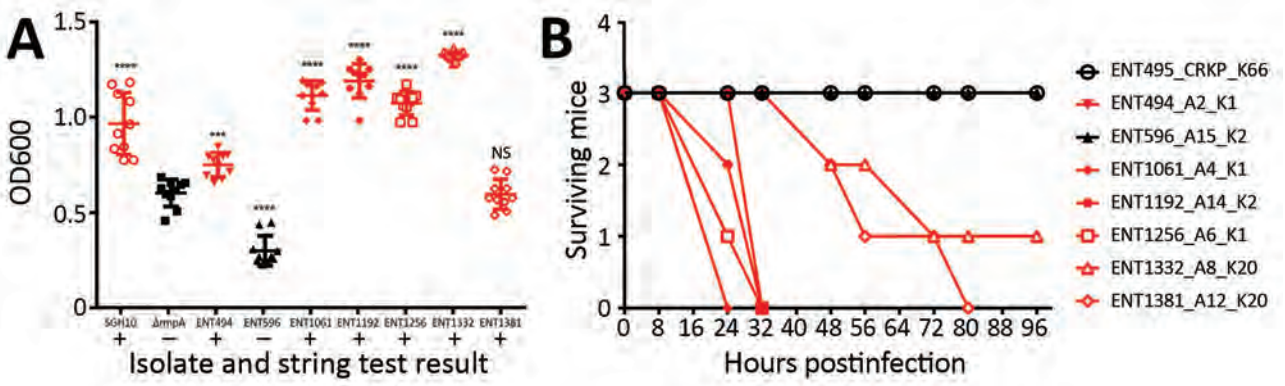

Figure 2. Hypervirulence assessment of first isolates from 7 patients with CRKP infections, Singapore, 2013–2015. A) Hypermucoviscosity of isolates as indicated by a low-speed centrifugation assay and the string test. For the centrifugation assay, *Klebsiella pneumoniae* isolates were grown in Luria broth overnight at 37°C and centrifuged (10 minutes at 2,000 × *g*), and OD600s of supernatants were measured. Each symbol represents the value for an individual clone (n = 10) from 3 independent experiments. Horizontal bars indicate means and error bars SDs. For the string test, *K. pneumoniae* were grown on sheep blood agar (2 days at 37°C). Red indicates a positive string test result. B) In vivo virulence in mice. Female C57BL/6J mice (7–8 weeks old, 3 mice/isolate) were injected with 1×10^5 CFU of bacteria by the intraperitoneal route. Every 8 or 16 hours, mice were checked and scored for death. If necessary, they were euthanized and counted as dead. The experiment was stopped at 96 hours postinfection. For each isolate, patient number and K serotype is indicated. CRKP, carbapenem-resistant *Klebsiella pneumoniae*; OD, optical density; NS, not significant. ***p = 0.0001; ****p<0.0001.

(Table 1; Figure 2), which might have been caused by the loss of expression of the virulence genes. The average length of hospitalization of the 7 patients harboring these isolates was 97 days, which was much longer than the average length of stay for 249 patients with carbapenem-resistant *Enterobacteriaceae* infection (38 days) (*8*). Taking into account all our evidence, we conclude that the isolates from 6 of 7 patients (A2, A4, A6, A8, A12, and A14) are phenotypically hypervirulent, and the isolates from patient A15 are phenotypically nonhypervirulent (although these isolates have a hypervirulent genetic background).

Highly Conserved Plasmid Harboring *bla*$_{KPC-2}$ on All Carbapenem-Resistant Hypervirulent *K. pneumoniae* Isolates

We screened the assemblies of all 18 carbapenem-resistant hypervirulent *K. pneumoniae* isolates for acquired antimicrobial resistance genes using ResFinder (*25*) and CARD (*26*). Except for endogenous penicillin resistance, hypervirulent *K. pneumoniae* isolates are generally considered to be susceptible to antimicrobial drugs. Our search results showed that SGH10 harbored the β-lactam resistance gene *bla*$_{SHV-11}$ and resistance genes against fluoroquinolones (*oqxA* and *oqxB*) and fosfomycins (*fosA6*) (Table 2). In total, 17 of 18 isolates carried these 3 resistance genes; 1 isolate from patient A15 (ENT686) did not have the *oqxA* and *oqxB* genes, and these genes were also not detectable by PCR. All isolates carried an identical set of the following 4 genes: *bla*$_{KPC-2}$, *bla*$_{TEM-1A}$, *bla*$_{TEM-1B}$, and *mph*(A). In the 5 completely sequenced genomes (ENT494, ENT646, and ENT1734 [patient A2]; ENT1192 [patient A14]; and ENT607 [patient A15]; Appendix Table), we located these 4 genes on a 71,861-bp plasmid, which we named pKPC2. The sequences of the pKPC2s in the 4 isolates from patients A2 and A14 were identical. The pKPC2 in ENT607 from patient A15 had only 1-bp difference.

A blastn search for pKPC2 revealed that the highest hit was a plasmid from *Salmonella enterica* (pSA20021456.2, GenBank accession no. CP030221), which covered 74% of pKPC2 with >99% identity (Figure 3). No attribute information was available for the *Salmonella* strain, and pSA20021456.2 carries no antimicrobial drug resistance genes. No incompatibility groups were detected on either plasmid by PlasmidFinder.

We performed a phylogenetic analysis of the pKPC2 sequences carried in the first isolates and other select isolates from all 7 patients, including the pKPC2 from ENT494 (i.e., pKPC2_494) as reference (Figure 4). This analysis revealed that all isolates carried sequences almost identical to pKPC2_494 (coverage and identity >99%). Because all isolates carried the 4-gene set, they probably had a plasmid closely related to pKPC2_494. Three patients had multiple isolates with pKPC2. The clinical records show long time-interval gaps of antimicrobial drug nonexposure between some isolates. The comparison also shows that the pKPC2-related plasmids were remarkably stable; they were maintained in bacteria with few changes for 90–281 days in the patients not undergoing antimicrobial drug treatment (Figure 4).

Table 2. Isolation date, sampling site, and resistance genes of carbapenem-resistant hypervirulent *Klebsiella pneumoniae* isolates, Singapore, 2013–2015

Isolate	Patient no.	Date of isolation	Sampling site	β-lactam resistance genes	Other resistance genes
ENT494	A2	2013 Jun 7	Sputum	*bla*$_{SHV-11}$, *bla*$_{KPC-2}$, *bla*$_{TEM-1A}$, *bla*$_{TEM-1B}$	*oqxA*, *oqxB*, *fosA6*, *mph*(A)
ENT646	A2	2013 Sep 18	Blood	*bla*$_{SHV-11}$, *bla*$_{KPC-2}$, *bla*$_{TEM-1A}$, *bla*$_{TEM-1B}$, *bla*$_{OXA-1}$	*oqxA*, *oqxB*, *fosA6, mph*(A), *qnrB1*, *aac(6')-Ib-cr, catB3*, *dfrA14*
ENT1734	A2	2014 Dec 19	Rectum	*bla*$_{SHV-11}$, *bla*$_{KPC-2}$, *bla*$_{TEM-1A}$, *bla*$_{TEM-1B}$, *bla*$_{OXA-1}$	*oqxA*, *oqxB*, *fosA6*, *mph*(A), *catB3*, *aac(6')-Ib-cr*
ENT1061	A4	2014 Mar 13	Blood	*bla*$_{SHV-11}$, *bla*$_{KPC-2}$, *bla*$_{TEM-1A}$, *bla*$_{TEM-1B}$	*oqxA*, *oqxB*, *fosA6*, *mph*(A)
ENT1256	A6	2014 Jun 20	Rectum	*bla*$_{SHV-11}$, *bla*$_{KPC-2}$, *bla*$_{TEM-1A}$, *bla*$_{TEM-1B}$	*oqxA*, *oqxB*, *fosA6*, *mph*(A)
ENT1332	A8	2014 Jul 13	Rectum	*bla*$_{SHV-1}$, *bla*$_{KPC-2}$, *bla*$_{TEM-1A}$, *bla*$_{TEM-1B}$, *bla*$_{CTX-M-15}$	*oqxA*, *oqxB*, *fosA6*, *mph*(A), *aac(6')-Ib-cr*, *aadA16*, *qnrB6*, *arr-3*, *sul1*, *tet*(A), *dfrA27*
ENT1381	A12	2014 Aug 10	Midstream urine	*bla*$_{SHV-75}$, *bla*$_{KPC-2}$, *bla*$_{TEM-1A}$, *bla*$_{TEM-1B}$, *bla*$_{OXA-1}$	*oqxA*, *oqxB*, *fosA6*, *mph*(A)
ENT1192	A14	2014 May 24	Rectum	*bla*$_{SHV-1}$, *bla*$_{KPC-2}$, *bla*$_{TEM-1A}$, *bla*$_{TEM-1B}$, *bla*$_{OXA-1}$	*oqxA*, *oqxB*, *fosA5*, *mph*(A), *aac(6')-Ib-cr*, *qnrB1*, *catB3*, *tet*(A), *dfrA14*
ENT1988	A14	2015 Apr 16	Feces, rectum	*bla*$_{SHV-1}$, *bla*$_{KPC-2}$, *bla*$_{TEM-1A}$, *bla*$_{TEM-1B}$, *bla*$_{OXA-1}$	*oqxA*, *oqxB*, *fosA5*, *mph*(A), *aac(6')-Ib-cr*, *qnrB1*, *catB3*, *tet*(A), *dfrA14*
ENT596	A15	2013 Aug 22	Urine	*bla*$_{SHV-11}$, *bla*$_{KPC-2}$, *bla*$_{TEM-1A}$, *bla*$_{TEM-1B}$	*oqxA*, *oqxB*, *fosA6*, *mph*(A)
ENT607	A15	2013 Aug 22	Sputum	*bla*$_{SHV-11}$, *bla*$_{KPC-2}$, *bla*$_{TEM-1A}$, *bla*$_{TEM-1B}$	*oqxA*, *oqxB*, *fosA6*, *mph*(A), *aadA1*, *cmlA1*, *arr-2*, *sul1*
ENT686	A15	2013 Oct 4	Tracheostomy aspirate	*bla*$_{SHV-11}$, *bla*$_{KPC-2}$, *bla*$_{TEM-1A}$, *bla*$_{TEM-1B}$	*fosA6, mph*(A)
ENT715	A15	2013 Oct 17	Trachea aspirate	*bla*$_{SHV-11}$, *bla*$_{KPC-2}$, *bla*$_{TEM-1A}$, *bla*$_{TEM-1B}$	*oqxA*, *oqxB*, *fosA6*, *mph*(A)
ENT750	A15	2013 Oct 31	Blood	*bla*$_{SHV-11}$, *bla*$_{KPC-2}$, *bla*$_{TEM-1A}$, *bla*$_{TEM-1B}$	*oqxA*, *oqxB*, *fosA6*, *mph*(A)
ENT758	A15	2013 Oct 31	Tracheal aspirate	*bla*$_{SHV-11}$, *bla*$_{KPC-2}$, *bla*$_{TEM-1A}$, *bla*$_{TEM-1B}$	*oqxA*, *oqxB*, *fosA6*, *mph*(A)
ENT883	A15	2013 Dec 14	Sputum	*bla*$_{SHV-11}$, *bla*$_{KPC-2}$, *bla*$_{TEM-1A}$, *bla*$_{TEM-1B}$	*oqxA*, *oqxB*, *fosA6*, *mph*(A)
ENT1072	A15	2014 Mar 26	Sputum	*bla*$_{SHV-11}$, *bla*$_{KPC-2}$, *bla*$_{TEM-1A}$, *bla*$_{TEM-1B}$	*oqxA*, *oqxB*, *fosA6*, *mph*(A)
ENT1077	A15	2014 Mar 28	Rectum	*bla*$_{SHV-11}$, *bla*$_{KPC-2}$, *bla*$_{TEM-1A}$, *bla*$_{TEM-1B}$	*oqxA, oqxB*, *fosA6*, *mph*(A), *tet*(A), *dfrA14*
ENT495*		2013 Jun 8	Not known	*bla*$_{OKP-B-6}$, *bla*$_{KPC-2}$, *bla*$_{TEM-1A}$, *bla*$_{TEM-1B}$, *bla*$_{OXA-1}$	*oqxA*, *oqxB*, *fosA6*, *mph*(A), *tet*(A), *dfrA14*, *aac(6')-Ib-cr*, *aadA1*, *arr-2*, *cmlA5*, *ereA*, *qnrB1*, *sul1*
SGH10		Not applicable	Blood	*bla*$_{SHV-11}$	*oqxA*, *oqxB*, *fosA6*

*Control carbapenem-resistant *K. pneumoniae* isolate (classified as *K. quasipneumoniae* by GenBank).

Besides resistance genes, pKPC2 had a complete set of conjugative machinery with all 4 essential modules (*oriT*, relaxase, type IV coupling protein, and a type IV secretion system cluster), suggesting the plasmid is self-transmissible. The *Salmonella* plasmid pSA20021456.2 has a relaxase, type IV coupling protein, and type IV secretion system cluster similar to pKPC2 but no *oriT* site. We selected 3 isolates that had only 1 antimicrobial drug resistance plasmid to assess the transmissibility of pKPC2. We performed filter mating on LB agar using the kanamycin-resistant *E. coli* strain SLC568 as the recipient. After 4 hours of incubation, ≈80% of recipients (≈0.8 × 100 transconjugate/recipient) had received pKPC2 from ENT596 and ENT1061 (Figure 5). The conjugation frequency was ≈0.2% (≈2.0 × 10^{-4} transconjugate/recipient) when ENT494 was the donor. We confirmed the transconjugants acquired the *bla*$_{KPC-2}$ gene by PCR (using 10 colonies for each donor). K serotype, sequence type, and hypermucoviscosity of

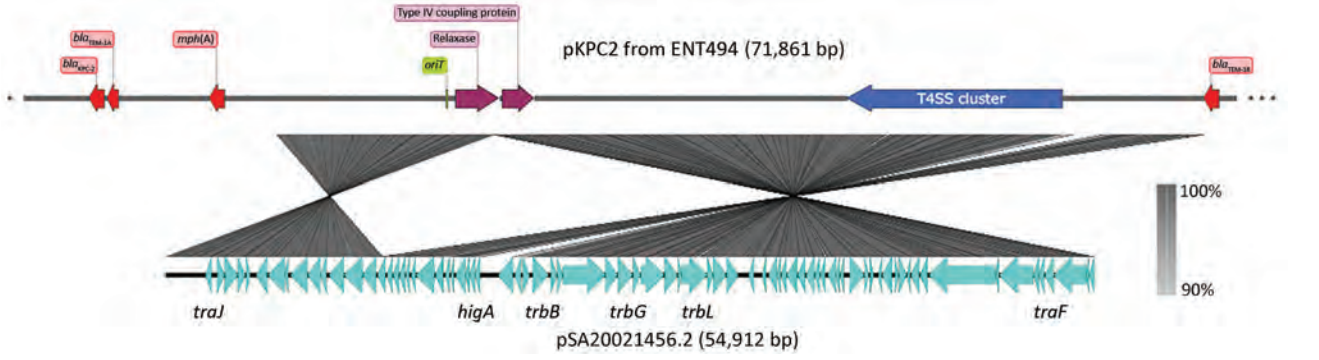

Figure 3. Main features of pKPC2 from *Klebsiella pneumoniae* isolate ENT494, Singapore, 2013, and comparison with pSA20021456.2. Image was generated by using SnapGene Viewer (https://www.snapgene.com) and Easyfig (https://github.com/mjsull/Easyfig). KPC, *Klebsiella pneumoniae* carbapenemase; *oriT*, origin of transfer; T4SS, type IV secretion system.

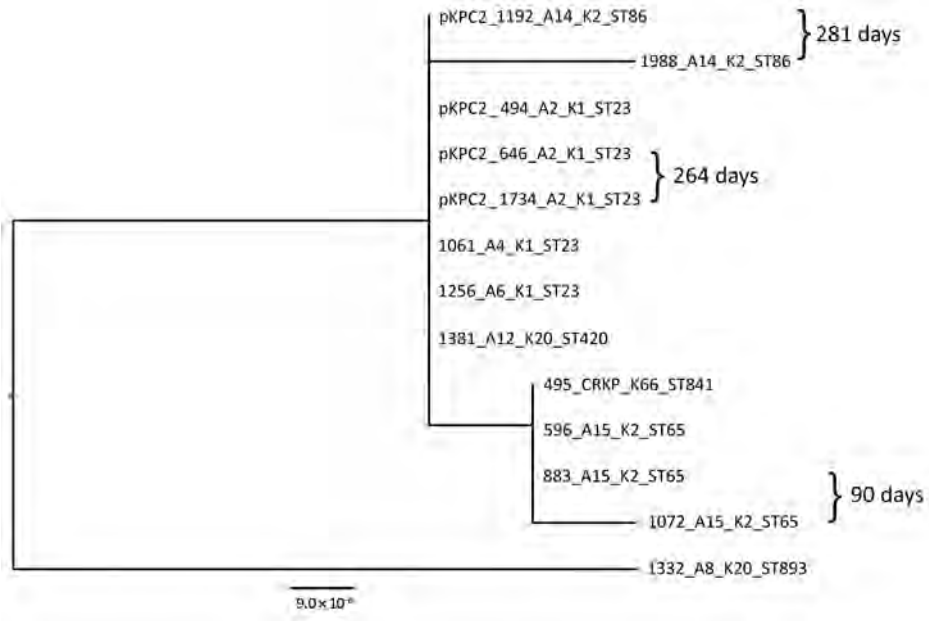

Figure 4. Maximum-likelihood analysis of pKPC2 plasmids from carbapenem-resistant hypervirulent *Klebsiella pneumoniae* isolates, Singapore, 2013–2015. pKPC2_494 was used as reference. Labels indicate isolate no._patient no._K serotype_sequence type. Days between isolate collection are indicated. Scale bar indicates nucleotide changes per base pair. KPC, *Klebsiella pneumoniae* carbapenemase; ST, sequence type.

donors could not explain the observed differences in conjugation efficiency.

To assess the role of pKPC2 in conferring antimicrobial drug resistance to host strains, we measured the MICs of antimicrobial drugs against the 3 isolates from patient A2 and compared with SGH10 (Table 3). SGH10 was resistant to penicillins and fosfomycin but susceptible to the 2 fluroquinolones tested, even though the strain carried the fluroquinolone efflux pump genes *oqxA* and *oqxB* (Table 2). This finding is consistent with the low *oqxB* expression seen for most *K. pneumoniae* strains (*42*). SGH10 was susceptible to cephems and carbapenems. In contrast, all 3 isolates from patient A2 were resistant to ceftriaxone, imipenem, and meropenem (Table 3), most likely because of the presence of pKPC2. These data show that pKPC2 is a highly transmissible plasmid that confers resistance to all 3 types of β-lactams.

Within-Patient Microevolution of Carbapenem-Resistant Hypervirulent *K. pneumoniae* Isolates

Using multiple isolates from the same patient, we set out to determine the changes that occurred in the genome of 1 carbapenem-resistant hypervirulent *K. pneumoniae* population over the course of an infection. This analysis enabled us to track the carriage of genes conferring carbapenem resistance and MDR in the bacteria versus antimicrobial drug exposure over time. With the available clinical data from patient A2, we reconstructed a timeline of the evolution of the 3 isolates from this patient, showing their plasmid content and antimicrobial drug exposure (Figure 6).

In addition to the chromosome, *K. pneumoniae* virulence plasmid, and pKPC2, all 3 isolates from patient A2 carried 2 or 3 additional plasmids (Appendix Table). Isolates were of the same infecting strain but lost or gained MDR plasmids over time. The *K. pneumoniae* virulence plasmid and pKPC2 were stable, showing few changes over a year. Treatment with gentamicin and ciprofloxacin correlated with the appearance of an MDR plasmid in ENT646 that encoded resistance genes to both classes of antimicrobial drugs. This 165-kb MDR plasmid (named pMDR646) carried *aac*(6′)-*Ib-cr*, bla_{OXA-1},

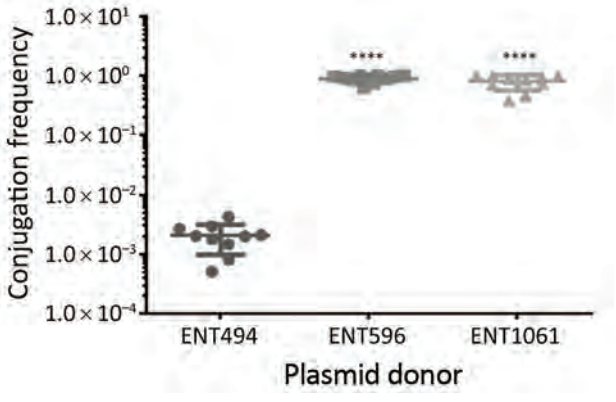

Figure 5. Conjugation ability of pKPC2 from carbapenem-resistant hypervirulent *Klebsiella pneumoniae* isolates, Singapore, 2013–2014, to *Escherichia coli* SLC568. Filter matings were performed for 4 h. The conjugation frequency is the number of CFUs of transconjugants divided by the number of CFUs of recipients. Each symbol represents the value for an individual clone (n = 10) from 3 independent experiments. Horizontal bars indicate means and error bars SD. KPC, *Klebsiella pneumoniae* carbapenemase. ****p<0.0001.

Table 3. MICs of antimicrobial drugs against 3 carbapenem-resistant hypervirulent *Klebsiella pneumoniae* isolates from patient A2, Singapore, 2013–2014, compared with reference strain SGH10*

Antimicrobial drug group and drug	SGH10	ENT494	ENT646	ENT1734
Penicillins				
Ampicillin	**>64**	**>64**	**>64**	**>64**
Piperacillin	**32**	**>64**	**>64**	**>64**
Cephems				
Ceftriaxone	≤1	**>64**	**>64**	**>64**
Carbapenems				
Imipenem	≤1	**>64**	**>64**	**>64**
Meropenem	≤1	**8**	**16**	**8–16**
Aminoglycosides				
Amikacin	≤1	≤1	2–4	4–8
Gentamicin	≤1	≤1	≤1	≤1
Kanamycin	2	4	**16**	**32**
Tetracyclines				
Doxycycline	≤1	2	2	2
Fluoroquinolones				
Ciprofloxacin	≤1	≤1	**8**	≤1
Levofloxacin	≤1	≤1	≤1	≤1
Folate pathway antagonists				
Sulfamethoxazole	128	**512**	**512**	**>512**
Trimethoprim	≤1	≤1	**>64**	≤1
Phenicols				
Chloramphenicol	4	4–8	4–8	4
Fosfomycins				
Fosfomycin	**>64**	**>64**	**>64**	**>64**
Lipopeptides				
Colistin	4	2	2–4	2–4
Polymyxin B	4	4	4	4

*Bold numbers indicate resistance as interpreted by Clinical and Laboratory Standards Institute interpretative criteria for MICs (*38*).

qnrB1, *catB3*, and *dfrA14*. In the third isolate from patient A2 (ENT1734), the MDR plasmid downsized to 100 kb (pMDR1734) and carried only *aac*(6′)*-lb-cr*, *bla*OXA-1, and *catB3*. The downsizing appeared to be the result of extensive deletion and reorganization (Appendix Figure). Antimicrobial susceptibility testing data also showed that this bacterium was resistant to fewer antimicrobial drugs; isolate ENT646 was resistant to 7 classes of antimicrobial drugs, and ENT1734 was resistant to 6 classes of drugs (Table 3). Both ENT646 and ENT1734 carried the broad-range resistance gene *aac(6′)-lb-cr*, which confers resistance against aminoglycoside and fluoroquinolone antimicrobial drugs. This gene was likely responsible for the observed resistance to kanamycin, and *qnrB1* (in ENT646) was likely responsible for resistance to ciprofloxacin (Table 3). Both isolates were also resistant to sulfamethoxazole, which we could not attribute to any resistance gene or mutation. All 3 isolates carried a 95-kb plasmid with unknown virulence or resistance attributes (Figure 6). The sizes of the chromosome and *K. pneumoniae* virulence plasmid gradually increased over time, mainly through the acquisition of mobile genetic elements.

Nine isolates were collected from patient A15 at various time points and from different anatomic sites (Table 2); all were identical in their core genomes (0 SNP differences). Two A15 isolates acquired antimicrobial drug resistance genes in addition to those on pKPC2; 1 of the first isolates, ENT607, had *aadA1*, *mph*(A), *cmlA1*, *arr-2*, and *sul1*, which were all on a 105-kb plasmid (named pMDR607). This plasmid appeared unstable and was absent in later isolates. The last isolate, ENT1077, had acquired tetracycline and trimethoprim resistance genes not seen in the other isolates.

Discussion

We report the coexistence of hypervirulence and carbapenem resistance within the same *K. pneumoniae* isolates in Singapore. These isolates dated back to 2013; however, their existence could have occurred even earlier because collection started in 2010. All carbapenem-resistant hypervirulent *K. pneumoniae* isolates in this study harbored a bla_{KPC-2} gene. In studies conducted in China, most patients infected with carbapenem-resistant hypervirulent *K. pneumoniae* also carried the bla_{KPC-2} gene (*16*,*43*–*45*). We and others have described hypervirulent *K. pneumoniae* in community-acquired liver abscesses in Singapore, where most isolates are capsular serotypes K1 and K2 (*6*,*46*). Most (>80%) liver abscess isolates are estimated to belong to sublineage CG23-I (includes reference strain SGH10) (*39*). The carbapenem-resistant hypervirulent *K. pneumoniae* isolates from 5 of 7 patients in this study were K1 or K2 serotype and 6 of 7 isolates were highly virulent, as predicted. Our results suggest that pKPC2 can be stably maintained in a hypervirulent *K. pneumoniae* bacterial host. Thus, the possible dissemination of the bla_{KPC-2} gene to hypervirulent strains present in a carriage state within communities is a concern.

In a study in China, 1,838 isolates were analyzed, and 21 carbapenem-resistant hypervirulent *K. pneumoniae* isolates were found and classified as ST11, ST65, ST268, ST595, and ST692 (*44*). In another report, 5 ST11 CRKP isolates were documented as having acquired *K. pneumoniae* virulence plasmids (*16*). In these reports, a *K. pneumoniae* virulence plasmid or parts of one was probably co-opted into the prevalent CRKP strain in that region, which was an ST11 strain carrying the bla_{KPC-2} gene. According to our previous study, only 5% of CRKP isolates in Singapore were ST11 (*8*). However, in another study, 7 carbapenem-resistant hypervirulent *K. pneumoniae* isolates were identified, 4 of which were ST23 and serotype K1 (*47*). In 2 case studies, ST23 (hypervirulent) isolates were

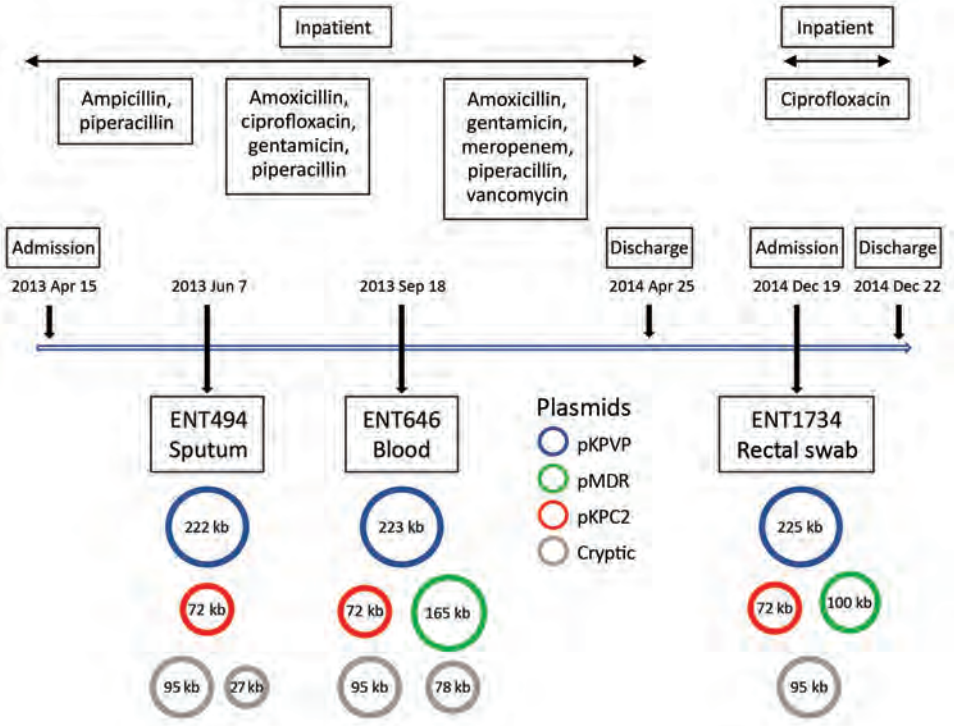

Figure 6. Timeline showing antimicrobial drug exposure and plasmid changes in 3 carbapenem-resistant hypervirulent *Klebsiella pneumoniae* isolates from patient A2, Singapore, 2013–2014. pMDR646 contains genes *aac(6')-Ib-cr*·bla_{OXA-1}, *qnrB1*, *catB3*, and *dfrA14*. pMDR1734 contains genes *aac(6')-Ib-c*^{r}, bla_{OXA-1}, and *catB3*. pKPC2 contains genes bla_{KPC-2}, blaT$_{EM-1A}$, bla_{TEM-1B}, and *mph*(A). KPC, *Klebsiella pneumoniae* carbapenemase; KPVP, *Klebsiella pneumoniae* virulence plasmid; MDR, multidrug resistance.

reported to have acquired carbapenem-resistance genes (*14*,*48*). All our isolates in this investigation had the hypervirulence background and acquired carbapenem-resistance and MDR genes; the MDR genes appeared to move in and out of the parental strain over time within the patient. Our observations are consistent with earlier reports in China involving ST65 isolates, which were likely hypervirulent, indicating that hypervirulent isolates can acquire antimicrobial drug resistance. Therefore, whether a superbug is more likely to arise from a carbapenem-resistant isolate acquiring a *K. pneumoniae* virulence plasmid or some of its genes versus a hypervirulent isolate acquiring MDR genes is unclear. Both ways of exchange appear possible, perhaps depending on the prevalence of the circulating sequence type in a particular setting and in vivo selection pressures.

We also show that, although isolates from different patients were similar in terms of the virulence and carbapenem-resistance plasmids, these isolates do not arise from transmission events. For patients with multiple isolates, the core genomes were highly conserved, suggesting a single infecting isolate gained or lost various antimicrobial drug resistance genes over time. For patient A2, our longitudinal data suggest that the use of distinct antimicrobial drugs drove the acquisition of resistance, though we have no direct proof of cause and effect. Of note, in patient A15, the rectal isolate had additional antimicrobial drug resistance, perhaps reflecting that the colon might serve as a reservoir where genetic exchange can take place. Six of the 18 isolates, including the last acquired isolates from the 3 patients with multiple isolates, were collected from feces or rectal swab specimens, suggesting that the intestines are a likely reservoir for persistent carriage. Last, we demonstrated as a proof-of-principle that pKPC2 can be transferred from the *K. pneumoniae* isolates to *E. coli* in vitro with high efficiency. Determining the particular characteristics of pKPC2 that make it so transmissible and stable, particularly during interactions with hypervirulent isolates, and how pKPC2 is acquired by the recipient is essential.

Therefore, this report serves to alert infectious disease clinicians to the possible presence of hypervirulence in MDR or carbapenem-resistant colonizing isolates; patients harboring these isolates are at risk of developing invasive infections. With timely (rather than retrospective) whole-genome sequencing of bacteria, identifying patients harboring hypervirulent and multidrug-or carbapenem-resistant isolates at high risk for death should be possible. These patients can be selected for appropriate infection control measures, treatment, and close monitoring. Developing strategies to decolonize the gastrointestinal tracts of patients with such isolates would help minimize the release of these potential superbugs into the community.

Acknowledgments

We thank the CaPES study group for their support. This group included Benjamin Cherng, Deepak Rama Narayana, Douglas Chan Su Gin, De Partha Pratim, Hsu Li Yang, Indumathi Venkatachalam, Jeanette Teo, Kalisvar Marimuthu, Koh Tse Hsien, Nancy Tee, Nares Smitasin, Ng Oon Tek, Ooi Say Tat, Raymond Fong, Raymond Lin Tzer Pin, Surinder Kaur Pada, Tan Thean Yen, and Thoon Koh Cheng. We thank Ewan M. Harrison for his critical reading of the manuscript.

This work was supported by the National University of Singapore, Yong Loo Lin School of Medicine Aspiration Fund (NUHSRO/2014/068/AF New Idea/03), and National Medical Research Council (NMRC) collaborative grant Collaborative Solutions Targeting Antimicrobial Resistance Threats in Health Systems (CoSTAR-HS, HS/ARGSeedGrant/2017/03) to Y.-H.G. Additional grant support was provided by CoSTAR-HS (NMRC CGAug16C005), NMRC Clinician Scientist Award (NMRC/CSA-INV/0007/2016), and NMRC Clinician Scientist Award (MOH-000276).

About the Author

Mr. Chen is a research associate at the Yong Loo Lin School of Medicine at National University of Singapore, Singapore. His main research interests are regulation of virulence and antimicrobial drug resistance in bacterial pathogens, including *K. pneumoniae*.

References

1. Willyard C. The drug-resistant bacteria that pose the greatest health threats. Nature. 2017;543:15. https://doi.org/10.1038/nature.2017.21550
2. David S, Reuter S, Harris SR, Glasner C, Feltwell T, Argimon S, et al.; EuSCAPE Working Group; ESGEM Study Group. Epidemic of carbapenem-resistant *Klebsiella pneumoniae* in Europe is driven by nosocomial spread. Nat Microbiol. 2019;4:1919–29. https://doi.org/10.1038/s41564-019-0492-8
3. Munoz-Price LS, Poirel L, Bonomo RA, Schwaber MJ, Daikos GL, Cormican M, et al. Clinical epidemiology of the global expansion of *Klebsiella pneumoniae* carbapenemases. Lancet Infect Dis. 2013;13:785–96. https://doi.org/10.1016/S1473-3099(13)70190-7
4. Government of the United Kingdom. Review on antimicrobial resistance. tackling drug-resistant infections globally: an overview of our work. 2016 Mar [cited 2019 Aug 22]. https://amr-review.org/sites/default/files/Tackling%20drug-resistant%20infections%20-%20An%20overview%20of%20our%20work_IncHealth_LR_NO%20CROPS.pdf
5. World Health Organization. Worldwide country situation analysis: response to antimicrobial resistance. 2015 Apr 29 [cited 2019 Aug 22]. https://www.who.int/drugresistance/documents/situationanalysis
6. Lee IR, Molton JS, Wyres KL, Gorrie C, Wong J, Hoh CH, et al. Differential host susceptibility and bacterial virulence factors driving *Klebsiella l*iver abscess in an ethnically diverse population. Sci Rep. 2016;6:29316. https://doi.org/10.1038/srep29316
7. Chew KL, Lin RTP, Teo JWP. *Klebsiella pneumoniae* in Singapore: hypervirulent infections and the carbapenemase threat. Front Cell Infect Microbiol. 2017;7:515. https://doi.org/10.3389/fcimb.2017.00515
8. Marimuthu K, Venkatachalam I, Khong WX, Koh TH, Cherng BPZ, Van La M, et al. Clinical and molecular epidemiology of carbapenem-resistant *Enterobacteriaceae* among adult inpatients in Singapore. Clin Infect Dis. 2017;64(suppl 2):S68–75.
9. Siu LK, Yeh KM, Lin JC, Fung CP, Chang FY. *Klebsiella pneumoniae* liver abscess: a new invasive syndrome. Lancet Infect Dis. 2012;12:881–7. https://doi.org/10.1016/S1473-3099(12)70205-0
10. Russo TA, Marr CM. Hypervirulent *Klebsiella pneumoniae.* Clin Microbiol Rev. 2019;32:e00001-19. https://doi.org/10.1128/CMR.00001-19
11. Lee CR, Lee JH, Park KS, Kim YB, Jeong BC, Lee SH. Global dissemination of carbapenemase-producing *Klebsiella pneumoniae:* epidemiology, genetic context, treatment options, and detection methods. Front Microbiol. 2016;7:895. https://doi.org/10.3389/fmicb.2016.00895
12. Paczosa MK, Mecsas J. *Klebsiella pneumoniae:* going on the offense with a strong defense. Microbiol Mol Biol Rev. 2016;80:629–61. https://doi.org/10.1128/MMBR.00078-15
13. Lee CR, Lee JH, Park KS, Jeon JH, Kim YB, Cha CJ, et al. Antimicrobial resistance of hypervirulent *Klebsiella pneumoniae:* epidemiology, hypervirulence-associated determinants, and resistance mechanisms. Front Cell Infect Microbiol. 2017;7:483. https://doi.org/10.3389/fcimb.2017.00483
14. Roulston KJ, Bharucha T, Turton JF, Hopkins KL, Mack DJF. A case of NDM-carbapenemase-producing hypervirulent *Klebsiella pneumoniae s*equence type 23 from the UK. JMM Case Rep. 2018;5:e005130. https://doi.org/10.1099/jmmcr.0.005130
15. Andrade LN, Vitali L, Gaspar GG, Bellissimo-Rodrigues F, Martinez R, Darini AL. Expansion and evolution of a virulent, extensively drug-resistant (polymyxin B-resistant), QnrS1-, CTX-M-2-, and KPC-2-producing *Klebsiella pneumoniae* ST11 international high-risk clone. J Clin Microbiol. 2014;52:2530–5. https://doi.org/10.1128/JCM.00088-14
16. Gu D, Dong N, Zheng Z, Lin D, Huang M, Wang L, et al. A fatal outbreak of ST11 carbapenem-resistant hypervirulent *Klebsiella pneumoniae* in a Chinese hospital: a molecular epidemiological study. Lancet Infect Dis. 2018;18:37–46. https://doi.org/10.1016/S1473-3099(17)30489-9
17. Wyres KL, Wick RR, Judd LM, Froumine R, Tokolyi A, Gorrie CL, et al. Distinct evolutionary dynamics of horizontal gene transfer in drug resistant and virulent clones of *Klebsiella pneumoniae.* PLoS Genet. 2019;15:e1008114. https://doi.org/10.1371/journal.pgen.1008114
18. Khong WX, Marimuthu K, Teo J, Ding Y, Xia E, Lee JJ, et al.; Carbapenemase-Producing Enterobacteriaceae in Singapore (CaPES) Study Group. Tracking inter-institutional spread of NDM and identification of a novel NDM-positive plasmid, pSg1-NDM, using next-generation sequencing approaches. J Antimicrob Chemother. 2016;71:3081–9. https://doi.org/10.1093/jac/dkw277
19. Bankevich A, Nurk S, Antipov D, Gurevich AA, Dvorkin M, Kulikov AS, et al. SPAdes: a new genome assembly algorithm and its applications to single-cell sequencing. J Comput Biol. 2012;19:455–77. https://doi.org/10.1089/cmb.2012.0021
20. Wick RR, Judd LM, Gorrie CL, Holt KE. Unicycler: resolving bacterial genome assemblies from short and long sequencing reads. PLOS Comput Biol. 2017;13:e1005595. https://doi.org/10.1371/journal.pcbi.1005595

21. Lam MMC, Wick RR, Wyres KL, Gorrie CL, Judd LM, Jenney AWJ, et al. Genetic diversity, mobilisation and spread of the yersiniabactin-encoding mobile element ICEKp in *Klebsiella pneumoniae* populations. Microb Genom. 2018;4. https://doi.org/10.1099/mgen.0.000196
22. Lam MMC, Wyres KL, Judd LM, Wick RR, Jenney A, Brisse S, et al. Tracking key virulence loci encoding aerobactin and salmochelin siderophore synthesis in *Klebsiella pneumoniae*. Genome Med. 2018;10:77. https://doi.org/10.1186/s13073-018-0587-5
23. Wyres KL, Wick RR, Gorrie C, Jenney A, Follador R, Thomson NR, et al. Identification of *Klebsiella* capsule synthesis loci from whole genome data. Microb Genom. 2016;2:e000102. https://doi.org/10.1099/mgen.0.000102
24. Deatherage DE, Barrick JE. Identification of mutations in laboratory-evolved microbes from next-generation sequencing data using breseq. Methods Mol Biol. 2014; 1151:165–88. https://doi.org/10.1007/978-1-4939-0554-6_12
25. Zankari E, Hasman H, Cosentino S, Vestergaard M, Rasmussen S, Lund O, et al. Identification of acquired antimicrobial resistance genes. J Antimicrob Chemother. 2012;67:2640–4. https://doi.org/10.1093/jac/dks261
26. Jia B, Raphenya AR, Alcock B, Waglechner N, Guo P, Tsang KK, et al. CARD 2017: expansion and model-centric curation of the comprehensive antibiotic resistance database. Nucleic Acids Res. 2017;45(D1):D566–73. https://doi.org/10.1093/nar/gkw1004
27. Carattoli A, Zankari E, García-Fernández A, Voldby Larsen M, Lund O, Villa L, et al. In silico detection and typing of plasmids using PlasmidFinder and plasmid multilocus sequence typing. Antimicrob Agents Chemother. 2014;58:3895–903. https://doi.org/10.1128/AAC.02412-14
28. Treangen TJ, Ondov BD, Koren S, Phillippy AM. The Harvest suite for rapid core-genome alignment and visualization of thousands of intraspecific microbial genomes. Genome Biol. 2014;15:524. https://doi.org/10.1186/s13059-014-0524-x
29. Langmead B, Salzberg SL. Fast gapped-read alignment with Bowtie 2. Nat Methods. 2012;9:357–9. https://doi.org/10.1038/nmeth.1923
30. Bertels F, Silander OK, Pachkov M, Rainey PB, van Nimwegen E. Automated reconstruction of whole-genome phylogenies from short-sequence reads. Mol Biol Evol. 2014;31:1077–88. https://doi.org/10.1093/molbev/msu088
31. Price MN, Dehal PS, Arkin AP. FastTree 2—approximately maximum-likelihood trees for large alignments. PLoS1. 2010;5:e9490. https://doi.org/10.1371/journal.pone.0009490
32. Li X, Xie Y, Liu M, Tai C, Sun J, Deng Z, et al. oriTfinder: a web-based tool for the identification of origin of transfers in DNA sequences of bacterial mobile genetic elements. Nucleic Acids Res. 2018;46(W1):W229–34. https://doi.org/10.1093/nar/gky352
33. Fang CT, Chuang YP, Shun CT, Chang SC, Wang JT. A novel virulence gene in *Klebsiella pneumoniae* strains causing primary liver abscess and septic metastatic complications. J Exp Med. 2004;199:697–705. https://doi.org/10.1084/jem.20030857
34. Lai YC, Peng HL, Chang HY. RmpA2, an activator of capsule biosynthesis in *Klebsiella pneumoniae* CG43, regulates K2 cps gene expression at the transcriptional level. J Bacteriol. 2003; 185:788–800. https://doi.org/10.1128/JB.185.3.788-800.2003
35. Hardiman CA, Weingarten RA, Conlan S, Khil P, Dekker JP, Mathers AJ, et al. Horizontal transfer of carbapenemase-encoding plasmids and comparison with hospital epidemiology data. Antimicrob Agents Chemother. 2016;60:4910–9. https://doi.org/10.1128/AAC.00014-16
36. Khetrapal V, Mehershahi K, Rafee S, Chen S, Lim CL, Chen SL. A set of powerful negative selection systems for unmodified *Enterobacteriaceae*. Nucleic Acids Res. 2015;43:e83. https://doi.org/10.1093/nar/gkv248
37. Clinical and Laboratory Standards Institute. Methods for dilution antimicrobial susceptibility tests for bacteria that grow aerobically (M07-A10). Wayne (PA): The Institute; 2015.
38. Clinical and Laboratory Standards Institute. Performance standards for antimicrobial susceptibility testing (M100-S28). Wayne (PA): The Institute; 2018.
39. Lam MMC, Wyres KL, Duchêne S, Wick RR, Judd LM, Gan YH, et al. Population genomics of hypervirulent *Klebsiella pneumoniae* clonal-group 23 reveals early emergence and rapid global dissemination. Nat Commun. 2018;9:2703. https://doi.org/10.1038/s41467-018-05114-7
40. Chen YT, Chang HY, Lai YC, Pan CC, Tsai SF, Peng HL. Sequencing and analysis of the large virulence plasmid pLVPK of *Klebsiella pneumoniae CG43*. Gene. 2004;337:189–98. https://doi.org/10.1016/j.gene.2004.05.008
41. Yu WL, Ko WC, Cheng KC, Lee CC, Lai CC, Chuang YC. Comparison of prevalence of virulence factors for *Klebsiella pneumoniae* liver abscesses between isolates with capsular K1/K2 and non-K1/K2 serotypes. Diagn Microbiol Infect Dis. 2008;62:1–6. https://doi.org/10.1016/j.diagmicrobio.2008.04.007
42. Zheng JX, Lin ZW, Sun X, Lin WH, Chen Z, Wu Y, et al. Overexpression of OqxAB and MacAB efflux pumps contributes to eravacycline resistance and heteroresistance in clinical isolates of *Klebsiella pneumoniae*. Emerg Microbes Infect. 2018;7:139. https://doi.org/10.1038/s41426-018-0141-y
43. Yao B, Xiao X, Wang F, Zhou L, Zhang X, Zhang J. Clinical and molecular characteristics of multi-clone carbapenem-resistant hypervirulent (hypermucoviscous) *Klebsiella pneumoniae* isolates in a tertiary hospital in Beijing, China.Int J Infect Dis. 2015;37:107–12. https://doi.org/10.1016/j.ijid.2015.06.023
44. Zhan L, Wang S, Guo Y, Jin Y, Duan J, Hao Z, et al. Outbreak by hypermucoviscous *Klebsiella pneumoniae* ST11 Isolates with carbapenem resistance in a tertiary hospital in China. Front Cell Infect Microbiol. 2017;7:182. https://doi.org/10.3389/fcimb.2017.00182
45. Lin YT, Siu LK, Lin JC, Chen TL, Tseng CP, Yeh KM, et al. Seroepidemiology of *Klebsiella pneumoniae* colonizing the intestinal tract of healthy Chinese and overseas Chinese adults in Asian countries. BMC Microbiol. 2012;12:13. https://doi.org/10.1186/1471-2180-12-13
46. Zhang R, Lin D, Chan EW, Gu D, Chen GX, Chen S. Emergence of carbapenem-resistant serotype K1 hypervirulent *Klebsiella pneumoniae* strains in China. Antimicrob Agents Chemother. 2016;60:709–11. https://doi.org/10.1128/AAC.02173-15
47. Cejas D, Fernández Canigia L, Rincón Cruz G, Elena AX, Maldonado I, Gutkind GO, et al. First isolate of KPC-2-producing *Klebsiella pneumonaie* sequence type 23 from the Americas. J Clin Microbiol. 2014;52:3483–5. https://doi.org/10.1128/JCM.00726-14
48. Zhang Y, Zeng J, Liu W, Zhao F, Hu Z, Zhao C, et al. Emergence of a hypervirulent carbapenem-resistant *Klebsiella pneumoniae* isolate from clinical infections in China. J Infect. 2015;71:553–60. https://doi.org/10.1016/j.jinf.2015.07.010

Address for correspondence: Yunn-Hwen Gan, National University of Singapore, Yong Loo Lin School of Medicine, Department of Biochemistry, 8 Medical Dr, 117596, Singapore; email: bchganyh@nus.edu.sg

Long-Term Rodent Surveillance after Outbreak of Hantavirus Infection, Yosemite National Park, California, USA, 2012

Mary E. Danforth, Sharon Messenger, Danielle Buttke, Matthew Weinburke, George Carroll, Gregory Hacker, Michael Niemela, Elizabeth S. Andrews, Bryan T. Jackson, Vicki Kramer, Mark Novak

In 2012, a total of 9 cases of hantavirus infection occurred in overnight visitors to Yosemite Valley, Yosemite National Park, California, USA. In the 6 years after the initial outbreak investigation, the California Department of Public Health conducted 11 rodent trapping events in developed areas of Yosemite Valley and 6 in Tuolumne Meadows to monitor the relative abundance of deer mice (*Peromyscus maniculatus*) and seroprevalence of Sin Nombre orthohantavirus, the causative agent of hantavirus pulmonary syndrome. Deer mouse trap success in Yosemite Valley remained lower than that observed during the 2012 outbreak investigation. Seroprevalence of Sin Nombre orthohantavirus in deer mice during 2013–2018 was also lower than during the outbreak, but the difference was not statistically significant (p = 0.02). The decreased relative abundance of *Peromyscus* spp. mice in developed areas of Yosemite Valley after the outbreak is probably associated with increased rodent exclusion efforts and decreased peridomestic habitat.

A disease outbreak in North America caused by a hantavirus occurred in 1993 in the Four Corners area of the southwestern United States (*1*). Deer mice (*Peromyscus maniculatus*) were identified as the primary reservoir of Sin Nombre virus (SNV) (*2*), an orthohantavirus and the etiologic agent of hantavirus pulmonary syndrome (HPS) (*3*). That outbreak might have been associated with an El Niño weather event the preceding winter, which could have led to increases in deer mouse infestations in buildings (*4*). Investigations into the outbreak and subsequent HPS cases found most cases had probable indoor exposures (*5,6*) and almost one fourth of all human case exposures were associated with a recreational setting (*7*).

During the summer of 2012, a total of 10 persons subsequently given a diagnosis of hantavirus infection visited Yosemite National Park in California, USA (*8,9*). SNV exposure for 9 case-patients was associated with staying overnight in a signature tent cabin, a canvas tent structure with interior insulated walls, located in Curry Village in Yosemite Valley (*8,9*); the tenth infection was associated with lodging in regular tent cabins in the Tuolumne Meadows area. The subsequent environmental investigation found that most of the signature tent cabins had rodent infestations in the insulated walls. A high overnight trap success rate (51%) for *Peromyscus* spp. mice and a 14% (10/73) SNV seroprevalence in deer mice were observed in Curry Village during the initial trapping event in August 2012 (*8*). The park responded by closing and subsequently removing the signature tent cabins, increasing staff and visitor education for HPS prevention, enhancing mouse control measures in and around human-made structures (*8,9*), and applying rodent exclusion measures to other buildings (*8*). In September 2012, the *Peromyscus* spp. trap success rate in Curry Village was substantially lower (14%), and no (0/10) deer mice were positive for SNV (*8*).

We summarize rodent trappings and SNV serosurveys for *Peromyscus* mice in Yosemite Valley and Tuolumne Meadows after the outbreak of infection with hantavirus during 2012. These activities were conducted to monitor relative abundance of deer mice, help assess the peridomestic rodent control efforts in the park, and reduce HPS risk in this heavily used recreational area. We compared *Peromyscus* spp. mouse overnight trap success rates and captured *Peromyscus* mouse species

Author affiliations: California Department of Public Health, Sacramento, California, USA (M.E. Danforth, G. Hacker, M. Niemela, E.S. Andews, B.T. Jackson, V. Kramer, M. Novak); California Department of Public Health, Richmond, California, USA (S. Messenger); National Park Service, Fort Collins, Colorado, USA (D. Buttke); National Park Service, El Portal, California, USA (M. Weinburke, G. Carroll)

DOI: https://doi.org/10.3201/eid2603.191307

composition and SNV seroprevalence in deer mice from peridomestic sites in Yosemite Valley during 2013–2018 with findings from the initial outbreak investigation in August–September 2012 and with findings of similar trapping events conducted in developed areas of Tuolumne Meadows. We also evaluated whether location or climatic factors influenced relative rodent abundance and SNV seroprevalence. Finally, we sought to identify demographic characteristics of SNV-positive deer mice captured in Yosemite National Park.

Methods

Site Selection, Description of Study Areas, and Study Period

Yosemite National Park is in the Sierra Nevada mountain range in California. Yosemite Valley (37.745570, –119.593604) is located in the west-central portion of the park (Figure 1) and covers ≈18 km^2 at an average elevation of 1,209 m. The primary habitat of Yosemite Valley is lower montane forest, dominated by California black oak (*Quercus kelloggii*), ponderosa pine (*Pinus ponderosa*), incense cedar (*Calocedrus decurrens*), and white fir (*Abies concolor*) (*10*). Curry Village is located near the eastern end of Yosemite Valley in a highly developed area that contains other visitor lodging, park administration buildings, and staff housing.

During May 2013–October 2018, rodent surveillance by the California Department of Public Health (CDPH) Vector-Borne Disease Section was conducted 11 times at Curry Village and other nearby peridomestic sites on the basis of park staff requests (Figure 1). In 2013, trapping was conducted in Yosemite

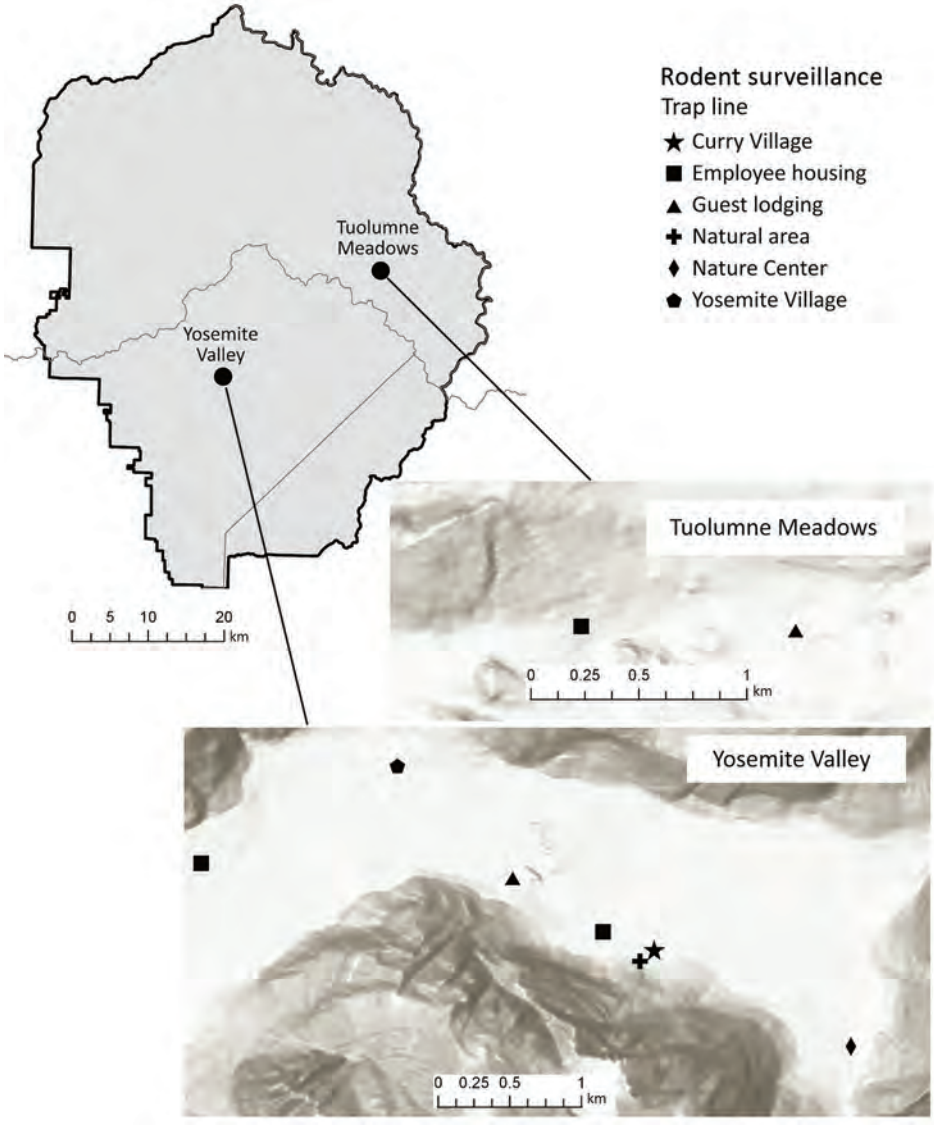

Figure 1. Yosemite National Park, California, USA, and trapping sites, with hillside shading, in Yosemite Valley and Tuolumne Meadows. Sources of mapping data were Esri (https://www.esri.com), Airbus Defence and Space, US Geological Survey, National Geospatial-Intelligence Agency, National Aeronautics and Space Administration, Consultative Group on International Agricultural Research, N. Robinson, National Center for Ecological Analysis and Synthesis, National Library Service, Ordnance Survey, National Mapping Association, Geodatastryelsen, Rijkswaterstaat, General Services Administration, Geoland, Federal Emergency Management Agency, Intermap, and the Geographic Information System user community.

Valley only in May. In subsequent years, trapping was conducted twice annually, in spring (May–June), to assess peridomestic deer mouse abundance and identify potential problem areas before peak tourist visitation, and fall (October–November) (Table 1), when peridomestic deer mouse trap success typically peaks (CDPH and National Park Service [NPS], unpub. data).

Six additional rodent trapping events were conducted annually during 2013–2018 in developed areas of Tuolumne Meadows (37.873107, –119.435709), where previous HPS case-patients have been exposed (*8*); Tuolumne Meadows is located ≈26 km northeast of Yosemite Valley (Figure 1) at an elevation of 2,602 m. The primary habitat is upper montane-subalpine, dominated by Sierra lodgepole (*Pinus contorta murryana*), Ross sedge (*Carex rossii*), western white pine (*Pinus monticola*), and mountain hemlock (*Tsuga mertensiana*) (*10*). Trapping in Tuolumne Meadows was conducted in and around guest lodging and employee housing (Figure 1). With the exception of June 2016, trapping events in Tuolumne Meadows were conducted in August or September, months when this area was most likely to be accessible and facilities open.

Trapping Protocol

All rodent trapping and handling was conducted according to protocols of the CDPH Institutional Animal Care and Use Committee (ACUP no. 2013-14–no. 2018-14). Rodent trapping used Sherman live traps (H.B. Sherman Traps, https://www.sherman-traps.com). Each event consisted of a single overnight trapping period, with 100–200 traps in Yosemite Valley or 44–180 traps in Tuolumne Meadows. Traps were primarily placed outside buildings and tent cabins and left open from ≈5:00 PM to 8:00 AM the following day. A total of 75–81 traps were set outdoors in Curry Village during each Yosemite Valley trapping event. A limited number of traps (0–26/event) were placed indoors to evaluate potential for rodent ingress or in response to reported mouse activity. Beginning in November 2014, a total of 25 traps/event were also set on a transect through a natural habitat adjacent to Curry Village, 25–75 m from any human-made structure, for comparison to peridomestic locations.

Traps were baited with a mixture of corn, oats, and barley, and a ball of polystyrene fill was placed inside as nesting material. Captured rodents were anesthetized with isoflurane, identified to species, sex, and age group, measured for weight, and assessed for the presence of ear scars or notches. Approximately 100 μL of blood was collected into a heparinized capillary tube from the retro-orbital sinus, then stored on ice or refrigerated before transport to the laboratory. All *Peromyscus* mice collected in or near a building were humanely euthanized. *P. boylii* (brush mice) trapped in the natural area adjacent to Curry Village and all other rodent species trapped were released at their point of capture.

Sample Testing

Peromyscus mouse blood samples were submitted to the CDPH Viral and Rickettsial Disease Laboratory to screen for evidence of antibodies against SNV and SNV RNA. Serum or whole blood was analyzed for SNV IgG by using an ELISA (*2*) to detect antibody directed against a purified recombinant Sin Nombre nucleocapsid protein that is strongly recognized by antibodies against orthohantaviruses associated with subfamily *Sigmondontinae* rodents. Rodent blood samples were also screened for evidence of SNV RNA by using a real-time reverse transcription PCR (RT-PCR) targeting an 81-nt region of the small segment of the genome (GenBank accession no. L33816) (*11*), which is highly conserved across known SNV strains.

Data Analysis

We excluded all non-*Peromyscus* rodent captures from data analyses. We estimated relative *Peromyscus* rodent abundance by using trap success (no. *Peromyscus* rodents trapped/no. traps set) for each trapping event at each site type and calculated the proportion of captured *Peromyscus* mice that were deer mice for each site type at each trapping event (no. deer mice/no. all *Peromyscus* rodent captures). We estimated seroprevalence by the percentage of deer mice sampled that were positive for SNV antibodies. We obtained climate data from the PRISM climate group (*12*); variables used were mean monthly temperature for the month of the trapping event (°C), mean monthly temperature from 6 months before (°C), mean monthly temperature from 12 months before (°C), current water year (total precipitation from the preceding October 1 through April 30, mm), and the previous water year (Table 1).

We analyzed data by using R statistical software (*13*). We made comparisons for trap success, proportions of *Peromyscus* species captures that were deer mice, and deer mouse seroprevalence in Yosemite Valley during June 2013–October 2018 to those from August 2012 and September 2012 in Yosemite Valley, in the natural area adjacent to Curry Village (2014–2018 for both datasets), and in Tuolumne Meadows by using χ^2 analysis. Because we made 5 comparisons, we

Table 1. Dates, locations, and climate data for Sin Nombre virus surveillance, Yosemite National Park, California, USA, 2013–2018

Trap date	Location	Mean monthly temperature, °C			Total water year, mm	Total water year, mm, from year before
		Trapping month	6 months before	1 year before		
2013 May 30	Yosemite Valley	12.9	7.0	16.9	643.01	547.43
2013 Sep 10	Tuolumne Meadows	9.2	0.7	10.5	541.02	426.65
2014 Jun 26	Yosemite Valley	18.2	7.5	18.4	451.25	643.01
2014 Sep 9	Tuolumne Meadows	9.9	−0.8	9.2	384.94	541.02
2014 Nov 13	Yosemite Valley	7.6	18.3	7.5	451.25	643.01
2015 May 19	Yosemite Valley	11.2	7.6	13.2	398.61	451.25
2015 Aug 26	Tuolumne Meadows	12.6	1.4	11.4	316.54	384.94
2015 Oct 22	Yosemite Valley	13.7	8.8	14.6	398.61	451.25
2016 May 25	Yosemite Valley	11.7	4.1	11.2	956.50	398.61
2016 Jun 22	Tuolumne Meadows	10.6	−5.5	11.4	744.60	316.54
2016 Oct 12	Yosemite Valley	11.4	9.3	13.7	956.50	398.61
2017 May 24	Yosemite Valley	12.9	7.3	11.7	1,871.10	956.50
2017 Aug 9	Tuolumne Meadows	12.9	−0.9	12.5	1,637.41	744.60
2017 Oct 18	Yosemite Valley	12.7	7.8	11.4	1,871.10	956.50
2018 May 17	Yosemite Valley	12.6	7.6	12.9	731.19	1,871.10
2018 Aug 22	Tuolumne Meadows	12.8	−3.7	12.9	648.49	1,637.41
2018 Oct 9	Yosemite Valley	12.0	9.0	12.7	731.19	1,871.10

applied the Bonferroni correction to χ^2 analyses; only $p \leq 0.01$ was considered significant. If a cell size was <5 by any χ^2 analysis, we then used the Fisher exact test.

We conducted regression analyses on all data collected for Yosemite Valley and Tuolumne Meadows after 2013. We used multivariate linear regression to find associations between relative rodent abundance and time as a continuous variable, season as a categorical variable (spring or fall), site (Curry Village, Curry Village natural area, other Yosemite Valley peridomestic sites, and Tuolumne Meadows), current and previous climatic variables, and current and previous relative rodent abundance. We also used multivariate linear regression to determine whether the proportion of *Peromyscus* captures at an event that were deer mice was associated with time, season, site, current and previous climatic variables, and current and previous proportions of deer mouse captures. We analyzed the relationship between seroprevalence and date, season, peridomestic versus natural area, current and previous relative rodent abundance and dominance by using multivariate linear regression. We then used multivariate logistic regression to identify which demographic variables (age, sex, weight, presence of ear notches/scars) were associated with detecting positive deer mice.

Results

Summary Statistics

During May 2013–October 2018, CDPH conducted 11 trapping events (1,574 trap nights of surveillance) at peridomestic sites in Yosemite Valley, and captured 231 rodents (overall trap success rate 14.7%); there were no recaptures. Thirty-one (2.0%) traps were set inside buildings, and only 1 deer mouse was captured

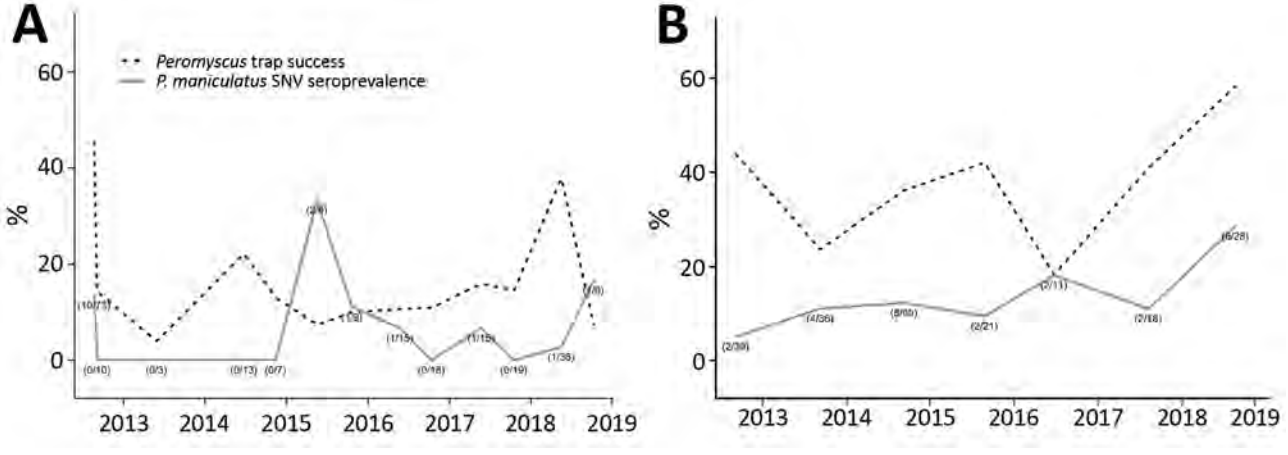

Figure 2. *Peromyscus* rodent trap success and seroprevalence (with sample sizes) of SNV in deer mice (*Peromyscus maniculatus*), Yosemite National Park, California, USA, 2012–2018. A) Yosemite Valley; B) Tuolumne Meadows. Numbers in parentheses indicate no. positive deer mice/no. tested. Figures include data from the August–September 2012 outbreak investigation (*8*) for reference. SNV, Sin Nombre virus.

indoors (trap success rate 3.2%). Deer mice represented 148 (64.1%) of all captures; the remainder consisted of 70 (30.3%) brush mice, 2 shrews (*Sorex* spp.), 5 house mice (*Mus musculus*), 2 roof rats (*Rattus rattus*), and 4 unidentified *Peromyscus* rodents that escaped before processing.

Blood samples were collected from 147 deer mice (Table 2), and 7 (4.8%) were positive for antibodies to SNV (Figure 2, panel A). We also tested 67 brush mice blood samples for SNV antibodies, and all were negative. We retested 6 deer mouse blood samples that had SNV antibodies and 131 that did not have SNV antibodies for SNV RNA by real-time RT-PCR. Three (50%) of the 6 antibody-positive deer mice were also positive for SNV RNA, and only 1 (0.8%) of 131 seronegative deer mice showed positive results. We also tested 34 brush mice by using real-time RT-PCR; all were negative for SNV RNA.

The natural area adjacent to Curry Village was trapped during 9 events from November 2014 through October 2018 for 223 trap nights. Thirty-three *Peromyscus* mice and 1 shrew were captured (overall trap success rate 15.2%). One brush mouse was captured twice. Deer mice represented 7 (20.6%) of the captures; 26 (76.5%) of captures were brush mice. We tested blood samples from 7 deer mice (Table 2) and 13 brush mice for antibodies to SNV; all were negative. We retested 6 deer mice and all 13 brush mice by using real-time RT-PCR; all were negative for SNV RNA.

Table 2. Characteristics of *Peromyscus maniculatus* rodents tested for Sin Nombre virus in Yosemite National Park, California, USA, 2013–2018*

Characteristic category	Value
Sex	
M	21/147 (14.3)†
F	12/186 (6.5)
Age	
Adult	24/189 (12.7)
Subadult	9/107 (8.4)
Juvenile	0/37 (0)
Ear scarred, torn, or notched‡	3/13 (18.8)
Location	
Curry Village	4/88 (4.5)
Other Yosemite Valley periodomestic area	3/59 (5.1)
Curry Village natural area	0/7 (0)
Tuolumne Meadows	26/179 (14.5)†
Mean weight, g	
Antibody negative	
M	14.7
F	15.9
Antibody positive	
M	17.1§
F	17.2§

*Values are no. antibody positive/no. tested (%) unless otherwise indicated.
†Significantly greater than others in category.
‡Observations about the presence of ear scars, tears, or notches were not systematically recorded.
§Significant difference between antibody positive and antibody negative.

During September 2013–October 2018, a total of 534 trap nights during 6 surveillance events in Tuolumne Meadows captured 195 rodents (trap success rate 36.5%); there were no recaptures. Deer mice represented 179 captures (91.8%), and the remaining 16 captures consisted of 8 wood rats (*Neotoma cinerea*), 3 chipmunks (*Tamias* spp.), 4 golden-mantled ground squirrels (*Callospermophilus lateralis*), and 1 long-tailed vole (*Microtus longicaudus*). Blood samples were collected from all 179 deer mice (Table 2) and 26 (14.5%) were positive for SNV antibodies (Figure 2, panel B).

Trends in *Peromyscus* spp. Trap Success

The overall *Peromyscus* trap success rate at peridomestic sites in Yosemite Valley (14.1%) (Figure 2, panel A) was significantly lower during 2013–2018 than that during the initial August 2012 outbreak investigation (χ^2 142.6; p<0.01), although not from the September 2012 surveillance event (χ^2 <0.1; p = 0.99). Within Yosemite Valley, we found no significant difference in the *Peromyscus* trap success between Curry Village (14.2%) and other peridomestic sites in Yosemite Valley (13.9%; χ^2 <0.1; p = 0.88). We also noted no significant difference in trap success rates between all Yosemite Valley peridomestic locations combined and the natural area adjacent to Curry Village (14.8%; χ^2 0.1; p = 0.78). However, *Peromyscus* trap success in Yosemite Valley during the study was significantly lower than that in Tuolumne Meadows (33.7%; χ^2 11.8; p<0.01) (Figure 2, panel B). When we performed analysis by using by multivariate regression, we found no significant association between relative rodent abundance and date, season, and any current or previous climatic variable.

Trends in *Peromyscus* spp. Rodent Captures

The proportion of *Peromyscus* spp. rodent captures that were *P. maniculatus* deer mice (82.2%) at peridomestic locations in Yosemite Valley during 2013–2018 was not different from those observed in August 2012 (73.3%; χ^2 3.2; p = 0.07) and September 2012 (52.6%; χ^2 1.8; p = 0.18) (Figure 3). Although most *Peromyscus* rodent captures at peridomestic sites in Yosemite Valley were deer mice (75.4%), deer mice were significantly less likely to be trapped in the natural area adjacent to Curry Village (24.2%; χ^2 33.1; p<0.01). The proportion of *Peromyscus* rodent captures that were deer mice did not have a significant linear relationship with time, season, site, current and previous climate variables, or current and previous trap success.

Trends in SNV Seroprevalence

SNV antibody seroprevalence in deer mice sampled at peridomestic sites in Yosemite Valley was not

significantly different than that observed during August 2012 (χ^2 5.4; p = 0.02) or September 2012 (p = 1.00 by Fisher exact test). Within Yosemite Valley, no significant difference occurred in detection of SNV-positive deer mice in peridomestic areas compared with the natural area (p = 1.00 by Fisher exact test). However, seroprevalence was significantly lower at peridomestic sites in Yosemite Valley than in Tuolumne Meadows during the study (χ^2 32.9; p<0.01). We found no relationship between seroprevalence in Yosemite Valley deer mice and time, season, peridomestic versus natural area, or concurrent or previous relative *Peromyscus* rodent abundance and *P. maniculatus* mouse dominance. When analyzed by logistic regression, we found that seropositive deer mice from Yosemite Valley and Tuolumne Meadows were significantly more likely to be male (β = 1.09; p = 0.02) and have higher body weights (β = 0.16; p = 0.01); no other demographic variables were significant.

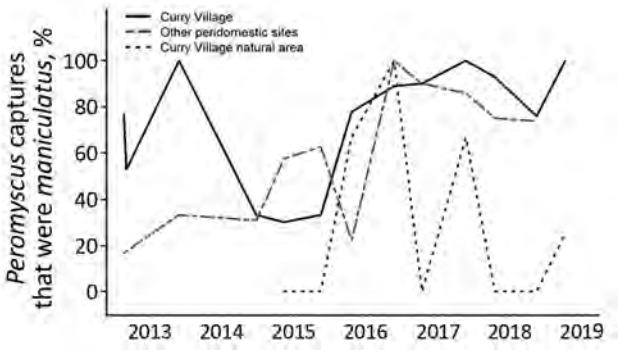

Figure 3. Proportion of *Peromyscus* rodent captures that were *P. maniculatus* from areas of Yosemite Valley, Yosemite National Park, California, USA, 2012–2018. Figure includes data from the August–September 2012 outbreak investigation (*8*) for reference. SNV, Sin Nombre virus.

Discussion

During the initial Yosemite hantavirus outbreak investigation in August 2012, a robust population of deer mice in Curry Village was identified, although SNV seroprevalence was not unusually increased (*8*). Just a few weeks later, after the signature tent cabins were closed and rodent control and exclusion measures were enacted, trap success for deer mice was substantially lower (*8*). Our study found that overall trap success during May 2013–October 2018 in Yosemite Valley remained lower than that observed during August 2012. The rodent control measures implemented by the park and concessionaires have likely contributed to lower *Peromyscus* rodent trap success in these peridomestic locations. To a lesser degree, the cumulative effect of removing *Peromyscus* mice from peridomestic locations during our surveillance events might have also contributed to the control effort. Although current and previous precipitation amounts were not associated with *Peromyscus* rodent trap success, we cannot rule out the effects of the historic drought in California during 2011–2015 (*12*). The end of the drought might have contributed to the trend of increasing trap success rates seen during 2016–2018. Although a few SNV-seropositive deer mice have continued to be detected since 2012, rodent control measures that limit the number of deer mice around and in buildings have likely decreased HPS exposure risk (*14*,*15*).

Overall, deer mice represented a similar proportion of the *Peromyscus* rodent captures from peridomestic locations during 2013–2018 as during the outbreak investigation in 2012. However, the proportion of deer mouse and brush mouse captures from these locations fluctuated after 2012, suggesting the relative abundance of these species changed over time. Interspecific competition between these sympatric species (*16*), climatic factors, or some combination of these effects probably contributed to the observed trends in trap success, but habitat preferences might also affect local abundance. Deer mice are the most common *Peromyscus* species in California, found in almost any habitat, and commonly enter buildings (*17*). Brush mice are found mainly below an elevation of 2,000 m (*17*) and have a preference for rocky areas in brush or woodlands (*18*), although they will readily enter human-made structures. Although preferred habitats for both species occur in Yosemite Valley, highly developed locations providing human-made harborage and food sources might favor deer mouse abundance.

Although deer mice predominated at peridomestic sites, brush mice were captured more frequently at the natural area sampled. This trap line was only 25–75 m from tent cabins and other buildings in Curry Village, both locations potentially within typical home ranges of deer mice (41–4,452 m^2) and brush mice (162–3,845 m^2) (*19*). Despite the proximity of these habitats, brush mice were the dominant, often only, *Peromyscus* species trapped in the natural area. This finding supports the need for minimizing peridomestic harborage that might favor deer mouse abundance. In addition, maintaining natural environments to the extent possible in Yosemite Valley could increase competition from brush mice, which are not known reservoirs of SNV (*20*). Increasing rodent diversity could also reduce SNV prevalence in deer mice (*21*,*22*).

We were unable to detect many major trends in deer mouse seroprevalence. Although SNV seroprevalence in Yosemite Valley decreased during August–September 2012 and typically remained lower in

subsequent years, we found no significant differences in seroprevalence between either month during 2012 and that observed during 2013–2018 because of Bonferroni adjustment for multiple comparisons and low p value threshold. Other, much larger, studies have detected relationships between deer mouse seroprevalence and previous rodent population density (*14,23,24*) or age (*14,21,23,25,26*), neither of which we observed, probably because of our smaller sample size. Also, potentially because of inconsistent collection of qualitative observations of body condition, we were unable to determine whether seropositive deer mice were more likely to have wounds (*14,23,25–27*). However, we did find that male and heavier deer mice were more likely to be seropositive, as seen in other studies (*14,21,23,25–27*).

We also compared trapping results and SNV seroprevalence from Yosemite Valley during 2013–2018 to Tuolumne Meadows. Despite trapping around similar types of buildings, the deer mouse trap success rate and SNV seroprevalence were higher in Tuolumne Meadows. This location is 1,400 m higher in elevation, outside the range of brush mice, and no other *Peromyscus* rodent species have been trapped here during previous CDPH surveillance events (CDPH, unpub. data). Tuolumne Meadows is also less developed than Yosemite Valley, and most buildings are used only seasonally, typically during June–September. Given the absence of other *Peromyscus* rodent species and abundance of seasonally used buildings in an otherwise natural montane habitat, the consistent abundance of deer mice and higher SNV seroprevalence at Tuolumne Meadows is not surprising. Higher SNV seroprevalence rates relative to Yosemite Valley were observed in previous surveillance events in this area (CDPH, unpub. data) and in deer mice sampled at other higher elevations in California (*28*). This area was associated with 3 previous HPS cases during 2000, 2010, and 2012 (*8*), and although more cases of infection with hantavirus have been associated with Yosemite Valley, all 9 cases were linked with the 2012 outbreak and the subsequently removed signature tent cabins. Our surveillance results and the sporadic occurrence of HPS cases underscore the need for maintaining hantavirus awareness and prevention measures in the Tuolumne Meadows area.

Since 2012, the NPS and concessionaires have expanded their efforts beyond Curry Village to improve rodent exclusion in other buildings, reduce rodent harborage in peridomestic habitats, and conduct regular mouse trapping in developed areas of the park (*8*). A previous study in Yosemite found that rodent-proofed homes are less likely to be infested with mice and, if infested, have fewer mice (*29*). In addition to snap-trapping indoors, Yosemite staff conduct routine outdoor snap-trapping around buildings that are difficult to exclude, which assists in peridomestic rodent control and provides monitoring for spatiotemporal increases in *Peromyscus* rodent abundance. Early indications of increases in rodent abundance prompt the initiation of specified actions to reduce human risk for exposure to SNV (*30*). To assist the park and concessionaire with identifying rodent exclusion issues, CDPH has conducted >300 building evaluations during 2013–2018.

After the outbreak during 2012, NPS and concessionaires expanded their public education programs to reduce the risk for HPS. NPS added hantavirus information to its Yosemite website, placed educational posters in central locations, and offers informational brochures to visitors (*8*). Visitors at Curry Village and other tent cabin lodgings are provided with information about hantavirus at check-in and prevention methods are posted in each tent cabin (*8*). These efforts, combined with improvements in rodent exclusion and control measures and ongoing rodent surveillance, have helped to strongly reduce peridomestic abundance of deer mice and the risk for exposure to HPS for visitors and staff in Yosemite.

Acknowledgments

We thank the CDPH Vector-Borne Disease Section staff for their assistance with rodent surveillance, particularly Lawrence Bronson, James Tucker, Renjie Hu, Joseph Burns, Marco Metzger, Sarah Billeter, and Robert Dugger. We also extend our appreciation to the staff of the CDPH Viral and Rickettsial Disease Laboratory who tested all rodent samples, especially Barryett Enge, Kristina Hsieh, Kim Hansard, and Mojgan Deldari. We also thank the Delaware North Corporation and Yosemite Hospitality for their cooperation with rodent surveillance and facility evaluations.

This study was partially supported by the NPS to Public Health Foundation Enterprises (doing business as Heluna Health) as part of a 5-year cooperative agreement (No. P13AC00320). Heluna Health staff carried out specific activities required by the contract in partnership with CDPH staff. For the purposes of this manuscript, we have included the activities of Heluna Health staff as part of the overall monitoring work of CDPH.

About the Author

Dr. Danforth is an epidemiologist with Heluna Health assigned to the California Department of Public Health, Sacramento, CA. Her primary research interest is the epidemiology of vectorborne diseases and their impact on public health.

References

1. Centers for Disease Control and Prevention. Hantavirus pulmonary syndrome—United States, 1993. MMWR Morb Mortal Wkly Rep. 1994;43:45–8.
2. Childs JE, Ksiazek TG, Spiropoulou CF, Krebs JW, Morzunov S, Maupin GO, et al. Serologic and genetic identification of *Peromyscus maniculatus* as the primary rodent reservoir for a new hantavirus in the southwestern United States. J Infect Dis. 1994;169:1271–80. https://doi.org/10.1093/infdis/169.6.1271
3. Elliott LH, Ksiazek TG, Rollin PE, Spiropoulou CF, Morzunov S, Monroe M, et al. Isolation of the causative agent of hantavirus pulmonary syndrome. Am J Trop Med Hyg. 1994;51:102–8. https://doi.org/10.4269/ajtmh.1994.51.102
4. Hjelle B, Jenison S, Mertz G, Koster F, Foucar K. Emergence of hantaviral disease in the southwestern United States. West J Med. 1994;161:467–73.
5. Hjelle B, Tórrez-Martínez N, Koster FT, Jay M, Ascher MS, Brown T, et al. Epidemiologic linkage of rodent and human hantavirus genomic sequences in case investigations of hantavirus pulmonary syndrome. J Infect Dis. 1996;173:781–6. https://doi.org/10.1093/infdis/173.4.781
6. Hjelle B, Glass GE. Outbreak of hantavirus infection in the Four Corners region of the United States in the wake of the 1997–1998 El Nino-southern oscillation. J Infect Dis. 2000;181:1569–73. https://doi.org/10.1086/315467
7. de St Maurice A, Ervin E, Schumacher M, Yaglom H, VinHatton E, Melman S, et al. Exposure characteristics of hantavirus pulmonary syndrome patients, United States, 1993–2015. Emerg Infect Dis. 2017;23:733–9. https://doi.org/10.3201/eid2305.161770
8. Núñez JJ, Fritz CL, Knust B, Buttke D, Enge B, Novak MG, et al.; Yosemite Hantavirus Outbreak Investigation Team. Hantavirus infections among overnight visitors to Yosemite National Park, California, USA, 2012. Emerg Infect Dis. 2014;20:386–93. https://doi.org/10.3201/eid2003.131581
9. Centers for Disease Control and Prevention. Hantavirus pulmonary syndrome in visitors to a national park—Yosemite Valley, California, 2012. MMWR Morb Mortal Wkly Rep. 2012;61:952.
10. Mayer KE, Laudenslayer WF, editors. A guide to wildlife habitats of California. Sacramento (CA): State of California, Resources Agency, Department of Fish and Game; 1988.
11. Bagamian KH, Towner JS, Kuenzi AJ, Douglass RJ, Rollin PE, Waller LA, et al. Transmission ecology of Sin Nombre hantavirus in naturally infected North American deermouse populations in outdoor enclosures. PLoS One. 2012;7:e47731. https://doi.org/10.1371/journal.pone.0047731
12. PRISM Climate Group. Northwest Alliance for Computational Science & Engineering (NACSE), Oregon State University. 2018 [cited 2019 Nov 27]. http://www.prism.oregonstate.edu
13. R Core Team. R: a language and environment for statistical computing. Vienna: R Foundation for Statistical Computing; 2018.
14. Mills JN, Ksiazek TG, Peters CJ, Childs JE. Long-term studies of hantavirus reservoir populations in the southwestern United States: a synthesis. Emerg Infect Dis. 1999;5:135–42. https://doi.org/10.3201/eid0501.990116
15. Calisher CH, Mills JN, Root JJ, Doty JB, Beaty BJ. The relative abundance of deer mice with antibody to Sin Nombre virus corresponds to the occurrence of hantavirus pulmonary syndrome in nearby humans. Vector Borne Zoonotic Dis. 2011;11:577–82. https://doi.org/10.1089/vbz.2010.0122
16. Holbrook SJ. Habitat utilization, competitive interactions, and coexistence of three species of Cricetine rodents in east-central Arizona. Ecology. 1979;60:758–69. https://doi.org/10.2307/1936613
17. Jameson, EW, Peeters, HJ. Mammals of California. Berkeley (CA): University of California Press; 2004.
18. Baker RH. Habitats and distribution. In: King JA, editor. Biology of *Peromyscus* (Rodentia). Topeka (KS): The American Society of Mammalogists; 1968. p. 98–126.
19. Stickel LF. Home range and travels. In: King JA, editor. Biology of *Peromyscus* (Rodentia). Topeka (KS): The American Society of Mammalogists; 1968. p. 373–411.
20. Sanchez AJ, Abbott KD, Nichol ST. Genetic identification and characterization of limestone canyon virus, a unique *Peromyscus-borne* hantavirus. Virology. 2001;286:345–53. https://doi.org/10.1006/viro.2001.0983
21. Calisher CH, Root JJ, Mills JN, Rowe JE, Reeder SA, Jentes ES, et al. Epizootiology of Sin Nombre and El Moro Canyon hantaviruses, southeastern Colorado, 1995–2000. J Wildl Dis. 2005;41:1–11. https://doi.org/10.7589/0090-3558-41.1.1
22. Dearing MD, Clay C, Lehmer E, Dizney L. The roles of community diversity and contact rates on pathogen prevalence. Journal of Mammalogy. 2015;96:29–36. https://doi.org/10.1093/jmammal/gyu025
23. Madhav NK, Wagoner KD, Douglass RJ, Mills JN. Delayed density-dependent prevalence of Sin Nombre virus antibody in Montana deer mice (*Peromyscus maniculatus)* and implications for human disease risk. Vector Borne Zoonotic Dis. 2007;7:353–64. https://doi.org/10.1089/vbz.2006.0605
24. Davis S, Calvet E, Leirs H. Fluctuating rodent populations and risk to humans from rodent-borne zoonoses. Vector Borne Zoonotic Dis. 2005;5:305–14. https://doi.org/10.1089/vbz.2005.5.305
25. Kuenzi AJ, Morrison ML, Swann DE, Hardy PC, Downard GT. A longitudinal study of Sin Nombre virus prevalence in rodents, southeastern Arizona. Emerg Infect Dis. 1999;5:113–7. https://doi.org/10.3201/eid0501.990113
26. Calisher CH, Wagoner KD, Amman BR, Root JJ, Douglass RJ, Kuenzi AJ, et al. Demographic factors associated with prevalence of antibody to Sin Nombre virus in deer mice in the western United States. J Wildl Dis. 2007;43:1–11. https://doi.org/10.7589/0090-3558-43.1.1
27. Calisher CH, Sweeney W, Mills JN, Beaty BJ. Natural history of Sin Nombre virus in western Colorado. Emerg Infect Dis. 1999;5:126–34. https://doi.org/10.3201/eid0501.990115
28. Jay M, Ascher MS, Chomel BB, Madon M, Sesline D, Enge BA, et al. Seroepidemiologic studies of hantavirus infection among wild rodents in California. Emerg Infect Dis. 1997;3:183–90. https://doi.org/10.3201/eid0302.970213
29. Glass GE, Johnson JS, Hodenbach GA, Disalvo CL, Peters CJ, Childs JE, et al. Experimental evaluation of rodent exclusion methods to reduce hantavirus transmission to humans in rural housing. Am J Trop Med Hyg. 1997;56:359–64. https://doi.org/10.4269/ajtmh.1997.56.359
30. Mills JN, Amman BR, Glass GE. Ecology of hantaviruses and their hosts in North America. Vector Borne Zoonotic Dis. 2010;10:563–74. https://doi.org/10.1089/vbz.2009.0018

Address for correspondence: Mary E. Danforth, California Department of Public Health, 1616 Capitol Ave, Mailstop 7307, Sacramento, CA 95899, USA; email: mary.danforth@cdph.ca.gov

Mycobacterium tuberculosis Beijing Lineage and Risk for Tuberculosis in Child Household Contacts, Peru

Chuan-Chin Huang,[1] Alexander L. Chu,[1] Mercedes C. Becerra, Jerome T. Galea, Roger Calderón, Carmen Contreras, Rosa Yataco, Zibiao Zhang, Leonid Lecca, Megan B. Murray

Few studies have prospectively compared the relative transmissibility and propensity to cause disease of *Mycobacterium tuberculosis* Beijing strains with other human-adapted strains of the *M. tuberculosis* complex. We assessed the effect of Beijing strains on the risk for *M. tuberculosis* infection and disease progression in 9,151 household contacts of 2,223 culture-positive pulmonary tuberculosis (TB) patients in Lima, Peru. Child contacts exposed to Beijing strains were more likely than child contacts exposed to non-Beijing strains to be infected at baseline, by 12 months of follow-up, and during follow-up. We noted an increased but nonsignificant tendency for child contacts to develop TB. Beijing strains were not associated with TB in adult contacts. These findings suggest that Beijing strains are more transmissible in children than are non-Beijing strains.

Tuberculosis (TB) remains the leading cause of death worldwide from a single infectious disease; in 2017, ≈10 million incident cases and 1.7 million deaths were reported (*1*). The causative pathogen, *Mycobacterium tuberculosis*, is divided into 7 human-adapted phylogenetic lineages, of which some are geographically restricted and others are widespread throughout the world, possibly because they are better adapted to environments of high human density (*2*). One of the widespread groups, lineage 2, includes a widely distributed genotype, the Beijing strain, that has been repeatedly implicated in outbreaks and in the evolution of drug resistance (*3*–*6*). The global distribution of Beijing strains and their precipitous rise in some populations have led researchers to speculate that it may be more transmissible and more likely to cause disease than other less widely distributed *M. tuberculosis* lineages (*7*–*9*).

However, the few direct assessments of the relative transmissibility of Beijing strains have been inconclusive. Although some studies found that exposure to Beijing strains was more likely than exposure to other strains to lead to TB (*10*–*15*), others reported no difference (*16*,*17*). Several studies have suggested that the Beijing genotype is more common among young persons and that its frequency declines with age (*18*–*21*). To explore these factors, we directly compared the relative transmissibility and propensity to cause disease of Beijing strains with other strains in a cohort study of household contacts of patients with pulmonary TB in Lima, Peru.

Methods

Ethics Statement

The Institutional Review Board of Harvard School of Public Health and the Research Ethics Committee of the National Institute of Health of Peru approved the study. All study participants or their guardians provided written informed consent, and children <18 years of age provided assent.

Setting, Study Design, and Participant Recruitment and Follow-Up

The study design and methods were previously described in detail (*22*). In brief, we conducted a prospective cohort study of household contacts of pulmonary TB patients in Lima, Peru. The study area comprised 20 districts inhabited by ≈3.3 million residents living in urban areas and in periurban, informal shantytown settlements.

Author affiliations: Brigham and Women's Hospital, Boston, Massachusetts, USA (C.-C. Huang, M.C. Becerra, Z. Zhang, M.B. Murray); Harvard Medical School, Boston (C.-C. Huang, M.C. Becerra, M.B. Murray); Harvard University Division of Continuing Education, Cambridge, Massachusetts, USA (A.L. Chu); University of South Florida, Tampa, Florida, USA (J.T. Galea); Socios En Salud Sucursal, Lima, Peru (R. Calderón, C. Contreras, R. Yataco, L. Lecca)

DOI: https://doi.org/10.3201/eid2603.191314

[1]These authors contributed equally to this article.

During September 2009–August 2012, we identified patients ≥15 years of age who had received a diagnosis of clinically presumptive pulmonary TB at any of 106 participating health centers. We confirmed the microbiological status of their disease with either a positive sputum smear or mycobacterial culture. We also recorded the index patient's sociodemographic data; baseline smear status; presence or absence of cavitary disease; tobacco and alcohol use; HIV status; time from symptom onset until initiation of treatment; and, for patients, with drug-resistant TB, the time from TB diagnosis until start of an effective treatment (i.e., a drug regimen deemed appropriate for the index patient's drug-resistant profile).

Within 2 weeks after index patient diagnosis, we enrolled all consenting household contacts. We assessed baseline *M. tuberculosis* infection status with the tuberculin skin test (TST) in household contacts with no history of a positive TST or TB. Household contacts who had signs or symptoms of TB underwent clinical evaluation and, if indicated, initiated treatment under Peru's National Tuberculosis Program guidelines (*23*). We offered HIV testing to all study participants. In accordance with Peru's National Tuberculosis Program guidelines, isoniazid preventive therapy (IPT) was offered to household contacts ≤19 years of age and persons with specified concurrent conditions. At the time of household contact enrollment, we collected age, sex, sociodemographic, and occupational information; height and weight; alcohol and tobacco use information; HIV status; self-reported diabetes mellitus; history and presence of *M. bovis* BCG vaccination scars; use of IPT; history of TB; and housing features. We repeated the TST 6 and 12 months after initial evaluation among household contacts who had previously tested negative; 2, 6, and 12 months after initial evaluation, we reevaluated them for pulmonary and extrapulmonary TB. We also accessed the medical records of health centers in the catchment areas to identify household contacts whose TB was diagnosed at a health center during the follow-up period.

Whole-Genome Sequencing

Among 3,027 index patients with culture-positive isolates at baseline, 2,143 had isolates that also underwent whole-genome sequencing (WGS) using the Illumina HiSeq 4000 platform (Illumina, https://www.illumina.com) with a read length of 100–150 bp and ≥50-fold coverage. The raw sequence data were trimmed using the sickle package (*24*) and mapped to the H37Rv reference genome using the BWA-MEM algorithm (*25*). We used a coverage-based approach, specifically SAMtools (default settings) (*26*) and pilon (*27*), to identify single-nucleotide polymorphisms across the whole genome. We assigned a call as missing if the valid depth of coverage at a specific site was <8 reads, if the mean read-mapping quality at the site did not reach 9, or if none of the alternative alleles accounted for ≥85% of the valid coverage.

Table 1. Baseline characteristics of *Mycobacterium tuberculosis* culture-positive index patients, Lima, Peru, September 2009–August 2012

Variable	No. (%), N = 2,223*
Age, y	
16–30	1,363 (61)
31–45	465 (21)
≥46	395 (18)
Sex	
M	1,289 (58)
F	934 (42)
Concurrent condition	
HIV seropositive	59 (3)
Self-reported diabetes	111 (6)
Current smoker	60 (3)
M. tuberculosis lineage	
L2 (Beijing)	255 (12)
L4.1	951 (43)
L4.3	775 (35)
Other	242 (11)
Sputum smear status†	
Negative	548 (25)
+	639 (29)
++	431 (19)
+++	596 (27)
Cavitary disease	655 (30)
Drug resistance profile	
Pansusceptible	1,442 (67)
Resistant	726 (33)

*Numbers might not add to total because of missing data.
†+, 1–99 acid-fast bacilli (AFB) in 100 observed fields; ++, 1–10 AFB per field in 50 observed fields; +++, ≥10 AFB per field in 20 observed fields.

Lineage Identification of *M. tuberculosis* Strains

Among index patients for whom WGS data were available, we identified *M. tuberculosis* lineages and sublineages on the basis of a previously published barcode that differentiates the groups on the basis of single-nucleotide polymorphisms (*28*). For index patients without available WGS data, we genotyped their *M. tuberculosis* isolates using 24-locus mycobacterial interspersed repetitive units–variable-number tandem repeats (MIRU-VNTR) (*29*). We used the best-match algorithm from the MIRU-VNTR*plus* online database (http://www.miru-vntrplus.org) to identify the lineages of the typed samples by cross-referencing them with reference lineages stored on the database (*30*).

Outcomes

We considered 4 distinct outcomes: *M. tuberculosis* infection at baseline, time to TST conversion during the 12 months of follow-up, *M. tuberculosis* infection by

Table 2. Baseline characteristics of household contacts exposed to a *Mycobacterium tuberculosis* culture-positive index tuberculosis patient, Lima, Peru, September 2009–August 2012

Variable	Total no. (%), N = 9,151*	Age ≤15 y, no. (%)	Age >15 y, no. (%)
Age, y			
≤15	3,225 (35)	3,225 (100)	Not applicable
>15	5,926 (65)	Not applicable	5,926 (100)
Sex			
M	4,147 (45)	1,620 (50)	2,527 (43)
F	5,004 (55)	1,605 (50)	3,399 (53)
Concurrent condition			
HIV seropositive	33 (<1)	3 (<1)	30 (1)
Self-reported diabetes	165 (2)	2 (<1)	163 (3)
Current smoker	559 (6)	4 (<1)	555 (10)
M. tuberculosis lineage exposure			
L2 (Beijing)	1,041 (11)	349 (11)	692 (12)
L4.1	3,733 (41)	1,332 (41)	2,401 (41)
L4.3	3,416 (37)	1,202 (37)	2,214 (37)
Other	961 (11)	342 (11)	619 (10)
Presence of *M. bovis* BCG vaccination scar	8,110 (89)	2,876 (89)	5,253 (89)
Nutritional status			
Normal weight	5,261 (58)	2,527 (79)	2,734 (47)
Underweight	163 (2)	95 (3)	68 (1)
Overweight	3,636 (40)	565 (18)	3,071 (52)
Socioeconomic status			
Low	3,112 (35)	1,253 (40)	1,859 (33)
Middle	3,991 (45)	1,384 (44)	2,607 (45)
High	1,828 (21)	514 (16)	1,314 (23)
Isoniazid preventive therapy recipient	2,090 (23)	1,542 (48)	490 (7)

*Numbers might not add to total because of missing data.

12 months of follow-up, and incident disease during the 12-month follow-up time. We classified household contacts as infected at baseline if they reported a history of TB, reported a previous positive TST result within 6 months after study enrollment, or had a positive TST (induration size ≥10 mm [≥5 mm for HIV-positive household contacts]) at baseline. We considered initially TST-negative household contacts to have undergone TST conversion if their TST status converted from negative to positive or if TB developed during follow-up. We considered household contacts to be infected with *M. tuberculosis* by 12 months of follow-up if contacts were infected at baseline or had a TST conversion during the 12-month follow-up period (*22*). We considered household contacts to have co-prevalent TB if it was diagnosed within 2 weeks after the diagnosis in the index patient. If household contacts received diagnoses 2 weeks–15 months (1-year follow-up plus a 3-month buffer period) after index patient diagnosis, we considered incident TB to have developed in those contacts during follow-up. We based TB diagnosis among contacts ≥18 years of age on the same criteria we used for index patients; the diagnosis among household contacts <18 years was based on published consensus guidelines from an expert panel on classifying TB in children (*31*).

Statistical Analysis

We made an a priori decision to analyze child household contacts (≤15 years) and adult household contacts (>15 years) separately for several reasons. First, we considered child contacts to be a more representative age group for household-based TB transmission than their more mobile, socially active adult counterparts. Second, several previous studies suggest that Beijing strains more commonly affect children than adults (*18*–*20*). We used complete data analyses in all multivariate adjustment models and conducted all statistical analyses in R version 3.5.1 (https://www.r-project.org).

Table 3. Effect of the *Mycobacterium tuberculosis* Beijing lineage on the risk for infection at baseline in child and adult household contacts of culture-positive index patients, Lima, Peru, September 2009–August 2012

	Age ≤15 y, n = 3,115*			Age >15 y, n = 5,663*		
	Prevalence,	Risk ratio (95% CI)		Prevalence,	Risk ratio (95% CI)	
Lineage	no. (%)†	Univariate	Multivariate‡	no. (%)†	Univariate	Multivariate‡
Non-Beijing	731 (26)	Referent	Referent	2,654 (53)	Referent	Referent
Beijing	110 (33)	1.27 (1.06–1.53)	1.23 (1.02–1.50)	353 (53)	0.99 (0.91–1.08)	1.00 (0.91–1.09)

*Likelihood ratio test for the interaction between age (≤15 or >15) and index patient *M. tuberculosis* lineage: p = 0.025.
†Prevalence of baseline *M. tuberculosis* infection in the univariate model.
‡Multivariate model adjusted for index patient drug resistance profile; index patient age (16–30, 31–45, 46–60, and >60 y); index patient HIV status; household contact age (0–5, 6–10, 11–15, 16–30, 31–45, 46–60, and >60 y); household contact *M. bovis* BCG vaccination status; household contact socioeconomic status; household contact nutritional status.

Table 4. Effect of the *Mycobacterium tuberculosis* Beijing lineage on the risk for infection by 12 months of follow-up in child and adult household contacts of culture-positive index patients, Lima, Peru, September 2009–August 2012

	Age ≤15 y, n = 2,521*			Age >15 y, n = 4,921*		
	Prevalence,	Risk ratio (95% CI)		Prevalence,	Risk ratio (95% CI)	
Lineage	no. (%)†	Univariate	Multivariate‡	no. (%)†	Univariate	Multivariate‡
Non-Beijing	1,098 (49)	Referent	Referent	3,546 (82)	Referent	Referent
Beijing	173 (59)	1.20 (1.08–1.35)	1.22 (1.09–1.38)	474 (82)	1.00 (0.96–1.05)	1.01 (0.97–1.06)

*Likelihood ratio test for the interaction between age (≤15 or >15 y) and index patient *M. tuberculosis* lineage: p = 0.003.
†Prevalence of *M. tuberculosis* infection by 12 months for the univariate model.
‡Adjusted for index patient drug resistance profile; index patient age (16–30, 31–45, 46–60, and >60 y); index patient HIV status; household contact age (0–5, 6–10, 11–15, 16–30, 31–45, 46–60, and >60 y); household contact *M. bovis* BCG vaccination status; household contact socioeconomic status; household contact nutritional status.

TB at Baseline and by 12 Months of Follow-Up

We used a modified Poisson generalized estimating equation to measure the association between exposure to index patients infected with Beijing strains and the likelihood of infection at baseline and by 12-months of follow-up. To account for correlation within households, we specified an exchangeable working correlation structure for observations within the same household and obtained empirical SE estimates for robust inference. We constructed univariate and multivariate models to compare the effect of exposure to Beijing and non-Beijing strains on the risk for TB infection at baseline and at 12 months. In the multivariate models, we included covariates from index patients (age, drug resistance profile, and HIV status) and their household contacts (age, diabetes status, BCG vaccination status, socioeconomic status, and nutritional status). We conducted sensitivity analyses in which we excluded household contacts who reported a history of TB, a previous positive TST result within 6 months after study enrollment, or a history of receiving TB treatment.

Time to TST Conversion and to Incident Disease

We assessed the time to TST conversion among household contacts who were uninfected at baseline by defining the date of infection as the midpoint between the date of enrollment and the date of a first positive TST result or TB diagnosis. We excluded from analysis household contacts who remained TST negative at the date of their last TST result. For the time to TB analysis, we excluded household contacts with co-prevalent TB and excluded from analysis household contacts in whom TB had not been diagnosed by the time of their death or at the end of the study. We first plotted Kaplan-Meier survival curves to visually evaluate the association between the index patient's *M. tuberculosis* genotype and the 2 time-to-event outcomes. We then used Cox frailty proportional hazards model to evaluate risk factors for time to TST conversion and time to incident disease while accounting for clustering within households. We constructed univariate and multivariate models to compare the effect of exposure to Beijing and non-Beijing strains on the risk for TST conversion and incident disease during follow-up. In the multivariate models, we included covariates from index patients (age, drug resistance profile, and HIV status) and their household contacts (age, diabetes status, BCG vaccination status, socioeconomic status, and nutritional status). We further adjusted for the use of IPT and TB history in the multivariate model of the time to incident disease analyses. We verified the proportional hazards assumptions for each covariate by including an interaction term for the covariate and time and stratifying by covariates for which the assumption did not hold. We conducted 2 sensitivity analyses, 1 in which we defined TST conversion using an increment of ≥6-mm induration size in repeat TST measurements during follow-up and 1 in which we restricted the analysis to household contacts in whom active TB developed during follow-up and who received their diagnoses within ≥30 days after index patient enrollment.

Effect of Index Patient *M. tuberculosis* Lineage on Protective Efficacy of BCG Vaccination

We also considered the possibility that index patient *M. tuberculosis* lineage might modify the protective

Table 5. Hazard ratios of tuberculin skin test conversion comparing contacts exposed to a *Mycobacterium tuberculosis* Beijing lineage with those exposed to a non-Beijing lineage, Lima, Peru, September 2009–August 2012

	Age ≤15 y*			Age >15 y*		
		Hazard ratio (95% CI)			Hazard ratio (95% CI)	
Lineage	Incidence, %†	Univariate	Multivariate‡	Incidence, %†	Univariate	Multivariate‡
Non-Beijing	0.26 (356/1,396)	Referent	Referent	0.69 (845/1,236)	Referent	Referent
Beijing	0.39 (62/160)	1.53 (1.09–2.14)	1.65 (1.17–2.33)	0.73 (118/162)	1.02 (0.80–1.30)	1.03 (0.80–1.33)

*Likelihood ratio test for the interaction between age (≤15 or >15 y) and index patient *M. tuberculosis* lineage: p = 0.048.
†Per person-year for the univariate model.
‡Adjusted for index patient drug resistance profile; index patient age (16–30, 31–45, 46–60, and >60 y); index patient HIV status; household contact age (0–5, 6–10, 11–15, 16–30, 31–45, 46–60, and >60 y); household contact *M. bovis* BCG vaccination status; household contact socioeconomic status; household contact nutritional status.

Table 6. Hazard ratios of incident tuberculosis among contacts exposed to a *Mycobacterium tuberculosis* Beijing lineage and a non-Beijing lineage, Lima, Peru, September 2009–August 2012

	Age ≤15 y*			Age >15 y*		
		Hazard ratio (95% CI)			Hazard ratio (95% CI)	
Lineage	Incidence, %†	Univariate	Multivariate‡	Incidence, %†	Univariate	Multivariate‡
Non-Beijing	3,043 (84/2,760)	Referent	Referent	2,874 (156/4,993)	Referent	Referent
Beijing	4,478 (15/335)	1.42 (0.78–2.59)	1.45 (0.77–2.72)	3,124 (19/661)	0.93 (0.57–1.52)	1.06 (0.64–1.77)

*Likelihood ratio test for the interaction between age (≤15 or >15 y) and index patient *M. tuberculosis* lineage: p = 0.231.
†Per 100,000 person-years in the univariate model.
‡Adjusted for index patient drug resistance profile; index patient age (16–30, 31–45, 46–60, and >60 y); index patient HIV status; household contact age (0–5, 6–10, 11–15, 16–30, 31–45, 46–60, and >60 y); household contact *M. bovis* BCG vaccination status; household contact SES; household contact nutritional status; household contact use of isoniazid preventive therapy; household contact TB history.

efficacy of BCG vaccine. To examine whether index patient *M. tuberculosis* strain type modified the association between BCG vaccination and outcomes of our study, we added in our model an interaction term that included index patient *M. tuberculosis* lineage and the BCG vaccination status of household contacts.

Results

We enrolled 9,151 household contacts of 2,223 culture-positive pulmonary TB index patients. The study enrollment rates were 85.5% for index patients and 94.6% for their household contacts. The retention rates for enrolled household contacts were 92.0% at 6 months and 94.7% at 12 months of follow-up. At baseline, 841 (27.0%) of 3,115 child household contacts and 3,007 (53.1%) of 5,663 adult household contacts were infected. A total of 951 (43%) index patients had lineage 4.1 strain isolates, 775 (35%) had lineage 4.3 strain isolates, 255 (12%) had lineage 2 isolates (all of which were of the Beijing strain), and 242 (11%) had other strain isolates (Table 1). We determined the baseline characteristics for household contacts, stratified by age at ≤15 and >15 years (Table 2; Appendix Tables 1–4, https://wwwnc.cdc.gov/EID/article/26/3/19-1314-App1.pdf).

M. tuberculosis Infection at Baseline and After 12 Months of Follow-up

Child contacts exposed to Beijing strains were more likely than those exposed to non-Beijing strains to be infected at baseline (risk ratio [RR] 1.27 [95% CI 1.06–1.53]; adjusted RR [aRR] 1.23 [95% CI 1.02–1.50]) (Table 3) and by 12 months of follow-up (RR 1.20 [95% CI 1.08–1.35]; aRR 1.22 [95% CI 1.09-1.38]) (Table 4). The prevalence of *M. tuberculosis* infection at baseline (RR 0.99 [95% CI 0.91–1.08]; aRR 1.00 [95% CI 0.91–1.09]) and by 12 months (RR 1.00 [95% CI 0.96–1.05]; aRR 1.01 [95% CI 0.97–1.06]) did not vary by index patient *M. tuberculosis* strain in adult household contacts (Tables 3, 4). In the sensitivity analyses, we obtained almost identical results when we excluded household contacts who reported a history of TB, a previous positive TST result within 6 months after study enrollment, or a history of TB treatment (Appendix Tables 5, 6).

TST Conversion

The TST status of children exposed to Beijing strains were more likely than that of children exposed to other strains to convert from negative to positive during 12 months of follow-up in both the univariate and

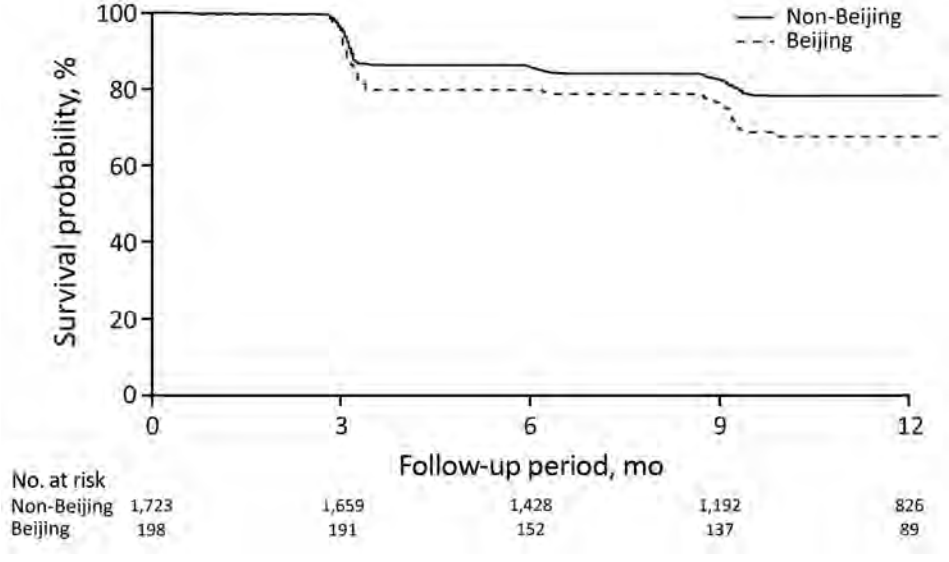

Figure 1. Survival curves for incident *Mycobacterium tuberculosis* infection in child household contacts by index patient *M. tuberculosis* lineage, Lima, Peru, September 2009–August 2012.

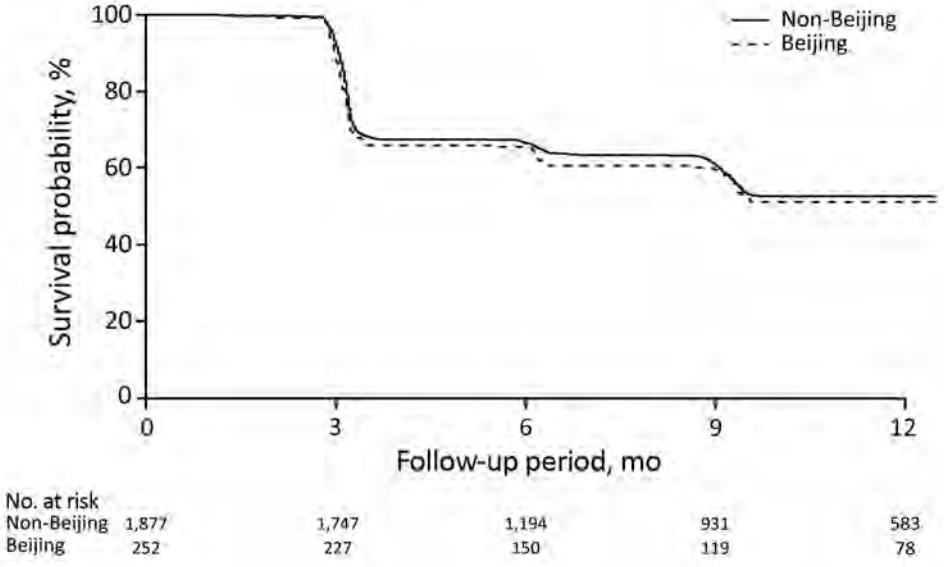

Figure 2. Survival curves for incident *Mycobacterium tuberculosis* infection in adult household contacts by index patient *M. tuberculosis* lineage, Lima, Peru, September 2009–August 2012.

multivariate analyses (hazard ratio [HR] 1.53 [95% CI 1.09–2.14]; adjusted HR [aHR] 1.65 [95% CI 1.17–2.33]). Exposure to Beijing strains had no differential effect in adults (HR 1.02 [95% CI 0.80–1.30]; aHR 1.03 [95% CI 0.80–1.33]) (Table 5; Figures 1, 2). In the sensitivity analyses, we defined TST conversion by an increment of ≥6 mm in TST induration size during follow-up, and the results changed by <5% (Appendix Table 7).

Progression to Active TB

After we adjusted for potential confounders, we found the HR for TB among child contacts exposed to an index patient with Beijing strains compared with non-Beijing strains to be 1.45 (95% CI 0.77–2.7). We found no evidence that exposure to Beijing strains affected the risk for incident TB in adult contacts (aHR 1.06 [95% CI 0.64–1.77]) (Table 6; Figures 3, 4). The results persisted when we restricted the analysis to household contacts in whom TB was diagnosed within ≥30 days after index patient diagnosis (Appendix Table 8).

Effect of Index Patient *M. tuberculosis* Lineage on the Protective Efficacy of BCG Vaccine

Although they lacked statistical significance, the aRRs for TB outcomes were higher for BCG-vaccinated children exposed to Beijing strains than for non–BCG-vaccinated children exposed to Beijing strains (aRR 1.01 [95% CI 0.69–1.49] for *M. tuberculosis* infection at baseline; aRR 1.21 [95% CI 0.90–1.63] for infection by 12 months; aRR 1.84 [95% CI 0.77–4.39] for TST conversion; aRR 1.96 [95% CI 0.41–9.39] for incident TB). This finding raises the possibility that BCG vaccination might be less efficacious in children exposed to Beijing strains than in those exposed to other strains

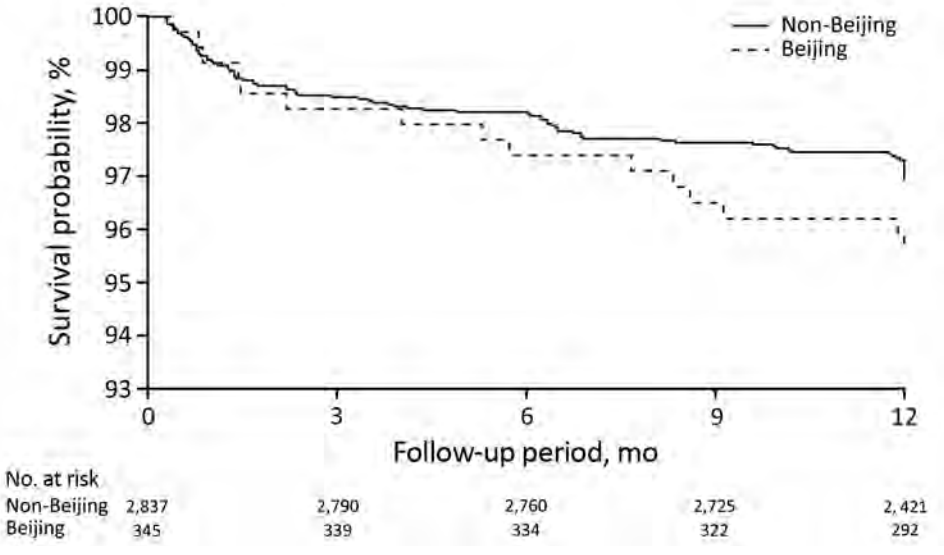

Figure 3. Survival curves for incident tuberculosis in child household contacts by index patient *Mycobacterium tuberculosis* lineage, Lima, Peru, September 2009–August 2012.

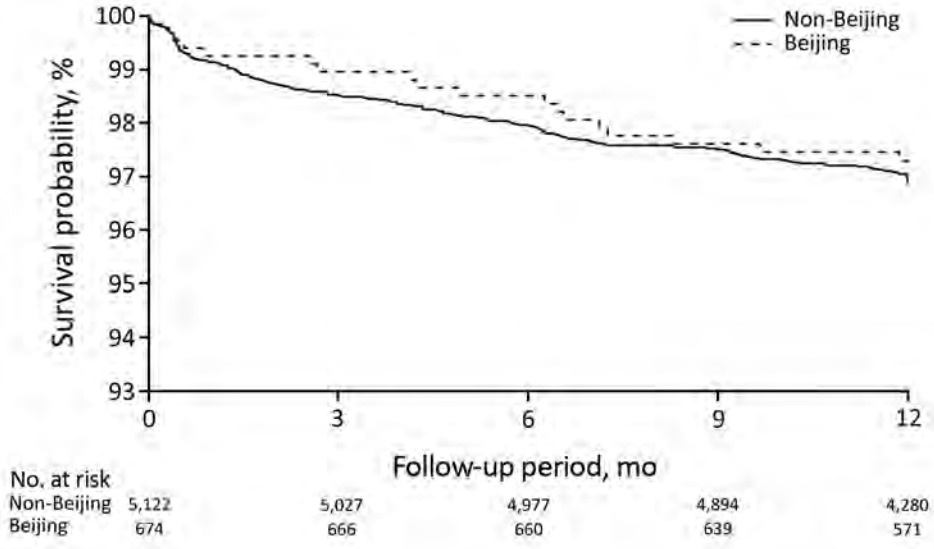

Figure 4. Survival curves for incident tuberculosis in adult household contacts by index patient *Mycobacterium tuberculosis* lineage, Lima, Peru, September 2009–August 2012.

(Table 7). Among BCG-vaccinated adult household contacts exposed to Beijing strains, the aRRs were 1.00 (95% CI 0.78–1.29) for *M. tuberculosis* infection at baseline, 1.02 (95% CI 0.89–1.16) for infection by 12 months, 1.00 (95% CI 0.48–2.06) for TST conversion, and 0.53 (95% CI 0.17–1.68) for incident TB (Table 7).

Discussion

In our study, children exposed to strains of *M. tuberculosis* Beijing sublineage were more likely than were those exposed to strains of other lineages to become infected. In addition, children exposed to Beijing strains were more likely than children exposed to other strains to progress to TB, although the relative risk of disease progression was not statistically significant (type 1 error rate of 0.05). We did not observe these effects among adult contacts.

Our results are consistent with those from previous studies that assessed the relative transmissibility of the Beijing strain through cohort-based studies or molecular epidemiology. In a study in South Africa, Marais et al. found that children <5 years of age who had household exposure to Beijing strains were 1.5 times more likely than those exposed to other strains to be TST-positive at baseline (*13*). In a prospective cohort study of household contacts in The Gambia, de Jong et al. found that Beijing lineage–exposed contacts were 7 times more likely than those exposed to the *M. africanum* lineage to progress to TB after 2 years of follow-up but were equally likely to be TST-positive at baseline or convert at 3 months (*12*). In the De Jong et al. study, the proportion of TST-positive household contacts at baseline and the incidence of TST conversion and disease did not differ significantly between Beijing and other strains within *M. tuberculosis* sensu strictu.

Although some molecular epidemiologic studies have found that Beijing strains are more likely than other strains to form genotypic clusters, other studies have not supported this conclusion. Many of these studies assumed that patients within a chain of recent *M. tuberculosis* transmission will share molecular fingerprints (*32*–*36*) and that clustering of genotypes is therefore a proxy for transmissibility and disease progression. In China, Yang et al. reported that patients infected with Beijing strains were 1.56 times more likely than those infected with other lineages to share molecular fingerprints with other patients (*15*). Similar findings have been reported from Lima; in a study by Imawoto et al., 80% of Beijing strains were in clusters, although clustering among other strains was not reported (*14*). In Vietnam, Holt et al. reported that, although the Beijing strains accounted for 58% of the total study sample, they constituted 70% of all clustered strains (*21*). In Papua New Guinea, Bainomugisa et al. found that 82% of isolates with Beijing strains were found in clusters, compared with 43% of isolates with strains from other lineages (*37*). In China, Yang et al. reported that the proportions of clustering were 34% for Beijing and 18% for non-Beijing strains (*38*). However, in Canada, Langlois-Klassen et al. found that Beijing was less likely to be found in clusters than other strains (21% vs. 37%) (*16*), and in the Netherlands, Nebenzahl-Guimaraes et al. showed that Beijing strains were no more transmissible than strains of other lineages, after adjustment for host factors using an approach that controlled for the propensity of a strain to propagate (*17*).

Some animal studies have provided evidence to support the hypothesis that Beijing strains are more

Table 7. Effects of BCG vaccination on *M. tuberculosis* infection and TB outcomes by lineage exposure for child and adult household contacts of culture-positive pulmonary tuberculosis patients, Lima, Peru, September 2009–August 2012*

	Non-Beijing lineage		Beijing lineage		
Category and BCG vaccination status	Infection prevalence, no. (%)	RR (95% CI)	Infection prevalence, no. (%)	RR (95% CI)	p value
Children, ≤15 y					
Baseline *M. tuberculosis* infection, n = 2,949					0.691
Without BCG vaccination	137 (27)	Referent	19 (32)	Referent	
With BCG vaccination	552 (26)	0.94 (0.81–1.09)	83 (32)	1.01 (0.69–1.49)	
M. tuberculosis infection by 12 months of follow-up, n = 2,417					0.405
Without BCG vaccination	187 (45)	Referent	26 (50)	Referent	
With BCG vaccination	853 (50)	1.07 (0.97–1.19)	139 (60)	1.21 (0.90–1.63)	
	Incidence†	HR (95% CI)	Incidence†	HR (95% CI)	
Time to TST conversion					0.579
Without BCG vaccination	0.18 (48/260)	Referent	0.21 (7/32)	Referent	
With BCG vaccination	0.27 (292/1,065)	1.5 (1.08–2.08)	0.45 (53/119)	1.84 (0.77–4.39)	
Time to TB					0.168
Without BCG vaccination	4,585 (25/545)	Referent	3,098 (2/65)	Referent	
With BCG vaccination	2,619 (60/2291)	0.58 (0.35–0.96)	4,639 (13/280)	1.96 (0.41–9.39)	
	Infection prevalence, no. (%)	RR (95% CI)	Infection prevalence, no. (%)	RR (95% CI)	
Adults, >15 y					
Baseline *M. tuberculosis* infection, n = 5,381					0.611
Without BCG vaccination	260 (47)	Referent	27 (51)	Referent	
With BCG vaccination	2,263 (54)	1.07 (0.98–1.18)	313 (54)	1.00 (0.78–1.29)	
M. tuberculosis infection by 12 months of follow-up, n = 4,716					0.315
Without BCG vaccination	334 (72)	Referent	39 (81)	Referent	
With BCG vaccination	3,042 (82)	1.10 (1.04–1.16)	419 (82)	1.02 (0.89–1.16)	
	Incidence†	HR (95% CI)	Incidence†	HR (95% CI)	
Time to TST conversion					0.315
Without BCG vaccination	0.41 (70/172)	Referent	0.77 (10/13)	Referent	
With BCG vaccination	0.72 (728/1,020)	1.55 (1.18–2.04)	0.73 (105/144)	1.00 (0.48–2.06)	
Time to TB					0.732
Without BCG vaccination	4,813 (28/582)	Referent	6,574 (4/61)	Referent	
With BCG vaccination	2,860 (129/4511)	0.66 (0.43–1.02)	2,434 (15/616)	0.53 (0.17–1.68)	

*BCG, *M. bovis* BCG; HR, hazard ratio; RR, risk ratio; TB, tuberculosis; TST, tuberculin skin test.
†Cases per person-year (no. converted/no. tested).

likely than other lineages to cause disease. Mice experimentally infected with Beijing strains not only died earlier and had higher death rates but also had more lung tissue damage than controls (*39*–*42*). Some in vitro studies of macrophages have also found that the Beijing strain can downregulate the expression of pathogen recognition receptors and major histocompatibility complex class II, modify the secretion of inflammatory cytokines, and induce the necrosis of host immune cells (*43*–*46*).

We considered possible explanations for the difference in the effect of the Beijing strain in children and adults. Given their mixing patterns, adults may be more likely than children to be infected within the community rather than in the household. If the household contacts in the cohort reported here had been infected by someone other than the household index patient, strain-specific exposure status might have been misclassified. Such misclassification would have been more likely in adults and would have biased the results for this group toward the null of no effect. However, another possibility is that Beijing strains might lead to earlier disease progression in younger persons with newly acquired *M. tuberculosis*. Several studies from Vietnam report that Beijing strains make up the highest proportion of incident cases in persons <20 years of age and that the prevalence of Beijing strains declines with increasing age (*18*,*19*). In Iran, Erie et al. similarly showed that 27% of patients ≤20 years of age were infected by Beijing strains and that the prevalence of Beijing strains among patients ≥20 years of age was 13% (*20*). The increasing prevalence of Beijing strains in children may be related to use of BCG vaccine. This explanation would be consistent with our finding that that the protective efficacy of BCG vaccine against Beijing strains was reduced in children but not in adults. Possible explanations for these observations include a decrease in the protective efficacy of BCG vaccination with increasing age, a shift in the administered BCG strain in Peru's recent history, or a reduction in the immunogenicity of BCG vaccine over time (*47*–*49*).

Our study had several notable limitations. First, within a high-transmission setting such as Lima, children still could have been infected outside the household. Misclassification of the lineage exposure

status in children also would have led to an underestimation of the effect. Second, discrepancies between 24-locus MIRU-VNTR genotyping and WGS have been noted previously (*50*), and some lineages assigned on the basis of MIRU-VNTR could have been inaccurate, again leading to a misclassification error that could have underestimated the true effect of Beijing strains.

In conclusion, we found that exposure to household index patients infected with Beijing strains was associated with increased risk for TST conversion and disease in children ≤15 years of age but not in adults. These findings raise the possibility that genotypic variation in *M. tuberculosis* may have important phenotypic effects that should be further studied. In particular, it will be essential to determine whether BCG vaccination provides less protection against Beijing strains than strains from other lineages and whether the efficacy of any newly developed vaccines varies by *M. tuberculosis* genoype.

Acknowledgments

We thank the patients and their families who gave their time and energy to contribute to this study, the National Strategy for Tuberculosis Control at the Peruvian Ministry of Health, and the healthcare personnel at the 106 participating health centers in Lima.

This work was supported by the National Institute of Allergy and Infectious Diseases U19AI076217 and TBRU U19AI111224.

About the Author

Dr. Huang is an epidemiologist and biostatistician at Brigham and Women's Hospital and an instructor at Harvard Medical School. His primary research interest is in epidemiologic investigation of TB.

References

1. World Health Organization. Global tuberculosis report 2018. Geneva: The Organization; 2018.
2. Stucki D, Brites D, Jeljeli L, Coscolla M, Liu Q, Trauner A, et al. *Mycobacterium tuberculosis* lineage 4 comprises globally distributed and geographically restricted sublineages. Nat Genet. 2016;48:1535–43. https://doi.org/10.1038/ng.3704
3. Bifani PJ, Mathema B, Kurepina NE, Kreiswirth BN. Global dissemination of the *Mycobacterium tuberculosis* W-Beijing family strains. Trends Microbiol. 2002;10:45–52. https://doi.org/10.1016/S0966-842X(01)02277-6
4. Glynn JR, Whiteley J, Bifani PJ, Kremer K, van Soolingen D. Worldwide occurrence of Beijing/W strains of *Mycobacterium tuberculosis*: a systematic review. Emerg Infect Dis. 2002;8:843–9. https://doi.org/10.3201/eid0805.020002
5. European Concerted Action on New Generation Genetic Markers and Techniques for the Epidemiology and Control of Tuberculosis. Beijing/W genotype *Mycobacterium tuberculosis* and drug resistance. Emerg Infect Dis. 2006;12:736–43. https://doi.org/10.3201/eid1205.050400
6. Merker M, Blin C, Mona S, Duforet-Frebourg N, Lecher S, Willery E, et al. Evolutionary history and global spread of the *Mycobacterium tuberculosis* Beijing lineage. Nat Genet. 2015;47:242–9. https://doi.org/10.1038/ng.3195
7. Agerton TB, Valway SE, Blinkhorn RJ, Shilkret KL, Reves R, Schluter WW, et al. Spread of strain W, a highly drug-resistant strain of *Mycobacterium tuberculosis*, across the United States. Clin Infect Dis. 1999;29:85–92, discussion 93–5. https://doi.org/10.1086/520187
8. Caminero JA, Pena MJ, Campos-Herrero MI, Rodríguez JC, García I, Cabrera P, et al. Epidemiological evidence of the spread of a *Mycobacterium tuberculosis* strain of the Beijing genotype on Gran Canaria Island. Am J Respir Crit Care Med. 2001;164:1165–70. https://doi.org/10.1164/ajrccm.164.7.2101031
9. Cowley D, Govender D, February B, Wolfe M, Steyn L, Evans J, et al. Recent and rapid emergence of W-Beijing strains of *Mycobacterium tuberculosis* in Cape Town, South Africa. Clin Infect Dis. 2008;47:1252–9. https://doi.org/10.1086/592575
10. Cox HS, Kubica T, Doshetov D, Kebede Y, Rüsch-Gerdess S, Niemann S. The Beijing genotype and drug resistant tuberculosis in the Aral Sea region of Central Asia. Respir Res. 2005;6:134. https://doi.org/10.1186/1465-9921-6-134
11. Hanekom M, van der Spuy GD, Streicher E, Ndabambi SL, McEvoy CRE, Kidd M, et al. A recently evolved sublineage of the *Mycobacterium tuberculosis* Beijing strain family is associated with an increased ability to spread and cause disease. J Clin Microbiol. 2007;45:1483–90. https://doi.org/10.1128/JCM.02191-06
12. de Jong BC, Hill PC, Aiken A, Awine T, Antonio M, Adetifa IM, et al. Progression to active tuberculosis, but not transmission, varies by *Mycobacterium tuberculosis* lineage in The Gambia. J Infect Dis. 2008;198:1037–43. https://doi.org/10.1086/591504
13. Marais BJ, Hesseling AC, Schaaf HS, Gie RP, van Helden PD, Warren RM. *Mycobacterium tuberculosis* transmission is not related to household genotype in a setting of high endemicity. J Clin Microbiol. 2009;47:1338–43. https://doi.org/10.1128/JCM.02490-08
14. Iwamoto T, Grandjean L, Arikawa K, Nakanishi N, Caviedes L, Coronel J, et al. Genetic diversity and transmission characteristics of Beijing family strains of *Mycobacterium tuberculosis* in Peru. PLoS One. 2012;7:e49651. https://doi.org/10.1371/journal.pone.0049651
15. Yang C, Shen X, Peng Y, Lan R, Zhao Y, Long B, et al. Transmission of *Mycobacterium tuberculosis* in China: a population-based molecular epidemiologic study. Clin Infect Dis. 2015;61:219–27. https://doi.org/10.1093/cid/civ255
16. Langlois-Klassen D, Senthilselvan A, Chui L, Kunimoto D, Saunders LD, Menzies D, et al. Transmission of *Mycobacterium tuberculosis* Beijing strains, Alberta, Canada, 1991–2007. Emerg Infect Dis. 2013;19:701–11. https://doi.org/10.3201/eid1905.121578
17. Nebenzahl-Guimaraes H, Borgdorff MW, Murray MB, van Soolingen D. A novel approach—the propensity to propagate (PTP) method for controlling for host factors in studying the transmission of *Mycobacterium tuberculosis*. PLoS One. 2014;9:e97816. https://doi.org/10.1371/journal.pone.0097816
18. Anh DD, Borgdorff MW, Van LN, Lan NT, van Gorkom T, Kremer K, et al. *Mycobacterium tuberculosis* Beijing g enotype emerging in Vietnam. Emerg Infect Dis. 2000; 6:302–5. https://doi.org/10.3201/eid0603.000312

19. Buu TN, Huyen MN, Lan NTN, Quy HT, Hen NV, Zignol M, et al. The Beijing genotype is associated with young age and multidrug-resistant tuberculosis in rural Vietnam. Int J Tuberc Lung Dis. 2009;13:900–6.
20. Erie H, Kaboosi H, Javid N, Shirzad-Aski H, Taziki M, Kuchaksaraee MB, et al. The high prevalence of *Mycobacterium tuberculosis* Beijing strain at an early age and extra-pulmonary tuberculosis cases. Iran J Microbiol. 2017;9:312–7.
21. Holt KE, McAdam P, Thai PVK, Thuong NTT, Ha DTM, Lan NN, et al. Frequent transmission of the *Mycobacterium tuberculosis* Beijing lineage and positive selection for the EsxW Beijing variant in Vietnam. Nat Genet. 2018;50:849–56. https://doi.org/10.1038/s41588-018-0117-9
22. Becerra MC, Huang CC, Lecca L, Bayona J, Contreras C, Calderon R, et al. Transmissibility and potential for disease progression of drug resistant *Mycobacterium tuberculosis:* prospective cohort study. BMJ. 2019;367:l5894. https://doi.org/10.1136/bmj.l5894
23. Ministerio de Salud. Norma técnica de salud para el control de la tuberculosis. Lima, Peru. 2006 [cited 2018 Oct 10]. ftp://ftp2.minsa.gob.pe/descargas/dgsp/ESN-tuberculosis/normaspublicaciones/NTSTBC.pdf
23. Joshi N, Fass J. A sliding-window, adaptive, quality-based trimming tool for FastQ files. 2011 [cited 2018 Dec 15]. https://github.com/najoshi/sickle
24. Li H. Toward better understanding of artifacts in variant calling from high-coverage samples. Bioinformatics. 2014;30:2843–51. https://doi.org/10.1093/bioinformatics/btu356
25. Li H, Handsaker B, Wysoker A, Fennell T, Ruan J, Homer N, et al.; 1000 Genome Project Data Processing Subgroup. The Sequence Alignment/Map format and SAMtools. Bioinformatics. 2009;25:2078–9. https://doi.org/10.1093/bioinformatics/btp352
26. Walker BJ, Abeel T, Shea T, Priest M, Abouelliel A, Sakthikumar S, et al. Pilon: an integrated tool for comprehensive microbial variant detection and genome assembly improvement. PLoS One. 2014;9:e112963. https://doi.org/ 10.1371/journal.pone.0112963
27. Coll F, McNerney R, Guerra-Assunção JA, Glynn JR, Perdigão J, Viveiros M, et al. A robust SNP barcode for typing *Mycobacterium tuberculosis* complex strains. Nat Commun. 2014;5:4812. https://doi.org/10.1038/ncomms5812
28. Supply P, Lesjean S, Savine E, Kremer K, van Soolingen D, Locht C. Automated high-throughput genotyping for study of global epidemiology of *Mycobacterium tuberculosis* based on mycobacterial interspersed repetitive units. J Clin Microbiol. 2001;39:3563–71. https://doi.org/10.1128/JCM.39.10.3563-3571.2001
29. Allix-Béguec C, Harmsen D, Weniger T, Supply P, Niemann S. Evaluation and strategy for use of MIRU-VNTRplus, a multifunctional database for online analysis of genotyping data and phylogenetic identification of *Mycobacterium tuberculosis* complex isolates. J Clin Microbiol. 2008;46:2692–9. https://doi.org/10.1128/JCM.00540-08
30. Verrall AJ, Netea MG, Alisjahbana B, Hill PC, van Crevel R. Early clearance of *Mycobacterium tuberculosis*: a new frontier in prevention. Immunology. 2014;141:506–13. https://doi.org/10.1111/imm.12223
31. Graham SM, Ahmed T, Amanullah F, Browning R, Cardenas V, Casenghi M, et al. Evaluation of tuberculosis diagnostics in children: 1. Proposed clinical case definitions for classification of intrathoracic tuberculosis disease. Consensus from an expert panel. J Infect Dis. 2012;205(Suppl 2):S199–208. https://doi.org/10.1093/infdis/jis008
32. Toungoussova OS, Mariandyshev A, Bjune G, Sandven P, Caugant DA. Molecular epidemiology and drug resistance of *Mycobacterium tuberculosis* isolates in the Archangel prison in Russia: predominance of the W-Beijing clone family. Clin Infect Dis. 2003;37:665–72. https://doi.org/10.1086/377205
33. Dou H-Y, Tseng F-C, Lin C-W, Chang J-R, Sun J-R, Tsai W-S, et al. Molecular epidemiology and evolutionary genetics of *Mycobacterium tuberculosis* in Taipei. BMC Infect Dis. 2008;8:170. https://doi.org/10.1186/1471-2334-8-170
34. Wada T, Fujihara S, Shimouchi A, Harada M, Ogura H, Matsumoto S, et al. High transmissibility of the modern Beijing *Mycobacterium tuberculosis* in homeless patients of Japan. Tuberculosis (Edinb). 2009;89:252–5. https://doi.org/10.1016/j.tube.2009.05.007
35. Yang C, Luo T, Sun G, Qiao K, Sun G, DeRiemer K, et al. *Mycobacterium tuberculosis* Beijing strains favor transmission but not drug resistance in China. Clin Infect Dis. 2012;55:1179–87. https://doi.org/10.1093/cid/cis670
36. Aleksic E, Merker M, Cox H, Reiher B, Sekawi Z, Hearps AC, et al. First molecular epidemiology study of *Mycobacterium tuberculosis* in Kiribati. PLoS One. 2013;8:e55423. https://doi.org/10.1371/journal.pone.0055423
37. Bainomugisa A, Pandey S, Donnan E, Simpson G, Foster J, Lavu E, et al. Cross-border movement of highly drug-resistant *Mycobacterium tuberculosis* from Papua New Guinea to Australia through Torres Strait Protected Zone, 2010–2015. Emerg Infect Dis. 2019;25:406–15. https://doi.org/10.3201/eid2503.181003
38. Yang C, Luo T, Shen X, Wu J, Gan M, Xu P, et al. Transmission of multidrug-resistant *Mycobacterium tuberculosis* in Shanghai, China: a retrospective observational study using whole-genome sequencing and epidemiological investigation. Lancet Infect Dis. 2017;17:275–84. https://doi.org/10.1016/S1473-3099(16)30418-2
39. Manca C, Tsenova L, Bergtold A, Freeman S, Tovey M, Musser JM, et al. Virulence of a *Mycobacterium tuberculosis* clinical isolate in mice is determined by failure to induce Th1 type immunity and is associated with induction of IFN-α/β. Proc Natl Acad Sci U S A. 2001;98:5752–7. https://doi.org/10.1073/pnas.091096998
40. López B, Aguilar D, Orozco H, Burger M, Espitia C, Ritacco V, et al. A marked difference in pathogenesis and immune response induced by different *Mycobacterium tuberculosis genotypes*. Clin Exp Immunol. 2003;133:30–7. https://doi.org/10.1046/j.1365-2249.2003.02171.x
41. Dormans J, Burger M, Aguilar D, Hernandez-Pando R, Kremer K, Roholl P, et al. Correlation of virulence, lung pathology, bacterial load and delayed type hypersensitivity responses after infection with different *Mycobacterium tuberculosis* genotypes in a BALB/c mouse model. Clin Exp Immunol. 2004;137:460–8. https://doi.org/10.1111/j.1365-2249.2004.02551.x
42. Aguilar D, Hanekom M, Mata D, Gey van Pittius NC, van Helden PD, Warren RM, et al. *Mycobacterium tuberculosis* strains with the Beijing genotype demonstrate variability in virulence associated with transmission. Tuberculosis (Edinb). 2010;90:319–25. https://doi.org/10.1016/j.tube.2010.08.004
43. Rocha-Ramírez LM, Estrada-García I, López-Marín LM, Segura-Salinas E, Méndez-Aragón P, Van Soolingen D, et al. *Mycobacterium tuberculosis* lipids regulate cytokines, TLR-2/4 and MHC class II expression in human macrophages. Tuberculosis (Edinb). 2008;88:212–20. https://doi.org/10.1016/j.tube.2007.10.003

44. Chacón-Salinas R, Serafín-López J, Ramos-Payán R, Méndez-Aragón P, Hernández-Pando R, Van Soolingen D, et al. Differential pattern of cytokine expression by macrophages infected in vitro with different *Mycobacterium tuberculosis* genotypes. Clin Exp Immunol. 2005;140:443–9. https://doi.org/10.1111/j.1365-2249.2005.02797.x
45. Sohn H, Lee K-S, Kim S-Y, Shin D-M, Shin S-J, Jo E-K, et al. Induction of cell death in human macrophages by a highly virulent Korean Isolate of *Mycobacterium tuberculosis* and the virulent strain H37Rv. Scand J Immunol. 2009;69:43–50. https://doi.org/10.1111/j.1365-3083.2008.02188.x
46. van Laarhoven A, Mandemakers JJ, Kleinnijenhuis J, Enaimi M, Lachmandas E, Joosten LAB, et al. Low induction of proinflammatory cytokines parallels evolutionary success of modern strains within the *Mycobacterium tuberculosis Beijing genotype*. Infect Immun. 2013;81:3750–6. https://doi.org/10.1128/IAI.00282-13
47. Sterne JA, Rodrigues LC, Guedes IN. Does the efficacy of BCG decline with time since vaccination? Int J Tuberc Lung Dis. 1998;2:200–7.
48. Luca S, Mihaescu T. History of BCG vaccine. Maedica (Buchar). 2013;8:53–8.
49. Behr MA. BCG—different strains, different vaccines? Lancet Infect Dis. 2002;2:86–92. https://doi.org/10.1016/S1473-3099(02)00182-2
50. Roetzer A, Diel R, Kohl TA, Rückert C, Nübel U, Blom J, et al. Whole genome sequencing versus traditional genotyping for investigation of a *Mycobacterium* tuberculosis outbreak: a longitudinal molecular epidemiological study. PLoS Med. 2013;10:e1001387. https://doi.org/10.1371/journal.pmed.1001387

Address for correspondence: Megan B. Murray, Harvard Medical School, 641 Huntington Ave, Boston, MA 02115, USA; email: megan.murray.epi@gmail.com

Risk Factors for Complicated Lymphadenitis Caused by Nontuberculous Mycobacteria in Children

Martin Kuntz, Daniela S. Kohlfürst, Cornelia Feiterna-Sperling, Renate Krüger, Ulrich Baumann, Laura Buchtala, Roland Elling, Veit Grote, Johannes Hübner, Markus Hufnagel, Petra Kaiser-Labusch, Johannes Liese, Eva-Maria Otto, Markus A. Rose,[1] Christian Schneider, Volker Schuster, Maximilian Seidl, Olaf Sommerburg, Markus Vogel,[2] Horst von Bernuth, Michael Weiß, Theodor Zimmermann, Alexandra Nieters, Werner Zenz, Philipp Henneke, for the NTMkids Consortium

Nontuberculous mycobacteria (NTM) are an emerging cause of infections, including chronic lymphadenitis in children. To identify risk factors for NTM lymphadenitis, particularly complicated disease, we collected epidemiologic, clinical, and microbiological data on 138 cases of NTM lymphadenitis in children across 13 centers in Germany and Austria. We assessed lifestyle factors but did not identify specific risk behaviors. We noted that more cases of NTM lymphadenitis occurred during cold months than during warm months. Moreover, we noted female sex and age ≤5.5 years as potential risk factors. Complete extirpation of the affected lymph node appeared to be the best therapeutic measure. We integrated the study data to develop a simple risk score to predict unfavorable clinical outcomes for NTM lymphadenitis.

Author affiliations: University of Freiburg, Freiburg, Germany (M. Kuntz, R. Elling, M. Hufnagel, C. Schneider, M. Seidl, A. Nieters, P. Henneke); Medical University of Graz, Graz, Austria (D.S. Kohlfürst, W. Zenz); Charité–Universitätsmedizin Berlin, Berlin, Germany (C. Feiterna-Sperling, R. Krüger, H. von Bernuth); Hannover Medical School, Hannover, Germany (U. Baumann); Professor-Hess-Kinderklinik, Bremen, Germany (L. Buchtala, P. Kaiser-Labusch); Dr. von Hauner Children's Hospital, Munich, Germany (V. Grote, J. Hübner); University Children's Hospital, Würzburg, Germany (J. Liese), Children's Hospital, Cologne, Germany (E.-M. Otto, M. Weiß); Goethe University of Frankfurt, Frankfurt, Germany (M.A. Rose); University of Leipzig, Leipzig, Germany (V. Schuster); University of Heidelberg, Heidelberg, Germany (O. Sommerburg); Heinrich Heine University, Düsseldorf, Germany (M. Vogel); Friedrich-Alexander-Universität Erlangen-Nürnberg, Erlangen, Germany (T. Zimmermann)

DOI: https://doi.org/10.3201/eid2603.191388

Nontuberculous mycobacteria (NTM) are common in the environment. NTM frequently are found in soil and are the most common bacteria on showerhead surfaces (*1*,*2*). Although many children likely have daily exposure to NTM, symptomatic infections are rare. Among children ≤2.5 years of age, the most frequently affected group, the annual NTM incidence in Germany has been estimated to be 3.1 cases/100,000 population (*3*). Some authors suggest the incidence of NTM infections in immunocompetent persons has been increasing in recent years (*4*–*7*), but little longitudinal data in well-defined epidemiologic contexts have been reported.

In children ≤5 years of age, NTM infections usually manifest as localized cervical lymphadenitis, and many resolve spontaneously. However, the median time to resolution is 40 weeks, differential diagnosis can be challenging, and recurrence and scarring are frequent complications (*8*). NTM infections are hallmarks of several immunodeficiency disorders, especially those involving the interleukin 12 and interferon-γ pathways (*9*–*11*). However, cervical lymphadenitis caused by NTM usually occurs in otherwise immunocompetent children who are not reported to be prone to opportunistic infections later in life. Host and environmental factors that could predispose a child to NTM lymphadenitis remain unclear. To identify potential risk factors for NTM lymphadenitis, we performed a prospective evaluation of childhood NTM lymphadenitis cases across 13 centers in Germany and Austria during 2010–2016. We collected detailed clinical information from the study centers and

[1]Current affiliation: Olga Children's Hospital, Stuttgart, Germany.

[2]Current affiliation: Hospital Neuwerk, Mönchengladbach, Germany.

documented socioeconomic features by using parent-directed questionnaires.

Materials and Methods

During 2010–2016, the 13 participating centers enrolled all patients ≤18 years of age who were evaluated for NTM lymphadenitis into the study registry. Most patients were recruited prospectively, but 1 center in Graz, Austria, recruited patients retrospectively from a local registry containing comprehensive data on NTM cases dating back to 2001. In addition to NTM cases, we enrolled a control cohort of patients without chronic illnesses (i.e., with infectious, malignant, or immunologic diseases) who were treated in the same institutions. We matched NTM cases with controls for age, sex, and center.

For comparison with the general population of Germany, we used the nearest neighbor method to match the age and sex of the control cohort with 17,641 participants in the German Health Interview and Examination Survey for Children and Adolescents (KiGGS), 2003–2006 (*12*,*13*). We used 7-fold oversampling to achieve the most accurate matches, resulting in an age- and sex-matched healthy control cohort of 966 children. We compared data on body mass, breast-feeding history, allergies, number of siblings in the same household, smoking during pregnancy, and parents' education level between the KiGGS-derived and the NTM cohorts.

We considered NTM likely for patients with the following symptoms: cervical lymphadenitis for >3 weeks; a lymph node size of >2 cm; exclusion of other causes, such as bartonellosis, toxoplasmosis, infectious mononucleosis, and lymphoma; and a positive tuberculin skin test (cutoff of 5 mm). We considered NTM to be the definitive diagnosis in patients with typical histology, such as presence of granuloma with or without necrosis or positive Ziehl-Neelsen staining or positive culture or PCR from lymph node samples. We documented the course of disease, including all diagnostic and therapeutic measures, antimicrobial drug therapy, associated clinical problems, prior medical history, vaccination status, and underlying conditions. Parents provided sociodemographic data, including ethnicity, place of birth, duration of breast-feeding, number of patient siblings, daycare attendance, cigarette smoke exposure, and parents' education and employment, as well as factors potentially increasing NTM exposure, such as animal contact, exposure to water and soil sources, and travel. We tracked patients until they recovered completely. When symptoms remained at the last documented visit, we conducted telephone interviews to assess the remainder of the disease course.

We obtained parental informed consent for all children included in this study. Each participating center's ethics committee granted ethics approval. The institutional review board of the University Medical Center, University of Freiburg, Freiburg, Germany, was the lead approval agency under IRB no. 232/10. All data were anonymized before analysis.

We performed data analysis by using R 3.5.3 (*14*). We used univariate analysis to screen for potential associations of individual disease history, socioeconomic factors, potential exposure to mycobacteria, and the clinical course of NTM and filtered for a correlation coefficient >0.2 and $p<0.05$ by using Pearson or Spearman correlations, depending on the variables. We subsequently examined the results for biological plausibility. We compared data from various categories by using the Fisher exact test and compared continuous and ordinal variables by using the Wilcoxon rank-sum test or Welch *t*-test. We analyzed seasonality of NTM by fitting a generalized linear regression model assuming a sinusoid Poisson distribution over the year (cosinor). Using no seasonal pattern as the null hypothesis, we assessed significance of seasonal variance by using the cosinor test (*15*). We considered $p<0.05$ statistically significant. For some analyses, we combined centers with <20 patients into a single group to attain meaningful comparisons and to ensure appropriate case anonymization.

Results

Cohort

During 2010–2016, we recruited 138 patients; 29 were from Graz, Austria, and the rest from Germany, including 35 from Berlin; 27 from Freiburg; 10 each from Leipzig and Munich; 8 from Bremen; 6 from Cologne; 3 each from Düsseldorf, Erlangen, and Heidelberg; 2 from Würzburg; and 1 each from Frankfurt and Hannover. We found suitable controls for 36 patients; 12 cases (9%) remained probable NTM, according to the case definition in the study protocol. We defined the remaining 102 cases as definite NTM.

Most NTM case-patients (61%; $p = 0.01$) were female. Median age at symptom onset was 28 months (range 8–151 months), with no difference between male and female sex ($p = 0.659$) (Figure 1). Age and sex distribution were similar between centers (data not shown). Most (86%) patients had parents from Germany or Austria; 14% had parents from a variety of other countries. Most (99.3%) patients were born in Germany or Austria; 1 was born in the Netherlands. Sociodemographic information, history of

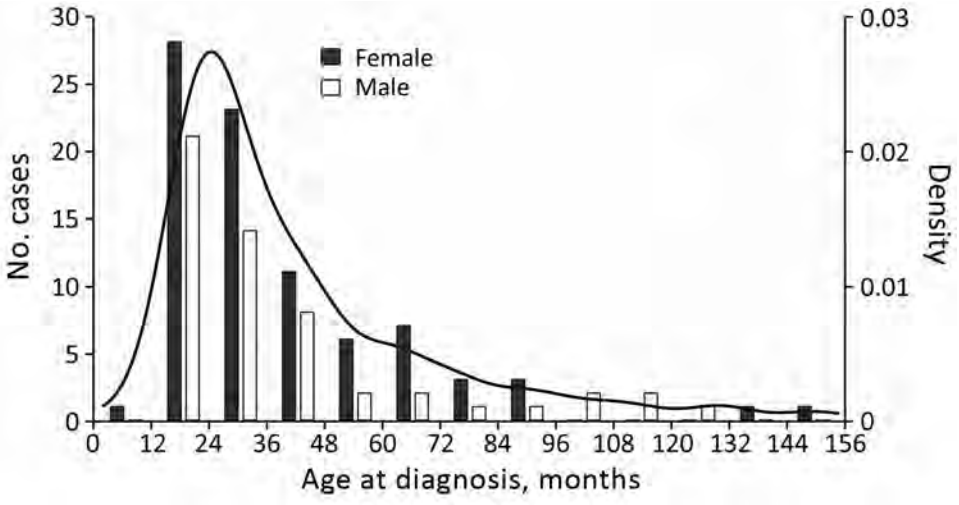

Figure 1. Histogram and density plot of patients' ages at diagnosis of nontuberculous mycobacteria lymphadenitis across 13 centers in Germany and Austria, 2010–2016.

prior diseases, and behavior related to possible NTM exposure did not differ substantially between female and male patients (data not shown). Boys were reported to play outside in summer longer than girls (p = 0.004); however, the difference was small (median 2 h/d for both sexes and mean 2.1 h/d for boys versus 1.6 h/d for girls). We did not detect any differences between male and female case-patients for any other factors. Of note, none of the patients had received the bacillus Calmette-Guérin vaccine.

Seasonal Variance

We noted more patients sought initial treatment during colder seasons than in warm seasons. Because many patients experienced symptoms long before visiting the clinic, we assessed and documented duration of symptoms at the initial visit. We saw a statistically significant difference between centers for symptom onset and initial visit in the study center (p = 0.019; Figure 2). However, we noted the seasonal pattern for the onset of symptoms across all centers. When we fit a sinusoidal yearly pattern for the reported onset of symptoms, seasonality was statistically significant (p<0.025; Figure 3, panel A). To minimize uncertainty in reporting the duration of symptoms, we analyzed the subgroup of patients with the shortest reported duration of symptoms, <4 weeks. The seasonal pattern remained the same, but statistical significance was lost due to the smaller sample size. In addition, peak incidence differed depending on patients' ages. For patients ≤24 months of age, peak incidence occurred in December, but peak incidence occurred 2 months later for older patients (Figure 3, panel B). However, the difference did not reach statistical significance.

NTM Species

NTM species were reported in 96/138 (70%) cases. In 2 cases, only *M. avium* complex was reported; 9 other cases were listed as NTM unspecified. Cultures were performed on samples from 106 cases; 58% were NTM positive by culture, but NTM species were identified by PCR in 35 culture-negative cases. The longer symptoms lasted before diagnosis, the less likely culture was to be positive. No cases with symptoms that lasted >6 months before diagnosis were culture-positive, compared with 65% of cases that had symptom onset <4 weeks before culture and 57% that had symptom onset in the previous 4 weeks–6 months (p = 0.004). Most (84%) cases were *M. avium* complex, and all centers reported similar rates of *M. avium* (75%–89%). We did not see statistically significant differences in species distribution among centers (p = 0.194; Table 1).

Localization and Symptoms

In most cases, cervical (33%), submandibular (35%), and preauricular (6%) lymph nodes were affected.

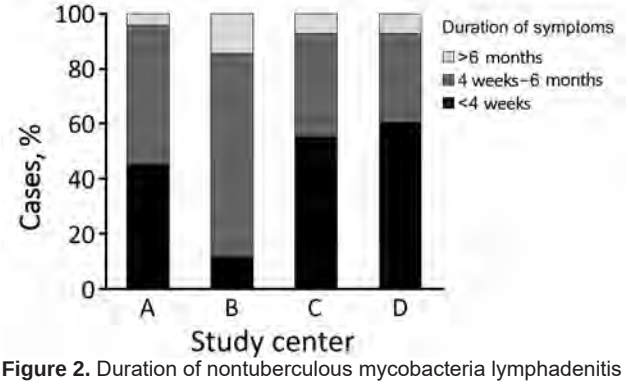

Figure 2. Duration of nontuberculous mycobacteria lymphadenitis symptoms after patients' first visit to a participating study center across 13 centers in Germany and Austria, 2010–2016. A represents combined data from the 10 smaller centers; B–D represent the 3 largest centers.

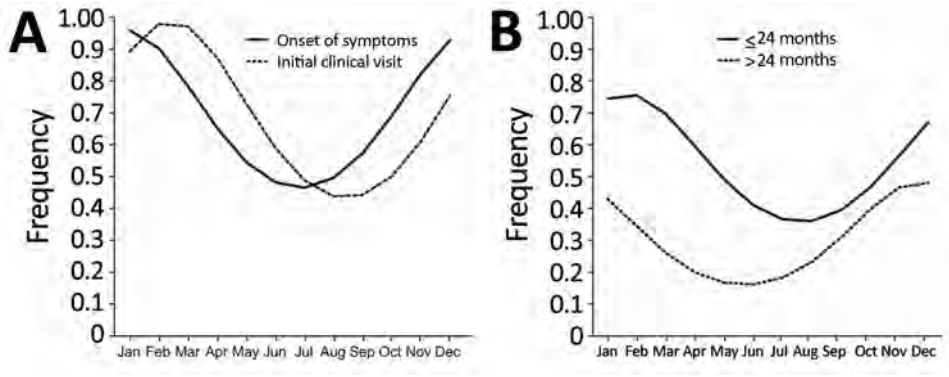

Figure 3. Seasonality of nontuberculous mycobacteria lymphadenitis in children across 13 centers in Germany and Austria, 2010–2016. Curves created by fitting a generalized linear regression model assuming a sinusoid Poisson distribution over the year (cosinor). A) Month of symptom onset and initial visit at a study center. B) Month of symptom onset for patients ≤24 months and >24 months of age.

Only 5% of cases involved lymph nodes in other regions, such as inguinal. Of note, 21% of cases had >1 affected region, such as same-sided cervical and submandibular lymph nodes; 9% of cases had bilateral involvement, mainly occurring as cervical and nuchal localization. We also noted additional local symptoms, such as discoloration, in 59% of cases. Only 17% of cases reported systemic symptoms; most were unspecific, and fever was reported most frequently.

Diagnosis and Treatment

During the initial workup, most (97%) patients had an ultrasound; 32% had magnetic resonance imaging (MRI), but MRI use was highly variable between centers (range 11%–78%; p<0.001); and 59% (43%–80%; p = 0.005) of patients had a chest radiograph. Tuberculin skin testing was done in 65% (49%–100%; p<0.001) of cases, and 61% of tests were positive. Most (94%) patients received surgical treatment; 49% (32%–69%; p = 0.03) had complete extirpation of the affected lymph node, and 40% had >1 operation, mainly due to impaired wound healing (Table 2). Histologic characteristics of affected lymph nodes included necrosis (61%), granuloma (60%), and giant cells (43%), among other findings (Table 3).

Apart from surgery, treatment varied considerably among centers (Table 2). Only 34% of patients received appropriate mycobacteria-targeted antimicrobial therapy that included a macrolide for ≥3 months (10%–52% across centers; p<0.001) (*16*,*17*). Only 23% of patients with complete extirpation of the affected lymph node received appropriate antimycobacterial therapy, compared with 49% undergoing other types of surgery (p = 0.006). The percentage of patients receiving antimycobacterial therapy declined over the course of the study (data not shown).

Clinical Course and Outcomes

We used univariate and multivariate analyses to search for risk factors associated with surgical complications, relapse after surgery, and length of time to full recovery. In addition to single factors, we created a surrogate, "unfavorable outcome," which we defined as illness lasting >12 months, >1 surgical intervention at the same site, or occurrence of major complications, such as substantial scarring or facial nerve palsy. We found 65% of the cohort had an unfavorable outcome and that differences between centers were statistically significant, ranging from 41% to 90% (p<0.01). However, we did not note any statistically significant difference between the 3 largest centers, where unfavorable outcomes averaged 78% (p = 0.19). The difference in the rate

Table 1. Number and distribution of patients identified with various *Mycobacteria* species by culture and PCR across 13 centers in Germany and Austria*

Mycobacteria species	Total no.	Negative culture, no.	Participating center			
			A	B	C	D
M. avium	73	18	29	14	15	15
M. intracellulare	6	2	2	2	2	0
MAI complex, nonspecified	2	0	0	0	1	1
M. malmoense	4	3	1	0	3	0
M. kansasii	4	2	2	0	1	1
M. haemophilum	2	2	0	0	2	0
M. austroamericanum	1	1	0	1	0	0
M. bohemicum	1	0	0	0	0	1
M. celatum	1	0	0	1	0	0
M. gordunae	1	0	0	1	0	0
M. stomatepiae	1	0	1	0	0	0

*Culture remained negative in some cases and nontuberculous mycobacteria were identified only by PCR. Combined data from the 10 smaller centers are represented in A and the 3 largest centers are represented by B, C, and D. MAI, mycobacterium avium-intracellular infection.

Table 2. Patient characteristics, treatment, and outcome for cases of complicated lymphadenitis caused by nontuberculous mycobacteria across 13 centers in Germany and Austria*

Characteristics	Total	Participating center				p value†
		A	B	C	D	
Patient sex, no. (%)	138	47	35	27	29	NS
F	84 (60.9)	29 (61.7)	21 (60)	15 (55.6)	18 (62.1)	NS
M	54 (39.1)	18 (38.3)	14 (40)	12 (44.4)	11 (37.9)	NS
Median patient age, mo	28	28	27	27	37	NS
Treatment, %						
Surgery	94	100	91	89	92	NS
Complete extirpation	49	48	69	42	32	0.03
Antimycobacterial therapy	44	62	21	30	55	<0.001
Outcome, %						
Unfavorable	65	41	68	74	90	0.006
Impaired wound healing	25	19	17	37	34	NS
Facial nerve palsy	7	2	6	0	24	0.002
Mean risk score‡	2.3	1.9	2.6	2.8	2.3	0.004

*Combined data from 10 smaller centers are represented in A and the 3 largest centers are represented by B, C, and D. NS, not significant.
†p values are based on original count data and calculated by using the Fisher exact test.
‡Risk scores calculated by using the Kruskal-Wallis test.

of transient or persistent facial nerve palsy was statistically significant between centers, ranging up to 24% (p<0.01). The incidence of facial nerve palsy did not correlate with the size of the study center, which we measured by the number of cases included from a center (Table 2).

The factor most strongly associated with unfavorable outcome was the presence of liquefaction in the affected lymph node identified by ultrasound or MRI. Most (73%) patients with liquefaction had an unfavorable outcome, compared with only 40% of patients who did not (p = 0.009).

Surgical procedures also affected outcomes. Overall, 51% of patients who had complete primary extirpation had an unfavorable outcome, compared with 75% of patients who had other types of surgery (p = 0.028). Only 19% of patients who had primary extirpation had impaired wound healing, compared with 35% of patients who had other types of surgery (p = 0.049). Complete extirpation also was associated with a lower incidence of other complications; only 3% of these patients had facial nerve palsy compared with 12% who had other surgical procedures (Table 3). Of patients who had the affected lymph node drained, 60% experienced impaired wound healing and an unfavorable outcome (p = 0.024), compared with 25% of patients who received other therapies (p = 0.027).

Mycobacteria-targeted antimicrobial therapy was not associated with improved clinical outcomes. When we used multivariate analysis to correct for the influence of the treatment center, complete extirpation of the affected lymph node still predicted a favorable clinical outcome (p = 0.029), good primary wound healing after surgery (p = 0.026), and a low rate of postsurgical complications, such as facial nerve palsy (p = 0.01). We saw impaired wound healing more often in connection with local skin symptoms, such as discoloration (p = 0.027), increased size of the affected lymph node (p = 0.036), and >1 affected location (p = 0.039). Taken together, complete extirpation was associated with an overall favorable clinical outcome and a lower rate of local complications compared with other types of surgical intervention.

Using these results, we developed a score for estimating the risk for an unfavorable clinical course before surgery. We grouped factors associated with adverse outcomes. Because the sample size was small, we could not calculate effect sizes reliably. Instead, we assigned each of the following items 1 point: skin discoloration, lymph node >2 cm, liquefaction on ultrasound or MRI, and >1 affected location. The resulting score helped us demonstrate a statistically significant association between outcomes and local complications, such as impaired wound healing, which has a Pearson score of $r = 0.23$ (p = 0.036) (Figure 4).

Risk Factors for NTM Lymphadenitis

To identify candidate risk factors for NTM lymphadenitis, we recruited control patients matched for age, sex, and center. In addition, we selected an age- and sex-matched control cohort from the KiGGS 2003–2006 (*13*). We compared sociodemographic factors,

Table 3. Histologic characteristics of lymph nodes from children infected with nontuberculous mycobacteria across 13 centers in Germany and Austria*

Finding	All samples, %
Fibrosis	6
Necrosis	61
Granulomatous infiltration	19
Granuloma	60
Giant cells	43
Epithelial cells	18
Acid-fast bacilli	15

*Multiple findings possible.

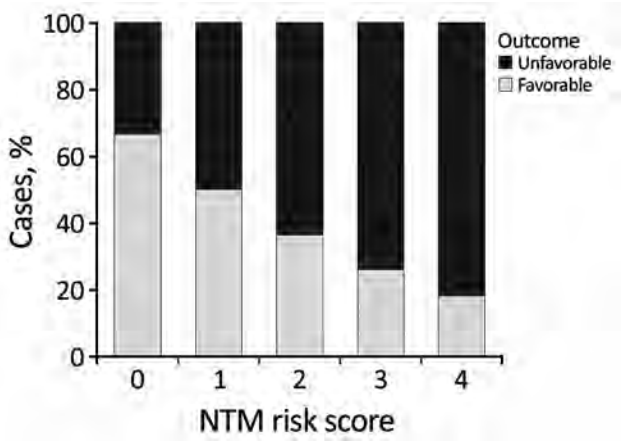

Figure 4. Correlation of NTM risk score and surrogate clinical outcome in a study of NTM lymphadenitis in children across 13 centers in Germany and Austria, 2010–2016. Scores represent 1 point each for skin discoloration, lymph node >2 cm, liquefication of lymph node on ultrasound or magnetic resonance imaging, and >1 affected location. Outcome percentages calculated by Pearson correlation are dependent on the assigned score (r = 0.23, p = 0.036). NTM, nontuberculous mycobacteria.

medical history, and data relating to potential exposure to mycobacteria, such as contact with animals and water sources, between patients and controls. Sociodemographic characteristics, such as parents' level of education, a child's presence in daycare, household smoking, and number of siblings, did not differ between patients and controls. We saw no difference in height and weight, the rate or duration of breastfeeding (mean 5.7 months for NTM patients and 5.5 months for control cohort; p = 0.590), or adherence to recommended vitamin D supplementation in the first year of life (94% for NTM patients and 81% for control cohort; p = 0.151).

We detected no difference between groups in health-related factors, such as frequency of antimicrobial drug treatment, typical childhood infections, or allergies. We also did not detect any difference in factors related to possible exposure to NTM, such as number of hours playing outside per day, exposure to natural bodies of water or swimming pools, or contact with pets and farm animals.

Discussion

In this study, we found that girls 18–36 months of age were at highest risk for NTM lymphadenitis, which aligns with findings of studies conducted in other geographic locations (*3*,*4*,*7*,*18*–*21*). The underlying cause for the predominance of NTM in girls remains unclear. We speculate that exposure to soil-residing NTM could be associated with the increased risk for NTM infection. However, the amount of time girls spent outside did not correspond to disease risk. Moreover, the predominance of NTM in female patients in varying geographic and climatic regions suggests that differences in immunity or host–pathogen interaction are more likely to be responsible for sex-related differences in NTM lymphadenitis incidence, rather than differences in exposure to NTM.

We also found a seasonal incidence pattern that peaked during colder months. Other studies reported an increase in new cases during winter (*7*,*20*), but peak incidence in relation to temperature and length of daylight hours varied among studies in different geographic regions. To expand on other studies, we recorded the duration of symptoms at each patient's initial visit to participating centers. Using this information, we were able to correct for the time between onset of symptoms and diagnosis because differences in referral and availability of appointments might influence the seasonal pattern. We noticed that time from onset of symptoms to the first physical examination at a clinic varied greatly between centers. Year-round differences in NTM exposure also could affect disease incidence. For example, seasonal NTM occurrence in drinking water has been reported (*22*,*23*).

Furthermore, the low incidence of NTM infections in warmer months could be linked to seasonal variations in vitamin D levels. Variations in vitamin D metabolism previously have been linked to NTM susceptibility (*24*,*25*). However, in our study, patients and healthy controls did not differ in sunlight exposure, and vitamin D supplementation in the first year of life occurred more often in the NTM-infected cohort than in controls.

Given the slow replication of NTM, incubation time for NTM lymphadenitis is unknown. Thus, a critical timeframe for infection is difficult to establish from the seasonal pattern seen in our cohort. In addition, unknown host factors, such as concurring infections, might affect seasonal incidence.

M. avium causes the majority of NTM lymphadenitis cases in countries as far removed from each other as Germany, Sweden, and Australia (*3*,*4*,*7*,*18*). By contrast, NTM species isolated in pulmonary infections have much more pronounced regional differences (*26*). Other than *M. avium*, we noted variations in NTM species between centers, but the small number of cases precluded a more detailed analysis. Nevertheless, the relatively high number of rare species underlines the need for improved PCR and culture techniques for reliable diagnosis of uncommon NTM species.

Therapeutic procedures, disease outcomes, and complications varied substantially among centers

and over the course of the study. Overall, patients frequently had complicated clinical courses that lasted >12 months or major complications, even after complete extirpation, the treatment most associated with a favorable outcome. More than 75% of patients in the 3 most experienced study centers had complicated clinical courses, which is a striking contrast to a report by Lindeboom et al. (*16*) in which early complete lymph node extirpation cured >90% of lymphadenitis cases. However, lymphadenitis frequently is caused by factors other than NTM. Our data might reflect more on clinical practices in which early extirpation is more the exception than the rule, a hypothesis further supported by the fact that clinical outcomes did not correlate with center size in our study. Consequently, surgical experience might not explain the unfavorable outcomes in our study. However, because only specialized centers participated in the study and inclusion criteria were strict, complicated surgical cases probably were overrepresented in our cohort. This finding is supported by evidence that some patients underwent primary surgery elsewhere and were referred to our participating centers after they received a definitive NTM diagnosis.

The rate of facial nerve palsy in our study was within the range reported elsewhere (*7*), but we saw variations among centers. Because our study relied on local clinical data, we cannot rule out differences in sensitivity thresholds. However, differences in the surgical approach reflected by the varying rates of complete extirpation most likely explain this observation. Primary complete lymph node extirpation was associated with a lower rate of facial nerve palsy than other surgical procedures. However, this observation could have a high bias because complete extirpation is performed more frequently when the affected lymph node is farther from the facial nerve. Antimicrobial therapy for NTM lymphadenitis decreased over the course of the study, which might reflect the increasing number of studies questioning the therapeutic benefit of antimicrobial drugs to treat NTM lymphadenitis.

Our study has several limitations. First, the limited number of disease controls precluded a more detailed analysis of possible individual risk factors. Second, our cohort probably does not reflect the full variety of NTM lymphadenitis phenotypes. Our strict inclusion criteria and registry-like design likely overrepresented severe cases, which are seen more frequently in secondary and tertiary health centers, and underrepresented less severe cases. Third, because we relied on data acquired by local centers and did not collect detailed information on PCR methods, we cannot rule out differences in laboratory methods or interpretation of clinical findings.

In conclusion, the NTM lymphadenitis risk profile for female patients ≤5 years of age, the chronic (albeit usually benign) course of disease, the worldwide predominance of *M. avium*, and the seasonal variability we noted in our study suggest a complex contribution of host, pathogen, environmental, and potential microbiome factors. Individual factors are insufficient to grasp the risk for unfavorable clinical outcomes. Our proposed risk score comprises multiple items and could be useful in estimating NTM lymphadenitis risk and stratifying patients to therapeutic modalities, if its validity is confirmed in a prospective study. Until then, early and complete extirpation of a suspicious lymph node remains a mainstay of NTM diagnosis and therapy.

Acknowledgments

We thank Christina Kronthaler for her excellent technical support and Natalie Diffloth for her English editing help. We also thank the participating centers in the following cities: Berlin, Charité–Universitätsmedizin Berlin; Bremen, Professor-Hess-Kinderklinik, Hospital Bremen Mitte; Düsseldorf, University Children's Hospital, Heinrich Heine University; Erlangen, University Children's Hospital, Friedrich-Alexander-University Erlangen-Nürnberg; Frankfurt, University Children's Hospital, Goethe University of Frankfurt; Freiburg, Center for Pediatrics and Adolescent Medicine, University Medical Center Freiburg; Graz, Medical University of Graz, Department of General Pediatrics; Hannover, Children's Hospital, Hannover Medical School; Heidelberg, University of Heidelberg, Department of Pediatrics; Cologne, Children's Hospital, City of Cologne; Leipzig, Hospital for Children and Adolescents, University of Leipzig; Munich, Dr. von Hauner Children's Hospital, Ludwig-Maximilians-University; Würzburg, University Children's Hospital.

Funding was provided in part by the German Research Council under grant no. DFG HE3127/9-2 to P.H., and by the German Ministry of Education and Research under grant nos. 01EO0803, 01GL1746A, and 535 01EK1602A to P.H. Data from the German Health Interview and Examination Survey for Children and Adolescents 2003–2006 (KiGGS Basiserhebung) was provided by the data research center of the Robert Koch Institute and was part of the advanced data usage program (no. 5.04.04/0002#148).

About the Author

Dr. Kuntz is a pediatrician at the University Medical Center, Freiburg, Germany. His research focuses on innate immunity and age-dependent host–pathogen interactions.

References

1. Feazel LM, Baumgartner LK, Peterson KL, Frank DN, Harris JK, Pace NR. Opportunistic pathogens enriched in showerhead biofilms. Proc Natl Acad Sci U S A. 2009;106:16393–9. https://doi.org/10.1073/pnas.0908446106
2. Thomson R, Tolson C, Carter R, Coulter C, Huygens F, Hargreaves M. Isolation of nontuberculous mycobacteria (NTM) from household water and shower aerosols in patients with pulmonary disease caused by NTM. J Clin Microbiol. 2013;51:3006–11. https://doi.org/10.1128/JCM.00899-13
3. Reuss AM, Wiese-Posselt M, Weissmann B, Siedler A, Zuschneid I, An der Heiden M, et al. Incidence rate of nontuberculous mycobacterial disease in immunocompetent children: a prospective nationwide surveillance study in Germany. Pediatr Infect Dis J. 2009;28:642–4. https://doi.org/10.1097/INF.0b013e3181978e8e
4. Romanus V, Hallander HO, Wåhlén P, Olinder-Nielsen AM, Magnusson PH, Juhlin I. Atypical mycobacteria in extrapulmonary disease among children. Incidence in Sweden from 1969 to 1990, related to changing BCG-vaccination coverage. Tuber Lung Dis. 1995;76:300–10. https://doi.org/10.1016/S0962-8479(05)80028-0
5. Nasiri MJ, Dabiri H, Darban-Sarokhalil D, Hashemi Shahraki A. Prevalence of non-tuberculosis mycobacterial infections among tuberculosis suspects in Iran: systematic review and meta-analysis. PLoS One. 2015;10:e0129073. https://doi.org/10.1371/journal.pone.0129073
6. Arend SM, van Soolingen D, Ottenhoff THM. Diagnosis and treatment of lung infection with nontuberculous mycobacteria. Curr Opin Pulm Med. 2009;15:201–8. https://doi.org/10.1097/MCP.0b013e3283292679
7. Tebruegge M, Pantazidou A, MacGregor D, Gonis G, Leslie D, Sedda L, et al. Nontuberculous mycobacterial disease in children–epidemiology, diagnosis & management at a tertiary center. PLoS One. 2016;11:e0147513. https://doi.org/10.1371/journal.pone.0147513
8. Lindeboom JA. Conservative wait-and-see therapy versus antibiotic treatment for nontuberculous mycobacterial cervicofacial lymphadenitis in children. Clin Infect Dis. 2011;52:180–4. https://doi.org/10.1093/cid/ciq070
9. Casanova JL. Mendelian susceptibility to mycobacterial infection in man. Swiss Med Wkly. 2001;131:445–54.
10. Haverkamp MH, van de Vosse E, van Dissel JT. Nontuberculous mycobacterial infections in children with inborn errors of the immune system. J Infect. 2014;68(Suppl 1):S134–50. https://doi.org/10.1016/j.jinf.2013.09.024
11. Wu U-I, Holland SM. Host susceptibility to non-tuberculous mycobacterial infections. Lancet Infect Dis. 2015;15:968–80. https://doi.org/10.1016/S1473-3099(15)00089-4
12. Kurth B-M. The German health interview and examination survey for children and adolescents (KiGGS): an overview of its planning, implementation and results taking into account aspects of quality management [in German]. Bundesgesundheitsblatt Gesundheitsforschung Gesundheitsschutz. 2007;50:533–46. https://doi.org/10.1007/s00103-007-0214-x
13. Kurth BM, Dölle R, Stolzenberg H.; Robert Koch-Institute, Department of Epidemiology and Health Monitoring. KiGGS baseline study on the health of children and adolescents in Germany [in German]. Robert Koch Institute; 2013 [cited 2019 May 30]. http://www.kiggs-studie.de/deutsch/studie/kiggs-basiserhebung.html
14. R Core Team. R: a language and environment for statistical computing. Vienna, Austria: R Foundation for Statistical Computing; 2019. https://www.R-project.org
15. Barnett AG, Dobson AJ. Analysing seasonal health data. Heidelberg: Springer-Verlag; 2010. https://doi.org/10.1007/978-3-642-10748-1
16. Lindeboom JA, Kuijper EJ, Bruijnesteijn van Coppenraet ES, Lindeboom R, Prins JM. Surgical excision versus antibiotic treatment for nontuberculous mycobacterial cervicofacial lymphadenitis in children: a multicenter, randomized, controlled trial. Clin Infect Dis. 2007;44:1057–64. https://doi.org/10.1086/512675
17. Griffith DE, Aksamit T, Brown-Elliott BA, Catanzaro A, Daley C, Gordin F, et al.; ATS Mycobacterial Diseases Subcommittee; American Thoracic Society; Infectious Disease Society of America. An official ATS/IDSA statement: diagnosis, treatment, and prevention of nontuberculous mycobacterial diseases. Am J Respir Crit Care Med. 2007;175:367–416. https://doi.org/10.1164/rccm.200604-571ST
18. Haverkamp MH, Arend SM, Lindeboom JA, Hartwig NG, van Dissel JT. Nontuberculous mycobacterial infection in children: a 2-year prospective surveillance study in the Netherlands. Clin Infect Dis. 2004;39:450–6. https://doi.org/10.1086/422319
19. Schaad UB, Votteler TP, McCracken GH Jr, Nelson JD. Management of atypical mycobacterial lymphadenitis in childhood: a review based on 380 cases. J Pediatr. 1979;95:356–60. https://doi.org/10.1016/S0022-3476(79)80506-5
20. Thegerström J, Romanus V, Friman V, Brudin L, Haemig PD, Olsen B. *Mycobacterium avium* lymphadenopathy among children, Sweden. Emerg Infect Dis. 2008;14:661–3. https://doi.org/10.3201/eid1404.060570
21. Wolinsky E. Mycobacterial lymphadenitis in children: a prospective study of 105 nontuberculous cases with long-term follow-up. Clin Infect Dis. 1995;20:954–63. https://doi.org/10.1093/clinids/20.4.954
22. Mishra PS, Narang P, Narang R, Goswami B, Mendiratta DK. Spatio-temporal study of environmental nontuberculous mycobacteria isolated from Wardha district in Central India. Antonie van Leeuwenhoek. 2018;111:73–87. https://doi.org/10.1007/s10482-017-0927-2
23. Whiley H, Keegan A, Fallowfield H, Bentham R. The presence of opportunistic pathogens, *Legionella spp.*, *L. pneumophila* and *Mycobacterium* avium complex, in South Australian reuse water distribution pipelines. J Water Health. 2015;13:553–61. https://doi.org/10.2166/wh.2014.317
24. Gelder CM, Hart KW, Williams OM, Lyons E, Welsh KI, Campbell IA, et al. Vitamin D receptor gene polymorphisms and susceptibility to *Mycobacterium malmoense* pulmonary disease. J Infect Dis. 2000;181:2099–102. https://doi.org/10.1086/315489
25. Jeon K, Kim S-Y, Jeong B-H, Chang B, Shin SJ, Koh W-J. Severe vitamin D deficiency is associated with non-tuberculous mycobacterial lung disease: a case-control study. Respirology. 2013;18:983–8. https://doi.org/10.1111/resp.12109
26. Hoefsloot W, van Ingen J, Andrejak C, Angeby K, Bauriaud R, Bemer P, et al.; Nontuberculous Mycobacteria Network European Trials Group. The geographic diversity of nontuberculous mycobacteria isolated from pulmonary samples: an NTM-NET collaborative study. Eur Respir J. 2013;42:1604–13. https://doi.org/10.1183/09031936.00149212

Address for correspondence: Philipp Henneke, Center for Chronic Immunodeficiency, Breisacher Strasse 117, 79106 Freiburg, Germany; email address: philipp.henneke@uniklinik-freiburg.de

Human Exposure to Hantaviruses Associated with Rodents of the *Murinae* Subfamily, Madagascar

Harinirina Aina Rabemananjara,[1] Vololoniaina Raharinosy,[1] Ravo Michèle Razafimahefa, Jean Pierre Ravalohery, Jean Théophile Rafisandratantsoa, Soa Fy Andriamandimby, Minoarisoa Rajerison, Soanandrasana Rahelinirina, Aina Harimanana, Judickaelle Irinantenaina, Marie-Marie Olive, Christophe Rogier, Noël Tordo, Rainer G. Ulrich, Jean-Marc Reynes, Stéphane Petres, Jean-Michel Heraud,[2] Sandra Telfer,[2] Claudia Filippone[2]

We conducted a national human serologic study of a hantavirus detected in Madagascar rodents using a commercial kit and a new ELISA targeting the virus. Our results suggest a conservative estimate of 2.7% (46/1,680) IgG seroprevalence. A second single-district study using the new ELISA revealed a higher prevalence (7.2%; 10/139).

Hantaviruses belonging to the genus *Orthohantavirus*, family *Hantaviridae*, are frequently zoonotic. Rodents are the usual reservoirs of human pathogenic hantaviruses and typically do not show obvious signs of disease (*1*,*2*). Transmission to humans usually occurs by inhalation of aerosols contaminated with urine or feces of infected reservoir animals (*3*). Hantaviruses are responsible for the severe illness hemorrhagic fever with renal syndrome (HFRS) and a milder form, nephropathia epidemica (NE), as well as for hantavirus cardiopulmonary syndrome (HCPS) (*1*).

Recent studies have described the geographic distribution and host range of novel hantaviruses in Africa and the Indian Ocean (*4*–*6*). In Madagascar, hantavirus RNA was identified by molecular analysis in *Rattus rattus* and *Eliurus majori* rats from a forest site in Anjozorobe district. The virus was named Anjozorobe virus (ANJZV) and is a genetic variant of Thailand orthohantavirus (THAIV) (*5*). In a more recent national study, Raharinosy et al. detected hantavirus RNA in 12% (n = 897) of *R. rattus* rats, and all the sequences obtained grouped with ANJZV (*7*), but they did not detect hantavirus RNA in *R. norvegicus* rats (0%; n = 124) (*7*), a species commonly associated with the cosmopolitan Seoul orthohantavirus (*1*). Because THAIV may cause HFRS in Southeast Asia (*8*), ANJZV could also be a human pathogen in Madagascar. In 1986, a limited study that used an immunofluorescence assay with Hantaan orthohantavirus (HTNV) and Puumala orthohantavirus antigens was conducted in areas around the capital and reported low titer hantavirus antibodies in the serum samples of 7/18 rat catchers in Madagascar (*9*).

We conducted a national study to assess hantavirus exposure in the general population of Madagascar. Sampling took place in conjunction with a recent rodent survey (*7*). In addition, because the original molecular hantavirus detection in Madagascar was from forest rodents (*5*), we also collected and analyzed human and rat samples from 4 sites close to forests.

The Study

As part of a retrospective national study on zoonoses, we collected human serum samples from 2011–2013. We then randomly recruited 1,680 asymptomatic participants (851 female and 829 male; average age 37 years; range 18–99 years). We conducted sampling in 28 sites, each with urban and rural zones;

Author affiliations: Institut Pasteur de Madagascar, Antananarivo, Madagascar (H.A. Rabemananjara, V. Raharinosy, R.M. Razafimahefa, J.P. Ravalohery, J.T. Rafisandratantsoa, S.F. Andriamandimby, M. Rajerison, S. Rahelinirina, A. Harimanana, J. Irinantenaina, M.-M. Olive, C. Rogier, J.-M. Heraud, C. Filippone); Central Directorate of the French Military Health Service, Paris, France (C. Rogier); Institut Pasteur, Conakry, Guinea (N. Tordo); Institut Pasteur, Paris (N. Tordo, J.-M. Reynes, S. Petres); Federal Research Institute for Animal Health, Greifswald-Insel Riems, Germany (R.G. Ulrich); German Center for Infection Research, Hamburg-Luebeck-Borstel-Insel Riems, Germany (R.G. Ulrich); University of Aberdeen, Aberdeen, Scotland, UK (S. Telfer)

DOI: https://doi.org/10.3201/eid2603.190320

[1]These first authors contributed equally to this article.

[2]These authors were co–principal investigators.

Table 1. Seroprevalence of hantavirus in humans in the 28 sites used for national study, Madagascar*

Site no.	Site	No. positive/total no. participants (%; 95% CI)
1	Antananarivo	8/60 (13.3; 6.3–25.1)
2	Antsirabe	0/60 (0.0; 0.0–7.5)
3	Anjozorobe	1/60 (1.7; 0.0–10.1)
4	Tsiroanomandidy	3/60 (5.0; 1.3–14.8)
5	Antsiranana	0/60 (0.0; 0.0–7.5)
6	Sambava	2/60 (3.3; 0.5–12.5)
7	Nosy-be	2/60 (3.3; 0.5–12.5)
8	Mananjary	1/60 (1.7; 0.0–10.1)
9	Ambositra	3/60 (5.0; 1.3–14.8)
10	Farafangana	4/60 (6.7; 2.1–17.0)
11	Ihosy	0/60 (0.0; 0.0–7.5)
12	Fianarantsoa	1/60 (1.7; 0.0–10.1)
13	Antsohihy	1/60 (1.7; 0.0–10.1)
14	Mandritsara	0/60 (0.0; 0.0–7.5)
15	Maevatanana	4/60 (6.7; 2.1–17.0)
16	Ambato Boeny	0/60 (0.0; 0.0–7.5)
17	Mahajanga	2/60 (3.3; 0.5–12.5)
18	Moramanga	0/60 (0.0; 0.0–7.5)
19	Toamasina	2/60 (3.3; 0.5–12.5)
20	Ambatondrazaka	0/60 (0.0; 0.0–7.5)
21	Miandrivazo	1/60 (1.7; 0.0–10.1)
22	Ejeda	2/60 (3.3; 0.5–12.5)
23	Morombe	1/60 (1.7; 0.0–10.1)
24	Toliary	2/60 (3.3; 0.5–12.5)
25	Taolagnaro	2/60 (3.3; 0.5–12.5)
26	Ambovombe	2/60 (3.3; 0.5–12.5)
27	Belo sur Tsiribihina	0/60 (0.0; 0.0–7.5)
28	Morondava	2/60 (3.3; 0.5–12.5)
Total		46/1,680 (2.7; 2.0–3.7)

*Results from IgG testing by commercial ELISA and custom ELISA developed for Anjozorobe virus.

we sampled 60 persons per site, with 30 persons per zone (*10*). In addition, we used samples collected during 2015–2016 from 4 rural sites close to natural forest areas in Moramanga district, which is close to Anjozorobe district. For this study, we randomly selected 139 asymptomatic participants (31–36 persons per site; average age 29 years, range 5–75 years). We also conducted trapping of the rat population in these 4 sites and randomly selected 237 *R. rattus* rats (58–61 per site).

The national ethics committee of Madagascar authorized human studies (authorization no. 066-MSANP/CE on July 26, 2011; no. 049-MSANT/CE on July 03, 2012). We conducted animal studies in accordance with Pasteur Institute animal use guidelines (https://www.pasteur.fr/en/file/2626/download?token=YgOq4QW7). A committee of the Institut Pasteur de Madagascar approved the studies.

For the national study, we performed initial screening using the commercial Dobrava-Hantaan IgG EIA kit (Reagena Ltd, https://www.reagena.com) based on the recombinant nucleocapsid (N) protein from HTNV. HTNV and THAIV, along with other *Murinae*-associated hantaviruses (Appendix Table 1, https://wwwnc.cdc.gov/EID/article/26/3/19-0320-App1.pdf), exhibit close antigenic relationship (*11*). However, because 2-way cross-reactivity is not complete (*12*), we developed a new IgG ELISA based on ANJZV recombinant N protein produced by a baculovirus-mediated insect cell expression system. We used this assay to test all samples testing positive or borderline by the commercial kit and a subset of negative samples (Appendix). Based on the apparent increased detection ability of the ANJZV ELISA, we only used ANJZV ELISA for testing the human samples from the 4 sites close to forest areas.

After screening 1,680 serum samples with the commercial ELISA, we found 36 (2.1%) positive and 26 (1.5%) borderline samples. Using the custom ANJZV ELISA on these samples and a subset of 62 negative samples, we found 46 positive and 15 borderline (Appendix Tables 2, 3). Thus, the ELISA we developed specifically for ANJZV appeared to be more sensitive. To obtain a conservative estimate of seroprevalence, only samples testing positive by both assays or positive by 1 assay and borderline by the other were considered positive; testing yielded an overall prevalence of 2.7% (46/1,680; 95% CI 2.0%–3.7%) in the population; 30 male (1.8%) and 16 female (0.9%) participants tested positive.

Seropositive participants came from 20 of the 28 study sites (0–13.3% per site) distributed all over Madagascar (Table 1; Figure). Univariate generalized linear mixed models with site-zone as random effect indicated no effect of age, sex, or location (urban or rural), but we did find a slight suggestion of increased exposure in sites where our previous study (*7*) had detected infected rats (OR 3.0, 95% CI 0.78–11.5; p = 0.11).

The Moramanga sites, situated close to forest, had significantly higher seroprevalence rates (7.2%: 10/139; 95% CI 3.7%–13.2%; range 3.2%–11.1%) than the national study sites (Kruskal-Wallis test $\chi^2_1 = 4.65$; p = 0.03) (Table 2; Figure). This finding may partly reflect the apparent higher sensitivity of the ANJZV ELISA used for the regional study. Because 2 (n = 62, 3.2%) national samples tested negative by the commercial ELISA were positive by ANJZV ELISA, and 1,558 national samples were not tested by ANJZV ELISA, the overall national seroprevalence could be >2.7% (3.2% × 1,558 = 50; (50 + 46)/1,680 = 5.7%). Of interest, when we tested *R. rattus* rats from the 4 Moramanga sites by nested reverse transcription PCR using a protocol described previously (Appendix) (*7*), we also observed significantly higher infection rates than those for the national study sites; 77 of 237 rat samples were positive (32.5%; 95% CI 26.7%–38.9%; range 19.0%–43.3%; Kruskal-Wallis test

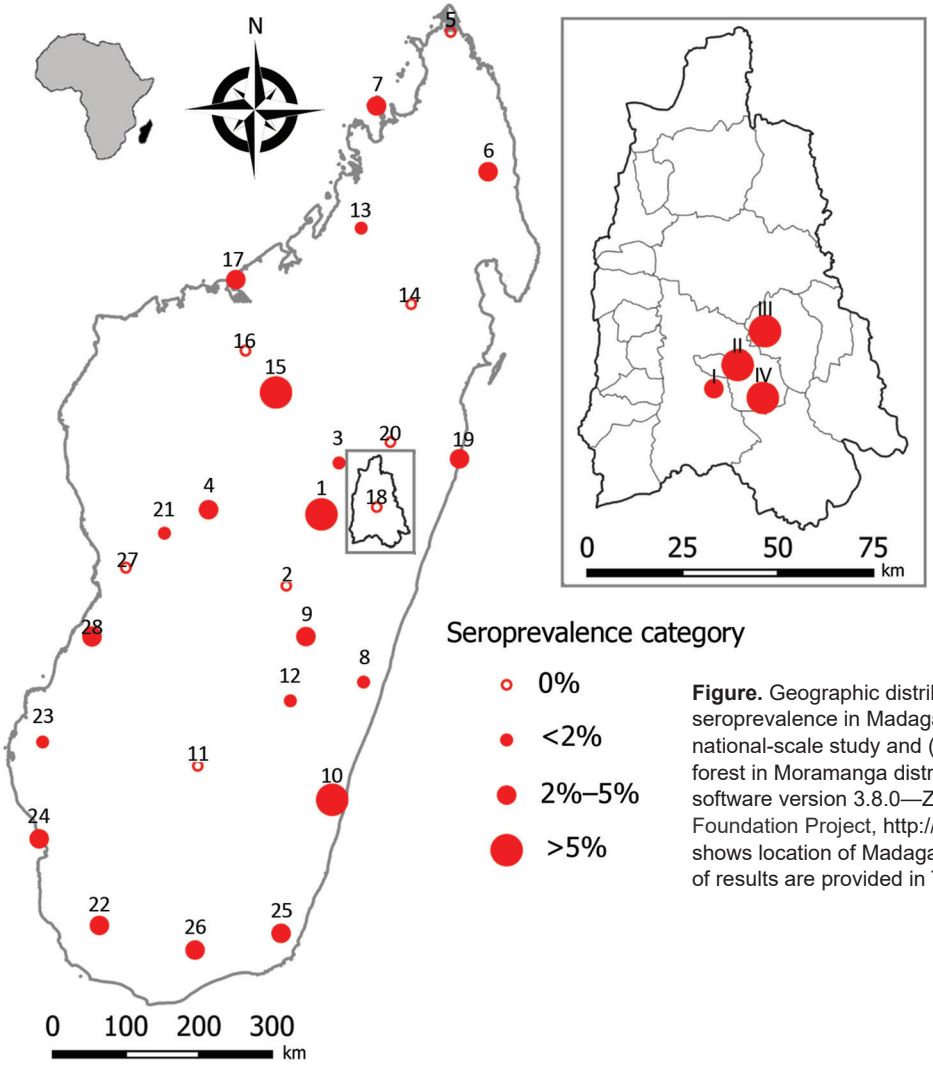

Figure. Geographic distribution of IgG hantavirus human seroprevalence in Madagascar for the 28 sites of the national-scale study and (inset) for the 4 sites close to forest in Moramanga district. Maps were built with QGIS software version 3.8.0—Zanzibar (Open Source Geospatial Foundation Project, http://qgis.osgeo.org). Small inset map shows location of Madagascar off the coast of Africa. Details of results are provided in Tables 1 and 2.

χ^2_1 = 5.55; p = 0.02). These results further confirm a relatively high infection rate in the most abundant and widespread rodent in Madagascar. The small number of samples (2/61; 3%) negative by ANJZV ELISA but seropositive by the commercial ELISA could be explained by other *Murinae*-associated hantaviruses circulating in Madagascar.

Conclusions

Our results suggest the population of Madagascar is exposed to hantaviruses associated with the *Murinae* subfamily of rodents. The overall conservative prevalence estimate of 2.7% from the national-scale study, obtained using 2 ELISA assays, is similar to results from studies in some Africa countries where other confirmatory tests were used (3.9% in Cote d'Ivoire and 2.4% in the Democratic Republic of the Congo) (*4*,*13*). Although we believe some seropositive persons may have been exposed to other *Murinae*-associated hantaviruses, considering both ELISA results in humans and rodent infection data together (*7*), our observations are consistent with evidence that most were exposed to ANJZV. Specifically, the ANJZV ELISA detected more seropositive persons than the commercial kit, and the cosmopolitan Seoul virus, if present in rodents in Madagascar, is at low prevalence or patchily

Table 2. Seroprevalence of hantavirus in humans in the 4 sites close to forest in Moramanga district, Madagascar

Site no.	Site	No. positive/total no. participants (%; 95% CI)
I	Mangidifoza	1/31 (3.2; 0.1–18.5)
II	Atsahatsaka	4/36 (11.1; 3.6–27.0)
III	Sahamalotra	3/36 (8.3; 2.1–23.6)
IV	Ambalafary	2/36 (5.5; 1.0–20.0)
Total		10/139 (7.2; 3.7–13.2)

*Results from IgG testing by custom ELISA developed for Anjozorobe virus.

distributed (*7*). Because hantavirus infection rates in *R. rattus* rats appear higher at sites close to forest, more widespread testing with the ELISA developed for Anjozorobe virus is needed to confirm whether human communities in such areas are also at higher risk for infection. In addition, hospital surveillance studies are needed in Madagascar to determine if hantavirus infection occurs in patients, with testing focused on those with fever with unknown etiology, renal failure, or both.

Acknowledgments

We thank all colleagues from the Virology, Plague and Epidemiology Units of the Institut Pasteur de Madagascar who aided with field and laboratory work. We thank Corinne Jallet for help with some ELISA assays and Rasa Petraityte-Burneikiene and Aurelija Zvirbliene for providing antigen for additional analysis. We thank Reagena for constructive exchanges during provision of the kits.

This work was supported by Wellcome Trust Fellowships (no. 081705 and 095171 to S.T.) and Institut Pasteur de Madagascar, and by PTR (Progamme Transversal de Recherche) HANTAREV at Institut Pasteur, Paris.

About the Author

Mr. Rabemananjara is a PhD student at the Virology Unit of Institut Pasteur de Madagascar. His research interests include hantaviruses in animal reservoirs (bats and other small mammals) and humans, as well as the circulation of arboviruses in Madagascar.

References

1. Jonsson CB, Figueiredo LT, Vapalahti O. A global perspective on hantavirus ecology, epidemiology, and disease. Clin Microbiol Rev. 2010;23:412–41. https://doi.org/10.1128/CMR.00062-09
2. Vaheri A, Strandin T, Hepojoki J, Sironen T, Henttonen H, Mäkelä S, et al. Uncovering the mysteries of hantavirus infections. Nat Rev Microbiol. 2013;11:539–50. https://doi.org/10.1038/nrmicro3066
3. Muranyi W, Bahr U, Zeier M, van der Woude FJ. Hantavirus infection. J Am Soc Nephrol. 2005;16:3669–79. https://doi.org/10.1681/ASN.2005050561
4. Witkowski PT, Klempa B, Ithete NL, Auste B, Mfune JKE, Hoveka J, et al. Hantaviruses in Africa. Virus Res. 2014;187:34–42. https://doi.org/10.1016/j.virusres.2013.12.039
5. Reynes JM, Razafindralambo NK, Lacoste V, Olive MM, Barivelo TA, Soarimalala V, et al. Anjozorobe hantavirus, a new genetic variant of Thailand virus detected in rodents from Madagascar. Vector Borne Zoonotic Dis. 2014;14:212–9. https://doi.org/10.1089/vbz.2013.1359
6. Filippone C, Castel G, Murri S, Beaulieux F, Ermonval M, Jallet C, et al. Discovery of hantavirus circulating among *Rattus rattus* in French Mayotte island, Indian Ocean. J Gen Virol. 2016;97:1060–5. https://doi.org/10.1099/jgv.0.000440
7. Raharinosy V, Olive MM, Andriamiarimanana FM, Andriamandimby SF, Ravalohery JP, Andriamamonjy S, et al. Geographical distribution and relative risk of Anjozorobe virus (*Thailand orthohantavirus*) infection in black rats (*Rattus rattus*) in Madagascar. Virol J. 2018;15:83. https://doi.org/10.1186/s12985-018-0992-9
8. Pattamadilok S, Lee BH, Kumperasart S, Yoshimatsu K, Okumura M, Nakamura I, et al. Geographical distribution of hantaviruses in Thailand and potential human health significance of Thailand virus. Am J Trop Med Hyg. 2006;75:994–1002. https://doi.org/10.4269/ajtmh.2006.75.994
9. Rollin PE, Mathiot C, Nawrocka E, Ravaoalimalala VE, Coulanges P, Sureau P, et al. Hemorrhagic fever with renal syndrome in Madagascar. First seroepidemiologic survey of rat populations [in French]. Arch Inst Pasteur Madagascar. 1986;52:181–6.
10. Olive MM, Chevalier V, Grosbois V, Tran A, Andriamandimby SF, Durand B, et al. Integrated analysis of environment, cattle, and human serological data: risk and mechanisms of transmission of Rift Valley fever in Madagascar. PLoS Negl Trop Dis. 2016;10:e0004827. https://doi.org/10.1371/journal.pntd.0004827
11. Yoshimatsu K, Arikawa J. Serological diagnosis with recombinant N antigen for hantavirus infection. Virus Res. 2014;187:77–83. https://doi.org/10.1016/j.virusres.2013.12.040
12. Chu YK, Rossi C, Leduc JW, Lee HW, Schmaljohn CS, Dalrymple JM. Serological relationships among viruses in the *Hantavirus* genus, family *Bunyaviridae*. Virology. 1994;198:196–204. https://doi.org/10.1006/viro.1994.1022
13. Witkowski PT, Leendertz SAJ, Auste B, Akoua-Koffi C, Schubert G, Klempa B, et al. Human seroprevalence indicating hantavirus infections in tropical rainforests of Côte d'Ivoire and Democratic Republic of Congo. Front Microbiol. 2015;6:518. https://doi.org/10.3389/fmicb.2015.00518

Address for correspondence: Claudia Filippone, Institut Pasteur de Madagascar–Virology Unit, Ambatofotsikely, BP 1274 Antananarivo, Madagascar; email: cla.filippone@gmail.com; Sandra Telfer, University of Aberdeen, Institute of Biological and Environmental Sciences, Aberdeen, Scotland AB24 2TZ, UK; email: s.telfer@abdn.ac.uk

Avian Influenza Virus Detection Rates in Poultry and Environment at Live Poultry Markets, Guangdong, China

Kit Ling Cheng,[1] Jie Wu,[1] Wei Ling Shen, Alvina Y.L. Wong, Qianfang Guo, Jianxiang Yu, Xue Zhuang, Wen Su, Tie Song, Malik Peiris, Hui-Ling Yen,[2] Eric H.Y. Lau[2]

We report the use of environmental samples to assess avian influenza virus activity in chickens at live poultry markets in China. Results of environmental and chicken samples correlate moderately well. However, collection of multiple environmental samples from holding, processing, and selling areas is recommended to detect viruses expected to have low prevalence.

Live poultry markets (LPMs) can serve as hubs for avian influenza virus (AIV) amplification in poultry and pose a risk for human zoonotic infections (*1*–*4*). Adopting efficient sampling strategies to monitor AIVs with human zoonotic potential at LPMs is essential for zoonotic disease prevention and pandemic preparedness. Recommendations regarding routine surveillance that would robustly and efficiently inform AIV activity at LPMs have been limited (*5*).

Handling of live poultry interrupts the vending process; moreover, such routine surveillance is difficult to implement. Environmental samples have been collected to monitor AIV activity at LPMs (*5*–*9*). There have been limited parallel comparisons of AIV detection rates among poultry and environmental samples (*7*,*10*). Without frequent cleaning, the environment often permits AIV accumulation; environmental samples may thus overestimate AIV prevalence in poultry. Subtype-specific detection rates among different environmental samples may also vary. To inform the development of effective sampling strategies for AIV surveillance, we compared monthly detection rates for AIV subtypes H5, H7, and H9 in chickens and various environmental samples at LPMs in Guangzhou, China.

The Study

During December 2015–July 2018, we performed sampling twice per month at 1 wholesale (52 stalls) and 1 retail (8 stalls) LPM, from 2 randomly selected stalls per sampling event. We collected paired oropharyngeal and cloacal swab samples (n = 3,119 chickens) and environmental samples (n = 3,008) in viral transport medium at the LPMs (Appendix Figure 1, https://wwwnc.cdc.gov/EID/article/26/3/19-0888-App1.pdf). We randomly collected samples from all chickens at the selected stalls. We rarely observed sick chickens but we sampled them when identified. We also collected environmental samples from 3 key activity areas: poultry holding zones (fecal droppings, drinking water, and poultry feed), slaughtering zones (defeathering machines and surrounding defeathering working areas), and selling zones (chopping boards and display tables) near the selected chickens whenever possible (*5*–*9*). (Stalls sampled at the wholesale LPM [wLPM] have only poultry holding zones.) We sampled air using BC-251 cyclone-based NIOSH bioaerosol samplers that fractionate airborne particles into >4 μm, 1–4 μm, and <1 μm size fractions (*11*). We applied quantitative real-time reverse transcription PCR to detect the matrix gene segment of AIV; we analyzed positive samples by the hemagglutinin gene to determine the AIV subtype (H5, H7, or H9) using specific primers and probes (*12*,*13*).

H5, H7, and H9 detection rates in environmental samples (median monthly difference 6.2% for H5,

Author affiliations: University of Hong Kong, Hong Kong, China (K.L. Cheng, A.Y.L. Wong, W. Su, M. Peiris, H.-L. Yen, E.H.Y. Lau); Guangdong Provincial Center for Disease Control and Prevention, Guangdong, China (J. Wu, W.L. Shen, Q. Guo, J. Yu, X. Zhuang, T. Song)

DOI: https://doi.org/10.3201/eid2603.190888

[1]These authors contributed equally to this article.

[2]These senior authors contributed equally to this article.

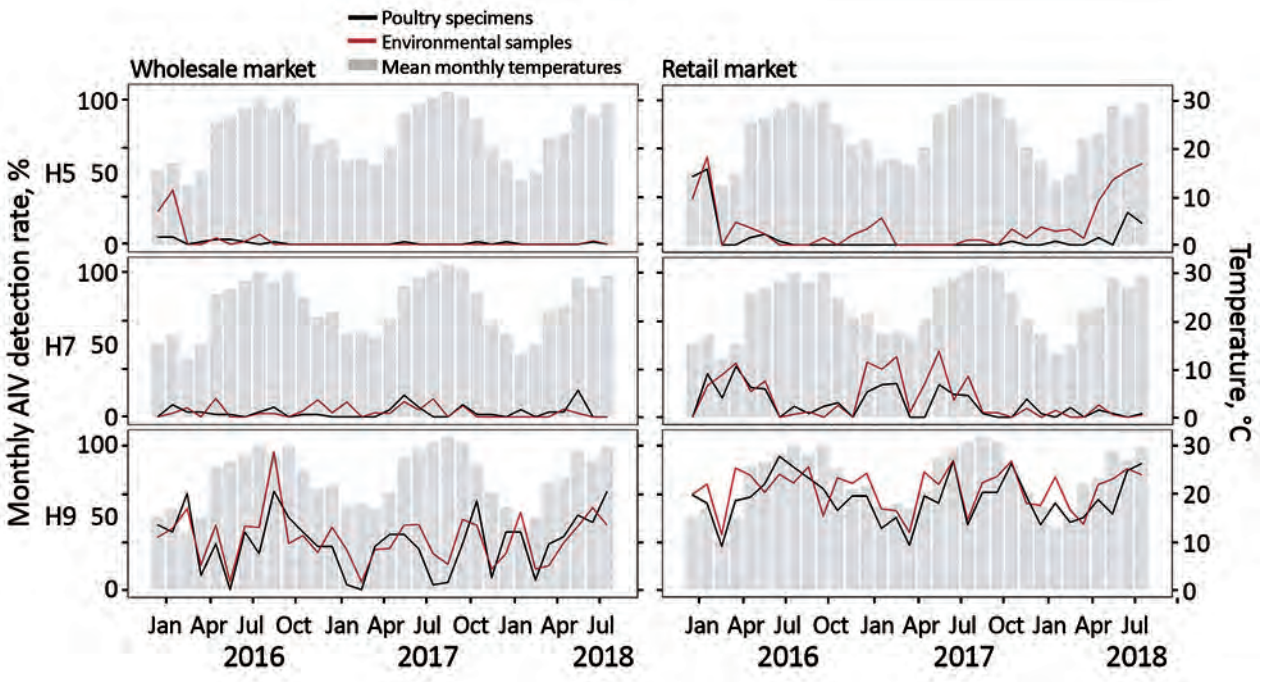

Figure 1. Monthly AIV H5, H7, and H9 positivity rates detected in poultry and environmental samples at live poultry markets (LPMs), Guangdong, China, December 2015–July 2018. Chicken (oropharyngeal and cloacal swab specimens) and environmental (swab specimens and air samples) samples were collected monthly from 1 retail and 1 wholesale LPM in Guangzhou and tested for H5, H7, and H9 AIV by real-time RT-PCR. Gray bars indicate mean temperatures recorded on the sampling date in Guangzhou. AIV, avian influenza virus.

3.1% for H7, and 34.1% for H9; all p<0.02 by Mann-Whitney test) were much higher at the retail LPM (rLPM) than that at the wLPM (Figure 1), probably because of poultry mixing, aggregation, and extended stay at retail settings. Human H5 or H7 zoonotic infections clustered in winter, but we observed no correlation (p>0.215 for both) between temperature (*14*) and H5 or H7 detection rates in chickens or environmental samples at both markets. We did not assess other confounding factors, including market interventions and poultry holding duration.

We evaluated correlations between monthly AIV detection rates in chickens and environmental samples (moderate correlation for r_s>0.5, at which point environmental samples are considered useful to monitor AIV in chickens). We observed a positive correlation for H5 (Spearman r_s = 0.569, p<0.001) and H9 viruses (r_s = 0.702, p<0.001) at the wLPM and for H5 (r_s = 0.581, p<0.001), H7 (r_s = 0.760, p<0.001), and H9 viruses (r_s = 0.685, p<0.001) at the rLPM. We examined the use of environmental samples to assess AIV activity in poultry (Table 1). Environmental

Table 1. Sensitivity and specificity of applying environmental samples to assess AIV activity in poultry, based on monthly AIV detection, Guangdong, China, December 2015–July 2018*

Market type	Subtype	Sensitivity, % (95% CI)†	Specificity, % (95% CI) †	Positive predictive value, % (95% CI)†	Negative predictive value, % (95% CI)†	Accuracy, % (95% CI)†
Wholesale	H5	45.5 (16.8–76.6)	95.2 (76.2–99.9)	83.3 (39.9–97.4)	76.9 (65.8–85.2)	78.1 (60.0–90.7)
	H7	68.4 (43.5–87.4)	69.2 (38.6–90.9)	76.5 (57.6–88.6)	60.0 (41.4–76.1)	68.8 (50.0–83.9)
	H9‡	100 (88.4–100)	0 (0–84.2)	93.8	NA	93.8 (79.2–99.2)
Retail	H5	90.0 (55.5–99.8)	45.5 (24.4–67.8)	42.9 (32.7–53.7)	90.9 (59.6–98.6)	59.4 (40.6–76.3)
	H7	87.0 (66.4–97.2)	66.7 (29.9–92.5)	87.0 (72.3–94.5)	66.7 (38.7–86.4)	81.3 (63.6–92.8)
	H9§	100 (89.1–100)	NA	100 (89.1–100)	NA	100 (89.1–100)

*Test results from reverse transcription PCR on bird samples were assumed to be the standard in the analysis. The results may not be applicable to other surveillance systems with more intensive sampling or accurate laboratory testing. AIV, avian influenza virus; NA, not applicable.
†Sensitivity: probability that the environmental samples will test positive when the subtype of AIV is present in chickens on site (true positive rate). Specificity: probability that the environmental samples will test negative when the subtype of AIV is not present (true negative rate). Positive predictive value: probability that the subtype of AIV is present in poultry when environmental samples are tested positive. Negative predictive value: probability that the subtype of AIV is not present in poultry when the environmental samples are tested negative. Accuracy: probability that the presence or absence of AIV in poultry will be correctly determined based on the test results of environmental samples.
‡H9 was detected during every month during the study period in the environmental samples (monthly data can be found in Appendix Table 1, https://wwwnc.cdc.gov/EID/article/26/3/19-0888-App1.pdf).
§H9 was detected during every month during the study period in both the poultry and the environmental samples (monthly data can be found in Appendix Table 2).

samples collected at the rLPM provided higher sensitivity in detecting H5, H7, or H9 viruses in poultry than those from the wLPM. Environmental samples were less likely to detect H5 and H7 viruses in poultry at the wLPM than at the rLPM (Appendix Tables 1, 2), possibly because of the low prevalence of infection in birds, a higher poultry turnover rate, and comparatively thorough daily cleaning practices at the wLPM. The lower specificity for H5 at the rLPM may be the result of carryover contamination at the poultry slaughtering area caused by processing birds of other species. The probabilities of accurately detecting the presence or absence of H5, H7, and H9 subtypes in poultry from environmental samples were comparable for the wLPM (68.8%–93.8%) and the rLPM (59.4%–100%) (Table 1). This finding suggests that environmental samples provided a useful indication of AIV activity in chickens at LPMs. Nevertheless, for H5 and H7 viruses at the wLPM, in only 1 month did all environment samples test positive when bird samples were also positive, demonstrating the need to take a wide range of environment samples.

We investigated correlations between specific environmental samples and monthly H5, H7, and H9 detection rates in chickens (Figure 2; Appendix Figure 2). At the wLPM, positive rates for H5 (r_s = 0.515, p = 0.003), H7 (r_s = 0.514, p = 0.003), and H9 (r_s = 0.508,

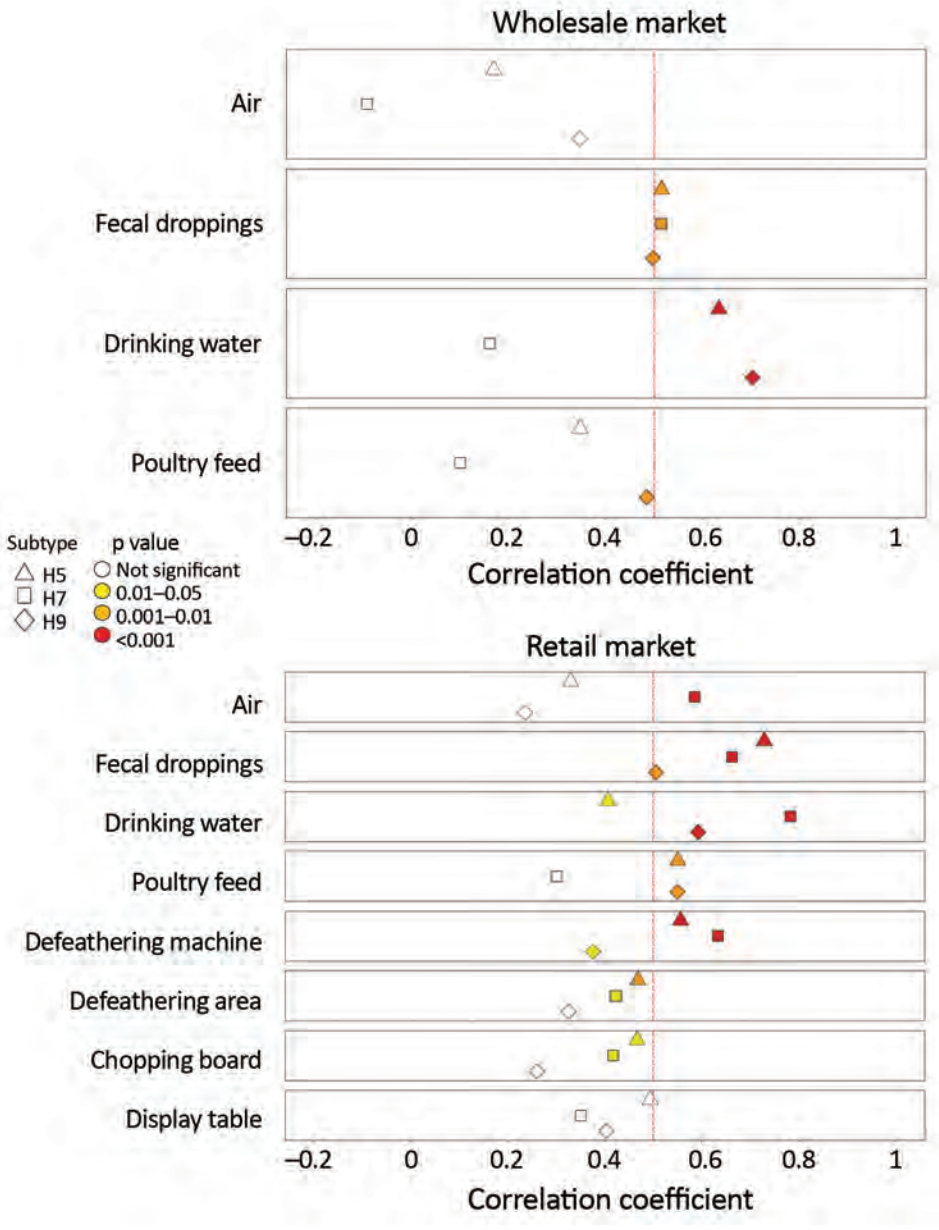

Figure 2. Correlation between AIV detection rates in poultry and environmental samples at live poultry markets (LPMs), Guangdong, China, December 2015–July 2018. Monthly AIV, H5, H7, and H9 detection rates in chicken and environmental samples were analyzed using Spearman's rank correlation. The vertical red dashed line indicates correlation coefficient (r_s) at 0.5. Subtypes and significance levels are indicated. AIV, avian influenza virus.

Table 2. AIV detection rates from chicken and environmental samples collected at a retail LPM, Guangdong, China, December 2015–July 2018*

Type of samples	No. samples	Median monthly positive rate, % (95% CI)		
		H5	H7	H9
Poultry samples†	1,239	0.0 (0.0–2.5)	5.8 (0.0–15.0)	64.6 (55.0–67.5)
Oropharyngeal	1,239	0.0 (0.0–2.5)	5.8 (0.0–13.3)	60.0 (52.5–67.5)
Cloacal	1,239	0.0 (0.0–2.5)	0.0 (0.0–2.5)	20.0 (13.2–26.5)
Environmental samples	1,734	6.2 (0.0–11.8)	4.2 (1.6–22.0)	73.8 (60.0–79.4)
Poultry holding zone‡	965	2.9 (0.0–6.3)	3.0 (0–20.0)	68.2 (56.0–75.9)
Fecal droppings	424	0.0 (0.0–7.7)	0.0 (0.0–11.1)	58.3 (50.0–66.7)
Drinking water	364	0.0 (0.0–8.3)	3.3 (0.0–15.4)	83.3 (66.7–100.0)
Poultry feed	177	0.0 (0.0–11.1)	0.0 (0.0–9.1)	50.0 (33.3–70.0)
Poultry slaughtering zone	457	2.2 (0.0–25.0)	6.1 (0.0–22.2)	78.6 (59.5–87.5)
Defeathering machine	250	0.0 (0.0–20.0)	0.0 (0.0–20.0)	86.2 (70.0–100.0)
Defeathering area	207	0.0 (0.0–25.0)	0.0 (0.0–12.5)	73.2 (50.0–87.5)
Poultry selling zone	194	27.9 (0.0–50.0)	0.0 (0.0–14.3)	91.2 (60.0–100.0)
Chopping board	141	33.0 (0.0–50.0)	0.0 (0.0–25.0)	100.0 (71.4–100.0)
Display table	53	0.0 (0.0–66.7)	0.0 (0.0–14.3)	92.9 (25.0–100.0)
Air§	118	0.0 (0.0–25.0)	0.0 (0.0–16.7)	75.0 (50.0–100.0)

*AIV, avian influenza virus; LPM, live poultry market; qRT-PCR, quantitative reverse transcription PCR.
†A positive poultry sample may detect AIV in the oropharyngeal samples, cloacal samples, or both by qRT-PCR.
‡Environmental swab specimens were collected within the same poultry stall at LPMs but may not be from the same cage where the chickens were sampled. Fecal droppings were collected from the ground or cages, drinking water was collected from the water troughs, and poultry feed was sampled from the surface of the bowls or feeders.
§A positive air sample may be positive for AIV by qRT-PCR in any of the 3 size fractions collected by a NIOSH sampler (*11*). Two to 6 NIOSH samplers were applied monthly to sample air at the retail markets.

p = 0.003) in fecal droppings correlated moderately well with viral prevalence in chickens, whereas drinking water provided the best correlation for H5 (r_s = 0.633, p<0.001) and H9 (r_s = 0.702, p<0.001) (Figure 2) and was more sensitive for H9 (Appendix Figure 3). At the rLPM, H9 detection rates in drinking water (r_s = 0.593, p<0.001), poultry feed (r_s = 0.550, p = 0.002), and fecal droppings (r_s = 0.506, p = 0.003) best correlated with H9 prevalence in chickens; drinking water was most sensitive (Appendix Figure 3). H7 detection rates in drinking water (r_s = 0.784, p<0.001), fecal droppings (r_s = 0.663, p<0.001), defeathering machines (r_s = 0.634, p<0.001), and air (r_s = 0.585, p<0.001) best correlated with H7 prevalence in chickens. The H5 detection rates in fecal droppings (r_s = 0.729, p<0.001), defeathering machines (r_s = 0.556, p<0.001), and poultry feed (r_s = 0.550, p = 0.02) best correlated with H5 prevalence in chickens. Collectively, these results suggest that fecal droppings may provide a good estimation for H5, H7, and H9 prevalence in chickens at LPMs and that drinking water can be more sensitive in some settings and useful for determining virus contamination in LPMs. For viruses present at low prevalence (e.g., H5), low sensitivity is expected.

We summarized H5, H7, and H9 detection rates in various environmental samples at the rLPM (Table 2). H5 virus was most frequently detected from poultry selling zones (median monthly positive rate 27.9%, 95% CI 0%–50%), especially from chopping boards (33%, 95% CI 0%–50%), whereas H7 virus was most frequently detected from poultry slaughtering zones (6.1%, 95% CI 0%–22.2%), especially from defeathering machines. H9 virus was frequently detected from all sampling sites. However, we found no clear difference in environmental sites for detecting H5, H7, or H9 (Appendix Tables 1,2).

Conclusions

AIV detection rates in environmental samples correlated moderately with AIV activity in chickens at LPMs. Environmental sampling at rLPMs provides greater sensitivity in detecting H5, H7, and H9 AIV in poultry than that at the wLPMs and should be included as routine surveillance to monitor AIV activity. At the rLPM, H5 and H7 viruses were most frequently detected from poultry selling and poultry slaughtering areas, whereas the highly prevalent H9 viruses were detected frequently at poultry holding, slaughtering, and selling areas. Environmental samples with the highest detection rate for H5, H7, and H9 viruses may not provide the best indication of virus activity in poultry, however. Some market stalls containing viruses with low prevalence would be misclassified if only environmental or bird samples were collected. To detect viruses expected to be present at low prevalence, environmental samples should be collected from multiple sites in each market stall, including samples from holding, processing, and selling areas.

This study was supported by contract HHSN272201400006C from the United States Department of Health and Human Services and the Theme-based Research Scheme (project no. T11-705/14N) from the Research Grants Council, Hong Kong SAR, China.

About the Author

Ms. Cheng is a postgraduate student at the University of Hong Kong. Her primary research interest is avian influenza epidemiology at live poultry markets. Dr. Wu is the chief technician for respiratory pathogens at Guangdong Provincial Center for Disease Control and Prevention, Guangdong, China. Her research interest is in monitoring human infection risk by avian influenza viruses at the human–poultry interface.

References

1. Peiris JS, Cowling BJ, Wu JT, Feng L, Guan Y, Yu H, et al. Interventions to reduce zoonotic and pandemic risks from avian influenza in Asia. Lancet Infect Dis. 2016;16:252–8. https://doi.org/10.1016/S1473-3099(15)00502-2
2. Cowling BJ, Jin L, Lau EHY, Liao Q, Wu P, Jiang H, et al. Comparative epidemiology of human infections with avian influenza A H7N9 and H5N1 viruses in China: a population-based study of laboratory-confirmed cases. Lancet. 2013;382:129–37. https://doi.org/10.1016/S0140-6736(13)61171-X
3. Jiang H, Wu P, Uyeki TM, He J, Deng Z, Xu W, et al. Preliminary epidemiologic assessment of human infections with highly pathogenic avian influenza A(H5N6) virus, China. Clin Infect Dis. 2017;65:383–8. https://doi.org/10.1093/cid/cix334
4. Wu J, Ke C, Lau EHY, Song Y, Cheng KL, Zou L, et al. Influenza H5/H7 virus vaccination in poultry and reduction of zoonotic infections, Guangdong Province, China, 2017–18. Emerg Infect Dis. 2019;25:116–8. https://doi.org/10.3201/eid2501.181259
5. Leung YHC, Zhang LJ, Chow CK, Tsang CL, Ng CF, Wong CK, et al. Poultry drinking water used for avian influenza surveillance. Emerg Infect Dis. 2007;13:1380–2. https://doi.org/10.3201/eid1309.070517
6. Wang X, Wang Q, Cheng W, Yu Z, Ling F, Mao H, et al. Risk factors for avian influenza virus contamination of live poultry markets in Zhejiang, China during the 2015–2016 human influenza season. Sci Rep. 2017;7:42722. https://doi.org/10.1038/srep42722
7. Yuan J, Lau EH, Li K, Leung YH, Yang Z, Xie C, et al. Effect of live poultry market closure on avian influenza A(H7N9) virus activity in Guangzhou, China, 2014. Emerg Infect Dis. 2015;21:1784–93. https://doi.org/10.3201/eid2110.150623
8. Kang M, He J, Song T, Rutherford S, Wu J, Lin J, et al. Environmental sampling for avian influenza A(H7N9) in live-poultry markets in Guangdong, China. PLoS One. 2015;10:e0126335. https://doi.org/10.1371/journal.pone.0126335
9. Fang S, Bai T, Yang L, Wang X, Peng B, Liu H, et al. Sustained live poultry market surveillance contributes to early warnings for human infection with avian influenza viruses. Emerg Microbes Infect. 2016;5:1–8. https://doi.org/10.1038/emi.2016.75
10. Kim Y, Biswas PK, Giasuddin M, Hasan M, Mahmud R, Chang YM, et al. Prevalence of avian influenza A(H5) and A(H9) viruses in live bird markets, Bangladesh. Emerg Infect Dis. 2018;24:2309–16. https://doi.org/10.3201/eid2412.180879
11. Lindsley WG, Green BJ, Blachere FM, Martin SB, Law BF, Jensen PA, et al. Sampling and characterization of bioaerosols. In: NIOSH manual of analytical methods, 5th edition. Cincinnati: National Institute for Occupational Safety and Health, Centers for Disease Control and Prevention; 2017.
12. Chinese Center for Diseases Control and Prevention. Avian influenza surveillance programme [cited 2019 June 17]. http://www.chinaivdc.cn/cnic/zyzx/jcfa/201605/W020160520546618208788.pdf
13. World Health Organization. WHO information for the molecular detection of influenza viruses; 2017 [cited 2019 June 8]. https://www.who.int/influenza/gisrs_laboratory/WHO_information_for_the_molecular_detection_of_influenza_viruses_20171023_Final.pdf
14. National Oceanic and Atmosphere Administration. Station data inventory, access and history [cited 2019 June 8]. https://www.ncdc.noaa.gov/cdo-web/datasets/GHCND/stations/GHCND:CHM00059287/detail

Address for correspondence: Hui-Ling Yen or Eric Ho-Yin Lau, The University of Hong Kong School of Public Health, Li Ka Shing Faculty of Medicine, 21 Sassoon Road, Hong Kong SAR, China; email: hyen@hku.hk or ehylau@hku.hk

Diphtheria Outbreaks in Schools in Central Highland Districts, Vietnam, 2015–2018

Noriko Kitamura, Thao T.T. Le, Lien T. Le, Luong D. Nguyen, Anh T. Dao, Thanh T. Hoang, Keisuke Yoshihara, Makiko Iijima, Tran M. The, Hung M. Do, Huy X. Le, Hung T. Do, Anh D. Dang, Mai Q. Vien, Lay-Myint Yoshida

During 2015–2018, seven schools in rural Vietnam experienced diphtheria outbreaks. Multilocus sequence types were the same within schools but differed between schools. Low vaccine coverage and crowded dormitories might have contributed to the outbreaks. Authorities should consider administering routine vaccinations and booster doses for students entering the school system.

Diphtheria is a serious childhood disease with a high mortality rate (*1*). After a diphtheria–tetanus–pertussis vaccine (DTP) was introduced in the early 20th century, the number of cases dramatically decreased. Incidence reached a low of 4,333 cases in 2006, but more recently, the number of reported cases has increased, with incidence reaching 16,648 cases in 2018 (*2*).

In 1981, Vietnam introduced a vaccination program in which participants received 3 primary doses of DTP (DTP3) vaccine; in 2011, a booster shot (DTP4) to be given 18 months after the initial doses was added (*3*). Although diphtheria cases had become sporadic by 2010, beginning in 2013, outbreaks occurred in the western and central highland areas of Vietnam, which prompted our study (*4*).

The Study

During June 2015–April 2018, the Pasteur Institute in Nha Trang, Vietnam, and the provincial health authority investigated 46 cases involving patients with suspected diphtheria, 8 of whom died, and 49 asymptomatic contacts in the provinces of Quang Nam and Quang Ngai in the central highlands region of Vietnam (Figure 1). We used standard case investigation forms to collect demographic and clinical information. We collected throat swab specimens from 93 patients and contacts but were unable to collect samples from 2 patients who had died. No cutaneous diphtheria was reported.

We used sheep blood agar and tellurite medium cultures to identify *Corynebacterium diphtheriae* and extracted DNA with a QIAGEN DNA Mini Kit (QIAGEN, https://www.qiagen.com), following a standard protocol. We used 2 sets of primers, Tox1/Tox2 and Dipht6F/Dipht6R, for PCR testing (*5*). The Elek test for diphtheria is not available in Vietnam.

Laboratory testing confirmed diphtheria in 22 of 46 suspected cases: 17 patients, including 4 who died, tested positive in both culture and PCR tests, whereas 5 patients, including 1 who died, tested positive only by PCR. We categorized diagnosis as epidemiologic for 10 patients for whom PCR results were not available, 7 suspected cases and 3 in which the person died. We confirmed 2 of 49 asymptomatic contacts as carriers of diphtheria (*6*).

We used Api Coryne (bioMérieux, https://www.biomerieux.com) to identify biotypes of *C. diphtheriae* isolates; 15 of 17 culture-positive isolates were biotype *mitis* and 1 each was *gravis* and *intermedius*. We conducted multilocus sequence typing (MLST) by using 7 primer sets for *C. diphtheriae* housekeeping genes according to reported protocol (*7*). Using the *C. diphtheriae* MLST database (https://pubmlst.org/cdiphtheriae), we detected 4 sequence types (STs): ST67 (n = 7), ST209 (n = 9), ST243 (n = 7), and ST244 (n = 1).

Among the 31 patients with confirmed or suspected diphtheria, 21 (60%) were male; age range was 1–45 years (median 10 years). We summarized case

Author affiliations: Nagasaki University, Nagasaki, Japan (N. Kitamura, K. Yoshihara, L.-M. Yoshida); Pasteur Institute in Nha Trang, Nha Trang, Vietnam (T.T.T. Le, L.T. Le, L.D. Nguyen, A.T. Dao, T.T. Hoang, T.M. The, H.M. Do, H.X. Le, H.T. Do, M.Q. Vien); World Health Organization Representative Office for Vietnam, EPI, Hanoi, Vietnam (M. Iijima); National Institute of Hygiene and Epidemiology, Hanoi (A.D. Dang)

DOI: https://doi.org/10.3201/eid2603.191027

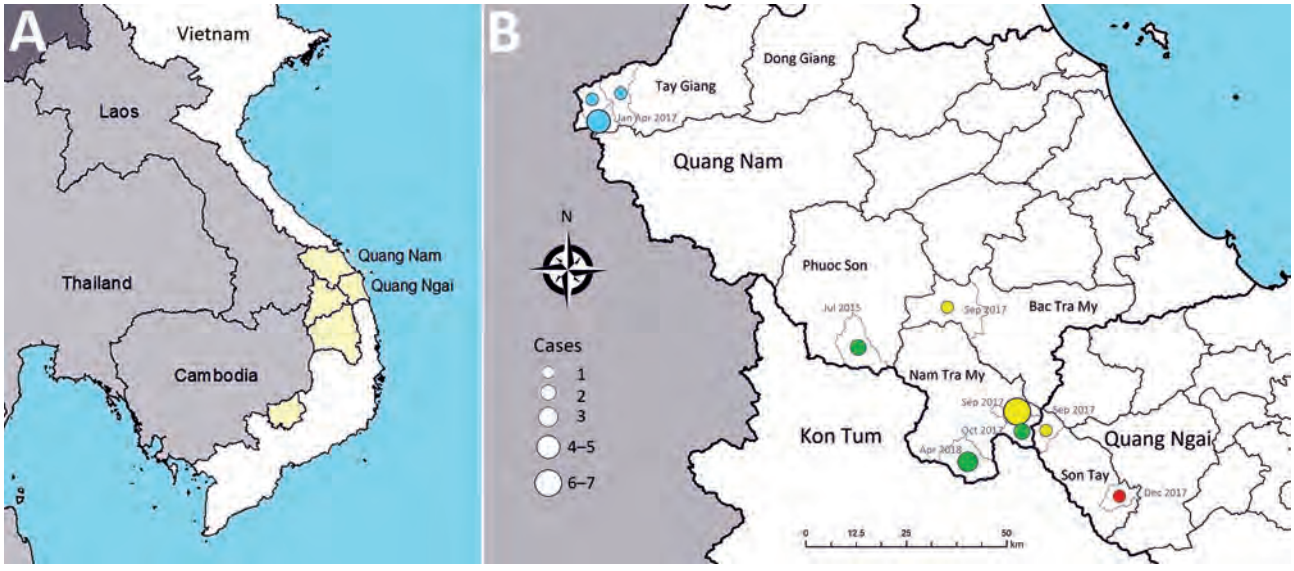

Figure 1. A) Provinces where diphtheria cases were identified in Vietnam in 2010s. Diphtheria cases were reported from provinces (shaded) neighboring Laos or Cambodia. B) Laboratory-confirmed diphtheria cases in the central highlands region of Quang Nam Province and Quang Ngai Province, central Vietnam, 2015–2018. Colored circles indicate separate outbreaks. Source: https://gadm.org/download_country_v3.html

characteristics (Table 1) and epidemiologic links and STs by cluster (Table 2). The most common symptoms recorded were fever (82%), followed by pseudomembrane and difficulty swallowing (76%).

We determined geographic areas in which cases were identified (Figure 1). Most residents in the central highlands area were in ethnic minority groups. Healthcare access is limited because of mountainous terrain and social barriers. In this area, each commune has a primary and a secondary school, but 10 communes share 1 district-level high school. All students, from primary through high school, live in dormitories during the week, and 30–50 students might live in a ≈50 m^2 room.

Table 1. Characteristics of confirmed and epidemiologically linked cases of diphtheria, central highlands of Vietnam, 2015–2018*

Characteristic	Confirmed	Epidemiologically linked	Epidemiologically linked asymptomatic carriers	Total
Age, y				
<1	0 (0)	0 (0)	0 (0)	0 (0)
1–4	2 (9)	1 (10)	1 (50)	4 (12)
5–9	7 (32)	2(20)	1 (50)	10 (29)
10–14	9 (41)	0 (0)	0 (0)	9 (26)
15–19	3 (14)	4(40)	0 (0)	7 (21)
≥20	1 (5)	3(30)	0 (0)	4 (12)
Sex				
M	14 (64)	6 (55)	1 (50)	21 (60)
F	9 (36)	4 (45)	1 (50)	14 (40)
Vaccination history, no. doses				
0	9 (41)	9 (90)	0 (0)	18 (51)
1	0 (0)	0 (0)	1 (50)	1 (3)
2	1 (5)	0 (0)	0 (0)	1 (3)
≥3	3 (14)	0 (0)	1 (50)	4 (11)
Unknown	9 (41)	1 (10)	0 (0)	11 (31)
Symptoms				
Fever	18 (81)	10 (100)	NA	28 (82)
Sore throat	15 (68)	10 (100)	NA	25 (74)
Pseudomembrane	17 (77)	9 (90)	NA	26 (76)
Difficulty swallowing	14 (64)	10 (100)	NA	26 (76)
Submandibular LN swelling	14 (64)	6 (60)	NA	20 (59)
Death	5 (23)	3 (30)	NA	8 (24)
Total no./no. persons investigated (%)	22/46 (48)	10/46 (22)	2/49 (4)	34/95 (36)

*Values are no. (%) except as indicated; total no. indicated number of patients with confirmed or suspected diphtheria or with diphtheria carrier status. LN, lymphadenopathic.

Table 2. Epidemiologic link and MLST results for 34 confirmed or epidemiologically linked case-patients with diphtheria, central highlands of Vietnam, 2015–2018*

District	Date of symptom onset	Patient age, y/sex	Epidemiologic link	Vaccine status†	Died	Culture result	PCR	ST	Biotype	Case
Phuoc Son	2015 Jun 30	26/F	Patient 1	UNK	X	‡	‡			Linked
	2015 Jun 30	18/M		UNK		–	§			Linked
	2015 Jul 4	17/F		UNK	X	–	§			Linked
	2015 Jul 4	27/M	Patient 1's husband	UNK		+	+§	67	*mitis*	Confirmed
	2015 Jul 4	16/M		UNK		–	§			Linked
	2015 Jul 5	7/M	Patient 1's son	UNK		–	§			Linked
	2015 Jul 5	20/M		UNK		–	§			Linked
	2015 Jul 8	45/M		UNK		–	§			Linked
	2015 Jul 9	1/F		UNK		–	§			Linked
	2015 Jul 14	14/M		UNK		+	+§	67	*mitis*	Confirmed
	2015 Jul 14	9/F		UNK		–	§			Linked
Tay Giang	2017 Jan 10	16/M	Tay Giang HS	UNK	X	‡	‡			Linked
	2017 Jan 10	17/M		UNK	X	+	+	243	*mitis*	Confirmed
Son Tay	2017 Mar 15	13/M		3	X	+	+	209	*mitis*	Confirmed
Tay Giang	2017 Apr 20	7/M		4	X	+	+	243	*mitis*	Confirmed
	2017 Apr 22	15/F		UNK		+	+	243	*mitis*	Confirmed
	2017 Apr 25	7/M	Gari PS	UNK		+	+	243	*mitis*	Confirmed
	2017 May 20	10/M	Patient 2 (Gari SS)	UNK		+	+	243	*mitis*	Confirmed
	2017 May 20	10/M	Gari SS	3		+	+	243	*mitis*	Confirmed
	2017 May 23	15/M	Patient 2's brother's friend	0		+	+	243	*mitis*	Confirmed
Bac Tra My	2017 Sep 5	5/F		UNK		–	+	209		Confirmed
Nam Tra My	2017 Sep 27	12/M	Tra Van SS	UNK		+	+	209	*mitis*	Confirmed
	2017 Sep 27	8/M	Tra Van PS	0	X	+	+	209	*mitis*	Confirmed
	2017 Sep 30	9/F		0		–	+	209		Confirmed
	2017 Sep 30	10/F		0		–	+	209		Confirmed
	2017 Sep 30	8/F		0		–	+	209		Confirmed
	2017 Oct 3	11/F		0		+	+	209	*mitis*	Confirmed
	2017 Oct 3	10/M		0		+	+	209	*mitis*	Confirmed
Nam Tra My	2017 Oct 8	12/F	Tra Vinh SS	UNK		–	+	67		Confirmed
	2017 Oct 12	13/M		UNK		+	+	67	*mitis*	Confirmed
Son Tay	2017 Dec 24	3/F		UNK		+	+	244	*gravis*	Confirmed
Nam Tra My	2018 Apr 17	4/M	Man Di NS	2	X	–	+	67	*intermed*	Confirmed
	2018 Apr 24	4/M		3 + 1 SIA		+	+	67		Linked
	2018 Apr 24	5/F		1 + 1 SIA		–	+	67		Linked

*Biotypes are of *Corynebacterium diphtheriae* bacteria. HS, high school; MLST, multilocus sequence typing; NS, nursery school; PS, primary school; SIA, supplemental immunization activity; SS, secondary school; ST, sequence type; UNK, unknown; –, negative; +, positive.
†The time of last vaccination was infancy or at 1 y of age according to the vaccination program in Vietnam. SIA dose was given October 30, 2017, for the last 2 case-patients.
‡Culture and PCR were not performed for these persons because their samples were not collected.
§PCR was not conducted for these 10 case-patients because this technique was not available during 2015. Stored isolates from 2 culture-positive case-patients were tested by PCR in 2017.

After January 2017, in each commune, diphtheria clusters formed mainly by school; cases in each school-based cluster shared the same ST. School clusters of the same ST in 2 communes in Tay Giang District were linked by a student who commuted between the communes. We could not identify any other epidemiologic links between clusters. An epidemic curve (Figure 2) showed the ST and outcome of cases by their onset. A long gap between clusters might indicate that the disease was transmitted through asymptomatic or skin carriers. However, further genomic testing is necessary to clarify the transmission pathway.

Of 8 persons who died, 3 were vaccinated, 1 each with 2, 3, and 4 doses. However, the vaccination history of 85% of patients was unknown. To compensate for the lack of vaccination history, we obtained administrative details of vaccination coverage in Nam Tra My District during 2013–2016. Of the 10 communes, only 3 (Tra Van, Tra Vinh, and Tra Nam) reported cases. We compared the ratios of vaccinated and unvaccinated children and found a significantly smaller proportion of children had received DTP3 in the outbreak communes than in nonoutbreak communes (57% [95% CI 53.3%–61.2%] vs. 77% [95% CI 87.0%–90.1%]; $p<0.05$ by χ^2 test).

Conclusions

Our investigation detected 22 patients with laboratory-confirmed *C. diphtheriae* cases during 2015–2018 in this region of Vietnam, 83% of whom were >5

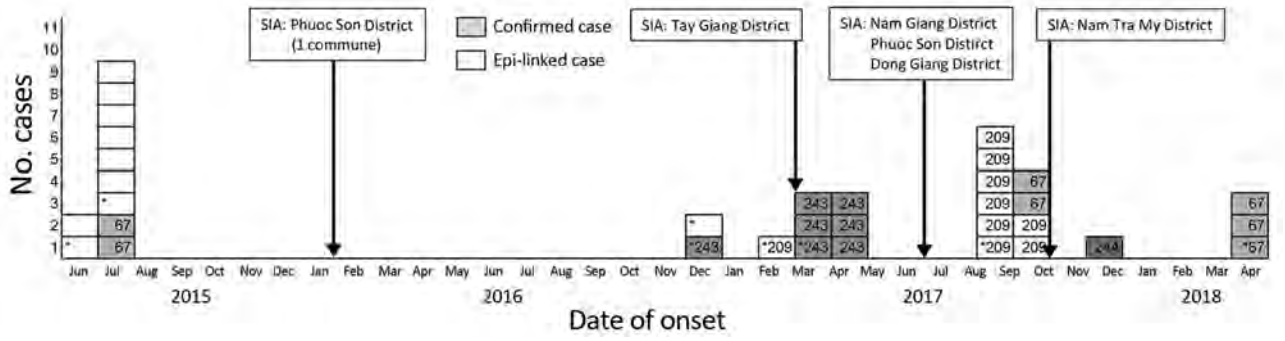

Figure 2. Confirmed and probable cases of diphtheria identified during June 2015–April 2018 in Vietnam. Numbers indicate multilocus sequencing type of confirmed cases with sequence types (STs) ST67, ST 243, ST209, and ST244 (gray shading). White indicates epidemiologically linked cases, and asterisks indicate cases in which the patient died. Epi, epidemiologically; SIA, supplemental immunization activity.

years of age. It has been predicted that age of diphtheria case-patients could increase after introduction of DTP because a high proportion of older persons will be susceptible to the disease due to reduced circulation of bacteria, especially when no booster dose is provided (*8*). The 4 MLST types identified in this study (ST67, ST209, ST243, and ST244) were also identified in Thailand, Cambodia, the Philippines, and Binh Phuoc Province in Vietnam in the 2010s (*4*,*9*,*10*). We found only 1 ST in each cluster location, which might indicate 1 person as the source of infection in each location. In addition, we identified no clear epidemiologic link among clusters. Detecting different STs between clusters indicates that multiple strains of *C. diphtheriae* were circulating in Vietnam, as well as in neighboring countries. This transmission pattern might not have changed since the prevaccination era when diphtheria was reported to spread from school to school or neighborhood to neighborhood (*11*).

The reemergence of diphtheria in Vietnam raises several concerns. Administrative coverage, although not always accurate, indicated DTP3 coverage of 57%, possibly creating a larger pool of susceptible people. In 2013, the health service temporarily suspended DTP immunization during a severe adverse event case investigation, which halved DTP3 coverage in the country (*2*) and potentially led to outbreaks. Students also share crowded school dormitories, which is a major factor for spreading disease. Moreover, students go home on weekends, increasing the chance of transmission between their schools and homes. Our finding of vaccinated people dying is particularly alarming because it might indicate a waning of vaccine-derived immunity.

Several interventions were conducted to control outbreaks. Erythromycin tablets were distributed to all contacts of diphtheria patients. However, only 2 asymptomatic carriers were identified among 49 contacts, lower than expected considering that 97% of case-patients could be asymptomatic in a vaccinated population (*12*). However, the sensitivity of laboratory testing might have been low because of the length of time required to collect and transport samples or because of prior antimicrobial drug use, so some carriers likely were not identified.

Supplemental immunization activities were conducted in the outbreak area and 2 neighboring districts (Nam Giang and Dong Giang). Healthcare agencies initiated 2 campaigns: the first, targeting persons 5–40 years of age, sought to administer 3 doses of tetanus–diphtheria vaccine and achieved >90% coverage. Simultaneously, a second campaign was conducted to administer DPT to previously unvaccinated children 1–4 years of age. However, 1 unvaccinated person with diphtheria and 2 asymptomatic carriers who had received 1 dose of DPT were reported 6 months after the supplemental immunization activity. This finding was probably because diphtheria toxoid vaccine does not prevent transmission but prevents respiratory disease (*13*); thus, carriage of the organism persists.

Although Vietnam has maintained high DTP3 coverage nationally, efforts should be intensified to increase coverage in specific areas of the country (*14*). Persistent immunity resulting from DTP3 alone is not apparent (*14*), and immunity might wane before children start school (*15*). The World Health Organization recommends that students receive a booster vaccination when entering school (*15*). However, even if this recommendation is adopted, maintaining high uptake of primary and booster doses remains critical.

Acknowledgments

We thank staff who were designated to the infectious disease surveillance program in central Vietnam for collecting and summarizing information, and healthcare workers at the Pasteur Institute in Nha Trang and Quang Nam Provincial Health Services for conducting multiple investigations.

This study was partly supported by Japan Agency for Medical Research and Development (grant no. JP19fm0108001: Japan Initiative for Global Research Network on Infectious Diseases) for research activities of Nagasaki University in Vietnam and the Joint Usage/Research Center on Tropical Disease, Institute of Tropical Medicine, Nagasaki University.

About the Author

Dr. Kitamura is an assistant professor in the Department of Pediatric Infectious Diseases, Institute of Tropical Medicine, Nagasaki University, Nagasaki, Japan, who has been stationed at the Pasteur Institute in Nha Trang, Vietnam, since 2016. Her primary research interest is epidemiology and control of infectious diseases, especially vaccine-preventable diseases.

References

1. Hardy IR, Sutter RW, Dittmann S. Current situation and control strategies for resurgence of diphtheria in newly independent states of the former Soviet Union. Lancet. 1996;347:1739–44. https://doi.org/10.1016/S0140-6736(96)90811-9
2. Immunization, vaccines and biologicals: data, statistics and graphics. Geneva: World Health Organization; 2019 [cited 2020 Jan 18]. http://www.who.int/immunization/monitoring_surveillance/data
3. Ministry of Health Expanded Program of Immunization. 25 years of expanded program of immunization in Vietnam. Hanoi (Vietnam): The Ministry; 2012.
4. Vo TT, Phan VT, Pham TH, Ho NL, Pham DQ, Nguyen VT, et al. Surveillance of *Corynebacterium diphtheriae*-caused diphtheria in Binh Phuoc province, June 2016 [in Vietnamese]. Vietnam Journal of Preventive Medicine. 2017;2017:11.
5. Nakao H, Popovic T. Development of a direct PCR assay for detection of the diphtheria toxin gene. J Clin Microbiol. 1997;35:1651–5. https://doi.org/10.1128/JCM.35.7.1651-1655.1997
6. Immunization, vaccines and biologicals: vaccine preventable disease surveillance standard. Geneva: World Health Organization; 2018 [cited 2020 Jan 19]. https://www.who.int/immunization/monitoring_surveillance/burden/vpd/standards
7. Bolt F, Cassiday P, Tondella ML, Dezoysa A, Efstratiou A, Sing A, et al. Multilocus sequence typing identifies evidence for recombination and two distinct lineages of *Corynebacterium diphtheriae.* J Clin Microbiol. 2010;48:4177–85. https://doi.org/10.1128/JCM.00274-10
8. Clarke KE, MacNeil A, Hadler S, Scott C, Tiwari TS, Cherian T. Global epidemiology of diphtheria, 2000–2017. Emerg Infect Dis. 2019;25:1834–42. https://doi.org/10.3201/eid2510.190271
9. Pailin P, Sittisak S, Pimrat K, Junti K, Jivapaisarnpong T, Paveenkittiporn W, et al. Epidemiological and serological study of re-emerging diphtheria in Dansai District, Loei Province, Thailand, June to October 2012. Surveillance and Investigation Reports. 2015;8:13–21.
10. Doyle CJ, Mazins A, Graham RMA, Fang NX, Smith HV, Jennison AV. Sequence analysis of toxin gene–bearing *Corynebacterium diphtheriae* strains, Australia. Emerg Infect Dis. 2017;23:105–7. https://doi.org/10.3201/eid2301.160584
11. Doull JA, Lara H. The epidemiological importance of diphtheria carriers. Am J Epidemiol. 1925;5:508–29. https://doi.org/10.1093/oxfordjournals.aje.a119677
12. Miller LW, Older JJ, Drake J, Zimmerman S. Diphtheria immunization. Effect upon carriers and the control of outbreaks. Am J Dis Child. 1972;123:197–9. https://doi.org/10.1001/archpedi.1972.02110090067004
13. Plotkin S, Orenstein W, Offit P, Edwards KM, editors. Vaccines, 7th ed. Philadelphia: Elsevier; 2018.
14. Immunization, vaccines and biologicals: the immunological basis for immunization series module 2: diphtheria. Geneva: World Health Organization; 2009 [cited 2020 Jan 24]. https://www.who.int/immunization/documents/ISBN9789241597869
15. World Health Organization. Diphtheria vaccine: WHO position paper, August 2017—recommendations. Vaccine. 2018; 36:199–201. https://doi.org/10.1016/j.vaccine.2017.08.024

Address for correspondence: Lay-Myint Yoshida, Nagasaki University, Institute of Tropical Medicine, Department of Pediatric Infectious Diseases, 1-12-4 Sakamoto, Nagasaki-City, Nagasaki 852-8523, Japan; email: lmyoshi@nagasaki-u.ac.jp

Progressive Vaccinia Acquired through Zoonotic Transmission in a Patient with HIV/AIDS, Colombia

Katherine Laiton-Donato,[1] Paola Ávila-Robayo,[1] Andrés Páez-Martinez, Paula Benjumea-Nieto, José A. Usme-Ciro, Nicole Pinzón-Nariño, Ivan Giraldo, Diego Torres-Castellanos, Yoshinori Nakazawa, Nishi Patel, Kimberly Wilkins, Yu Li, Whitni Davidson, Jillybeth Burgado, Panayampalli Subbian Satheshkumar, Ashley Styczynski, Matthew R. Mauldin, Martha Gracia-Romero, Brett W. Petersen

In March 2015, a patient in Colombia with HIV/AIDS was hospitalized for disseminated ulcers after milking cows that had vesicular lesions on their udders. Vaccinia virus was detected, and the case met criteria for progressive vaccinia acquired by zoonotic transmission. Adherence to an optimized antiretroviral regimen resulted in recovery.

Vaccinia virus (VACV) belongs to the genus *Orthopoxvirus* (OPXV) and was the main component of vaccines used during the 1960s and 1970s against smallpox (*1*). More recently, VACV has caused several zoonotic outbreaks in South America (*2*,*3*), where human cases are mainly associated with occupational exposure of farmworkers to infected cows. Progressive vaccinia is a severe and often lethal condition caused by infection and uncontrolled replication of VACV in immunocompromised patients (*4*,*5*).

The Study

In November 2014, a 30-year-old man with HIV/AIDS living and working at a rural dairy cattle farm in the department of Cundinamarca, Colombia, with no prior hospitalizations for opportunistic infections sought treatment for a suppurative ulcer with initial sharply raised defined edges on his right hand (Figure 1, panel A), right ear, and distal left leg that appeared 1 week after he had milked cows with similar lesions on their udders. He had recently interrupted antiretroviral therapy after onset of depression because of his father's death 4 months before. Despite treatment with self-formulated antimicrobial drugs and home therapies (application of alcohol, methylene blue, and herbs), the lesions continued and spread within 1 month to his nostrils, glans penis, right leg, right knee, and ankles. On November 14, 2014, the patient was treated with antimicrobial drugs at a local hospital and instructed to comply with his antiretroviral therapy. On December 9, 2014, after failing to respond to treatment, the patient was referred to the Hospital Universitario Mayor Méderi in Bogotá, Colombia. Laboratory tests showed a CD4 cell count of 11 cells/mL and HIV viral load of 44,201 copies/mL. The patient was treated with acyclovir after suspected initial diagnosis of alphaherpesvirus infection and was discharged on December 23, 2014, with antimicrobial therapy prophylaxis for opportunistic infections (trimethoprim/sulfamethoxazole) and persuaded to continue his previous antiretroviral therapy (lamivudine/zidovudine and efavirenz).

The patient was readmitted to the hospital on March 24, 2015, because of a deteriorating clinical condition that included deep, severe, and extended foul-smelling ulcers with raised and undefined edges throughout his face and extremities (Figure 1, panels B and C), as well as fever, tachycardia, hearing and vision impairment, anemia, and leukopenia. He received a blood transfusion, prophylactic antimicrobial drugs against opportunistic infections, analgesics, and supportive care. The case was suggestive of poxvirus infection because the patient had not received smallpox vaccination, the pathologic study showed

Author affiliations: Instituto Nacional de Salud, Bogotá, Colombia (K. Laiton-Donato, J.A. Usme-Ciro, M. Gracia-Romero); Hospital Universitario Mayor Méderi-Universidad del Rosario, Bogotá (P. Ávila-Robayo, P. Benjumea-Nieto, N. Pinzón-Nariño, I. Giraldo, D. Torres-Castellanos); Universidad de La Salle, Bogotá (A. Páez-Martínez); Universidad Cooperativa de Colombia, Santa Marta, Colombia (J.A. Usme-Ciro); Centers for Disease Control and Prevention, Atlanta, Georgia, USA (Y. Nakazawa, N. Patel, K. Wilkins, Y. Li, W. Davidson, J. Burgado, P.S. Satheshkumar, A. Styczynski, M.R. Mauldin, B.W. Petersen)

DOI: https://doi.org/10.3201/eid2603.191365

[1]These authors contributed equally to this article.

Figure 1. Clinical progression of vaccinia virus infection in a patient with HIV/AIDS, Colombia. A) On December 9, 2014, the patient was referred to the Hospital Universitario Mayor Méderi because of a suppurative ulcer with sharply raised, defined edges on his right hand. B, C) In March 2015, lesions increased in size and disseminated over his face and extremities. D) In July 2015, most lesions completely healed, with mild scarring and depigmentation.

the presence of cytoplasmic B-type inclusion bodies, and the patient reported previous contact with cattle with vesicular lesions in their udders. Therefore, biological samples were remitted to the Instituto Nacional de Salud for viral diagnostics, and, subsequently, to the US Centers for Disease Control and Prevention for confirmation of VACV diagnosis and further characterization.

On March 30, 2015, HIV resistance to antiretroviral drugs was confirmed, and the pharmacologic therapy was changed to raltegravir and darunavir/ritonavir. Within 2 weeks, the lesions had healed considerably, and the patient was discharged from the hospital on April 20. Follow-up visits revealed complete healing of the lesions, mild scarring, and depigmentation (Figure 1, panel D), with the exception of a persistent ulcer on the patient's left leg. This lesion did not respond to initial antimicrobial treatment or a 2-week course of topical imiquimod.

Experimental assays included ELISA and neutralization tests for OPXV IgM and IgG detection, virus isolation in BSC-40 cells, and molecular detection through OPXV-generic and VACV-specific real-time PCR (Appendix, https://wwwnc.cdc.gov/EID/

Table. Laboratory testing for orthopoxvirus diagnosis in an HIV/AIDS patient who acquired progressive vaccinia through zoonotic transmission, Colombia*

	Serology			PCR		
Sample date and type	IgM ELISA	IgG ELISA	Neutralization titer	OPXV-specific (C_t)	Vaccinia-specific	Viral culture
2015 Mar						
Serum	Pos	Pos	1:517			
Scab				Pos (31.9)	Pos	Pos
Scab				Pos (28.6)	Pos	Pos
2015 Jul						
Serum	Neg	Pos	1:223			
Scab, left leg				Pos (36.2)	Pos	Pos†
Swab, left leg				Pos (29.2)	Pos	Pos†
2016 Apr						
Paraffin block, left leg				Neg		
Paraffin block, left leg				Neg		
Paraffin block, left leg				Neg		

*C_t, cycle threshold; Neg, negative; Pos, positive.
†Slow-growing.

article/26/3/19-1365-App1.pdf). OPXV IgM and IgG antibodies were detected in serum in March 2015 (5 months after illness onset). IgG but not IgM was in serum in July 2015 (9 months after illness onset). Viral neutralization assays had 50% effective concentration values of 1:517 for the March sample and 1:223 for the July sample (Table). VACV persisted in lesions despite the presence of OPXV IgM and IgG, suggesting that humoral immunity alone might be insufficient to clear infection, as demonstrated previously (*6*). Recovery occurred only after improving adherence and optimizing antiretroviral therapy on the basis of antiretroviral-resistance testing. This finding suggests that cell-mediated immunity is required for complete VACV clearance and that reversing any underlying immunosuppressive condition should be pursued whenever possible for recovery from progressive vaccinia (*7*) (Appendix Figure).

Molecular tests performed on serum and scab samples were positive for OPXV and VACV in March 2015 and remained positive in July 2015 (Table). To better characterize the VACV strain, we used specific primers targeting the A56R hemagglutinin gene (1,134 bp) for amplification and sequencing (*3*). Phylogenetic analysis (Appendix) confirmed infection with a VACV strain whose A56R gene sequence was closely related to those recently reported in Colombia and grouped as a sister lineage of the VACV group 1 in Brazil (Figure 2).

A biopsy of the persistent leg lesion collected in April 2016 tested negative for OPXV DNA by real-time PCR (Table) and positive for *Pseudomonas aeruginosa* and *Escherichia coli* by classic microbiological assays. The lesion healed after focused antimicrobial treatment.

Conclusions

The clinical case we describe meets all criteria for progressive vaccinia (*4*): immunodeficiency from HIV infection was documented with a CD4 cell count of

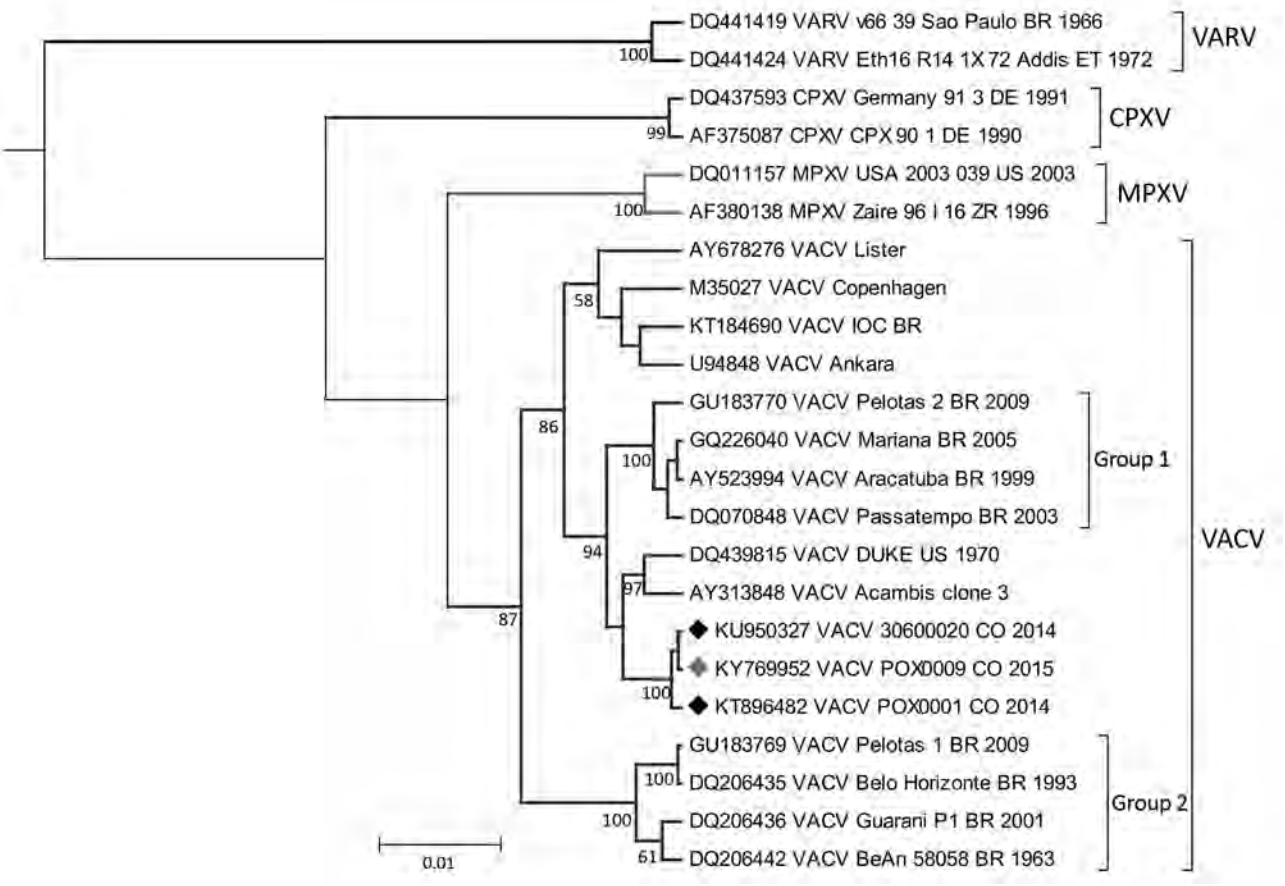

Figure 2. Phylogenetic inference of *Orthopoxvirus* genus based on the A56R hemagglutinin gene. Nucleotide sequences of 829 bp representing the different species were aligned and used for Bayesian inference (Appendix, https://wwwnc.cdc.gov/EID/article/26/3/19-1365-App1.pdf). Black diamonds indicate previously reported sequences of VACV in Colombia; red diamond indicates sequence from the strain from the patient in this study (POX0009). GenBank accession numbers are provided for reference sequences. CPXV, cowpox virus; MPXV, monkeypox virus; VACV, vaccinia virus; VARV, variola virus.

<50 cells/mL; multiple lesions developed and failed to heal despite antimicrobial therapy; and VACV infection was confirmed by several laboratory methods. Our results document progressive vaccinia acquired through zoonotic transmission.

Because smallpox eradication led to the discontinuation of routine smallpox vaccination before the global spread of HIV, little is known about VACV infections in persons with HIV (*8*,*9*). Progressive vaccinia is thought to occur only in patients with substantial cell-mediated immunodeficiency (*4*). This hypothesis is further supported by the observation that VACV infection (through smallpox vaccination) in 10 HIV-infected persons with CD4 cell counts >200 cells/mL did not lead to progressive vaccinia (*10*). In the case we describe, VACV lesions persisted despite the documentation of VACV neutralizing antibodies. The lesions resolved only after immune reconstitution, indicating that cell-mediated immunity is required for complete viral clearance.

The persistent leg lesion was unexpected given the resolution of the patient's other lesions and because latent VACV infection has not been described previously. Although testing of this lesion in July 2015 detected VACV, previous studies have demonstrated that VACV can be isolated from smallpox vaccination site lesions even after the separation of scab when the viral infection is presumably recovered (*11*). The positive bacterial cultures and absence of evidence of VACV in the lesion biopsy in April 2016 suggest that this lesion was most likely attributable to secondary bacterial infection resulting from the compromised dermal barrier rather than persistence or reactivation of latent VACV infection.

Our findings suggest that, in VACV infection cases, reversing any underlying immunosuppressive condition should be pursued whenever possible because of the potential role of the cellular immune response in clearing the infection. Because of waning global immunity against OPXVs (*12*), increasing immunosuppressed populations (*13*), and the potential nosocomial (*14*) and demonstrated zoonotic transmission of VACV (*3*), additional infection prevention, treatment, and control strategies are needed.

Acknowledgments

We thank the following persons who provided essential assistance during the case investigation and subsequent laboratory testing of samples: Luis Ernesto Ayala, Faiber Antonio Gutierrez Lozada, Alberto de la Ossa, Rodrigo Posada and Juan Manuel Peláez Serna.

This work was supported by the Public Health Network at the Instituto Nacional de Salud, Colombia, and the US Centers for Disease Control and Prevention.

This study was performed in accordance with the ethical standards noted in the 1964 Declaration of Helsinki and its later amendments, and followed the national regulation contained in the 1993 resolution no. 008430 related to the ethical aspects of scientific research involving human beings where it is categorized as a minimal risk research. Samples were remitted to the Colombian National Institute of Health as part of the active virologic surveillance of potentially emerging threats.

About the Author

Ms. Laiton-Donato is a researcher in the Sequencing and Genomic Unit, Virology Group, at the Instituto Nacional de Salud, Colombia. Her research is focused on molecular virology of emerging viruses. Dr. Ávila-Robayo is a medical doctor at Hospital Universitario Mayor Méderi, Colombia. Her work focuses on the care of patients with infectious diseases.

References

1. Fenner F, Henderson DA, Arita I, Jezek Z, Ladnyi ID. Smallpox and its eradication. 1988 [cited 2019 Sep 19]. https://apps.who.int/iris/handle/10665/39485
2. Trindade GS, Emerson GL, Carroll DS, Kroon EG, Damon IK. Brazilian vaccinia viruses and their origins. Emerg Infect Dis. 2007;13:965–72. https://doi.org/10.3201/eid1307.061404
3. Usme-Ciro JA, Paredes A, Walteros DM, Tolosa-Pérez EN, Laiton-Donato K, Pinzón MD, et al. Detection and molecular characterization of zoonotic poxviruses circulating in the Amazon region of Colombia, 2014. Emerg Infect Dis. 2017;23:649–53. https://doi.org/10.3201/eid2304.161041
4. Bray M, Wright ME. Progressive vaccinia. Clin Infect Dis. 2003;36:766–74. https://doi.org/10.1086/374244
5. Redfield RR, Wright DC, James WD, Jones TS, Brown C, Burke DS. Disseminated vaccinia in a military recruit with human immunodeficiency virus (HIV) disease. N Engl J Med. 1987;316:673–6. https://doi.org/10.1056/NEJM198703123161106
6. Bray M. Henry Kempe and the birth of vaccinia immune globulin. Clin Infect Dis. 2004;39:767–9. https://doi.org/10.1086/423005
7. Letz AG, McFarland RW, Dice JP. Delay of chemotherapy to prevent progressive vaccinia. Mil Med. 2006;171:788–9. https://doi.org/10.7205/MILMED.171.8.788
8. Amorosa VK, Isaacs SN. Separate worlds set to collide: smallpox, vaccinia virus vaccination, and human immunodeficiency virus and acquired immunodeficiency syndrome. Clin Infect Dis. 2003;37:426–32. https://doi.org/10.1086/375823
9. Bartlett JG. Smallpox vaccination and patients with human immunodeficiency virus infection or acquired

immunodeficiency syndrome. Clin Infect Dis. 2003;36:468–71. https://doi.org/10.1086/368093
10. Tasker SA, Schnepf GA, Lim M, Caraviello HE, Armstrong A, Bavaro M, et al.; US Department of Defense Tri-Service AIDS Clinical Consortium. Unintended smallpox vaccination of HIV-1-infected individuals in the United States military. Clin Infect Dis. 2004;38:1320–2. https://doi.org/10.1086/420938
11. Pittman PR, Garman PM, Kim SH, Schmader TJ, Nieding WJ, Pike JG, et al. Smallpox vaccine, ACAM2000: sites and duration of viral shedding and effect of povidone iodine on scarification site shedding and immune response. Vaccine. 2015;33:2990–6. https://doi.org/10.1016/j.vaccine.2015.04.062
12. Reynolds MG, Carroll DS, Karem KL. Factors affecting the likelihood of monkeypox's emergence and spread in the post-smallpox era. Curr Opin Virol. 2012;2:335–43. https://doi.org/10.1016/j.coviro.2012.02.004
13. Parrino J, Graham BS. Smallpox vaccines: past, present, and future. J Allergy Clin Immunol. 2006;118:1320–6. https://doi.org/10.1016/j.jaci.2006.09.037
14. Zafar A, Swanepoel R, Hewson R, Nizam M, Ahmed A, Husain A, et al. Nosocomial buffalopoxvirus infection, Karachi, Pakistan. Emerg Infect Dis. 2007;13:902–4. https://doi.org/10.3201/eid1306.061068

Address for correspondence: Katherine Laiton-Donato, Virology Group, Department of Public Health Network, Instituto Nacional de Salud, Av Calle 26 No 51-20, Bogotá, Colombia; email: kdlaitond@unal.edu.co

Suspected Locally Acquired Coccidioidomycosis in Human, Spokane, Washington, USA

Hanna N. Oltean, Mark Springer, Jolene R. Bowers, Riley Barnes, George Reid, Michael Valentine, David M. Engelthaler, Mitsuru Toda, Orion Z. McCotter

The full geographic range of coccidioidomycosis is unknown, although it is most likely expanding with environmental change. We report an apparently autochthonous coccidioidomycosis patient from Spokane, Washington, USA, a location to which *Coccidioides* spp. are not known to be endemic.

Coccidioides immitis is a rare but emerging fungal pathogen in Washington, USA; <5 autochthonous infections are reported annually (*1*). Coccidioidomycosis ranges from asymptomatic infection and mild pulmonary disease to potentially fatal severe disease (*2*,*3*). Infection typically results from inhaling environmental arthroconidia (*3*–*8*).

Only the south-central region of Washington has been established as an area to which *Coccidioides* spp. are endemic; *C. immitis* has been detected in soil from Benton, Yakima, and Kittitas Counties (Figure). In addition, human and canine cases from local exposure have been reported from Franklin, Walla Walla, and Asotin Counties (*8*–*10*). Ecologic models predict a larger endemic area, but no models predict high endemicity in Spokane County (*11*,*12*). We report a possible autochthonous coccidioidomycosis case from Spokane.

The Study

An 87-year-old woman came to an urgent care center because of a 4-day history of productive cough, fatigue, chest pain, and dyspnea. Chest radiography showed right middle lobe pneumonia; levofloxacin was prescribed without further testing. Four days later (day 8 from symptom onset), she had worsening symptoms and an erythematous maculopapular rash. Antimicrobial drug therapy was switched to concurrent courses of azithromycin for 5 days and cephalexin for 10 days. Repeat chest radiography showed worsening pneumonia and a new pleural effusion. Follow-up visits documented persistent fatigue and productive cough. On day 49, repeat chest radiography showed new bilateral reticular opacities with mild peribronchial wall thickening but no evidence of pleural effusion or worsening infiltrates; a 7-day course of doxycycline was prescribed. Clinical improvement was noted 2 weeks later (day 66): there was resolution of cough, dyspnea, and chest pain.

On day 80, she again had 4 days of congestion and productive cough and received a 5-day course of azithromycin. On day 89, she reported dyspnea, decreased appetite, and weight loss; an albuterol inhaler was prescribed. Three weeks later, she was given a diagnosis of a rectal adenocarcinoma detected by colonoscopy. Positron emission tomography scan (day 109) identified hypermetabolic activity, indicating a right lung mass, which was diagnosed as lung metastasis. A lung biopsy specimen of this mass (day 127) showed no malignant cells but documented spherules morphologically consistent with *Coccidioides* spp.

On day 137, an infectious disease consultant collected serum and prescribed fluconazole, noting pneumonia and 5 months of persistent symptoms consistent with coccidioidomycosis. Results of tests performed at the University of California Davis Serology Laboratory (Davis, CA, USA) (day 146) were positive for IgG and IgM by immunodiffusion and negative by complement fixation; these results were interpreted as indicating a primary coccidioidal infection not well focalized.

Author affiliations: Washington State Department of Health, Shoreline, Washington, USA (H.N. Oltean); Spokane Regional Health District, Spokane, Washington, USA (M. Springer); Translational Genomics Research Institute, Flagstaff, Arizona, USA (J.R. Bowers, R. Barnes, G. Reid, M. Valentine, D.M. Engelthaler); Centers for Disease Control and Prevention, Atlanta, Georgia, USA (M. Toda, O.Z. McCotter)

DOI: https://doi.org/10.3201/eid2603.191536

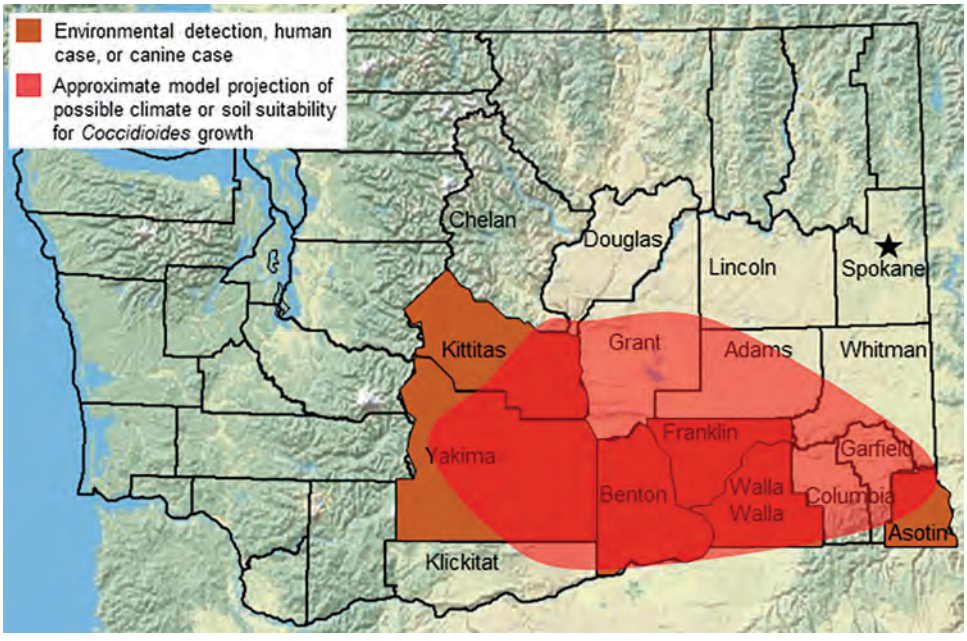

Figure. Known and suspected range of *Coccidioides immitis* in Washington, USA. Star indicates residence of case-patient with suspected locally acquired coccidioidomycosis.

Medical records for the patient indicated no recent travel to *Coccidioides* spp.–endemic areas, including south-central Washington. Three months of fluconazole therapy were completed; 13 months after her diagnosis, complement fixation remained negative and symptoms had resolved.

The case-patient was reported to Spokane Regional Health District on day 149. An in-person interview (day 178) elicited lifetime travel history, which included California (2 visits 15–20 years earlier), Oregon (>25 years earlier), and southern Idaho (>3 years earlier). She also reported travel within Washington, including Benton County (>8 years earlier) and Walla Walla County (>8 years earlier). She reported contact with friends who had traveled to Arizona but denied receiving goods from their travel. Her only outdoor activities in the year before onset were nearby walks and scenic drives; she denied gardening or other soil exposures.

Her home was inspected for possible exposure sources, and building employees were interviewed regarding construction and landscaping. No specific exposures were identified; no new landscaping was identified; indoor plants were limited, and central air filters were regularly replaced. Road construction occurred nearby during her exposure period, which could represent a possible infection source.

Record review and patient interview medical history included iliopsoas corticosteroid injections for 2 years before onset; no other immunosuppressing conditions or medications were noted. Records indicated outpatient treatment for pneumonia in 2006 and hospitalization for pneumonia in 2011.

Fixed tissue from lung biopsy specimens was sent to Translational Genomics Research Institute (https://www.tgen.org), where we extracted DNA by using the GeneRead DNA Formalin-Fixed Paraffin-Embedded Kit (QIAGEN, https://www.qiagen.com). We identified *Coccidioides* spp. by using quantitative PCR, as described (*9*,*13*). We performed amplicon sequencing targeting the quantitative PCR region and 10 distinct canonical single-nucleotide polymorphisms (canSNPs) that define the previously described Washington clade (*10*). Sequence reads aligned with the quantitative PCR target at 1,900× depth of coverage, and reads aligned with 2 canSNP targets, at 10× and 6× depth, both suggesting that the sample fits within the Washington *C. immitis* clade. The genomic regions containing the remaining canSNPs had no coverage in these metagenomic samples, limiting a high degree of confidence for true phylogenetic placement.

Conclusions

We report an apparently autochthonous case of coccidioidomycosis in a woman from Spokane, Washington, a location not known to have *Coccidioides* spp. This patient had many clinical setbacks commonly described with coccidioidomycosis, including 5 unsuccessful antibacterial courses, misdiagnosed lung cancer, and 131 days of healthcare encounters before an accurate diagnosis was obtained.

At least 4 possible hypotheses could explain how this patient became infected. *Coccidioides* infections might be asymptomatic or involve subclinical

disease until a reactivation occurs, typically after immunosuppression. First, she could have been infected during travel to south-central Washington (>8 years earlier). Findings of canSNPs matching the known Washington clade support this hypothesis. Second, infection could have occurred during travel to California reported >15 years before onset, although the SNP analysis does not support this hypothesis. The negative complement fixation and positive IgM results suggest more recent infection (*14*), which, along with no calcified lesions observed by chest radiography, would argue against reactivation of infection acquired during previous travel. Third, she could have been exposed through fomite transmission, which has been described (*15*). The patient had visitors who traveled to Arizona; however, no gifts or goods were brought back, and *C. posadasii* would be expected in fomites from Arizona. Plants or soil purchased from another disease-endemic area around her residence are hypothetical sources of exposure, although none were identified. Fourth, it is possible that exposure happened locally in Spokane. Nearby road construction in the weeks before symptom onset could represent a possible source. However, coccidioidomycosis exposures have not been reported from Spokane, and ecologic niche models predict low likelihood of *Coccidioides* habitat (*12*). The nearest known location of detection of *Coccidioides* spp. in soil was ≈130 miles from Spokane. Windborne spores from south-central Washington or through fomite transmission from intrastate commerce or visitors are alternative possibilities. Sequence alignment with 2 canSNP targets and laboratory findings consistent with primary disease support a hypothesis of recent exposure to the Washington clade.

Recent exposure in Spokane County is the most plausible explanation of illness. However, clear documentation of *Coccidioides* spp. endemicity in Spokane will require additional clinical cases or environmental detections.

The environmental range of *Coccidioides* spp. is not fully understood, and is possibly expanding in arid climates (*11*). This possible expansion creates a diagnosis and surveillance challenge because raising and maintaining clinical awareness in low-incidence or emerging settings is difficult. Although determining a definitive exposure source for this case-patient is not possible, the potential for coccidioidomycosis acquisition in new locations cannot be ignored.

Healthcare providers should consider the risk for coccidioidomycosis in patients who reside in or travel to *Coccidioides*-endemic regions (*3*). In addition, healthcare providers should consider fungal infections in patients who have respiratory symptoms that do not respond to antibacterial therapy and should be aware that the geographic risk for coccidioidomycosis is evolving. Ongoing public health surveillance is required to clarify the range of *Coccidioides* spp. and to improve messaging to healthcare providers and the public.

Acknowledgments

We thank Marcia Goldoft, Tom Chiller, and Brendan R. Jackson for critically reviewing the manuscript.

About the Author

Ms. Oltean is the zoonotic and vectorborne disease epidemiologist for the Washington State Department of Health, in the Office of Communicable Disease Epidemiology, Shoreline, WA. Her primary research interests are design, implementation, and evaluation of zoonotic disease surveillance systems.

References

1. Washington State Department of Health. Washington State communicable disease report, 2017 [cited 2019 Dec16]. https://www.doh.wa.gov/Portals/1/Documents/5100/420-004-CDAnnualReport2017.pdf
2. Brown J, Benedict K, Park BJ, Thompson GR III. Coccidioidomycosis: epidemiology. Clin Epidemiol. 2013;5:185–97.
3. Valley Fever Center for Excellence, The University of Arizona. Valley fever (coccidioidomycosis) tutorial for primary care professionals, 2015 [cited 2019 Dec 16]. http://vfce.arizona.edu/sites/vfce/files/tutorial_for_primary_care_professionals_1.pdf
4. Cordeiro RA, Brilhante RSN, Rocha MFG, Bandeira SP, Fechine MAB, de Camargo ZP, et al. Twelve years of coccidioidomycosis in Ceará State, northeast Brazil: epidemiologic and diagnostic aspects. Diagn Microbiol Infect Dis. 2010;66:65–72. https://doi.org/10.1016/j.diagmicrobio.2008.09.016
5. Wilken JA, Sondermeyer G, Shusterman D, McNary J, Vugia DJ, McDowell A, et al. Coccidioidomycosis among workers constructing solar power farms, California, USA, 2011–2014. Emerg Infect Dis. 2015;21:1997–2005. https://doi.org/10.3201/eid2111.150129
6. Pappagianis D; Coccidioidomycosis Serology Laboratory. Coccidioidomycosis in California state correctional institutions. Ann N Y Acad Sci. 2007;1111:103–11. https://doi.org/10.1196/annals.1406.011
7. Colson AJ, Vredenburgh L, Guevara RE, Rangel NP, Kloock CT, Lauer A. Large-scale land development, fugitive dust, and increased coccidioidomycosis incidence in the Antelope Valley of California, 1999–2014. Mycopathologia. 2017;182:439–58. https://doi.org/10.1007/s11046-016-0105-5
8. Marsden-Haug N, Goldoft M, Ralston C, Limaye AP, Chua J, Hill H, et al. Coccidioidomycosis acquired in Washington State. Clin Infect Dis. 2013;56:847–50. https://doi.org/10.1093/cid/cis1028

9. Litvintseva AP, Marsden-Haug N, Hurst S, Hill H, Gade L, Driebe EM, et al. Valley fever: finding new places for an old disease: *Coccidioides immitis* found in Washington State soil associated with recent human infection. Clin Infect Dis. 2015;60:e1–3. https://doi.org/10.1093/cid/ciu681
10. Oltean HN, Etienne KA, Roe CC, Gade L, McCotter OZ, Engelthaler DM, et al. Utility of whole-genome sequencing to ascertain locally acquired cases of coccidioidomycosis, Washington, USA. Emerg Infect Dis. 2019;25:501–6. https://doi.org/10.3201/eid2503.181155
11. Gorris ME, Treseder KK, Zender CS, Randerson JT. Expansion of coccidioidomycosis endemic regions in the United States in response to climate change. GeoHealth. 2019;3:308–27. https://doi.org/10.1029/2019GH000209
12. Dobos R, McCotter O. Modeling and mapping of *Coccidioides* soil habitat. In: Proceedings of the 61st Annual Coccidioidomycosis Study Group Meeting, Stanford, California, 2017 Aug 10–13. Stanford (CA): 2017 [cited 2019 Dec 27]. http://coccistudygroup.com/wp-content/uploads/2017/11/CSG-61st-Annual-Proceedings-11-27-17.pdf
13. Bowers JR, Parise KL, Kelley EJ, Lemmer D, Schupp JM, Driebe EM, et al. Direct detection of coccidioides from Arizona soils using CocciENV, a highly sensitive and specific real-time PCR assay. Med Mycol. 2019;57:246–55. https://doi.org/10.1093/mmy/myy007
14. Pappagianis D, Zimmer BL. Serology of coccidioidomycosis. Clin Microbiol Rev. 1990;3:247–68. https://doi.org/10.1128/CMR.3.3.247
15. Stagliano D, Epstein J, Hickey P. Fomite-transmitted coccidioidomycosis in an immunocompromised child. Pediatr Infect Dis J. 2007;26:454–6. https://doi.org/10.1097/01.inf.0000259231.95285.bc

Address for correspondence: Hanna N. Oltean, Washington State Department of Health, 1610 NE 150th St, Shoreline, WA 98155, USA; email: hanna.oltean@doh.wa.gov

Pulmonary *Nocardia ignorata* Infection in Gardener, Iran, 2017

Hossein A. Rahdar, Mehrnaz A. Gharabaghi, Abbas Bahador, Shahram Shahraki-Zahedani, Morteza Karami-Zarandi, Shahram Mahmoudi, Mohammad M. Feizabadi

Author affiliation: Iranshahr University of Medical Sciences, Iranshahr, Iran (H.A. Rahdar) Tehran University of Medical Sciences, Tehran, Iran (M.A. Gharabaghi, A. Bahador, M. Karami-Zarandi, S. Mahmoudi, M.M. Feizabadi); Zahedan University of Medical Sciences, Zahedan, Iran (S. Shahraki-Zahedani)

DOI: https://doi.org/10.3201/eid2603.180725

Nocardia ignorata, which was first described in 2001, is a rare human pathogen. We report a case of pulmonary nocardiosis caused by this bacterium in a 55-year-old man from Iran. The patient, a gardener, had frequent exposure to soil and may have acquired the infection from that source.

Since the description of *Nocardia ignorata* in 2001 (*1*), 4 respiratory isolates in Europe and 3 corneal isolates in India have been reported (*2*,*3*). Among the respiratory isolates, only 2 were confirmed as the cause of disease (*2*). We report a case of pulmonary nocardiosis that was caused by *Nocardia ignorata* in a person from Iran.

The patient, a 55-year-old man, smoked, had multiple myeloma, and had a history of opium use for 3 years. He was consuming methadone syrup daily at the time of hospitalization but had no history of corticosteroid consumption. He had frequent exposure to dust because of working in a garden.

The recent course of disease began ≈4 months earlier, initially as a feeling of heaviness and pain in the anterior chest (no clear distribution) and shortness of breath (functional class II level). However, coronary disease was rejected as a possible diagnosis during examination. The patient had night sweats and a weight loss of 5% in the past 4 months.

Two months after initial symptoms began, he had had fever, chills, and gradually productive coughs. During a visit to a different hospital, he was given a diagnosis of bacterial pneumonia and received azithromycin and cefixime, which initially reduced the symptoms but did not completely resolve them. When he sought care at Imam Khomeini Hospital (Tehran, Iran) because he had symptoms including cramping abdominal pain, fever, and shortness of breath 4–7 days before the visit, he was first admitted to the emergency department and then transferred to the lung unit.

Vital signs of the patient at the time of hospitalization were temperature 37.6°C, blood pressure 135/75 mm Hg, heart rate 80 beats/min, respiratory rate 18 breaths/min, and O_2 saturation 90%. Laboratory findings were increased leukocyte count (12,210 cells/mm^3 with 68.8% neutrophils) and C-reactive protein level 65 mg/L (reference value <5 mg/L); thyroid function test results were within reference ranges. Examination of abdominal organs did not show organomegaly or any other indications of disease; prostate size and consistency were unremarkable by testicular and digital rectal examinations. Heart sounds were unremarkable, and cervical, axillary, and extracorporeal lymph nodes were also unremarkable. Examination of the lungs showed fine end inspiratory crackles in both lungs.

Chest radiograph showed a mediastinal mass from the periphery of the right main bronchus to the medial and lower branches and an extension to the posterior part (vertebral trunk and adjacent to the esophagus). The maximum size of the mass was 31 × 74 mm, and an air bronchogram showed opacities near the mass, suggesting postobstructive pneumonia.

The patient was given empirical pneumonia treatment with levofloxacin (750 mg/d) and ceftriaxone (1 g, 2×/d) for 8 days. For the mediastinal mass, the patient underwent endoscopic ultrasonography and bronchoscopy, but his symptoms did not resolve. In a spiral computed tomography scan of the thorax, we found patchy ground glass and nodular opacities that were spread in both lungs, especially in the posterior and lateral segments of the left lower lobe, the posterior segment of the right lower lobe, lingular, and the right upper lobe. Thus, nocardiosis and tuberculosis examinations were recommended.

We performed a tuberculin skin test, and the intraderm response to tuberculin was absent. Moreover, mucosal erythema with inflammation were seen on a right lung bronchoscopic examination. We found abundant mucoid secretions, no endobronchial ulcers, and a white discharge without endobronchial ulcer in the left lung.

We then subjected a bronchoalveolar lavage specimen for microbiological cultures. No *Mycobacterium* growth was seen, but colonies suspected of being *Nocardia* species appeared on blood agar plates after 4 days of incubation. A modified Kinyoun acid-fast stain confirmed the partial acid-fast staining feature of the colonies.

We performed DNA extraction by using the modified Pitcher method (*4*–*6*) and a *Nocardia*-specific PCR

with primers NG1 (5′-ACCGACCACAAGGGGG-3′) and NG2 (5′-GGTTGTAAACCTCTTTCGA-3′). We obtained positive results with this PCR and a resistance-to-lysozyme test, and confirmed the presence of *Nocardia* species. For accurate identification, we PCR amplified 16S rRNA and partial DNA gyrase B (*gyrB*) genes (*4*) and subjected PCR products to direct sequencing (GenBank accession nos. KY817987.1 for 16S rRNA and MN159177 for *gyrB*).

We performed a BLAST analysis (https://blast.ncbi.nlm.nih.gov/Blast.cgi) by using the megablast algorithm. This analysis confirmed the identity as *N. ignorata* (16S rRNA coverage 100% and 99% identity with GenBank accession no. KM113026.1; *gyrB* coverage 100% and 100% identity with GenBank accession no. GQ496109.1).

Antimicrobial drug susceptibility testing (broth microdilution method) showed that the isolate was susceptible to trimethoprim/sulfamethoxazole, imipenem, amikacin, doxycycline, and linezolid and resistant to erythromycin, ceftriaxone, and ciprofloxacin. At this point, we gave the patient cotrimoxazole and imipenem for 20 days and then trimethoprim/sulfamethoxazole for 6 months. The clinical, biological, and radiologic outcomes of the treatment were optimal, and no recurrence occurred after 8 months.

N. ignorata is a rare human pathogen. However, soil samples have been described as a possible reservoir (*2*,*7*,*8*). Accordingly, this patient, who had frequent exposure to soil through his work as a gardener, might have acquired the infection from that source.

About the Author

Dr. Rahdar is an assistant professor in the Department of Microbiology, School of Medicine, Iranshahr University of Medical Sciences, Iranshahr, Iran. His research interests are rare bacterial pathogens and antimicrobial resistance.

References

1. Yassin AF, Rainey FA, Steiner U. *Nocardia ignorata* sp. nov. Int J Syst Evol Microbiol. 2001;51:2127–31. https://doi.org/10.1099/00207713-51-6-2127
2. Rodríguez-Nava V, Couble A, Khan ZU, Pérouse de Montclos M, Brasme L, Villuendas C, et al. *Nocardia ignorata*, a new agent of human nocardiosis isolated from respiratory specimens in Europe and soil samples from Kuwait. J Clin Microbiol. 2005;43:6167–70. https://doi.org/10.1128/JCM.43.12.6167-6170.2005
3. Lalitha P, Srinivasan M, Rajaraman R, Ravindran M, Mascarenhas J, Priya JL, et al. *Nocardia keratitis*: clinical course and effect of corticosteroids. Am J Ophthalmol. 2012;154:934–9. http://dx.doi.org/10.1016/j.ajo.2012.06.001
4. Pitcher D, Saunders N, Owen R. Rapid extraction of bacterial genomic DNA with guanidium thiocyanate. Letters in Applied Microbiology. 1989;8:151–6. https://doi.org/10.1111/j.1472-765X.1989.tb00262.x
5. Rahdar HA, Azadi D, Shojaei H, Daei-Naser A. Molecular analysis and species diversity of *Nocardia* in the hospital environment in a developing country, a potential health hazard. J Med Microbiol. 2017;66:334–41. https://doi.org/10.1099/jmm.0.000436
6. Laurent FJ, Provost F, Boiron P. Rapid identification of |clinically relevant *Nocardia* species to genus level by 16S rRNA gene PCR. J Clin Microbiol. 1999;37:99–102. http://dx.doi.org/10.1128/JCM.37.1.99-102.1999
7. Habibnia S, Nasab MR, Heidarieh P, Bafghi MF, Pourmand MR, Eshraghi SS. Phenotypic characterization of *Nocardia* spp. isolated from Iran soil microflora. International Journal of Environmental Health Enginering. 2015;4:20. https://doi.org/10.4103/2277-9183.158388
8. Salimi F, Hamedi J, Motevaseli E, Mohammadipanah F. Isolation and screening of rare Actinobacteria, a new insight for finding natural products with antivascular calcification activity. J Appl Microbiol. 2018;124:254–66. https://doi.org/10.1111/jam.13605

Address for correspondence: Mohammad M. Feizabadi, Department of Medical Microbiology, School of Medicine, Tehran University of Medical Sciences, Keshavarz Blvd, Poursina St, Tehran 1416753955, Iran; email: mfeizabadi@tums.ac.ir

Mycobacterium senegalense Infection after Implant-Based Breast Reconstruction, Spain

Octavio Carretero, Carmen Reyes, Rafael San-Juan, Fernando Chaves, Paula López-Roa

Author affiliation: Hospital Universitario 12 de Octubre, Madrid, Spain

DOI: https://doi.org/10.3201/eid2603.190230

Bacterial infection is a well-known complication of breast implant surgery. We identified *Mycobacterium senegalense*, the principal pathogen of bovine farcy of cattle, in a woman after implant-based breast reconstruction. This finding indicates that unusual pathogens should be considered as an etiology of infected breast prostheses.

Mycobacterium senegalense is a rapidly growing mycobacterium that belongs to the *M. fortuitum* complex. These opportunistic pathogens cause post-traumatic skin and soft tissue infections, including postsurgical wound infections (*1*). *M. senegalense* is the principal pathogen of bovine farcy, which is endemic to eastern and central Africa (*2*). Few human cases have been described (*3*–*5*).

In 2014, a 44-year-old woman in Spain had a right breast mastectomy with lymph node dissection, radiotherapy and chemotherapy for breast carcinoma, followed by bilateral breast augmentation in November 2016. Her postoperative course was uneventful until January 2017, when a serous discharge appeared on the right breast. Consequently, she underwent removal of her right breast implant, drainage, and sample collection. Standard bacteriologic cultures were sterile.

In August 2017, the patient underwent repeat implant-based breast reconstruction. Three months after surgery, she sought care for edema and erythema of her right breast. Nuclear magnetic resonance imaging showed inflamed fistulous tracts. Serous fluid obtained during the implant surgery was sent to the microbiological laboratory at Hospital Universitario 12 de Octubre (Madrid. Spain). After 48 hours of incubation, the blood agar grew slow-growing tiny colonies identified as *M. senegalense* by using matrix-assisted laser desorption/ionization time-of-flight (MALDI-TOF) mass spectrometry (Bruker Daltonics, https://www.bruker.com) with a score of 2.1 (scores ≥1.8 are accepted for mycobacterial species assignment). Before MALDI-TOF mass spectrometry analysis, bacteria were heat-inactivated in a dry water bath at 95°C for 30 min and submerged in ethanol to a final concentration of 75%. The cells were then physically disrupted by using a protein-extraction protocol recommended by the manufacturer (MycoEx version 3.0; Bruker Daltonics).

We performed partial sequencing of the 16S ribosomal RNA and *rpoB* genes of the isolate (*6*). The partial sequence of 16S rRNA showed 100% identity to the sequences deposited in GenBank of 7 *Mycobacterium* species: *M. farcinogenes*, *M. senegalense*, *M. houstonense*, *M. conceptionense*, *M. fortuitum*, *M. mucogenicum*, and *M. phocaicum*. Partial *rpoB* gene sequencing showed 99% identity with the *M. senegalense* and *M. conceptionense* sequences. The latest update of MALDI-TOF mass spectrometry database includes *M. conceptionense*, but we did not find this species among the top matches. Therefore, using a combination of 16S rRNA/rpoB gene sequencing and MALDI-TOF mass spectrometry, we identified the isolate as *M. senegalense*. By using the Etest method, we determined the isolate was susceptible to cefoxitin, amikacin, ciprofloxacin, clarithromycin, trimethoprim/sulfamethoxazole, and minocycline.

After prostheses removal and debridement of the fistulous tract, an extended treatment was scheduled with moxifloxacin (400 mg/d for 4 weeks). The patient's clinical course was uneventful until May 2018, when she sought care for fistulization of the surgical wound. *M. senegalense* exhibiting an identical antimicrobial drug susceptibility pattern was again isolated from the wound fluid. Nuclear magnetic resonance imaging showed bone impairment and new fistulous tracts. The patient was then treated over a 3-month period with a combination of clarithromycin (500 mg 2×/d) and trimethoprim/ sulfamethoxazole (160.800 mg 2×/d). After finishing the combination therapy, she completed 3 months of clarithromycin monotherapy. At a follow-up examination 6 months later, she had no signs or symptoms of infection, and ultrasound detected nothing relevant.

No clear habitat for human strains of *M. senegalense* outside of Africa has been reported. We do not know how this patient's breast prosthesis became infected with *M. senegalense*, but we speculate the infection occurred during implant-based breast reconstruction.

Limited studies have reported *M. senegalense* as the causal agent of human diseases (*3*–*5*). In the case reported here, the absence of other pathogens and its repeated isolation from clinical specimens suggests the clinical significance of this species.

MALDI-TOF mass spectrometry identified *M. senegalense* with a score of 2.1, which is considered high-confidence identification at species level. 16S rRNA sequencing did not enable us to discriminate between 7 closely related species. Although *rpoB* gene sequencing has higher discrimination power, it could not distinguish between *M. senegalense and M. conceptionense*. These findings suggest that the combination of 16S rRNA/rpoB partial gene sequencing and MALDI-TOF mass spectrometry is useful and reliable for identifying this species.

Because previous experience with this organism is limited, no specific treatment guidelines exist. Therefore, the treatment course was based on current recommendations for breast implant infection caused by *M. fortuitum*. Although some reports have suggested success with single-agent treatment, combination therapy is recommended to avoid the emergence of resistance. No standard duration of therapy is reported, and treatment may last ≥6 months (*6*–*8*). In this case, the complete removal of prosthetic material was considered curative, and an extended antimicrobial treatment with moxifloxacin was prescribed. After relapse, a combined treatment was administered,

followed by prolonged treatment with clarithromycin, which was finally curative.

In conclusion, the case reported here is a reminder that unusual pathogens, such as *M. senegalense*, should be considered as an etiology of infected breast prosthesis. Molecular techniques confirmed the accuracy of MALDI-TOF mass spectrometry to identify this emerging mycobacterial species. Patients should undergo prolonged treatment for ≥3 months, ideally with combined therapy, even with adequate surgical treatment.

About the Author

Dr. Carretero is on the faculty of the Department of Microbiology, Hospital Universitario 12 de Octubre, Madrid. His primary research interests include nontuberculosis mycobacteria and prosthesis infections.

References

1. Brown BA, Wallace RJ Jr, Onyi GO, De Rosas V, Wallace RJ III. Activities of four macrolides, including clarithromycin, against *Mycobacterium fortuitum*, *Mycobacterium chelonae*, and *M. chelonae*–like organisms. Antimicrob Agents Chemother. 1992;36:180–4. https://doi.org/10.1128/AAC.36.1.180
2. Oh WS, Ko KS, Song JH, Lee MY, Ryu SY, Taek S, et al. Catheter-associated bacteremia by *Mycobacterium senegalense* in Korea. BMC Infect Dis. 2005;5:107. https://doi.org/10.1186/1471-2334-5-107
3. Talavlikar R, Carson J, Meatherill B, Desai S, Sharma M, Shandro C, et al. *Mycobacterium senegalense* tissue infection in a child after fish tank exposure. Can J Infect Dis Med Microbiol. 2011;22:101–3. https://doi.org/10.1155/2011/206532
4. Wallace RJ Jr, Brown-Elliott BA, Brown J, Steigerwalt AG, Hall L, Woods G, et al. Polyphasic characterization reveals that the human pathogen *Mycobacterium peregrinum* type II belongs to the bovine pathogen species *Mycobacterium senegalense*. J Clin Microbiol. 2005;43:5925–35. https://doi.org/10.1128/JCM.43.12.5925-5935.2005
5. Adékambi T, Colson P, Drancourt M. *rpoB*-based identification of nonpigmented and late-pigmenting rapidly growing mycobacteria. J Clin Microbiol. 2003;41:5699–708. https://doi.org/10.1128/JCM.41.12.5699-5708.2003
6. Wallace RJ Jr, Steele LC, Labidi A, Silcox VA. Heterogeneity among isolates of rapidly growing mycobacteria responsible for infections following augmentation mammaplasty despite case clustering in Texas and other southern coastal states. J Infect Dis. 1989;160:281–8. https://doi.org/10.1093/infdis/160.2.281
7. Brown-Elliott BA, Wallace RJ Jr. Clinical and taxonomic status of pathogenic nonpigmented or late-pigmenting rapidly growing mycobacteria. Clin Microbiol Rev. 2002; 15:716–46. https://doi.org/10.1128/CMR.15.4.716-746.2002
8. Betal D, Macneill FA. Chronic breast abscess due to *Mycobacterium fortuitum*: a case report. J Med Case Reports. 2011;5:188. https://doi.org/10.1186/1752-1947-5-188

Address for correspondence: Paula López-Roa, Hospital Universitario 12 de Octubre, Department of Clinical Microbiology, Avenida de Córdoba, s/n, 28041 Madrid, Spain; email: plroa@salud.madrid.org

Low Prevalence of *Mycobacterium bovis* in Tuberculosis Patients, Ethiopia

Muluwork Getahun, H.M. Blumberg, Waganeh Sinshaw, Getu Diriba, Hilina Mollalign, Ephrem Tesfaye, Bazezew Yenew, Mengistu Taddess, Aboma Zewdie, Kifle Dagne, Dereje Beyene, Russell R. Kempker, Gobena Ameni

Author affiliations: Ethiopian Public Health Institute, Addis Ababa, Ethiopia (M. Getahun, W. Senshaw, G. Diriba, H. Mollalign, E. Tesfaye, B. Yenew, M. Taddess); Addis Ababa University, Addis Ababa (M. Getahun, A. Zewdie, K. Dagne, D. Beyene, G. Ameni); Emory University, Atlanta, Georgia, USA (H.M. Blumberg, R.R. Kempker)

DOI: https://doi.org/10.3201/eid2603.190473

An estimated 17% of all tuberculosis cases in Ethiopia are caused by *Mycobacterium bovis*. We used *M. tuberculosis* complex isolates to identify the prevalence of *M. bovis* as the cause of pulmonary tuberculosis. Our findings indicate that the proportion of pulmonary tuberculosis due to *M. bovis* is small (0.12%).

In 2016, the World Health Organization (WHO) estimated that there were 147,000 cases and 12,500 deaths worldwide from tuberculosis, which is predominantly caused by *Mycobacterium bovis*. However, because of the lack of comprehensive surveillance data, particularly from developing countries, actual illness and death could exceed this estimate (*1*,*2*). To enhance efforts at addressing zoonotic TB, multiple international organizations collaboratively developed and recently released the Roadmap for Zoonotic Tuberculosis (*1*). The roadmap states 3 objectives, the first of which is to collect more accurate scientific evidence on zoonotic TB through improved surveillance efforts.

In Ethiopia, ≈80% of persons live in rural areas, where most of the population harvests crops or raises livestock (*3*). Because of the pastoral lifestyle, the burden of zoonotic TB is thought to be high in such rural communities because of a perceived higher risk of acquiring *M. bovis* infection (*2*). In 2013, Müller et al. estimated the proportion of all forms of TB cases caused by *M. bovis* in Ethiopia to be 17% (*4*). For this study, we evaluated the contribution of *M. bovis* toward causing pulmonary TB in Ethiopia.

We obtained a total of 1,785 stored *M. tuberculosis* complex isolates collected from patients testing

positive in smear tests. These tests were performed in 32 health facilities across Ethiopia during November 2011–June 2013 as part of a drug resistance survey. Among the 32 sites enrolled in the drug resistance survey, 30 sites had participated in an earlier survey in 2003–2005; two additional sites were selected from the Gambella and Benishangul Gumuz regions to ensure that ≥1 health facility from each region was included (Table). We included data from all patients with positive results for TB on consecutive sputum smear tests.

To identify species, region of difference (RD) 9- and RD4-based PCR procedures were performed using HVD primers and QIAGEN HotStarTaq Master Mix reagents (QIAGEN, https://www.qiagen.com), which were described in earlier studies (*5*–*8*). The Capilia TB-Neo test (Goffin Molecular Technologies, http://www.goffinmoleculartechnologies.com) was used to distinguish *M. tuberculosis*–complex species from other nontuberculous mycobacterial (NTM) species. The same standard operating procedures were used to interpret the results.

Of the 1,785 isolates collected, 1,735 were available for typing. Among those typed, 1,599 (92%) yielded visible bands of *M. tuberculosis* complex. RD9 typing identified 1,597 (99.87%) of 1,599 isolates as *M. tuberculosis*, and RD4 typing identified only 2 (0.13%) of 1,599 of the isolates as *M. bovis*. These findings indicate that pulmonary TB due to *M. bovis* is rare in Ethiopia.

This study has certain limitations. We used *M. tuberculosis* complex isolates collected from a sentinel drug resistance survey. Data from smears testing negative for pulmonary TB cases, which account for some proportion of PTB and extrapulmonary TB cases, were not included.

One possible alternative explanation for finding few cases of *M. bovis* as a pathogen in pulmonary TB is that *M. bovis* may have been acquired through ingestion of food from livestock infected with extrapulmonary TB (*7*). In that case, sputum might not have been the ideal technique for isolating *M. bovis* samples. Previous studies in Ethiopia reported variable (0%–16%) prevalence of *M. bovis* in extrapulmonary TB patients (*8*,*9*). A second possible reason could be the low prevalence of bovine TB in zebu cattle, which comprise >95% of the cattle population of Ethiopia (*10*) and have been reported to have lower infection rates with *M. bovis* than other types of cattle. In addition, most cattle husbandry in Ethiopia is on extensively managed small farms in open fields, which poses a low risk for the spread of bovine TB (*7*). Thus, a low prevalence of bovine TB in the Ethiopia cattle population could result in a limited rate of transmission to humans.

This study included samples from all regions of Ethiopia to identify the prevalence of bovine TB among patients with pulmonary TB. We found that *M. bovis* was an etiologic agent of human pulmonary TB in only a small fraction of cases, a lower proportion than previously estimated. This finding indicates that aerosol transmission of *M. bovis* from livestock to humans is rare. A useful focus for future efforts might be to implement or strengthen pasteurization programs in *M. bovis*–prevalent areas to limit possible transmission of bovine TB through the consumption of dairy products.

This work was supported in part by the Ethiopian Public Health Institute, Aklilu Lemma Institute of Pathobiology of Addis Ababa University, and the National Institutes of Health Fogarty International Center (D43TW009127).

This study received ethics approval from the IRBs of the Ethiopian Public Health Institute and Addis Ababa University.

RD9 and RD4 typing were performed at the Ethiopian Public Health Institute (EPHI).

Table. Number of cases by region and results of *Mycobacterium tuberculosis* testing for isolates in study of contribution of *M. bovis* to pulmonary tuberculosis, Ethiopia*

		M. tuberculosis positive		*M. tuberculosis* negative	
Region	Total no. cases	Culture positive	Culture negative/ contaminated	Culture positive	Culture negative/ contaminated
Addis Ababa	181	166	10	1	4
Afar	68	58	4	3	3
Amhara	138	121	6	5	6
Benishangul Gumuz	21	19	1	0	1
Dire Dawa	103	86	1	6	10
Gambella	121	105	4	7	5
Harar	52	50	2	0	0
Oromia	518	469	22	12	15
SNNPR	352	315	19	10	8
Somali	104	101	2	1	0
Tigray	77	62	10	2	3
Total	1,735	1,552	81	47	55

*Of the 1,735 isolates available for typing, 1,599 yielded positive results for *M. tuberculosis* complex; of those, 1,597 (99.87%) were *M. tuberculosis* positive by RD9 testing and 2 (0.13%) were *M. bovis* positive by RD4 testing. Of the 2 RD4 positive results, 1 was from culture-positive and the other from smear-positive (culture negative) sediment. RD, region of difference.

About the Author

Dr. Getahun works at the national reference laboratory for Ethiopia. Her main areas of work include conducting research on priority public health problems, providing technical assistance on TB research, and providing supportive supervision for surveillance and program evaluation.

References

1. World Health Organization, Food and Agriculture Organization of the United Nations, and World Organisation for Animal Health. Roadmap for zoonotic tuberculosis. Geneva: WHO Press; 2017 [cited 2019 Feb 1]. http://www.fao.org/3/a-i7807e.pdf
2. Olea-Popelka F, Muwonge A, Perera A, Dean AS, Mumford E, Erlacher-Vindel E, et al. Zoonotic tuberculosis in human beings caused by *Mycobacterium bovis*—a call for action. Lancet Infect Dis. 2017;17:e21–5. https://doi.org/10.1016/S1473-3099(16)30139-6
3. Central Statistical Agency, World Bank. Ethiopia rural socioeconomic survey. 2013 [cited 2019 Feb 1]. http://siteresources.worldbank.org/INTLSMS/Resources/3358986-1233781970982/5800988-1367841456879/9170025-1367841502220/ERSS_Survey_Report.pdf
4. Müller B, Dürr S, Alonso S, Hattendorf J, Laisse CJ, Parsons SD, et al. Zoonotic *Mycobacterium bovis*–induced tuberculosis in humans. Emerg Infect Dis. 2013;19:899–908. https://doi.org/10.3201/eid1906.120543
5. Parsons LM, Brosch R, Cole ST, Somoskövi A, Loder A, Bretzel G, et al. Rapid and simple approach for identification of *Mycobacterium tuberculosis* complex isolates by PCR-based genomic deletion analysis. J Clin Microbiol. 2002;40:2339–45. https://doi.org/10.1128/JCM.40.7.2339-2345.2002
6. Mamo G, Bayleyegn G, Sisay Tessema T, Legesse M, Medhin G, Bjune G, et al. Pathology of camel tuberculosis and molecular characterization of its causative agents in pastoral regions of Ethiopia. PLoS One. 2011;6:e15862. https://doi.org/10.1371/journal.pone.0015862
7. Portillo-Gómez L, Sosa-Iglesias EG. Molecular identification of *Mycobacterium bovis* and the importance of zoonotic tuberculosis in Mexican patients. Int J Tuberc Lung Dis. 2011;15:1409–14. https://doi.org/10.5588/ijtld.10.0608
8. Firdessa R, Berg S, Hailu E, Schelling E, Gumi B, Erenso G, et al. Mycobacterial lineages causing pulmonary and extrapulmonary tuberculosis, Ethiopia. Emerg Infect Dis. 2013;19:460–3. https://doi.org/10.3201/eid1903.120256
9. Regassa A, Medhin G, Ameni G. Bovine tuberculosis is more prevalent in cattle owned by farmers with active tuberculosis in central Ethiopia. Vet J. 2008;178:119–25. https://doi.org/10.1016/j.tvjl.2007.06.019
10. Sibhat B, Asmare K, Demissie K, Ayelet G, Mamo G, Ameni G. Bovine tuberculosis in Ethiopia: a systematic review and meta-analysis. Prev Vet Med. 2017;147:149–57. https://doi.org/10.1016/j.prevetmed.2017.09.006

Address for correspondence: Muluwork Getahun, Ethiopian Public Health Institute, National TB Reference Laboratory, Addis Ababa, 1242, Ethiopia; email: mimishaget@yahoo.com

Metagenomics of Imported Multidrug-Resistant *Mycobacterium leprae*, Saudi Arabia, 2017

Qingtian Guan, Talal S. Almutairi, Tahani Alhalouli, Arnab Pain,[1] Faisal Alasmari[1]

Author affiliations: King Abdullah University of Science and Technology, Thuwal-Jeddah, Saudi Arabia (Q. Guan, A. Pain); King Saud University Medical City, Riyadh, Saudi Arabia (T.S. Almutairi); King Fahad Medical City, Riyadh (T.S. Almutairi, T. Alhalouli, F. Alasmari)

DOI: https://doi.org/10.3201/eid2603.190661

Using shotgun metagenomics, we identified an imported case of multidrug-resistant *Mycobacterium leprae* in a Filipino resident of Saudi Arabia in 2017. We determined the phylogenomic lineage (3K1) and identified mutations in *rpoB* and *rrs* corresponding to the multidrug-resistance phenotype clinically observed. Metagenomics sequencing can be used to identify multidrug-resistant *M. leprae*.

Leprosy is a chronic dermatologic and neurologic disease caused by the infectious agent *Mycobacterium leprae* and can lead to severe disabilities; >200,000 new cases are reported annually worldwide, according to the World Health Organization. A total of 242 leprosy cases were reported in Saudi Arabia during 2003–2012; however, little is known about the subtypes and prevalence of drug resistance among these *M. leprae* cases (*1*).

In May 2017, a 30-year-old woman from the Philippines sought treatment at the dermatology clinic of King Fahad Medical City (KFMC) Hospital in Riyadh, Saudi Arabia, for painful systemic skin nodules and joint pain without joint swelling. She had no medical history of leprosy. The initial clinical diagnosis of this patient was inconclusive, but her initial signs and symptoms were suggestive of a connective tissue disease such as systemic lupus erythematosus, and initial clinical improvement was recorded after a short course of empiric steroids and hydroxychloroquine treatment. Other suspected diagnoses included lepromatous leprosy with type 2 erythema nodosum leprosum reaction or other nontuberculosis mycobacterial infection.

We performed a punch skin biopsy of the extensor surface of the forearm and performed Ziehl-Neelsen staining; we observed a florid histiocytic

[1]These senior authors contributed equally to this article.

proliferation containing numerous *Mycobacterium* bacilli without an obvious granuloma (Appendix Figure 1, https://wwwnc.cdc.gov/EID/article/26/3/19-0661-App1.pdf). We referred the patient to the infectious disease clinic, which performed QuantiFERON-TB Gold (QIAGEN, https://www.quantiferon.com) and took a biopsy for bacterial and fungal culture, and all test results were negative. Mycobacterial culture showed >9 acid-fast bacilli/high-power field on smears, and no growth was observed on Lowenstein-Jensen slants after 8 weeks of incubation.

Her treatment started with a daily regimen of clofazimine (50 mg), dapsone (100 mg), and rifampin (600 mg). Treatment with moxifloxacin (400 mg/d) and macrolides was briefly added (clarithromycin and azithromycin were both stopped because of gastrointestinal side effects) in case of possible nontuberculosis mycobacterial infection. The patient had multiple relapses during 12 months of follow-up and became steroid dependent (i.e., her skin lesions reappeared shortly after steroid treatment ended).

Because initial test reports were inconclusive and the etiologic agent was unconfirmed, we attempted to confirm the etiology by subjecting the patient's skin biopsy sample to metagenomic sequencing; a DNA sequencing protocol without target DNA–enrichment steps (*2*) was needed to unambiguously identify the etiologic agent. From the metagenomics datasets, we reconstructed the near-complete genome of the *M. leprae* species (which we named KFMC-1) at 99.2% completeness when compared with *M. leprae* TN, a strain commonly used for reference (*3*). We assembled the 3.24-Mb genome of *M. leprae* KFMC-1 in 19 DNA segments, and average coverage was 20.02× (Appendix Table 1, Figure 2, panel A). A single-nucleotide polymorphism comparison of *M. leprae* KFMC-1 with a globally representative set of *M. leprae* revealed KFMC-1 was most closely related to 3K1 Ryukyu-2 (Appendix Figure 2, panel B), which was originally isolated in Japan (*4*).

We identified 158 polymorphic sites in the genome (Appendix Table 2), which corresponded to 136 single-nucleotide polymorphisms and 22 insertion/deletions. In total, 53 of the 158 changes were new, and 63 appeared within gene-coding regions, a couple of which helped us predict the multidrug-resistance profile. We identified a G→T nucleotide change, which leads to a nonsynonymous change (Q438H) in the *rpoB* gene (Appendix Figure 2, panel C). This substitution results in rifampin resistance (*5*), matching our clinical records. The C1414A mutation in the *rrs* locus is predicted to confer capreomycin resistance, as observed previously in *M. tuberculosis* (*6*).

After we confirmed the clinical diagnosis as an *M. leprae* infection, we halted moxifloxacin treatment and kept the patient on 3 standard antimicrobial drugs (clofazimine, dapsone, and rifampin). Afterward, the patient left Saudi Arabia and continued her antimicrobial drug course in her country of origin.

The predominant genotypes of *M. leprae* strains in the Middle East are subtypes 2 and 3 (*7*). Most 3K cases are found in countries of East Asia, such as China (*8*), Japan (*9*), Korea (*2*), and the Philippines (*8*). In addition, >37% of the leprosy cases in Saudi Arabia occur in persons from other countries (*1*). Our results suggest that this case of leprosy was imported from the patient's country of origin. Saudi Arabia hosts a massive number of expatriates from all over the world, including persons from *M. leprae*–endemic countries, and also hosts one of the largest recurring religious gatherings in the world. Therefore, genomics-guided infection control efforts are needed to monitor the potential importation and prevent the spread of *M. leprae* infections in the region.

About the Author

Mr. Guan is a graduate student in the Pathogen Genomics Laboratory of King Abdullah University of Science and Technology. His research focuses on the applications of bioin-formatics tools in understanding of pathogens and infectious diseases.

References

1. Alotaibi MH, Bahammam SA, Ur Rahman S, Bahnassy AA, Hassan IS, Alothman AF, et al. The demographic and clinical characteristics of leprosy in Saudi Arabia. J Infect Public Health. 2016;9:611–7. https://doi.org/10.1016/j.jiph.2015.12.015
2. Schuenemann VJ, Avanzi C, Krause-Kyora B, Seitz A, Herbig A, Inskip S, et al. Ancient genomes reveal a high diversity of *Mycobacterium leprae* in medieval Europe. PLoS Pathog. 2018;14:e1006997. https://doi.org/10.1371/journal.ppat.1006997
3. Cole ST, Eiglmeier K, Parkhill J, James KD, Thomson NR, Wheeler PR, et al. Massive gene decay in the leprosy bacillus. Nature. 2001;409:1007–11. https://doi.org/10.1038/35059006
4. Hosokawa A. A clinical and bacteriological examination of *Mycobacterium leprae* in the epidermis and cutaneous appendages of patients with multibacillary leprosy. J Dermatol. 1999;26:479–88. https://doi.org/10.1111/j.1346-8138.1999.tb02032.x
5. Kai M, Nguyen Phuc NH, Nguyen HA, Pham THBD, Nguyen KH, Miyamoto Y, et al. Analysis of drug-resistant strains of *Mycobacterium leprae* in an endemic area of Vietnam. Clin Infect Dis. 2011;52:e127–32. https://doi.org/10.1093/cid/ciq217
6. Suzuki Y, Katsukawa C, Tamaru A, Abe C, Makino M, Mizuguchi Y, et al. Detection of kanamycin-resistant

Mycobacterium tuberculosis by identifying mutations in the 16S rRNA gene. J Clin Microbiol. 1998;36:1220–5.
7. Monot M, Honoré N, Garnier T, Zidane N, Sherafi D, Paniz-Mondolfi A, et al. Comparative genomic and phylogeographic analysis of *Mycobacterium leprae*. Nat Genet. 2009;41:1282–9. https://doi.org/10.1038/ng.477
8. Weng X, Xing Y, Liu J, Wang Y, Ning Y, Li M, et al. Molecular, ethno-spatial epidemiology of leprosy in China: novel insights for tracing leprosy in endemic and non endemic provinces. Infect Genet Evol. 2013;14:361–8. https://doi.org/10.1016/j.meegid.2012.12.009
9. Benjak A, Avanzi C, Singh P, Loiseau C, Girma S, Busso P, et al. Phylogenomics and antimicrobial resistance of the leprosy bacillus *Mycobacterium leprae*. Nat Commun. 2018; 9:352. https://doi.org/10.1038/s41467-017-02576-z

Address for correspondence: Arnab Pain, King Abdullah University of Science and Technology, BESE Division, Thuwal-Jeddah, 239556900, Saudi Arabia; email: arnab.pain@kaust.edu.sa

Three New Cases of Melioidosis, Guadeloupe, French West Indies

Bénédicte Melot, Sylvaine Bastian, Nathalie Dournon, Eric Valade, Olivier Gorgé, Anne Le Fleche, Charlotte Idier, Mireille Vernier, Elisabeth Fernandes, Bruno Hoen, Sébastien Breurec, Michel Carles

Author affiliations: University Hospital of Guadeloupe, Pointe-à-Pitre, France (B. Melot, S. Bastian, N. Dournon, C. Idier, B. Hoen, S. Breurec, M. Carles); Ecole du Val-de-Grâce, Paris, France (E. Valade); Aix Marseille University, Marseille, France (E. Valade, O. Gorgé); Institut Pasteur, Paris (A. Le Fleche); Hospital of Basse-Terre, Basse-Terre, France (M. Vernier, E. Fernandes); Pasteur Institute of Guadeloupe, Pointe-à-Pitre (S. Breurec); University of the French West Indies and French Guiana, Pointe-à-Pitre (B. Hoen, S. Breurec, M. Carles)

DOI: https://doi.org/10.3201/eid2603.190718

Melioidosis has been detected in the Caribbean, and an increasing number of cases has been reported in the past few decades, but only 2 cases were reported in Guadeloupe during the past 20 years. We describe 3 more cases that occurred during 2016–2017 and examine arguments for increasing endemicity.

Melioidosis, caused by the telluric gram-negative rod *Burkholderia pseudomallei*, is endemic in Southeast Asia and northern Australia (*1*) but may be underdiagnosed in other tropical regions (*2*). Increasing occurrences have been reported in the Caribbean during the past few decades among persons with no exposure to known endemic areas (*3*–*5*). Tropical environmental conditions and the presence of this bacterium in soil samples in the Caribbean support the plausibility of endemicity (*3*). We describe 3 new cases detected in Guadeloupe during 2016–2017.

Patient 1 was a 54-year-old man, receiving renal replacement therapy, with a history of hypertensive vascular nephropathy. He developed a pulmonary form of melioidosis in November 2016. Thoracoabdominal computed tomography (CT) scan showed bilateral nodular lesions. *B. pseudomallei* grew from bronchoalveolar lavage fluid obtained by fiberoptic bronchoscopy. Treatment with ceftazidime (6 g/d intravenously) was given for 2 weeks and switched to trimethoprim/sulfamethoxazole (TMP/SMX) (320/1,600 mg 2×/d orally) for 1 month, then changed to doxycycline because rash developed. The patient complied poorly with treatment; he died in March 2017 under unknown circumstances.

Patient 2 was a 66-year-old woman with a history of arterial hypertension and diabetes mellitus, a subcutaneous abscess in the prepubic area surgically treated without microbiological identification (June 2016), a lumbar hematoma (March 2017), and bacteremic obstructive pyelonephritis caused by *Escherichia coli* (April 2017). In April 2017, she developed a severe and disseminated form of melioidosis with pneumonia, bacteremia, and deep abscess. CT scan showed multiple pulmonary nodes consistent with hematogenous pneumonia, a deep abscess between kidney and psoas, and splenic emboli. *B. pseudomallei* was isolated from blood cultures performed at admission and from the abscess. The patient developed multiple complications: acute respiratory distress syndrome, systemic candidiasis, renal failure, hemodynamic failure, nonspecific encephalopathy, refractory septic shock related to catheter infection, and bacteremia caused by extended spectrum β-lactamase *Klebsiella pneumoniae*. In the intensive care unit, she was treated with ceftazidime (6 g/d for 24 d), then with meropenem (1 g 3×/d) plus TMP/SMX (320/1,600 mg 2×/d). Blood cultures grew *B. pseudomallei* until day 40. The patient died on day 60 from multiple organ failure.

Patient 3 was a 52-year-old man with a history of chronic alcoholism. He developed pneumonia in April 2017. Thoracic tomography showed an excavated condensation of the right middle lobe, right

lower infiltrates, and multiple right hilar nodes. Bronchoalveolar lavage fluid contained *B. pseudomallei*. Intravenous ceftazidime (2 g 3×/d) for 40 days followed by oral TMP/SMX (320/1,600 mg 2×/d) slowly improved the clinical status, but 1 month after starting oral antimicrobial drug therapy, he had a drug reaction that caused eosinophilia and systematic symptoms. He died a year later despite appropriate treatment.

All patients were born and had always lived in the western part of Guadeloupe and Les Saintes islands, the rainiest places in Guadeloupe (1,500–5,500 mm of rainfall per year in 2017 [Météo France, http://www.meteofrance.gp/climat/pluies-annuelles/rr_an_guadeloupe]). The patients reported no travel history to endemic countries. All had a history of potential occupational or recreational exposure to *B. pseudomallei* (as farmers, gardeners) and predisposing risk factors, such as diabetes mellitus, chronic renal diseases, and alcoholism (*1*). The clinical manifestations of disease were classical, but all patients experienced severe side effects during their treatments, and the mortality rate was 100% (Table), which is much higher than in most series of reported cases, underlining the severity of this disease.

These 3 cases of melioidosis were identified over a 6-month period, in contrast with only 2 cases diagnosed and reported during the previous 20 years in Guadeloupe. The identification of the isolate from the first case was performed locally by the API-20NE system (bioMérieux, https://www.biomerieux.com) and confirmed by matrix-assisted laser desorption/ionization time-of-flight (MALDI-TOF) mass spectrometry and by real-time PCR (*6*) at a reference laboratory in France. The isolates from the other cases were not identified correctly by the API-20NE system, as often described (*7*). However, after the first case, we were aware that a wrinkled colony-forming, oxidase-positive, gram-negative bacillus resistant to colistin and aminoglycosides could be *B. pseudomallei.* Thus, the strains were sent to the reference laboratory for confirmation. All the isolates were genotyped by multilocus sequence typing (*8*). They belonged to sequence type (ST) 92 (n = 2) and 95 (n = 1), 2 clones previously described in Central and South America and Caribbean islands: Brazil (ST92), Puerto Rico (ST95), Martinique, and Mexico (ST92 and ST95 in both areas) (*9*). This finding highlights the potential role of this region as a reservoir for these clones.

Our experience suggests that the incidence of *B. pseudomallei* infection is probably underestimated in the Caribbean because of inadequate diagnostic laboratory facilities and the lack of knowledge about melioidosis among physicians and microbiologists. The tropical climate in this region provides suitable conditions for bacterial survival, and elevated alcoholism and diabetes rates among Caribbean populations cause weakened immunity that could lead to increased infection risk (*10*). Therefore, investigation of soil samples should be undertaken to identify the most likely sources of human infection in this area.

Table. Main comparative data for 3 cases of melioidosis in Guadeloupe, French West Indies*

Characteristic	Patient 1	Patient 2	Patient 3
Age, y	54	66	52
Sex	M	F	M
Place of birth	Guadeloupe	Guadeloupe	Guadeloupe
Place of residence	Bouillante	Deshaies	Les Saintes
Rainfall, mm/y	2,500–3,000	1,500–2,000	1,500–2,000
Concurrent conditions	Chronic renal failure (vascular nephropathy)	Diabetes	Chronic alcohol intake
Possible means of inoculation	Gardening without gloves	Animals breeding, gardening without gloves	Animals breeding, gardening without shoes
Clinical presentation according to the Infectious Disease Association of Thailand†	1: Multifocal infection with bacteremia (45% of cases, 87% mortality)	3: Localized infection (42% of cases, 9% mortality)	3: Localized infection (42% of cases, 9% mortality)
Time from first clinical signs to death	11 mo	2 mo	16 mo
Organ involvement	Pneumonia	Disseminated (psoas abscess, lung abscesses, bacteremia)	Pneumonia
MLST	ST92	ST95	ST92
Treatment	Ceftazidime + TMP/SMX, then doxycycline; TMP/SMX discontinued due to rash	Ceftazidime, meropenem, TMP/SMX	Ceftazidime + TMP/SMX; TMP/SMX discontinued due to DRESS syndrome
Outcome	Death	Death	Death

*DRESS, drug reaction with eosinophilia and systematic symptoms; MLST, multilocus sequence typing; ST, sequence type; TMP/SMX, trimethoprim/sulfamethoxazole.
†Punyagupta S. Melioidosis: review of 686 cases and presentation of a new clinical classification. In: Punyagupta S, Sirisanthana T, Stapatayavong B, eds. Melioidosis. Bangkok: Bangkok Medical; 1989:217–29; Leelarasamee A, Bovornkitti S. Melioidosis: review and update. Rev Infect Dis. 1989; 11:413–25.

Acknowledgments

We acknowledge the Departments of Infectious Diseases and Tropical Medicine, Intensive Care Medicine, and Microbiology of Pointe-à-Pitre University Hospital; L'Institut de Recherche Biomédicale des Armées, Brétigny-sur-Orge, France; and Cellule d'Intervention Biologique d'Urgence, Paris, France, for their valuable collaboration in the medical care, investigation, and participation for each case report.

About the Author

Dr. Melot is a medical doctor in infectious and tropical diseases at University Hospital of Guadeloupe, Pointe-à-Pitre, France, and holds a master's degree in public health and epidemiology. Her primary research interests include the study of tropical endemic infections.

References

1. Currie BJ, Ward L, Cheng AC. The epidemiology and clinical spectrum of melioidosis: 540 cases from the 20 year Darwin prospective study. PLoS Negl Trop Dis. 2010;4:e900. https://doi.org/10.1371/journal.pntd.0000900
2. Limmathurotsakul D, Golding N, Dance DAB, Messina JP, Pigott DM, Moyes CL, et al. Predicted global distribution of *Burkholderia pseudomallei* and burden of melioidosis. Nat Microbiol. 2016;1:15008. https://doi.org/10.1038/nmicrobiol.2015.8
3. Torres AG, Montufar FE, Gee JE, Hoffmaster AR, Elrod MG, Duarte-Valderrama C, et al. Melioidosis is in the Americas: a call to action for diagnosing and treating the disease. Am J Trop Med Hyg. 2018;99:563–4. https://doi.org/10.4269/ajtmh.18-0418
4. Sanchez-Villamil JI, Torres AG. Melioidosis in Mexico, Central America, and the Caribbean. Trop Med Infect Dis. 2018;3:24. https://doi.org/10.3390/tropicalmed3010024
5. Benoit TJ, Blaney DD, Doker TJ, Gee JE, Elrod MG, Rolim DB, et al. A review of melioidosis cases in the Americas. Am J Trop Med Hyg. 2015;93:1134–9. https://doi.org/10.4269/ajtmh.15-0405
6. Thibault FM, Valade E, Vidal DR. Identification and discrimination of *Burkholderia pseudomallei*, *B. mallei*, and *B. thailandensis* by real-time PCR targeting type III secretion system genes. J Clin Microbiol. 2004;42:5871–4. https://doi.org/10.1128/JCM.42.12.5871-5874.2004
7. Glass MB, Popovic T. Preliminary evaluation of the API 20NE and RapID NF plus systems for rapid identification of *Burkholderia pseudomallei* and *B. mallei*. J Clin Microbiol. 2005;43:479–83. https://doi.org/10.1128/JCM.43.1.479-483.2005
8. Godoy D, Randle G, Simpson AJ, Aanensen DM, Pitt TL, Kinoshita R, et al. Multilocus sequence typing and evolutionary relationships among the causative agents of melioidosis and glanders, *Burkholderia pseudomallei* and *Burkholderia mallei*. J Clin Microbiol. 2003;41:2068–79. https://doi.org/10.1128/JCM.41.5.2068-2079.2003
9. Hall CM, Jaramillo S, Jimenez R, Stone NE, Centner H, Busch JD, et al. *Burkholderia pseudomallei*, the causative agent of melioidosis, is rare but ecologically established and widely dispersed in the environment in Puerto Rico. PLoS Negl Trop Dis. 2019;13:e0007727. https://doi.org/10.1371/journal.pntd.0007727
10. Carrère P, Fagour C, Sportouch D, Gane-Troplent F, Hélène-Pelage J, Lang T, et al. Diabetes mellitus and obesity in the French Caribbean: a special vulnerability for women? Women Health. 2018;58:145–59. https://doi.org/10.1080/03630242.2017.1282396

Address for correspondence: Bénédicte Melot, Delocalized Centers for Prevention and Care, Hospital of Cayenne, Av des Flamboyants, Cayenne 97306, French Guiana; email: melotb@gmail.com

Coccidioidomycosis Skin Testing in a Commercially Insured Population, United States, 2014–2017[1]

Kaitlin Benedict, Orion Z. McCotter, Brendan R. Jackson

Author affiliation: Centers for Disease Control and Prevention, Atlanta, Georgia, USA

DOI: https://doi.org/10.3201/eid2603.190798

Coccidioidomycosis skin testing appears to be uncommon, based on US health insurance claims data. Patient demographic features were consistent with the approval of the test for adults, but few patients had previous coccidioidomycosis diagnosis codes supporting its use for detecting delayed-type hypersensitivity in those with a history of pulmonary coccidioidomycosis.

Coccidioidal skin testing has been a valuable epidemiologic and clinical tool for estimating the prevalence of previous *Coccidioides* spp. exposure and monitoring treatment response (*1*–*3*). Such testing could also be useful for evaluating healthy persons' risk of developing coccidioidomycosis (*3*). The skin test became commercially available again in 2014 after more than a decade; it is approved for adults 18–64 of age who have a history of pulmonary coccidioidomycosis (*3*,*4*). However, little is known about its use

[1]This work was presented in part at the 63rd Annual Coccidioidomycosis Study Group Conference, Sacramento, California, USA, April 5–6, 2019.

in the general population with unknown exposure to *Coccidioides*. We describe features of patients who have employer-sponsored insurance who received a *Coccidioides* skin test.

We used the IBM MarketScan Research Databases (https://www.ibm.com/products/marketscan-research-databases) to identify patients with a Current Procedural Terminology (CPT; https://www.ama-assn.org/amaone/cpt-current-procedural-terminology) code for a coccidioidomycosis skin test during 2014–2017. MarketScan health insurance claims data include outpatient visits and prescriptions and hospitalizations for employees, dependents, and retirees, representing >25% of all employer-sponsored beneficiaries throughout the United States. This analysis was not subject to review by the Centers for Disease Control and Prevention institutional review board because the data are fully deidentified.

We accessed the data through MarketScan Treatment Pathways, a web-based platform that includes data from persons with health insurance plans that contribute prescription drug data to MarketScan. We limited the analysis to patients continuously enrolled during the 3 months before and after the skin test. We examined periods up to 3 years before and 1 year after; because the primary features of interest did not change substantially, we focused on the smaller period to retain a larger study population.

We analyzed patient demographics; visits within 3 days to estimate the proportion who returned to have their test results read after 48 hours (compared with patients with a CPT code for tuberculosis skin testing); coccidioidomycosis diagnoses (International Classification of Diseases [ICD], 9th Revision, Clinical Modification, codes 115.00–115.99; ICD, 10th Revision, Clinical Modification, code B38); laboratory testing; and fluconazole prescriptions. We also examined certain underlying medical conditions and assessed the cost of skin test claims to patients and insurers among patients with noncapitated health plans.

Among ≈57 million MarketScan enrollees, 505 had a coccidioidomycosis skin test; 407 of those were continuously enrolled. Of those 407, most (n = 391, 89%) were 18–64 years of age, female (n = 243, 60%), and in California (n = 367, 90%) (Table). Thirty-five percent had a code for a subsequent visit within 3 days, compared with 24% of 1,061,118 patients who had a tuberculosis skin test. Test results were not available.

Table. Characteristics of patients who received a coccidioidomycosis skin test, 2014–2017, USA

Characteristic	Value	Diagnosis or procedure codes
Age, median, y (range)	46 (2–85)	
0–17	20 (5)	
18–34	73 (18)	
35–44	67 (16)	
45–54	105 (26)	
55–64	116 (29)	
≥65	26 (6)	
Sex		
M	164 (40)	
F	243 (60)	
Primary beneficiary's residence		
California	367 (90)	
Arizona	16 (4)	
Other or unknown state	24 (6)	
Underlying conditions		
Immune-mediated inflammatory disease	44 (11)	ICD-9-CM codes 555, 556, 696.0, 696.1, 696.8, 714.0, 714.2; ICD-10-CM codes K50, K51, L40, M023, M05, M06, M08, M33, M352, M45
Chronic obstructive pulmonary disease	40 (10)	ICD-9-CM codes 490–492, 494, 496; ICD-10-CM codes J41–J44
Diabetes	39 (10)	ICD-9-CM codes 249–250; ICD-10 codes E08–E11
HIV/AIDS	5 (1)	ICD-9-CM code 042; ICD-10-CM code B20
Solid organ or stem cell transplant	4 (1)	ICD-9-CM codes V42 (excluding V42.3–V42.5), 996.8; ICD-10-CM codes T86, Z94 (excluding Z94.5– Z94.7)
Hematologic malignancy	4 (1)	ICD-9-CM codes 200–208; ICD-10-CM codes C81–C86, C88, C90–C96
Fungal laboratory testing in the 3 mo before skin test		
Coccidioidomycosis serologic test	20 (5)	CPT codes 86331, 86171, 86635
Fungal culture	5 (1)	CPT codes 87101, 87102, 87103, 87106, 87107
Fungal smear	11 (3)	CPT codes 87205, 87206, 87210
Fungal laboratory testing on the day of or in the 3 mo after skin test		
Coccidioidomycosis serologic test	63 (15)	CPT codes 86331, 86171, 86635
Fungal culture	34 (8)	CPT codes 87101, 87102, 87103, 87106, 87107
Fungal smear	42 (10)	CPT codes 87205, 87206, 87210

*Values are no. (%) except as indicated. CPT, Current Procedural Terminology; ICD-9-CM, International Classification of Diseases, 9th Revision, Clinical Modification; ICD-10-CM, International Classification of Diseases, 10th Revision, Clinical Modification.

In the 3 months before the skin test, 5% had a coccidioidomycosis diagnosis code, 5% had a coccidioidomycosis serologic test code, and 5% had a fluconazole prescription. On the skin test date and in the 3 months after, 7% had a coccidioidomycosis diagnosis code, 15% had a serologic test, and 9% had a fluconazole prescription. Forty-four patients (11%) had noncapitated health plans; among those, the mean cost of skin test claims was $43.66 (range $0–$264). Mean costs were $31.57 (range $0–$184) to insurers and $12.09 (range $0–$264) to patients.

In the context of the large at-risk population in *Coccidioides*-endemic areas, coccidioidomycosis skin testing appears to be uncommon in this privately insured population. Real-world data on the test's use and performance in the general population are lacking, although it performs well for risk-stratifying prison inmates (*5*). Reasons for its low use could be its limited approved clinical indication to detect delayed-type hypersensitivity to *Coccidioides* in persons with a known history of disease or that the clinical implications of such testing may be unclear. Cost may also play a role, although it is unclear why most patients had capitated health plans. Reasons why most tests were performed in California rather than in Arizona (states where most coccidioidomycosis cases occur) are unknown.

Patient age was consistent with the test's approval for use in adults. However, few patients had coccidioidomycosis diagnosis codes, suggesting possible use of this test to screen for immunity in those with unknown exposure to *Coccidioides*, which has not been evaluated. Another explanation for the low frequency of coccidioidomycosis diagnosis codes in the 3 months before testing is a more distant coccidioidomycosis history. We observed laboratory testing and fluconazole prescription patterns that suggest that the test might be occasionally used as a supplemental diagnostic tool.

Patient return visit rate (35%) was comparable to that of tuberculosis skin testing. This proportion could appear falsely low if providers chose not to bill for reading the test results. In addition to lack of test results, limitations of this analysis include potential coding misclassification.

In summary, skin testing could be useful for evaluating healthy persons' risk of developing coccidioidomycosis but appears to be rare, even in endemic areas. Determining features of patients who receive a coccidioidomycosis skin test and assessing clinicians' knowledge and attitudes could provide insight into the test's clinical and epidemiologic value.

About the Author

Ms. Benedict is an epidemiologist in the Mycotic Diseases Branch, Division of Foodborne, Waterborne, and Environmental Diseases, National Center for Emerging and Zoonotic Infectious Diseases, Centers for Disease Control and Prevention, Atlanta, Georgia, USA. Her research interests include the epidemiology and prevention of fungal infections.

References

1. Edwards PQ, Palmer CE. Prevalence of sensitivity to coccidioidin, with special reference to specific and nonspecific reactions to coccidioidin and to histoplasmin. Dis Chest. 1957;31:35–60. https://doi.org/10.1378/chest.31.1.35
2. Smith CE, Whiting EG, Baker EE, Rosenberger HG, Beard RR, Saito MT. The use of coccidioidin. Am Rev Tuberc. 1948; 57:330–60.
3. Wack EE, Ampel NM, Sunenshine RH, Galgiani JN. The return of delayed-type hypersensitivity skin testing for coccidioidomycosis. Clin Infect Dis. 2015;61:787–91. https://doi.org/10.1093/cid/civ388
4. Johnson R, Kernerman SM, Sawtelle BG, Rastogi SC, Nielsen HS, Ampel NM. A reformulated spherule-derived coccidioidin (Spherusol) to detect delayed-type hypersensitivity in coccidioidomycosis. Mycopathologia. 2012;174:353–8. https://doi.org/10.1007/s11046-012-9555-6
5. Wheeler C, Lucas KD, Derado G, McCotter O, Tharratt RS, Chiller T, et al. Risk stratification with coccidioidal skin test to prevent Valley fever among inmates, California, 2015. J Correct Health Care. 2018;24:342–51. https://doi.org/10.1177/1078345818792679

Address for correspondence: Kaitlin Benedict, Centers for Disease Control and Prevention, 1600 Clifton Rd NE, Mailstop H24-9, Atlanta, GA 30329-4027, USA; email: jsy8@cdc.gov

Geographic Expansion of Sporotrichosis, Brazil

Isabella Dib Ferreira Gremião, Manoel Marques Evangelista Oliveira, Luisa Helena Monteiro de Miranda, Dayvison Francis Saraiva Freitas, Sandro Antonio Pereira

Author affiliation: Oswaldo Cruz Foundation, Rio de Janeiro, Brazil

DOI: https://doi.org/10.3201/eid2603.190803

Brazil has experienced geographic expansion of zoonotic sporotrichosis. Social problems in the country contribute substantially to the expansion. A comprehensive sporotrichosis control program is beyond the sphere of public health. A One Health approach is needed to control the disease in animals and humans.

High rates of human cases of sporotrichosis caused by *Sporothrix brasiliensis* transmitted by cats have been reported in Brazil since 1998 (*1*). The main referral center for the treatment of this mycotic disease, Oswaldo Cruz Foundation (Fiocruz) in Rio de Janeiro, recorded ≈5,000 human cases during 1998–2015 (D.F.S. Freitas, unpub. data) and 5,113 feline cases during 1998–2018 (S.A. Pereira, unpub. data). However, these numbers only represent cases diagnosed at 1 institution, and actual incidence rates likely are higher.

During 1998–2017, Brazil experienced a geographic expansion of sporotrichosis. The southeast region had the largest occurrence of human and animal cases (*1*,*2*), but outbreaks and case reports of feline sporotrichosis have been described from other regions (*3*,*4*,*5*) (Figure). In regions only reporting feline cases, zoonotic transmission probably is going unnoticed.

Zoonotic sporotrichosis also has been reported in the United States, India, Malaysia, Argentina, Mexico, and Panama (*2*). In Malaysia, isolates from cases caused by *S. schenckii* sensu stricto (*6*) have included clonal reproduction, which could indicate ongoing emergence of a genotype that is adapting to the feline host (*7*), similar to what was reported for *S. brasiliensis* in Brazil (*1*). Also, the occurrence of zoonotic sporotrichosis due to *S. brasiliensis* in Argentina is alarming because it points to a potential transboundary expansion of this virulent species to other regions in Latin America. Despite rules implemented for pet travel, poor control over road transportation might contribute to the spread of sporotrichosis in Brazil and could pose a risk for spread beyond its borders (*8*).

Fungal infections generally are neglected (*9*), and public health policies and strategic plans for prioritizing such infections are lacking. Inadequate surveillance of fungal infections leads to unnoticed emergence, such as seen with zoonotic sporotrichosis.

The rise and spread of sporotrichosis cases in Brazil were overlooked for several years, making a

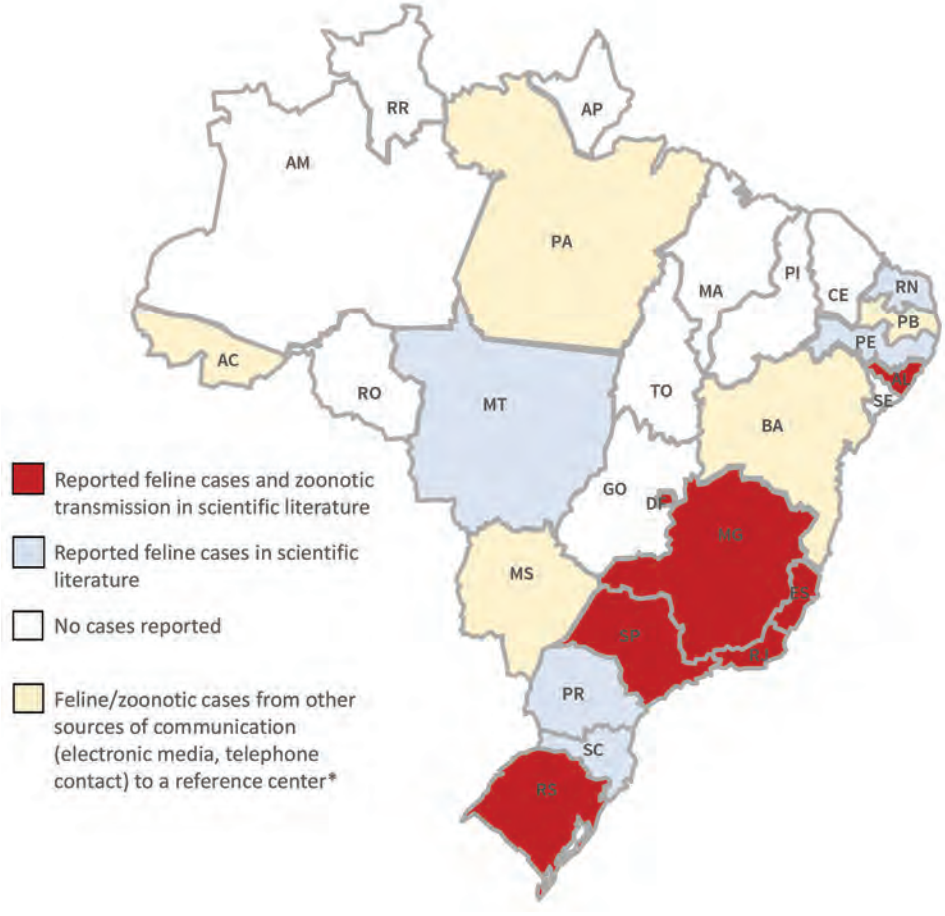

Figure. Occurrence of feline sporotrichosis and cases of zoonotic transmission in Brazil. *Reference center is the Laboratory of Clinical Research on Dermatozoonoses in Domestic Animals, Evandro Chagas National Institute of Infectious Diseases, Oswaldo Cruz Foundation (Fiocruz), Rio de Janeiro, Brazil. AC, Acre; AL, Alagoas; AM, Amazonas; AP, Amapá; BA, Bahia; CE, Ceará; DF, Federal District; ES, Espírito Santo; GO, Goiás; MA, Maranhão; MG, Minas Gerais; MS, Mato Grosso do Sul; MT, Mato Grosso; PA, Pará; PB, Paraíba; PE, Pernambuco; PI, Piauí; PR, Paraná; RJ, Rio de Janeiro; RN, Rio Grande do Norte; RO, Rondônia; RR, Roraima; RS, Rio Grande do Sui; SC, Santa Catarina; SE, Sergipe; SP, São Paulo; TO, Tocantins.

previously rare disease frequent and uncontrolled in many regions. Continuing socioeconomic and environmental difficulties, such as economic and social inequality, poverty, unemployment, urban agglomeration, and poor basic sanitation, coupled with scarce and inadequate health services, are fueling this expansion. In Rio de Janeiro, despite the high number of cases and the strain sporotrichosis puts on public health services, an animal sporotrichosis control program that included free diagnosis and treatment was not implemented until 16 years after the epidemic began. Nevertheless, given the chaotic situation in this region, the control measures used were insufficient. Even with the spread of the disease to other states in Brazil, compulsory notification is performed by only a few specific municipalities.

The absence of a comprehensive feline sporotrichosis control program in Brazil, the multifactorial difficulty in managing sick cats, and the lack of knowledge of sporotrichosis control measures by most of the population have contributed to the growing number of human and animal cases. A One Health approach is key for effective surveillance and successful control. Coordinated actions among veterinarians, laboratory practitioners, surveillance authorities, and other healthcare workers will ensure broader investigations and promote prevention, detection, and assistance for human and animal cases.

Early diagnosis of feline sporotrichosis is essential to guarantee appropriate prevention for owners, especially those at higher risk for infection, such as persons with immunosuppression. In addition, prompt treatment in felines can rapidly reduce the fungal load and risk for transmission of *Sporothrix* by cats (*10*). Thus, the availability of itraconazole, the first-line treatment for humans and animals, is essential in health units of affected areas.

The pattern of feline sporotrichosis appears to be changing in the world, with new cases of zoonotic transmission by other *Sporothrix* species appearing (*1*). Health authorities from neighboring countries should be aware of the signs and symptoms of disease to identify cases early and rapidly implement prevention and control measures. Atypical cases and treatment failures emphasize the need for studies focusing on the detection of potential antifungal resistance and alternative therapeutic strategies. The emergence of new species or changes in the behavior of known species also should be assessed, to identify variations in the ecoepidemiology and in host–pathogen interactions.

If health authorities in Rio de Janeiro had taken measures to control and prevent sporotrichosis in the feline population at the first appearance of human cases, the current scenario could be different and likely would have cost less to the health system in the long term. Considering the remarkable spread of sporotrichosis in the past decade, effective public health actions, including free medication and service for animals, are urgently needed to prevent additional cases in affected areas. We encourage a One Health approach to curb further expansion of sporotrichosis in humans and animals in Brazil.

Acknowledgments

The authors thank the Laboratory of Clinical Research on Dermatozoonoses in Domestic Animals, Evandro Chagas National Institute of Infectious Diseases, Oswaldo Cruz Foundation (Fiocruz), Rio de Janeiro, Brazil.

S.A.P. was supported in part by Jovem Cientista do Nosso Estado 2019 (JCNE) – FAPERJ (grant no. E-26/202.737/2019) and Conselho Nacional de Desenvolvimento Científico e Tecnológico (CNPq) (grant no. 309657/2016-4). M.M.E. O. was supported in part by FAPERJ (grant nos. INST E-26/010.001784/2016 and JCNE E-26/203.301/2017).

About the Author

Dr. Gremião is a veterinarian and researcher in the Laboratory of Clinical Research on Dermatozoonoses in Domestic Animals, Evandro Chagas National Institute of Infectious Diseases, Oswaldo Cruz Foundation (Fiocruz), Rio de Janeiro. Her areas of interest include epidemiology, diagnosis, and treatment of fungal diseases in animals, including sporotrichosis and cryptococcosis.

References

1. Lopes-Bezerra LM, Mora-Montes HM, Zhang Y, Nino-Vega G, Rodrigues AM, de Camargo ZP, et al. Sporotrichosis between 1898 and 2017: The evolution of knowledge on a changeable disease and on emerging etiological agents. Med Mycol. 2018;56(suppl_1):126–43. https://doi.org/10.1093/mmy/myx103
2. Gremião ID, Miranda LH, Reis EG, Rodrigues AM, Pereira SA. Zoonotic Epidemic of Sporotrichosis: Cat to Human Transmission. PLoS Pathog. 2017;13:e1006077. https://doi.org/10.1371/journal.ppat.1006077
3. Fernandes CGN, Moura ST, Dantas AFM, Blatt, MCS. Feline sporotrichosis–clinical and epidemiological aspects: case reports (Cuiabá, Mato Grosso, Brazil) [in Portuguese]. MedVep Rev Cient Med Vet Peq An. 2004;2:39–43.
4. Figueira KD, Nunes GDL. Feline sporotrichosis: first report in the city of Mossoró, Rio Grande do Norte, Brazil [in Portuguese]. MedVep Rev Cient Med Vet Peq An. 2010;8:715–18.
5. Silva GM, Howes JCF, Leal CAS, Mesquita EP, Pedrosa CM, Oliveira AAF, et al. Feline sporotrichosis outbreak in the metropolitan region of Recife [in

Portuguese]. Pesq Vet Bras. 2018;38:1767–71. http://dx.doi.org/10.1590/ 1678-5150-pvb-5027
6. Kano R, Okubo M, Siew HH, Kamata H, Hasegawa A. Molecular typing of *Sporothrix schenckii* isolates from cats in Malaysia. Mycoses. 2015;58:220–4. https://doi.org/10.1111/myc.12302
7. Siew HH. The current status of feline sporotrichosis in Malaysia. Med Mycol J. 2017;58:E107–13. https://doi.org/10.3314/mmj.17.014
8. Ministry of Agriculture, Livestock and Food Supply, Brazil. Traveling with pets [in Portuguese]. 2017 Nov 24 [cited 2019 Nov 08]. http://www.agricultura.gov.br/assuntos/vigilancia-agropecuaria/animais-estimacao
9. Seyedmousavi S, Guillot J, Tolooe A, Verweij PE, de Hoog GS. Neglected fungal zoonoses: hidden threats to man and animals. Clin Microbiol Infect. 2015;21:416–25. https://doi.org/10.1016/j.cmi.2015.02.031
10. de Miranda LHM, Silva JN, Gremião IDF, Menezes RC, Almeida-Paes R, Dos Reis EG, et al. Monitoring fungal burden and viability of *Sporothrix* spp. in skin lesions of cats for predicting antifungal treatment response. J Fungi (Basel). 2018;4:E92. https://doi.org/10.3390/jof4030092

Address for correspondence: Isabella D.F. Gremião, Evandro Chagas National Institute of Infectious Diseases, Fiocruz, Avenida Brasil, 4365 Rio de Janeiro 21040-360, Brazil; email: isabella.dib@ini.fiocruz.br

Need for BCG Vaccination to Prevent TB in High-Incidence Countries and Populations

Shalini Pooransingh, Sateesh Sakhamuri

Author affiliation: The University of the West Indies, St. Augustine, Trinidad and Tobago

DOI: https://doi.org/10.3201/eid2603.191232

An estimated one quarter of persons worldwide are infected with *Mycobacterium tuberculosis*. In 2018, the World Health Organization issued revised guidance on bacille Calmette-Guérin (BCG) vaccine for high-risk groups. The World Health Organization should consider guiding countries on a case-by-case basis in developing appropriate BCG policies to deliver equitable healthcare and protect public health.

In 1993, the World Health Organization (WHO) recognized tuberculosis (TB) as a global emergency (*1*). Twenty-five years later, TB remains a major public health challenge. It is the single leading infectious cause of death globally. An estimated one quarter of the world's population is infected with *Mycobacterium tuberculosis* (*2*). In 2017, 10 million persons became ill with TB, and 1.6 million died of it. That year, an estimated 1 million children became ill with TB, and 230,000 died (*3*).

Ending the TB epidemic by 2030 is a primary goal of WHO and, if achieved, will contribute to WHO's Sustainable Development Goal 3, which is concerned with health (*4*). In keeping with Pillar 1 of the End TB Strategy, no opportunity to control TB should be missed. The treatment for latent infection in combination with treatment measures for active disease or with preexposure vaccination can substantially decrease TB incidence (*5*).

Until a new TB vaccine is developed, *M. bovis* bacille Calmette-Guérin (BCG) remains the only effective vaccine for TB (*6*,*7*). BCG's overall efficacy, including cost-effectiveness, has been questioned by studies that were confounded by the cross-reactivity of antigens and the absence of measures to exclude latent infection before vaccination. None of these studies considered BCG's primary preventive effect on drug-resistant TB and tangential benefits, such as avoidance of prolonged treatment and unwanted adverse effects. BCG's importance is again increasing in light of new, encouraging evidence about its efficacy and because of the limited availability of alternative new anti-TB strategies.

BCG effectiveness in preventing the life-threatening forms of TB in children is unquestionable. Vaccination at birth or shortly thereafter protects against disseminated and pulmonary TB in young children (*4*). Vaccination is cost-effective in the following groups: infants in settings where TB incidence rates are >20 cases/100,000 population or 5 cases/100,000 smear-positive cases per year; school-aged children in high-risk settings in school-based catch-up programs; and settings with low TB incidence where vaccination of specific populations, such as immigrants from high-incidence countries and healthcare workers, is selectively administered. High global coverage and widespread use of BCG in routine infant vaccination programs could prevent >115,000 TB deaths per birth cohort during the first 15 years of life (*8*).

WHO therefore recommends that, in countries with a high incidence of TB, a single dose of BCG should be provided to all infants at or soon after birth as part of the national schedule. In countries with low TB incidence, BCG may be limited to neonates and infants in recognized high-risk groups or to older children who are skin test–negative for TB infection.

Despite clear evidence and WHO recommendations, however, global BCG administration practices appear to be arbitrary (*9*). Among 180 countries, 154 (86%) reported universal BCG vaccination. Of the other 26 countries, 20 reported having had a national BCG policy for everyone in the past, and the remaining 6 countries reported having selective vaccination for persons in high-risk groups. Among the 30 high TB–incidence countries globally, BCG coverage ranged from 53% to 99%; coverage was <80% in 6 high-incidence countries (*3*).

Governments committed to achieving universal health coverage should revise their national BCG vaccination policies to reflect newly available evidence. If health is genuinely considered a human right, this right might be realized only if governments provide the necessary services for equitable healthcare for all sectors of society. Equitable healthcare would mean BCG vaccine for all in high-incidence countries and selective vaccination for high-risk populations in low-incidence countries.

WHO is unfailing in its technical support to countries through activities such as developing guidelines, standards, and checklists, as well as supporting national and regional workshops. However, what might be needed is for regional and country WHO offices to perhaps be more proactive and more prescriptive in assisting with the adaptation of global strategies to the local country situation and with their follow up. Such action by WHO regional and country offices may assist countries with weak health information and surveillance systems and limited human resource technical capacity, both of which might limit the timely adaptation of national policies to international best practice guidance and to rapidly changing country demographics.

The WHO Multisectoral Accountability Framework to Accelerate Progress to End Tuberculosis (*10*) is timely; it supports accountability of stakeholders at all levels (global, regional, and country). However, critical indicators concerning screening and vaccination appear to be missing.

Neglecting End TB Strategy initiatives should no longer be accepted. Countries should not abandon BCG entirely. WHO should take an active role in guiding countries on a case-by-case basis in developing appropriate BCG policies to deliver equitable healthcare, thereby protecting public health and achieving the goals of the End TB Strategy.

About the Authors

Dr. Pooransingh is a lecturer in the Paraclinical Sciences Department, Faculty of Medical Sciences, The University of the West Indies. Her primary research interests include communicable disease control and healthcare quality.

Dr. Sakhamuri is a lecturer in the Clinical Medical Sciences Department, Faculty of Medical Sciences, The University of the West Indies. His primary research interests include airways disease and tuberculosis.

References

1. WHO Global Tuberculosis Program. TB: a global emergency. WHO report on the TB epidemic [cited 2019 Sep 27]. https://apps.who.int/iris/handle/10665/58749
2. Houben RM, Dodd PJ. The global burden of latent tuberculosis infection: a re- estimation using mathematical modelling. PLoS Med. 2016;13:e1002152. http://dx.doi.org/10.1371/journal.pmed.1002152
3. World Health Organization. Global tuberculosis report 2018 [cited 2019 Aug 4]. https://apps.who.int/iris/handle/10665/274453
4. World Health Organization. The End TB Strategy [cited 2019 Aug 4]. http://www.who.int/tb/strategy/end-tb
5. Roy A, Eisenhut M, Harris RJ, Rodrigues LC, Sridhar S, Habermann S, et al. Effect of BCG vaccination against *Mycobacterium tuberculosis* infection in children: systematic review and meta-analysis. BMJ. 2014;349(aug04 5):g4643. http://dx.doi.org/10.1136/bmj.g4643
6. Colditz GA, Brewer TF, Berkey CS, Wilson ME, Burdick E, Fineberg HV, et al. Efficacy of BCG vaccine in the prevention of tuberculosis. Meta-analysis of the published literature. JAMA. 1994;271:698–702. http://dx.doi.org/10.1001/jama.1994.03510330076038
7. Van Der Meeren O, Hatherill M, Nduba V, Wilkinson RJ, Muyoyeta M, Van Brakel E, et al. Phase 2b placebo controlled trial of M72/ASO1E candidate vaccine to prevent tuberculosis. N Engl J Med. 2018;379:1621–34. http://dx.doi.org/10.1056/NEJMoa1803484
8. BCG vaccines: WHO position paper – February 2018. Wkly Epidemiol Rec. 2018;93:73–96.
9. Zwerling A, Behr MA, Verma A, Brewer TF, Menzies D, Pai M. The BCG World Atlas: a database of global BCG vaccination policies and practices. PLoS Med. 2011; 8:e1001012. http://dx.doi.org/10.1371/journal.pmed.1001012
10. World Health Organization. Multisectoral accountability framework to accelerate progress to end tuberculosis by 2030 [cited 2019 Aug 3]. https://www.who.int/tb/publications/MultisectoralAccountability

Address for correspondence: Shalini Pooransingh, The University of the West Indies, Paraclinical Sciences, Mount Hope Trinidad and Tobago, St. Augustine, Trinidad and Tobago; email: shalini.pooransingh@sta.uwi.edu

Invasive *Candida bovina* Infection, France

Kévin Brunet, Alida Minoza, Blandine Rammaert, Vincent Portet-Sulla, Florent Hubert, Jean-Claude Lorenzo, Marie-Hélène Rodier, Estelle Cateau

Author affiliations: Poitiers University Hospital, Poitiers, France (K. Brunet, A. Minoza, B. Rammaert, V. Portet-Sulla, F. Hubert, J.-C. Lorenzo, M.-H. Rodier, E. Cateau); INSERM U1070, Poitiers (K. Brunet, B. Rammaert); University of Poitiers, Poitiers (K. Brunet, B. Rammaert, M.-H. Rodier, E. Cateau); CNRS 7267, Poitiers (M.-H. Rodier, E. Cateau)

New *Candida* species such as *Candida auris* have emerged recently as important invasive fungal diseases. We report a case of *C. bovina* bloodstream infection in a 94-year-old patient in France. The species led to identification issues because it was misidentified by phenotypic and matrix-assisted laser desorption/ionization time-of-flight mass spectrometry methods.

DOI: https://doi.org/10.3201/eid2603.191371

A 94-year-old patient in France with no remarkable medical history was hospitalized because of a fall. During hospitalization, the patient had digestive disorders with postprandial regurgitations, leading to undernutrition. At hospital day 24, we performed an abdominal computed tomography scan, which indicated a dolicho-mega esophagus. Because of undernutrition, we introduced parenteral nutrition through peripheral venous catheter on day 36. We performed endoscopic pneumatic dilation to treat achalasia of the esophagus lower sphincter on day 51. One day later (day 52), the patient had a fever, triggering a bloodstream culture, which was positive after 24 hours (day 53) for *Streptococcus mitis/oralis* and *S. gordonii*. Parenteral nutrition was stopped, the peripheral catheter was removed, and the patient received piperacillin/tazobactam. On day 56, a catheter culture was positive for *S. mitis/oralis* and for a yeast. We identified this yeast by using matrix-assisted laser desorption/ionization time-of-flight (MALDI-TOF) mass spectrometry with the Vitek MS 3.2 system (bioMérieux, https://www.biomerieux-diagnostics.com), which revealed *Candida slooffiae* with a maximal score of probability.

We performed bloodstream cultures on day 57. Aerobic culture was positive on day 58 for a yeast again, which we identified as *C. slooffiae* by using Vitek MS, and anaerobic culture was positive for *S. anginosus*. We initiated treatment with caspofungin (70 mg loading dose, then 50 mg/d). Three days later, the patient was nonpyretic, and the inflammatory syndrome regressed. Results of blood cultures performed on day 63 were negative. Caspofungin was continued for 14 days after the negative culture, and no valvular disease or cardiac failure was noted. Moreover, funduscopic examination revealed no abnormalities.

Although Vitek MS indicated a MALDI-TOF mass spectrometry high score of identification, we performed sequencing of *Candida* 18S ribosomal DNA to confirm identification of this rare species. This sequencing identified the isolate as *C. bovina* (GenBank accession no. MN704805). Sequence analysis showed 100% similarity with ribosomal DNA sequences (internal transcribed spacer [ITS] 1–5.8S through ITS2–28S) of 2 *C. bovina* isolates from 2 different collection centers (GenBank nos. KY103626.1 and KP132306.1). After 90 days of monitoring, the patient showed improvement and had no relapse of infection.

The prevalence of healthcare-associated *Candida* bloodstream infections has increased over recent decades in many countries, mainly because of use of immunosuppressive drugs and critical care therapies (*1*). Among involved species, non–*C. albicans Candida* have emerged, especially because of use of fluconazole as a prophylactic drug, which promotes emergence of fluconazole nonsusceptible *Candida* (*1*,*2*). Moreover, new *Candida* species have emerged, such as *C. auris* (*3*). Enhanced use of antifungal agents in susceptible patients might lead to an increase of candidiasis because of uncommon *Candida* species. The ability to identify and treat infections with these organisms, which might have high antifungal MICs, is critical.

C. bovina, first described in 1957 from bovine cecum (*4*), is a member of the *Kazachstania* (*Arxiozyma*) *telluris* complex, which includes *C.* (*Kazachstania*) *bovina*, *C.* (*Kazachstania*) *pintolopesii*, *C.* (*Kazachstania*) *sloofiae*, *K. heterogenica*, and *K. telluris* (*5*). Members of the *K. telluris* complex are known to cause infections in rodents and birds and, less frequently, in horses, pigs, and cows (*5*). *C. bovina* has been isolated from cows, birds, and, rarely, humans (*5*), but human disease has not been previously reported.

C. bovina yeast grows on usual yeast culture media (i.e., Sabouraud, Sabouraud gentamicin chloramphenicol, and potato dextrose agar) in 24 hours and forms small colonies. This yeast was inhibited by cycloheximide and was found to be white on a chromogenic CAN2 medium (bioMérieux). Attention must be paid to misidentification through use of

Table. Antifungal susceptibility of *Candida bovina* from a patient in France, evaluated by using EUCAST broth microdilution*

Antifungal agent	MIC, mg/L
Fluconazole	2
Posaconazole	≤0.016
Voriconazole	0.03
Isavuconazole	0.015
Amphotericin B	0.03
Caspofungin	0.06
Micafungin	0.03

*EUCAST, European Committee on Antimicrobial Susceptibility Testing.

MALDI-TOF mass spectrometry technology, which appears unable to distinguish yeasts inside the *Kazachstania (Arxiozyma) telluris* complex. Vitek MS 3.2 identified the organism as *C. slooffiae*; identification was *K. telluris* by using Bruker Biotyper MS 4.1.80 (Bruker Daltonics, https://www.bruker.com). Phenotypic identification using the Vitek2 YST card (bioMérieux) was unable to identify fungi. Sequencing of ITS1 and ITS4 (18S ribosomal DNA) must be performed and appears able to effectively differentiate species inside this complex.

We evaluated MICs by using European Committee on Antimicrobial Susceptibility Testing broth microdilution (*6*) (Table). Among azoles, fluconazole showed MICs of 2 mg/L, considered susceptible because the breakpoint for all non–*C. glabrata Candida* is 2 mg/L. However, this MIC is higher than those of common *Candida*, such as *C. albicans* (MIC_{90} ≤0.25 mg/L) (*7*). For other antifungal agents, interpretation of MICs is complicated in the absence of specific clinical breakpoints. However, MICs were comparable to those of common species (*7*). In the case of this patient, catheter removal and caspofungin treatment led to recovery.

In conclusion, this case illustrates the emergence of an uncommon *Candida* species about which laboratory staff are advised to be aware. These new species might lead to issues with identification and antifungal susceptibility. Clinicians should remain skeptical of infections with uncommon yeast species and consider confirmation through DNA sequencing.

Acknowledgments

We thank Lauranne Broutin and Laureen Leduc-Aumerle for their participation in identification testing, Jeffrey Arsham for help the English revision of the manuscript, and Marie Desnos-Ollivier for identification and antifungal susceptibility expertise.

The strain was deposited in the National Reference Center for Invasive Mycoses and Antifungals (CNRMA), Institut Pasteur, Paris, France. It was also deposited in the CBS-KNAW Collections (Westerdijk Fungal Biodiversity Institute). The nucleotide sequence was deposited in GenBank (accession no. MN704805).

About the Author

Dr. Brunet is a microbiologist at the University Hospital of Poitiers and a PhD student at the University of Poitiers. His primary research interests include invasive fungal infections.

References

1. Koehler P, Stecher M, Cornely OA, Koehler D, Vehreschild MJGT, Bohlius J, et al. Morbidity and mortality of candidaemia in Europe: an epidemiologic meta-analysis. Clin Microbiol Infect. 2019;25:1200–12. https://doi.org/10.1016/j.cmi.2019.04.024
2. Kullberg BJ, Arendrup MC. Invasive candidiasis. N Engl J Med. 2015;373:1445–56. https://doi.org/10.1056/NEJMra1315399
3. Jeffery-Smith A, Taori SK, Schelenz S, Jeffery K, Johnson EM, Borman A, et al.; Candida auris Incident Management Team. *Candida auris*: a review of the literature. Clin Microbiol Rev. 2017;31:e00029–17. https://doi.org/10.1128/CMR.00029-17
4. Van Uden N, Do Sousa LC. Yeasts from the bovine caecum. J Gen Microbiol. 1957;16:385–95. https://doi.org/10.1099/00221287-16-2-385
5. Kurtzman CP, Robnett CJ, Ward JM, Brayton C, Gorelick P, Walsh TJ. Multigene phylogenetic analysis of pathogenic *Candida* species in the *Kazachstania* (*Arxiozyma*) *telluris* complex and description of their ascosporic states as *Kazachstania bovina* sp. nov., *K. heterogenica* sp. nov., *K. pintolopesii* sp. nov., and *K. slooffiae* sp. nov. J Clin Microbiol. 2005;43:101–11. https://doi.org/10.1128/JCM.43.1.101-111.2005
6. European Committee on Antimicrobial Susceptibility Testing (EUCAST). Method for the determination of broth dilution minimum inhibitory concentrations of antifungal agents for yeast. 2017 [cited 2019 Dec 1]. http://www.eucast.org/fileadmin/src/media/PDFs/EUCAST_files/AFST/Files/EUCAST_E_Def_7_3_1_Yeast_testing__definitive.pdf
7. Castanheira M, Deshpande LM, Davis AP, Rhomberg PR, Pfaller MA. Monitoring antifungal resistance in a global collection of invasive yeasts and molds: application of CLSI epidemiological cutoff values and whole-genome sequencing analysis for detection of azole resistance in *Candida albicans*. Antimicrob Agents Chemother. 2017;61:e00906–17. https://doi.org/10.1128/AAC.00906-17

Address for correspondence: Kévin Brunet, CHU de Poitiers, Bâtiment UBM, Laboratoire de Parasitologie et Mycologie Médicale, 86021 Poitiers, CEDEX, France; email: kevin.brunet@univ-poitiers.fr

Chlamydia abortus in Pregnant Woman with Acute Respiratory Distress Syndrome

Nicolas Pichon, Laure Guindre, Karine Laroucau, Muriel Cantaloube, Agathe Nallatamby, Simon Parreau

Author affiliations: Hospital Dubois, Brive La Gaillarde, France (N. Pichon, L. Guindre, M. Cantaloube); ANSES, Maisons-Alfort, France (K. Laroucau); University Hospital Dupuytren, Limoges, France (A. Nallatamby, S. Parreau)

DOI: https://doi.org/10.3201/eid2603.191417

We describe a case of *Chlamydia abortus* in a woman in rural France who was pregnant, developed severe generalized infection, and suffered fetal loss. The case stresses the need for healthcare personnel to perform thorough anamnesis in pregnant women in farming areas and to advise them to avoid contact with small ruminants.

A 27-year-old pregnant woman in week 23 of gestation with no other known medical conditions was admitted to a hospital in rural France for influenza-like illness, headache, dry cough, and fever (38.3°C). Ultrasound examination showed a single viable unaffected fetus and no abnormalities in the placenta or amount of amniotic fluid. Laboratory data revealed a raised C-reactive protein of 159 mg/L (reference <12 mg/L) and pronounced thrombocytopenia (platelet count 27 G/L [reference range 150–350 G/L]) without leukocytopenia. Results of urinalysis and blood cultures, including routine bacterial diagnosis, were negative, as were maternal serologic tests for toxoplasmosis, cytomegalovirus, rubella, and syphilis. Results of serologic tests for parvovirus B19, Epstein-Barr virus, and varicella zoster virus were positive for IgG. PCR results for *Chlamydia trachomatis* were negative from vaginal swab specimens, and results of an amniocentesis were negative.

Probabilistic treatment was started with cefotaxime and metronidazole, but the patient's condition did not improve over the next 48 hours. She had arterial hypotension (96/55 mm Hg), acute respiratory distress syndrome (PaO_2/FiO_2 114 mm Hg), and hypercapnia ($PaCO_2$ 68 mm Hg). She was admitted to the intensive care unit, where she was intubated and placed on a ventilator. Her chest radiographs were consistent with acute respiratory distress syndrome (Figure, panel A). A follow-up pelvic ultrasound showed death of the fetus in utero, and clinicians conducted a delivery.

When we queried the patient's husband on her history, we learned he was a goat farmer. He also informed us about an increased number of abortions among the herd during the previous 2 years and that the goats were not vaccinated against *Chlamydia abortus*. Despite absence of direct contact between his wife and the animals, we immediately changed the patient's antimicrobial drug therapy to doxycycline. The patient improved clinically and biologically and was discharged from the hospital 3 weeks later.

Histopathologic examination of the placenta showed acute villitis and intervillitis on the maternal side (Figure, panels B–D). Immunohistochemistry using antichlamydial lipopolysaccharide antibody and *C. abortus*–specific antibody did not identify chlamydia in the placenta. However, high-resolution melt PCR analysis of isolates from placenta tissue was positive for a wild-type *C. abortus* but not for the live vaccine strain.

Human infection with *C. abortus* is rare but devastating (*1*). *C. abortus* induces pelvic inflammatory disease in pregnant women and replicates in the trophoblast epithelium, which leads to placental dysfunction and late-term fetal death (*2*–*4*). The infection in pregnant women often requires hospitalization in an intensive care unit and causes fetal death (*5*). Most reported cases of human infection involve direct contact of pregnant women with infected animals, but indirect contact by visiting or living on or close to a farm affected by enzootic abortion also has been described (*6*). When pregnant women, especially those who live in rural areas, arrive in the emergency department with rapidly worsening influenza-like illness, a thorough patient history is necessary, and clinicians should give special attention to possible contact with animals from an infected herd (*5*). In this case, delayed information on the husband's occupation and the high rate of abortions in the herd explained why zoonotic infection, especially *C. abortus*, was not included in initial diagnostic tests and treatment until chlamydia was excluded.

The route of transmission to humans for *C. abortus* is uncertain, but direct contact with infected placenta and infective secretions are likely routes. The risk is limited mainly to those actively working with small ruminants, including veterinarians, and their immediate families. Large amounts of *C. abortus* are discharged through vaginal fluids of infected animals ≤2 weeks before and ≤2 weeks after abortion. Even without abortion, bacteria are eliminated through the placenta and vaginal fluids during

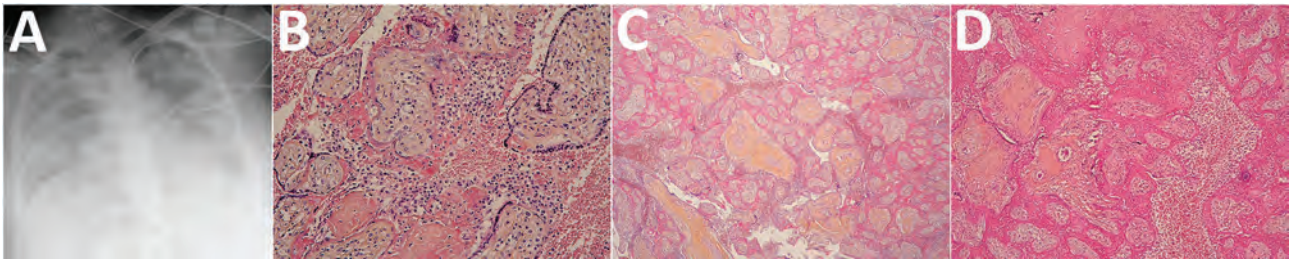

Figure. Radiographic and histologic images from a pregnant woman in rural France infected with *Chlamydia abortus*. A) Chest radiograph demonstrating bilateral pulmonary edema consistent with acute respiratory distress syndrome; B) hematoxylin and eosin (H&E) stained section of placenta showing acute histiocytic intervillitis zones (original magnification ×200); C) H&E stained section of placenta showing intervillitis hemorrhage (original magnification ×100); D) H&E stained section of placenta showing necrotizing mural arteritis (original magnification ×100).

labor in infected animals. Urine, milk, and feces also can contain small amounts of the bacteria following abortion. Women are at risk if they have close contact with small ruminants, but infection also has been associated with handling contaminated clothing and boots. We believe this patient had an indirect mode of transmission.

No effective human chlamydia vaccines are available (*7*). An early, phase 1 clinical trial assessed the safety and immunogenicity of a novel *C. trachomatis* vaccine in humans (*8*,*9*), but that vaccine would not be effective against *C. abortus*. An attenuated *C. abortus* vaccine is available for use in small ruminants but is not safe or approved for use in humans. Developing a human vaccine or adapting the existing veterinary vaccine to humans for such a rare zoonotic infection is not cost-effective. Instead, healthcare personnel should be educated on the importance of thorough anamnesis, and pregnant women living in farming areas should be informed about zoonotic infections. Prevention is the best course against human infection with *C. abortus*, but early recognition, targeted laboratory diagnosis, and appropriate treatment can reduce miscarriage and other effects in pregnant women.

Acknowledgments

We thank Marie Carrier, Laura Mesturoux, and Caroline Lavignac for assisting with histopathologic findings.

About the Author

Dr. Pichon is an intensivist in the medical-surgical critical care department, Hospital Dubois, Brive La Gaillarde. His primary research interest is sepsis in critical care medicine.

References

1. Walder G, Hotzel H, Brezinka C, Gritsch W, Tauber R, Würzner R, et al. An unusual cause of sepsis during pregnancy: recognizing infection with *chlamydophila abortus*. Obstet Gynecol. 2005;106:1215–7. https://doi.org/10.1097/01.AOG.0000161060.69470.9c
2. Cohen CR, Brunham RC. Pathogenesis of chlamydia induced pelvic inflammatory disease. Sex Transm Infect. 1999;75:21–4. https://doi.org/10.1136/sti.75.1.21
3. Walder G, Meusburger H, Hotzel H, Oehme A, Neunteufel W, Dierich MP, et al. *Chlamydophila abortus* pelvic inflammatory disease. Emerg Infect Dis. 2003;9:1642–4. https://doi.org/10.3201/eid0912.020566
4. Pospischil A, Thoma R, Hilbe M, Grest P, Gebbers JO. Abortion in woman caused by caprine *Chlamydophila abortus* (*Chlamydia psittaci* serovar 1). Swiss Med Wkly. 2002;132:64–6. https://doi.org/10.4414/smw.2002.09911
5. Meijer A, Brandenburg A, de Vries J, Beentjes J, Roholl P, Dercksen D. *Chlamydophila abortus* infection in a pregnant woman associated with indirect contact with infected goats. Eur J Clin Microbiol Infect Dis. 2004;23:487–90. https://doi.org/10.1007/s10096-004-1139-z
6. Cheong HC, Lee CYQ, Cheok YY, Tan GMY, Looi CY, Wong WF. *Chlamydiaceae*: diseases in primary hosts and zoonosis. Microorganisms. 2019;7:146. https://doi.org/10.3390/microorganisms7050146
7. de la Maza LM, Zhong G, Brunham RC. Update on *Chlamydia trachomatis* vaccinology. Clin Vaccine Immunol. 2017;24:e00543-16. https://doi.org/10.1128/CVI.00543-16
8. Poston TB, Darville T. First genital chlamydia vaccine enters in-human clinical trial. Lancet Infect Dis. 2019;19:1039–40. https://doi.org/10.1016/S1473-3099(19)30290-7
9. Abraham S, Juel HB, Bang P, Cheeseman HM, Dohn RB, Cole T, et al. Safety and immunogenicity of the chlamydia vaccine candidate CTH522 adjuvanted with CAF01 liposomes or aluminium hydroxide: a first-in-human, randomised, double-blind, placebo-controlled, phase 1 trial. Lancet Infect Dis. 2019;19:1091–1100. https://doi.org/10.1016/S1473-3099(19)30279-8

Address for correspondence: Nicolas Pichon, Hospital Dubois, Department of Intensive Care Medicine, Boulevard du Docteur Verlhac, 19100 Brive La Gaillarde, France; email: nicolas.pichon@ch-brive.fr

Novel Techniques for Detection of *Mycobacterium bovis* Infection in a Cheetah

Tanya J. Kerr, Rachiel Gumbo, Wynand J. Goosen, Peter Rogers, Robert D. Last, Michele A. Miller

Author affiliations: Stellenbosch University, Cape Town, South Africa (T.J. Kerr, R. Gumbo, W.J. Goosen, M.A. Miller); Provet Wildlife Services, Hoedspruit, South Africa (P. Rogers); VetDiagnostix, Veterinary Pathology Services, Pietermaritzburg, South Africa (R.D. Last)

DOI: https://doi.org/10.3201/eid2603.191542

In South Africa, bovine tuberculosis threatens some of Africa's most iconic wildlife species, including the cheetah (*Acinonyx jubatus*). The lack of antemortem diagnostic tests for this species strongly hinders conservation efforts. We report use of antemortem and postmortem diagnostic assays to detect *Mycobacterium bovis* infection in a cheetah.

Charismatic carnivore species such as the cheetah (*Acinonyx jubatus*) are considered a priority within conservation areas. However, the global population of cheetahs is decreasing; they are classified as vulnerable to extinction by the International Union for Conservation of Nature Red List of Threatened Species (*1*). Infectious diseases, such as bovine tuberculosis, pose a threat to wild carnivore populations, especially those that are small and fragmented (*2*). Bovine tuberculosis, caused by *Mycobacterium bovis*, affects multiple wildlife species in South Africa. Although fatal *M. bovis* infection has been described in a cheetah in Greater Kruger National Park, South Africa (*3*), reports of antemortem diagnosis in this species in South Africa have not been published. We report use of antemortem and postmortem diagnostic assays to detect *M. bovis* infection in a cheetah.

The study protocol was approved by the Stellenbosch University Research Ethics Committee (protocol no. SU-ACU-2019–10286). In January 2019, an adult female cheetah from a breeding center showed signs of chronic pneumonia. A positive test result was observed for an intradermal comparative cervical tuberculin test, based on the protocol described for African lions (*Panthera leo*) (*4*).

Thereafter, blood was collected for additional immunologic tests, including the *CXCL9* gene expression assay (GEA) and the Dual Path Platform (DPP) Vet TB Serologic Assay (Chembio Diagnostic Systems, Inc., http://chembio.com). The use of these assays has been reported for African lions (*5,6*). In brief, we performed the *CXCL9* GEA by adding whole blood into QuantiFERON-TB Gold Plus tubes (QIAGEN, https://www.qiagen.com) and incubating for 24 hours at 37°C. We stabilized whole blood cell pellets by using RNALater Solution (Ambion, https://www.thermofisher.com), after which we extracted RNA by using the RiboPure Blood Kit (Ambion) and reverse transcribed this RNA by using the Quantitect Reverse Transcription Kit (QIAGEN). We performed quantitative PCR as described for lions (*5*). Using previously determined cutoff values calculated for lions, we interpreted the mycobacterial peptide-specific response for the cheetah as *CXCL9* GEA positive ($2^{-\Delta\Delta Cq}$ = 90.09; cutoff value ≥27).

In addition, we tested serum by using a commercial DPP serologic assay (*6*). We detected antibodies to the antigen MBP83 (relative light units = 52.5, cutoff value ≥5). On the basis of these antemortem test results, the cheetah was suspected to be infected with *M. bovis* and was euthanized.

The postmortem examination and histopathologic findings showed a severe multifocal to coalescent, necrotizing, caseous, granulomatous bronchopneumonia. Lung tissues were processed for mycobacterial culture, and culture isolates were genetically speciated by using genomic regions of difference PCR and spoligotyping, as described (*7,8*). Using this approach, we confirmed that the cheetah was infected with *M. bovis* isolate SB0121, a strain commonly found in Greater Kruger National Park.

We also detected *M. tuberculosis* complex (MTBC) DNA in lung tissues before mycobacterial culture results were obtained by using the GeneXpert MTB/RIF Ultra Assay (Cepheid, https://www.cepheid.com) (*9*). GeneXpert PCR machines are widely available in numerous human tuberculosis clinics and laboratories across South Africa to enable rapid identification of human MTBC infections (*9*). Therefore, this tool might also be useful for MTBC diagnosis in wildlife if samples can be taken to these clinics.

Within the borders of South Africa, most cheetahs are found in fragmented populations, resulting in development of an actively managed metapopulation, which is currently composed of 60 reserves (V. van der Merwe, Endangered Wildlife Trust, pers. comm., 2019 Nov 8). The primary goal of the metapopulation is to maintain genetic diversity by translocating animals between reserves. One of the current challenges facing cheetah conservation is quarantine and restricted movement of cheetahs from premises that have known *M. bovis*–infected species present. Because movement of cheetahs from these populations requires tuberculosis testing, the lack of antemortem

diagnostic tests, which can distinguish between *M. bovis*–infected and uninfected animals, strongly hinders conservation efforts.

Although tuberculosis diagnostic tests for other species rely predominantly on detection of the adaptive immune response of the host, only a few studies investigated immunoassays for wild felids (*6*). In this instance, the tuberculin skin test response was key to promoting further investigation. The decision to use the lion *CXCL9* GEA for this cheetah was based on its previously reported sensitivity of 87.5% for lions (*10*) and the assumption that various cytokine mRNA transcripts were homologous between wild felid species. This assumption was strongly supported when it appeared to be an accurate indicator of *M. bovis* infection after confirmation by mycobacterial culture. In addition, the DPP serologic assay detected a strong antibody response to *M. bovis* antigen MPB83 during antemortem screening of this cheetah. Because these findings are limited to 1 case, further investigation in a larger cohort is required before drawing conclusions about the ability of these diagnostic assays to discriminate between *M. bovis*–infected and uninfected cheetahs.

In conclusion, novel antemortem immunoassays (*CXCL9* GEA and DPP) and a postmortem PCR (GeneXpert Ultra) appear to be promising tools for detection of *M. bovis* infection in cheetahs. Tests that can accurately identify *M. bovis*–infected cheetahs are crucial to supporting conservation efforts and tuberculosis control.

This study was supported by the South African Medical Research Council, the National Research Foundation, South African Research Chair Initiative (SARChI grant no. 86949), and the Stellenbosch University Faculty of Medicine and Health Science.

About the Author

Dr. Kerr is a postdoctoral researcher in the Animal TB Research Group at Stellenbosch University, Cape Town, South Africa. Her primary research interest is developing tools with diagnostic potential for tuberculosis detection in wildlife species including large felids (African lion, leopard, and cheetah), African elephants, and various antelope species.

References

1. Durant S, Mitchell N, Ipavec A, Groom R. *Acinonyx jubatus*, cheetah. In: The IUCN red list of threaten species. Version 2019–2 [cited 2019 Jun 6]. https://www.iucnredlist.org
2. Higgitt RL, Louis van Schalkwyk O, de Klerk-Lorist L-M, Buss PE, Caldwell P, Rossouw L, et al. *Mycobacterium bovis* infection in African wild dogs, Kruger National Park, South Africa. Emerg Infect Dis. 2019;25:1425–7. https://doi.org/10.3201/eid2507.181653
3. Keet DF, Kriek NP, Penrith ML, Michel A, Huchzermeyer H. Tuberculosis in buffaloes (*Syncerus caffer*) in the Kruger National Park: spread of the disease to other species. Onderstepoort J Vet Res. 1996;63:239–44.
4. Keet DF, Michel AL, Bengis RG, Becker P, van Dyk DS, van Vuuren M, et al. Intradermal tuberculin testing of wild African lions (*Panthera leo*) naturally exposed to infection with Mycobacterium bovis. Vet Microbiol. 2010;144:384–91. https://doi.org/10.1016/j.vetmic.2010.01.028
5. Olivier TT, Viljoen IM, Hofmeyr J, Hausler GA, Goosen WJ, Tordiffe ASW, et al. Development of a gene expression assay for the diagnosis of *Mycobacterium bovis* infection in African lions (*Panthera leo*). Transbound Emerg Dis. 2017;64:774–81. https://doi.org/10.1111/tbed.12436
6. Miller MA, Buss P, Sylvester TT, Lyashchenko KP, deKlerk-Lorist L-M, Bengis R, et al. *Mycobacterium bovis* in free-rangng lions (*Panthera leo*): evaluation of serological and tuberculin skin tests for detection of infection and disease. J Zoo Wildl Med. 2019;50:7–15. https://doi.org/10.1638/2017-0187
7. Goosen WJ, Miller MA, Chegou NN, Cooper D, Warren RM, van Helden PD, et al. Agreement between assays of cell-mediated immunity utilizing *Mycobacterium bovis*–specific antigens for the diagnosis of tuberculosis in African buffaloes (*Syncerus caffer*). Vet Immunol Immunopathol. 2014;160:133–8. https://doi.org/10.1016/j.vetimm.2014.03.015
8. Kamerbeek J, Schouls L, Kolk A, van Agterveld M, van Soolingen D, Kuijper S, et al. Simultaneous detection and strain differentiation of *Mycobacterium tuberculosis* for diagnosis and epidemiology. J Clin Microbiol. 1997;35:907–14.
9. Chakravorty S, Simmons AM, Rowneki M, Parmar H, Cao Y, Ryan J, et al. The New Xpert MTB/RIF Ultra: improving detection of *Mycobacterium tuberculosis* and resistance to rifampin in an assay suitable for point-of-care testing. MBio. 2017;8:1–12. https://doi.org/10.1128/mBio.00812-17
10. Sylvester TT, Martin LER, Buss P, Loxton AG, Hausler GA, Rossouw L, et al. Prevalence and risk factors for *Mycobacterium bovis* infection in African lions (*Panthera leo*) in the Kruger National Park. J Wildl Dis. 2017;53:372–6. https://doi.org/10.7589/2016-07-159

Address for correspondence: Michele A. Miller, Department of Science and Technology–National Research Foundation Centre of Excellence for Biomedical Tuberculosis Research, South African Medical Research Council Centre for Tuberculosis Research, Division of Molecular Biology and Human Genetics, Faculty of Medicine and Health Sciences, Stellenbosch University, PO Box 241, Cape Town 8000, South Africa; email: miller@sun.ac.za

Global Estimates of Invasive *Mycobacterium chimaera* Infections after Cardiac Surgery

Theresa L. Lamagni, André Charlett, Nick Phin, Maria Zambon, Meera Chand

Author affiliations: Public Health England, London, UK (T.L. Lamagni, A. Charlett, N. Phin, M. Zambon, M. Chand); Imperial College, London (M. Zambon, M. Chand); Guy's & St. Thomas' NHS Foundation Trust, London (M. Chand)

DOI: https://doi.org/10.3201/eid2603.180452

To the Editor: In their recent assessment of *Mycobacterium chimaera* risk in patients undergoing heart valve surgery, Sommerstein et al. compare their findings to our prior risk assessment for UK patients (*1*,*2*). In their article, the authors note their assessed risk as "4 to 7" times higher than our risk estimate and suggest this relates to differences in case-finding methodology. Our study reported incidence density (cases per 10,000 person-years) to account for the differing lengths of postoperative follow-up in each successive annual cohort of surgical patients. In contrast, Sommerstein et al. calculated crude risk based on annual procedure numbers. Since our published assessment was undertaken some years before the authors' assessment, additional cases have been diagnosed, in keeping with the long incubation period for these infections, a median of 15 months but up to 5 years (*3*). Recalculation of risk and 95% (binomial) CIs, limited to 2008–2014 to match the authors' assessment, would yield a crude risk estimate of 0.24 (0.15–0.35) per 1,000 procedures (24/102,234); the risk in Switzerland (11/14,054) would be estimated at 0.78 (0.39–1.40), just over 3 times higher.

Whether the observed differences between the United Kingdom and Switzerland represent a true difference in *M. chimaera* risk in patients undergoing heart valve surgery is subject to debate. Both countries based case finding on results from routine diagnostic investigation; however, awareness of the risk in Switzerland predates that in other countries, potentially increasing the likelihood of investigation for mycobacterial infection. We have observed considerable variation in risk between cardiac centers, from 0 cases rising to 1 per 100 patients for 1 center in their year of highest estimated risk (*4*). Our pooled estimate covering 33 centers may encompass a wider selection of risk profiles, compared with the smaller number of centers in Switzerland.

References

1. Sommerstein R, Hasse B, Marschall J, Sax H, Genoni M, Schlegel M, et al.; Swiss Chimaera Taskforce. Global health estimate of invasive *Mycobacterium chimaera* infections associated with heater-cooler devices in cardiac surgery. Emerg Infect Dis. 2018;24:576–8. https://doi.org/10.3201/eid2403.171554
2. Chand M, Lamagni T, Kranzer K, Hedge J, Moore G, Parks S, et al. Insidious risk of severe *Mycobacterium chimaera* infection in cardiac surgery patients. Clin Infect Dis. 2017;64:335–42. https://doi.org/10.1093/cid/ciw754
3. Scriven JE, Scobie A, Verlander NQ, Houston A, Collyns T, Cajic V, et al. *Mycobacterium chimaera* infection following cardiac surgery in the United Kingdom: clinical features and outcome of the first 30 cases. Clin Microbiol Infect. 2018;24:1164–70. https://doi.org/10.1016/j.cmi.2018.04.027
4. Public Health England. Infections associated with heater cooler units used in cardiopulmonary bypass and ECMO. Information for healthcare providers in the UK. 2017 [cited 2018 Mar 13]. https://www.gov.uk/government/publications/infections-associated-with-heater-cooler-units-used-in-cardiopulmonary-bypass-and-ecmo

Address for correspondence: Theresa L. Lamagni, Public Health England—National Infection Service, 61 Colindale Avenue, London NW9 5EQ, UK; email: theresa.lamagni@phe.gov.uk

Rami Sommerstein, Barbara Hasse, Andreas F. Widmer

Author affiliations: Bern University Hospital, Bern, Switzerland (R. Sommerstein); University Hospital Zurich, Zurich, Switzerland (B. Hasse); Basel University Hospital, Basel, Switzerland (A.F. Widmer)

DOI: https://doi.org/10.3201/eid2603.191818

In Response: We would like to thank Lamagni et al. (*1*) for including additional cases from the period of 2008–2014 and for recalculating the UK cumulative incidence risk by matching our assessment. We agree that the observed 3 times higher risk in Switzerland of *Mycobacterium chimaera* infection for a patient undergoing heart valve surgery cannot be explained unambiguously. The most likely explanation is indeed increased awareness of the risk in Switzerland compared with other countries, potentially improving likelihood of investigation for mycobacterial infection. We think that the early formation of a national and interdisciplinary working group (*M. chimaera* Task Force), which included representatives of the involved (para-)medical disciplines, authorities, and professional associations, has contributed greatly to raising this awareness.

We want to emphasize that approximately half of the patients in Switzerland were treated for suspected sarcoidosis or other rheumatic diseases. It was via the active case finding mechanisms that these cases were identified. Furthermore, we would like to point out that, since the publication of our report (2), only one case known to the Task Force has been identified in Switzerland (in a patient whose surgery was performed in 2014). This finding could indicate that the formation of the national task force not only increased awareness but also ensured that the remaining infectious risk was reduced to a minimum within a very short time.

References

1. Lamagni T, Charlett A, Phin N, Zambon M, Chand M. Invasive *Mycobacterium chimaera* infections hand heater–cooler devices in cardiac surgery. Emerg Infect Dis. 2020 Mar [*date cited*]. https://doi.org/10.3201/eid2603.180452
2. Sommerstein R, Hasse B, Marschall J, Sax H, Genoni M, Schlegel M, et al.; Swiss Chimaera Taskforce. Global health estimate of invasive *Mycobacterium chimaera* infections associated with heater-cooler devices in cardiac surgery. Emerg Infect Dis. 2018;24:576–8. https://doi.org/10.3201/eid2403.171554

Address for correspondence: Rami Sommerstein, Bern University Hospital, Department of Infectious Diseases, Freiburgstrasse, 3010 Bern, Switzerland; email: rami.sommerstein@insel.ch

Confusion in the Genesis of Art and Disease—Charles Laval, Paul Gauguin, and Tuberculosis

Terence Chorba and John Jereb

Charles Laval (1861–1894) was a Parisian painter whose brief life ended in an untimely death from underlying tuberculosis. He was a colleague and contemporary of two other post-Impressionists: Vincent van Gogh (1853–1890) and Paul Gauguin (1848–1903). In part because of misattribution, Laval's work has receded into a historical footnote to the career of Gauguin, whose output far exceeded that of Laval. Gauguin, among the most renowned of the late 19th century European artists, was a pioneer of the Synthetist school of painting. This post-Impressionist movement encouraged artists to depict their emotions about the subject, beyond its outward appearance, with bold displays of color, relaxation of exactitude, and portrayal of form based on memory.

Laval studied under realist painter Léon Bonnat at the École des Beaux-Arts in Paris. In the summer of 1886, he became acquainted with van Gogh and Gauguin at Pont-Aven, a growing artist colony in Brittany. In April 1887, Laval and Gauguin set sail for Panama, an adventure that was ostensibly pursued for employment at the invitation of Gauguin's brother-in-law, a Chilean with business interests in Panama. In June 1887, after several misadventures, Laval and Gauguin left Panama for Martinique, where they painted together before returning to France in November of the same year.

The emergence of Laval's eccentric, flamboyant style coincided with Gauguin's. The astonishing similarity of their works from that period has led art historians to conclude that a few of Laval's paintings were incorrectly attributed to Gauguin, whose signature was added later to inflate market value. *Femmes et Chevre dans le Village* (Women and Goat in the Village), presented on the next page, was undertaken in Martinique and bears a Gauguin signature but has been attributed by some to Laval. The ascendance of Gauguin's legacy and the neglect of Laval's, in the context of their matching styles, could tempt us to surmise that Laval imitated Gauguin, but their paintings and their life stories leave open the possibility that their visions converged as they influenced each other. Only Laval's early death deprived him, and us, of his potential for greater recognition.

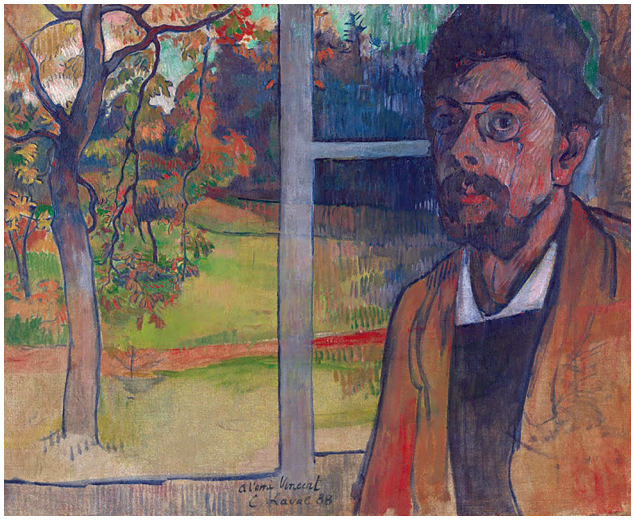

Charles Laval (1861–1894, *Self-Portrait, Pont-Aven*, 1888. Oil on canvas, 20 in x 23.8 in/50.7 cm × 60.4 cm. Van Gogh Museum, Amsterdam, Vincent van Gogh Foundation.

During the brief sojourn in Martinique, Gauguin wrote to a painter friend back in Paris, Émile Schuffenecker, that he would be returning with a dozen of his own works, presumably to sell. However, in the various editions of the definitive Gauguin catalogue raisonné, a total of 18 works has been attributed to him from Martinique. The leading explanation for the surfeit of Gauguin-attributed works relative to the number that he reported to Schuffenecker is that some of these works may be those of Laval or other painters. Only six original remaining paintings are signed by and

Author affiliation: Centers for Disease Control and Prevention, Atlanta, Georgia, USA

DOI: https://doi.org/10.3201/eid2603.AC2603

Paul Gauguin (1848–1903), *Women and Goat in the Village* (*Femmes et Chevre dans le Village*), 1887. Oil on canvas, 45.7 x 71 cm. The Israel Museum, Jerusalem, America-Israel Cultural Foundation.

attributed to Laval, and all these date from after their time in Martinique.

Laval and Gauguin both returned to the school at Pont-Aven, but the friendship dissolved when Gauguin fell in love with Madeleine Bernard, sister of Émile Bernard, another Synthetist painter and van Gogh's best friend, but Laval became engaged to her. Soon after the return to Pont-Aven, Laval developed tuberculosis. In 1890, he set sail for Cairo in search of a more favorable climate but returned to Paris and succumbed to an acute illness in 1894 at age 33. Tuberculosis patients easily fell prey to other illnesses because of their impaired pulmonary function and weakened constitution. Influenza was notoriously lethal for them. Madeleine also acquired tuberculosis and died in 1895. In our era of curative therapy, we forget the chronic natural course of tuberculosis: in the preantibiotic era, a third of its victims would survive longer than 5 years, perpetuating the epidemic and the dread that it evoked.

An infamously capricious agent of death, tuberculosis has taken away a great many artists prematurely. Through their creations, they could mourn the burden of mortality or conceal it defiantly. Laval seems to have traveled both pathways: his *Self Portrait,* inspired in an exchange with van Gogh in 1888 and praised by Gauguin, is featured on this month's cover. In it, Laval gave us a brilliant exterior window view alive with splashes of color; he relegated his own face to one side, hauntingly somber, gaunt, peering out from cyan shadows wistfully. Does the gnarled tree reflect how Laval imagined himself, beaten down by tuberculosis?

In an 1895 letter, Gauguin mused that "in art, there are only two types of people: revolutionaries and plagiarists." The resemblance of Laval's work to Gauguin's brought criticism to Laval. How fitting that tuberculosis, the source of Laval's demise, is sometimes called "the great imitator" when clinicians are challenged by differentiating it from other diseases. Pulmonary tuberculosis and lung cancer commonly mimic each other, indistinguishable radiographically, sharing symptoms of cough, fevers, chills, loss of weight, and even similar presentations of metastasis. Similarly, intestinal tuberculosis mimics chronic inflammatory bowel disease, including Crohn's disease and ulcerative colitis.

Although Gauguin's most widely discussed, reproduced, and exhibited paintings were undertaken in Tahiti over a 10-year period toward the end of his life, the greater body of his work spanned a 35-year career. In contrast, Laval painted for barely a decade before tuberculosis halted the trajectory of his career. Had he fared better in his fight with tuberculosis, his artistic style could have matured independently, and his renown might have rivaled that of Gauguin. Had that happened, differentiating the work of these two artists would be easier.

Bibliography

1. Benezit Dictionary of Artists. Charles Laval. Oxford (UK): Oxford University Press; 2006.
2. Faci M, Cavazza A, Ferrari G, Filice A, Sgarbi G. Pulmonary tuberculosis mimicking lung metastasis. J Thorac Oncol. 2008;3:660–1. https://doi.org/10.1097/JTO.0b013e3181757ad4
3. Gecse KB, Vermeire S. Differential diagnosis of inflammatory bowel disease: imitations and complications. Lancet Gastroenterol Hepatol. 2018;3:644–53. https://doi.org/10.1016/S2468-1253(18)30159-6
4. Guérin D, editor. Paul Gauguin: The writings of a savage. Levieux E, translator. New York: Da Capo Press; 1996.
5. Malingue M, editor. Paul Gauguin: letters to his wife and friends. Paris: Bernard Grasset; 1949.
6. Pope KR. Gauguin and Martinique [doctoral dissertation]. Austin (TX): University of Texas; 1981.
7. Sweetman D. Paul Gauguin: a complete life. London: Hodder and Stoughton, 1995.
8. van Dijk M, van der Hoeven J. Gauguin and Laval in Martinique. Bussum (The Netherlands): Thoth Publishers; 2018.
9. Vickers P. Martinique: in Gauguin's footsteps. Contemporary Review. 1997;270:313–4.
10. Wildenstein G. Paul Gauguin: catalogue raisonné, 1st ed. Paris: Les Beaux-Arts; 1964.

Address for correspondence: Terence Chorba, Centers for Disease Control and Prevention, 1600 Clifton Rd NE, Mailstop US12-4, Atlanta, GA 30329-4027, USA; email: tlc2@cdc.gov

EMERGING INFECTIOUS DISEASES®

Upcoming Issue

- Stemming the Increase in Human-Biting Ticks and Tickborne Diseases, United States
- Decreased Susceptibility to Azithromycin in Clinical Shigella Isolates Associated with HIV and Sexually Transmitted Bacterial Diseases, Minnesota, USA, 2012–2015
- Ecology and Epidemiology of Tickborne Pathogens, Washington State, USA, 2011–2016
- Severe Dengue Epidemic, Sri Lanka, 2017
- High Incidence of Active Tuberculosis in Asylum Seekers from Eritrea and Somalia in the First 5 Years after Arrival in the Netherlands
- Severe Fever with Thrombocytopenia Syndrome, Japan, 2013–2017
- Comprehensive Profiling of Zika Virus Risk with Natural and Artificial Mitigating Strategies, United States
- Intensified Short Symptom Screening Program for Dengue Infection during Pregnancy, India
- Genomic Insight into the Spread of Meropenem-Resistant *Streptococcus pneumoniae* Spain-ST81, Taiwan
- Isolation of Drug-Resistant *Gallibacterium anatis* from Calves with Unresponsive Bronchopneumonia
- Prevalence of Antibodies to Crimean-Congo Hemorrhagic Fever Virus in Ruminants, Nigeria, 2015
- Confirmation of Person-to-Person Transmission of Andes Virus in Persons with Hantavirus Pulmonary Syndrome, Argentina, 2014
- Detection of Zoonotic Bartonella Pathogens in Rabbit Fleas, Colorado, USA
- Tickborne Crimean-Congo Hemorrhagic Fever Virus in Humans and Livestock, Pakistan
- Outbreak of *Dirkmeia churashimaensis* Fungemia in a Neonatal Intensive Care Unit, India
- Pruritic Cutaneous Nematodiasis Caused by Avian Eyeworm Oxyspirura Larvae, Vietnam
- Recurrent Herpes Simplex Virus 2 Lymphocytic Meningitis in a Patient with Immunoglobulin G Subclass 2 Deficiency

Complete list of articles in the April issue at http://www.cdc.gov/eid/upcoming.htm

Upcoming Infectious Disease Activities

March 8–11, 2020
Conference on Retroviruses and Opportunistic Infections
Boston, MA, USA
https://www.croiconference.org/

March 9–13, 2020
African Society for Laboratory Medicine
7th African Network for Influenza Surveillance Epidemiology
Livingstone, Zambia
https://www.anise2020.org

March 18–20, 2020
International Conference on Reemerging Infectious Diseases
Addis Ababa, Ethiopia
http://www.icreid.com

March 26–30, 2020
Society for Healthcare Epidemiology of America Decennial 2020
6th International Conference on Healthcare Associated Infections
Atlanta, GA, USA
https://decennial2020.org

April 18–21, 2020
The European Congress of Clinical Microbiology and Infectious Diseases
Paris, France
https://www.eccmid.org/eccmid_2020/

May 3–6, 2020
ASM Clinical Virology Symposium
West Palm Beach, FL, USA
https://asm.org/Events/2019-Clinical-Virology-Symposium/Home

June 18-22, 2020
American Society for Microbiology ASM Microbe 2020
Chicago, Il, USA
https://asm.org/Events/ASM-Microbe

Announcements
Email announcements to EIDEditor (eideditor@cdc.gov). Include the event's date, location, sponsoring organization, and a website.

Earning CME Credit

To obtain credit, you should first read the journal article. After reading the article, you should be able to answer the following, related, multiple-choice questions. To complete the questions (with a minimum 75% passing score) and earn continuing medical education (CME) credit, please go to http://www.medscape.org/journal/eid. Credit cannot be obtained for tests completed on paper, although you may use the worksheet below to keep a record of your answers.

You must be a registered user on http://www.medscape.org. If you are not registered on http://www.medscape.org, please click on the "Register" link on the right hand side of the website.

Only one answer is correct for each question. Once you successfully answer all post-test questions, you will be able to view and/or print your certificate. For questions regarding this activity, contact the accredited provider, CME@medscape.net. For technical assistance, contact CME@medscape.net. American Medical Association's Physician's Recognition Award (AMA PRA) credits are accepted in the US as evidence of participation in CME activities. For further information on this award, please go to https://www.ama-assn.org. The AMA has determined that physicians not licensed in the US who participate in this CME activity are eligible for *AMA PRA Category 1 Credits*™. Through agreements that the AMA has made with agencies in some countries, AMA PRA credit may be acceptable as evidence of participation in CME activities. If you are not licensed in the US, please complete the questions online, print the AMA PRA CME credit certificate, and present it to your national medical association for review.

Article Title

Clinical Characteristics of Disseminated Strongyloidiasis, Japan, 1975–2017

CME Questions

1. Your patient is a 60-year-old man with human T-cell lymphotropic virus type 1 (HTLV-1) infection who was admitted for suspected strongyloidiasis. According to the Japanese case series by Mukaigawara and colleagues, which of the following statements about classification of disseminated strongyloidiasis into 3 clinical phenotypes is correct?

A. Most patients had occult dissemination with meningitis caused by enteric organisms
B. Mortality was greatest among patients with occult dissemination with culture-negative suppurative meningitis
C. Sepsis occurred in 40.6% of patients with dissemination
D. The number of reported cases increased each year

2. According to the Japanese case series by Mukaigawara and colleagues, which of the following statements about clinical and laboratory findings in disseminated strongyloidiasis is correct?

A. Common symptoms included fever (52.9%), headache (32.9%), mental status changes (24.3%), and nausea/vomiting (14.3%)
B. Half of patients tested for HTLV-1 with serological assay had positive findings
C. Predominant clinical syndromes were sepsis caused by nonenteric organisms, heart failure, and disseminated rash
D. *Enterococcus* spp. were the most frequent isolates from blood and cerebrospinal fluid (CSF) cultures

3. According to the Japanese case series by Mukaigawara and colleagues, which of the following statements about treatment of disseminated strongyloidiasis is correct?

A. Before 2002, most patients were treated with pyrvinium pamoate 20 mL/d
B. After 2003, patients were treated with ivermectin, 200 μg/kg/d, either 1 to 2 weeks apart or consecutively until clinical improvement or disappearance of larvae from stool
C. Patients with occult dissemination should be observed and treated only if they deteriorate
D. Treatment should be limited to antihelmintic agents

Earning CME Credit

To obtain credit, you should first read the journal article. After reading the article, you should be able to answer the following, related, multiple-choice questions. To complete the questions (with a minimum 75% passing score) and earn continuing medical education (CME) credit, please go to http://www.medscape.org/journal/eid. Credit cannot be obtained for tests completed on paper, although you may use the worksheet below to keep a record of your answers.

You must be a registered user on http://www.medscape.org. If you are not registered on http://www.medscape.org, please click on the "Register" link on the right hand side of the website.

Only one answer is correct for each question. Once you successfully answer all post-test questions, you will be able to view and/or print your certificate. For questions regarding this activity, contact the accredited provider, CME@medscape.net. For technical assistance, contact CME@medscape.net. American Medical Association's Physician's Recognition Award (AMA PRA) credits are accepted in the US as evidence of participation in CME activities. For further information on this award, please go to https://www.ama-assn.org. The AMA has determined that physicians not licensed in the US who participate in this CME activity are eligible for *AMA PRA Category 1 Credits*™. Through agreements that the AMA has made with agencies in some countries, AMA PRA credit may be acceptable as evidence of participation in CME activities. If you are not licensed in the US, please complete the questions online, print the AMA PRA CME credit certificate, and present it to your national medical association for review.

Article Title

Epidemiology of Cryptosporidiosis, New York City, New York, USA, 1995–2018

CME Questions

1. Which of the following statements regarding cryptosporidiosis is most accurate?

A. It is usually transmitted through either the respiratory or fecal-oral route
B. Recreational water use is a risk factor for cryptosporidiosis
C. All patients with cryptosporidiosis require antiparasitic treatment
D. The best means to neutralize *Cryptosporidium* oocytes in drinking water is low levels of chlorine

2. What does the current study by Alleyne and colleagues find regarding the epidemiology of cryptosporidiosis in New York, New York?

A. The median annual age-adjusted incidence of cryptosporidiosis cases was 536/100,000 population
B. There was a gradual increase in the incidence of cryptosporidiosis from 1995 to 2018
C. Cryptosporidiosis was most active in January and February
D. There were no outbreaks of cryptosporidiosis related to New York, New York, tap water

3. Which of the following statements regarding individuals with documented cryptosporidiosis in the current study is most accurate?

A. Most patients were male between the ages of 20 and 59 years
B. Most patients were nonwhite
C. The incidence of cryptosporidiosis among individuals living with HIV infection increased steadily from 1995 to 2018
D. There was no geographic pattern of cryptosporidiosis cases

4. Which of the following statements regarding other trends in the epidemiology of cryptosporidiosis in the current study is most accurate?

A. Most patients reported international travel during their incubation period
B. Cryptosporidiosis related to international travel declined in incidence between 2010 and 2018
C. Syndromic multiplex panels were associated with an increase in the incidence of cryptosporidiosis
D. The introduction of syndromic multiplex panels led to an increase in cases of cryptosporidiosis among individuals living with HIV infection

Earning CME Credit

To obtain credit, you should first read the journal article. After reading the article, you should be able to answer the following, related, multiple-choice questions. To complete the questions (with a minimum 75% passing score) and earn continuing medical education (CME) credit, please go to http://www.medscape.org/journal/eid. Credit cannot be obtained for tests completed on paper, although you may use the worksheet below to keep a record of your answers.

You must be a registered user on http://www.medscape.org. If you are not registered on http://www.medscape.org, please click on the "Register" link on the right hand side of the website.

Only one answer is correct for each question. Once you successfully answer all post-test questions, you will be able to view and/or print your certificate. For questions regarding this activity, contact the accredited provider, CME@medscape.net. For technical assistance, contact CME@medscape.net. American Medical Association's Physician's Recognition Award (AMA PRA) credits are accepted in the US as evidence of participation in CME activities. For further information on this award, please go to https://www.ama-assn.org. The AMA has determined that physicians not licensed in the US who participate in this CME activity are eligible for *AMA PRA Category 1 Credits*™. Through agreements that the AMA has made with agencies in some countries, AMA PRA credit may be acceptable as evidence of participation in CME activities. If you are not licensed in the US, please complete the questions online, print the AMA PRA CME credit certificate, and present it to your national medical association for review.

Article Title

Methicillin-Resistant *Staphylococcus aureus* Bloodstream Infections and Injection Drug Use, Tennessee, USA, 2015–2017

CME Questions

1. You are advising a public health department in Tennessee about anticipated needs and potential preventive strategies for methicillin-resistant *Staphylococcus aureus* (MRSA) bloodstream infections (BSI). According to the analysis of data from the National Healthcare Safety Network (NHSN) and the Tennessee Hospital Discharge Data System by Parikh and colleagues, which of the following statements about the prevalence of life-threatening injection drug use (IDU)–related MRSA BSI in Tennessee in 2015–2017 is correct?

A. 10% of identified MRSA BSI were IDU-related
B. IDU-related BSI increased by nearly 50%
C. The number of MRSA BSI cases overall remained stable from 2015 to 2017
D. Among IDU-related cases stratified by onset type, 62.9% were community-onset (CO), with positive culture drawn in the emergency department (CO-ED)

2. According to the analysis of data from the NHSN and the Tennessee Hospital Discharge Data System by Parikh and colleagues, which of the following statements about the demographics and clinical characteristics of IDU-related MRSA BSI in Tennessee in 2015–2017 is correct?

A. IDU-related MRSA BSI more often occurred in older black men
B. Non-IDU BSI had higher use of Medicare (63.5%) and commercial insurance (11.21%); IDU cases had higher self-pay/uninsured (33.3%) and Medicaid (31%) status
C. Among all MRSA BSI, one-quarter had ≥1 IDU-related diagnosis documented within 6 months of MRSA onset
D. Prevalence of endocarditis and hepatitis C infections was not significantly different for IDU-related vs IDU-unrelated MRSA BSI

3. According to the analysis of data from the NHSN and the Tennessee Hospital Discharge Data System by Parikh and colleagues, which of the following statements about clinical and public health implications of the association of IDU practices with life-threatening MRSA BSI in Tennessee is correct?

A. Targeted harm reduction strategies for persons at high risk for IDU are needed to lower the burden of MRSA BSI in acute care settings, as IDU can lead to life-threatening MRSA BSI
B. The increase in the burden of all MRSA BSI in Tennessee from 2015 to 2017 is not likely related to the drug use crisis
C. Most public health MRSA BSI prevention and treatment strategies currently target CO infections
D. The findings are unlikely to affect ED management of MRSA BSI

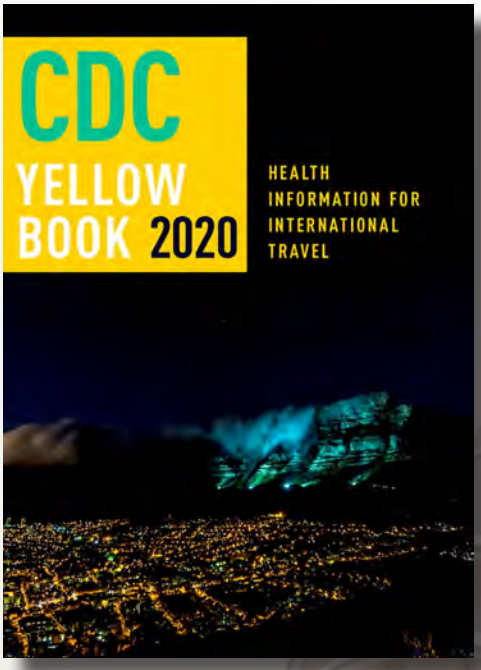

Available Now
Yellow Book 2020

The fully revised and updated CDC Yellow Book 2020: Health Information for International Travel codifies the US government's most current health guidelines and information for clinicians advising international travelers, including pretravel vaccine recommendations, destination-specific health advice, and easy-to-reference maps, tables, and charts.

ISBN: 978-0-19-006597-3 | $115.00 | May 2019 | Hardback | 720 pages

ISBN: 978-0-19-092893-3 | $55.00 | May 2019 | Paperback | 687 pages

Yellow Book 2020 includes important travel medicine updates

- **The latest information on emerging infectious disease threats, such as Zika, Ebola, and henipaviruses**
- **Considerations for treating infectious diseases in the face of increasing antimicrobial resistance**
- **Legal issues facing clinicians who provide travel health care**
- **Special considerations for unique types of travel, such as wilderness expeditions, work-related travel, and study abroad**

OXFORD
UNIVERSITY PRESS

Order your copy at:
www.oup.com/academic